Synaptic plasticity in stochastic neuronal networks

Gaëtan Vignoud

▶ **To cite this version:**

Gaëtan Vignoud. Synaptic plasticity in stochastic neuronal networks. Probability [math.PR]. Sorbonne Université, 2022. English. NNT : 2022SORUS068 . tel-03640150v2

HAL Id: tel-03640150
https://theses.hal.science/tel-03640150v2

Submitted on 6 Jul 2022

HAL is a multi-disciplinary open access archive for the deposit and dissemination of scientific research documents, whether they are published or not. The documents may come from teaching and research institutions in France or abroad, or from public or private research centers.

L'archive ouverte pluridisciplinaire **HAL**, est destinée au dépôt et à la diffusion de documents scientifiques de niveau recherche, publiés ou non, émanant des établissements d'enseignement et de recherche français ou étrangers, des laboratoires publics ou privés.

Sorbonne Université
ED 386 - Paris Centre

MAMBA - Modelling and Analysis for Medical and Biological Applications
Inria de Paris, LJLL (UMR 7598) - Laboratoire Jacques-Louis Lions

Équipe Dynamic and Pathophysiology of Neuronal Networks
Center for Interdisciplinary Research in Biology (CIRB), College de France, CNRS, INSERM, Université PSL, Paris, France

ÉTUDE DE LA PLASTICITÉ SYNAPTIQUE DANS LES RÉSEAUX STOCHASTIQUES DE NEURONES

SYNAPTIC PLASTICITY IN STOCHASTIC NEURAL NETWORKS

Par Gaëtan Vignoud

Thèse de doctorat de Mathématiques

Dirigée par Philippe Robert et Laurent Venance
Présentée et soutenue publiquement le 15 mars 2022
Devant un jury composé de :

- Pr. Nicolas Brunel (Rapporteur, Professor of Neurobiology, Duke University)
- Dr. Fabien Campillo (Rapporteur, DR INRIA)
- Dr. Srdjan Ostojic (Examinateur, DR CNRS)
- Pr. Lea Popovic (Rapportrice, Associate Professor, Mathematics and Statistics, Concordia)
- Dr. Philippe Robert (Directeur de thèse, DR INRIA)
- Pr. Michèle Thieullen (Examinatrice, MC Sorbonne Université)
- Pr. Jonathan D. Touboul (Invité, Associate Professor of Mathematics, Brandeis University)
- Dr. Laurent Venance (Directeur de thèse, DR INSERM)

Acknowledgements

Une longue liste de remerciements se prépare, et c'est tout dire que je n'aurai pu apprécier les quatre dernières années, rédiger ce manuscrit sans l'aide et le support de nombreuses personnes.

Je me permettrai de commencer par remercier grandement mes trois rapporteurs, Nicolas Brunel, Fabien Campillo et Lea Popovic, qui ont accepté de lire mon (très) long manuscrit et rédigé des rapports qui m'ont été d'une grande aide. Par la même occasion, j'exprime toute ma gratitude aux autres membres du jury, Srdjan Ostojic et Michèle Thieullen pour avoir accepté de m'évaluer lors de ma soutenance publique. Je ne peux que vous faire part de ma reconnaissance pour le travail que vous avez tous et toutes produit afin de juger mon travail, et la grande honnêteté avec laquelle cela fut réalisé.

Cette thèse est le résultat d'un impressionnant travail d'équipe, au cours duquel mes deux fantastiques directeurs de thèse m'ont guidé, aidé et parfois même supporté (dans les deux sens du terme). Philippe, merci pour ta pédagogie et ta rigueur, qui m'ont permis au cours de ces années de découvrir et de finir par adhérer totalement à ta vision des mathématiques. Je ne pourrai mentionner toutes nos discussions, qui pouvaient très facilement déborder du cadre de la science, lorsque nous débations de sports, de littérature, de politique, à table, autour d'un thé, ou lors d'un footing au Parc de Vincennes. Ces deux ans passés seul à tes côtés ne sont remplis que de souvenirs agréables, et depuis que notre petite équipe s'est agrandie, je ne peux qu'apprécier encore plus toutes tes qualités. Laurent, tu me suis depuis maintenant presque sept ans, ce beau rapprochement que l'on doit à Jonathan, m'a permis d'exaucer mon rêve de jeunesse de pouvoir travailler au contact des neurosciences et de la médecine. Je ne te remercierai jamais assez pour m'avoir invité dans ton équipe, et m'avoir permis d'interagir avec tous les expérimentalistes de talent que tu aiguilles au jour le jour. Nos longues discussions, la liberté que tu m'as laissé et ton soutien tout au long de ma thèse sont autant de guides sur lesquels je me suis reposé au cours des ces années. Tu diriges une équipe pleine de vie, à ton image, qui m'a accueilli avec une affection presque familiale, et avec qui j'ai partagé tant de bon moments, à base de bonnes bières et de champagne. Je tenais à terminer en insistant sur le fait que malgré vos domaines d'expertise très éloignés, ce fut toujours un grand plaisir pour moi de participer à nos réunions communes, où je pouvais observer, dans la bonne humeur, la rencontre entre deux mondes scientifiques très différents. Votre ouverture d'esprit partagée m'impressionne encore tout autant, et je vous remercie de m'avoir permis de faire cette aventure à vos côtés.

Cette rencontre, nous te la devons Jonathan et c'est une des raisons pour lesquelles je tenais à t'exprimer toute la gratitude que je te dois. Tu fus présent dès mes premiers pas dans le monde de la recherche, et m'auras accompagné tout le long de mon parcours, jusqu'à cette soutenance, où tu as accepté de faire partie de mon jury. Sans toi, sans tes idées, sans ta motivation et ton intuition, je ne serai pas allé bien loin, et c'est avec grand plaisir que j'ai pu venir travailler directement à tes côtés durant ma thèse. J'ai été honoré de partager ce long segment de ma vie avec toi, et en regardant en arrière, je peux apprécier comment ta présence m'a permis de grandir tant scientifiquement que personnellement.

Je me dois maintenant de porter un toast à toute l'équipe DPRN (et oui c'est çà son nom), comme nous avons pu le faire dans à peu près toutes les salles du Collège de

France (à base de kro, saucissons, chips au vinaigre) sous la houlette de Sylvie, grande organisatrice et cuisinière talentueuse. Bertrand, Marie, Mérie, Nathalie, Nicolas, Seb, Yulia, Willy et tant d'autres, vous avez participé par tous nos échanges, moments de folie et de jeux, à rendre cette période inoubliable. Charlotte et Elodie, nous aurons tout fait ensemble, en passant pas la Californie et ses chemins dangereux, je vous remercie de m'avoir supporté (surtout quand je conduisais), et je tiens à vous faire part de mon admiration la plus totale quant au travail que vous produisez tous les jours, tout en restant disponibles pour un bon burger. Jana et Lucie, vous êtes venues nous rejoindre avec Philippe et avez apporté votre vivacité et votre éclat lors de cette période difficile du COVID. Merci pour toutes ces discussions où nous ne pouvions nous empêcher quelques fois de martyriser le pauvre Philippe, ces bonnes patisseries et macarons. Je regrette juste que nous n'ayons pu vous convertir à la course à pied, mais bon votre thèse est encore longue . . . Je tenais aussi remercier les personnes que j'ai pu rencontrer à Brandeis, notamment Denis, Kana, Subhadra, Daniel, grâce à qui le temps passé en Goldsmith 118 reste chargé de bons souvenirs. Un grand merci enfin à tous les services administratifs et de gestion avec qui j'ai eu à interagir, tout particulièment au CIRB, Nicole et France, à l'INRIA, Meriem, pour votre efficacité et la bonne humeur avec laquelle tous les problèmes étaient résolus.

Je me tourne maintenant vers toutes celles et ceux que j'ai la chance d'appeler mes amis, et qui tout au long de ces années ont fait preuve d'une grande résilience et compréhension. Toujours là pour me changer les idées et me remonter le moral, leur contribution à cette thèse, bien qu'indirecte, est de premier plan. Chacune de ces "teams", symbolisée par un groupe messenger associé, où j'ai bien souvent abusé de mon talent de spammeur, a une place bien claire dans mon coeur et y restera pour longtemps, je l'espère. Tout d'abord, la *Team Escape* avec qui j'ai pu enchaîner escape games, restaurants, repas Top Chef et cinéma, en passant par les Fêtes de Bayonne. Vous êtes une deuxième famille pour moi, et je ne vous remercierai jamais assez pour tous ces moments. Pour ce qui est de la partie sportive, il me faut remercier la *Team Rando* avec qui j'ai parcouru une bonne partie de la France avec comme point culminant ce GR20 si attendu. Nos footings, parties de switch et repas délicieux ont rythmé ces dernières années et j'espère qu'ils ne s'arrêteront pas de si tôt. Pour continuer dans le "sport", je dois remercier *Chambre Ski*, cette géniale équipe composées des BDS 2014/2015/2016 de l'ENS, avec qui le lien est toujours très fort, surtout pour aller manger chez Oi ou danser sur du Lady Gaga. Heureusement, mes deux *teams MacDo* étaient toujours présentes pour me rappeler que l'essentiel restait de bien manger, en bonne compagnie et de collecter des verres. On va arriver à vaincre le Monopoly, j'ai confiance en nous. La *team HP* m'a permis de m'évader à Londres (et Paris), lors de petits thés, de séances de théâtre, de brunchs, dans une ambiance digne d'Harry Potter. Bon il faut être honnête, les Serdaigles dominent le monde, mais les Poufsouffles ne sont pas si méchants. Je pense aussi à la *team Nico*, la *team Ski Ginette*, les *Tata du Mila*, et j'en oublie certainement d'autres ... Je m'estime heureux de pouvoir aujourd'hui compter sur autant de personnes, rencontrées au cours de mes très longues études, et je vous remercie tous et toutes pour ce que vous m'avez apporté.

Enfin, le reste de mes remerciements est pour ma famille, qui me soutient depuis mon plus jeune âge, grâce à une éducation exceptionnelle et un amour inconditionnel. Que ca soit mes oncles, tantes, cousins, cousines, du côté paternel comme maternel, vous avez tous toujours tout fait pour moi, dans un cadre que je m'estime chanceux de fréquenter, sur les pentes d'Orelle ou à la Fenouille. En particulier, ma cousine

Camille, ma jumelle, j'espère qu'on continuera à se supporter jusqu'àu bout. De mes grand-parents qui m'ont chacun servi d'exemples à leur manière, Grand-mère tu es la dernière représentante et je voudrais te dédier cette thèse, toi qui me soutient chaque jour. Papa, Maman, je voudrais vous remercier pour tous les sacrifices que vous avez fait pour moi, l'amour que vous me témoignez quotidiennement. Avec le temps qui passe, je réalise tout ce que je vous dois et vous pouvez compter sur moi pour ne pas l'oublier. Pour finir, je tenais à remercier mon frère et ma soeur pour nos différentes cohabitations, que cela soit à Lyon chez les parents, où à Paris, dans notre petit appart' du Montparnasse. J'ai toujours pu compter sur vous, comme compagnons de jeu et de vie, et ces liens forts qui nous unissent persisteront contre vents et marées.

SUMMARY

Synaptic plasticity is a biological mechanism, integrating neuronal activity in the evolution of recurrent connections between neurons. Several studies from biology and computational neuroscience have explored the influence of spike-timing dependent plasticity (STDP) on learning and memory. This PhD work is based on experimental data about STDP in the striatum, and studies its implications, first in mathematical models of neuronal networks seen as stochastic processes, and then in a learning task based on the functional role of the striatum.

We have developed a general class of models to reproduce different STDP rules in a stochastic setting, modeling spike trains as point processes. Synaptic plasticity is a slow process, compared to neuronal activity, supporting an analysis of this system using slow-fast theory. After having characterized the dynamics of complex shot-noise processes, and introduced several auxiliary models, we prove that the scaled system wis tight, and that stochastic averaging principles are verified. Adding regularity hypotheses, we prove a convergence theorem in the slow-fast limit, and apply it to different sets of STDP rules. The simplest STDP rule consists in updating the synaptic weights as a function of the time between pre- and postsynaptic spikes. These models also depend a lot on the choice of which spikes to consider when updating the synaptic weight. Using the previously proven averaging principle, we study the influence of different models of synaptic dynamics. A theoretical and numerical analysis of the synaptic weight asymptotic behavior is performed and has led us to conclude on the potential impact of each STDP rule on a simple network.

Neuronal dynamics can be represented using auto-exciting stochastic processes, called Hawkes processes. We develop a new formalism to study these objects, by representing them as Markov processes in the space of non-negative real sequences. Using a Markovian approach, we prove results on the existence of stationary Hawkes processes for a simple subclass of Hawkes processes.

At the same time, we also study the influence of anti-Hebbian STDP in networks inspired from the striatum, a subcortical nucleus involved in procedural learning. Anti-Hebbian STDP is specific to the striatum, and we investigated its implication when learning sequences of cortical spikes. We found that the striatal network with anti-Hebbian STDP is able to discriminate rewarded and non-rewarded patterns. Other properties of striatal neurons are subsequently added to the model and improve the network performance. In particular, with collateral inhibition, which is displayed between striatal neurons, the system learns more patterns than classical algorithms. Finally, experimental results have recently shown that two regions of the dorsal striatum, the dorsolateral (DLS) and the dorsomedial (DMS) striatum display different kinds of STDP. Using a simple model accounting for these region-specific STDPs, we study the influence of STDP rules on learning in a complex task, composed by a learning phase, a maintenance phase where the network is subject to random activity, and a relearning phase. We show that STDP present at DMS synapses leads to a quicker forgetting of learned patterns and consequently to higher flexibility, while STDP at DLS synapses helps maintaining these patterns in memory.

RÉSUMÉ

La plasticité synaptique est un mécanisme biologique intégrant l'activité neuronale dans l'évolution des connections récurrentes entre différents neurones. De nombreuses études de biologie et de neurosciences computationelles ont exploré l'influence de la *spike-timing dependent plasticity* (STDP, plasticité fonction du temps d'occurrence des impulsions) sur l'apprentissage et la consolidation de la mémoire. Ces travaux de thèse s'appuient sur des données expérimentales de STDP dans le striatum, et étudie la dynamique associée dans des réseaux de neurones vue comme des processus stochastiques, puis dans une tâche d'apprentissage inspirée du rôle du striatum.

Nous avons développé une classe générale de modèles, pour reproduire différentes règles de STDP dans un cadre stochastique, en modélisant notamment les ensembles de potentiels d'action par des processus ponctuels. La plasticité synaptique est un processus lent comparé à l'activité neuronale, justifiant une analyse de ce système avec des arguments de la théorie lent-rapide. Après avoir caractérisé le comportement de processus de type *shot-noise* et introduit différents systèmes auxiliaires, il a été possible de démontrer que le système dimensionné était relativement compact et par conséquent, que la propriété d'homogénéisation était vérifiée. En ajoutant des hypothèses de régularité, un théorème de convergence dans la limite lent-rapide est énoncé et appliqué à différentes règles de STDP. La plus simple des règles de STDP consiste à mettre à jour les poids synaptiques en fonction de l'intervalle de temps entre les potentiels d'action présynaptique et postsynaptique. Le choix du modèle implique aussi de choisir quels potentiels d'action prendre en compte dans l'évolution du poids synaptique. En utilisant le théorème d'homogénéisation prouvé précédemment, nous avons étudié l'influence de ces différentes modélisations sur la dynamique des poids synaptiques. Une analyse théorique et numérique de l'évolution des poids synaptiques nous a amené à conclure sur l'impact des différents types de STDP sur un système neuronal simple.

Les neurones peuvent être modélisés par des processus stochastiques auto-excitants, appelés processus de Hawkes. Nous avons développé un formalisme nouveau pour étudier ces objets en les représentant comme des processus de Markov dans l'espace des suites réelles positives. En utilisant des arguments de théorie markovienne, nous avons pu montrer l'existence de versions stationnaires d'une sous-classe des processus de Hawkes.

En parallèle de ces travaux d'essence mathématique, nous avons étudié l'influence de la STDP de type anti-Hebienne dans des réseaux reproduisant certaines propriétés du striatum, un noyau sous-cortical impliqué dans l'apprentissage procédural. La plasticité anti-Hebbienne est une spécificité du striatum, et nous avons donc analysé son implication dans l'apprentissage de séquences de motifs corticaux. Nous avons montré que seul ce type de plasticité permet de discriminer les motifs associés à une récompense et ceux sans. D'autres propriétés des neurones striataux ont ensuite été ajoutées au modèle et ont amélioré la performance du réseau. En particulier, l'inhibition collatérale présente entre les neurones striataux permet d'atteindre des performances supérieures à certains algorithmes classiques d'apprentissage. Enfin, des résultats expérimentaux

ont récemment démontré que deux régions du striatum dorsal, le striatum dorsolatéral (DLS) et le striatum dorsomédial (DMS) sont caractérisées par deux types de STDP de polarités différentes. En utilisant un modèle simple prenant en compte ces spécificités, nous avons étudié l'influence des règles de STDP sur la dynamique d'apprentissage dans une tâche complexe, combinant une phase d'apprentissage, suivie d'une phase d'activité aléatoire pour mesurer la maintenance des motifs dans la mémoire du système et d'une phase de ré-apprentissage. Les conclusions de cette étude mettent en avant que la plasticité présente dans le DMS permet au réseau d'oublier rapidement tous motifs précédemment acquis, alors que la STDP du DLS participe à la maintenance de ces mêmes motifs.

CONTENTS

The following document will be decomposed as follows: a general introduction, a general presentation of my contributions, wo parts gathering a total of seven different chapters, each chapter corresponding to a publication, and a discussion. Each chapter will contain its own appendix and a local bibliography.

Introduction

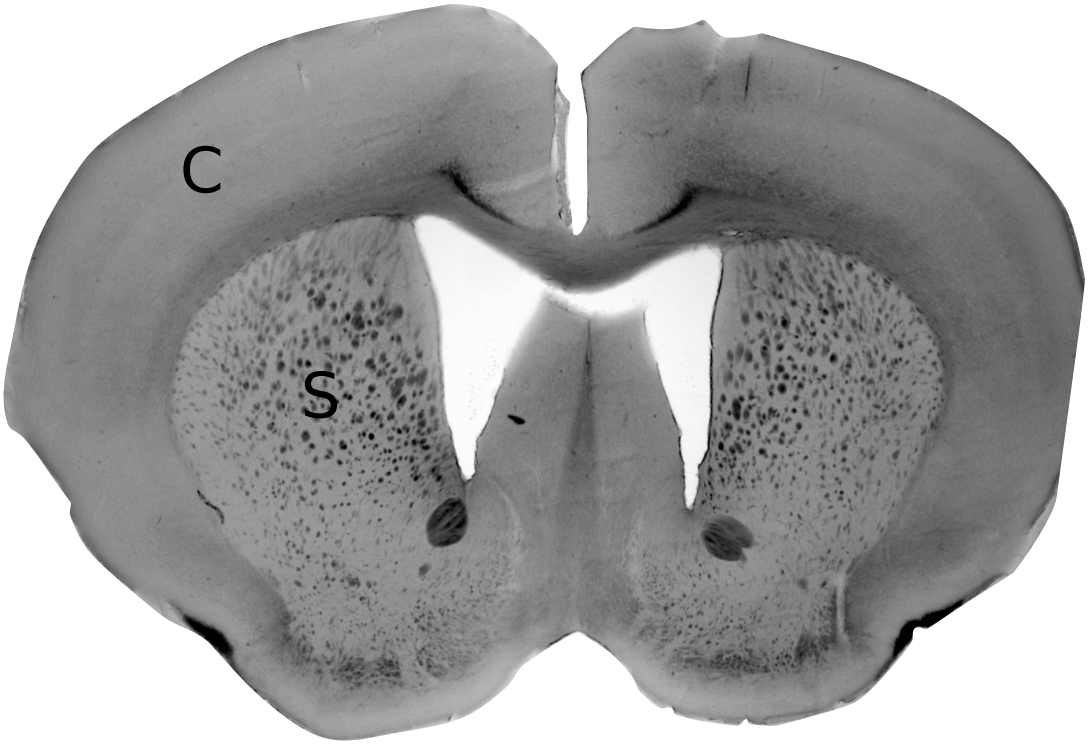

Coronal slice of mouse brain with cortex (C) and striatum (S). [C. Piette].

Evolution, development, learning ... everything changes along generations, through life, during experiments as a result of complex processes that are direct consequences of interactions between the subject and its environment. All species have been shown to evolve on long timescales following Darwinism and other intricate laws, that still motivate many studies in both ecology and evolution. Similarly, all animals adapt their behavior throughout their life thanks to numerous mechanisms, most of them implicating the nervous system. Biology, and more specifically neuroscience have studied such long-term changes, and the processes from which those transformations originate. Directly at the cellular level, experimental studies have shown that activity-induced adjustments in neuronal connectivity are correlated with behavioral changes and learning. In particular, spike-timing dependent plasticity (STDP) is defined as plasticity mechanisms that are based on the spike timings of the neighboring neurons. It has been the focus of a wide range of studies starting from neurophysiology to computational neuroscience, and even having implications in computer science.

In **Chapter 1**, I present synaptic plasticity, as a mechanism for shaping brain activity during learning. I detail how STDP was defined, first as a timing-based learning rule in computational neuroscience, and then how experimental works have proven its existence in brain slices, and then in awake animals. Several models of STDP are then described ranging from phenomenological pair-based rules and their extensions, to biophysical calcium-based models. I conclude by exploring different theoretical assumptions that have been made by physicists when investigating the influence of STDP on neuronal network dynamics.

Then, in **Chapter 2**, I develop a general stochastic setting, that will prove necessary to investigate the influence of STDP on stochastic networks. Using a simple network with two neurons connected by one synapse, I will introduce integrate-and-fire models, and different mechanisms for random spike generation. Considering that spikes trains are the principal object of interest when studying simple neuronal networks, I introduce the notions of point processes, and detail how random spiking can be modeled using non-homogeneous Poisson processes. Finally, since STDP happens at longer timescales than neuronal activity, a simple slow-fast approximation is established, based on the proofs of stochastic averaging principles.

Finally, in **Chapter 3**, I shortly introduce a neuronal system, the striatum, where STDP has been proven to exist, and which has an important role in procedural learning. In particular, the striatum is characterized by its principal neurons, the medium-sized spiny neurons (MSNs), whose connections with cortex exhibit a quite distinctive property known as anti-Hebbian STDP. I briefly present how heterogeneities in MSNs and synaptic plasticity are necessary for the implementation of action selection and procedural learning in a more global system called the basal ganglia. The influence of different types of STDP, presented in Chapter 1, in such networks is detailed, both from an experimental and a computational point of view.

CHAPTER 1

LEARNING IN NEURONAL NETWORKS WITH SPIKE-TIMING DEPENDENT PLASTICITY

1.1 Synaptic plasticity as a primary substrate for learning and memory

Complex mechanisms account for the establishment of memory

Interacting with others and the environment lead to the accumulation of knowledge, the development of memory and of characteristic skills. This process is commonly referred to as learning, and is crucial to many aspects of life. How do we learn?

This simple question has led to more than a century of research, honoured by several Nobel Prizes in a large array of different fields. It has long been hypothesized that learning occurs, partly at least, through the adaptation of neuronal maps in the brain. A crude simplification of the brain system would be to model it as a combination of several areas, involved in specific tasks, ranging from the integration of sensory inputs to motor skill implementation. Sensations, context, feelings are all integrated during brain processing, through the involvement of different circuits. Each of these areas is composed by numerous cells, critical to all nervous mechanisms and called neurons. They can convey information through electrical and chemical signaling. These large networks of neurons, recurrently connected at synaptic junctions, are the basis of brain activity, and as such have been the focus of the neuroscientific community since its beginning.

Coming back to learning, it is now accepted that most learning processes result from modifications of neuronal activity [Ath+18]. The development of the *engram* (physical means by which memories are stored) at the neuronal level, and its storage over time is complex and rests on several mechanisms that still motivate many experimental and computational works.

Memory can be characterized by several assertions from a computational point of view [CF16]. First, learning needs to create persistence from memory-less components, through positive/negative feedbacks or biological multistable systems. Second, these changes must be robust to noise, considering the fact the brain always exhibits spontaneous random activity. Using these two assertions, it is then possible to define the network capacity, as the quantity of information that can be stored in the system during learning and recollected later.

Computers now challenge humans in many tasks, and part of this success results from hypotheses based on biological learning. Deep learning in particular has been influenced by several properties of neuronal networks. Would it then be possible to see the brain as a gigantic computer, where learning is the result of supervised algorithms, as defined by classical machine learning [Hen+21]? We dare say here that this restrictive view may be of interest, to analyze brain behavior, but will not enable us to understand the brain and its mechanisms in their full extent.

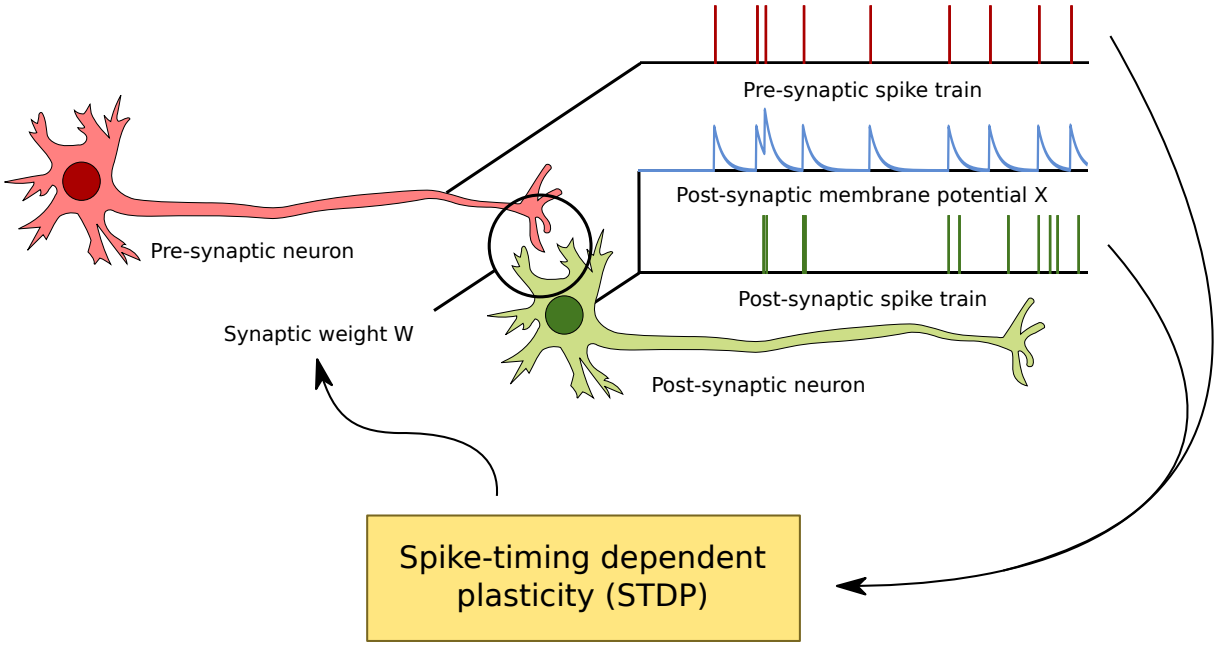

Figure 1.1: **A simple neural network with two neurons.**

The critical role of neuronal maps does not end once memory is stored. In fact, accumulating evidence and patterns along life is not the sole purpose of the brain. Each action taken during life is the result of a complex decision process that happens in the brain using previously stored information, and the current context. Each decision will lead to consequences, and to a subsequent remodeling of neuronal circuits. Learning is therefore an ongoing and online process, which makes it complex to grasp and to model [Gar19].

Synaptic plasticity or how the brain shapes itself to encode memory

Different mechanisms may modify neuronal activity in order to store memory as part of learning. As defined before, neuronal cells transmit chemical/electrical signals at synapses, mainly in a unidirectional way.

In the following, I will consider a simple neuronal network, only composed of two neurons: the *presynaptic* neuron and the *postsynaptic* neuron located on either side of the synapse, see Figure 1.1. The presynaptic neuron conveys large depolarizations of its membrane potential, called spikes (and represented by the presynaptic spike train), towards the synapse where neurotransmitters are released and cross the synaptic cleft. On the other side of the synapse, they induce local changes in the postsynaptic membrane potential X. The intensity W of this connection, rendering the amplitude of the changes, is determinant for the triggering of postsynaptic spikes and more generally for neuronal network dynamics. More complex neuronal systems are just multidimensional versions of this simple model, where the synaptic weight is described by the connectivity matrix $(W_{i,j})$ where (i, j) represents a pair of two neurons.

It has been postulated and proven that information can be stored following the modifications of these synaptic weights. All processes related to this are gathered under the name *synaptic plasticity* [Nab+14]. Activity-dependent changes in synaptic weight is therefore a crucial part of learning and encoding memory.

Different types of synaptic plasticity have been discovered and studied experimentally, in many species, in various environments [SBD18]. It is common to distinguish plasticity mechanisms based on the timescale on which they modify neuronal dynamics. Short-term synaptic plasticity leads to modulation of the synaptic weight on the neuronal timescale, usually around several milliseconds up to seconds [ZR02]. Conversely, long-term synaptic plasticity relates to changes that lasts for hours, days and even longer. Another distinction is made between synaptic changes that results in a reinforced connection (synaptic *potentiation*) or its reverse (synaptic *depression*)

Although synaptic plasticity results from complex processes, general principles have been inferred from experimental data and previous modeling studies. In 1949, Donald Hebb postulated that synaptic changes should result from correlated activity from presynaptic and postsynaptic neurons, or in Carla Shatz's words [Sha92] as, "*Cells that fire together wire together*". This hypothesis was later on confirmed by many experimental studies, and is still today a widely accepted fact in neuroscience [Seu00].

Of course, this simple postulate does not account for all brain dynamics and is therefore regularly questioned. In particular, supposing that only pre- and postsynaptic activity are actors in synaptic plasticity leads to the neglect of other resources that the brain uses to develop memory maps. Neuromodulators (e.g. dopamine, serotonin or acetylcholine) are known to influence, not only neuronal dynamics but most definitely also synaptic weights changes [Fon+18; BMP19; MG20]. The greatest example of neuromodulation is the control of goal-directed behavior and reward signaling by dopamine. Indeed, it has been shown that dopamine shapes also synaptic plasticity, and is one of its necessary components.

Spike-timing dependent plasticity, an insight in complex mechanisms of synaptic plasticity

Following Hebbian theory, many experimental studies have shown that synaptic weight changes were correlated to pre- and postsynaptic neuronal activity, usually quantified through the firing rate of each neuron. If both neurons exhibit high firing rates and are recurrently activated together, synaptic transmission between both neurons should be enhanced, or in other words going through long-term potentiation.

Some computational studies went even further and hypothesized that spikes timing should also play a role in improving learning capacities [Ger+96]. It is quite logical to consider that individual spikes, at the order of their apparition and the duration between spiking events is a lot more resourceful than only looking at averaged spiking activity.

This computational hypothesis was later experimentally demonstrated, in several experimental studies, in different brain areas [Fel12] and has been characterized ever since as STDP. Under this name are gathered all plasticity processes that depend on the timing of pre- and postsynaptic spikes, see Figure 1.1.

Numerous experimental protocols have been developed to study STDP since its discovery. Most study the evolution of synaptic transmission, usually through the size of the excitatory post-synaptic currents (EPSCs), after a protocol composed of sequences of paired spikes from either side of a specific synapse, at a certain frequency and with a certain delay [Fel12]. The delay Δt between the pre- and postsynaptic spikes is the quantity of interest in such studies, with $\Delta t = t_{\text{post}} - t_{\text{pre}}$, t_{pre} (resp., t_{post}) the timing of the presynaptic spike (resp., the postsynaptic one).

Studies have shown that the synaptic weight changes depend on Δt, and have led to a reformulation of Hebb's postulate in terms of STDP. *Hebbian STDP* plasticity is the result of a pre-post pairing, i.e. $t_{\text{pre}}<t_{\text{post}}$ leads to potentiation; and a post-pre pairing, i.e. $t_{\text{post}}<t_{\text{pre}}$, leads to depression. An example of Hebbian STDP taken from [BP98] is given in Figure 1.2a. Experiments have shown that this type of plasticity occurs at several synapses [BP98; BP01]. Plasticity protocols following this principle are characterized as "Hebbian" because they follow some parts of Hebb's postulate: (i) when a presynaptic neuron actively participate, through its spiking activity to the initiation of a spike in the postsynaptic neuron, the synaptic weight should be enhanced (ii) when the postsynaptic neuron spikes before correlated activity from the presynaptic neuron, it should lead to depression.

Other forms of STDP have been discovered experimentally see [Fel12]. *Anti-Hebbian STDP* follows the opposite sequence: pre-post pairings lead to depression, and post-pre pairings lead to potentiation. This has been observed experimentally in the striatum, see [FGV05] for example, see Figure 1.2b.

The protocols used to induce STDP are of a great importance in the final form of plasticity that is observed experimentally. Changes in the number of spike pairings or their frequency usually lead to different results. The first studies were performed *in vitro* using brain slices, and electrophysiological recordings [Fel12]. The use of different slice preparations techniques as well as the presentation of different neuromodulators such as dopamine or GABA, have also highlighted that STDP depends on numerous parameters [Pai+13]. Later on, STDP protocols were also realized *in vivo*, in anesthetized and awake animals [Mor+19] , showing that STDP is a mechanism that needs to be taken into account when building models for learning.

1.2 Models of spike-timing dependent plasticity

STDP was first studied as a model before being discovered experimentally [Ger+96]. Experimental confirmations of this synaptic plasticity rule have considerably increased the interest of the computational neuroscience community. Indeed, a large literature of computational models of STDP emerged at the beginning of the 21st century. This introduction will not be an exhaustive review of all existing works on STDP, but will instead detail how STDP models have emerged and why they currently represent a pool of interesting update rules for learning systems.

STDP models developed in computational neurosciences range from detailed biophysical descriptions of the synaptic plasticity mechanisms [GB10] to simple phenomenological models directly based on experimental data [MDG08].

From experiments to models: pair-based rules of STDP

Most experimental studies about STDP are based on pairing protocols, where pre- and postsynaptic spikes are repeated at a certain frequency for a given number of repetitions. This gives in fact a map $\Phi(\Delta t)$ of the synaptic weight changes as a function of Δt, two examples of such STDP curves are given in Figure 1.2.

Accordingly, a large class of models has been developed on the principle that the synaptic weight change due to a pair $(t_{\text{pre}}, t_{\text{post}})$ of instants of pre- and post-synaptic spikes, only depends on $\Delta t = t_{\text{post}} - t_{\text{pre}}$ through some generic function $\Phi(\Delta t)$, inferred from experimental data.

In most models, the plasticity curve is taken as an exponential one, see Figure 1.2c:

$$\Phi(\Delta t) = \begin{cases} A_{\text{post-pre}} \exp(\Delta t/\tau_{\text{post-pre}}), & \Delta t<0, \\ A_{\text{pre-post}} \exp(-\Delta t/\tau_{\text{pre-post}}), & \Delta t>0, \end{cases}$$

where $A_{\text{post-pre}}$ (resp., $A_{\text{pre-post}}$) represent the maximum amplitude of the synaptic weight update after a post-pre (resp., pre-post) pairing. Both constants can be taken as negative or positive. $\tau_{\text{post-pre}}$ (resp., $\tau_{\text{pre-post}}$) represents the STDP temporal window for post-pre (resp., pre-post) pairings.

Exponential STDP curves are quite close to experimental data and are widely used in computational neuroscience because, they are convenient to simulate in computational models [MDG08] and can lead to analytical studies.

Another study [GK02a] propose, starting from classical Hebbian rate-based rules, to extend synaptic plasticity by taking into account the neuronal membrane potential instead of the firing rate. Using this hypothesis, and approximating the membrane potential by spiking activity, they derive synaptic plasticity rules that are similar to pair-based STDP as defined above.

An important part of modeling STDP in pair-based rules focuses on the choice of which pairings to consider when updating the synaptic weight. Indeed, when the postsynaptic neuron spikes, it is possible to devise several schemes to define the associated synaptic weight update ΔW as the sum over a certain set of previous presynaptic spikes of the plasticity curve $\Phi(\Delta t)$. A similar choice needs to be made about the other types of updates, happening at presynaptic spikes. Many pair-based models have been developed over the years [MDG08], but three schemes are used in the majority of theoretical works.

We start with the simplest rule, the *all-to-all* version (following [MDG08] terminology), where all pairs of spikes give an update of the synaptic weight. The all-to-all scheme leads the synaptic weight being updated at each postsynaptic spike, occurring at time t_{post} by the sum over all previous presynaptic spikes occurring at time $t_{\text{pre}}<t_{\text{post}}$ of the quantity $\Phi(t_{\text{post}} - t_{\text{pre}})$. Switching the role of pre- and postsynaptic spikes, the synaptic weight is updated in the same way at presynaptic spikes. An example of which pairings to consider for the all-to-all case is given in Figure 1.2c (bottom left).

A second intuitive scheme is the *nearest neighbor symmetric* model: whenever one neuron spikes, the synaptic weight is updated by only considering the last (and thus closest) spike of the other neuron. If the postsynaptic neuron fires at time t_{post}, the contribution to the synaptic update is reduced to $\Phi(t_{\text{post}} - t_{\text{pre}})$, where t_{pre} is the last presynaptic spike before t_{post}. See Figure 1.2c (top right), for an example of the nearest neighbor symmetric model.

Finally, the *nearest neighbor reduced symmetric* model has also some important properties and is defined as a restriction of the *nearest neighbor symmetric* model to consecutive pairings. A postsynaptic spike at t_{post} is paired with the last presynaptic spike at $t_{\text{pre}}<t_{\text{post}}$, only if there are no other postsynaptic spikes in the time interval $(t_{\text{pre}}, t_{\text{post}})$. See Figure 1.2c (bottom right), for an example of the nearest neighbor reduced symmetric model.

Several studies have investigated the role of these different pairing interactions [ID03; MAD07; MDG08], but its influence on the synaptic weight dynamics has not been discussed in theoretical works, except in [BMG04].

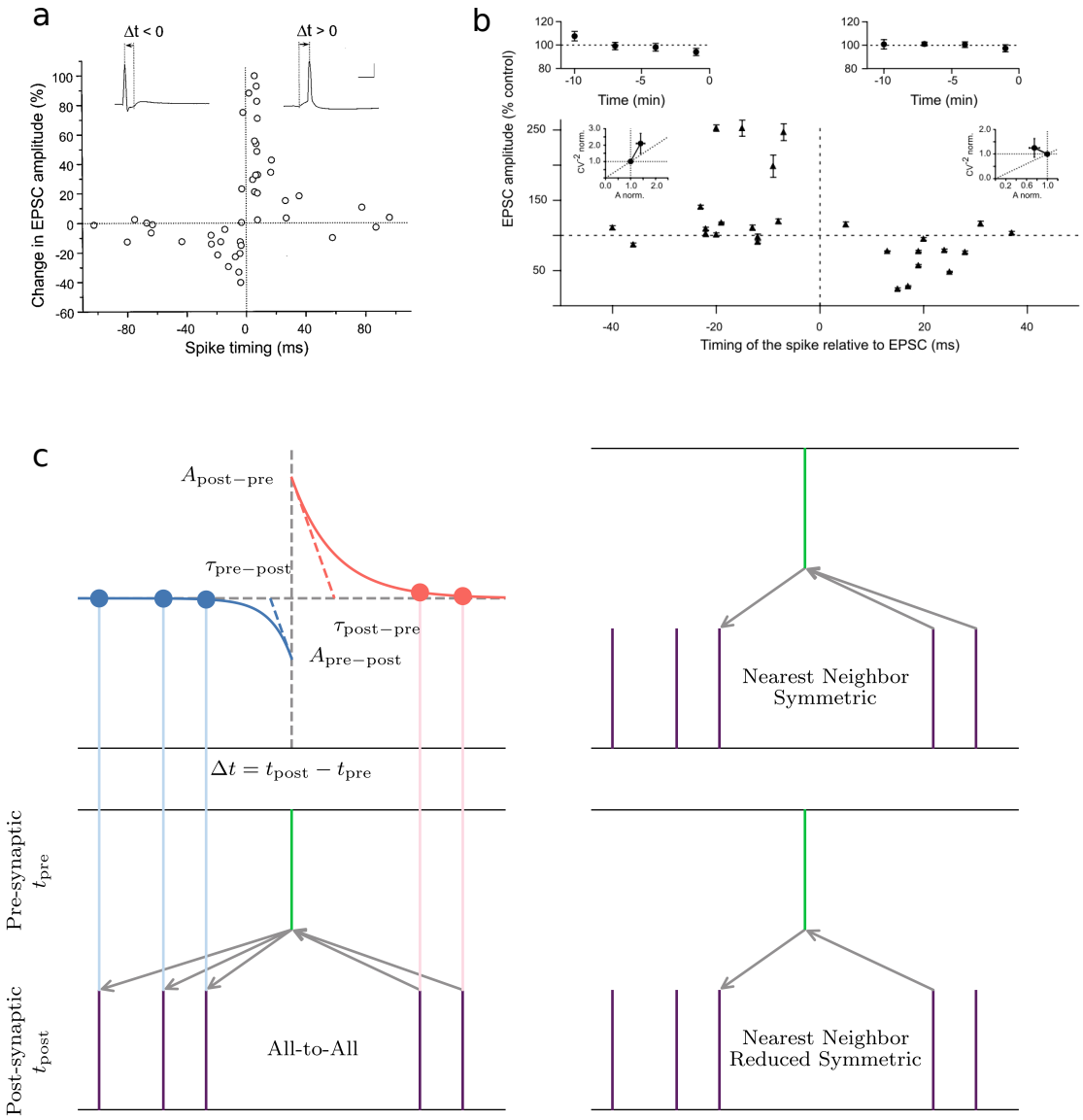

Figure 1.2: **Spike-timing dependent plasticity, from experiments to pair-based rules.**
(a) Hebbian STDP, taken from [BP98]
(b) Anti-Hebbian STDP, taken from [FGV05]
(c) Pair-based STDP rules, models based on the choice of two parameters, the STDP curve (top left) and the pairing scheme.
EPSC [excitatory post-synaptic current]

Extensions of pair-based models: how to fit to biology by adding new components to a simple model

Pair-based STDP relies on very few assumptions, mainly the shape of the STDP curve and the pairing scheme, and would therefore have some difficulty to match experimental data produced when studying STDP. In particular, more complex protocols of pairings have been tested, including triplets of spikes or changes in frequency where pair-based STDP does not account for the diversity of behaviors observed experimentally. These limitations have led computational neuroscientists to develop more complex STDP rules, that better fit experimental data. A large literature has been built on these variations of canonical pair-based models, and it is sometimes quite difficult to find one's way in the variety of new hypotheses that have emerged from this process.

The first variation of pair-based STDP models occurred when neuroscientists started to investigate the influence of the current value of the synaptic weight W on the synaptic update ΔW. Indeed, it seemed logical to suppose that synaptic weights that were almost null, would undergo a smaller synaptic depression than stronger synaptic weights. Early experimental data from [BP98] highlighted that long-term depression scaled with the synaptic weight value, whereas long-term potentiation did not. In order to take this fact into account, several studies introduced multiplicative STDP,

$$\Delta W = F(W)\Phi(\Delta t)$$

where $F(W)$ represent the multiplicative influence of the current synaptic weight value. Several papers have studied the influence of multiplicative rules, compared to additive ones [RLS01], and the influence of the exponent of $F(W)$ was studied in more details by [Güt+03].

A second important fact that was added to pair-based STDP models was the existence of delays in cellular signaling pathways that could lead to shifts in the plasticity curves $\Phi(\Delta t)$. In particular, the backpropagating action potentials need some time, after being elicited at the cell soma, to retropropagate and ultimately influence distal synapses. Similarly, when the presynaptic neuron spikes, there is a delay due to chemical transmission and channel dynamics before seeing a quantitative effect at the level of the synapse. For all these reasons, translated plasticity curves were the focus of several works [LS08; BA10].

Pair-based rules have been shown to poorly fit with experimental data when more complex protocols are used. This is the case for example in protocols repeating sequences of three spikes (called triplets) from the presynaptic and postsynaptic neurons [FD02; PG06a] where protocols repeating sequences of three spikes from the presynaptic and postsynaptic neurons are presented to the synapse. For this reason, more detailed models that take into account the influence of several pre- and postsynaptic spikes have been proposed. These models vary a lot in their hypotheses, mainly because they are based on different experimental data.

First, it was observed, using triplet-based protocols, that previous pre- and postsynaptic spikes have a "suppressive" effect on the induction of Hebbian STDP observed [FD02]. A new model of STDP integrating this suppression effect was proposed in the same study [FD02]. A few years later, [PG06a] showed that previous pre-synaptic spikes enhance the depression obtained for a *post-pre* pairing, whereas previous postsynaptic spikes lead to a bigger potentiation than in a classical pre-post pairing. This led to the formulation of the triplets model [PG06a].

It is interesting to note that these two models are derived from opposite experimental conclusions. Indeed, they are based on data obtained from different brain regions: visual cortex in [FD02], and hippocampus in [PG06a]. A global model considering both mechanisms, the *NMDA-model*, is defined in [BA16].

More recently the influence of neuromodulators has been shown to radically change STDP curves. Three-factor learning rules have been developed to take this new experimental data into account, leading to a great variety of new models. A large literature focuses on multiplicative influence of neuromodulators on STDP synaptic updates [FG16; KIT17; Ger+18], mainly by supposing that,

$$\Delta W = F(d)\Phi(\Delta t)$$

where $F(d)$ represents the influence of the neuromodulator d. More complex models directly add the dependence of the STDP rules on neuromodulators inside the plasticity function [GHR15], i.e., taking

$$\Delta W = \Phi_d(\Delta t).$$

All those models require a large amount of experimental data when fitting biologically-relevant parameters. A last, simpler, approach consists in including the influence of neuromodulators as an additive process,

$$\Delta W = \Phi(\Delta t) + F(d).$$

Over the years a large diversity of STDP pair-based rules were developed in order to reproduce new experimental protocols and results, leading to a profusion of such models.

From models to experiments: biophysical models of STDP

Pair-based models can be characterized as phenomenological models of STDP in the sense that experimental STDP curves are taken as a core parameter of the models. Another important class of plasticity models is derived from biological phenomena and aims at reproducing experimental STDP curves using biological mechanisms.

Biophysical models gather all the current knowledge on how synaptic plasticity is implemented at the synaptic level and integrate all biological mechanisms that are relevant in plasticity modelling. In particular, chemical reactions and protein interactions are described in details leading to gigantic systems with numerous parameters, most of them chosen from experimental data. The general idea in using such models is to explain using such models, how STDP as observed, in pairings protocols, can be elicited and to identify the underlying mechanisms. For STDP, most biophysical models are based on the CamKII protein system, or the endocannabinoid network, see [GB07; Cui+16]. These models, as biologically grounded as they can be, are hard to simulate and even more complex to integrate in large neuronal networks. However, their conclusions are useful when building simpler models which can then be used in more complex systems.

Many experimental studies have pointed out the crucial role of calcium transients in the establishment of plasticity. At the same time, biophysical models have studied the importance of calcium concentration in the dynamics of plasticity. All these works have led to the development of many STDP models based on the postsynaptic calcium

concentration [GB10; ID21]. These models are able to reproduce experimental results from pair-based protocols but also more complex ones, such as triplets. The general dependency on postsynaptic calcium concentration can be integrated in plasticity updates using

$$\Delta W = F(C)$$

where C is the postsynaptic calcium concentration.

A simple phenomenological calcium-based model [GB12] was able to reproduce most of the experimental STDP curves with only a few parameters which made it ideal to fit with electrophysiological data. Recent works have extended this model by adding the influence of the number of pairings, and of different signaling pathways [VVT18] or by modeling heterosynaptic plasticity thanks to local calcium diffusion at the synaptic level [Men+20]. The influence of neurotransmitters such as GABA has also been taken into account in calcium-based models [HF17].

Instead of supposing that STDP rules are dependent on the postsynaptic calcium concentration, another class of models are based on the hypothesis that the postsynaptic membrane potential X is the quantity of interest. These models were shown to also reproduce the results of STDP protocols [GK02a; CG10], with

$$\Delta W = F(X).$$

Numerous models were developed over the years to reproduce STDP, a significant part of which are simple enough to be implemented in large neuronal networks and can be studied using tools from statistical physics and mathematics.

1.3 Theoretical study of STDP

Pair-based models of STDP have attracted quite early the interest of physicists, because of their simplicity. They can be studied theoretically, using either dynamical systems theory, stochastic processes or statistical physics.

Three main approaches have been developed in order to gain theoretical insights on the role of STDP in neuronal networks. Most studies consider a feedforward network of neurons, with a (sometimes large) collection of presynaptic neurons, and a single postsynaptic cell that integrates all these inputs. Pair-based STDP, most of the time with the all-to-all formulation, is then applied to the synaptic weights between the pre- and the postsynaptic cells. The asymptotic behavior of the neuronal network is often studied, with most works mostly aiming at characterizing the distribution of the synaptic weights for large windows of time.

Slow-fast analysis

An important feature of long-term synaptic plasticity, as STDP, is that there are essentially two different timescales in action.

On the one hand, the decay time of the membrane potential, and the mean duration between two presynaptic spikes or two postsynaptic spikes are of the order of several milliseconds. Consequently, interacting pairs of spikes are on the same timescale. Accordingly, pair-based models also integrate this fast timescale with an exponential decay time around 50 milliseconds, see [BP98; FGV05]. Similarly, in calcium-based

models, the interaction between pre- and postsynaptic spikes is integrated at the calcium level, and its concentration decays with a time constant of about 20 milliseconds, see [GB12]. On the other hand, the effect of STDP on synaptic weights takes place on a slower timescale, where it can take seconds and even minutes for changes to occur see [BP98; FGV05]

Most computational models of synaptic plasticity incorporate this timescale difference by implementing small updates of the synaptic weights. A first example is [KGH99], who "introduced a small parameter η [..] with the idea in mind that the learning process is performed on a much slower time scale than the neuronal dynamics." Similarly, [Rob99] defines two timescales (t, x) such that "the measurable changes in behavior occur during the course of several training cycles (t), whereas the neuronal activity modulation that is responsible for synaptic change is greatest within each cycle (x).", with t representing the long timescales of synaptic plasticity, and x neuronal activity. Other models also make this assumption, sometimes mixing it with a mean-field approximation leading to a Fokker-Plank equation [RLS01; RBT00a].

It should be noted that models using this assumption do not seem to agree with observations from numerous experimental studies, see [BP98; FGV05; Fel12]. Classically (in experimental works), the protocol to induce plasticity consists in stimulating both neurons at a certain frequency a fixed number of times with a fixed delay Δt, over a period of one or two minutes (60-150 pairings at 1 Hz for example). This part is designed to reproduce conditions of correlations between the two neurons, when mechanisms of plasticity are known to be triggered. However, measurements of the synaptic weight show that changes take place on a different timescale: after the protocol, it is observed that at least several minutes are necessary to have a significant and stable effect on the synaptic weight. In other words, the change in synaptic weights happens long after the end of the plasticity induction.

To tackle this added complexity, an approach consists in updating the synaptic weights with a fixed, or random, delay. This is not completely satisfactory since the evolution of the synaptic weight is generally believed to be an integrative process of past events rather than a delayed action. Another approach which I will use consists in implementing this delay through an exponentially filtered process to represent the accumulation of past information. A recent article [RBS16] also takes this fact into account by adding an "induction" function to canonical models of STDP.

Separating the timescales into two components leads to a simplification of the dynamical system. Indeed, it is then possible to find theoretical estimates by studying the fast system, in our case plasticity induction, by supposing that the slow variables, the synaptic weights, are constant. Once the behavior for fixed slow variables has been studied, it is possible to solve the slow dynamics using the estimates of the fast processes. In particular, one can consider that the fast system is only present in the slower dynamics through averaged functionals. Similar principles are used in theoretical studies of STDP leading to simpler dynamics that are then studied analytically see [KGH99; KH00; KGH01].

A story of correlations

The first thorough study of pair-based STDP was developed in [KGH99], and used the previously defined slow-fast approximation. Their analysis led to the conclusion that a fundamental quantity in the study of STDP was the cross-correlation between the pre-

and postsynaptic neurons. The asymptotic behavior of the synaptic weight dynamics, Relation (4) of [KGH99] is given by,

$$\frac{\mathrm{d}w}{\mathrm{d}t}(t) = \int_{-\infty}^{+\infty} \Phi(s)\mu(s,t)\,\mathrm{d}s,$$

where,

— $\Phi(\cdot)$ represents the STDP curve;

— $\mu(\cdot,t)=\overline{\langle S^1(t+s)S^2(t)\rangle}$, the correlation between the spike trains at time t.

The quantity $\overline{\langle\cdots\rangle}$ is defined in terms of *temporal and ensemble averages*, $\langle\cdots\rangle$ is the ensemble average and $\overline{\cdots}$ the temporal average over the spike trains. Therefore, $\mu(s,t)=\overline{\langle S^1(t+s)S^2(t)\rangle}$ represents the cross-correlogram of the pre- and postsynaptic neurons, i.e the distribution of presynaptic spikes relative to postsynaptic ones.

It is quite striking to see that in the slow-fast approximation, the synaptic weight update is solely determined by the convolution of the plasticity curve Φ and the correlation function. This quantity can either be directly taken from electrophysiological data, where cross-correlograms are commonly drawn, or can be computed based on neuronal models used in the system. Many studies have tried to analytically compute this quantity, and only succeed using some approximations. In [KH00] for example, the authors use the integrate-and-fire model and employ themselves to compute this correlation function under some assumptions.

One interesting fact about this equation is that one can study the influence of highly correlated inputs in this framework [KGH99; KGH01; GK02a], leading to estimations of the synaptic weight dynamics with biologically inspired inputs.

It is however important to stress here, that this framework supposes that all pre- and postsynaptic spikes are taken into account at each pairing, therefore restricting its use only to the all-to-all pairing scheme.

Mean-field analysis

Another approximation is sometimes made, usually in addition to the timescale separation, and relates to having a large number of independent presynaptic neurons N in a stochastic context. Under the approximation of N being large, and therefore after scaling each single synaptic weight by a factor $1/N$, it is possible to obtain a Fokker-Plank equation for the weight distribution [RBT00a; RLS01; BMG04]. In this case, the temporal evolution of each synaptic strength is assumed to follow a diffusion process and, consequently, verifies the Markovian property. The analysis is done with the associated Fokker-Planck equations, and the corresponding equilibrium distribution when it exists, see [RLS01; RBT00a].

This approach can also be compared with mean-field analysis, in the sense that usually, limit equations lead to dynamics that depends on the mean synaptic weight, see [RBT00a]. This approximation leads to the characterization of asymptotic synaptic weight distribution, in simple cases, usually with independent presynaptic inputs, and as such, is a great tool to study STDP in a theoretical setting.

However, the scaling of each synaptic weight by the factor $1/N$ is not biologically plausible. Indeed, in that case, the importance of a single pairing is diluted over the

large number of inputs in the mean-field limit, whereas by definition STDP relies on the repetition of such correlated pairings. Furthermore, for the postsynaptic neurons to spike, one may expect it to receive highly correlated inputs. The Fokker-Planck approach would not be able to take into account these types of inputs, and it therefore greatly limits its potential application to more biologically-plausible neuronal networks. An extension of this formalism to higher orders, the *Kramers-Moyal* expansion, is also used in this context for some non-Markovian models, see [LF12].

CHAPTER 2

A PROBABILISTIC APPROACH TO NEURONAL NETWORKS

2.1 Stochastic models for neuronal activity

Neurons are complex cells that integrate many different biological processes in order to emit action potentials and transmit them to other neuronal cells. Modeling neurons has been an active topic of research for the past century, and many books have reviewed large classes of models. We refer to them for a general presentation of neuronal dynamics in computational neuroscience [Izh07; ET10; Ger+14].

The following sections will be devoted to building a stochastic model for neuronal activity, using different mathematical tools, starting with point processes and then slow-fast analysis.

Neuronal dynamics

Neurons can be modeled through complex systems, where different compartments interact to reproduce neuronal dynamics. These compartments are related to functionally diverse parts of the neuron, and are of interest when studying in details how action potentials are generated and how they travel along the axons to convey information to other neurons.

When modeling neuronal networks with numerous neurons, those complex models do not scale well in numerical complexity and are hard to study using theoretical tools. Most of the research therefore focuses on reducing neuronal dynamics to a system with only one scalar variable to represent cell activity and usually define it as the membrane potential X of the neuron. The equivalence between the membrane potential used in models and the actual membrane potential in biological experiments is not straightforward, as this potential greatly depends on where it is measured along the neuron's membrane. However, its repetitive use in computational neuroscience has proved that, even if it is not directly related to a specific biological quantity, it still enables neuroscientists to reproduce complex dynamics with a simple model of neuronal activity.

The membrane potential is subject to different ionics flows and depends on the dynamics of numerous channels, that open or close depending on the neuron's state and the signals it receives. A first simple hypothesis is to suppose that there exists a resting potential X_{eq}, to which the membrane potential decays when it is not stimulated, and that the membrane acts as a resistance-capacitance system. These *leaky-integrate* dynamics lead to the following equation for X,

$$\tau \, \mathrm{d}X/\mathrm{d}t = -(X(t) - X_{\text{eq}}) + RI$$

where τ represents a time constant, R the resistance of the neuron and I external input currents.

Regarding neuronal models, an important topic is spike generation, in particular in simple models as the leaky-integrate neuron, where all biological mechanisms that

trigger action potentials are not taken into account. It has been known for a long time that a neuron spikes when it depolarizes, i.e when its membrane potential is high. Most models in computational neuroscience [Izh07; ET10; Ger+14] use *integrate-and-fire* models, where a spike is emitted as soon as the membrane potential X reaches a specific value X_{th}. After the spike, the neuron resets to another value X_{reset}, that is often taken as the resting potential X_{eq}. In mathematical terms, this translates to:

$$\begin{cases} \tau \, \mathrm{d}X/\mathrm{d}t = -(X(t) - X_{\text{eq}}) + RI \text{ if } X < X_{\text{th}} \\ X(t) \to X_{\text{reset}} \text{ when } X(t-) = X_{\text{th}}. \end{cases}$$

This model leads to membrane potentials that are not continuous functions of time. In a mathematical setting, *càdlàg* functions model this type of dynamics[1].

The dynamics of X in the absence of spikes are said to be linear, in the sense that, for any type of inputs $I{=}I_1 + I_2$, it is possible to compute X through a linear combination of X_1 and X_2, i.e the membrane potentials with $I = I_1$ and $I = I_2$. Experimental neurons follow the same principles when their membrane potential is below the spike threshold, and as such, linear integrate-and-fire neurons are known to correctly model subthreshold dynamics.

However, upon neuronal depolarization (i.e membrane potential rise), linear approximations do not satisfyingly reproduce biological data. Indeed, spikes result from auto-exciting processes that take place in the soma and more complex models are needed to reproduce similar dynamics. The introduction of nonlinear models has solved this issue, by replacing the leaky term by more complex, nonlinear functionals of the membrane potential, leading to,

$$\begin{cases} \tau \, \mathrm{d}X/\mathrm{d}t = f(X(t)) + RI \text{ if } X < X_{\text{th}} \\ X(t) \to X_{\text{reset}} \text{ when } X(t-) = X_{\text{th}}. \end{cases}$$

where $f(X)$ is the nonlinear model. Two nonlinear models have emerged and established themselves as good approximations for neuronal dynamics, the first of them known as the *quadratic model* with $f(X) \propto X^2$, and the second one called the *exponential-integrate-and-fire neuron* with $f(X) \propto \exp(X)$.

These models are not sufficient to reproduce other neuronal patterns of activity, that are sometimes of interest in neuronal networks. Bursting for example, i.e the capacity of a neuron to fire discrete groups (i.e bursts) of spikes, cannot intrinsically be modeled under these simple assumptions (without any additional input). The same problem emerges when modelling adaptation: the fact that under constant input, a neuron is able to raise or decrease its firing rate over time.

A second variable needs to be added to the model to properly reproduce these behaviors. The adaptation variable U usually follows slower dynamics than X and represents many underlying ionic currents that are responsible for complex neuronal behaviors. Adaptive nonlinear integrate-and-fire models have therefore been introduced [Izh07; ET10; Ger+14] and their dynamics follow,

$$\begin{cases} \tau \, \mathrm{d}X/\mathrm{d}t = f(X(t)) + RI \text{ if } X < X_{\text{th}} \\ \tau_U \, \mathrm{d}U/\mathrm{d}t = g(U(t), X(t)) \text{ if } X < X_{\text{th}} \\ X(t) \to X_{\text{reset}}, U(t) \to U(t-) + U_{\text{reset}} \text{ when } X(t-) = X_{\text{th}}. \end{cases}$$

[1] a function f is said to be càdlàg if, it is right continuous and has a left limit at every point t, $f(t-)$ denotes the left limit of f at t.

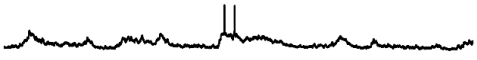

where $g(U, X)$ models the dynamics of the slow adaptation variable and τ_U the adaptation timescale. When the neuron spikes, the adaptation variable U can also be updated by U_{reset} or not, depending on the model.

When building a computational neuronal network, different arguments need to be considered to choose which neuronal models to use. Theoretical models, which aim at investigating neuronal dynamics using mathematical tools, need the simplest model that reproduces the studied phenomenon, in order to manipulate analytical expressions. Computational models, designed for computer experiments and therefore limited by computer capacity and complexity, are able to manipulate more complex descriptions. Overall, choosing the right model results from a complex balance between keeping a contiguous proximity to biological reality and using the best adapted technique to investigate neuronal dynamics.

Random generation of spikes

In the natural brain, spontaneous neuronal activity is abundant, which causes noisy spiking dynamics. It is important to distinguish extrinsic noisy activity, that is related to random spikes coming from external neurons, from intrinsic noise. Most models introduce noise using an extrinsic random current, sometimes in the form of random spikes and more often as a diffusive random noise, usually taken as a Gaussian process, to integrate the effect of large populations of neurons [Ger+14]. In integrate-and-fire models, where the firing mechanisms is deterministic, it is necessary to introduce such external noise in order to trigger spikes in a random fashion. In particular, when the external noise is taken as a diffusive process, spiking times are defined as the first time when the stochastic process X reaches a particular value, i.e its threshold potential X_{th}. There is an extensive on first passage times exists; which has investigated the distribution of spike timings in diffusive neuronal models.

However, neurons cut out from their networks also display randomness in their spiking mechanisms, highlighting the existence of noise inside the neuronal cell. Experimental data suggest that the firing process itself has a significant random component, which can lead to randomness in the spike trains even in the presence of deterministic input.

A first approach to model this intrinsic randomness was developed in Wilson-Cohan neuronal networks: neurons [Cow68] switch between different states: quiescent (corresponding to subthreshold dynamics), activated (to spikes) and refractory (the refractory period, i.e is caused by mechanisms that unable a neuron to generate another spike). Later on, in order to study neuronal dynamics, a stochastic version of this model was developed, in which neurons switch between states at a rate that depends on the membrane potential [Cow91]. Even if spikes in this model where modeled indirectly as a switch between two neuronal states, it is, to our knowledge the first introduction of a stochastic mechanism for spiking. Since then, several models have been built on this hypothesis, some of them keeping the Wilson-Cohan formalism of different neuronal states [BC07; Hel18].

Later on, some works have added variability in the threshold mechanisms, by adding a random component when generating spikes [GH92]. Extending this idea, spike generation can be modeled through a random variable that depends on the current value of the membrane potential, leading to the development of *Poisson* neurons. These neurons are characterized by their membrane potential X, usually defined as a simple

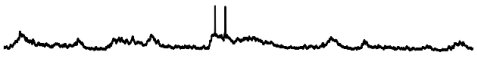

leaky-integrate process, but spike triggering results from a Poisson process. In other words, if the neuron state at time t is $X(t-)$, it is natural to assume that the probability that the neuron spikes between times t and $t+\mathrm{d}t$ is equal to $\beta(X(t-))\,\mathrm{d}t$, where β represents the *activation function*. This function is often taken as nondecreasing, because neurons tend to spike as their membrane potential rises. Under this hypothesis, spikes are generated through a random process, even in the presence of a constant input. Several models have used this approximation either with β as a linear function of the membrane potential [KGH99] or more complex nonlinear activation functions [Chi01]. The Poisson neuron model is able to reproduce intrinsic spike emissions and is a powerful tool for theoretical studies of stochastic neuronal networks [RT16].

2.2 Spiking trains as point processes

Spikes represent good estimates for neuronal activity, even if it would be overly simplistic to reduce neuronal dynamics to these events. Once a spiking mechanism is defined, either by using integrate-and-fire neurons or Poisson neurons, neuronal activity can be represented, under this approximation, by the sets of spiking events $(t_k)_{k\in\mathbb{N}}$. This can be completed by the definition of the neuron spike train $\mathcal{N}$, i.e the measure,

$$\mathcal{N}(\mathrm{d}t) = \sum_{k\in\mathbb{N}} \delta_{t_k}(\mathrm{d}t),$$

where δ_x is the Dirac measure at $t{=}x$.

$\mathcal{N}$ is a classical object in probability theory, and can be seen, under some supplementary assumptions as a *point measure*. A point measure on $\mathbb{R}_+$, is an integer-valued Borelian positive measure on $\mathbb{R}_+$ which is Radon (which has finite values on any compact set in $\mathbb{R}_+$). In particular, a point measure is carried by a subset of $\mathbb{R}_+$ which is at most countable and without any finite limiting point. It is however quite realistic to use these objects when considering biological neuronal dynamics such as refractoriness to suppose that explosion events do not occur.

As explained in the previous section, spike generation is a stochastic process and accordingly the measure $\mathcal{N}$ is also a random object. Indeed, simulating the same neuronal dynamics several times would result in distinct realizations of the spike train. It is possible to define a probability measure $(\mathbb{P},\Omega)$ on the point measures $\mathcal{N}$. Each realization $\mathcal{N}(w)$ would then be characterized by stochastic spikes timings $(t_k(w))_{k\in\mathbb{N}}$. The stochastic process $\mathcal{N}(\mathrm{d}w)$ is called *a point process*, and has led to many works in the probability community [Ver70; DV08]. Such processes have been used to model earthquake events, population dynamics, finance and of course, neuroscience.

In the following, the point process formalism is used for a simple system, composed by two neurons connected at one synapse. We only choose to model each spike train by a point process, with $\mathcal{N}_{\mathrm{pre}}$ for the presynaptic neuron and $\mathcal{N}_{\mathrm{post}}$ for the postsynaptic cell. We suppose that the postsynaptic cell follow leaky-integrate dynamics, and that its input is only defined by the presynaptic neuron spikes. In other words, at each presynaptic spike, the membrane potential X of the postsynaptic neuron is updated by a quantity W which represents the synaptic weight. This process can be formulated, setting aside the reset of the neuron after a spike and taking $X_{\mathrm{eq}}{=}0$, using a stochastic differential equation,

$$\mathrm{d}X(t) = -\frac{1}{\tau}X(t)\,\mathrm{d}t + W\mathcal{N}_{\mathrm{pre}}(\mathrm{d}t).$$

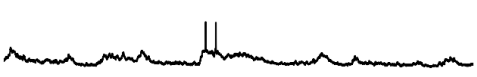

Poisson processes

In order to model the postsynaptic neuron spikes, *Poisson processes* need to be introduced. They represent a significant subset of point processes [Kin92] and are characterized by their intensity measure μ on $\mathbb{R}_+$, which appears when computing the number of points of the Poisson process in a measurable set A, i.e

$$\mathcal{N}(A) = \text{Poisson}(\mu(A)),$$

where Poisson(λ) is a Poisson law with parameter λ, i.e

$$\mathbb{P}\left(\mathcal{N}(A){=}k\right) = \frac{\mu(A)^k}{k!}e^{-\mu(A)}.$$

They also need to display an independence property, i.e for any disjoint subsets A and B, $\mathcal{N}(A)$ and $\mathcal{N}(B)$ must be independent random variables.

These processes are commonly used in stochastic theory because thanks to the independence property they share, they lead to simpler proofs and can then be used to build more complex objects.

Going back to our simple model of neuronal dynamics, I will assume that the presynaptic neuron spikes according to a homogeneous Poisson process, i.e their interspike times are taken as identically independent exponential variable of parameters λ. It corresponds to taking a Poisson process with an intensity measure proportional to the Lebesgue measure, $\mu(\mathrm{d}t) = \lambda\,\mathrm{d}t$. In particular, the following property is verified,

$$\mathbb{P}(\mathcal{N}_{\text{pre}}([t, t+\mathrm{d}t]){=}1) = \lambda\,\mathrm{d}t + o(\mathrm{d}t).$$

For the postsynaptic neuron, following the hypothesis developed in the previous section, I would need to build a nonhomogeneous Poisson process that verifies,

$$\mathbb{P}(\mathcal{N}_{\text{post}}([t, t+\mathrm{d}t]){=}1) = \beta(X(t{-}))\,\mathrm{d}t + o(\mathrm{d}t).$$

where $\beta(\cdot)$ is the activation function and represents the influence of the postsynaptic membrane potential on spiking.

In order to reproduce this property using homogenous Poisson processes, I need to introduce a Poisson point process $\mathcal{P}$ on $\mathbb{R}^2$ with rate 1 and define the firing instants of the output neuron $(t_{\text{post},k})$ as the jumps of the point process $\mathcal{N}_{\text{post}}$ defined by

$$\int_{\mathbb{R}_+} f(u)\mathcal{N}_{\text{post}}(\mathrm{d}u) \overset{\text{def.}}{=} \int_{\mathbb{R}_+} f(u)\mathcal{P}\left((0, \beta(X(u{-}))], \mathrm{d}u\right)$$
$$= \int_{\mathbb{R}_+^2} f(u)\mathbb{1}_{\{s\in(0,\beta(X(u-))]\}}\mathcal{P}(\mathrm{d}s, \mathrm{d}u), \quad (2.1)$$

for any non-negative Borelian function f on $\mathbb{R}_+$.

Classical properties of Poisson processes give that, for $t{>}0$ and $x{\in}\mathbb{R}$,

$$\mathbb{P}\left(\mathcal{N}_{\text{post}}(t, t{+}\,\mathrm{d}t){=}1 | X(t{-}){=}x\right) {=} \beta(x)\,\mathrm{d}t {+} o(\mathrm{d}t),$$

as expected, $\mathcal{N}_{\text{post}}$ is a Poisson process with intensity $(\beta(X(t)))$.

Poisson processes are natural objects to represent neuronal spike trains and their use in theoretical studies of neuronal networks benefit from the large amount of existing works on the subject.

Hawkes processes, a natural formulation for an auto-exciting process

The influence of postsynaptic spikes on the membrane potential results in its resetting to a constant value E_r, the reset potential. This property can be integrated easily in the stochastic differential equations developed in the last section,

$$\mathrm{d}X(t) = -\frac{1}{\tau}X(t)\,\mathrm{d}t + W\mathcal{N}_{\mathrm{pre}}(\mathrm{d}t) + (X_r - X(t-))\mathcal{N}_{\mathrm{post}}(\mathrm{d}t).$$

This dynamic is of real interest in probability because it produces a Poisson process whose intensity $\beta(X(t))$ depends on previous jumps. It could also be postulated that instead of being reset to a specific value, a postsynaptic spike just decreases (or increases) the membrane potential by a fixed value ΔX_r leading to

$$\mathrm{d}X(t) = -\frac{1}{\tau}X(t)\,\mathrm{d}t + W\mathcal{N}_{\mathrm{pre}}(\mathrm{d}t) + \Delta X_r\mathcal{N}_{\mathrm{post}}(\mathrm{d}t).$$

For most neurons, ΔX_r would be taken as negative modeling the inhibitory influence of a postsynaptic spike on the postsynaptic membrane potential. However, for bursting neurons one could imagine that ΔX_r may be taken as positive, in order to model the fact that after a first spike, a bursting neuron is more prone to spike again. These assumptions are of course only possible when using Poisson neurons, because of the absence of fixed spike threshold. In particular, the spiking rate of a neuron following this dynamic is equal to,

$$\lambda_{\mathrm{post}}(t) = \beta(X(t-)) = \beta\left(\int_{(-\infty,t)} W\exp(-(t-s)/\tau)\mathcal{N}_{\mathrm{pre}}(\mathrm{d}s) + \int_{(-\infty,t)} \Delta X_r \exp(-(t-s)/\tau)\mathcal{N}_{\mathrm{post}}(\mathrm{d}s)\right).$$

This formulation is close to the SRM (spike response model), see [Ger+14] for a review, where the impact of each spiking event (from the presynaptic and the postsynaptic neurons) are modeled by response kernels (here exponentials).

Such auto-exciting (or auto-inhibiting) processes have been studied in probability since their discovery by Hawkes in 1974 [HO74], and applied to various domains as finance, genetics or neuroscience.

A *Hawkes process* is a point process $\mathcal{N}_{\mathrm{Hawkes}}$ whose intensity is a function of previous jumps, i.e

$$\lambda_{\mathrm{Hawkes}}(t) = \beta\left(\int_{(-\infty,t)} h(t-s)\mathcal{N}_{\mathrm{Hawkes}}(\mathrm{d}s)\right).$$

It is quite evident from the previous expression that neuronal dynamics can fit, after small adaptations, under this formalism with h being an exponential function. These processes exhibit complex dynamics, and the existence of stationary processes verifying this definition has led to several works in stochastic process theory.

The first formulation of the Hawkes process dates back to [Haw71; HO74], and chose to focus on linear activation function β. This enabled the authors to study the existence of stationary Hawkes processes using cluster branching processes theory. Later on, the latter analysis was extended to nonlinear Hawkes processes, i.e with nonlinear activation function β, primarily in [BM96]. Hawkes processes can also be extended to study multidimensional recurrent systems. This approach has already been applied to the analysis of neuronal networks dynamics in [RRT13] for example.

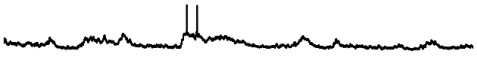

2.3 Synaptic plasticity and neuronal activity, a slow-fast system

Up until now, neuronal networks have been considered with fixed connections and therefore lacking any synaptic plasticity. In particular, the synaptic weight W is taken as a constant of the model. This is a simplistic model of neuronal activity, and to explain the influence of synaptic plasticity a more accurate version needs to be developed. We have introduce in the first chapter the notion of synaptic plasticity, the evolution of the synaptic strength as a function of neuronal activity, and would lead to stochastic differential equations of the following form,

$$\begin{cases} \mathrm{d}X(t) &= -\frac{1}{\tau}X(t)\,\mathrm{d}t + W(t-)\mathcal{N}_{\mathrm{pre}}(\mathrm{d}t), \\ \mathrm{d}W(t) &= F\left(X(t)\right)\mathrm{d}t. \end{cases} \tag{2.2}$$

where F represents synaptic plasticity mechanisms and is responsible for the fact that $W = (W(t), t{>}0)$ is now a function of time. We chose in this example to use synaptic plasticity that only depends on the value of the postsynaptic potential X.

When focusing on long-term synaptic plasticity, i.e synaptic changes that operate on longer timescales than neuronal dynamics, it is interesting to apply a slow-fast decomposition to this system.

Scaling of the neuronal and synaptic weight dynamics

In order to represent this timescale separation, most studies introduce a small scaling parameter ε.

Neuronal processes, associated to the point processes $\mathcal{N}_{\mathrm{pre}}$ and $\mathcal{N}_{\mathrm{post}}$, occur on a timescale which is much faster than the timescale of the evolution of $(W(t), t{>}0)$. For our simple model, after scaling, the SDE (2.2) becomes, for $\varepsilon{>}0$,

$$\begin{cases} \mathrm{d}X_\varepsilon(t) &= -\frac{1}{\tau}X(t)\frac{\mathrm{d}t}{\varepsilon} + W_\varepsilon(t-)\mathcal{N}_{\mathrm{pre},\varepsilon}(\mathrm{d}t), \\ \mathrm{d}W_\varepsilon(t) &= F\left(X_\varepsilon\right)\mathrm{d}t. \end{cases} \tag{2.3}$$

where $\mathcal{N}_{\mathrm{pre},\varepsilon}$ corresponds to the Poisson process $\mathcal{N}_{\mathrm{pre}}$ with the timescale change $t{\mapsto}t/\varepsilon$, Using this formulation, X_ε is the *fast variable*, in the sense that when ε goes to 0, it is sped up. The increments of the variable W are of order $O(1)$ and for this reason, $(W_\varepsilon(t), t{>}0)$ is described as a *slow process*. The corresponding scaling results, known as separation of timescales, are routinely used in mathematical models of computational neuroscience see, for example [KGH99].

Stochastic averaging

In a mathematical context, these types of results are referred to as averaging principles. See [PSV77] and Chapter 7 of [FW98] for general presentation. They aim at establishing a limit result, or averaging principle, for $(W_\varepsilon(t), t{>}0)$ when ε goes to 0 for certain types of dynamics.

In particular, in most formalisms, the stochastic systems studied verifies some Markovian property, in particular the system (2.3), can be formulated using martingale problems.

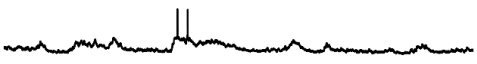

We denote by $(X^w(t), t>0)$ the solution of Relation (2.2) when the process $(W(t), t>0)$ is constant and equal to w. Under appropriate conditions, it has a unique equilibrium distribution Π_w. The averaging principle for the simple model can be expressed as follows. Under some conditions, the processes $(W_\varepsilon(t), t>0)$ is tight for the convergence in distribution when ε goes to 0, and any limiting point $(w(t), t>0)$ satisfies the following integral equation,

$$w(t) = w(0) + \int_0^t \int_{\mathbb{R}} F(x)\Pi_{w(s)}(\mathrm{d}x)\ \mathrm{d}s, \quad t \geqslant 0. \tag{2.4}$$

See Section 5 of Chapter 1 of [Bil99] for general results on tightness properties and convergence in distribution.

An important part of the proof using stochastic averaging principles is dedicated to the tightness of the slow variable $(W_\varepsilon, t>0)$ viewed as càdlàg processes. In particular, using that,

$$W_\varepsilon(t) = W_\varepsilon(0) + \int_0^t F(X_\varepsilon(s))\,\mathrm{d}s,$$

the tightness of the family of processes $(W_\varepsilon(t))$ is equivalent to the tightness of

$$\left(\int_0^t F(X_\varepsilon(s))\,\mathrm{d}s, t>0 \right).$$

A general approach to prove averaging principles is presented in [Kur92] for jump processes.

An elegant idea first developed in [PSV77] is to introduce the notion of occupation measure, it computes a local average of the fast variable value, as a measure defined by, for all $t>0$ and Borelian set B,

$$\nu_\varepsilon(A, [0,t]) = \int_0^t \mathbb{1}_{\{B\}}(X_\varepsilon(s))\,\mathrm{d}s,$$

where $\mathbb{1}_{\{B\}}$ is the indicator function of a Borelian B.

Indeed, it is then possible to rewrite the previous expression as,

$$\left(\int_0^t \int_{\mathbb{R}} F(x)\nu_\varepsilon(\mathrm{d}x, \mathrm{d}s), t>0 \right).$$

As expressed in [Kur92], an important hypothesis is that the process $(X_\varepsilon(t), t>0)$ verifies the compact containment condition, i.e that the set,

$$\{X_\varepsilon(t),\ t>0,\ \varepsilon>0\}$$

is relatively compact, which directly leads to the fact that the occupation measure ν_ε is also tight. If the function F is bounded, the resulting tightness of W_ε is straightforward. Most applications of slow-fast analysis need these two conditions to prove the stochastic averaging principles [KK+13]. This is also the case of [Hel18] for the time-elapsed model of plasticity for which this representation holds. Note that this is one of the few rigorous proofs I know of an averaging principle for a stochastic model of plasticity.

However, in a real biological system, the compact containment condition, and the boundedness of the slow variable dynamics may not be verified as easily, and would lead to more complex proofs.

Once tightness is proven, one last step is still needed to prove convergence of the scaled system to the averaged version described by equation (2.4). If Relation (2.4) has a unique solution for a given initial state, a result for the convergence in distribution of $(W_\varepsilon(t), t>0)$ when ε goes to 0 is therefore obtained. Uniqueness holds if the integrand, with respect to s, of the right-hand side of Relation (2.4) is locally Lipschitz as a function of $w(s)$. Regularity properties of the invariant distribution Π_w as a function of w need to be verified.

Stochastic averaging principles gather a set of tools that have been used to study slow-fast systems. However, several assumptions classically used on this subject are equivalent to the boundedness of the dynamics. In biological systems, such conditions may not be always verified and therefore applying slow-fast analysis is not as straightforward as it seems in a first approach.

CHAPTER 3

PROCEDURAL LEARNING IN THE STRIATUM

During my PhD, I was also part of the "Dynamic and Pathophysiology of Neuronal Networks" team at Collège de France, led by Dr. Laurent Venance. The experimentalists there are working on electrophysiological and behavioral approaches to examine the role of the dorsal striatum in procedural learning. Here, I will be referring to the dorsal striatum as the striatum, for simplification, leaving aside its ventral part, the nucleus accumbens. Most of the work I report here is focused on the striatal system, using mathematical tools and computational neuroscience to understand its dynamics and properties. In particular, the striatum displays a specific type of synaptic plasticity, anti-Hebbian STDP and I will develop several properties of anti-Hebbian STDP either in stochastic neuronal networks or in computational models of the striatum. In the following section, I will introduce the striatum as a core subcortical nucleus, that is part of a larger system, the basal ganglia, involved in action selection and procedural learning. Then, I will describe the different properties of the striatal neuronal network, in particular by defining its main constituents, the medium-spiny neurons (MSNs), that will be the basis of all the computational work in this report. Finally, I will detail how anti-Hebbian STDP has been discovered at corticostriatal synapses and what are the current views on the implication of anti-Hebbian STDP in models. Most information from this introduction has been taken from [Mil07; ST16] for the biological system and [PS95] for the computational part.

3.1 The striatum, a subcortical structure involved in procedural learning

The input nuclei of the basal ganglia

The striatum represents the entry system of the basal ganglia, a large group of subcortical nuclei involved in action selection, goal-directed behavior and procedural learning [ST16].

As the main input to the basal ganglia, the striatum is characterized by a convergence of a large array of excitatory neurons descending from the cortex or the thalamic nuclei. Cortical and thalamic glutamatergic (excitatory) axons converge at the level of the striatal neurons, and represent the main cause of neuronal activity in the striatum.

The striatum is of particular interest because of its capacity to integrate cortical inputs from all cortices, starting from the sensorimotor cortex (responsible for sensory integration and motor commands) to the limbic cortex (which supports diverse functions including emotion, behavior, long-term memory). The striatum uses this convergence of different sources of information to select correct associations and determine future actions based on this large collection of signals.

The striatum is primarily composed by projections neurons, called the medium-sized spiny neurons (MSNs) because of the size and shape of their dendritic tree.

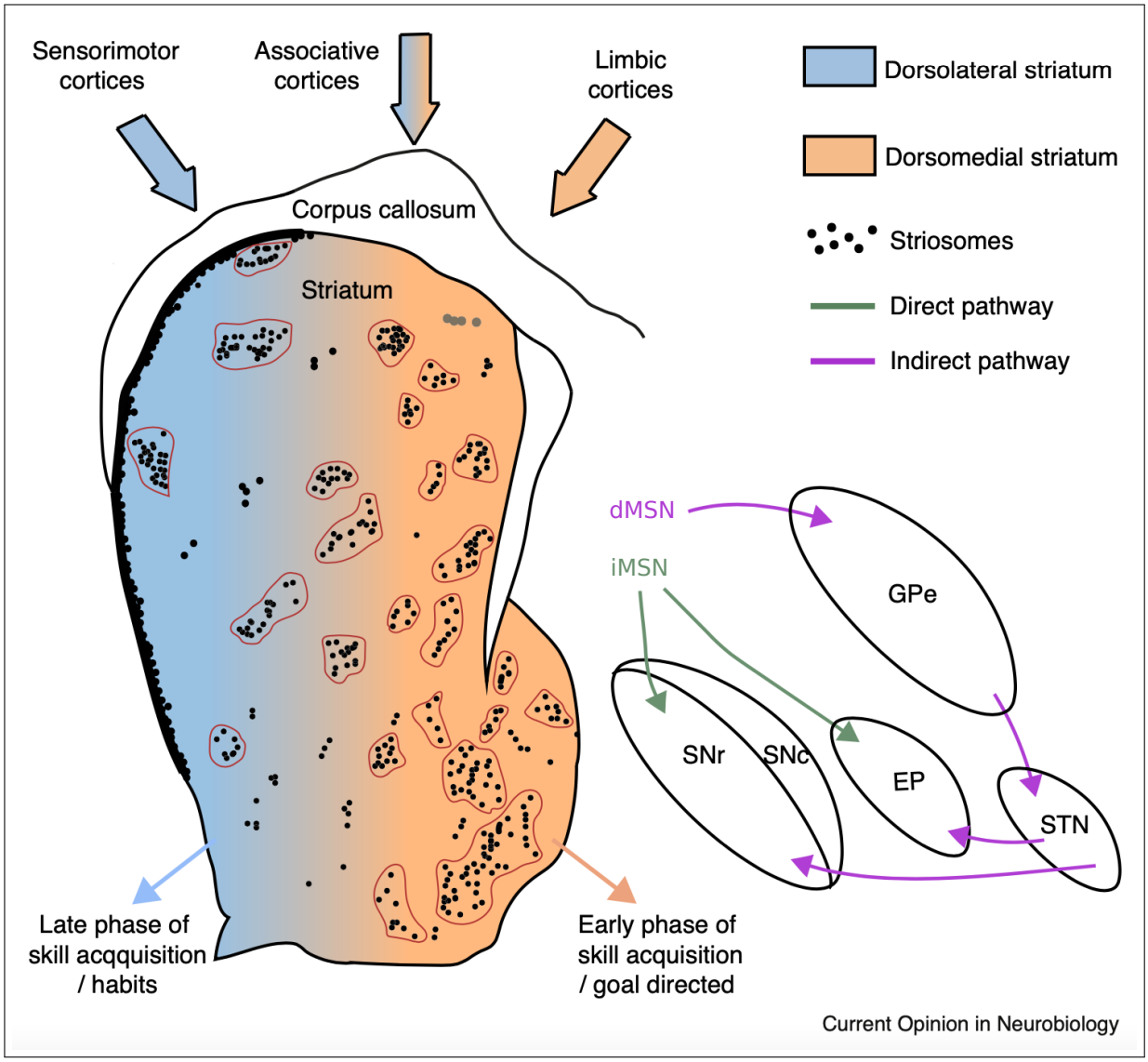

Figure 3.1: **Schematic representation of the striatal heterogeneity and the anatomo-functional compartments of the dorsal striatum, adapted from [PV19].**
Schematic representation of the direct and indirect trans-striatal pathways of the basal ganglia. Striosomes are shown with black dots distributed between the dorsolateral striatum (blue) and the dorsomedial striatum (orange). Grouped black dots represent striosomes surrounded by the annular compartment (red line, [BC15]), whereas isolated black dots illustrate the exo-patch [Smi+16]. Striosomal SPNs mainly project to SNc whereas SPNs from the matrix belong to the direct or indirect pathway. The direct and indirect pathways are represented, respectively, in green and purple.
GPe, external segment of the globus pallidus; EP, entopeduncular nucleus; STN: subthalamic nucleus; SNr, substantia nigra pars reticulata; SNc, substantia nigra pars compacta.

Because of their roles as the only neurons projecting outside of the striatum, they are also referred to as striatal projection neurons (SPNs). Accordingly, MSNs project to other parts of the basal ganglia, and two main pathways have been characterized in the past decade. For a simplified picture of the basal ganglia organization see Figure 3.1 (right). It has been shown that two subtypes of MSN differ in their target nuclei. *Direct-pathway* neurons, dMSNs, directly extend their axons into the EP (entopeduncular nucleus) and the SNr (substantia nigra pars reticulata), which represent the output nuclei of the basal ganglia. Conversely, *indirect-pathway* neurons, iMSNs, project to the GPe (external globus pallidum), whose neurons then project to the STN (subthalamic nucleus) as a final step before being received at the EP and SNr. Information traveling through this pathway goes to several intermediate steps before arriving at the output neurons of the basal ganglia. This simplistic view of the basal ganglia system is presented and discussed in [Mil07].

The basal ganglia are composed of nuclei whose projecting neurons share a quite uncommon property when comparing to the rest of the brain: all neurons are inhibitory and transmit information at synapses using the GABA (gamma-aminobutyric acid) neurotransmitter. An exception must be made for neurons from the STN which are excitatory. When comparing with the cortex, where the majority of the cells are excitatory, and inhibition is only present through local interneurons, it highlights the fact that the basal ganglia has its own dynamics, quite distinct from cortical ones. In particular, the MSNs have inhibitory projections to their target neurons, which exhibit tonic (spontaneous) firing activity, and modulate these rates through the intensity of inhibition.

The striatum, and more generally the basal ganglia, are linked to several neurological disorders, such as Parkinson's disease or Huntington's disease. The continuous effort of experimentalists and neuroscientists working on the basal ganglia, has mainly been driven by the understanding of these diseases and by the prospect to heal them.

Functional role of the striatum

The basal ganglia are a key structure for action selection, and the control of voluntary motor movements. The striatum, as the main input structure of this system, has distinct functional roles which can be linked to three of its main properties.

The striatum integrates numerous cortical inputs at each MSN, and a large number of those excitatory neurons need to be activated at the same time to trigger a spike at the MSN. Indeed, MSN are known to exhibit low rest potentials ($X_{\text{eq}} = -80\,mV$) and only spike when receiving enough excitatory currents concurrently to reach the spike potential ($X_{\text{th}} = -50\,mV$). Therefore, MSNs play a great part in filtering random cortical activity, and extracting from noise, relevant information, characterized by correlated cortical spiking. It is particularly interesting to notice that MSNs integrate excitatory inputs from variate cortical structures, which then "share" information at the level of the striatum to decide on which action to perpetrate in response to a particular situation. From the machine learning point of view, the striatal layer mimics the role of a perceptron, whose input layer would be represented by cortical neurons, and the output layer would be modeled by the MSNs [Wic93; PS95]. MSNs are then able to send this filtered information to the following stages of the circuit, leading to action selection and motor processing. This detection of coincidence is enhanced by the presence of collateral inhibition between MSNs, i.e they also project to neighboring MSNs, and

therefore inhibit them while spiking. This competition between inhibitory cells lead to *winner-take-all* dynamics, where a single active neuron shuts down the other MSNs, enhancing signal-to-noise ratio. This hypothesis, based on strong collateral inhibition has been tempered in recent works, where MSN inhibition has been shown to be weaker, leading to *winner-share-all* dynamics [WAS07].

A second important fact about the striatum is that its synaptic connections are highly plastic. In particular, corticostriatal synapses are modified following correlated activity from cortical and striatal neurons [PS95] and also display STDP [FV10]. Accordingly, the ability of MSNs to select important information from spontaneous cortical activity is shaped by synaptic plasticity. Indeed, corticostriatal synapses learn to modulate MSN activity to the right intensity to participate in the pattern detection task. Many synaptic mechanisms have been proven to be involved in different types of learning, and in particular for the striatum, in procedural learning. This particular type of learning refers to the process of acquiring skills in a motor task that is eventually can be performed automatically, without having to consciously remember the information. Learning to ride a bike is an example of procedural learning, in the sense that, when cycling, people do not move their feet with explicit, conscious, orders, but rather just replicate a sequence that they have learned to perform. It is usually opposed to declarative memory, where the subject is able to consciously recall particular information.

Finally, for learning to occur in the striatum, striatal neurons need to be taught through some mechanisms which cortical associations are contextually appropriate or not. Reward mechanisms are usually associated to dopaminergic signaling [SDM97], and the striatum is one of the brain areas where dopamine plays a major role. A subset of MSNs, mainly located at striosomes (patches of chemical compartments in the striatum, see Figure 3.1) are known to directly project to the SNc, one of the main pools of dopaminergic neurons in the brain. Striatal activity therefore greatly influences the release of dopamine in the rest of the brain, and in particular in the striatum. Indeed, neurons from the SNc are known to project directly to the dorsal striatum and therefore locally influence striatal activity, and even synaptic plasticity, with signals based on reward. Goal-directed learning in particular has been shown to rely on the influence of dopamine in the striatum [YK06; BO10]. More precisely, dopamine is a good candidate to represent reward or RPE (reward prediction error) directly at the level of the striatum.

Dichotomies in the dorsal striatum

As explained in the previous sections, the striatum has to perform several different tasks at the same time, keeping in mind that it only has a single type of projecting neurons, the MSNs. Several heterogeneities have been observed at the level of the striatum, both structurally and functionally that can explain its ability to "multitask".

Direct vs indirect pathways

As explained in Section 3.1, MSNs can be discriminated based on their output targets, and their belonging to the direct or indirect pathways. Furthermore, neurons from the direct and indirect pathways are associated with different dopaminergic receptors (D1-like for direct pathway neurons, and D2-like for indirect ones). Indirect pathway MSNs

also have a greater excitability (they are more prone to spike) than MSNs belonging to the direct pathway. Finally, [Per+22] have proven that in some regimes, MSNs may exhibit different STDP rules at their corticostriatal synapses. These neurons also have different functions, because direct and indirect pathways neurons tend to exert an opposite influence on the basal ganglia output. The differential influence of the direct, and the indirect pathways has been the focus of many studies. Excitatory inputs received by the direct MSNs lead to a decrease of activity in the output neurons of the basal ganglia, which in turn stop inhibiting key areas for motor processing, enabling motor activity. The direct pathway is therefore involved in the release of inhibition, necessary for the correct implementation of learned motor skills. The indirect pathway goes through one more inhibitory connection, and as such has the opposite influence on the output neurons of the basal ganglia. It has been shown that its role is to prevent actions from being processed. The balance resulting from the activity of both systems is key in order to perform action selection, and to correctly process complex motor programs. These facts have been used when modeling the action selection process [CJB10; Dun+19], or when studying the influence of the basal ganglia in Parkinsonian models [Rub17; HOD18]

The dorsolateral (DMS) vs dorsomedial (DMS) striata

The second duality that is present in the (dorsal) striatum consists in the distinction between the DLS and DMS regions of the striatum, see 3.1 (DLS in blue, DMS in orange). These two parts are not clearly segregated when looking at the dorsal striatum, but they integrate inputs from different cortical areas, sensorimotor cortices for the DLS and associative ones for the DMS. Again, MSNs display different properties in these two regions, in particular, at the level of their corticostriatal plasticity [Per+22]. Another important variation between those two regions is that striatal interneurons (neurons that only project inside the striatum) have different distributions [Fin+18]. It has been shown that these two regions also exhibit clear functional differences [BO10]: the DLS is involved in habit formation, i.e learning to associate stimulus to a succession of actions without taking into any rewards, whereas DMS participate in goal-directed learning (learning based on rewards). They are both involved when learning a new task, and their complementary action seems necessary for procedural learning. For a more detailed presentation on this topic, see Section IV.2.2.1.

Patch vs matrix compartments

Finally, the striatum can be subdivided in two types of chemically-distinct patterns. Striosomes are patches of MSNs which project to the SNc, and the matrix which forms the rest of the MSNs [BC15; Smi+16]. In the first models of the striatum, these two parts where supposed to represent the two systems in actor-critic model [PS95], where the matrix would be responsible for choosing an action based on current information (the actor) and the striosomes, thanks to their association with dopaminergic neurons of the SNc, would predict, using an internal model of the world, the reward that would result from doing a particular move (the critic). Dopamine would then be used to correctly update both systems (as is expected in the actor-critic model) because dopaminergic neurons project back to the whole striatum.

Even if at first view, the striatum seems to be quite restricted in its actions, due to the fact that its only influence is exerted through a single type of cells, the MSNs,

different local variations of the striatal network explain its ability to multitask efficiently, while sharing relevant information.

3.2 Corticostriatal STDP and importance of anti-Hebbian plasticity

STDP at corticostriatal synapses

The striatum, while integrating inputs from all cortical areas (from motor to limbic parts) and from some thalamic nuclei, is involved in both action selection and procedural learning. [Yin+09] proved that procedural learning depends on corticostriatal plasticity, leading to various studies to characterize the shape and role of corticostriatal plasticity [Kor+12; PV19]. Plasticity observed *in vitro* (using brain slices) and *in vivo* (in anesthetized or awake rodents) depend on several conditions, first of all the induction protocols (rate-based, STDP), then striatal heterogeneity, and finally the presence/absence of neuromodulators [PV19].

For a long time, corticostriatal plasticity was known to be depression-based, i.e leading to a decrease in the synaptic weight value. However, after applying STDP protocols at corticostriatal synapses, [FGV05] described that they displayed anti-Hebbian STDP. In short, pre-post pairings (a presynaptic spike followed by a postsynaptic spike) lead to long-term depression while reversed pairings trigger long-term potentiation. It is important to stress here that, anti-Hebbian STDP has not been as extensively studied as Hebbian one, even if it was discovered at the same time [Bel+97]. Several studies have later on confirmed the presence of anti-Hebbian STDP at corticostriatal synaspes [Pai+13; Val+17], and have studied the influence of the induction protocol on synaptic plasticity. Changes in frequency [Per+22], number of pairings [Cui+16], age of the rodents [Val+17] have shown that STDP is highly dependent on these parameters, leading to legitimate questions about its active role in *in vivo* synaptic plasticity, and of course in behavior. *In vivo* studies have confirmed that corticostriatal STDP could be elicited, while maintaining a biological level of activity [Mor+19].

It is to be noted that some works have reported Hebbian STDP at corticostriatal synapses. These conflicting observations have been explained by the use (or lack of use) of ionotropic GABA antagonists [Pai+13]. Moreover, the influence of dopamine on the shape of STDP is also of great importance [She+08], when starting to consider models of goal-directed learning [GHR15], or the influence of three-factor learning rules [KIT17; Ger+18; PV19].

I would like to stress here, that when talking about corticostriatal synapses, I am referring to synapses onto MSNs. However, several studies have also demonstrated that STDP could also be elicited at corticostriatal synapses located on the different types of interneurons present in the striatum. In particular, fast-spiking inhibitory interneurons (FS), cholinergic interneurons and low threshold-spiking interneurons (LTS) also exhibit different types of STDP [FV10]. Similarly, plasticity was also induced at thalamocortical synapses, i.e where thalamic afferents connect to striatal neurons [Men+20].

In conclusion, striatal neurons have highly plastic synapses, and various works have proven that anti-Hebbian plasticity has an important role to play in learning. However, few models have tried to study how anti-Hebbian STDP impacts neuronal dynamics, and this work aims at reporting some new principles for anti-Hebbian STDP.

Functions of anti-Hebbian STDP

In order to understand the role of anti-Hebbian STDP, modeling studies are often necessary and it is quite appalling to see that most computational works on synaptic plasticity only focus on Hebbian STDP. Theoretical studies analyzing different types of STDPs, even if scarce in numbers, exist [Rob00; CF03; RA04; ZD07; RL10; BK12].

An exception must be made for a sequence of publications on the role of anti-Hebbian STDP in electrosensory systems, in the mormyrid electric fish. These fish are known to have an electric organ located in their tail that generates a weak electric field. A motor command causes the electric organ to discharge in pulses and the animals can then navigate by detecting small distortions in the electrical field caused by external objects. Moreover, it has been shown that anti-Hebbian STDP was present at parallel fiber synapses [Bel+97] and several computational models have been built on this hypothesis [RL10]. They explain that anti-Hebbian STDP helps the system to create a *negative* image of the electrical field generated by a motor command. When this negative image is subtracted to the actual electric field sensed by the fish, small distortions are easily detected, helping the fish to navigate. Anti-Hebbian plasticity has been shown to be perfect in order to reproduce this phenomenon [RB00; WRL03] and this cancellation mechanisms has been studied both with computer simulations and theoretical studies [RL10]. An important point raised by several articles, is that anti-Hebbian STDP alone, is not able to generate sustained spiking activity. Indeed, as a causal pre-post pairing leads to depression, the synaptic weights will eventually converge to a situation where they are not large enough to trigger spiking activity. In order to counteract this phenomenon, and to reproduce experimental data, non-associative potentiation (only triggered by presynaptic activity) is often added to the associative anti-Hebbian STDP rule [RB00; WRL03; RA04].

Hebbian STDP is known to act as a correlation tool, in the sense that neurons whose firing are correlated, will be even more correlated after the action of synaptic plasticity. This auto-exciting process has been shown to be of great importance in the formation of neuronal assemblies and syncfire chains [GBV10], mainly in the cortex. Anti-Hebbian STDP follows the opposite principles, in the sense that as soon as the postsynaptic neuron spikes, it immediately reduces the value of the synaptic weights that have led to its spiking. Anti-Hebbian STDP therefore acts as a *homeostatic* mechanisms, that can limit the growth of the synaptic weights to a value sufficient to trigger spikes [RA04]. This view has also emerged in studies on learning temporal spiking sequences, where the goal is not only to spike in response to a pattern, but to spike at the right time. Theoretical studies have shown that algorithms needed to solve this task, as the Chronotron [Flo12] or ReSuMe [PK10] have dynamics similar to anti-Hebbian rules [Güt14]. For a more specific introduction on this topic see, Section IV.1.1.1.

BIBLIOGRAPHY

[Ath+18] V. R. Athalye, F. J. Santos, J. M. Carmena, and R. M. Costa. Evidence for a neural law of effect. *Science* **359** (Mar. 2018), 1024–1029.

[BA10] B. Babadi and L. F. Abbott. Intrinsic stability of temporally shifted spike-timing dependent plasticity. *PLoS computational biology* **6** (Nov. 2010), e1000961.

[BA16] B. Babadi and L. F. Abbott. Stability and Competition in Multi-spike Models of Spike-Timing Dependent Plasticity. *PLoS computational biology* **12** (Mar. 2016), e1004750.

[BC07] M. A. Buice and J. D. Cowan. Field-theoretic approach to fluctuation effects in neural networks. *Physical Review E* **75** (May 2007), 051919.

[BC15] K. R. Brimblecombe and S. J. Cragg. Substance P Weights Striatal Dopamine Transmission Differently within the Striosome-Matrix Axis. *The Journal of Neuroscience* **35** (June 2015), 9017–9023.

[Bel+97] C. C. Bell, V. Z. Han, Y. Sugawara, and K. Grant. Synaptic plasticity in a cerebellum-like structure depends on temporal order. *Nature* **387** (May 1997), 278–281.

[Bil99] P. Billingsley. Convergence of Probability Measures. John Wiley & Sons, 1999.

[BK12] K. S. Burbank and G. Kreiman. Depression-biased reverse plasticity rule is required for stable learning at top-down connections. *PLoS computational biology* **8** (2012), e1002393.

[BM96] P. Brémaud and L. Massoulié. Stability of Nonlinear Hawkes Processes. *The Annals of Probability* **24** (1996), 1563–1588.

[BMG04] A. N. Burkitt, H. Meffin, and D. B. Grayden. Spike-timing-dependent plasticity: the relationship to rate-based learning for models with weight dynamics determined by a stable fixed point. *Neural Computation* **16** (May 2004), 885–940.

[BMP19] Z. Brzosko, S. B. Mierau, and O. Paulsen. Neuromodulation of Spike-Timing-Dependent Plasticity: Past, Present, and Future. *Neuron* **103** (Aug. 2019), 563–581.

[BO10] B. W. Balleine and J. P. O'Doherty. Human and rodent homologies in action control: corticostriatal determinants of goal-directed and habitual action. *Neuropsychopharmacology: Official Publication of the American College of Neuropsychopharmacology* **35** (Jan. 2010), 48–69.

[BP01] G. Bi and M. Poo. Synaptic modification by correlated activity: Hebb's postulate revisited. *Annual Review of Neuroscience* **24** (2001), 139–166.

[BP98] G.-q. Bi and M.-m. Poo. Synaptic Modifications in Cultured Hippocampal Neurons: Dependence on Spike Timing, Synaptic Strength, and Postsynaptic Cell Type. *Journal of Neuroscience* **18** (Dec. 1998), 10464–10472.

[CF03] H. Câteau and T. Fukai. A stochastic method to predict the consequence of arbitrary forms of spike-timing-dependent plasticity. *Neural Computation* **15** (Mar. 2003), 597–620.

[CF16] R. Chaudhuri and I. Fiete. Computational principles of memory. *Nature Neuroscience* **19** (Mar. 2016), 394–403.

[CG10] C. Clopath and W. Gerstner. Voltage and Spike Timing Interact in STDP – A Unified Model. *Frontiers in Synaptic Neuroscience* **2** (July 2010).

[Chi01] E. Chichilnisky. A simple white noise analysis of neuronal light responses. *Network: Computation in Neural Systems* **12** (2001), 199–213.

[CJB10] V. S. Chakravarthy, D. Joseph, and R. S. Bapi. What do the basal ganglia do? A modeling perspective. *Biological Cybernetics* **103** (Sept. 2010), 237–253.

[Cow68] J. D. Cowan. Statistical Mechanics of Nervous Nets. *Neural Networks: Proceedings of the -School on Neural Networks - June 1967 in Ravello*. Ed. by E. R. Caianiello. Berlin, Heidelberg: Springer, 1968, 181–188.

[Cow91] J. Cowan. Stochastic Neurodynamics. *Advances in Neural Information Processing Systems*. Vol. 3. Morgan-Kaufmann, 1991.

[Cui+16] Y. Cui, I. Prokin, H. Xu, B. Delord, S. Genet, L. Venance, and H. Berry. Endocannabinoid dynamics gate spike-timing dependent depression and potentiation. *eLife* **5** (Feb. 2016), e13185.

[Dun+19] K. Dunovan, C. Vich, M. Clapp, T. Verstynen, and J. Rubin. Reward-driven changes in striatal pathway competition shape evidence evaluation in decision-making. *PLoS computational biology* **15** (May 2019), e1006998.

[DV08] D. J. Daley and D. Vere-Jones. An introduction to the theory of point processes. Vol. II. Second edition. Probability and its Applications (New York). New York: Springer, 2008, xviii+573.

[ET10] G. B. Ermentrout and D. H. Terman. Mathematical Foundations of Neuroscience. Springer Science & Business Media, July 2010.

[FD02] R. C. Froemke and Y. Dan. Spike-timing-dependent synaptic modification induced by natural spike trains. *Nature* **416** (Mar. 2002), 433–438.

[Fel12] D. E. Feldman. The spike-timing dependence of plasticity. *Neuron* **75** (Aug. 2012), 556–571.

[FG16] N. Frémaux and W. Gerstner. Neuromodulated Spike-Timing-Dependent Plasticity, and Theory of Three-Factor Learning Rules. *Frontiers in Neural Circuits* **9** (2016), 85.

[FGV05] E. Fino, J. Glowinski, and L. Venance. Bidirectional activity-dependent plasticity at corticostriatal synapses. *The Journal of Neuroscience: The Official Journal of the Society for Neuroscience* **25** (Dec. 2005), 11279–11287.

[Fin+18] E. Fino, M. Vandecasteele, S. Perez, F. Saudou, and L. Venance. Region-specific and state-dependent action of striatal GABAergic interneurons. *Nature Communications* **9** (Aug. 2018), 3339.

[Flo12] R. V. Florian. The Chronotron: A Neuron That Learns to Fire Temporally Precise Spike Patterns. *PLoS ONE* **7** (Aug. 2012), e40233.

[Fon+18] A. Foncelle, A. Mendes, J. Jędrzejewska-Szmek, S. Valtcheva, H. Berry, K. T. Blackwell, and L. Venance. Modulation of Spike-Timing Dependent Plasticity: Towards the Inclusion of a Third Factor in Computational Models. *Frontiers in Computational Neuroscience* **12** (2018), 49.

[FV10] E. Fino and L. Venance. Spike-timing dependent plasticity in the striatum. *Frontiers in Synaptic Neuroscience* **2** (2010), 6.

[FW98] M. I. Freidlin and A. D. Wentzell. Random perturbations of dynamical systems. Second Edition edition. New York: Springer-Verlag, 1998.

[Gar19] J. L. Gardner. Optimality and heuristics in perceptual neuroscience. *Nature Neuroscience* **22** (Apr. 2019), 514–523.

[GB07] M. Graupner and N. Brunel. STDP in a bistable synapse model based on CaMKII and associated signaling pathways. *PLoS computational biology* **3** (Nov. 2007), e221.

[GB10] M. Graupner and N. Brunel. Mechanisms of induction and maintenance of spike-timing dependent plasticity in biophysical synapse models. *Frontiers in Computational Neuroscience* **4** (2010).

[GB12] M. Graupner and N. Brunel. Calcium-based plasticity model explains sensitivity of synaptic changes to spike pattern, rate, and dendritic location. *Proceedings of the National Academy of Sciences of the United States of America* **109** (Mar. 2012), 3991–3996.

[GBV10] M. Gilson, A. Burkitt, and L. J. Van Hemmen. STDP in Recurrent Neuronal Networks. *Frontiers in Computational Neuroscience* **4** (2010).

[Ger+14] W. Gerstner, W. M. Kistler, R. Naud, and L. Paninski. Neuronal Dynamics: From Single Neurons to Networks and Models of Cognition. New York, NY, USA: Cambridge University Press, 2014.

[Ger+18] W. Gerstner, M. Lehmann, V. Liakoni, D. Corneil, and J. Brea. Eligibility Traces and Plasticity on Behavioral Time Scales: Experimental Support of NeoHebbian Three-Factor Learning Rules. *Frontiers in Neural Circuits* **12** (July 2018).

[Ger+96] W. Gerstner, R. Kempter, J. L. van Hemmen, and H. Wagner. A neuronal learning rule for sub-millisecond temporal coding. *Nature* **383** (Sept. 1996), 76–81.

[GH92] W. Gerstner and J. L. van Hemmen. Associative memory in a network of 'spiking' neurons. *Network: Computation in Neural Systems* **3** (Jan. 1992), 139–164.

[GHR15] K. N. Gurney, M. D. Humphries, and P. Redgrave. A new framework for cortico-striatal plasticity: behavioural theory meets in vitro data at the reinforcement-action interface. *PLoS biology* **13** (Jan. 2015), e1002034.

[GK02a] W. Gerstner and W. M. Kistler. Mathematical formulations of Hebbian learning. *Biological Cybernetics* **87** (Dec. 2002), 404–415.

[Güt+03] R. Gütig, R. Aharonov, S. Rotter, and H. Sompolinsky. Learning input correlations through nonlinear temporally asymmetric Hebbian plasticity. *The Journal of Neuroscience: The Official Journal of the Society for Neuroscience* **23** (May 2003), 3697–3714.

[Güt14] R. Gütig. To spike, or when to spike? *Current Opinion in Neurobiology* **25** (Apr. 2014), 134–139.

[Haw71] A. G. Hawkes. Spectra of Some Self-Exciting and Mutually Exciting Point Processes. *Biometrika* **58** (1971), 83–90.

[Hel18] P. Helson. A new stochastic STDP Rule in a neural Network Model. *arXiv:1706.00364 [math]* (Mar. 2018).

[Hen+21] J. A. Hennig, E. R. Oby, D. M. Losey, A. P. Batista, B. M. Yu, and S. M. Chase. How learning unfolds in the brain: toward an optimization view. *Neuron* (Oct. 2021).

[HF17] N. Hiratani and T. Fukai. Detailed Dendritic Excitatory/Inhibitory Balance through Heterosynaptic Spike-Timing-Dependent Plasticity. *The Journal of Neuroscience: The Official Journal of the Society for Neuroscience* **37** (Dec. 2017), 12106–12122.

[HO74] A. G. Hawkes and D. Oakes. A Cluster Process Representation of a Self-Exciting Process. *Journal of Applied Probability* **11** (1974), 493–503.

[HOD18] M. D. Humphries, J. A. Obeso, and J. K. Dreyer. Insights into Parkinson's disease from computational models of the basal ganglia. *Journal of Neurology, Neurosurgery, and Psychiatry* **89** (Nov. 2018), 1181–1188.

[ID03] E. M. Izhikevich and N. S. Desai. Relating STDP to BCM. *Neural Computation* **15** (July 2003), 1511–1523.

[ID21] Y. Inglebert and D. Debanne. Calcium and Spike Timing-Dependent Plasticity. *Frontiers in Cellular Neuroscience* **15** (2021), 374.

[Izh07] E. M. Izhikevich. Dynamical Systems in Neuroscience. MIT Press, 2007.

[KGH01] R. Kempter, W. Gerstner, and J. L. van Hemmen. Intrinsic stabilization of output rates by spike-based Hebbian learning. *Neural Computation* **13** (Dec. 2001), 2709–2741.

[KGH99] R. Kempter, W. Gerstner, and J. L. van Hemmen. Hebbian learning and spiking neurons. *Physical Review E* **59** (Apr. 1999), 4498–4514.

[KH00] W. M. Kistler and J. L. v. Hemmen. Modeling Synaptic Plasticity in Conjunction with the Timing of Pre- and Postsynaptic Action Potentials. *Neural Computation* **12** (Feb. 2000), 385–405.

[Kin92] J. F. C. Kingman. Poisson Processes. Clarendon Press, Dec. 1992.

[KIT17] Ł. Kuśmierz, T. Isomura, and T. Toyoizumi. Learning with three factors: modulating Hebbian plasticity with errors. *Current Opinion in Neurobiology* **46** (Oct. 2017), 170–177.

[KK+13] H.-W. Kang, T. G. Kurtz, et al. Separation of time-scales and model reduction for stochastic reaction networks. *The Annals of Applied Probability* **23** (2013), 529–583.

[Kor+12] A. C. Koralek, X. Jin, J. D. Long, R. M. Costa, and J. M. Carmena. Corticostriatal plasticity is necessary for learning intentional neuroprosthetic skills. *Nature* **483** (Mar. 2012), 331–335.

[Kur92] T. G. Kurtz. Averaging for martingale problems and stochastic approximation. *Applied Stochastic Analysis*. Ed. by I. Karatzas and D. Ocone. Vol. 177. Berlin/Heidelberg: Springer-Verlag, 1992, 186–209.

[LF12] T. K. Leen and R. Friel. Stochastic Perturbation Methods for Spike-Timing-Dependent Plasticity. *Neural Comput.* **24** (May 2012), 1109–1146.

[LS08] E. V. Lubenov and A. G. Siapas. Decoupling through synchrony in neuronal circuits with propagation delays. *Neuron* **58** (Apr. 2008), 118–131.

[MAD07] A. Morrison, A. Aertsen, and M. Diesmann. Spike-timing-dependent plasticity in balanced random networks. *Neural Computation* **19** (June 2007), 1437–1467.

[MDG08] A. Morrison, M. Diesmann, and W. Gerstner. Phenomenological models of synaptic plasticity based on spike timing. *Biological Cybernetics* **98** (June 2008), 459–478.

[Men+20] A. Mendes, G. Vignoud, S. Perez, E. Perrin, J. Touboul, and L. Venance. Concurrent Thalamostriatal and Corticostriatal Spike-Timing-Dependent Plasticity and Heterosynaptic Interactions Shape Striatal Plasticity Map. *Cerebral Cortex (New York, N.Y.: 1991)* **30** (June 2020), 4381–4401.

[MG20] J. C. Magee and C. Grienberger. Synaptic Plasticity Forms and Functions. *Annual Review of Neuroscience* **43** (2020), 95–117.

[Mil07] R. Miller. A Theory of the Basal Ganglia and Their Disorders. CRC Press, Aug. 2007.

[Mor+19] T. Morera-Herreras, Y. Gioanni, S. Perez, G. Vignoud, and L. Venance. Environmental enrichment shapes striatal spike-timing-dependent plasticity in vivo. *Scientific Reports* **9** (Dec. 2019), 19451.

[Nab+14] S. Nabavi, R. Fox, C. D. Proulx, J. Y. Lin, R. Y. Tsien, and R. Malinow. Engineering a memory with LTD and LTP. *Nature* **511** (July 2014), 348–352.

[Pai+13] V. Paille, E. Fino, K. Du, T. Morera-Herreras, S. Perez, J. H. Kotaleski, and L. Venance. GABAergic circuits control spike-timing-dependent plasticity. *The Journal of Neuroscience: The Official Journal of the Society for Neuroscience* **33** (May 2013), 9353–9363.

[Per+22] S. Perez, Y. Cui, G. Vignoud, E. Perrin, A. Mendes, Z. Zheng, J. Touboul, and L. Venance. Striatum expresses region-specific plasticity consistent with distinct memory abilities. *Cell Reports* **38** (2022), 110521.

[PG06a] J.-P. Pfister and W. Gerstner. Triplets of Spikes in a Model of Spike Timing-Dependent Plasticity. *Journal of Neuroscience* **26** (Sept. 2006), 9673–9682.

[PK10] F. Ponulak and A. Kasiński. Supervised learning in spiking neural networks with ReSuMe: sequence learning, classification, and spike shifting. *Neural Computation* **22** (Feb. 2010), 467–510.

[PS95] T. A. Poggio and T. J. Sejnowski. Models of Information Processing in the Basal Ganglia. MIT Press, 1995.

[PSV77] G. Papanicolalou, D. W. Stroock, and S. R. S. Varadhan. Martingale approach to some limit theorems. *Proc. 1976. Duke Conf. On Turbulence*. III. Duke Univ. Math, 1977.

[PV19] E. Perrin and L. Venance. Bridging the gap between striatal plasticity and learning. *Current Opinion in Neurobiology*. Neurobiology of Learning and Plasticity **54** (Feb. 2019), 104–112.

[RA04] C. C. Rumsey and L. F. Abbott. Equalization of synaptic efficacy by activity- and timing-dependent synaptic plasticity. *Journal of Neurophysiology* **91** (May 2004), 2273–2280.

[RB00] P. D. Roberts and C. C. Bell. Computational consequences of temporally asymmetric learning rules: II. Sensory image cancellation. *Journal of Computational Neuroscience* **9** (Aug. 2000), 67–83.

[RBS16] B. S. Robinson, T. W. Berger, and D. Song. Identification of Stable Spike-Timing-Dependent Plasticity from Spiking Activity with Generalized Multilinear Modeling. *Neural Comput.* **28** (Nov. 2016), 2320–2351.

[RBT00a] M. C. van Rossum, G. Q. Bi, and G. G. Turrigiano. Stable Hebbian learning from spike timing-dependent plasticity. *The Journal of Neuroscience: The Official Journal of the Society for Neuroscience* **20** (Dec. 2000), 8812–8821.

[RL10] P. D. Roberts and T. K. Leen. Anti-Hebbian spike-timing-dependent plasticity and adaptive sensory processing. *Frontiers in Computational Neuroscience* **4** (2010), 156.

[RLS01] J. Rubin, D. D. Lee, and H. Sompolinsky. Equilibrium properties of temporally asymmetric Hebbian plasticity. *Physical Review Letters* **86** (Jan. 2001), 364–367.

[Rob00] P. D. Roberts. Dynamics of temporal learning rules. *Phys. Rev. E* **62** (3 Sept. 2000), 4077–4082.

[Rob99] P. D. Roberts. Computational Consequences of Temporally Asymmetric Learning Rules: I. Differential Hebbian Learning. *Journal of Computational Neuroscience* **7** (Nov. 1999), 235–246.

[RRT13] P. Reynaud-Bouret, V. Rivoirard, and C. Tuleau-Malot. Inference of functional connectivity in Neurosciences via Hawkes processes. *2013 IEEE Global Conference on Signal and Information Processing*. Dec. 2013, 317–320.

[RT16] P. Robert and J. Touboul. On the Dynamics of Random Neuronal Networks. *Journal of Statistical Physics* **165** (Nov. 2016), 545–584.

[Rub17] J. E. Rubin. Computational models of basal ganglia dysfunction: the dynamics is in the details. *Current Opinion in Neurobiology* **46** (2017), 127–135.

[SBD18] J. Schiller, S. Berlin, and D. Derdikman. The Many Worlds of Plasticity Rules. *Trends in Neurosciences* **41** (Mar. 2018), 124–127.

[SDM97] W. Schultz, P. Dayan, and P. R. Montague. A neural substrate of prediction and reward. *Science (New York, N.Y.)* **275** (Mar. 1997), 1593–1599.

[Seu00] H. S. Seung. Half a century of Hebb. *Nature Neuroscience* **3** (Nov. 2000), 1166–1166.

[Sha92] C. J. Shatz. The Developing Brain. *Scientific American* **267** (1992), 60–67.

[She+08] W. Shen, M. Flajolet, P. Greengard, and D. J. Surmeier. Dichotomous dopaminergic control of striatal synaptic plasticity. *Science (New York, N.Y.)* **321** (Aug. 2008), 848–851.

[Smi+16] J. B. Smith, J. R. Klug, D. L. Ross, C. D. Howard, N. G. Hollon, V. I. Ko, H. Hoffman, E. M. Callaway, C. R. Gerfen, and X. Jin. Genetic-Based Dissection Unveils the Inputs and Outputs of Striatal Patch and Matrix Compartments. *Neuron* **91** (Sept. 2016), 1069–1084.

[ST16] H. Steiner and K. Y. Tseng. Handbook of Basal Ganglia Structure and Function. Academic Press, 2016.

[Val+17] S. Valtcheva, V. Paillé, Y. Dembitskaya, S. Perez, G. Gangarossa, E. Fino, and L. Venance. Developmental control of spike-timing-dependent plasticity by tonic GABAergic signaling in striatum. *Neuropharmacology* **121** (July 2017), 261–277.

[Ver70] D. Vere-Jones. Stochastic Models for Earthquake Occurrence. *Journal of the Royal Statistical Society. Series B (Methodological)* **32** (1970), 1–62.

[VVT18] G. Vignoud, L. Venance, and J. D. Touboul. Interplay of multiple pathways and activity-dependent rules in STDP. *PLoS computational biology* **14** (2018), e1006184.

[WAS07] J. R. Wickens, G. W. Arbuthnott, and T. Shindou. Simulation of GABA function in the basal ganglia: computational models of GABAergic mechanisms in basal ganglia function. *Progress in Brain Research* **160** (2007), 313–329.

[Wic93] J. Wickens. A Theory of the Striatum. New York, NY, USA: Elsevier Science Inc., 1993.

[WRL03] A. Williams, P. D. Roberts, and T. K. Leen. Stability of negative-image equilibria in spike-timing-dependent plasticity. *Physical Review E* **68** (Aug. 2003), 021923.

[Yin+09] H. H. Yin, S. P. Mulcare, M. R. F. Hilário, E. Clouse, T. Holloway, M. I. Davis, A. C. Hansson, D. M. Lovinger, and R. M. Costa. Dynamic reorganization of striatal circuits during the acquisition and consolidation of a skill. *Nature Neuroscience* **12** (Mar. 2009), 333–341.

[YK06] H. H. Yin and B. J. Knowlton. The role of the basal ganglia in habit formation. *Nature Reviews. Neuroscience* **7** (June 2006), 464–476.

[ZD07] Q. Zou and A. Destexhe. Kinetic models of spike-timing dependent plasticity and their functional consequences in detecting correlations. *Biological Cybernetics* **97** (July 2007), 81–97.

[ZR02] R. S. Zucker and W. G. Regehr. Short-term synaptic plasticity. *Annual Review of Physiology* **64** (2002), 355–405.

Contributions

*

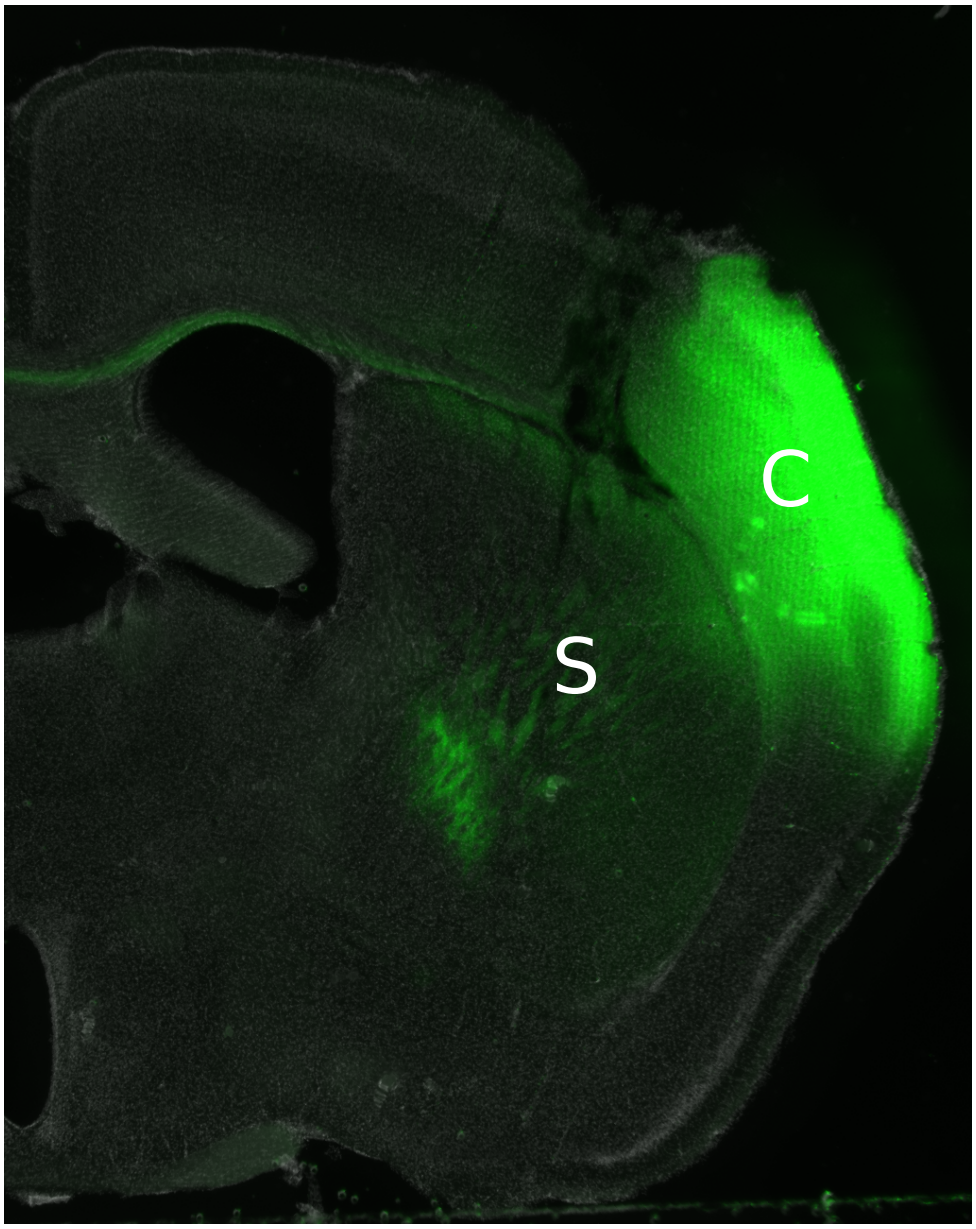

Corticostriatal projection from secondary somatosensory cortex to striatum. Axio Zoom image of sensory cortical axon terminals expressing ChR2-YFP in the striatum [E. Perrin].

This PhD is the result of an interdisciplinary collaboration between mathematics and neuroscience, where I have been working under the supervision of

— Dr Philippe Robert, in the MAMBA (Modelling and Analysis for Medical and Biological Applications) team from INRIA Paris;

— Dr Laurent Venance, in the DPRN (Dynamic and Pathophysiology of Neuronal Networks) team, in the CIRB (Center for Interdisciplinary Research in Biology) at Collège de France, Paris.

This work is built on experimental results, mainly the expression of anti-Hebbian STDP at corticostriatal synapses, observed in Laurent Venance's team. During my PhD, I have developed two main applications of this synaptic plasticity rule in neuronal networks models.

This report is divided in two parts, in order to present the different paths that I have pursued:

— **Part A** starts by studying STDP in stochastic neuronal networks, detailing a rigorous framework in which we have applied stochastic theory to synaptic plasticity. This line of research led to five articles: three published [RV21b; RV21c; RV21a], one submitted [RV22b] and one in last stages of redaction [RV22a]. In these five papers, the work was equally distributed between myself and my PhD supervisor Dr. Philippe Robert. In more details,

  – Chapter 1: P. Robert and G. Vignoud. Stochastic Models of Neural Plasticity. *SIAM Journal on Applied Mathematics* **81**.5 (Sept. 2021), 1821–1846 (reproduced fully in its published version, with minor orthographic and typographic corrections).

  – Chapter 2: P. Robert and G. Vignoud. Stochastic Models of Neural Synaptic Plasticity: A Scaling Approach. *SIAM Journal on Applied Mathematics* **81**.6 (2021), 2362–2386 (reproduced fully in its published version, with minor orthographic and typographic corrections).

  – Chapter 3: P. Robert and G. Vignoud. Averaging Principles for Markovian Models of Plasticity. *Journal of Statistical Physics* **183**.3 (June 2021), 47–90 (reproduced fully in its published version, with minor orthographic and typographic corrections).

  – Chapter 4: P. Robert and G. Vignoud. On the Spontaneous Dynamics of Synaptic Weights in Stochastic STDP Models. *revisions at Physical Review E* (2022) (reproduced in its current version, in review in PRE).

  – Chapter 5: P. Robert and G. Vignoud. A Markovian approach to Hawkes processes. In writing. 2022 (reproduced in its current version).

— **Part B** will implement anti-Hebbian STDP in simple models of the striatum, using computer simulations to study the influence of synaptic plasticity on different learning tasks. For this part, I have been directed, from the computational neuroscience side, by Pr. Jonathan Touboul (Brandeis University) and was partly funded by a Fulbright grant to work at Brandeis University for a five months period. Two articles emerged from these projects, the first has been accepted [Per+22] and the second in last writing stages [VTV22]. In both papers, I have designed the model,

the task, done the simulations, analyzed the results and written the paper under the tight supervision of Pr. Jonathan Touboul and my second PhD advisor Dr. Laurent Venance.

- Chapter 1: G. Vignoud et al. A synaptic theory for sequence learning in the striatum. Preprint. 2022 (reproduced in its current version).
- Chapter 2: S. Perez et al. Striatum expresses region-specific plasticity consistent with distinct memory abilities. *Cell Reports* **38**.11 (2022), 110521 (reproduced partially, with a general presentation of the experimental results, and my specific contribution in full). In this paper, the model is used to draw conclusion on the respective roles of different types of plasticity, studied in their full extent in the associated paper [Per+22], by my colleagues from Dr. Laurent Venance team.

Both lines of works were based on the same experimental mechanisms, but the collaboration between them did not end there. Indeed, the composition of a rigorous setting for synaptic plasticity in stochastic neuronal networks was enriched by several biologically plausible properties, after lengthy discussions with my advisors. Similarly, the analysis of synaptic weights dynamics in computational models of the striatum was greatly helped by theoretical results obtained in the stochastic framework. As a conclusion, although, both projects have been built together, and have influenced each other over the course of my PhD, I present them separately here, for clarity.

Stochastic neural networks and synaptic plasticity

If numerous models of neuronal cells have been proposed in the mathematical literature, few of them include a variable for the time-varying strength of the connection between two neurons. We introduce a general, mathematical framework to study synaptic plasticity. We develop and use this formalism in a serie of four articles, that I will detail sequentially.

In **Chapter A.1** [RV21b], we investigate a system composed of two neurons connected by a single synapse, and a stochastic process describing its dynamical behavior is presented and analyzed. The notion of *plasticity kernel* is introduced as a key component of plastic neuronal networks models, generalizing a notion used for pair-based models. We show that most STDP rules from computational neuroscience can be represented by this formalism. An important subclass of plasticity kernels, where cellular processes such as the neuronal membrane potential and the concentrations of chemical components have Markovian dynamics, is defined and investigated.

After having defined the general formalism needed to study STDP, we apply a slow-fast analysis to the dynamics of the associated neuronal network. This work is presented in **Chapter A.2** [RV21c]. In this chapter we develop and investigate a scaling approach of these models based on several biological assumptions. Experiments show that long-term synaptic plasticity evolves on a slower timescale than the cellular mechanisms driving the activity of neuronal cells. For this reason, a scaled version of the stochastic model is introduced, and an averaging principle is stated for a subclass of Markovian plasticity kernels. These averaging principles are used to study two important STDP models, *pair-based rules* and *calcium-based rules*, and are compared with the approximations of STDP models from computational neuroscience. Discrete

models of STDP rules are also investigated for the analytical tractability of their limiting dynamical system.

The proof of the averaging principle is developed in **Chapter A.3** [RV21a]. We consider a stochastic system with two connected nodes, whose unidirectional connection is variable and depends on point processes associated to each node, that represent the simple neuronal network defined before. We study the scaling regime when the rate of both point processes is large compared to the evolution of the connection. The central result of this chapter is the averaging principle for the connection dynamics. Mathematically, the key variable is the point process, associated to the output node, whose intensity depends on the past activity of the system. The proof rests on a detailed analysis of several of its unbounded additive functionals in the slow-fast limit, and technical results on interacting shot-noise processes.

In **Chapter A.4** [RV22b], we apply the timescale separation (consequence of [RV21c; RV21a]) to derive the long-time limits of a single synaptic weight subject to pair-based STDP. We show, using theoretical arguments and computer simulations, that the pairing scheme (choice of presynaptic and postsynaptic spikes to consider) controls the synaptic weight dynamics for small external input on an excitatory synapse. This result implies in particular that mean-field analysis of plasticity may miss some important properties of STDP. Anti-Hebbian STDP favors the emergence of a stable connection. In the case of an inhibitory synapse the pairing schemes matter less, and we observe convergence of the synaptic weight to a stable value only for Hebbian STDP. We study different asymptotic regimes for STDP rules, raising interesting questions for future works on adaptative neural networks and, more generally, on adaptative systems.

All previous chapters have highlighted the importance of stationary distributions of neuronal dynamics with constant synaptic weights. Considering that a neuron can be modeled as an auto-exciting process, we have developed an interest in the study of stationary Hawkes processes. In **Chapter A.5** [RV22a], we develop a new formalism for Hawkes process, where we prove that the sequence of jump timings can be seen as a Markovian chain on the space of positive real sequences. In addition, we study the transient behavior in details the case where each jump induces an exponential influence on the Hawkes intensity. Under this hypothesis, the system is described by a simpler Markov chain, and we prove several estimations on this type of Hawkes process, using Markovian theory, either for stationary or transient processes.

STDP in the striatum: implications on learning and memory

One of the focuses of this PhD was to build a simplified model of the striatum, with anti-Hebbian STDP and reward signaling, and thus investigate the impact of anti-hebbian forms of STDP on learning and memory. In particular, I have developed a simple numerical model of the striatum, integrating cortical spiking inputs to study the role of anti-Hebbian STDP in learning. I have tested this network on two different tasks, which I will present in this part.

In **Chapter B.1** [VTV22], we study the influence of anti-Hebbian STDP on a specific task, related to the striatum prominent role in procedural learning. Sequences of cortical spikes are presented to the striatal output neurons (MSN) and combined information from the output, reward and timing between the different spikes modify the intensity of each connection, through two mechanisms: anti-Hebbian STDP and reward signaling. The network learning capacity is measured by a score, based on

the prediction of rewarded and nonrewarded patterns. The learning dynamics and efficiency are compared between different settings (number of neurons, intensity of the plasticity, types of STDP, tolerance to random noise). Two important properties of the striatal networks, spiking latency and collateral inhibition have subsequently been added to the model and lead to an improvement of the global accuracy. In conclusion, we show that anti-Hebbian STDP favors the learning of complete sequence of spikes, such as is needed in the striatum, whereas, even if Hebbian STDP helps to correlate the spiking of two connected neurons, it is not sufficient to integrate long sequences of correlated input spikes.

Finally, in **Chapter B.2** [Per+22], I present a project where I have directly collaborated with experimentalists. Electrophysiological and behavioral experiments were performed to study the different properties of two regions of the striatum, who mediate different types of learning: goal-directed behavior in DMS and habits in DLS. We show that symmetric and asymmetric anti-Hebbian STDP exist in DMS and DLS, respectively, with opposite plasticity dominance upon increasing corticostriatal activity. In this chapter, I use the mathematical model, defined in Chapter B.1 to study the computational properties of these STDP rules in procedural learning. We developed a complex task, composed by a learning phase, followed by a period of random activity, and finally a relearning phase in order to investigate the influence of STDP on the maintenance of learned patterns. We found that symmetric anti-Hebbian STDP favored memory flexibility by allowing a rapid forgetting of patterns, while asymmetric anti-Hebbian STDP contributed to memory maintenance, consistent with memory processes at play in procedural learning.

Other PhD works, not presented in this document

During the course of my PhD, I have also been involved in several projects of data analysis, through local collaborations in Laurent Venance's team. These projects, which helped me to gain experience while closely working with experimentalists, are not reported in the main document, as they are not directly linked with my PhD subject. In the following section, I will shortly present four of those works to give a complete overview of my PhD.

First, using experimental data from the lab, I have developed a tool to discriminate between direct- and indirect-pathway MSNs using electrophysiological properties. I have first developed an algorithm to compute all interesting properties from AP (action potential) protocols, then I have trained several machine learning techniques to correctly classify both types of neurons. In particular, I have shown that using the combination of two algorithms leads to a good performance in the classification task. This work was presented at an international conference [Vig+19], and has been subsequently used in the lab by experimentalists to identify neurons, without having to use genetically-modified mouse lines.

In the second half of my PhD, I have also worked with Pr. Bertrand Degos (a neurologist that works part-time in Laurent Venance's team), and two of his interns on quantitatively measuring parkinsonian symptoms from videos. Bradykinesia is defined as a motor slowness and is associated with a decrease of the amplitude and speed of movement. As a key parkinsonian feature, it is currently assessed by the MDS-UPDRS score, a subjective protocol that lacks reproducibility and makes follow-up challenging. Using deep learning, we developed a tool to compute an objective score

of bradykinesia. A large database of videos showing parkinsonian patients performing MDS-UPDRS protocols has been acquired in a Movement Disorder unit, and several deep learning algorithms, including DeepLabCut [Mat+18], were applied to detect a 2D skeleton of the hand composed of 21 points, and transpose it into a 3D representation. A two- and three-dimensional semi-automated analysis tool was then developed to study the evolution of several key parameters during the protocol repetitions. This tool was presented at several medical conferences [Des+20], and a paper is currently being written. Both interns that have worked on this project, C. Desjardins and Q. Salardaine have received the APinnov 2021 Trophy.

Using the same deep learning network, DeepLabCut [Mat+18], I have developed, in the lab, a process to follow different points of interest in videos where mice are subject to behavioral experiments. In particular, I was involved in a project with S. Valverde on the Engrailed-1 homoprotein [Pez+22]. Engrailed-1 is a homeoprotein transcription factor able to transfer between cells and to regulate transcription, translation and chromatin epigenetic status. The goal here is to develop En1 as a therapeutic homeoprotein in a Parkinson's Disease mouse model by virally addressing it to mesencephalic dopaminergic neurons of the SNc and test if it exerts a long-lasting epigenetic protection and has pro-survival activity. By overexpressing En1 in the SNc following the local and unilateral injection of an AAV virus, we wanted to test En1's ability to protect dopaminergic neurons from degeneration by looking at rotational behavior amplified by amphetamine sensitization. Using DeepLabCut, we were able to automatically compute the number of turns, and the distance on which the mice had run.

Finally, I have supervised two interns, C. Richard and G. Yasmine-Degobert, who have worked on the influence of feedforward inhibition in a computational model of the striatal network. Results from both internships have highlighted the role of inhibition in the striatum, and its differential influence in DMS and DLS. A general model of the striatum, based on these works and on the results obtained during my PhD on the influence of STDP, is currently in formation, and will tackle several interesting issues about procedural learning in the basal ganglia.

Previous publications

[Men+20] A. Mendes, G. Vignoud, S. Perez, E. Perrin, J. Touboul, and L. Venance. Concurrent Thalamostriatal and Corticostriatal Spike-Timing-Dependent Plasticity and Heterosynaptic Interactions Shape Striatal Plasticity Map. *Cerebral Cortex (New York, N.Y.: 1991)* **30** (June 2020), 4381–4401.

[Mes+19] T. Mesnard, G. Vignoud, J. Sacramento, W. Senn, and Y. Bengio. Ghost Units Yield Biologically Plausible Backprop in Deep Neural Networks. 2019. arXiv: `1911.08585 [q-bio.NC]`.

[Mor+19] T. Morera-Herreras, Y. Gioanni, S. Perez, G. Vignoud, and L. Venance. Environmental enrichment shapes striatal spike-timing-dependent plasticity in vivo. *Scientific Reports* **9** (Dec. 2019), 19451.

[Si+19] G. Si, J. K. Kanwal, Y. Hu, C. J. Tabone, J. Baron, M. Berck, G. Vignoud, and A. D. Samuel. Structured Odorant Response Patterns across a Complete Olfactory Receptor Neuron Population. *Neuron* **101** (2019), 950–962.e7.

[VVT18] G. Vignoud, L. Venance, and J. D. Touboul. Interplay of multiple pathways and activity-dependent rules in STDP. *PLoS computational biology* **14** (2018), e1006184.

PhD publications (in this report)

[Per+22] S. Perez, Y. Cui, G. Vignoud, E. Perrin, A. Mendes, Z. Zheng, J. Touboul, and L. Venance. Striatum expresses region-specific plasticity consistent with distinct memory abilities. *Cell Reports* **38** (2022), 110521.

[RV21a] P. Robert and G. Vignoud. Averaging Principles for Markovian Models of Plasticity. *Journal of Statistical Physics* **183** (June 2021), 47–90.

[RV21b] P. Robert and G. Vignoud. Stochastic Models of Neural Plasticity. *SIAM Journal on Applied Mathematics* **81** (Sept. 2021), 1821–1846.

[RV22a] P. Robert and G. Vignoud. A Markovian approach to Hawkes processes. In writing. 2022.

[RV22b] P. Robert and G. Vignoud. On the Spontaneous Dynamics of Synaptic Weights in Stochastic STDP Models. *revisions at Physical Review E* (2022).

[VTV22] G. Vignoud, J. Touboul, and L. Venance. A synaptic theory for sequence learning in the striatum. Preprint. 2022.

PhD publications (not in this report)

[Des+20] C. Desjardins, Q. Salardaine, G. Vignoud, and B. Degos. Movement disorders analysis using a deep learning approach. *Movement Disorders*. Vol. 35. 2020.

[Vig+19] G. Vignoud, S. Perez, E. Perrin, C. Piette, A. Mendes, and L. Venance. D1/D2 detection from action-potential properties using machine learning approach in the dorsal striatum. *International Basal Ganglia Society Meeting (IBAGS)*. 2019.

FIRST PART

Stochastic neural networks and synaptic plasticity

CONTENTS

The following document will be decomposed as follows: a general introduction, a general presentation of my contributions, wo parts gathering a total of seven different chapters, each chapter corresponding to a publication, and a discussion. Each chapter will contain its own appendix and a local bibliography.

CHAPTER 1

STOCHASTIC MODELS OF NEURAL SYNAPTIC PLASTICITY

ABSTRACT

In neuroscience, learning and memory are usually associated to long-term changes of neuronal connectivity. In this context, *synaptic plasticity* refers to the set of mechanisms driving the dynamics of neuronal connections, called *synapses* and represented by a scalar value, the *synaptic weight*. Spike-Timing Dependent Plasticity (STDP) is a biologically-based model representing the time evolution of the synaptic weight as a functional of the past spiking activity of adjacent neurons.

If numerous models of neuronal cells have been proposed in the mathematical literature, few of them include a variable for the time-varying strength of the connection. A new, general, mathematical framework is introduced to study synaptic plasticity associated to different STDP rules. The system composed of two neurons connected by a single synapse is investigated and a stochastic process describing its dynamical behavior is presented and analyzed. The notion of *plasticity kernel* is introduced as a key component of plastic neural networks models, generalizing a notion used for pair-based models. We show that a large number of STDP rules from neuroscience and physics can be represented by this formalism. Several aspects of these models are discussed and compared to canonical models of computational neuroscience. An important sub-class of plasticity kernels with a Markovian formulation is also defined and investigated. In these models, the time evolution of cellular processes such as the neuronal membrane potential and the concentrations of chemical components created/suppressed by spiking activity has the Markov property.

1.1 Introduction

Central nervous systems, as the brain, are the main substrate for memory and learning, two essential concepts in the understanding of behavior.

It is widely accepted that neurons constitute the main relay for information in complex neural networks composing the brain. This multi-scale system, ranging from single neuronal cells to complex brain areas, is known to be the basis of memory consolidation, i.e. the transformation of a temporary information into a long-lasting stable memory. The memory trace, or *engram*, is the focus of studies in neuroscience, see [TMK18] for example. Biological, computational and mathematical models are developed to understand mechanisms by which an *engram* emerges during learning, maintains itself, and evolves with time.

Synapses are the key components for the transmission of information between connected neurons, and accordingly, it is assumed that the encoding of memory is integrated in the intensity of these connections. From a biological point of view, a synapse is a structure, located at the junction of two neurons, where the transmission of chemical/electrical signals is possible. A neuronal connection is unidirectional in the sense that the signal goes from an input neuron, called the *pre-synaptic neuron*, to the output one, *the post-synaptic neuron*. The intensity of the connection is referred to as the *synaptic efficacy/strength* and is represented by a scalar variable, the *synaptic weight*

W. The impact of an input signal, a *spike*, from the pre-synaptic neuron is modeled as a jump of the *membrane potential* X of the post-synaptic neuron. The amplitude of this jump is used to quantify the synaptic weight.

A synaptic plasticity mechanism is defined as a collection of activity-dependent cellular processes that modifies the synaptic connectivity. During learning, specific patterns of neural activity may elicit short, from milliseconds to seconds, and/or long, from minutes to hours, -term changes in the associated synaptic weights. In this context, it is conjectured that memory is directly associated to synaptic plasticity, see [TDM14].

The state of a neuronal cell

In this paper we will investigate stochastic models of the dynamic of the synaptic weight of a connection from a pre-synaptic neuron to a post-synaptic neuron.

The post-synaptic neuron is represented by its membrane potential X which is a key parameter to describe its current activity. In neuroscience numerous models of an individual neuronal cell and neuronal networks have been used to investigate learning abilities and plasticity. See [Ger+14] for a review.

The *leaky-integrate-and-fire model* describes the time evolution of the membrane potential as a resistor-capacitor circuit with a constant leaking mechanism. Due to different input currents, the membrane potential of a neuron may rise until it reaches some threshold after which a spike is emitted and transferred to the synapses of neighboring cells. A large class of neural models based on this hypothesis has been developed, see [Ger+14] and references within.

To take into account the important fluctuations within cells, due to the spiking activity and thermal noise in particular, a random component in the cell dynamics has to be included in mathematical models describing the membrane potential evolution. For several models this random component is represented as an independent additive diffusion component, like Brownian motion, of the membrane potential.

In our approach, the random component is at the level of the generation of spikes. When the value of the membrane potential of the output neuron is at $X{=}x$, a spike occurs at rate $\beta(x)$ where β is the *activation function*. See [Chi01] for a discussion. In particular the instants when the output neuron spikes are represented by an inhomogeneous Poisson process. Considering a constant synaptic weight W, the time evolution of the post-synaptic membrane potential $(X(t))$ is represented by the following stochastic differential equation (SDE):

$$\mathrm{d}X(t) = -\frac{1}{\tau}X(t)\,\mathrm{d}t + W\mathcal{N}_\lambda(\mathrm{d}t) - g\left(X(t-)\right)\mathcal{N}_{\beta,X}(\mathrm{d}t), \tag{1.1}$$

where $X(t-)$ is the left limit of X at $t{>}0$:

— τ is the exponential decay time constant of the membrane potential associated to the leaking mechanism.

— The sequence of firing instants of the pre-synaptic neuron is represented by a Poisson point process $\mathcal{N}_\lambda$ on $\mathbb{R}_+$ with rate λ. At each pre-synaptic spike, the membrane potential X is increased by the amount W.

— The sequence of firing instants of the post-synaptic neuron is an inhomogeneous Poisson point process $\mathcal{N}_{\beta,X}$ on $\mathbb{R}_+$ whose rate function is given by $(\beta(X(t-)))$.

— The drop of potential due to a post-synaptic spike is represented by the function g, i.e. after a post-synaptic spike, the membrane potential is reset to $X(t-)-g(X(t-))$.

Considering that the point process $\mathcal{N}_{\beta,X}$ depends on $(X(t))$, Relation (1.1) can be seen as a fixed point equation.

Synaptic plasticity

Synaptic plasticity refers to different mechanisms that leads to the modification of the synaptic weight. Consequently, we need to consider a time varying version of the synaptic strength $W(t)$. Although synaptic plasticity is a complex mechanism, general principles have been inferred from experimental data and previous modeling studies. One of the founding principles is Hebb's postulate (1949), later on summarized by [Sha92] as, "*Cells that fire together wire together*".

Synaptic *potentiation*, resp. *depression*, is associated to an increase, resp. a decrease, of the synaptic strength. Plasticity is described as a set of mechanisms controlling the potentiation and the depression of synapses. It usually depends on the pre-synaptic and post-synaptic signaling, i.e. of past instants of pre-synaptic and post-synaptic spikes. In the literature this class of mechanisms are referred to as *Spike-Timing Dependent Plasticity* (STDP). Several experimental protocols have been developed to elicit STDP at synapses: sequences of spikes pairing from either side of a specific synapse are presented, at a certain frequency and with a certain delay. Occurrence, magnitude and polarity of STDP have been shown to depend on protocols used in experiments: frequency, number of pairings, types of synapses where it is applied, the neuronal sub-population, brain area, just to cite a few key parameters, see [Fel12].

We now introduce two important classes of synaptic plasticity mechanisms. Most models of the literature belong to, or are a variation of, one of these two classes.

a. *Pair-based models.*
Each pair $t=(t_{\rm pre}, t_{\rm post})$ of instants of pre-synaptic and post-synaptic spikes is associated to an increment ΔW of the synaptic weight at time $\max(t_{\rm pre}, t_{\rm post})$,

$$\Delta W = \Phi(\Delta t), \tag{1.2}$$

where $\Delta t \overset{\text{def.}}{=} t_{\rm post} - t_{\rm pre}$ and Φ is the some function on $\mathbb{R}$, the *STDP curve*. The function Φ, usually taken from experimental data, is sharply decreasing to 0 as Δt goes to infinity, so that distant spikes have a negligible contribution.

Many variants and extensions of pair-based models have been developed over the years to fit with experimental results. Triplets-rules, described in Sections 1.A and 1.A, add a dependency between spikes of the same neuronal cell. Additional examples can be found in [BA16].

b. *Calcium-based models.*
Another class of models infers from explicit biological mechanisms the shape of the STDP curve. Post-synaptic calcium traces have been found experimentally to be critical in the establishment of plasticity, see [Fel12] and references therein. In a classical model, when the calcium concentration $C_{\rm ca}$ in the post-synaptic neuron

reaches some specific threshold, STDP is induced accordingly. The analogue of Relation (1.2) for calcium-based STDP rules is,

$$\mathrm{d}W(t) = F(C_{\mathrm{ca}}(t))\,\mathrm{d}t, \tag{1.3}$$

for some function F. The dynamics of C_{ca} is only driven by instants of pre- and post-synaptic spikes. Consequently, the dependence of plasticity on the instants of spikes is not expressed directly as in pair-based models, but through some intermediate biological variable. Several biophysical models are based on this calcium hypothesis, see [GB10] for a review.

It should be noted that there are other STDP models, such as the ones based on exponential filtered traces of the membrane potential, see [CG10]. Pair-based and calcium-based models are nevertheless the most widely used STDP rules in large-scale plastic neural networks.

Models of plasticity in the literature

To understand how synaptic plasticity may shape the brain, the study of STDP in neural networks has attracted a lot of interest in different domains:

a. *Experiments*, with measurements of a large variety of STDP rules.

b. *Computational models*, for numerical simulations of these protocols with several populations of neuronal cells.

c. *Mathematical models*, to investigate the qualitative properties of STDP rules.

Many computational models have been developed to investigate STDP rules in different contexts. See [KGH99] and [MAD07] and the references therein.

Mathematical studies of models of plasticity are quite scarce. Most models are centered on evolution equations of neural networks with a fixed synaptic weight. See Sections 1 and 2 of [RT16] for a review. [Hel18] investigates a Markovian model of a Nearest Neighbor Symmetric Model STDP rule. See Section 1.2. This is one of the few stochastic analyses in this domain.

Contributions

A mathematical model of plasticity describing a pre- and a post-synaptic neuron should include the spiking mechanisms of the two neuronal cells. It is given by the time evolution of the membrane potential X of the post-synaptic cell, as described by Equation (1.1). It must also include the dynamics of plasticity of the type (1.2) or (1.3) for the time evolution of the synaptic weight W.

The difficulty lies in the complex dependence of the evolution of W with respect to the instants of spikes of both cells, the processes $\mathcal{N}_\lambda$ and $\mathcal{N}_{\beta,X}$ of Equation (1.1). For pair-based models for example, this is a functional of all pairs of instants of both processes. In general, there does not exist a simple Markovian model to describe the membrane potential dynamics and the evolution of the synaptic weight.

In Section 1.2, we introduce the notion of *plasticity kernel* which describes in a general way how the spiking activity is taken into account in the synaptic weight dynamics

as a functional of the point processes $\mathcal{N}_\lambda$ and $\mathcal{N}_{\beta,X}$. A differential system associated to the dynamics of the variables X and W is presented. Under mild conditions, it is proved that it has a unique solution for a given initial state. It is, to the best of our knowledge, the first attempt to have a general mathematical framework that describes most STDP rules of the literature. A large set of examples is presented in Section 1.2 and Section 1.A: most STDP models of [MDG08; GB10; Clo+10; BA16] can be represented within this formalism. Section 1.C gives a graphical representation of several STDP rules, see Figures 1.3 and 1.4.

Section 1.3 is devoted to an important sub-class of STDP rules, *plasticity kernels of class* $\mathcal{M}$. These kernels have a representation in terms of a finite dimensional process whose coordinates can be interpreted as concentrations of chemical components created/suppressed by spiking activity. If a classical Markovian analysis of the associated stochastic processes is not really possible, their main advantage is that one can formulate a tractable model with two timescales, when the cellular dynamics are "fast". This approach is developed in the follow-up paper [RV21c]. For these models, when the synaptic weight is fixed, the fast stochastic processes have the Markov property. Section 1.3 discusses these aspects and several examples are presented in Section 1.D. Finally in Section 1.4, a discrete formulation of the stochastic system is defined and its fast processes invariant distribution is analyzed. The case of a calcium-based model is analyzed. Section 1.B discusses modeling issues on the incorporation of plasticity: via a time-smoothing kernel, as we do in the paper, or directly with an instantaneous information.

STDP in recurrent neural networks

In this paper, we consider only two neurons (the pre-synaptic neuron and the post-synaptic) that are connected by a single synapse. As it will be seen, a large variety of models have been used in the literature to describe the time evolution of a synaptic weight. Our goal is to propose a general, basic, mathematical framework where most of these models of plasticity can be investigated. The dynamics of the synaptic weight $(W(t))$ depends in an intricate way on the point process $\mathcal{N}_\lambda$ for pre-synaptic spikes and $\mathcal{N}_{\beta,X}$ for post-synaptic spikes.

For a neural network whose nodes are the vertices of a graph $\mathcal{G}$, an extension of this model would be as follows: the membrane potential process $(X_i(t))$ of node $i\in\mathcal{G}$ should satisfy the SDE,

$$\mathrm{d}X_i(t) = -\frac{1}{\tau}X_i(t)\,\mathrm{d}t + \sum_{j\to i} W_{j,i}(t-)\mathcal{N}_{\beta,X_j}(\mathrm{d}t) - g(X_i(t-))\mathcal{N}_{\beta,X_i}(\mathrm{d}t),$$

where $j\to i$ indicates that there is a synapse (j,i), from node j to node i, and $(W_{j,i}(t))$ is the corresponding process for the synaptic weight. The associated differential quantity $W(t-)\mathcal{N}_\lambda(\mathrm{d}t)$ for instants of pre-synaptic of the synapse (j,i) is given by

$$W_{j,i}(t-)\mathcal{N}_{\beta,X_j}(\mathrm{d}t).$$

Each synaptic weight $(W_{j,i}(t))$ will be subject to synaptic plasticity, with defined plasticity kernels $\Gamma_{p,i}$ and $\Gamma_{d,i}$ that can be different. For synaptic weight $(W_{j,i}(t))$, we will define $\mathcal{N}_{\beta,X_j}$ as the Poisson process representing the pre-synaptic neuron and similarly, $\mathcal{N}_{\beta,X_i}$ for the post-synaptic neuron.

The models and some results of our paper can be extended to the multidimensional case, in particular the existence and uniqueness result, Theorem 4. For simplicity and because of its importance as a generic model, we will restrict ourselves to the case of a network with two-nodes.

1.2 Models of neural plasticity

We consider two neurons connected by one *synapse*. A synapse is a unidirectional connection from the *input neuron* to the *output neuron* allowing the transmission of 'information'. When the input, or *pre-synaptic*, neuron spikes, some neurotransmitters are released at the level of the synapse, where they can interact with the output, or *post-synaptic*, neuron. Following synaptic transmission, a pre-synaptic spike increments the *membrane potential* X of the output neuron by a scalar value, the synaptic weight W.

The dynamics of neural plasticity is described in terms of the time evolution of $(X(t))$ and $(W(t))$. For $t\geqslant 0$,

a. $X(t)\in\mathbb{R}$ is the *membrane potential* of the output neuron at time t. This is the difference between the internal and the external electric potentials of the neuron. The dynamics of the process $(X(t))$ associated to the output neuron is a classical model of neuroscience. See [Ger+14] for a survey.

b. $W(t)\in\mathbb{R}$ represents the intensity of *synaptic transmission* at time t, i.e. the increment of the post-synaptic membrane potential X when the input neuron spikes at time t. The evolution of $(W(t))$ at time $t>0$ depends in general on the total sample path of $((X(s),W(s)),0\leqslant s\leqslant t)$, in an intricate way.

To take into account inhibitory mechanisms, these two variables are real-valued and, consequently, may have negative values. Real synapses have a constant sign: they can be either excitatory (with a non-negative synaptic weight) or inhibitory (with a non-positive synaptic weight). In the following sections, other variables will be added to formalize the evolution equations of $(X(t),W(t))$.

Definitions and notations

Sequences of pre- and post-synaptic spikes play an important role in the study of *spike-timing dependent* plasticity. Mathematically, it is convenient to describe them in terms of *point processes*. See [Daw93] for general definitions and results on point processes.

We denote by $\mathcal{M}_+(\mathbb{R}_+^d)$ the set of positive Radon measures on $\mathbb{R}_+^d$, i.e. with finite values on any compact subset of $\mathbb{R}_+^d$. A point measure on $\mathbb{R}_+^d$, $d\geqslant 1$, is an integer-valued Borelian positive measure on $\mathbb{R}_+^d$ which is Radon. A point measure is carried by a subset of $\mathbb{R}_+^d$ which is at most countable and without any finite limiting point. The set of point measures on $\mathbb{R}_+^d$ is denoted by $\mathcal{M}_p(\mathbb{R}_+^d)\subset\mathcal{M}_+(\mathbb{R}_+^d)$, it is endowed with the natural weak topology of $\mathcal{M}_+(\mathbb{R}_+^d)$ and its corresponding Borelian σ-field.

If $m\in\mathcal{M}_p(\mathbb{R}_+^d)$ and $A\in\mathcal{B}(\mathbb{R}_+^d)$ is a Borelian subset of $\mathbb{R}_+^d$, then $m(A)$ denotes the number of points of m in A, i.e.

$$m(A)=\int_{\mathbb{R}_+^d}\mathbb{1}_A(x)\,m(\mathrm{d}x).$$

A point process on $\mathbb{R}_+^d$ is a probability distribution on $\mathcal{M}_p(\mathbb{R}_+^d)$. Two independent Poisson point processes are assumed to be defined on a filtered probability space $(\Omega, \mathcal{F}, (\mathcal{F}_t), \mathbb{P})$, see [Kin92]:

a. A point process $\mathcal{N}_\lambda$ on $\mathbb{R}_+$ to represent the instants of pre-synaptic spikes is assumed to be Poisson with rate $\lambda>0$, $(t_{\mathrm{pre},n})$ is the increasing sequence of its jumps, i.e.

$$\mathcal{N}_\lambda = \sum_{n\geqslant 1} \delta_{t_{\mathrm{pre},n}}, \text{ with } 0\leqslant t_{\mathrm{pre},1}\leqslant t_{\mathrm{pre},2} \leqslant \cdots \leqslant t_{\mathrm{pre},n} \leqslant \cdots,$$

where δ_a is the Dirac measure at $a\in\mathbb{R}_+$.

b. A Poisson point process $\mathcal{P}$ on $\mathbb{R}_+^2$ with rate 1. It is used to define the inhomogeneous point process of post-synaptic spikes in Relation (1.5).

The variable t of the point processes $\mathcal{N}_\lambda(\mathrm{d}t)$ and $\mathcal{P}(\mathrm{d}x, \mathrm{d}t)$ is interpreted as the time variable. For $t\geqslant 0$, the σ-field $\mathcal{F}_t$ of the filtration $(\mathcal{F}_t)$ of the probability space is assumed to contain all events before time t for both point processes, i.e.

$$\sigma\left\langle \mathcal{P}_1\left(A\times(s,t]\right), \mathcal{P}_2\left(A\times(s,t]\right), A\in\mathcal{B}\left(\mathbb{R}_+\right), s\leqslant t\right\rangle \subset \mathcal{F}_t. \tag{1.4}$$

A stochastic process $(U(t))$ is *adapted* if, for all $t\geqslant 0$, $U(t)$ is $\mathcal{F}_t$-measurable. It is a *càdlàg process* if, almost surely, it is right continuous and has a left limit at every point $t>0$, $U(t-)$ denotes the left limit of $(U(t))$ at t. The Skorokhod space of càdlàg functions from $[0,T]$ to $\mathcal{S}$ is $\mathcal{D}([0,T],\mathcal{S})$. See [Bil99].

The set of real continuous bounded functions on the metric space $\mathcal{S}\subset\mathbb{R}^d$ is denoted by $\mathcal{C}_b(\mathcal{S})$, and $\mathcal{C}_b^k(\mathcal{S})\subset\mathcal{C}_b(\mathcal{S})$ is the set of bounded, k-differentiable functions on $\mathcal{S}$ with respect to each coordinate, with the respective derivatives bounded and continuous.

We conclude this preliminary section with an elementary but important lemma concerning the *filtering* of a stochastic process with an exponential function.

Lemma 1 (Exponential filtering)**.** *If μ is a non-negative Radon measure on $\mathbb{R}_+$, $\alpha>0$ and $h_0\in\mathbb{R}$, then*

$$H(t) = h_0 e^{-\alpha t} + \int_{(0,t]} e^{-\alpha(t-s)}\mu(\mathrm{d}s)$$

is the unique càdlàg solution of the differential equation,

$$\mathrm{d}H(t) = -\alpha H(t)\,\mathrm{d}t + \mu(\mathrm{d}t),$$

such that $H(0)=h_0$.

This type of process is a central object in mathematical models of neuroscience. It is used to represent *leaky-integrate phenomena* of chemical components within cells. See [Ger+14] for a general review.

The dynamics of the post-synaptic membrane potential

It is represented as a càdlàg stochastic process $(X(t))$ following leaky-integrate dynamics illustrated in Figure 1.1a:

a. It decays exponentially to 0 with a fixed characteristic decay time τ, set without loss of generality to $\tau=1$.

b. It is incremented by the current synaptic weight variable at each firing instant of the input neuron, i.e. at each instant of the Poisson point process $\mathcal{N}_\lambda$.

c. The firing mechanism of the output neuron is driven by a function β from $\mathbb{R}$ to $\mathbb{R}_+$, the activation function. When the membrane potential is x, the output neuron fires at rate $\beta(x)$. This function is usually assumed to be non-decreasing, in other words, the larger the membrane potential is, the more likely the neuron is to spike.

d. After a post-synaptic spike, the neuronal membrane potential X is decreased by the amount $g(x)$, where g is some function on $\mathbb{R}$. In general, the membrane potential is reset to 0 after a spike, i.e. $g(x)=x$, see [RT16]. However, in some cases, the reset potential may not depend on the membrane potential before the spike, g can be constant for example.

Post-synaptic spikes. If the instants of pre-synaptic spikes are represented by the Poisson process $\mathcal{N}_\lambda$, the firing instants of the output neuron $t_{post,n}$ are expressed as the jumps of the point process $\mathcal{N}_{\beta,X}$ on $\mathbb{R}_+$ defined by

$$\int_{\mathbb{R}_+} f(u)\mathcal{N}_{\beta,X}(\mathrm{d}u) \overset{\text{def.}}{=} \int_{\mathbb{R}_+} f(u)\mathcal{P}\left((0,\beta(X(u-))],\mathrm{d}u\right) = \int_{\mathbb{R}_+^2} f(u)\mathbb{1}_{\{s\in(0,\beta(X(u-))]\}}\mathcal{P}(\mathrm{d}s,\mathrm{d}u), \quad (1.5)$$

for any non-negative Borelian function f on $\mathbb{R}_+$.

Classical properties of Poisson processes give that, for $t>0$ and $x\in\mathbb{R}$,

$$\mathbb{P}\left(\mathcal{N}_{\beta,X}(t,t+\mathrm{d}t)\neq 0 \,\middle|\, X(t-)=x\right) = \beta(x)\,\mathrm{d}t + o(\mathrm{d}t),$$

as expected, $\mathcal{N}_{\beta,X}$ is Poisson process with intensity $(\beta(X(t)))$.

The following stochastic differential equation summarizes the description of the time evolution of $(X(t))$ given by a), b), c) and d),

$$\mathrm{d}X(t) = -X(t)\,\mathrm{d}t + W(t-)\mathcal{N}_\lambda(\mathrm{d}t) - g(X(t-))\mathcal{N}_{\beta,X}(\mathrm{d}t).$$

Time evolution of the synaptic weight

In this work, the synaptic weight W will stay in a defined real (not necessarily bounded) interval K_W. For several examples, the plasticity process leads to dynamics for which the process $(W(t))$ stays in K_W for all time t.

— Taking $K_W{=}\mathbb{R}$ leads to free dynamics of the synaptic weight, that can be either negative or positive, change its sign because of the plasticity rules. This situation occurs in models of neural networks where excitatory/inhibitory neurons are not separated in distinct classes..

— If $K_W{=}\mathbb{R}_+$, the synaptic weight is non-negative and plasticity processes cannot change its sign. This is a model for excitatory neurons whose spikes lead to the increase of the post-synaptic membrane potential.

— Conversely, if $K_W{=}\mathbb{R}_-$, the cell is an inhibitory neuron, which has the opposite effect on the post-synaptic membrane potential.

— Finally, K_W can also be bounded in order to represent saturation mechanisms, i.e. the synaptic weights needs to stay in a biological range of value. In that case, potentiation refers to a diminution of the amplitude of the negative jump, whereas depression indicates an augmentation. In experimental works, the denominations are inverted, for the sake of clarity we chose to stay with the previous names.

We can now introduce the notion of *plasticity kernels*.

Definition 2 (Plasticity kernel)**.** *A plasticity kernel is a measurable function*

$$\Gamma\colon \mathcal{M}_p(\mathbb{R}_+)^2 \longrightarrow \mathcal{M}_+(\mathbb{R}_+), \quad (m_1, m_2) \longrightarrow \Gamma(m_1, m_2),$$

$\mathcal{M}_+(\mathbb{R}_+)$ is the set of positive Radon measures on $\mathbb{R}_+$ and, for any $t{>}0$, the functional

$$(m_1, m_2) \longrightarrow \Gamma(m_1, m_2)(\mathrm{d}u \cap [0, t]) \tag{1.6}$$

is $\mathcal{G}_t{\otimes}\mathcal{G}_t$-measurable, where $\mu(\mathrm{d}u{\cap}[0,t])$ denotes the restriction of the Radon measure μ to the interval $[0,t]$ and $(\mathcal{G}_t)$ is the filtration on $\mathcal{M}_p(\mathbb{R}_+)$, such that for $t{\geqslant}0$, $\mathcal{G}_t$ is the σ-field generated by the functionals $m{\to}m((0,s])$, with $s{\leqslant}t$.

If Γ is a plasticity kernel and m_1, $m_2{\in}\mathcal{M}_p(\mathbb{R}_+)$, the measure $\Gamma(m_1,m_2)(\mathrm{d}u{\cap}[0,t])$ depends only on the variables $m_i([0,s])$, for $i{\in}\{1,2\}$ and $s{\leqslant}t$.

In our model, the infinitesimal elements at time t for the update of plasticity are expressed as $\Gamma(\mathcal{N}_\lambda, \mathcal{N}_{\beta,X})(\mathrm{d}t)$ for some plasticity kernel Γ. This quantifies how the interaction between the instants of pre-synaptic and of post-synaptic spikes, $\mathcal{N}_\lambda$ and $\mathcal{N}_{\beta,X}$ leads to specific synaptic changes. For example, the order and timing between instants of pre- and post-synaptic spikes may have an impact on plasticity.

In previous works [SWW10; FSG10; LS14; Fel12], the notion of STDP Temporal Kernels referred to the curve of synaptic weight change ΔW as a function of Δt for pair-based models. [PG06a] introduced more complex kernels, with multi-spikes interactions. The plasticity kernels defined above extend this notion to more general interactions between pre- and post-synaptic spikes.

Plasticity is represented as a process, integrating, with some decay, the past interactions of the spiking activity on either side of the synapse. Two non-negative process are introduced: $(\Omega_p(t))$ and $(\Omega_d(t))$, the first one is associated to potentiation (increase of W) and the other to depression (decrease of W). For $a{\in}\{p,d\}$,

$$\Omega_a(t) = \Omega_a(0)e^{-\alpha t} + \int_{(0,t]} e^{-\alpha(t-s)}\Gamma_a(\mathcal{N}_\lambda, \mathcal{N}_{\beta,X})(\mathrm{d}s), \tag{1.7}$$

where $\alpha>0$ and the variables Γ_p and Γ_d are plasticity kernels associated to potentiation and depression respectively. The process $(\Omega_a(t))$ can be seen as a exponential filtering of the random measure $\Gamma_a(\mathcal{N}_\lambda, \mathcal{N}_{\beta,X})(\mathrm{d}t)$ in the sense of Lemma 1. In Section 1.B of Supplementary Materials, another stochastic model of plasticity with no exponential filtering of the plasticity kernels is introduced and discussed.

As explained in the introduction of this section, the function M need to be chosen so that the synaptic weight W stays at all time in its definition interval K_W. The time evolution of $(W(t))$ depends then on the past activity of the input and output neurons, through $(\Omega_p(t))$ and $(\Omega_d(t))$ and is described by,

$$\frac{\mathrm{d}W(t)}{\mathrm{d}t} = M\left(\Omega_p(t), \Omega_d(t), W(t)\right), \tag{1.8}$$

with, M verifying, for any piecewise-continuous càdlàg functions $(\omega_p(t))$ and $(\omega_d(t))$ on $\mathbb{R}_+$, a solution $(w(t))$ of the ODE

$$\frac{\mathrm{d}w(t)}{\mathrm{d}t} = M(\omega_p(t), \omega_d(t), w(t)),$$

with $w(0)\in K_W$, is such that $w(t)\in K_W$, for all $t\geqslant 0$.

We now give some examples of functions M associated to different synaptic domains K_W. For $K_W=\mathbb{R}$, we can chose the additive implementation of STDP rules, where,

$$M(\omega_p, \omega_d, w) \overset{\text{def.}}{=} M(\omega_p, \omega_d) = \omega_p - \omega_d \tag{1.9}$$

In that case, the dynamics are unbounded and we see the update only depends on the potentiation/depression plasticity variables Ω_a.

If we want to model bounded synaptic weight in $K_W=[A_d, A_p]$, we can consider the function M given by

$$M(\omega_p, \omega_d, w) \overset{\text{def.}}{=} (A_p-w)^n\omega_p-(w-A_d)^n\omega_d - \mu(w - A_r), \quad w\in[A_d, A_p], \tag{1.10}$$

where $A_d\leqslant A_r\leqslant A_p$, and $n>0$. This corresponds to a multiplicative influence of W. See [Güt+03]. It is straightforward to see that in that case, the synaptic weight stays bounded between A_p and A_d for any plasticity processes Ω_a. The expression $-\mu(W(t)-A_r)$ is for the exponential decay of the synaptic weight W to A_r, its resting value. This term represents *homeostatic mechanisms*, i.e. mechanisms that maintain steady internal physical and chemical conditions to allow the functioning of the system. See [TN04].

Finally, an unbounded dynamics for an excitatory synapse, with $K_W=\mathbb{R}_+$ can be enforced by,

$$M(\omega_p, \omega_d, w) \overset{\text{def.}}{=} \omega_p-w\omega_d, \tag{1.11}$$

Examples of plasticity kernels

We show that several important STDP rules of the literature can be expressed with plasticity kernels Γ_p and Γ_d. Further extensions are presented in 1.A and Section 1.A

Pair-based models

For pair-based mechanisms, the synaptic weight is modulated according to the respective timing of pre-synaptic and post-synaptic spikes, as illustrated in Figure 1.1b. This follows the fact that most STDP experimental studies are based on pairing protocols, where pre- and post-synaptic spikes are repeated at a certain frequency for a given number of pairings.

Accordingly, a large class of models have been developed on the principle that the synaptic weight change due to a pair $(t_{\rm pre}, t_{\rm post})$ of instants of pre- and post-synaptic spikes, depends only on $\Delta t{=}t_{\rm post}{-}t_{\rm pre}$. The synaptic update is then taken proportional to $\Phi(\Delta t)$, where Φ is some function converging to 0 at infinity, that is referred to as the *STDP curve*. An example of exponential STDP curves is given in Figure 1.1b (top left). Many pair-based models have been developed over the years, varying mainly which pairs of spikes are taken into account when updating the synaptic weight.

We start with the simplest rule, the *all-to-all* version (following [MDG08] terminology), where all pairs of spikes give an update of the synaptic weight.

All-to-all model

The *all-to-all* scheme consists in updating the synaptic weight at each post-synaptic spike, occurring at time t by the sum over all previous pre-synaptic spikes occurring at time $s{<}t$ of the quantity $\Phi(t{-}s)$. Switching the role of pre- and post-synaptic spikes, the synaptic weight is updated in the same way with other constants. See Figure 1.1b (bottom left) for an example of *all-to-all* interactions.

The plasticity kernels are defined by, for m_1, $m_2{\in}\mathcal{M}_p(\mathbb{R}_+)$ and $a{\in}\{p,d\}$,

$$\Gamma_a^{\rm PA}(m_1,m_2)(\mathrm{d}t) \stackrel{\text{def.}}{=} \left(\int_{(0,t)} \Phi_{a,2}(t{-}s)m_2(\mathrm{d}s)\right) m_1(\mathrm{d}t) + \left(\int_{(0,t)} \Phi_{a,1}(t{-}s)m_1(\mathrm{d}s)\right) m_2(\mathrm{d}t), \quad a{\in}\{p,d\}. \tag{1.12}$$

The functions $\Phi_{a,i}$, $a{\in}\{p,d\}$ and $i{\in}\{1,2\}$ are non-negative and non-increasing functions functions converging to 0 at infinity.

If f is a non-negative Borelian function on $\mathbb{R}_+$, we have

$$\int_{\mathbb{R}_+} f(t)\Gamma_a^{\rm PA}(\mathcal{N}_\lambda,\mathcal{N}_{\beta,X})(\mathrm{d}t) = \sum_{t_{\rm pre}} f(u) \sum_{t_{\rm post}<t_{\rm pre}} \Phi_{a,2}(t_{\rm post}{-}t_{\rm pre}) + \sum_{t_{\rm post}} f(u) \sum_{t_{\rm pre}<t_{\rm post}} \Phi_{a,1}(t_{\rm pre}{-}t_{\rm post}).$$

Remarks.

a. The exponential STDP functions $\Phi(s){=}B\exp(-\gamma s)$, $s{\geqslant}0$, are often used in this context. See [MDG08]. Several studies also consider the case when Φ is a translated exponential kernel. See [LS08].

b. *Hebbian STDP* plasticity is said to occur when

— a pre-post pairing, i.e. $t_{\rm pre}<t_{\rm post}$ leads to potentiation, $\Delta W>0$;

— a post-pre pairing, $t_{\rm post}<t_{\rm pre}$, leads to depression, $\Delta W<0$.

Experiments have shown that this type of plasticity occurs for several populations of neuronal cells [BP98]. Early models can be found in [RBT00a; RLS01; MDG08] for a review.

Following Hebb's postulate, a 'causal' pre-post pairing (a post-synaptic spike occurs after a pre-synaptic one) should lead to potentiation,

$$\Gamma_p^{\rm PAH}(m_1,m_2)(\mathrm{d}t) = \left(\int_{(0,t)} \Phi_{p,1}(t-s)m_1(\mathrm{d}s)\right) m_2(\mathrm{d}t).$$

Conversely, a *post-pre* pairing (anti-causal activation) leads to depression,

$$\Gamma_d^{\rm PAH}(m_1,m_2)(\mathrm{d}t) = \left(\int_{(0,t)} \Phi_{d,2}(t-s)m_2(\mathrm{d}s)\right) m_1(\mathrm{d}t).$$

This corresponds to $\Phi_{p,2}=0$ and $\Phi_{d,1}=0$ in Equation (1.12).

c. Other forms of STDP have been discovered experimentally see [Fel12]. *Anti-Hebbian STDP* models follows the opposite principles: Pre-post pairings lead to depression, and post-pre pairings lead to potentiation. It has also been observed experimentally in the striatum, see [FGV05] for example.

It corresponds to the case where $\Phi_{p,1}=0$ and $\Phi_{d,2}=0$, and symmetric LTD rules to $\Phi_{p,1}=\Phi_{p,2}=0$ and, finally, symmetric LTP by $\Phi_{d,1}=\Phi_{d,2}=0$. This is the motivation of the general setting defined in Equation (1.12).

d. Pre/post-synaptic-only plasticity rules can also be expressed into this formalism. These models include a component to express the direct influence of the pre- or post-synaptic spikes on the plasticity without any interaction between the two spike trains. In that case, the kernel $\Gamma_a^{\rm PA_1}$ would have the following expression, for m_1, $m_2\in\mathcal{M}_p(\mathbb{R}_+)$ and $a\in\{p,d\}$,

$$\begin{aligned}\Gamma_a^{\rm PA_1}(m_1,m_2)(\mathrm{d}t) \overset{\text{def.}}{=} & \left(\int_{(0,t)} \Phi_{a,2}(t-s)m_2(\mathrm{d}s)\right) m_1(\mathrm{d}t) \\ & + \left(\int_{(0,t)} \Phi_{a,1}(t-s)m_1(\mathrm{d}s)\right) m_2(\mathrm{d}t) + D_{a,1}\, m_1(\mathrm{d}t) + D_{a,2}\, m_2(\mathrm{d}t), \quad (1.13)\end{aligned}$$

where the constants $D_{a,i}$, $a\in\{p,d\}$, $i\in\{1,2\}$, are non-negative.

Nearest neighbor symmetric model

In the *nearest neighbor symmetric* model, whenever one neuron spikes, the synaptic weight is updated by only taking into account the last spike of the other neuron, as can be seen in Figure 1.1b (top right). If the pre-synaptic neuron fires at time $t_{\rm pre}$, the contribution to the plasticity kernel is $\Phi_{a,2}(t_{\rm pre}-t_{\rm post})$, where $t_{\rm post}$ is the last post-synaptic spike before $t_{\rm pre}$.

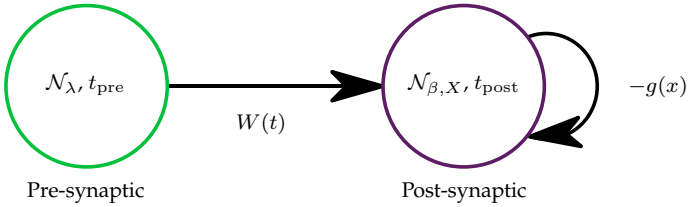

(a) **A simple stochastic model for a synaptic connection.**

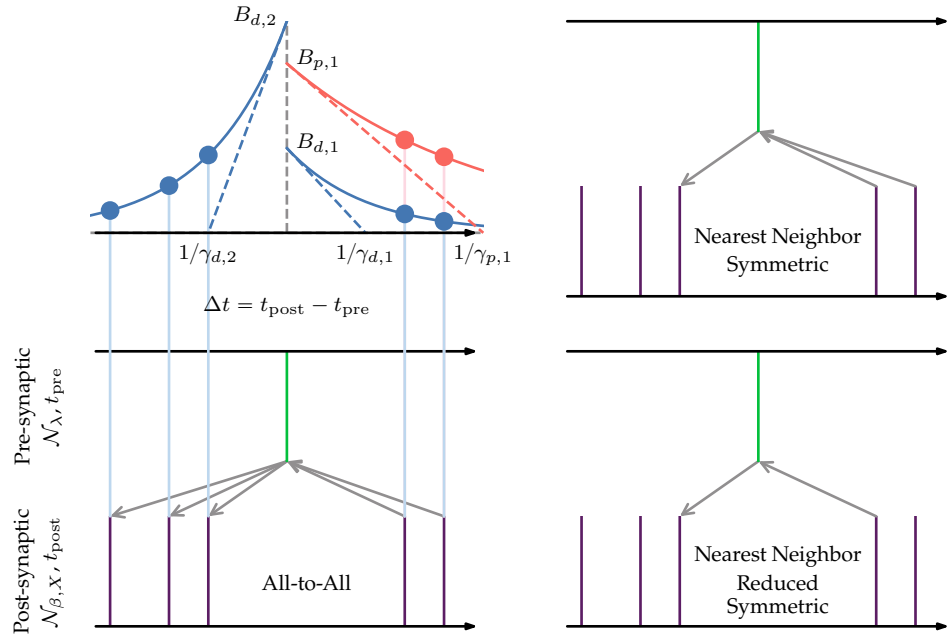

(b) **Synaptic plasticity kernels for pair-based rules.**
(Top left) *STDP curve:* update of the potentiation (in red) and depression (in blue) kernels as a function of $\Delta t{=}t_{\text{post}}{-}t_{\text{pre}}$. Exponential STDP curves of the form $\Phi_{a,i}(\Delta t){=}B_{a,i}\exp(-\gamma_{a,i}\Delta t)$ are used in this example.
(Bottom left) *All-to-all pair-based rules:* all pairings of pre-synaptic (in green) and post-synaptic (in purple) spikes are taken into account for the synaptic updates. Grey arrows indicate the interactions between the different spikes, see the associated updates as a function of the STDP curve above (blue and red points in (Top left)).
(Top right) *Nearest neighbor symmetric pair-based rules:* for each pre-synaptic spike (in green), only the interaction with the previous post-synaptic spike (in purple) is taken into account for the synaptic update, and conversely for post-synaptic spikes. Grey arrows indicate the interactions between the different spikes.
(Bottom right) *Nearest neighbor reduced symmetric pair-based rules:* only consecutive pairings of pre-synaptic (in green) and post-synaptic spikes (in purple) are taken into account for the synaptic update, and conversely for post-synaptic spikes. Grey arrows indicate the interactions between the different spikes.

Figure 1.1: **Stochastic models of STDP.**

The corresponding kernels Γ^{PS} are defined by, for $m_1, m_2{\in}\mathcal{M}_p(\mathbb{R}_+)$ and $a{\in}\{p,d\}$,

$$\Gamma^{\text{PS}}_a(m_1,m_2)(\mathrm{d}t) \stackrel{\text{def.}}{=} \Phi_{a,2}(t_0(m_2,t))\, m_1(\mathrm{d}t){+}\Phi_{a,1}(t_0(m_1,t))\, m_2(\mathrm{d}t), \tag{1.14}$$

with the following definition, for $m{\in}\mathcal{M}_p(\mathbb{R}_+)$ and $t{>}0$,

$$t_0(m,t) = t - \sup\{s : s{<}t, m(\{s\}){\neq}0\}, \tag{1.15}$$

with the convention that $t_0(m,0) = +\infty$. The quantity $t_0(m,t)$ is the delay between t and the last point of m before t.

Nearest neighbor reduced symmetric model

For the *nearest neighbor reduced symmetric*, a pre-synaptic spike at t is paired with the last post-synaptic spike at $s \leqslant t$, only if there are no pre-synaptic spikes in the time interval (s,t), and similarly for post-synaptic spikes. See Figure 1.1b (bottom right).

Accordingly, the kernels Γ^{PR} are defined, for $m_1, m_2 \in \mathcal{M}_p(\mathbb{R}_+)$ and $a \in \{p,d\}$, by

$$\Gamma_a^{\mathrm{PR}}(m_1,m_2)(\mathrm{d}t) \stackrel{\text{def.}}{=} \left(\Phi_{a,2}(t_0(m_2,t))\mathbb{1}_{\{t_0(m_2,t)\leqslant t_0(m_1,t)\}}\right) m_1(\mathrm{d}t) + \left(\Phi_{a,1}(t_0(m_1,t))\mathbb{1}_{\{t_0(m_1,t)\leqslant t_0(m_2,t)\}}\right) m_2(\mathrm{d}t), \quad (1.16)$$

with same notations as in (1.14). For $t>0$, the inequality $t_0(m_2,t)<t_0(m_1,t)$ is equivalent to the relation $m_1((t_0(m_2,t),t))=0$ so that there is a unique point of m_1 paired to $t_0(m_2,t)$ as expected, and similarly by switching m_1 and m_2. The updates of Relation (1.16) are therefore done only for consecutive pre- and post-synaptic spikes.

Calcium-based models

Pair-based models can be characterized as phenomenological models of STDP in the sense that experimental STDP curves are taken as a core parameter of the models. Another important class of synaptic models are derived from biological phenomenons and aims at reproducing experimental STDP curves using simple biological models. A common hypothesis is to use the calcium concentration in the post-synaptic neuron as a key parameter to model STDP, see [SBC02] and [GB12]. Several biophysical models have studied the link between calcium concentration, and its direct implication on the dynamics of plasticity. A calcium-based model with saturation mechanisms has investigated the dependency on the number of pairings and the existence of different mechanisms for plasticity in [VVT18].

For these models, synaptic plasticity is expressed as a functional of the post-synaptic calcium concentration. For $m_1, m_2 \in \mathcal{M}_p(\mathbb{R}_+)$, the points of m_1, resp. m_2, elicit calcium transfers of amplitudes C_1, resp. C_2, followed by an exponential decay with rate γ. If $(C_m(t))$ is the process of the calcium concentration associated to the couple $m=(m_1,m_2)$, it is therefore the solution of the differential equation

$$\mathrm{d}C_m(t) = -\gamma C_m(t)\,\mathrm{d}t + C_1 m_1(\mathrm{d}t) + C_2 m_2(\mathrm{d}t),$$

with some fixed initial condition. By Lemma 1, it can be expressed as

$$C_m(t) \stackrel{\text{def.}}{=} C_m(0)e^{-\gamma t} + C_1 \int_{(0,t]} e^{-\gamma(t-s)} m_1(\mathrm{d}s) + C_2 \int_{(0,t]} e^{-\gamma(t-s)} m_2(\mathrm{d}s). \quad (1.17)$$

The mechanisms for potentiation, resp. depression, are triggered depending on the calcium concentration. For $a \in \{p,d\}$, the plasticity kernel Γ_a^{C} is defined by,

$$\Gamma_a^{\mathrm{C}}(m_1,m_2)(\mathrm{d}t) \stackrel{\text{def.}}{=} h_a(C_m(t))\,\mathrm{d}t, \quad (1.18)$$

for some non-negative function h_a on $\mathbb{R}_+$. The function h_a is usually a threshold function of the type

$$h_a(x) \stackrel{\text{def.}}{=} B_a \mathbb{1}_{\{x \geqslant \theta_a\}}, \quad x \geqslant 0, \quad (1.19)$$

for some $B_a \in \mathbb{R}_+$ and $\theta_a \geqslant 0$, as done in [GB12]. In that case, the process $(\Omega_a(t))$ associated to Γ_a^C has therefore an impact on the synaptic weight as soon as the concentration of calcium is above level θ_a.

Further examples of STDP rules are presented in Section 1.A.

The plasticity process

This section is devoted to the formal definition of the stochastic process describing the time evolution of the synaptic weight.

Definition 3. *The stochastic process* $(X(t), \Omega_p(t), \Omega_d(t), W(t))$ *with the initial state* $(x_0, \omega_{0,p}, \omega_{0,d}, w_0)$*, is the solution in* $\mathcal{D}(\mathbb{R}_+, \mathbb{R}\times\mathbb{R}_+^2 \times K_W)$ *of the SDEs, for* $t>0$*,*

$$\begin{cases} \mathrm{d}X(t) = -X(t)\,\mathrm{d}t + W(t-)\mathcal{N}_\lambda(\mathrm{d}t) - g(X(t-))\mathcal{N}_{\beta,X}(\mathrm{d}t), \\ \mathrm{d}\Omega_a(t) = -\alpha\Omega_a(t)\,\mathrm{d}t + \Gamma_a(\mathcal{N}_\lambda, \mathcal{N}_{\beta,X})(\mathrm{d}t), \quad a\in\{p,d\}, \\ \mathrm{d}W(t) = M\left(\Omega_p(t), \Omega_d(t), W(t)\right)\mathrm{d}t, \end{cases} \tag{1.20}$$

where, Γ_p *and* Γ_d *are plasticity kernels and* $\mathcal{N}_{\beta,X}$ *is the point process defined by Relation* (1.5) *and the function* M *is expressed by Relation* (1.8)*.*

The system (1.20) can be interpreted as fixed point equation for the process $(X(t))$ with an intricate dependence due to the point process $\mathcal{N}_{\beta,X}$ as an argument of the plasticity kernels. Theorem 4 gives an existence and uniqueness result for the solutions of Equations (1.20). We now introduce the main assumptions on the parameters of our model which will be used throughout this paper.

Examples of different dynamics are presented in Section 1.C, for pair-based in Figure 1.3 and calcium-based in Figure 1.4.

Assumptions A

a. Firing rate function.
β is a non-negative, continuous function on $\mathbb{R}$ and $\beta(x)=0$ for $x\leqslant -c_\beta \leqslant 0$.

b. Drop of potential after firing.
g is continuous on $\mathbb{R}$ and $0\leqslant g(x)\leqslant \max(c_g, x)$ holds for all $x\in\mathbb{R}$, for $c_g\geqslant 0$.

c. Dynamic of plasticity.
The function M is such that, for any $w\in K_W$ and any càdlàg piecewise-continuous functions h_1 and h_2 on $\mathbb{R}_+$, the ODE

$$\frac{\mathrm{d}w(t)}{\mathrm{d}t} = M(h_1(t), h_2(t), w(t)) \text{ with } w(0)=w, \tag{1.21}$$

for all points of continuity of h_1 and h_2, has a unique continuous solution $(S[h_1,h_2](w,t))$ in K_W.

Theorem 4. *Under Assumptions A, the system* (1.20) *has a unique càdlàg adapted solution with initial state* $(x_0, \omega_{0,p}, \omega_{d,0}, w_0)$ *in* $\mathbb{R}\times\mathbb{R}_+^2\times K_W$*.*

Proof. The construction is done on the successive intervals between two consecutive instants of jump of the system. The non-decreasing sequence (s_n) of these instants is defined by induction.

The first jump of $(X(t))$ occurs at time s_1 and is defined as the minimum of the first jumps of the processes

$$(\mathcal{N}_\lambda((0,t])) \text{ and } \left(\int_{(0,t]} \mathcal{P}\left(\left(0,\beta\left(x_0e^{-u}\right)\right],\mathrm{d}u\right)\right). \tag{1.22}$$

With Relation (1.21), for $0\leqslant t<s_1$, we set $X(t)=x_0e^{-t}$ and $W(t)=S[\Omega_p^1,\Omega_d^1](w_0,t)$, with

$$\Omega_a^1(t) \stackrel{\text{def.}}{=} \omega_{0,a}+\int_{(0,t)} e^{-\alpha(t-s)}\Gamma_a(\underline{0},\underline{0})(\mathrm{d}s), \quad a\in\{p,d\},$$

and $W(s_1)=W(s_1-)$, where $\underline{0}$ is the null point process.

a. If s_1 is the first point of $\mathcal{N}_\lambda$, define

$$f_1 \stackrel{\text{def.}}{=} + \text{ and } X(s_1) = x_0e^{-s_1}+W(s_1-).$$

b. If s_1 is the first point of the second point process of Relation (1.22), set

$$f_1 \stackrel{\text{def.}}{=} - \text{ and } X(s_1) = x_0e^{-s_1}-g\left(x_0e^{-s_1}\right).$$

The mark f_1 indicates the nature of the jump occurring at time s_1, i.e. if the spike was fired by the pre- or post-synaptic neuron.

The process $(X(t),\Omega_p^1(t),\Omega_d^1(t),W(t))$ satisfies the equations (1.20) on the time interval $[0,s_1]$ and, by Relation (1.4), s_1 is a stopping time with respect to $(\mathcal{F}_t)$.

Assume by induction that, for $n\geqslant 0$, the variables $(s_k,f_k,1\leqslant k\leqslant n)$ and the adapted càdlàg process $(X(t),W(t),t\in[0,s_n])$ are defined, and s_n is a stopping time. For $a\in\{p,d\}$, let

$$\Omega_a^{n+1}(t) \stackrel{\text{def.}}{=} \omega_a+\int_{(0,t)} e^{-\alpha(t-s)}\Gamma_a\left(\sum_{k=1}^n \delta_{s_k}\mathbb{1}_{\{f_k=+\}},\sum_{k=1}^n \delta_{s_k}\mathbb{1}_{\{f_k=-\}}\right)(\mathrm{d}s). \tag{1.23}$$

In Definition 2, the $\mathcal{G}_t\otimes\mathcal{G}_t$ measurability property, gives that for any $n\geqslant 1$ and $k<n$, the process $(\Omega_a^j(t))$ does not depend on the index $j\in\{k,\ldots,n\}$ on $[0,s_k]$. The instant $s_{n+1}>s_n$ is defined as the minimum of the first jumps of the two point processes,

$$(\mathcal{N}_\lambda([s_n,t]),t>s_n),\left(\int_{[s_n,t]} \mathcal{P}\left[\left(0,\beta\left(X(s_n)e^{-(u-s_n)}\right)\right],\mathrm{d}u\right],t>s_n\right). \tag{1.24}$$

The fact that s_n is a stopping time and the strong Markov property of the Poisson processes $\mathcal{N}_\lambda$ and $\mathcal{P}$ give that s_{n+1} is also a stopping time. For $s_n\leqslant t<s_{n+1}$, set

$$W(t)=S[\Omega_p^{n+1},\Omega_d^{n+1}](W(s_n),t-s_n) \text{ and } X(t) \stackrel{\text{def.}}{=} X(s_n)e^{-(t-s_n)},$$

and $W(s_{n+1})=W(s_{n+1}-)$, and

a. If s_{n+1} is a point of $\mathcal{N}_\lambda$, define $f_{n+1}{=}+$, and

$$X(s_{n+1}) \stackrel{\text{def.}}{=} X(s_n)e^{-(s_{n+1}-s_n)}{+}W(s_{n+1}-).$$

b. Otherwise, we set $f_{n+1}{=}-$, and

$$X(s_{n+1}) \stackrel{\text{def.}}{=} X(s_n)e^{-(s_{n+1}-s_n)}{-}g\left(X(s_n)e^{-(s_{n+1}-s_n)}\right).$$

We have thus defined by induction a stochastic process $(X(t), W(t))$ on sequence of time intervals (s_n, s_{n+1}), $n{\geqslant}1$. We now prove that the process is defined on the whole real half-line, i.e. that the sequence (s_n) is almost surely converging to infinity. This is the object of the following lemma.

Lemma 5 (Non-explosive behavior)**.** *Under Assumptions A, the sequence of successive jump instants (s_n) is almost surely converging to infinity.*

Proof. Denote by $\mathcal{E}_0$ the event where the sequence (s_n) is bounded and assume that it has a positive probability. On the event $\mathcal{E}_0$, almost surely, only a finite number of points of the Poisson process $\mathcal{N}_\lambda$ may be points of the sequence (s_n). Therefore, there exists some $N_0{\in}\mathbb{N}$ and a subset $\mathcal{E}_1$ of $\mathcal{E}_0$ of positive probability such that for $n{\geqslant}N_0$, one has $f_n{=}-$, i.e. the jumps are due to the second point process of Relation (1.24) after time s_{N_0}.

On the event $\mathcal{E}_1$, for $n{\geqslant}N_0$ one has $X(s_n-){<}|X(s_{N_0})|$, almost surely, because $(|X(t)|)$ can only decrease when there are no pre-synaptic spikes. Consequently, as $\beta(x)$ is null for $x{<}{-}c_\beta$, we have that $\max(\beta(X(t)){:}t{>}s_{N_0}){<}+\infty$. Therefore, the successive jump instants $(s_n, n{\geqslant}N_0)$ cannot stay bounded on the event $\mathcal{E}_1$. This is a contradiction. The sequence (s_n) is therefore converging to infinity almost surely. □

A direct consequence of this result is that, from the very definition of the sequence (s_n), for any $t{>}0$, there exists n_0 such that if $n{\geqslant}n_0$ then

$$\sum_{k=1}^{n}\delta_{s_k}\mathbb{1}_{\{f_k=+\}}\cap[0,t]=\mathcal{N}_\lambda\cap[0,t] \text{ and } \sum_{k=1}^{n}\delta_{s_k}\mathbb{1}_{\{f_k=-\}}\cap[0,t]=\mathcal{N}_{\beta,X}\cap[0,t], \quad \text{a.s.},$$

recall that $\mu\cap[0,t]$ is the measure $\mu{\in}\mathcal{M}(\mathbb{R}_+)$ restricted to the interval $[0,t]$. For $a{\in}\{p,d\}$, again with the $\mathcal{G}_t{\otimes}\mathcal{G}_t$-measurability property of plasticity kernels, the quantity

$$\Omega_a^n(t){=}\Omega_a(0){+}\int_{(0,t)}e^{-\alpha(t-s)}\Gamma_a\left(\mathcal{N}_\lambda,\mathcal{N}_{\beta,X}\right)(\mathrm{d}s)$$

is constant for $n{\geqslant}n_0$, it is defined as $\Omega_a(t)$. Furthermore, for $s{\leqslant}t$ and $n{\geqslant}n_0$,

$$\mathrm{d}W(s)=M\left(\Omega_p^n(t),\Omega_d^n(s),W(s)\right)\mathrm{d}s=M\left(\Omega_p(t),\Omega_d(s),W(s)\right)\mathrm{d}s.$$

We have thus the existence of a solution to Relation (1.20). The uniqueness is clear on any time interval $[0,s_n]$, $n{\geqslant}1$, and therefore almost surely on $\mathbb{R}_+$.

□

1.3 Markovian plasticity kernels

In this section we introduce an important subclass $(\mathcal{M})$ of plasticity kernels that leads to a Markovian formulation of the whole plasticity process. In this context, it turns out that the associated synaptic weight process $(W(t))$ can be investigated with a scaling approach which is often used, sometimes implicitly, in the literature of physics in neuroscience. As it will be seen, plasticity kernels of pair-based models of Section 1.2 and of calcium-based models of Section 1.2 are of class $\mathcal{M}$. The follow-up paper [RV21c] is devoted to the scaling analysis of these plasticity kernels.

Definition 6 (Kernels of class $(\mathcal{M})$)**.** *A plasticity kernel Γ is of class $(\mathcal{M})$ if, for m_1, $m_2 \in \mathcal{M}_p(\mathbb{R}_+)$,*

$$\Gamma(m_1, m_2)(\mathrm{d}t) = n_0(z(t))\,\mathrm{d}t + n_1(z(t-))m_1(\mathrm{d}t) + n_2(z(t-))m_2(\mathrm{d}t), \tag{1.25}$$

where

a. For $i=0, 1, 2$, $n_{a,i}$ is a non-negative measurable function on $\mathbb{R}_+^\ell$, where $\ell \in \mathbb{N}_*$.

b. $(z(t))$ is a càdlàg function with values in $\mathbb{R}_+^\ell$, solution of the SDE

$$\mathrm{d}z(t) = (-\gamma \odot z(t) + k_0)\,\mathrm{d}t + k_1(z(t-))m_1(\mathrm{d}t) + k_2(z(t-))m_2(\mathrm{d}t). \tag{1.26}$$

— *$\gamma \in \mathbb{R}_+^\ell$, $a \odot b = (a_i \times b_i)$ if $a=(a_i)$ and $b=(b_i)$ in $\mathbb{R}_+^\ell$.*

— *$k_0 \in \mathbb{R}_+^\ell$ is a constant and k_1 and k_2 are measurable functions from $\mathbb{R}_+^\ell$ to $\mathbb{R}^\ell$. Furthermore, the (k_i) are such that the function $(z(t))$ has values in $\mathbb{R}_+^\ell$ whenever $z(0) \in \mathbb{R}_+^\ell$.*

It is important to note that the function $(z(t))$ is a functional of the pair (m_1, m_2). The fact that $z(t)$ stay non-negative is an important feature of class $(\mathcal{M})$ kernels. For example, we may have functions k_1 or k_2 of the form,

$$k_i(z) = B_i - b_i \odot z$$

where $B_i \in \mathbb{R}_+^\ell$, and $b_i \in \{0,1\}^\ell$.

If Γ is of class $(\mathcal{M})$ and $(z(t))$ is its associated càdlàg process, with Relation (1.26) it is easily seen that, for any $t>0$, the functional

$$\begin{cases} (\mathcal{M}_p(\mathbb{R}_+)^2, \mathcal{G}_t \otimes \mathcal{G}_t) & \longrightarrow (\mathcal{M}_+([0,t]), \mathcal{B}(\mathcal{M}_+([0,t]))) \\ (m_1, m_2) & \longrightarrow \Gamma(m_1, m_2)(\mathrm{d}u \cap [0,t]) \end{cases}$$

is indeed $\mathcal{G}_t$-measurable, where $(\mathcal{G}_t)$ is the filtration of Definition (2).

Proposition 7 (A Markovian formulation of plasticity)**.** *If Γ_a, $a \in \{p, d\}$, are plasticity kernels of class $(\mathcal{M})$ associated to $(n_{a,i}, k_i)$, $i \in \{0,1,2\}$, $a \in \{p,d\}$ and $\gamma \in \mathbb{R}_+^\ell$ and under Assumptions A, the solution of Relations* (1.20) *of Theorem 4 is such that the stochastic process $(U(t)) \overset{\text{def.}}{=} (X(t), Z(t), \Omega_p(t), \Omega_d(t), W(t))$ is a Markov process on $\mathcal{S}_{\mathcal{M}}(\ell) \overset{\text{def.}}{=} \mathbb{R} \times \mathbb{R}_+^\ell \times \mathbb{R}_+^2 \times K_W$, solution of the SDE,*

$$\begin{cases} \mathrm{d}X(t) & = -X(t)\,\mathrm{d}t + W(t)\mathcal{N}_\lambda(\mathrm{d}t) - g\left(X(t-)\right)\mathcal{N}_{\beta,X}\left(\mathrm{d}t\right), \\ \mathrm{d}Z(t) & = (-\gamma \odot Z(t) + k_0)\,\mathrm{d}t \\ & \qquad + k_1(Z(t-))\mathcal{N}_\lambda(\mathrm{d}t) + k_2(Z(t-))\mathcal{N}_{\beta,X}(\mathrm{d}t), \\ \mathrm{d}\Omega_a(t) & = -\alpha\Omega_a(t)\,\mathrm{d}t + n_{a,0}(Z(t))\,\mathrm{d}t \\ & \quad + n_{a,1}(Z(t-))\mathcal{N}_\lambda(\mathrm{d}t) + n_{a,2}(Z(t-))\mathcal{N}_{\beta,X}(\mathrm{d}t), \quad a \in \{p,d\}, \\ \mathrm{d}W(t) & = M(\Omega_p(t), \Omega_d(t), W(t))\,\mathrm{d}t \end{cases} \tag{1.27}$$

Proof. Theorem 4 shows the existence and uniqueness of such a process $(U(t))$. The process $(U(t))$ is a piecewise deterministic Markov process in the sense of [Dav93] and consequently has the Markov property. See Chapter 2 of [Dav93]. An expression of its infinitesimal generator is given in Section 1.D of Supplementary Materials. □

It should be noted that, due to the dimension of the state space, the Markov property of $(U(t))$ cannot be really used in practice in our analysis. The representation in terms of SDEs in Relation (1.27) turns out to be useful in the scaling approach presented in [RV21c].

Motivation for Markovian kernels

The processes $(\Omega_p(t))$ and $(\Omega_d(t))$ determining the synaptic plasticity depend on the process $(Z(t))$ in a non-linear way. The coordinates of $(Z(t))=(Z_i(t))$ may be interpreted as the concentration of chemical components created/suppressed by pre-synaptic and/or post-synaptic spikes, with some leaking mechanism. Calcium is such an example, see Relation (1.17). A simple case is when each coordinate of $(Z(t))$ is associated either to pre- or post-synaptic spikes, i.e. it satisfies

$$\mathrm{d}Z_i(t) = -\gamma_i Z_i(t)\,\mathrm{d}t + B_i\mathcal{N}_\lambda(\mathrm{d}t) \text{ or } \mathrm{d}Z_i(t) = -\gamma_i Z_i(t)\,\mathrm{d}t + B_i\mathcal{N}_{\beta,X}(\mathrm{d}t).$$

Moreover, if Z_i needs to be reset to B_i when one of the neurons spikes, we just need to replace B_i by $B_i - Z_i(t-)$ in these equations.

We now show that calcium-based models and several pair-based models, can be represented in such a setting, i.e. that their plasticity kernels are of class $(\mathcal{M})$.

Examples

Calcium-based models

For this set of models, the class $(\mathcal{M})$ property is fairly clear. Relations (1.17) and (1.18) give that, for $a\in\{p,d\}$ and $m_1, m_2\in\mathcal{M}_p(\mathbb{R}_+)$,

$$\Gamma_a^C\,(m_1,m_2)(\mathrm{d}t) \overset{\text{def.}}{=} h_a(C_m(t))\,\mathrm{d}t,$$

where, if $m=(m_1,m_2)$, $(C_m(t))$ is a càdlàg solution of the differential equation

$$\mathrm{d}C_m(t) = -\gamma C_m(t)\,\mathrm{d}t + C_1 m_1(\mathrm{d}t) + C_2 m_2(\mathrm{d}t).$$

The process $(Z(t))$ is simply the one-dimensional process $(C_{\mathcal{N}_\lambda,\mathcal{N}_{\beta,X}}(t))$. Markovian dynamics of the calcium-based model are illustrated in Figure 1.4-(a).

Pair-based models

Several kernels associated to pair-based models defined by Relation (1.12) are also of class $(\mathcal{M})$. This type of Markov property has been mentioned in [MDG08]. Markovian models including STDP models described in Section 1.2 are presented in Section 1.D of Supplementary Materials.

All-to-all model

The class $(\mathcal{M})$ holds when the STDP functions Φ are exponential, i.e. when, for $a\in\{p,d\}$ and $i\in\{1,2\}$,

$$\Phi_{a,i}(t)=B_{a,i}\exp(-\gamma_{a,i}t),\quad t\geqslant 0.$$

with $B_{a,i}\in\mathbb{R}_+$ and $\gamma_{a,i}>0$. For m_1 and $m_2\in\mathcal{M}_p(\mathbb{R}_+)$, denote by $(z_{a,i}(t))$, the càdlàg solution of the differential equation

$$\mathrm{d}z_{a,i}(t) = -\gamma_{a,i}z_{a,i}(t)\,\mathrm{d}t + B_{a,i}m_i(\mathrm{d}t),$$

with $z_{a,i}(0)=0$. Lemma 1 gives the relation

$$z_{a,i}(t) = B_{a,i}\int_{(0,t]} e^{-\gamma_{a,i}(t-s)}m_i(\mathrm{d}s).$$

The process $(z(t))$ is then defined as $(z_{p,1}(t), z_{p,2}(t), z_{d,1}(t), z_{d,2}(t))$. The plasticity kernel of this model, see Relation (1.12), can be expressed as

$$\Gamma_a^{\mathrm{PA}}(m_1,m_2) = n_{a,1}(z(t-))m_1(\mathrm{d}t)+n_{a,2}(z(t-))m_2(\mathrm{d}t),$$

the functions $(n_{a,i})$ are defined by, for $z=(z_{a,i})\in\mathbb{R}_+^4$, $n_{a,1}(z)=z_{a,2}$ and $n_{a,2}(z)=z_{a,1}$.

An example of dynamics with plasticity kernels and associated Markov process $(Z_{a,i})$ is presented in Figure 1.3-(a). Similar models, using auxiliary processes $(Z_{a,i})$ can be devised for nearest STDP rules. See Section 1.D of Supplementary Materials, Figure 1.3-(b) for the nearest neighbor symmetric STDP and Figure 1.3-(c) for the nearest neighbor reduced symmetric STDP.

Nearest neighbor models

For $m\in\mathcal{M}_p(\mathbb{R}_+)$ and $t>0$, the variable $t_0(m,t)$ of Relation (1.15) used in the two models presented in Section 1.2,

$$t_0(m,t) = t - \sup\{s : s<t, m(\{s\})\neq 0\},$$

can be expressed as the solution $(z_m(t))$ of the differential equation,

$$\mathrm{d}z_m(t) = \mathrm{d}t - z_m(t-)m(\mathrm{d}t),$$

with $z_m(0)=0$.

For m_1 and $m_2\in\mathcal{M}_p(\mathbb{R}_+)$, we define $(z(t))=(z_{m_1}(t), z_{m_2}(t))$, Relation (1.26) holds with $\gamma=(0,0)$, $k_0=(1,1)$ and, for $z=(z_1,z_2)$, $k_1(z)=(-z_1,0)$ and $k_2(z)=(0,-z_2)$.

In this setting, both nearest models are of class $\mathcal{M}$:

— The nearest neighbor symmetric model, Γ_a^{PS} of Relation (1.14), with $n_{a,0}(z)=0$, $n_{a,1}(z)=\Phi_{a,2}(z_2)$ and $n_{a,2}(z)=\Phi_{a,1}(z_1)$.

— The nearest neighbor reduced symmetric model, Γ_a^{PR} of Relation (1.16), with $n_{a,0}(z)=0$, $n_{a,1}(z)=\Phi_{a,2}(z_2)\mathbb{1}_{\{z_2\leqslant z_1\}}$ and $n_{a,2}(z)=\Phi_{a,1}(z_1)\mathbb{1}_{\{z_1\leqslant z_2\}}$.

Extensions

For all-to-all models, the exponential STDP function allows the representation of time evolution of plastic synapticity with a finite-dimensional process $(Z(t))$ and, therefore, the associated kernels are of class $\mathcal{M}$.

For a general function Φ, it is however possible to express the system as a Markovian system, by taking the instants of all past instants of spikes

$$(Z_{1,k}(t)) \stackrel{\text{def.}}{=} (t_k(\mathcal{N}_\lambda, t), k\geqslant 0) \text{ and } (Z_{2,k}(t)) \stackrel{\text{def.}}{=} (t_k(\mathcal{N}_{\beta,X}, t), k\geqslant 0)$$

with, for $k\geqslant 0$, $m\in\mathcal{M}_p(\mathbb{R}_+)$ and $t>0$,

$$t_k(m,t) = t - \sup\{s\leqslant t : m([s,t])>k\}$$

$t_k(m,t)$ represent the time between t and the kth last spike of m. In an analogous way as for Definition (1.15), we have, for $k\geqslant 1$,

$$\mathrm{d}t_k(m,t) = \mathrm{d}t + (t_k(m,t-) - t_{k-1}(m,t-))\, m(\mathrm{d}t),$$

so that the processes $(Z_{i,k}(t), k\geqslant 0)$, $i\in\{1,2\}$ would satisfy SDE as in Relation (1.27). Keeping track of *all* instant previous spikes, we can express the plasticity kernels with an infinite dimensional Markovian process. Unfortunately, there are fewer results, concerning equilibrium distributions for example, in such a context. This is why we restrict our study to finite-dimensional systems.

Markov processes associated to cellular processes

When the plasticity process $(W(t))$ is constant and equal to $w\in\mathbb{R}$, the associated solution $(X^w(t), Z^w(t))$ of the first two SDEs of Relations (1.27) is clearly a Markov process driven by the pre- and post-synaptic spikes. The invariant distribution of this Markov process plays in important role in the scaling analysis of the process $(W(t))$ developed in [RV21a; RV21c]. For reasons explained in the introduction of [RV21c], these processes are referred to as *fast processes*.

It is easily seen that its infinitesimal generator is defined by, if $f\in\mathcal{C}_b^1(\mathbb{R}\times\mathbb{R}_+^\ell)$ and $v=(x,z)\in\mathbb{R}\times\mathbb{R}_+^\ell$, then

$$\begin{aligned} B_w^F(f)(v) \stackrel{\text{def.}}{=} & -x\frac{\partial f}{\partial x}(x,z) + \left\langle -\gamma\odot z + k_0, \frac{\partial f}{\partial z}(x,z)\right\rangle \\ & + \lambda\left(f(x+w, z+k_1(z)) - f(v)\right) + \beta(x)\left(f(x-g(x), z+k_2(z)) - f(v)\right), \end{aligned} \quad (1.28)$$

with

$$\frac{\partial f}{\partial z}(x,z) = \left(\frac{\partial f}{\partial z_i}(x,z), i\in\{1,\dots,\ell\}\right).$$

Examples of fast processes for classical STDP rules are presented in Section 1.D of Supplementary Materials. The following proposition is proved in Section 5 of [RV21a].

Proposition 8. *Under the Assumptions A-a and A-b and if the functions k_1 and k_2 are bounded and all coordinates of γ are positive then the Markov process $(X^w(t), Z^w(t))$ has a unique invariant distribution Π_w.*

The explicit expression of Π_w is not known in general. For several STDP models, like calcium-based models, this is a limitation for a detailed analysis of the plasticity process $(W(t))$. See Section 4 of [RV21c]. The next section is devoted to a class of discrete models of synaptic plasticity for which the corresponding Π_w has an explicit expression for the analogue of calcium-based models.

1.4 Discrete models of STDP rules

In this section, we introduce a discrete model of plasticity associated to Relation (1.27), where the membrane potential X, the cellular processes Z and the synaptic weight W are integer-valued variables. It amounts to represent these quantities as multiple of a "quantum", instead of a continuous variable. For example, pre-/post-synaptic receptors (like the AMPA receptor for example) have a measurable influence on the membrane potential, where one quantum would represent the influence of a single receptor. This is a biologically plausible assumption for potential and cellular processes. The leaking mechanism ($-aU(t)\mathrm{d}t$ in the continuous model, $U{\in}\{X,Z,W\}$ and $a{>}0$, in the SDEs) is represented by the fact that each quantum leaves the cell/synapse at rate a.

$$\begin{cases} \mathrm{d}X(t) &= -\mathcal{N}_{I,X}(\mathrm{d}t) + W(t-)\mathcal{N}_{\lambda}(\mathrm{d}t) - \mathcal{N}_{I,\beta X}(\mathrm{d}t), \\ \mathrm{d}Z_j(t) &= -\mathcal{N}_{I,\gamma_j Z_j}(\mathrm{d}t) + k_{0,j}(Z(t-))\mathcal{N}_1^j(\mathrm{d}t) + k_{1,j}(Z(t-))\mathcal{N}_{\lambda}(\mathrm{d}t) \\ &\qquad + k_{2,j}(Z(t-))\mathcal{N}_{I,\beta X}(\mathrm{d}t), \quad j{=}1,\ldots,\ell, \\ \mathrm{d}W(t) &= -\mathcal{N}_{I,\mu W}(\mathrm{d}t) + A_p\mathcal{N}_{I,\Omega_p}(\mathrm{d}t) - A_d\mathbb{1}_{\{W(t-)\geqslant A_d\}}\mathcal{N}_{I,\Omega_d}(\mathrm{d}t). \end{cases} \tag{1.29}$$

The processes $(\Omega_a(t))$, $a{\in}\{p,d\}$ satisfy the same SDE as in Relation (1.27), the functions $n_{a,i}$ and k_i, $i\in\{0,1,2\}$ are defined on $\mathbb{N}^\ell$ with values in $\mathbb{N}^\ell$. The variables A_p and A_d are integers and $\gamma{=}(\gamma_j){\in}\mathbb{R}_+^\ell$.

For $\xi{>}0$, $\mathcal{N}_\xi$, resp. $(\mathcal{N}_\xi^i)$, is a Poisson process on $\mathbb{R}_+$ with rate ξ, resp. independent i.i.d. sequences of such point processes. As before, with Relation (1.5) and $I(x){=}x$ and a process $(U(t))$, the notation $\mathcal{N}_{I,U}(\mathrm{d}t)$ stands for $\mathcal{P}\left((0,U(t-)),\mathrm{d}t\right)$, where $\mathcal{P}$ is a Poisson process in $\mathbb{R}_+^2$ with rate 1. We have in particular

$$\mathbb{P}(\mathcal{N}_{I,U}(\mathrm{d}t){\neq}0|U(t-)){=}U(t-)\,\mathrm{d}t{+}o(\mathrm{d}t).$$

All Poisson processes are assumed to be independent.

We have taken $g(\cdot)$ as the constant function equal to 1. As it can be seen, the firing rate in the evolution of $(X(t))$ is the linear function $x{\mapsto}\beta x$. The time evolution of the discrete random variable $(W(t))$ is driven by two inhomogeneous Poisson processes, one for potentiation and the other for depression.

As before we define $(X^w(t),Z^w(t))$ as the Markov process $(X(t),Z(t))$ when $(W(t))$ is constant and equal to $w{\in}\mathbb{N}$. If $Q{=}(q((x,z),(x',z')))$ is the jump matrix of $(X^w(t),Z^w(t))$, we have,

$$\begin{cases} q((x,z),(x{-}1,z)){=}x, \quad q((x,z),(x,z{+}k_0(z))){=}1 \\ q((x,z),(x{+}w,z{+}k_1(z))){=}\lambda, \quad q((x,z),(x{-}1,z{+}k_2(z))){=}\beta x, \\ q((x,z),(x,z{-}e_i)){=}\gamma_i z_i, \quad i{\in}\{1,\ldots,\ell\}. \end{cases}$$

where e_i is the ith unit vector of $\mathbb{N}^\ell$. If f is a function on $\mathbb{N}{\times}\mathbb{N}^\ell$, with the notation $\nabla_{(a,b)}(f)(v){=}(f(v{+}(a,b)){-}f(v))$, for v, $(a,b){\in}\mathbb{Z}^{\ell+1}$, Q can be expressed as

$$\begin{aligned} Q(f)(x,z) &\stackrel{\text{def.}}{=} \sum_{(x',z')} q((x',z'),(x,z))f(x',z') \\ &= x\nabla_{(-1,0)}(f)(x,z) + \sum_{j=1}^{\ell}\gamma_j z_j\nabla_{(0,-e_j)}(f)(x,z) + \nabla_{(0,k_0(z))}(f)(x,z) \\ &\qquad + \lambda\nabla_{(w,k_1(z))}(f)(x,z) + \beta x\nabla_{(-1,k_2(z))}(f)(x,z). \end{aligned}$$

Proposition 9. *Under Assumptions A-a and A-b and if the coordinates of functions k_0, k_1 and k_2 are bounded and all coordinates of γ are positive then the Markov process $(X^w(t), Z^w(t))$ has a unique invariant distribution on $\mathbb{N}^{1+\ell}$.*

Proof. Since the state space is at most countable, the proof is simpler than its continuous counterpart, Proposition 9, where annoying technical intricacies hide the simplicity of the result. Let C_k be an upper bound for the coordinates of k_i, $i=0, 1, 2$. For $(x, z)\in\mathbb{N}^{\ell+1}$, define, for $\eta>0$, $f(x, z)=x+\eta(z_1+\cdots+z_\ell)$. We have

$$Q(f)(x,z) \leqslant -x + \lambda w - \beta x - \eta \sum_{j=1}^{\ell} \gamma_j z_j + \eta\ell(1+\lambda)C_k + \eta\ell\beta C_k x$$
$$\leqslant -\beta(1-\eta\ell C_k)x - \min(1, \gamma_j) f(x,z) + D,$$

with D a constant. If η is chosen so that $\eta<1/\ell C_k$, then there exists $\gamma>0$ and K such that $Q(f)(x, z)<-\gamma$ holds whenever $f(x, z)>K$. We can now use Proposition 8.14 of [Rob03] to conclude the proof of the proposition. □

A Discrete Version of Calcium-Based Models

A comparison between continuous and discrete models of calcium-based STDP is presented in Section 1.C, and illustrated by Figure 1.4. The state of the system corresponds to the case when $(Z(t))$ is a one-dimensional process $(C(t))$ solution of the SDE,

$$\begin{cases} \mathrm{d}C(t) &= -\mathcal{N}_{I,\gamma C}(\mathrm{d}t) + C_1\mathcal{N}_\lambda(\mathrm{d}t) + C_2\mathcal{N}_{I,\beta X}(\mathrm{d}t), \\ \mathrm{d}\Omega_a(t) &= (-\alpha\Omega_a(t) + h_a(C(t)))\,\mathrm{d}t, \quad a\in\{p,d\}, \end{cases}$$

where C_1, $C_2\in\mathbb{N}$ and, for $a\in\{p, d\}$, $A_a\in\mathbb{N}$ and h_a is a non-negative function.

Definition 10. *For a fixed $W=w$, the Markov process $(X^w(t), C^w(t))$ is defined by its transition rate matrix $Q_C=(q_C((x, c), (x', c')))$ is given by, for $(x, c)\in\mathbb{N}^2$,*

$$\begin{cases} q_C((x,c),(x+w,c+C_1))=\lambda, & q_C((x,c),(x-1,c))=x, \\ q_C((x,c),(x,c-1))=\gamma c, & q_C((x,c),(x-1,c+C_2))=\beta x. \end{cases}$$

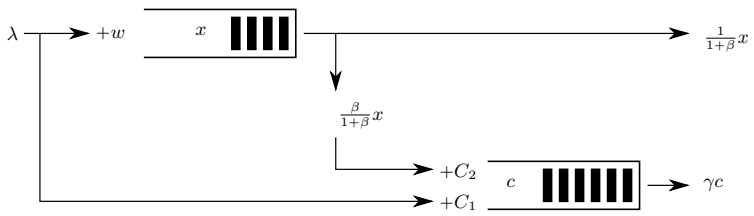

Figure 1.2: **Stochastic queue for the associated fast process of the discrete calcium-based model.**

This process can be seen as a network of two $M/M/\infty$ queues with simultaneous arrivals, see Chapter 6 of [Rob03], as illustrated in Figure 1.2.

Proposition 11 (Equilibrium of fast process). *For $w\in\mathbb{N}$, the Markov process on $\mathbb{N}^2$ of Definition 10 has a unique invariant distribution Π_w^{CQ}, and the generating function of C^w is given by, for $u\in[0,1]$,*

$$E\left(u^{C^w}\right) = \exp\left(-\lambda\int_0^{+\infty}(1-\Delta(u,s,w))\,\mathrm{d}s\right), \tag{1.30}$$

with

$$\Delta(u,s,w) = \Big(1+(u-1)p_1(s)\Big)^{C_1}\left(1+\sum_{i=1}^{C_2}(u-1)^k p_2(s,k)\right)^w$$

$$p_1(s) = e^{-\gamma s} \text{ and } p_2(s,k) = \frac{\beta}{\beta+1-\gamma k}\binom{C_2}{k}\left(e^{-\gamma k s}-e^{-(\beta+1)s}\right).$$

Due to its use in the scaling results of [RV21c], only the distribution of the calcium variable C^w is considered. The joint generating function of (X^w, C^w) could be obtained with the same approach.

It might be tempting to try to solve the equilibrium equations for the transition rates of Definition 10. It does not seem that there is a way to solve them with generating functions methods. The proof below relies in fact on a convenient representation of the Markov process with a Poisson marked point process, it then gives a satisfactory representation of the equilibrium distribution.

Proof. To each arrival instant t of the Poisson process $\mathcal{N}_\lambda$ on $\mathbb{R}$ is associated a vector of $\mathbb{N}^{2w+C_1+wC_2}$

$$\underline{u}=((x_i,1\leqslant i\leqslant w),(y_i,1\leqslant i\leqslant w),(z_{0,j},1\leqslant j\leqslant C_1),(z_{i,j},1\leqslant i\leqslant w,1\leqslant j\leqslant C_2))$$

We take $(\underline{U}_n)=((X_{n,i}),(Y_{n,i}),(Z_{n,i,j}))$, where $(X_{n,i})$, $(Y_{n,i})$ and $(Z_{n,i,j})$, sequences of i.i.d. exponentially distributed random variables with respective parameters 1, β and γ, and independent of $\mathcal{N}_\lambda$. The interpretation of these variables are as follows, for $1\leqslant i\leqslant w$, for the nth instant of the Poisson process $\mathcal{N}_\lambda$,

a. $X_{n,i}$ is the lifetime of the ith quantum of potential generated at time t (if any);

b. $Y_{n,i}$, the duration of time after which this ith quantum of potential initiates a firing of the neuron;

c. $Z_{n,0,j}$, the lifetime of the jth quantum of calcium generated at t, for $1\leqslant j\leqslant C_1$;

d. $Z_{n,i,j}$, the lifetime of the ith quantum of calcium created if the event described by (c) occurs, for $1\leqslant j\leqslant C_2$.

Define

$$\overline{\mathcal{N}}_\lambda(\mathrm{d}s,\mathrm{d}\underline{u}) \overset{\text{def.}}{=} \sum_{n\in\mathbb{Z}}\delta_{(t_n,\underline{U}_n)},$$

it is well known that $\overline{\mathcal{N}}_\lambda$ is a Poisson marked point process with intensity measure

$$\mu(\mathrm{d}s,\mathrm{d}\underline{u}) \overset{\text{def.}}{=} \lambda\,\mathrm{d}s\otimes_{i=1}^w E_1(\mathrm{d}x_i)\otimes_{i=1}^w E_\beta(\mathrm{d}y_i)\otimes_{j=1}^{C_1}E_\gamma(\mathrm{d}z_{0,j})\otimes_{i=1}^w\otimes_{j=1}^{C_2}E_\gamma(\mathrm{d}z_{i,j}), \tag{1.31}$$

where $E_\xi(\mathrm{d}x)$ is the exponential distribution with parameter $\xi>0$. See Chapter 5 of [Kin92] for example.

Assuming that $X^w(0)=C^w(0)=0$, with the interpretation of the coordinates of the mark $\underline{u}$, it is easy to get the representation, for $t\geqslant 0$,

$$X^w(t) = \int_{(0,t]} \sum_{i=1}^{w} \mathbb{1}_{\{s+x_i>t, s+y_i>t\}} \overline{\mathcal{N}}_\lambda(\mathrm{d}s, \mathrm{d}\underline{u}),$$

indeed, if there is an arrival at $s\leqslant t$, its ith quantum $i\in\{1,\dots,w\}$ of this arrival with lifetime x_i with firing time y_i is still present at t if $s+x_1>t$ and $s+y_i>t$. Similarly,

$$C^w(t) = \int_{(0,t]} \sum_{j=1}^{C_1} \mathbb{1}_{\{s+z_{0,j}>t\}} \overline{\mathcal{N}}_\lambda(\mathrm{d}s, \mathrm{d}\underline{u}) + \int_{(0,t]} \sum_{i=1}^{w} \sum_{j=1}^{C_2} \mathbb{1}_{\{x_i>y_i, s+y_i<t, s+y_i+z_{i,j}>t\}} \overline{\mathcal{N}}_\lambda(\mathrm{d}s, \mathrm{d}\underline{u}).$$

Using invariance by time-translation of the Poisson process $\overline{\mathcal{N}}_\lambda$, we get that the random variable $(X^w(t), C^w(t))$ has the same distribution as

$$\left(\overline{X}^w(t), \overline{C}_w(t)\right) \stackrel{\text{def.}}{=} \left(\int_{(-t,0]} \sum_{i=1}^{w} \mathbb{1}_{\{s+x_i>0, s+y_i>0\}} \overline{\mathcal{N}}_\lambda(\mathrm{d}s, \mathrm{d}\underline{u}) \,, \right.$$
$$\left. \int_{(-t,0]} \sum_{j=1}^{C_1} \mathbb{1}_{\{s+z_{0,j}>0\}} \overline{\mathcal{N}}_\lambda(\mathrm{d}s, \mathrm{d}\underline{u}) + \sum_{i=1}^{w} \sum_{j=1}^{C_2} \mathbb{1}_{\left\{\substack{x_i>y_i, s+y_i<0,\\ s+y_i+z_{i,j}>0}\right\}} \overline{\mathcal{N}}_\lambda(\mathrm{d}s, \mathrm{d}\underline{u}) \right).$$

The random variables $(\overline{X}^w(t), \overline{C}^w(t))$ are non-decreasing and converging to

$$\left(\overline{X}^w(\infty), \overline{C}_w(\infty)\right) \stackrel{\text{def.}}{=} \left(\int_{(-\infty,0]} \sum_{i=1}^{w} \mathbb{1}_{\{s+x_i>0, s+y_i>0\}} \overline{\mathcal{N}}_\lambda(\mathrm{d}s, \mathrm{d}\underline{u}) \,, \right.$$
$$\left. \int_{(-\infty,0]} \left[\sum_{j=1}^{C_1} \mathbb{1}_{\{s+z_{0,j}>0\}} + \sum_{i=1}^{w} \sum_{j=1}^{C_2} \mathbb{1}_{\{x_i>y_i, s+y_i<0, s+y_i+z_{i,j}>0\}} \right] \overline{\mathcal{N}}_\lambda(\mathrm{d}s, \mathrm{d}\underline{u}) \right). \quad (1.32)$$

The variable $\overline{X}^w(\infty)$ and $\overline{C}_w(\infty)$ are almost surely finite since, with standard calculations with Poisson processes, we obtain that

$$\mathbb{E}\left[\overline{X}^w(\infty)\right] = \frac{\lambda}{\beta+1} w, \quad \mathbb{E}\left[\overline{C}_w(\infty)\right] = \frac{\lambda}{\gamma}\left(C_1 + C_2 \frac{\beta w}{\beta+1}\right).$$

Recall the formula for Laplace transform of Poisson point processes,

$$\mathbb{E}\left[\exp\left(\int -f(s,\underline{u}) \overline{\mathcal{N}}_\lambda(\mathrm{d}s, \mathrm{d}\underline{u})\right)\right] = \exp\left(\int \left(1 - e^{-f(s,\underline{u})}\right) \mu(\mathrm{d}s, \mathrm{d}\underline{u})\right),$$

for any non-negative Borelian function f on $\mathbb{R}_+^{2w+C_1+wC_2}$, where μ is defined by Relation (1.31). See Proposition 1.5 of [Rob03] for example. For $u\in[0,1]$, we therefore get the relation

$$-\ln \mathbb{E}\left[u^{\overline{C}_w(\infty)}\right] =$$

$$\lambda \int_{\mathbb{R}_+} \left(1 - \mathbb{E}\left[u^{\sum_{j=1}^{C_1} \mathbb{1}_{\left\{E_{\gamma,0,j} > s\right\}}} \right] \mathbb{E}\left[u^{\sum_{i=1}^{w} \sum_{j=1}^{C_2} \mathbb{1}_{\left\{E_{1,i} > E_{\beta,i}, E_{\beta,i} < s < E_{\beta,i} + E_{\gamma,i,j}\right\}}} \right] \right) \mathrm{d}s =$$

$$\lambda \int_{\mathbb{R}_+} \left(1 - \left(1 - e^{-\gamma s} + u e^{-\gamma s}\right)^{C_1} \mathbb{E}\left[u^{\mathbb{1}_{\left\{E_{\beta,1} < s \wedge E_{1,1}\right\}} \sum_{j=1}^{C_2} \mathbb{1}_{\left\{s < E_{\beta,1} + E_{\gamma,1,j}\right\}}} \right]^w \right) \mathrm{d}s,$$

where $(E_{1,i})$, $(E_{\beta,i})$ and $(E_{\gamma,i,j})$ are independent i.i.d. exponentially distributed random variables with respective parameters 1, β and γ. We have

$$\mathbb{E}\left[u^{\sum_{j=1}^{C_2} \mathbb{1}_{\left\{E_{1,1} > E_{\beta,1}, E_{\beta,1} < s < E_{\beta,1} + E_{\gamma,1,j}\right\}}} \right] =$$

$$1 - p(s) + \mathbb{E}\left[\mathbb{E}\left[1 - q(s, E_{\beta,1}) + u q(s, E_{\beta,1})\right]^{C_2} \mathbb{1}_{\left\{E_{\beta,1} < s \wedge E_{1,1}\right\}} \right]$$

with

$$p(s) = \mathbb{P}\left(E_{\beta,1} < E_{1,1} \wedge s \right) = \frac{\beta}{\beta + 1} \left(1 - e^{-(\beta+1)s}\right),$$

and

$$q(s, E_{\beta,1}) = \mathbb{P}\left(s - E_{\beta,1} < E_{\gamma,1,1} \middle| E_{\beta,1} \right) = e^{-\gamma(s - E_{\beta,1})},$$

$$\mathbb{E}\left[\mathbb{E}\left[1 - q(s, E_{\beta,1}) + u q(s, E_{\beta,1})\right]^{C_2} \mathbb{1}_{\left\{E_{1,1} > E_{\beta,1}, E_{\beta,1} < s\right\}} \right] =$$

$$\sum_{k=0}^{C_2} (u-1)^k \left[\beta \binom{C_2}{k} e^{-\gamma k s} \int_0^s e^{-(\beta + 1 - \gamma k)h} \, \mathrm{d}h \right] = \sum_{k=0}^{C_2} (u-1)^k p_2(s, k)$$

with,

$$p_2(s, k) = \frac{\beta}{\beta + 1 - \gamma k} \binom{C_2}{k} \left(e^{-\gamma k s} - e^{-(\beta+1)s}\right)$$

Note that, $p_2(s, 0) = p(s)$ the proposition is thus proved. □

Appendix

1.A Additional examples of plasticity kernels

Suppression models

Computational models of pair-based rules of Section 1.2 are easy to implement in large neural networks and they capture some essentials properties of STDP.

Nevertheless, they have been shown to fit poorly with experimental data when more complex protocols are used. See [FD02; PG06a]. For this reason, more detailed models taking into account the influence of several pre- and post-synaptic spikes have been proposed. [BA16] is a review of these so-called 'triplet-based' rules and their influence on the stability of the synaptic weights distribution. The model of this section is a variant of the pair-based model with an additional dependence on earlier instants of post- and pre-synaptic spikes. Another variant is described in Section 1.A.

It was observed, using triplet-based protocols in [FD02], that preceding pre- and post-synaptic spikes have a 'suppression' effect on the Hebbian STDP observed. Motivated by these experiments, the following model, extending pair-based rules, has been proposed.

If there is a pre-synaptic spike, resp. post-synaptic spike, at time $t\geqslant 0$, we denote by $\ell_1(t)$ [resp. $\ell_2(t)$] the instant of the last pre-synaptic [resp. post-synaptic spike], before t. For this model, when a pre-synaptic spike occurs at time $t\geqslant 0$, the contribution to $\Gamma^{\mathrm{S}}_a(\cdot,\cdot)(\mathrm{d}t)$ is the sum over all post-synaptic spikes before time $s\leqslant t$ of the quantities

$$(1-\Phi_{\mathrm{S},1}(t-\ell_1(t)))\,(1-\Phi_{\mathrm{S},2}(s-\ell_2(s)))\,\Phi_{a,2}(t-s),$$

and similarly for post-synaptic spikes, where $\Phi_{\mathrm{S},i}$ is a non-negative non decreasing function verifying $\Phi_{\mathrm{S},i}(0)\leqslant 1$ and $\lim_{t\to+\infty}\Phi_{\mathrm{S},i}(t)=0$, for $i\in\{1,2\}$. In particular, if the instants t_1 and t_2 of consecutive pre-synaptic spikes are too close, i.e. $t_2-t_1=t_2-\ell_1(t)$ is small, the synaptic weight is not significantly changed at the instant t_2. And similarly for consecutive post-synaptic spikes.

The plasticity kernels Γ^{S}_a, $a\in\{p,d\}$, are defined by, for m_1, $m_2\in\mathcal{M}_p(\mathbb{R}_+)$,

$$\begin{aligned}\Gamma^{\mathrm{S}}_a(m_1,m_2)(\mathrm{d}t) \overset{\text{def.}}{=}\\ &\left[(1-\Phi_{\mathrm{S},1}(t_0(m_1,t))\int_{(0,t)}(1-\Phi_{\mathrm{S},2}(t_0(m_2,s)))\,\Phi_{a,2}(t-s)m_2(\mathrm{d}s)\right]m_1(\mathrm{d}t)\\ &+\left[(1-\Phi_{\mathrm{S},2}(t_0(m_2,t))\int_{(0,t)}(1-\Phi_{\mathrm{S},1}(t_0(m_1,s)))\,\Phi_{a,1}(t-s)m_1(\mathrm{d}s)\right]m_2(\mathrm{d}t)\end{aligned}$$

with the $t_0(m,t)$ defined by Equation (1.15).

Triplet-based models

[PG06a] shows that preceding pre-synaptic spikes enhance the depression obtained for a *post-pre* pairing, whereas preceding post-synaptic spikes lead to a bigger potentiation than in a classical pre-post pairing. The plasticity kernels Γ^{T}_a, $a\in\{p,d\}$ of the associated model are defined by, for m_1, $m_2\in\mathcal{M}_p(\mathbb{R}_+)$,

$$\Gamma_a^{\mathrm{T}}(m_1,m_2)(\mathrm{d}t) \stackrel{\text{def.}}{=} \left(1+\int_{(0,t)}\Phi_{\mathrm{T},a,1}(t-s)m_1(\mathrm{d}s)\right)\left(\int_{(0,t)}\Phi_{a,2}(t-s)m_2(\mathrm{d}s)\right)m_1(\mathrm{d}t) + \left(1+\int_{(0,t)}\Phi_{\mathrm{T},a,2}(t-s)m_2(\mathrm{d}s)\right)\left(\int_{(0,t)}\Phi_{a,1}(t-s)m_1(\mathrm{d}s)\right)m_2(\mathrm{d}t). \quad (1.33)$$

where, for $a\in\{p,d\}$, $i\in\{1,2\}$, $\Phi_{\mathrm{T},a,i}$ is a non-negative non-decreasing function converging to 0 at infinity.

It is interesting to note that this model is in contradiction with the suppression model described just before. Both models are based on experimental data from different neuronal cells: visual cortical in [FD02], and hippocampal in [PG06a]. A global model taking into account both mechanisms, the *NMDA-model*, is defined in [BA16].

Voltage-based models

In [CG10], another class of plasticity rules, voltage-based models, has been used to explain plasticity with biophysical mechanisms, similarly to calcium-based models.

In particular, filtered traces of the membrane potential X are used in the synaptic update. Adapting notations from [CG10], we have for depression,

$$\Gamma_d(\mathrm{d}t) = \left[B_d\left(\int_{(0,t)}e^{-\gamma_{d,2}(t-s)}X(t-s)\,\mathrm{d}s-\theta_d\right)^+\right]\mathcal{N}_\lambda(\mathrm{d}t),$$

and for potentiation,

$$\Gamma_p(\mathrm{d}t) = B_p\left(\int_{(0,t)}e^{-\gamma_{p,0}(t-s)}X(t-s)\,\mathrm{d}s-\theta_p\right)^+ \times\left(\int_{(0,t)}e^{-\gamma_{p,2}(t-s)}X(t-s)\,\mathrm{d}s-\theta_d\right)^+ \times\left(\int_{(0,t)}e^{-\gamma_{p,1}(t-s)}\mathcal{N}_\lambda(\mathrm{d}s)\right)\mathrm{d}t.$$

See Relations (1) and (2) of [CG10].

In their model, an adaptive-exponential integrate-and-fire model (AdEx) is used to represent the post-synaptic neuron, instead of a Poisson point process. They take θ_p above the threshold potential of the AdEx model, leading to a simple estimation in terms of the post-synaptic spike train:

$$\left(\int_{(0,t)}e^{-\gamma_{p,0}(t-s)}X(t-s)\,\mathrm{d}s-\theta_p\right)^+\mathrm{d}t \sim \mathcal{N}_{\beta,X}(\mathrm{d}t).$$

However, θ_d lies around the resting potential of the neuron, leading to synaptic update that are functions of X directly and not only of the spike-trains. This feature justifies the denomination *voltage-based* models and is not easily taken into account in the framework presented here. To include such a STDP rule, one could extend the definition of a plasticity kernel to $\Gamma(m_1,m_2,x)$ by adding a direct dependence on a càdlàg adapted process $(x(t))$.

We present a variation of the *voltage-based* model using filtered functionals of pre- and post-synaptic spike trains that fits in our formalism. Notice that both models are not equivalent in the sense that in [CG10], sub-threshold-activity can lead to plasticity, whereas our model needs post-synaptic spikes.

If there is a pre-synaptic spike at time $t>0$, the synaptic weight is depressed by the quantity

$$B_d\left(\int_{(0,t)} e^{-\gamma_{d,2}(t-s)}\mathcal{N}_{\beta,X}(\mathrm{d}s)-\theta_d\right)^+,$$

where, for $x\in\mathbb{R}$, $x^+=\max(x,0)$, and if some filtered variable is above some threshold θ_d at that time.

If there is a pre-synaptic spike at time t, the synaptic weight will be potentiated by a quantity involving the product of two filtered variables,

$$B_p\left(\int_{(0,t)} e^{-\gamma_{p,2}(t-s)}\mathcal{N}_{\beta,X}(\mathrm{d}s)-\theta_d\right)^+\int_{(0,t)} e^{-\gamma_{p,1}(t-s)}\mathcal{N}_{\lambda}(\mathrm{d}s),$$

The plasticity kernels are thus defined by, for m_1, $m_2\in\mathcal{M}_p(\mathbb{R}_+)$,

$$\Gamma_d^{\mathrm{V}}(m_1,m_2)(\mathrm{d}t)\stackrel{\text{def.}}{=}\left[B_d\left(\int_{(0,t)} e^{-\gamma_{d,2}(t-s)}m_2(\mathrm{d}s)-\theta_d\right)^+\right]m_1(\mathrm{d}t),$$

$$\Gamma_p^{\mathrm{V}}(m_1,m_2)(\mathrm{d}t)\stackrel{\text{def.}}{=}\left[B_p\left(\int_{(0,t)} e^{-\gamma_{p,2}(t-s)}m_2(\mathrm{d}s)-\theta_d\right)^+\left(\int_{(0,t)} e^{-\gamma_{p,1}(t-s)}m_1(\mathrm{d}s)\right)\right]m_2(\mathrm{d}t).$$

1.B Plasticity models without exponential filtering

In the model of Section 1.2, with Relation (1.7) we defined a filtering procedure with an exponential kernel of rate $\alpha>0$ for the function Ω_a, where $\Omega_p(t)$ and $\Omega_d(t)$ are used to quantify the past activity of input and output neurons leading to potentiation and depression respectively. It is given by, for $a\in\{p,d\}$,

$$\mathrm{d}\Omega_a(t)=-\alpha\Omega_a(t)\,\mathrm{d}t+\Gamma_a(\mathcal{N}_\lambda,\mathcal{N}_{\beta,X})(\mathrm{d}t),$$

where $\Gamma_a(\mathcal{N}_\lambda,\mathcal{N}_{\beta,X})(\mathrm{d}t)$ represents the plasticity kernels for potentiation, $a=p$, and, for depression, $a=d$.

Therefore, the update of the synaptic weight at time t depends on a functional of the synaptic processes that happened *before* t. The dynamic of the synaptic weight $(W(t))$ is defined by,

$$\mathrm{d}W(t)=M\left(\Omega_p(t),\Omega_d(t),W(t)\right)\mathrm{d}t,$$

Several studies of computational neuroscience have investigated the role of STDP in a stochastic setting. See [KGH99; KH00; Rob99; RLS01; MDG08] for example. These references use more "direct" dynamics for the synaptic weight. The update at time t depends only on the current synaptic plastic processes $\Gamma_a(\mathcal{N}_\lambda,\mathcal{N}_{\beta,X})(\mathrm{d}t)$ at time t, instead of a smoothed version over the past activity. The associated model can be defined so that the corresponding synaptic weight process $(\overline{W}(t))$ satisfies the relation

$$\mathrm{d}\overline{W}(t)=\overline{M}\left(\Gamma_p(\mathcal{N}_\lambda,\mathcal{N}_{\beta,\overline{X}}),\Gamma_d(\mathcal{N}_\lambda,\mathcal{N}_{\beta,\overline{X}}),\overline{W}(t-)\right)(\mathrm{d}t),$$

for some functional $\overline{M}$.

Biological arguments for exponential filtering

It should be noted that the model associated to $(\overline{W}(t))$ does not seem to be in agreement with observations of numerous experimental studies. See [BP98; FGV05; Fel12]. In a classical experiment, the protocol to induce plasticity consists in stimulating both neurons at a certain frequency a fixed number of times with a fixed delay Δt, over a period of up to one or two minutes (60-100 pairings at 1 Hz for example). This part is designed to reproduce conditions of correlations between the two neurons, when mechanisms of plasticity are known to be triggered. However, measurements of the synaptic weight show that changes take place on a different timescale. After the end of the protocol, it is observed that at least several minutes are necessary to have a significant and stable effect on the synaptic weight. In other words, the change in synaptic weights happens long after the end of the plasticity induction.

For this reason we have chosen to use a filter, possibly with an exponential kernel, on the past synaptic activity. Therefore it does not only depend on the instantaneous synaptic variable $\Gamma_d(\mathcal{N}_\lambda, \mathcal{N}_{\beta,X})(\mathrm{d}t)$ at time t, but on the whole past $\Gamma_d(\mathcal{N}_\lambda, \mathcal{N}_{\beta,X})(\mathrm{d}s)$, $s \leqslant t$, with a smoothing exponential kernel which gives the desired dynamical feature for the synaptic weight. Another recent article [RBS16] also takes this fact into account by adding an "ìnduction" function to the classical models of STDP.

A toy example

We define

$$\begin{cases} M(\omega_p, \omega_d, w) = \omega_p - \omega_d, & (\omega_p, \omega_d, w) \in \mathbb{R}_+^2 \times \mathbb{R}, \\ \overline{M}(\Gamma_1, \Gamma_2, w) = \Gamma_1 - \Gamma_2, & \Gamma_1, \Gamma_2 \in \mathcal{M}_+(\mathbb{R}_+), \\ \Gamma_p(\mathrm{d}t) - \Gamma_d(\mathrm{d}t) = (F - W(t))\,\mathrm{d}t, \end{cases}$$

with $F > 0$. The equations for the time evolution of synaptic weights are given by

$$\frac{\mathrm{d}\overline{W}(t)}{\mathrm{d}t} = \varepsilon\left(F - \overline{W}(t)\right) \text{ and } \frac{\mathrm{d}W(t)}{\mathrm{d}t} = \alpha^2 \int_0^t e^{-\alpha(t-s)}(F - W(s))\,\mathrm{d}s,$$

with the initial condition $W(0) = \overline{W}(0) = w_0 > 0$. We get that

$$\overline{W}(t) = F + (w_0 - F)e^{-\varepsilon t}, \quad t \geqslant 0,$$

so that $(\overline{W}(t))$ converges to F as t gets large, as it can be expected. By differentiating the relation for $(W(t))$ we obtain,

$$\frac{\mathrm{d}^2 W(t)}{\mathrm{d}t^2} + \alpha \frac{\mathrm{d}W(t)}{\mathrm{d}t} + W(t) = F,$$

with $W(0) = w_0$ and $W'(0) = 0$. If we take $\alpha = 2\varepsilon$ with $\varepsilon < 1$, we get that

$$W(t) = F + (w_0 - F)e^{-\varepsilon t}\left(\cos\left(t\sqrt{1-\varepsilon^2}\right) + \sqrt{\frac{\varepsilon^2}{1-\varepsilon^2}}\,\sin\left(t\sqrt{1-\varepsilon^2}\right)\right),$$

in particular $((W(t) - \overline{W}(t))e^{\varepsilon t}/(w_0 - F))$ is a periodic function with maximal value of the order of $1/\varepsilon$. Both functions $(W(t))$ and $(\overline{W}(t))$ converge to F as t goes to infinity at the same exponential rate but differ at the second order.

A comparison of both models is also done in Section 1.C of the Appendix and illustrated for pair-based rules in Figure 1.3 and for calcium-based ones in Figure 1.4.

1.C Graphical representation of models of plasticity

In this section, we will consider several examples of simple dynamics of the Markovian system defined in Section 1.3.

We will start by comparing the effect of three different Hebbian pair-based rules, both on model with, Section 1.3, and without, Section 1.B, exponential filtering. Then, we will focus on calcium-based models and show that the discrete model of Section 1.4 can be a good approximation of the continuous model of Section 1.3.

We consider two different timescales to compare the induction of plasticity in the model with/without exponential filtering:

— A fast timescale, on the order of the membrane potential dynamics (see plain black line under each row), where the input and output spike patterns are presented.

— A slow timescale (20 times slower in this example), on the order of the synaptic weight modifications (see dotted black line), where no input is presented.

Input and output spikes patterns are fixed in both Figures (see first row).

Pair-based STDP rules (Figure 1.3)

In this section, we describe the dynamics of the different stochastic processes involved in the pair-based STDP model.

In particular, we compare the various interpretation of the pair-based rules that are described in Section 1.2 in Figure 1.3,

a. all-to-all model;

b. nearest neighbor symmetric model;

c. nearest neighbor reduced symmetric model.

The different interactions are represented by grey arrows (first row).

Exponential STDP curves are considered with their associated Markovian description, see Section 1.D.

Finally, we focus on Hebbian STDP rules with $B_{d,1}{=}0$ and $B_{p,2}{=}0$.

In the second row, the time evolution of the membrane potential,

$$\mathrm{d}X(t) = -X(t)\,\mathrm{d}t + W(t-)\mathcal{N}_\lambda(\mathrm{d}t) - X(t-)\mathcal{N}_{\beta,X}(\mathrm{d}t),$$

is presented. Two interesting facts are to be noted here, at each pre-synaptic spike (green, first row), the current value of the synaptic weight $W(t-)$ is added to the membrane potential $X(t)$. It can be seen in this example that the size of the jump varies across time. In addition, a complete reset of X occurs after a post-synaptic spike (purple, first row), corresponding to $g(x){=}x$.

Then we focus on the instantaneous synaptic variables $Z_{p,1}$ (brown, third row) and $Z_{d,2}$ (brown, fourth row), that follows different dynamics depending on the rule chosen.

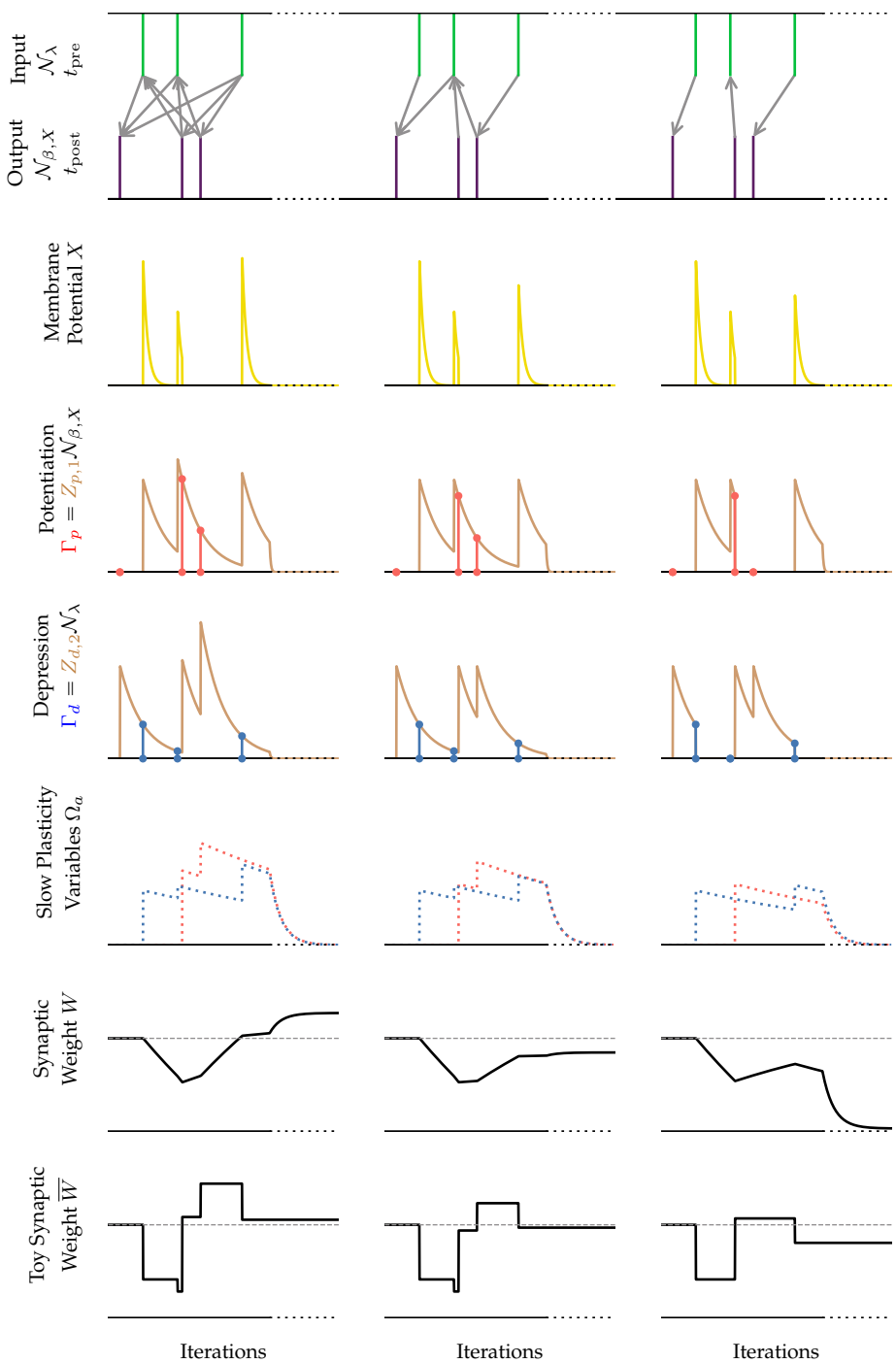

(a) Hebbian all-to-all pair-based rules Section 1.3

(b) Hebbian nearest neighbor symmetric pair-based rules Section 1.3

(c) Hebbian nearest neighbor reduced symmetric pair-based rules Section 1.3

Figure 1.3: **Synaptic plasticity kernels for pair-based rules.**

a. For *all-to-all* pairings, each synaptic spike is paired with all previous post-synaptic spikes, and conversely. They are already described in the main text, by the set of equations, for $a \in \{p, d\}$,

$$\begin{cases} \mathrm{d}Z_{p,1}(t) = -\gamma_{p,1} Z_{p,1}(t)\,\mathrm{d}t + B_{p,1}\mathcal{N}_\lambda(\mathrm{d}t), \\ \mathrm{d}Z_{d,2}(t) = -\gamma_{d,2} Z_{d,2}(t)\,\mathrm{d}t + B_{d,2}\mathcal{N}_{\beta,X}(\mathrm{d}t). \end{cases}$$

All pairs of pre-synaptic and post-synaptic spikes are taken into account.

b. For *nearest neighbor symmetric* scheme, each pre-synaptic spike is paired with the last post-synaptic spike, and conversely, the system changes slightly:

$$\begin{cases} \mathrm{d}Z_{p,1}(t) = -\gamma_{p,1} Z_{p,1}(t)\,\mathrm{d}t + (B_{p,1} - Z_{p,1}(t-))\mathcal{N}_\lambda(\mathrm{d}t), \\ \mathrm{d}Z_{d,2}(t) = -\gamma_{d,2} Z_{d,2}(t)\,\mathrm{d}t + (B_{d,2} - Z_{d,2}(t-))\mathcal{N}_{\beta,X}(\mathrm{d}t). \end{cases}$$

The variable $Z_{p,1}$, resp. $Z_{d,2}$ is reset to $B_{p,1}$, resp. $B_{d,2}$, after a pre-synaptic spike, resp. post-synaptic spike.

c. For *nearest neighbor reduced symmetric* scheme, where only immediate pairing matters, we have:

$$\begin{cases} \mathrm{d}Z_{p,1}(t) = -\gamma_{p,1} Z_{p,1}(t)\,\mathrm{d}t + (B_{p,1} - Z_{p,1}(t-))\mathcal{N}_\lambda(\mathrm{d}t) - Z_{p,1}(t-)\mathcal{N}_{\beta,X}(\mathrm{d}t), \\ \mathrm{d}Z_{d,2}(t) = -\gamma_{d,2} Z_{d,2}(t)\,\mathrm{d}t + (B_{d,2} - Z_{d,2}(t-))\mathcal{N}_{\beta,X}(\mathrm{d}t) - Z_{d,2}(t-)\mathcal{N}_\lambda(\mathrm{d}t), \end{cases}$$

The variable $Z_{p,1}$ is reset to $B_{p,1}$, after a pre-synaptic spike and to 0 after a post-synaptic spike, and conversely for $Z_{d,2}$.

This simple example shows how different pair-based rules shape the instantaneous plasticity variables Z. This dependence is subsequently transferred to the potentiation kernel Γ_p (red, third row) and the depression kernel Γ_d (blue, fourth row). With exponential pair-based models, we have $n_{a,0}(z)=0$, $n_{d,1}(z)=z_{d,2}$, $n_{p,1}(z)=0$, $n_{d,2}(z)=0$, $n_{p,2}(z)=z_{p,1}$, and therefore, they follow,

$$\begin{cases} \Gamma_p(\mathrm{d}t) = Z_{p,1}(t-)\mathcal{N}_{\beta,X}(\mathrm{d}t) \\ \Gamma_d(\mathrm{d}t) = Z_{d,2}(t-)\mathcal{N}_\lambda(\mathrm{d}t). \end{cases}$$

It is then not surprising to observe that for a same sequence of pre- and post-synaptic spikes the plasticity kernels are different.

Consequently, it is the same for the slow plasticity variables Ω_p (red, fifth row) and Ω_d (blue, fifth row), that follows,

$$\begin{cases} \mathrm{d}\Omega_p(t) = -\alpha\Omega_p(t)\,\mathrm{d}t + Z_{p,1}(t-)\mathcal{N}_{\beta,X}(\mathrm{d}t) \\ \mathrm{d}\Omega_d(t) = -\alpha\Omega_d(t)\,\mathrm{d}t + Z_{d,2}(t-)\mathcal{N}_\lambda(\mathrm{d}t), \end{cases}$$

We choose in this example a linear function M, leading to the following time evolution of the synaptic weight (sixth row),

$$\mathrm{d}W(t) = (\Omega_p(t) - \Omega_d(t))\,\mathrm{d}t.$$

This example shows that a simple change in the STDP rule can lead to very different dynamics for the synaptic weight. All-to-all rules lead to global potentiation (the dotted line represents the initial value) whereas nearest neighbor rules lead to depression.

Finally, as can be expected from the slow plasticity variables Ω_a that are still positive long after the end of the stimulus (see in the dotted part), the synaptic weight is modified long after the patterns of spikes.

On the contrary, considering the model without exponential filtering (seventh row),

$$\mathrm{d}\overline{W}(t) = \Gamma_p(\mathrm{d}t) - \Gamma_d(\mathrm{d}t),$$

we see that in that case, the synaptic weight is only updated during the stimulus. We notice that the polarity of the global plasticity is the same as with exponential filtering, but the dynamics are completely different, as showed with the toy model in Section 1.B.

Calcium-based STDP rules (Figure 1.4)

In this section, we focus on the dynamics of the calcium-based models,

a. the continuous version, described in Section 1.3;

b. the discrete version from Section 1.4.

The continuous membrane potential (second row, left) follows,

$$\mathrm{d}X(t) = -X(t)\,\mathrm{d}t + W(t-)\mathcal{N}_\lambda(\mathrm{d}t) - \mathcal{N}_{\beta,X}(\mathrm{d}t).$$

We consider a different function $g(x)=1$ than in the previous case. Its discrete analogue (second row, right) verifies,

$$\mathrm{d}X(t) = -\sum_{i=1}^{X(t-)} \mathcal{N}_{1,i}(\mathrm{d}t) + W(t-)\mathcal{N}_\lambda(\mathrm{d}t) - \sum_{i=1}^{X(t-)} \mathcal{N}_{\beta,i}(\mathrm{d}t).$$

It is plainly clear that both processes are almost identical, except that the exponential decay in the continuous model is replaced by a $M/M/\infty$ queue in the discrete case. In the case of large jumps, they lead to a similar dynamical evolution.

The same conclusions can be drawn for the calcium concentration, where the continuous version (third row, left) follows,

$$\mathrm{d}C(t) = -\gamma C(t)\,\mathrm{d}t + C_1\mathcal{N}_\lambda(\mathrm{d}t) + C_2\mathcal{N}_{\beta,X}(\mathrm{d}t),$$

and the discrete version (third row, right),

$$\mathrm{d}C(t) = -\sum_{i=1}^{C(t-)} \mathcal{N}_{\gamma,i}(\mathrm{d}t) + C_1\mathcal{N}_\lambda(\mathrm{d}t) + C_2 \sum_{i=1}^{X(t-)} \mathcal{N}_{\beta,i}(\mathrm{d}t).$$

In both cases, the plasticity kernels Γ_p (fourth row, red) and Γ_d (fourth row, blue) verify,

$$\begin{cases} \Gamma_p(\mathrm{d}t) = \mathbb{1}_{\{C(t-)\geqslant\theta_p\}}\,\mathrm{d}t \\ \Gamma_d(\mathrm{d}t) = \mathbb{1}_{\{C(t-)\geqslant\theta_d\}}\,\mathrm{d}t. \end{cases}$$

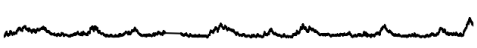

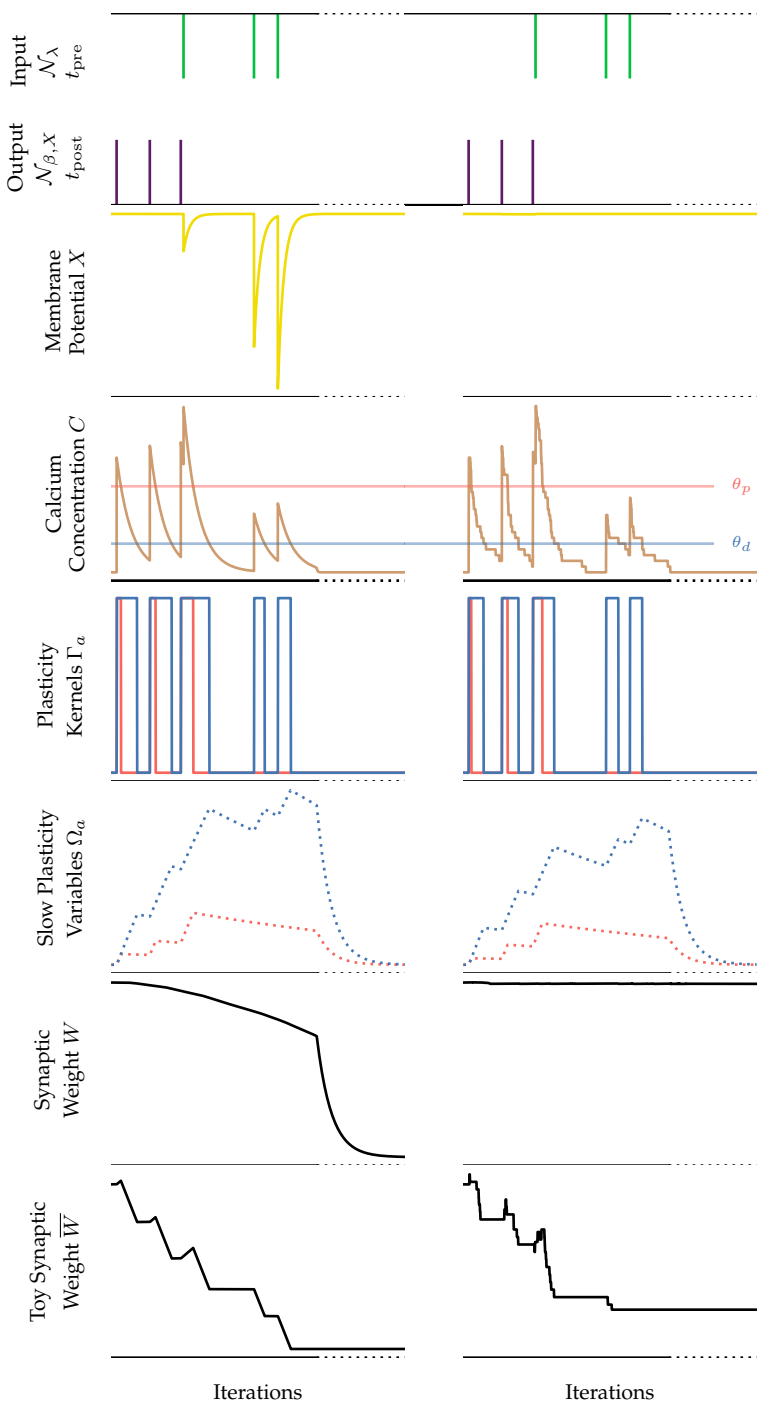

(a) Continuous calcium-based rules Section 1.3

(b) Stochastic queue calcium-based rules Section 1.4

Figure 1.4: **Synaptic plasticity kernels for calcium-based rules.**

When the calcium reaches the thresholds θ_p for potentiation (third row, red) and θ_d (third row, blue), the plasticity kernels are "activated" and are equal to $\mathrm{d}t$. We see that both models leads to similar values of the kernels, even if some discrepancies start to appear.

The slow plasticity variables (fifth row) are just obtained by integration of the kernels with an exponential filtering,

$$\begin{cases} \mathrm{d}\Omega_p(t) = -\alpha\Omega_p(t)\,\mathrm{d}t + \Gamma_p(\mathrm{d}t)\,\mathrm{d}t \\ \mathrm{d}\Omega_d(t) = -\alpha\Omega_d(t)\,\mathrm{d}t + \Gamma_d(\mathrm{d}t)\,\mathrm{d}t. \end{cases}$$

A second discretization is applied in the synaptic update, the continuous version (sixth row, left) verifies,

$$\mathrm{d}W(t) = \left(A_p\Omega_p(t) - A_d\mathbb{1}_{\{W(t-)\geqslant 0\}}\Omega_d(t)\right)\mathrm{d}t,$$

and the discrete one (sixth row, right),

$$\mathrm{d}W(t) = A_p\mathcal{N}_{\Omega_p(t-)}(\mathrm{d}t) - A_d\mathbb{1}_{\{W(t-)\geqslant A_d\}}\mathcal{N}_{\Omega_d(t-)}(\mathrm{d}t).$$

We note here that we need to force W to stay non-negative in order to have a valid description of the system. We observe that, even after two different discretizations, both synaptic weights follow a similar evolution.

Using a model without exponential filtering (seventh row) leads to a different dynamical evolution of the synaptic weight, for the continuous model,

$$\mathrm{d}\overline{W}(t) = A_p\Gamma_p(\mathrm{d}t) - A_d\mathbb{1}_{\{W(t-)\geqslant 0\}}\Gamma_d(\mathrm{d}t),$$

and the discrete one,

$$\mathrm{d}\overline{W}(t) = A_p\mathbb{1}_{\{C(t-)\geqslant\theta_p\}}\mathcal{N}_1^1(\mathrm{d}t) - A_d\mathbb{1}_{\{W(t-)\geqslant A_d, C(t-)\geqslant\theta_d\}}\mathcal{N}_1^2(\mathrm{d}t).$$

As a conclusion, the discrete models approximate well the continuous one and therefore, using the exact expressions of the discrete model can give an interesting insight on the dynamics of the continuous model.

1.D Fast systems of STDP models

We first start with the generator of a general STDP of class $\mathcal{M}$ as in Definition 6. For $u{=}(x,z,\omega_p,\omega_d,w){\in}\mathcal{S}_{\mathcal{M}}(\ell)$ and $f{\in}\mathcal{C}_b^1(\mathcal{S}_{\mathcal{M}}(\ell))$, i.e. f is a bounded $\mathcal{C}^1$-function, and all its respective derivatives are bounded, by using Equations (1.27), it is not difficult to show that the extended infinitesimal generator $\mathcal{A}$ of $(U(t))$ can be expressed as,

$$\begin{aligned}\mathcal{A}(f)(u) = {} & (-\alpha\omega_p{+}n_{p,0}(z))\,\frac{\partial f}{\partial\omega_p}(u){+}(-\alpha\omega_d{+}n_{d,0}(z))\,\frac{\partial f}{\partial\omega_d}(u)\\ & -x\frac{\partial f}{\partial x}(u){+}\left\langle -\gamma{\odot}z{+}k_0,\frac{\partial f}{\partial z}(u)\right\rangle{+}M(\omega_p,\omega_d,w)\frac{\partial f}{\partial w}(u)\\ & +\lambda\left[f\left(u{+}we_1{+}k_1(z){\odot}\overline{e}_2{+}n_{p,1}(z)e_{\ell+2}{+}n_{d,1}(z)e_{\ell+3}\right){-}f\left(u\right)\right]\\ & +\beta(x)\left[f\left(u{-}g(x)e_1{+}k_2(z){\odot}\overline{e}_2{+}n_{p,1}(z)e_{\ell+2}{+}n_{d,1}(z)e_{\ell+3}\right){-}f(u)\right]\end{aligned}$$

with the following notations, e_i is the unit vectors for the coordinates with index i. The notation

$$\left(\frac{\partial f}{\partial z}(u)\right) \stackrel{\text{def.}}{=} \left(\frac{\partial f}{\partial u_i}(u), 2 \leqslant i \leqslant \ell+1\right)$$

is for the gradient vector with respect to the coordinates associated to z, i.e. from index 2 to index $\ell+1$. Finally $\bar{e}_2$ is the vector whose coordinates are 1 for the indices associated to z and 0 elsewhere and, for $a \in \mathbb{R}_+^\ell$, the quantity $a \odot \bar{e}_2$ is the vector whose ith coordinate is a_{i-1}, for $2 \leqslant i \leqslant \ell+1$, and 0 otherwise.

For sake of completeness, we detail the processes of fast variables for the classical STDP rules described in Section 1.2.

Pair-based models with exponential kernels Φ

For pair-based mechanisms, we follow the classification discussed in [MDG08]:

— For *all-to-all* pairings, each synaptic spike is paired with all previous post-synaptic spikes, and conversely. They are already described in the main text, by the set of equations, for $a \in \{p, d\}$,

$$\begin{cases} \mathrm{d}X(t) = -X(t)\,\mathrm{d}t + w\mathcal{N}_\lambda(\mathrm{d}t) - g\left(X(t-)\right)\mathcal{N}_{\beta,X}\left(\mathrm{d}t\right), \\ \mathrm{d}Z_{a,1}(t) = -\gamma_{a,1} Z_{a,1}(t)\,\mathrm{d}t + B_{a,1}\mathcal{N}_\lambda(\mathrm{d}t), \\ \mathrm{d}Z_{a,2}(t) = -\gamma_{a,2} Z_{a,2}(t)\,\mathrm{d}t + B_{a,2}\mathcal{N}_{\beta,X}(\mathrm{d}t). \end{cases}$$

— In the *nearest neighbor symmetric* scheme each pre-synaptic spike is paired with the last post-synaptic spike, and conversely. The system changes slightly:

$$\begin{cases} \mathrm{d}X(t) = -X(t)\,\mathrm{d}t + w\mathcal{N}_\lambda(\mathrm{d}t) - g\left(X(t-)\right)\mathcal{N}_{\beta,X}\left(\mathrm{d}t\right), \\ \mathrm{d}Z_{a,1}(t) = -\gamma_{a,1} Z_{a,1}(t)\,\mathrm{d}t + (B_{a,1} - Z_{a,1}(t-))\mathcal{N}_\lambda(\mathrm{d}t), \\ \mathrm{d}Z_{a,2}(t) = -\gamma_{a,2} Z_{a,2}(t)\,\mathrm{d}t + (B_{a,2} - Z_{a,2}(t-))\mathcal{N}_{\beta,X}(\mathrm{d}t). \end{cases}$$

The variable $Z_{a,1}$, resp. $Z_{a,2}$ is reset to $B_{a,1}$, resp. $B_{a,2}$, after a pre-synaptic spike, resp. post-synaptic spike.

— For *nearest neighbor symmetric reduced* scheme, where only immediate pairing matters, we have:

$$\begin{cases} \mathrm{d}X(t) = -X(t)\,\mathrm{d}t + w\mathcal{N}_\lambda(\mathrm{d}t) - g\left(X(t-)\right)\mathcal{N}_{\beta,X}\left(\mathrm{d}t\right), \\ \mathrm{d}Z_{a,1}(t) = -\gamma_{a,1} Z_{a,1}(t)\,\mathrm{d}t + (B_{a,1} - Z_{a,1}(t-))\mathcal{N}_\lambda(\mathrm{d}t) - Z_{a,1}(t-)\mathcal{N}_{\beta,X}(\mathrm{d}t), \\ \mathrm{d}Z_{a,2}(t) = -\gamma_{a,2} Z_{a,2}(t)\,\mathrm{d}t + (B_{a,2} - Z_{a,2}(t-))\mathcal{N}_{\beta,X}(\mathrm{d}t) - Z_{a,2}(t-)\mathcal{N}_\lambda(\mathrm{d}t), \end{cases}$$

for exponential pair-based models, with $n_{a,0}(z)=0$, $n_{a,1}(z)=z_{a,2}$ and $n_{a,2}(z)=z_{a,1}$.

Nearest pair-based models with general kernels Φ

In the case of nearest pair-based models, we have a simple description of the system, based on the time since the last spike as detailed in Section 1.3. We define $(Z(t))=(Z_1(t), Z_2(t))$, such that,

$$\begin{cases} \mathrm{d}Z_1(t) = \mathrm{d}t - Z_1(t-)\,\mathcal{N}_\lambda(\mathrm{d}t), \\ \mathrm{d}Z_2(t) = \mathrm{d}t - Z_2(t-)\,\mathcal{N}_{\beta,X}(\mathrm{d}t). \end{cases}$$

In this setting, both nearest models are of class $\mathcal{M}$:

— The nearest neighbor symmetric model of Relation (1.14), with

$$n_{a,0}(z)=0, \quad n_{a,1}(z)=\Phi_{a,2}(z_2), \quad n_{a,2}(z)=\Phi_{a,1}(z_1).$$

— The nearest neighbor symmetric reduced model of Relation (1.16), with

$$n_{a,0}(z)=0, \quad n_{a,1}(z)=\Phi_{a,2}(z_2)\mathbb{1}_{\{z_2\leqslant z_1\}}, \quad n_{a,2}(z)=\Phi_{a,1}(z_1)\mathbb{1}_{\{z_1\leqslant z_2\}}.$$

In fact, we have here two different Markovian systems that represents the same dynamics for nearest exponential STDP rules.

Triplet-based models

Generator for triplet-based mechanisms can also be defined in a similar way, see [BA16] for a list of different implementations.

— The suppression model of Section 1.A from [FD02], where the Markovian system is given by:

$$\begin{cases} \mathrm{d}X(t) = -X(t)\,\mathrm{d}t+w\mathcal{N}_\lambda(\mathrm{d}t)-g\left(X(t-)\right)\mathcal{N}_{\beta,X}\left(\mathrm{d}t\right), \\ \mathrm{d}Z_{a,1}(t) = -\gamma_{a,1}Z_{a,1}(t)\,\mathrm{d}t+(1-Z_{s,1}(t-))B_{a,1}\mathcal{N}_\lambda(\mathrm{d}t), \\ \mathrm{d}Z_{a,2}(t) = -\gamma_{a,2}Z_{a,2}(t)\,\mathrm{d}t+(1-Z_{s,2}(t-))B_{a,2}\mathcal{N}_{\beta,X}(\mathrm{d}t), \\ \mathrm{d}Z_{s,1}(t) = -\delta_1 Z_{s,1}(t)\,\mathrm{d}t+(1-Z_{s,1}(t-))\mathcal{N}_\lambda(\mathrm{d}t), \\ \mathrm{d}Z_{s,2}(t) = -\delta_2 Z_{s,2}(t)\,\mathrm{d}t+(1-Z_{s,2}(t-))\mathcal{N}_{\beta,X}(\mathrm{d}t), \end{cases}$$

with $n_{a,0}(z)=0$, $n_{a,1}(z)=(1-z_{s,1})z_{a,2}$ and $n_{a,2}(z)=(1-z_{s,2})z_{a,1}$.

— The triplet-based model, see [PG06a], we have:

$$\begin{cases} \mathrm{d}X(t) = -X(t)\,\mathrm{d}t+w\mathcal{N}_\lambda(\mathrm{d}t)-g\left(X(t-)\right)\mathcal{N}_{\beta,X}\left(\mathrm{d}t\right), \\ \mathrm{d}Z_{a,1}(t) = -\gamma_{a,1}Z_{a,1}(t)\,\mathrm{d}t+B_{a,1}\mathcal{N}_\lambda(\mathrm{d}t), \\ \mathrm{d}Z_{a,2}(t) = -\gamma_{a,2}Z_{a,2}(t)\,\mathrm{d}t+B_{a,2}\mathcal{N}_{\beta,X}(\mathrm{d}t), \\ \mathrm{d}Z_{s,a,1}(t) = -\delta_{a,1}Z_{s,a,1}(t)\,\mathrm{d}t+D_{a,1}\mathcal{N}_\lambda(\mathrm{d}t), \\ \mathrm{d}Z_{s,a,2}(t) = -\delta_{a,2}Z_{s,a,2}(t)\,\mathrm{d}t+D_{a,2}\mathcal{N}_{\beta,X}(\mathrm{d}t), \end{cases}$$

with $n_{a,0}(z)=0$, $n_{a,1}(z)=(1+z_{s,a,1})z_{a,2}$ and $n_{a,2}(z)=(1+z_{s,a,2})z_{a,1}$.

Calcium-based models

For models of calcium-based plasticity, we have:

— Calcium transients as exponential traces in [GB12], which is the dynamics used as an example in this paper. The system is,

$$\begin{cases} \mathrm{d}X(t) = -X(t)\,\mathrm{d}t+w\mathcal{N}_\lambda(\mathrm{d}t)-g(X(t-))\mathcal{N}_{\beta,X}(\mathrm{d}t), \\ \mathrm{d}C(t) = -\gamma C(t)\,\mathrm{d}t+C_1\mathcal{N}_\lambda(\mathrm{d}t)+C_2\mathcal{N}_{\beta,X}(\mathrm{d}t). \end{cases}$$

— Calcium transients modeled in a discrete setting as for the example in Section 1.4. The associated Markov process has the following transitions transition rates, for $(x,c)\in\mathbb{N}^2$,

$$(x,c)\longrightarrow\begin{cases}(x+w,c+C_1) & \lambda,\\ (x-1,c) & x,\end{cases}\qquad\longrightarrow\begin{cases}(x,c-1) & \gamma c,\\ (x-1,c+C_2) & \beta x.\end{cases}$$

The functions of calcium-based models are given by, for $a\in\{p,d\}$, $n_{a,0}(c)=h_a(c)$, $n_{a,1}(x,c)=0$ and $n_{a,2}(c)=0$.

Voltage-based models

Models of Section 1.A, which are adaptations of [CG10] by replacing the direct dependence on filtered traces of X, can also be analyzed with this formalism. The dynamics are given by

$$\begin{cases}\mathrm{d}X(t) = -X(t)\,\mathrm{d}t+w\mathcal{N}_\lambda(\mathrm{d}t)-g\left(X(t-)\right)\mathcal{N}_{\beta,X}\left(\mathrm{d}t\right),\\ \mathrm{d}Z_{p,1}(t) = -\gamma_{p,1}Z_{p,1}(t)\,\mathrm{d}t+\mathcal{N}_\lambda(\mathrm{d}t),\\ \mathrm{d}Z_{a,2}(t) = -\gamma_{a,2}Z_{a,2}(t)\,\mathrm{d}t+\mathcal{N}_{\beta,X}(\mathrm{d}t),\end{cases}$$

with $n_{a,0}(z)=n_{p,1}(z)=n_{d,2}(z)=0$, $n_{p,2}(z)=B_pz_{p,1}(z_{p,2}-\theta_d)^+$, $n_{d,1}(z)=B_d(z_{d,2}-\theta_d)^+$.

BIBLIOGRAPHY

[BA16] B. Babadi and L. F. Abbott. Stability and Competition in Multi-spike Models of Spike-Timing Dependent Plasticity. *PLoS computational biology* **12** (Mar. 2016), e1004750.

[Bil99] P. Billingsley. Convergence of Probability Measures. John Wiley & Sons, 1999.

[BP98] G.-q. Bi and M.-m. Poo. Synaptic Modifications in Cultured Hippocampal Neurons: Dependence on Spike Timing, Synaptic Strength, and Postsynaptic Cell Type. *Journal of Neuroscience* **18** (Dec. 1998), 10464–10472.

[CG10] C. Clopath and W. Gerstner. Voltage and Spike Timing Interact in STDP – A Unified Model. *Frontiers in Synaptic Neuroscience* **2** (July 2010).

[Chi01] E. Chichilnisky. A simple white noise analysis of neuronal light responses. *Network: Computation in Neural Systems* **12** (2001), 199–213.

[Clo+10] C. Clopath, L. Büsing, E. Vasilaki, and W. Gerstner. Connectivity reflects coding: a model of voltage-based STDP with homeostasis. *Nature Neuroscience* **13** (Mar. 2010), 344–352.

[Dav93] M. H. A. Davis. Markov models and optimization. London: Chapman & Hall, 1993.

[Daw93] D. A. Dawson. Measure-valued Markov processes. *École d'Été de Probabilités de Saint-Flour XXI—1991*. Vol. 1541. Lecture Notes in Math. Berlin: Springer, Nov. 1993, 1–260.

[FD02] R. C. Froemke and Y. Dan. Spike-timing-dependent synaptic modification induced by natural spike trains. *Nature* **416** (Mar. 2002), 433–438.

[Fel12] D. E. Feldman. The spike-timing dependence of plasticity. *Neuron* **75** (Aug. 2012), 556–571.

[FGV05] E. Fino, J. Glowinski, and L. Venance. Bidirectional activity-dependent plasticity at corticostriatal synapses. *The Journal of Neuroscience: The Official Journal of the Society for Neuroscience* **25** (Dec. 2005), 11279–11287.

[FSG10] N. Frémaux, H. Sprekeler, and W. Gerstner. Functional Requirements for Reward-Modulated Spike-Timing-Dependent Plasticity. *Journal of Neuroscience* **30** (2010), 13326–13337. eprint: `https://www.jneurosci.org/content/30/40/13326.full.pdf`.

[GB10] M. Graupner and N. Brunel. Mechanisms of induction and maintenance of spike-timing dependent plasticity in biophysical synapse models. *Frontiers in Computational Neuroscience* **4** (2010).

[GB12] M. Graupner and N. Brunel. Calcium-based plasticity model explains sensitivity of synaptic changes to spike pattern, rate, and dendritic location. *Proceedings of the National Academy of Sciences of the United States of America* **109** (Mar. 2012), 3991–3996.

[Ger+14] W. Gerstner, W. M. Kistler, R. Naud, and L. Paninski. Neuronal Dynamics: From Single Neurons to Networks and Models of Cognition. New York, NY, USA: Cambridge University Press, 2014.

[Güt+03] R. Gütig, R. Aharonov, S. Rotter, and H. Sompolinsky. Learning input correlations through nonlinear temporally asymmetric Hebbian plasticity. *The Journal of Neuroscience: The Official Journal of the Society for Neuroscience* **23** (May 2003), 3697–3714.

[Hel18] P. Helson. A new stochastic STDP Rule in a neural Network Model. *arXiv:1706.00364 [math]* (Mar. 2018).

[KGH99] R. Kempter, W. Gerstner, and J. L. van Hemmen. Hebbian learning and spiking neurons. *Physical Review E* **59** (Apr. 1999), 4498–4514.

[KH00] W. M. Kistler and J. L. v. Hemmen. Modeling Synaptic Plasticity in Conjunction with the Timing of Pre- and Postsynaptic Action Potentials. *Neural Computation* **12** (Feb. 2000), 385–405.

[Kin92] J. F. C. Kingman. Poisson Processes. Clarendon Press, Dec. 1992.

[LS08] E. V. Lubenov and A. G. Siapas. Decoupling through synchrony in neuronal circuits with propagation delays. *Neuron* **58** (Apr. 2008), 118–131.

[LS14] Y. Luz and M. Shamir. The Effect of STDP Temporal Kernel Structure on the Learning Dynamics of Single Excitatory and Inhibitory Synapses. *PLoS ONE* **9** (July 2014), e101109.

[MAD07] A. Morrison, A. Aertsen, and M. Diesmann. Spike-timing-dependent plasticity in balanced random networks. *Neural Computation* **19** (June 2007), 1437–1467.

[MDG08] A. Morrison, M. Diesmann, and W. Gerstner. Phenomenological models of synaptic plasticity based on spike timing. *Biological Cybernetics* **98** (June 2008), 459–478.

[PG06a] J.-P. Pfister and W. Gerstner. Triplets of Spikes in a Model of Spike Timing-Dependent Plasticity. *Journal of Neuroscience* **26** (Sept. 2006), 9673–9682.

[RBS16] B. S. Robinson, T. W. Berger, and D. Song. Identification of Stable Spike-Timing-Dependent Plasticity from Spiking Activity with Generalized Multilinear Modeling. *Neural Comput.* **28** (Nov. 2016), 2320–2351.

[RBT00a] M. C. van Rossum, G. Q. Bi, and G. G. Turrigiano. Stable Hebbian learning from spike timing-dependent plasticity. *The Journal of Neuroscience: The Official Journal of the Society for Neuroscience* **20** (Dec. 2000), 8812–8821.

[RLS01] J. Rubin, D. D. Lee, and H. Sompolinsky. Equilibrium properties of temporally asymmetric Hebbian plasticity. *Physical Review Letters* **86** (Jan. 2001), 364–367.

[Rob03] P. Robert. Stochastic Networks and Queues. Stochastic Modelling and Applied Probability. Berlin Heidelberg: Springer-Verlag, 2003.

[Rob99] P. D. Roberts. Computational Consequences of Temporally Asymmetric Learning Rules: I. Differential Hebbian Learning. *Journal of Computational Neuroscience* **7** (Nov. 1999), 235–246.

[RT16] P. Robert and J. Touboul. On the Dynamics of Random Neuronal Networks. *Journal of Statistical Physics* **165** (Nov. 2016), 545–584.

[RV21a] P. Robert and G. Vignoud. Averaging Principles for Markovian Models of Plasticity. *Journal of Statistical Physics* **183** (June 2021), 47–90.

[RV21c] P. Robert and G. Vignoud. Stochastic Models of Neural Synaptic Plasticity: A Scaling Approach. *SIAM Journal on Applied Mathematics* **81** (2021), 2362–2386.

[SBC02] H. Z. Shouval, M. F. Bear, and L. N. Cooper. A unified model of NMDA receptor-dependent bidirectional synaptic plasticity. *Proceedings of the National Academy of Sciences of the United States of America* **99** (Aug. 2002), 10831–10836.

[Sha92] C. J. Shatz. The Developing Brain. *Scientific American* **267** (1992), 60–67.

[SWW10] H. Shouval, S. Wang, and G. Wittenberg. Spike Timing Dependent Plasticity: A Consequence of More Fundamental Learning Rules. *Frontiers in Computational Neuroscience* **4** (2010), 19.

[TDM14] T. Takeuchi, A. J. Duszkiewicz, and R. G. M. Morris. The synaptic plasticity and memory hypothesis: encoding, storage and persistence. *Philosophical Transactions of the Royal Society of London. Series B, Biological Sciences* **369** (Jan. 2014), 20130288.

[TMK18] S. Tonegawa, M. D. Morrissey, and T. Kitamura. The role of engram cells in the systems consolidation of memory. *Nature Reviews Neuroscience* **19** (Aug. 2018), 485–498.

[TN04] G. G. Turrigiano and S. B. Nelson. Homeostatic plasticity in the developing nervous system. *Nature Reviews. Neuroscience* **5** (Feb. 2004), 97–107.

[VVT18] G. Vignoud, L. Venance, and J. D. Touboul. Interplay of multiple pathways and activity-dependent rules in STDP. *PLoS computational biology* **14** (2018), e1006184.

CHAPTER 2

STOCHASTIC MODELS OF NEURAL PLASTICITY: A SCALING APPROACH

ABSTRACT

In neuroscience, *synaptic plasticity* refers to the set of mechanisms driving the dynamics of neuronal connections, called *synapses* and represented by a scalar value, the *synaptic weight*. A Spike-Timing Dependent Plasticity (STDP) rule is a biologically-based model representing the time evolution of the synaptic weight as a functional of the past spiking activity of adjacent neurons. A general mathematical framework has been introduced in [RV21b].

In this paper we develop and investigate a scaling approach of these models based on several biological assumptions. Experiments show that long-term synaptic plasticity evolves on a much slower timescale than the cellular mechanisms driving the activity of neuronal cells, like their spiking activity or the concentration of various chemical components created/suppressed by this spiking activity. For this reason, a scaled version of the stochastic model of [RV21b] is introduced and a limit theorem, an averaging principle, is stated for a large class of plasticity kernels. A companion paper [RV21a] is entirely devoted to the tightness properties used to prove these convergence results.

These averaging principles are used to study two important STDP models: *pair-based rules* and *calcium-based rules*. Our results are compared with the approximations of neuroscience STDP models. A class of discrete models of STDP rules is also investigated for the analytical tractability of its limiting dynamical system.

2.1 Introduction

In [RV21b] we have introduced a general class of mathematical models to represent and study synaptic plasticity mechanisms. Their purpose is to investigate the synaptic weight dynamics, i.e. the evolution of the unilateral connection between two neurons. These models rely on two clearly stated hypotheses: the effect of plasticity is seen on the synaptic strength on *long timescales* and it only depends on the *relative timing of the spikes*. This type of plasticity, known as Spike-Timing-Dependent Plasticity (STDP), has been extensively studied in experimental and computational neuroscience, see [Fel12; MDG08] for references.

This paper is devoted to a scaling analysis of an important subclass of STDP rules, *Markovian plasticity kernels*. These kernels have a representation in terms of finite dimensional vectors whose coordinates are shot-noise processes. See Section 3 of [RV21b] and Section 2.2 below.

We start with a simple example of the models investigated in this paper. See Section 2.2 for a detailed presentation. The stochastic process can be represented by the following variables,

a. the membrane potential X of the output cell;

b. the synaptic weight W, modeling the strength of the connection from the input neuron to the output neuron.

When the input neuron is spiking (a *presynaptic spike*), a chemical/electrical signal is transmitted to the output neuron through the synapse. If the couple of variables (X, W) is (x, w) just before this event, it is then updated to $(x+w, w)$.

In state $X=x$, the output neuron emits a spike at rate $\beta(x)$, where β is *the activation function*. This is a *postsynaptic spike*. It is usually assumed that β is a nondecreasing function of the membrane potential X.

Consequently, after a presynaptic spike and the associated rise in membrane potential X, the probability that a postsynaptic spike occurs is increased. As seen in [RV21b], STDP synaptic mechanisms depend, in a complex way, on past spiking times of both adjacent neurons.

More formally, in our simple example, the time evolution is described by the following set of stochastic differential equations (SDEs),

$$\begin{cases} \mathrm{d}X(t) &= -X(t)\,\mathrm{d}t + W(t)\mathcal{N}_\lambda(\mathrm{d}t), \\ \mathrm{d}Z(t) &= -\gamma Z(t)\,\mathrm{d}t + B_1\mathcal{N}_\lambda(\mathrm{d}t) + B_2\mathcal{N}_{\beta,X}(\mathrm{d}t), \\ \mathrm{d}W(t) &= Z(t-)\mathcal{N}_{\beta,X}(\mathrm{d}t), \end{cases} \tag{2.1}$$

where $h(t-)$ is the left-limit of the function h at $t>0$ and, for $i=\{1,2\}$, $B_i\in\mathbb{R}_+$. Throughout the paper, the notation $(Y(t))$ is used to represent the stochastic process $t\mapsto Y(t)$ on $\mathbb{R}_+$.

We discuss briefly the random variables involved.

a. The point processes $\mathcal{N}_\lambda$ and $\mathcal{N}_{\beta,X}$.
These random variables are point processes representing the sequences of spike times of the pre- and postsynaptic neurons.

In the present work, $\mathcal{N}_\lambda$ is assumed to be a Poisson process with rate λ. It can be represented either as a nondecreasing sequence of points $(t_n, n\geqslant 1)$ of $\mathbb{R}_+$, or as nonincreasing function, the *counting measure*

$$t\mapsto\mathcal{N}_\lambda((0,t]) = \sum_{n\geqslant 1} \mathbb{1}_{\{t_n\leqslant t\}}$$

with jumps of size 1, or, finally as a random measure, the sum of Dirac measures at the points (t_n),

$$\mathcal{N}_\lambda(\mathrm{d}x) = \sum_{n\geqslant 1} \delta_{t_n}.$$

Each point t_n of $\mathcal{N}_\lambda(\mathrm{d}t)$ is associated to a presynaptic spike and the consequent increment of the postsynaptic membrane potential $X(t-)$ by $W(t)$.

The point process $\mathcal{N}_{\beta,X}$ accounts for the instants of the postsynaptic spikes.

It is a nonhomogeneous Poisson process with (random) intensity function $(\beta(X(t-)))$. See Relation (2.3) for a formal definition. See [Kin92] for an extensive introduction to Poisson processes and [Daw93] for theoretical aspects of random measures.

b. The process $(Z(t))$.
$(Z(t))$ encodes the past spiking activity of both neurons through an additive functional of $\mathcal{N}_\lambda$ and $\mathcal{N}_{\beta,X}$ with an exponential decay factor $\gamma>0$. It is not difficult to see that, for $t\geqslant 0$,

$$Z(t) = Z(0)+B_1\int_0^t e^{-\gamma(t-s)}\mathcal{N}_\lambda(\mathrm{d}s)+B_2\int_0^t e^{-\gamma(t-s)}\mathcal{N}_{\beta,X}(\mathrm{d}s).$$

See Lemma 2.1 of [RV21b]. In our general model, $(Z(t))$ is a multidimensional process which can be thought as a vector of cellular processes associated to the concentration of chemical components created/suppressed by the spiking activity of both neurons. See also [AK15] for a general presentation of stochastic processes in the context of biochemical systems.

c. The processes $(W(t))$. The synaptic weight W is increased at each jump of $\mathcal{N}_{\beta,X}$ by the value of $(Z(t))$.

From a biological point of view, the relevant process is $(W(t))$, because it describes the synaptic strength, i.e. the intensity of transmission between two connected neurons. This value can be measured through electrophysiological experiments for example. Many computational models have been developed to investigate synaptic plasticity in different contexts. See [MDG08; GB10; Clo+10; BA16; KGH99] and the references therein.

From a mathematical perspective, the variables $(X(t), Z(t), W(t))$, solutions of SDE (2.1) are central to the model. However, as will be seen in this article, the point process of instants of postsynaptic spikes $\mathcal{N}_{\beta,X}$ is the key component of the system since it drives the time evolution of $(Z(t))$ and $(W(t))$ and, consequently, of $(X(t))$.

Mathematical models of plasticity in the literature

Numerous works in physics have investigated mathematical models of plasticity. We quickly review some of them. Most studies focus on the dynamics of a collection of synaptic weights projecting to a single postsynaptic cell. There are basically two types of approximations used.

a. Separation of timescales.
The cellular processes are averaged to give a simpler dynamical system for the evolution of the synaptic weight. This is a classical approach in the literature. See [KGH99; RKO18; Eur+99; Rob00]. [ARJ20] uses an analogous description of the evolution of synaptic weights in the context of a mean-field approximation of several populations of neurons. This is the approach of the paper, see Section 2.1 below.

b. Fokker-Planck approach.
In this case, the time evolution of the synaptic strength alone is assumed to follow a diffusion process and, consequently, has the Markovian property. The analysis is done with the associated Fokker-Planck equations and the corresponding equilibrium distribution when it exists. See [RLS01; Hor+00; KH00; RBT00a]. An extension, the *Kramers-Moyal* expansion is also used in this context for some non-Markovian models, see [LF12]. We refer to [Paw67; Gar10] for general properties of the *Kramers-Moyal* expansion.

Mathematical studies of models of plasticity are quite scarce. Most models are centered on evolution equations of neural networks with a fixed synaptic weight. See Sections 1 and 2 of [RT16] for a review. In [AFH12] and [PSW17], an ODE/PDE approach for a population of leaky integrate-and-fire neurons is presented for a specific pair-based STDP rule. See [Che+15] for the connection between stochastic models and PDE models. [Hel18] investigates a Markovian model of a pair-based STDP rule. This is one of the few stochastic analyses in this domain.

Multiple timescales

An important feature of long-term neural plasticity explored in this paper is that there are essentially two different timescales in action.

On the one hand, the decay time of the membrane potential and the mean duration between two presynaptic spikes or two postsynaptic spikes are of the order of several milliseconds. See [GK02b]. Consequently, interacting pairs of spikes are on the same timescale. For example, pair-based models have an exponential decay whose inverse is around 50 milliseconds. See [BP98; FGV05]. Similarly, for calcium-based models, the calcium concentration decays with a time constant of the order of 20 milliseconds. See [GB12]. The stochastic process $(Z(t))$ represents fast cellular mechanisms associated to STDP and accordingly, its timescale is also of the same order.

On the other hand, the synaptic weight process $(W(t))$ changes on a much slower timescale. It can take seconds and even minutes to observe an effect of an STDP rule on the synaptic weight. See [BP98]. Computational models of synaptic plasticity have used similar scaling principles. Kempter et al. [KGH99] for the equation (1) of this reference for plasticity updates and with different neuronal dynamics, but built in the same framework, [KH00]. We can mention also [RBT00a], [Rob99; Rob00] where a separation of the timescales is also assumed. A final example is [RLS01] where the parameter λ speeds up the rate of pre- and postsynaptic spikes in the equation for plasticity updates.

Computational models of plasticity incorporate this timescale difference by only implementing small updates of the synaptic weights. However, it does not really take into account the fact that significant changes occur *after* the end of the experiment. To take into account this phenomenon, a possible approach consists in updating the synaptic weights with a fixed, or random, delay. This is not completely satisfactory since the evolution of the synaptic weight is generally believed to be an integrative process of past events rather than a delayed action. A more thorough analysis is done in Section SM2 of [RV21b]. Another approach which we will use consists in implementing this delay through an exponentially filtered process to represent the accumulation of past information.

It is important to stress here, that even if synaptic plasticity depends on the immediate timing of individual spikes, which happens on a fast timescale, it has a slow and delayed impact on the synaptic weight. This justifies the term of long-term plasticity and the fact that we can consider a separation of the timescales. Fast synaptic plasticity processes also exist, in the sense that they modulate the synaptic weight on the same timescale as the fast neuronal processes (spikes, membrane potential). This is referred to as *short-term* synaptic plasticity. See [ZR02]. For this type of dynamics, the timescale is of the order of milliseconds, much faster than the plasticity considered in this paper which can last several hours. This is not investigated in this paper. [Gal+19] analyzes

such models; in this case, separation of the timescales does not occur, and a mean-field approximation is developed.

The scaling approach of this paper represents the model as a *slow-fast* system. Neuronal processes, associated to the point processes $\mathcal{N}_\lambda$ and $\mathcal{N}_{\beta,X}$, occur on a timescale which is much faster than the timescale of the evolution of $(W(t))$. For our simple model, with the scaling, the SDE (2.1) becomes, for $\varepsilon{>}0$,

$$\begin{cases} \mathrm{d}X_\varepsilon(t) &= -X_\varepsilon(t)\,\mathrm{d}t/\varepsilon + W_\varepsilon(t)\mathcal{N}_{\lambda/\varepsilon}(\mathrm{d}t), \\ \mathrm{d}Z_\varepsilon(t) &= -\gamma Z_\varepsilon(t)\,\mathrm{d}t/\varepsilon + B_1\mathcal{N}_{\lambda/\varepsilon}(\mathrm{d}t) + B_2\mathcal{N}_{\beta/\varepsilon,X_\varepsilon}(\mathrm{d}t), \\ \mathrm{d}W_\varepsilon(t) &= Z_\varepsilon(s{-})\varepsilon\mathcal{N}_{\beta/\varepsilon,X_\varepsilon}(\mathrm{d}t). \end{cases}$$

As can be seen, the variables $(X_\varepsilon(t))$ and $(Z_\varepsilon(t))$ evolve on the timescale $t{\mapsto}t/\varepsilon$, with ε small; they are *fast variables*. The increments of the variable W are scaled with the parameter ε, and the integration of the differential element $\varepsilon\mathcal{N}_{\beta/\varepsilon,X_\varepsilon}(\mathrm{d}s)$ on a bounded time-interval is $O(1)$. For this reason, $(W_\varepsilon(t))$ is described as a *slow process*. This is a classical assumption in the corresponding models of statistical physics. Approximations of $(W_\varepsilon(t))$ when ε is small are discussed and investigated with ad hoc methods. The corresponding scaling results, known as separation of timescales, are routinely used in approximations in mathematical models of computational neuroscience; see, for example, [KGH99].

Mathematical proofs of averaging principles

In a mathematical context, these types of results are referred to as averaging principles. See [PSV77] and Chapter 7 of [FW98] for general presentation. They have been used to study various biochemical systems, see for example [Bal+06] and [KK+13]. See also the general presentation [BG06] in the context of dynamical systems and recent developments in [KP17]. We discuss the specific difficulties to prove such convergence results in our stochastic models of STDP rules:

a. Tightness of functionals of occupation measures.
Recall that the fast process is $(X_\varepsilon(t), Z_\varepsilon(t))$. Part of the technical problems of the proof of an averaging principle is related to the tightness properties of linear functionals of the fast process occupation measures.

The main difficulty originates, as could be expected, from the scaled point process $\varepsilon\mathcal{N}_{\beta/\varepsilon,X_\varepsilon}(\mathrm{d}s)$ associated to postsynaptic spikes and, more precisely, from the tightness of families of processes of the form

$$\left(\int_0^t Z_\varepsilon(s)\varepsilon\mathcal{N}_{\beta/\varepsilon,X_\varepsilon}(\mathrm{d}s)\right). \tag{2.2}$$

This is done in the paper by [RV21a]. If the model was expressed in terms of functionals of the occupation measure of type

$$\left(\int_0^t F(X_\varepsilon(s), Z_\varepsilon(s))\,\mathrm{d}s\right),$$

where $s{\to}F(X_\varepsilon(s), Z_\varepsilon(s))$ is a bounded continuous function on $\mathbb{R}_+$, as it is usually the case, the proof of this tightness property would be quite simple. From this

point of view, this is the case of [Bal+06], Kang and Kurtz [KK+13]. In these papers the proof of the tightness results associated to occupation measures is essentially achieved through a quite direct use of [Kur92]. There are technical difficulties, of course, but they are not related to these functionals of occupation measures. The only (unpublished) paper we know that establishes an averaging principle for a specific pair-based rule of Wilson-Cowan models of neural networks is [Hel18] and here too, this is a quite direct application of [Kur92].

Due to our quite general framework it does not seem to be possible to handle functionals of the form (2.2) with this approach. The process $(Z_\varepsilon(s))$ is not bounded, and neither is the differential element $\mathcal{N}_{\beta/\varepsilon,X_\varepsilon}(\mathrm{d}s)$ since $(\beta(X_\varepsilon(s))$ is also not bounded. The proof of this tightness result motivates a large part of the most technical estimates of [RV21a].

For our general models of [RV21a] the tightness properties are stated on an a priori, *bounded time interval* $[0, S_0)$ only. More specifically, it is shown that it may happen that the limit in distribution of $(W_\varepsilon(t_0))$ as ε goes to 0 blows up, i.e., hits infinity in finite time t_0. Contrary to all slow-fast results mentioned above where this phenomenon does not occur, convergence is proved on the real half-line. This is an indication perhaps that some stochastic processes have to be controlled carefully and that the difficulty of the tightness results mentioned above is not an artifact of the method used.

b. Regularity properties.
The results of the paper by [RV21a] do not provide convergence results as such. This is the purpose of the present paper of having convergence results and explicit expressions of the asymptotic dynamical system. To have a convergence result as in this paper, regularity properties of the invariant distribution Π_w of the fast process $(X_\varepsilon(t), Z_\varepsilon(t))$ when the synaptic weight is fixed at w have to be established. A typical property is that

$$w \longrightarrow \int_{\mathbb{R}_+^{\ell+1}} G(x,z)\pi_w(\mathrm{d}x,\mathrm{d}z)$$

is locally Lipschitz for some function G on $\mathbb{R}_+^{\ell+1}$. This is a delicate question in general, and there are very few cases where an explicit expression of Π_w is known. This type of result can be proved if there exists a "uniform" Lyapunov function on a neighborhood of w, see [Has80]. Sections 3 and 4 of our paper are devoted to the proof of these type of results. Different arguments are used.

Contributions

A scaled version of Markovian plasticity kernels as introduced in [RV21b] is presented in Section 2.2. The difficulty is to take into account the two different timescales mentioned above. This is done by assuming that the membrane potential X is a "fast" variable, i.e. that it evolves on a fast timescale. An averaging principle for the synaptic weight process has to be established in this context.

Under convenient assumptions, an averaging principle, Theorem 12, shows that the evolution equation of the synaptic weight $(W(t))$ converges to a deterministic dynamical

system as ε goes to 0. The proof of this quite technical result uses tightness results proved in the companion paper by [RV21a].

Sections 2.3 and 2.4 investigate the implications of averaging principles for classical models of pair-based and calcium-based STDP rules. In particular, we work out explicit results for the time evolution of the synaptic weight for several pair-based rules. Related results of the literature in physics are discussed in Section 2.3.

For calcium-based STDP models, the situation is more complicated since an explicit representation of invariant distributions of a class of Markov processes is required to express the asymptotic time evolution of the synaptic weight. Section 2.5 considers an analytically tractable discrete model of calcium-based STDP rules introduced in [RV21b]. With a scaling approach similar to that of Section 2.2, the dynamical system verified by the asymptotic synaptic weight can be investigated and an explicit representation of the invariant distributions of the corresponding Markov processes has been obtained in [RV21b].

2.2 A scaling approach

We begin with some formal definitions. Two independent point processes are defined on the probability space,

a. $\mathcal{N}_\lambda$ is the Poisson process with rate $\lambda{>}0$;

b. $\mathcal{P}$ is an homogeneous Poisson point process on $\mathbb{R}_+^2$ with rate 1.

If h is a càdlàg function and $(V(t))$ a càdlàg process, we define $\mathcal{N}_{h,V}$ the point process on $\mathbb{R}_+$ by

$$\int_{\mathbb{R}_+} f(u)\mathcal{N}_{h,V}(\mathrm{d}u) \stackrel{\text{def.}}{=} \int_{\mathbb{R}_+^2} f(u)\mathbb{1}_{\{s\in(0,h(V(u-))]\}}\mathcal{P}(\mathrm{d}s,\mathrm{d}u), \tag{2.3}$$

for any nonnegative Borelian function f on $\mathbb{R}_+$, where $\mathcal{P}$ is a homogeneous Poisson point process on $\mathbb{R}_+^2$ with rate 1. The filtration of the space contains the natural filtrations of $\mathcal{N}_\lambda$ and $\mathcal{P}$. See [RV21b].

Markovian plasticity kernels

We go back to the general Markovian formulation of STDP developed in [RV21b]. Important features are added to the simple model described in the introduction:

— The dynamics of the membrane potential X is unchanged, except for the influence of a postsynaptic spike on X, which is now modeled by a general decrease $x{\to}g(x){\geqslant}0$.

— We consider a multidimensional fast plasticity process $(Z(t))$ in $\mathbb{R}_+^\ell$, that can encode the activity of several chemical components. They can be defined as *shot-noise processes*. A shot-noise process $(S(t))$ associated to a point process $\mathcal{P}$ on $\mathbb{R}_+$ with amplitude $k(\cdot)$ and exponential decay $\alpha{>}0$ is a solution of the SDE,

$$\mathrm{d}S(t) = -\alpha S(t){+}k(S(t-))\mathcal{P}(\mathrm{d}t).$$

See [GP60] for the corresponding definition. In our case $(Z(t))$ is a vector of shot-noise processes associated to $\mathcal{N}_\lambda$ and/or $\mathcal{N}_{\beta,X}$, with amplitude $(k_i(\cdot))$, $i{=}1$, 2. See Relation (2.4) below. In this paper, the term "shot-noise process" will refer to the stochastic process defined in this reference, and not to a specific source of neuronal noise, as is usually the case in neurosciences.

— The influence of these fast plasticity variables is integrated through general functionals $z{\to}n_{a,i}(z){\geqslant}0$ with exponential decay into two slow variables Ω_a. In particular, the process $(\Omega_p(t))$ (resp., $(\Omega_d(t))$) encodes in some way the memory of the spiking activity leading to potentiation, i.e., increasing the synaptic weight (resp., to depression, i.e., decreasing the synaptic weight).

— The synaptic weight W is updated thanks to a functional M of both slow plasticity variables and its current value.

More rigorously, the random variable $(X(t), Z(t), \Omega_p(t), \Omega_d(t), W(t))$ is a Markov process, solution of the SDE

$$\left\{\begin{array}{ll} \mathrm{d}X(t) & = -X(t)\,\mathrm{d}t + W(t)\mathcal{N}_\lambda(\mathrm{d}t) - g\left(X(t-)\right)\mathcal{N}_{\beta,X}\left(\mathrm{d}t\right), \\ \mathrm{d}Z(t) & = (-\gamma \odot Z(t) + k_0)\,\mathrm{d}t \\ & \qquad\qquad +k_1(Z(t-))\mathcal{N}_\lambda(\mathrm{d}t) + k_2(Z(t-))\mathcal{N}_{\beta,X}(\mathrm{d}t), \\ \mathrm{d}\Omega_a(t) & = -\alpha\Omega_a(t)\,\mathrm{d}t + n_{a,0}(Z(t))\,\mathrm{d}t \\ & \quad +n_{a,1}(Z(t-))\mathcal{N}_\lambda(\mathrm{d}t) + n_{a,2}(Z(t-))\mathcal{N}_{\beta,X}(\mathrm{d}t), \quad a{\in}\{p,d\}, \\ \mathrm{d}W(t) & = M\left(\Omega_p(t), \Omega_d(t), W(t)\right)\mathrm{d}t. \end{array}\right. \tag{2.4}$$

where $(Z(t))$ is a nonnegative ℓ-dimensional process, $\ell{\geqslant}1$, and the following hold:

— $\gamma{\in}\mathbb{R}_+^\ell$, $a{\odot}b{=}(a_i{\times}b_i)$ if $a{=}(a_i)$ and $b{=}(b_i)$ in $\mathbb{R}_+^\ell$.

— $k_0{\in}\mathbb{R}_+^\ell$ is a constant and k_1 and k_2 are measurable functions from $\mathbb{R}_+^\ell$ to $\mathbb{R}^\ell$. Furthermore, the (k_i) are such that the function $(z(t))$ has values in $\mathbb{R}_+^\ell$ whenever $z(0){\in}\mathbb{R}_+^\ell$.

— For $i{=}0$, 1, 2, $n_{a,i}$ is a nonnegative measurable function on $\mathbb{R}_+^\ell$.

— M is a general measurable function.

The firing instants of the output neuron are the jumps of the point process $\mathcal{N}_{\beta,X}$ on $\mathbb{R}_+$, and the presynaptic spikes are represented by the Poisson process $\mathcal{N}_\lambda$.

See [RV21b] for more details. Recall the set of assumptions used in this reference.

Assumptions A

a. Firing rate function.
β is a nonnegative, continuous function on $\mathbb{R}$, and $\beta(x){=}0$ for $x{\leqslant}{-}c_\beta{\leqslant}0$.

b. Drop of potential after firing.
g is continuous on $\mathbb{R}$ and $0{\leqslant}g(x){\leqslant}\max(c_g, x)$ holds for all $x{\in}\mathbb{R}$, for $c_g{\geqslant}0$.

c. Dynamic of plasticity.
There exists an interval $K_W \subset \mathbb{R}$ such that, for any càdlàg piecewise-continuous functions h_1 and h_2 on $\mathbb{R}_+$, the ODE

$$\frac{\mathrm{d}w(t)}{\mathrm{d}t} = M(h_1(t), h_2(t), w(t)) \tag{2.5}$$

for all points of continuity of h_1 and h_2 has a unique continuous solution $(w(t))$ such that $w(t) \in K_W$ for all $t \geqslant 0$ when $w(0) \in K_W$.

A scaled model of Markovian plasticity of kernels

To take into account the multiple timescales mentioned in the introduction, a scaling parameter $\varepsilon > 0$ is introduced for stochastic processes following (2.4):

a. The exponential decay of $(X(t))$, $(Z(t))$ and the rates λ and $\beta(\cdot)$ are scaled with the factor $1/\varepsilon$.

b. The functions $n_{a,i}$, $a \in \{p, d\}$, $i \in \{1, 2\}$, associated to synaptic updates due to neuronal spikes are scaled by ε.

The initial condition of $(U_\varepsilon(t))$ is assumed to be fixed:

$$U_\varepsilon(0) = U_0 = (x_0, z_0, \omega_{0,p}, \omega_{0,d}, w_0). \tag{2.6}$$

This leads to the definition of a scaled version of the system (2.4), where we denote $(U_\varepsilon(t)) = (X_\varepsilon(t), Z_\varepsilon(t), \Omega_{\varepsilon,p}(t), \Omega_{\varepsilon,d}(t), W_\varepsilon(t))$:

$$\begin{cases} \mathrm{d}X_\varepsilon(t) &= -\dfrac{1}{\varepsilon} X_\varepsilon(t)\,\mathrm{d}t + W_\varepsilon(t)\mathcal{N}_{\lambda/\varepsilon}(\mathrm{d}t) - g\left(X_\varepsilon(t-)\right)\mathcal{N}_{\beta/\varepsilon, X_\varepsilon}\left(\mathrm{d}t\right), \\ \mathrm{d}Z_\varepsilon(t) &= \dfrac{1}{\varepsilon}\Big(-\gamma \odot Z_\varepsilon(t) + k_0\Big)\,\mathrm{d}t \\ &\qquad + k_1(Z_\varepsilon(t-))\mathcal{N}_{\lambda/\varepsilon}(\mathrm{d}t) + k_2(Z_\varepsilon(t-))\mathcal{N}_{\beta/\varepsilon, X_\varepsilon}(\mathrm{d}t), \\ \mathrm{d}\Omega_{\varepsilon,a}(t) &= -\alpha\Omega_{\varepsilon,a}(t)\,\mathrm{d}t + n_{a,0}(Z_\varepsilon(t))\,\mathrm{d}t \\ &\qquad + \varepsilon\Big(n_{a,1}(Z_\varepsilon(t-))\mathcal{N}_{\lambda/\varepsilon}(\mathrm{d}t) + n_{a,2}(Z_\varepsilon(t-))\mathcal{N}_{\beta/\varepsilon, X_\varepsilon}(\mathrm{d}t)\Big), \; a \in \{p, d\}, \\ \mathrm{d}W_\varepsilon(t) &= M\left(\Omega_{\varepsilon,p}(t), \Omega_{\varepsilon,d}(t), W_\varepsilon(t)\right)\mathrm{d}t. \end{cases} \tag{2.7}$$

From Relations (2.7), the dynamics of the processes $(\Omega_{\varepsilon,p}(t))$, $(\Omega_{\varepsilon,d}(t))$ and $(W_\varepsilon(t))$ is slow in the sense that the fluctuations within a bounded time-interval are limited either because of the deterministic differential element $\mathrm{d}t$ with a locally bounded coefficient, or via a driving Poisson process with rate of order $1/\varepsilon$ but with jumps of size proportional to ε. The processes $(X_\varepsilon(t))$ and $(Z_\varepsilon(t))$ are fast, for each of them the fluctuations are driven either by the deterministic differential element $\mathrm{d}t/\varepsilon$, or the jumps of Poisson point processes with rates of the order of $1/\varepsilon$.

Averaging principles

We are interested in the limiting behavior of the synaptic weight process $(W_\varepsilon(t))$ when the scaling parameter ε goes to 0. An intuitive, rough picture of the results that can be obtained is as follows: for ε small enough, on a small time-interval, the slow process $(\Omega_{p,\varepsilon}(t), \Omega_{d,\varepsilon}(t), W_\varepsilon(t))$ is almost constant, and, due to its fast timescale, the process $(X_\varepsilon(t), Z_\varepsilon(t))$ is "almost" at its equilibrium distribution Π_w associated to the current value of $(W_\varepsilon(t))$. If this statement holds in an appropriate way, we can then write a deterministic ODE for the time evolution of a possible limit of $(\Omega_{p,\varepsilon}(t), \Omega_{d,\varepsilon}(t), W_\varepsilon(t))$.

We now introduce the framework of our main theorem concerning averaging principles. If we set the process $(W_\varepsilon(t))$ to be a constant equal to w, the time evolution of $(X_\varepsilon(t), Z_\varepsilon(t))$ in Relation (2.7) has the Markov property. The corresponding process will be referred to as the fast process. Its infinitesimal generator is defined as follows: if $f \in \mathcal{C}_b^1\left(\mathbb{R}_+ \times \mathbb{R}^\ell\right)$, $w \in K_W$ and $(x,z) \in \mathbb{R} \times \mathbb{R}_+^\ell$, then

$$B_w^F(f)(x,z) \stackrel{\text{def.}}{=} -x\frac{\partial f}{\partial x} + \left\langle -\gamma \odot z + k_0, \frac{\partial f}{\partial z}(x,z) \right\rangle + \lambda \Big[f(x+w, z+k_1(z)) - f(x,z) \Big] + \beta(x) \Big[f(x-g(x), z+k_2(z)) - f(x,z) \Big]. \quad (2.8)$$

We now introduce a set of general assumptions driving the system (2.4).

Assumptions B

a. There exists $C_\beta \geqslant 0$ such that

$$\beta(x) \leqslant C_\beta(1+|x|) \quad \forall x \in \mathbb{R}. \quad (2.9)$$

b. All coordinates of the vector γ are positive. There exists $C_k \geqslant 0$ such that $0 \leqslant k_0 \leqslant C_k$ and the functions k_i, $i=1, 2$, in $\mathcal{C}_b^1(\mathbb{R}_+^\ell, \mathbb{R}_+^\ell)$, are upper-bounded by $C_k \geqslant 0$.

c. There exists a constant C_n such that, for $j \in \{0,1,2\}$, $a \in \{p,d\}$, the function $n_{a,j}$ is assumed to be nonnegative and Borelian such that

$$n_{a,j}(z) \leqslant C_n(1+\|z\|)$$

for $z \in \mathbb{R}_+^\ell$, where $\|z\| = z_1 + \cdots + z_\ell$. Additionally, for any $w \in K_W$, the discontinuity points of

$$(x,z) \mapsto (n_{a,0}(z), n_{a,1}(z), \beta(x) n_{a,2}(z))$$

for $a \in \{p,d\}$ are negligible for the probability distribution Π_w of the operator defined by Relation (2.8).

d. M can be decomposed as, $M(\omega_p, \omega_d, w) = M_p(\omega_p, w) - M_d(\omega_d, w) - \mu w$, where $M_a(\omega_a, w)$ is nonnegative continuous function, nondecreasing on the first coordinate for a fixed $w \in K_w$, and,

$$M_a(\omega_a, w) \leqslant C_M(1+\omega_a),$$

for all $w \in K_W$, for $a \in \{p,d\}$.

Note that, in the (large) list of STDP models presented in [RV21b], only the fast processes of triplet-based and voltage-based models may not verify these assumptions; in particular, the functions $n_{a,i}$ depend on the product of different shot-noises $Z(t)$. Nevertheless, Assumptions B result mainly from technical arguments, and is in any way necessary to obtain Theorem 12. An extension using quadratic functions $n_{a,i}$ instead of linear ones may be proved using the stronger analytical estimations in the proof.

We can now state the main result concerning the scaled model. Its proof is the main result of the paper by [RV21a].

Theorem 12 (Averaging principle)**.** *Under Assumptions A and B and for initial conditions satisfying Relation* (2.6)*, there exists $S_0 \in (0, +\infty]$, such that the family of processes $(\Omega_{p,\varepsilon}(t), \Omega_{d,\varepsilon}(t), W_\varepsilon(t), t<S_0)$, $\varepsilon \in (0,1)$, of the system* (2.7)*, is tight for the convergence in distribution.*

As ε goes to 0, any limiting point $(\omega_p(t), \omega_a(t), w(t), t<S_0)$, satisfies the ODEs, for $a \in \{p, d\}$,

$$\begin{cases} \dfrac{\mathrm{d}\omega_a(t)}{\mathrm{d}t} = -\alpha\omega_a(t) + \displaystyle\int_{\mathbb{R}\times\mathbb{R}_+^\ell} \Big[n_{a,0}(z) + \lambda n_{a,1}(z) + \beta(x) n_{a,2}(z) \Big] \, \Pi_{w(t)}(\mathrm{d}x, \mathrm{d}z), \\ \dfrac{\mathrm{d}w(t)}{\mathrm{d}t} = M(\omega_p(t), \omega_d(t), w(t)), \end{cases} \tag{2.10}$$

where, for $w \in K_W$, Π_w is the unique invariant distribution Π_w on $\mathbb{R}\times\mathbb{R}_+^\ell$ of the Markovian operator B_w^F defined by Relation (2.8)*.*

If K_W is bounded, then $S_0 = +\infty$ almost surely.

Remarks

We quickly discuss several aspects of these results.

a. Uniqueness.
If Relation (2.10) has a unique solution for a given initial state, the convergence in distribution of $(W_\varepsilon(t))$ when ε goes to 0 is therefore obtained. Such a uniqueness result holds if the integrand, with respect to s, of the right-hand side of Relation (2.10) is locally Lipschitz as a function of $w(s)$. One therefore has to investigate regularity properties of the invariant distribution Π_w as a function of w. This is a quite technical topic; however, methods based on classical results of perturbation theory and their generalizations in a stochastic context (see [Has80]), can be used to prove this type of properties. These problems are investigated for several important examples in Sections 2.3, 2.4, and 2.5.

b. Blow-up phenomenon.
The convergence properties are stated on a fixed time interval $[0, S_0)$. The reason is that, for some of our models the variable S_0 is finite. The limit in distribution of $(W_\varepsilon(t))$, as ε goes to 0, blows up, i.e., hits infinity in finite time. An analog property holds for some mathematical models of large nonplastic random neural networks. In this case, the blow-up phenomenon is the result of mutually exciting dynamics. In our case, the strengthening of the connection may grow without bounds when the function $z \mapsto n_2(z)$ exhibits some linear growth with respect to z and when the activation function β also has a linear growth. See [RV21a].

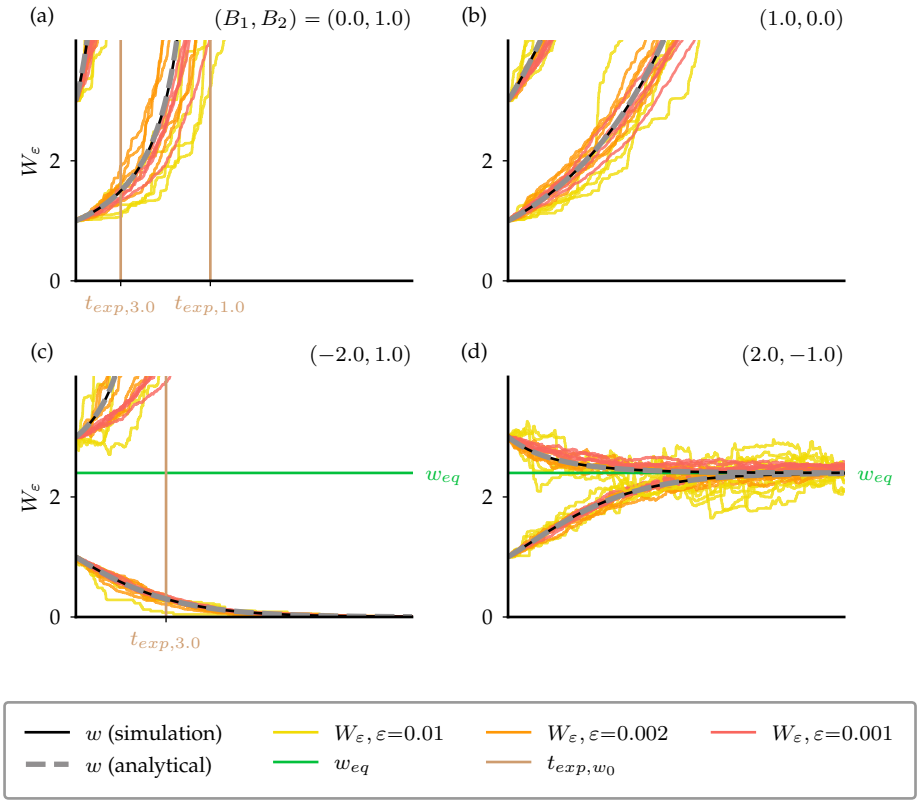

Figure 2.1: **Applications of Theorem 12 to the simple model of Section 2.1.**

Simple model dynamics

To illustrate Theorem 12, we go back to the simple model detailed in Section 2.1. We present in Figure 2.1 different possible behaviors of the asymptotic dynamics, for different values of B_1 and B_2. We represent the scaled process for different values of ε (in yellow, orange and red), the simulated ODE of the asymptotic dynamics (in black) and the analytical solution of the same ODE (in grey, dotted line). In all cases, the scaled processes converge indeed towards the solution of the ODE. We simulated the different processes starting from two deterministic initial values w_0=1.0 and w_0=3.0. In particular, we observe different asymptotic regimes:

(a) The scaled system converges to an ODE that explodes in finite time for all initial conditions. The time of explosion t_{exp,w_0} depends on the initial condition.

(b) The limiting ODE leads to solutions of $w(t)$ that diverge towards $+\infty$ but that do not explode.

(c) Depending on the initial condition (relative to w_{eq}), the asymptotic $w(t)$ either converges to 0 ($w_0 < w_{eq}$) or explodes in finite time ($w_0 > w_{eq}$).

(d) The scaled processes converge to an ODE that has a stable fixed point w_{eq}, and all the asymptotic processes w converge to this value.

We have shown with this simple example that the blow-up phenomenon does not only result from technical arguments but does indeed take place for some systems.

Moreover, we also highlight the fact that depending on the initial conditions, several behaviors are possible as in Figure 2.1(c).

Several important examples of pair-based and calcium-based models are now investigated in light of Theorem 12. In order to have simpler expressions, we restrict our study in the following sections to the linear neuron without reset receiving excitatory inputs, leading to the following set of assumptions,

Assumptions L (Linear)

a. The initial conditions of Relation (2.6) are such that $U_0{=}(0, 0_\ell, 0, 0, 0)$.

b. The output neuron is without reset; i.e., the function g is null. The SDE associated to the membrane potential is

$$\mathrm{d}X^w(t) = -X^w(t)\,\mathrm{d}t + w\,\mathcal{N}_\lambda(\mathrm{d}t). \tag{2.11}$$

c. There are only excitatory inputs, i.e., $0{\subset}K_W{\subset}\mathbb{R}_+$.

d. M verifies Assumptions A-c and B-d and is L_M-Lipschitz.

e. The activation function is linear, $\beta(x){=}\nu{+}\beta x$, $x{\geqslant}0$ for $\nu{\geqslant}0$ and $\beta{>}0$.

In that case, X stays in $\mathbb{R}^+$ and we can have an explicit expression of the stationary distribution of the important point process $\mathcal{N}_{\beta,X^w}$.

Proposition 13. *Under Assumptions L, if $(X^w_\infty(t), -\infty{\leqslant}t{\leqslant}{+}\infty)$ is a stationary version of SDE* (2.11)*, then the point process $\mathcal{N}_{\beta,X^w_\infty}$ of Relation* (2.3) *extended on the real line is stationary, and if f is a bounded Borelian function with compact support on $\mathbb{R}$, then*

$$\begin{aligned}-\ln\mathbb{E}\left[\exp\left(-\int_{-\infty}^{+\infty} f(s)\mathcal{N}_{\beta,X^w_\infty}(\mathrm{d}s)\right)\right]\\ = \nu\int_{-\infty}^{+\infty}\left(1{-}e^{-f(s)}\right)\mathrm{d}s{+}\lambda\int_{-\infty}^{+\infty}\left(1{-}\exp\left(-\beta w\int_0^{+\infty}\left(1{-}e^{-f(s+t)}\right)e^{-t}\,\mathrm{d}t\right)\right)\mathrm{d}s.\end{aligned} \tag{2.12}$$

Proof. Setting

$$(X^w_\infty(t)) \overset{\text{def.}}{=} \left(w\int_{-\infty}^{t} e^{-(t-s)}\mathcal{N}_\lambda(\mathrm{d}s)\right), \tag{2.13}$$

it is easily seen that this process is almost surely defined and that it satisfies Relation (2.11). The stationarity property of $(X^w_\infty(t))$ and, consequently of $\mathcal{N}_{\beta,X^w_\infty}$, comes from the invariance by translation of the distribution of $\mathcal{N}_\lambda$.

The independence of $\mathcal{P}$ and $\mathcal{N}_\lambda$, and the formula for the Laplace transform of Poisson point processes (see Proposition 1.5 of [Rob03]) give the relation

$$\mathbb{E}\left[\exp\left(-\int_{-\infty}^{+\infty} f(s)\mathcal{N}_{\beta,X^w_\infty}(\mathrm{d}s)\right)\right] = \mathbb{E}\left[\exp\left(-\int_{-\infty}^{+\infty}\left(1{-}e^{-f(s)}\right)\beta(X^w_\infty(s))\,\mathrm{d}s\right)\right].$$

If F is a nonnegative bounded Borelian function with compact support on $\mathbb{R}$, with Relation (2.13) and Fubini's theorem, we get

$$\int_{-\infty}^{+\infty} F(s)X^w_\infty(s)\,\mathrm{d}s = \int_{-\infty}^{+\infty}\left(w\int_0^{+\infty} F(u{+}s)e^{-s}\,\mathrm{d}s\right)\mathcal{N}_\lambda(\mathrm{d}u). \tag{2.14}$$

We conclude the proof by using again the formula for the Laplace transform of $\mathcal{N}_\lambda$

$$\mathbb{E}\left[\exp\left(-\int_{-\infty}^{+\infty} g(s)\mathcal{N}_\lambda(\mathrm{d}u)\right)\right] = \mathbb{E}\left[\exp\left(-\lambda\int_{-\infty}^{+\infty}\left(1-e^{-g(u)}\right)\mathrm{d}u\right)\right].$$

where the function g is defined by

$$g(u) \stackrel{\text{def.}}{=} \beta w \int_0^{+\infty}\left(1-e^{-f(s+u)}\right)e^{-s}\,\mathrm{d}s, \quad u\geqslant 0.$$

The proposition is proved.

□

2.3 Pair-based rules

We investigate scaled models of pair-based rules (see [RV21a]) with Assumptions L. In this setting, we are able to derive a closed form expression of the asymptotic equation (2.10).

All-to-all model

We recall the Markovian formulation of the all-to-all pair-based model with exponential functions Φ. All pairs of pre- and postsynaptic spikes are taken into account in the processes $(\Omega_a(t))$, $a\in\{p,d\}$. See Section 3.1.3 of [RV21b]. In our framework, this is defined as follows.

Assumptions PA
For $w\geqslant 0$, the fast process associated to the operator B_w^F of Relation (2.8) is expressed as $(X^w(t), Z^w(t))$, where $(X^w(t))$ is the solution of Relation (2.11) and

$$\begin{cases}\mathrm{d}Z_{a,1}^w(t) = -\gamma_{a,1}Z_{a,1}^w(t)\,\mathrm{d}t + B_{a,1}\,\mathcal{N}_\lambda(\mathrm{d}t),\\ \mathrm{d}Z_{a,2}^w(t) = -\gamma_{a,2}Z_{a,2}^w(t)\,\mathrm{d}t + B_{a,2}\,\mathcal{N}_{\beta,X^w}(\mathrm{d}t),\end{cases} \tag{2.15}$$

for $a\in\{p,d\}$, where $\gamma=(\gamma_{a,i})>0$ and $B=(B_{a,i})$ in $\mathbb{R}_+^4$. For $a\in\{p,d\}$ the process $(\Omega_a(t))$ is such that

$$\mathrm{d}\Omega_a(t) = -\alpha\Omega_a(t)\,\mathrm{d}t + Z_{a,2}(t-)\mathcal{N}_\lambda(\mathrm{d}t) + Z_{a,1}(t-)\mathcal{N}_{\beta,X}(\mathrm{d}t).$$

i.e., $n_{a,0}\equiv 0$, $n_{a,1}(z)=z_{a,2}$, and $n_{a,2}(z)=z_{a,1}$ for $z\in\mathbb{R}_+^4$.

We denote Π_w^{PA} the invariant distribution of the process $(X^w(t), Z^w(t))$. The existence of Π_w^{PA} is given by Proposition 4 of Section 5 of [RV21a].

Proposition 14. *Under Assumptions L and PA, then for* $a\in\{p,d\}$,

$$\int_{\mathbb{R}\times\mathbb{R}_+^4}(n_{a,0}(z)+\lambda n_{a,1}(z)+\beta(x)n_{a,2}(z))\Pi_w^{\mathrm{PA}}(\mathrm{d}x,\mathrm{d}z) = \frac{\nu}{\beta\lambda}\Lambda_{a,1} + (\Lambda_{a,1}+\Lambda_{a,2})\,w.$$

with

$$\Lambda_{a,1} = \beta\lambda^2\left(\frac{B_{a,1}}{\gamma_{a,1}}+\frac{B_{a,2}}{\gamma_{a,2}}\right) \text{ and } \Lambda_{a,2}=\beta\lambda\frac{B_{a_1}}{1+\gamma_{a,1}}. \tag{2.16}$$

Proof. Assume that the initial point of SDE (2.15) is a random variable (X^w, Z^w) with distribution Π_w^{PA}.

For $a{\in}\{p,d\}$, it is easily seen that $\mathbb{E}\left[Z_{a,1}^w\right]{=}\lambda B_{a,1}/\gamma_{a,1}$ and $\mathbb{E}\left[X^w\right]{=}\lambda w$. Denote $(Y^w(t)){=}(X^w(t)Z_{a,1}^w(t))$; then with Relation (2.15), we get

$$\mathrm{d}Y^w(t) = -(1{+}\gamma_{a,1})Y^w(t)\,\mathrm{d}t + \Big(wZ_{a,1}^w(t-){+}B_{a,1}X^w(t-){+}wB_{a,1}\Big)\,\mathcal{N}_\lambda(\mathrm{d}t).$$

By integrating this ODE on $[0,t]$ and taking the expected value, we obtain

$$(1{+}\gamma_{a,1})\mathbb{E}\left[X^wZ_{a,1}^w\right] = \lambda w\mathbb{E}\left[Z_{a,1}^w\right] + \lambda B_{a,1}\mathbb{E}\left[X^w\right] + \lambda wB_{a,1}$$
$$= \frac{(1{+}\gamma_{a,1})}{\gamma_{a,1})}\lambda^2 B_{a,1}w + \lambda wB_{a,1}.$$

By integrating the second SDE of Relation (2.15) on $[0,t]$ and taking the expected value, we have

$$-\gamma_{a,2}\mathbb{E}(Z_{a,2}^w)\,\mathrm{d}t + B_{a,2}\mathbb{E}(\beta(X^w)) = 0,$$

and, with

$$\mathbb{E}\left[\beta(X^w)\right] = B_{a,2}(\nu{+}\beta\mathbb{E}(X^w)) = B_{a,2}(\nu{+}\lambda\beta w),$$

the proposition is proved. □

Theorem 15. *Under Assumptions L and PA, as ε goes to 0, the family of processes $(\Omega_{\varepsilon,p}(t), \Omega_{\varepsilon,d}(t), W_\varepsilon(t))$ of Relation* (2.7) *converges in distribution to the unique solution $(\omega_p(t), \omega_d(t), w(t))$ of the relations*

$$\begin{cases} \omega_a(t) &= \dfrac{\nu}{\lambda\beta}\Lambda_{a,1}\dfrac{1{-}e^{-\alpha t}}{\alpha} + (\Lambda_{a,1}{+}\Lambda_{a,2})\,e^{-\alpha t}\displaystyle\int_0^t e^{\alpha s}w(s)\,\mathrm{d}s, \quad a{\in}\{p,d\}, \\ \dfrac{\mathrm{d}w(t)}{\mathrm{d}t} &= M\left(\omega_p(t),\omega_d(t),w(t)\right), \end{cases}$$

where $\Lambda_{a,i}$, $i{\in}\{1,2\}$, $a{\in}\{p,d\}$ are defined by Relation (2.16).

Proof. This is a direct consequence of Theorem 12 and of Proposition 14. □

Note that, for $a{\in}\{p,d\}$, the parameter $\Lambda_{a,1}$ is proportional to the area under the two STDP curves $\Phi_{a,i}(x){=}B_{a,i}\exp(-\gamma_{a,i}(x))$, $i{=}1,2$. It represents the averaged potentiation/depression rate as if we had considered two neurons without any interactions. Two important facts results from this property,

— the term in the dynamics for the constant firing rate of the output neuron, ν, is proportional to $\Lambda_{a,1}$, as expected;

— the term $\Lambda_{a,2}$ reflects the dependence between pre- and postsynaptic spikes.

Nearest neighbor symmetric model

Similar results can be obtained for the nearest neighbor symmetric scheme of Section 3.1.4 of [RV21a] with general STDP curves Φ. For this class of models, whenever one neuron spikes, the synaptic weight is updated by only taking into account the last spike of the other neuron. In our framework, this is defined as follows.

Assumptions PNS For $w\geqslant 0$, the fast process associated to the operator B_w^F of Relation (2.8) can be expressed as $(X^w(t), Z^w(t))$, where $(Z^w(t))$ is the solution of the SDEs,

$$\begin{cases} \mathrm{d}Z_1^w(t) = \mathrm{d}t - Z_1^w(t-)\,\mathcal{N}_\lambda(\mathrm{d}t), \\ \mathrm{d}Z_2^w(t) = \mathrm{d}t - Z_2^w(t-)\,\mathcal{N}_{\beta,X^w}(\mathrm{d}t). \end{cases} \tag{2.17}$$

It it easily seen that for $Z_1^w(t)=t_0(\mathcal{N}_\lambda, t)$ when t is greater than the first point of $\mathcal{N}_\lambda$ and, similarly, $Z_2^w(t)=t_0(\mathcal{N}_{\beta,X^w}, t)$ under an analogue condition, with

$$t_0(m,t)=t-\sup\{s : s<t : m(\{s\})\neq 0\}, \tag{2.18}$$

the distance between the first point of m at the left of t and t. For $a\in\{p,d\}$, the process $(\Omega_a(t))$ is such that

$$\mathrm{d}\Omega_a(t) = -\alpha\Omega_a(t)\,\mathrm{d}t + \Phi_{a,2}(Z_2(t-))\mathcal{N}_\lambda(\mathrm{d}t) + \Phi_{a,1}(Z_1(t-))\mathcal{N}_{\beta,X}(\mathrm{d}t),$$

i.e., $n_{a,0}(z)=0$, $n_{a,1}(z)=\Phi_{a,2}(z_2)$, and $n_{a,2}(z)=\Phi_{a,1}(z_1)$ for $z\in\mathbb{R}_+^2$.

The functions $\Phi_{a,1}$ and $\Phi_{a,2}$ are quite general nonnegative, nonincreasing, and differentiable functions, instead of exponential functions, as is usually assumed for tractable models of many STDP rules.

Proposition 16. *For $w\geqslant 0$, the Markov process $(X^w(t), Z^w(t))$ has a unique invariant distribution Π_w^{PS}. If f is a bounded Borelian function on $\mathbb{R}_+^2$ and $a\geqslant 0$, then*

$$\int_{\mathbb{R}\times\mathbb{R}_+^2} f(x,z_1)\Pi_w^{\mathrm{PS}}(\mathrm{d}x,\mathrm{d}z) = \mathbb{E}\left[f\left(we^{-E_\lambda}(1+S), E_\lambda\right)\right],$$

$$\int_{\mathbb{R}\times\mathbb{R}_+^2} \mathbb{1}_{\{z_2\geqslant a\}}\Pi_w^{\mathrm{PS}}(\mathrm{d}x,\mathrm{d}z) = \exp\left(-\nu a - \lambda\int_0^a \left(1-\exp\left(-\beta w\left(1-e^{s-a}\right)\right)\right)\mathrm{d}s \right.$$
$$\left. -\lambda\int_{-\infty}^0 \left(1-\exp\left(-\beta w\left(1-e^{-a}\right)e^s\right)\right)\mathrm{d}s\right),$$

where E_λ and S are independent random variables, E_λ has an exponential distribution with rate λ, and, for $\xi\geqslant 0$,

$$\mathbb{E}\left[e^{-\xi S}\right] = \exp\left(-\xi\lambda\int_0^{+\infty} ue^{-u}e^{-\xi e^{-u}}\,\mathrm{d}u\right).$$

Proof. The first condition of Assumption B-a is clearly not satisfied, the coordinates of the vector γ being -1. This is not a concern since this condition is only used to construct a Lyapunov function as in the proof of Proposition 4 of Section 5 of [RV21a]. We only show that one can construct such a function for this model. Set, for $(x,z)\in\mathbb{R}\times\mathbb{R}_+^2$,

$$H(x,z) \stackrel{\text{def.}}{=} \frac{1}{x^\delta} + x + z_1 + z_2,$$

for some $\delta>0$; then,

$$B_F^w(H) \leqslant \frac{1}{x^\delta}\left(\delta+\lambda\left(\frac{x^\delta}{(x+w)^\delta}-1\right)\right)+\lambda w+2-x-\lambda z_1-(\nu+\beta x)z_2,$$

Choosing $\delta<\lambda/4$, we set $x_0=\min(x_1,x_2)$, where

$$x_1=\frac{w}{2^{1/\delta}-1},\quad x_2=\left(\frac{\lambda}{4(\lambda w+3)}\right)^{1/\delta},$$

such that if $x\leqslant x_0$, then $B_F^w(H)\leqslant -1$.

Moreover, if $x\geqslant x_0$, we also have $B_F^w(H)\leqslant -1$ for $H(x,z)\geqslant K_0$, where

$$K_0=\left(\frac{\delta}{x_0^\delta}+\lambda w+3\right)/\min(1,\lambda,\nu+\beta x_0).$$

In particular, H is a Lyapunov function for B_w^F. Consequently, there exists a unique invariant distribution.

We denote by (X^w,Z_1^w,Z_2^w) a random variable with distribution Π_w^{PS}. It is easily checked that, for $t>0$,

$$(X^w(t),Z_1^w(t))=\left(w\int_0^t e^{-(t-s)}\mathcal{N}_\lambda(\mathrm{d}s),t_0(\mathcal{N}_\lambda,t)\right)\stackrel{\text{dist.}}{=}\left(w\int_{-t}^0 e^s\mathcal{N}_\lambda(\mathrm{d}s),t_0(\mathcal{N}_\lambda,0)\right),$$

where $t_0(\cdot,\cdot)$ is defined by Relation (2.18). By letting t go to infinity, we thus get, with $t_0\stackrel{\text{def.}}{=}t_0(\mathcal{N}_\lambda,0)$,

$$(X^w,Z_1^w)\stackrel{\text{dist.}}{=}\left(w\int_{-\infty}^0 e^s\mathcal{N}_\lambda(\mathrm{d}s),t_0(\mathcal{N}_\lambda,0)\right)=\left(we^{-t_0}\left(1+\int_{(-\infty,-t_0)}e^{s+t_0}\mathcal{N}_\lambda(\mathrm{d}s)\right),t_0\right).$$

The strong Markov property of $\mathcal{N}_\lambda$ gives the desired relation for the representation of the law of (X^w,Z_1^w). Again, with the formula of the Laplace transform of Poisson point processes, we have

$$\mathbb{E}\left[\exp\left(-\xi\int_{(-\infty,-t_0)}e^{s+t_0}\mathcal{N}_\lambda(\mathrm{d}s)\right)\right]=\mathbb{E}\left[\exp\left(-\xi\int_{-\infty}^0 e^s\mathcal{N}_\lambda(\mathrm{d}s)\right)\right]$$
$$=\exp\left(-\lambda\int_0^{+\infty}\left(1-e^{-\xi e^{-s}}\right)\mathrm{d}s\right).$$

The stationary distribution of $(Z_2(t))$ is the distribution of the distance of the first point of $\mathcal{N}_{\beta,X}$ at the left of 0 at equilibrium, and hence, for $a\geqslant 0$,

$$\mathbb{P}(Z_2^w\geqslant a)=\mathbb{P}\left(\mathcal{N}_{\beta,X_\infty^w}((-a,0))=0\right)=\mathbb{P}\left(\mathcal{N}_{\beta,X_\infty^w}((0,a))=0\right).$$

Relation (2.12) gives, for $\xi\geqslant 0$,

$$-\ln\mathbb{E}\left[e^{-\xi\mathcal{N}_{\beta,X_\infty^w}((0,a))}\right]=\nu a\left(1-e^{-\xi}\right)+\lambda\int_0^a\left(1-\exp\left(-\beta w\left(1-e^{-\xi}\right)\left(1-e^{s-a}\right)\right)\right)\mathrm{d}s$$
$$+\lambda\int_{-\infty}^0\left(1-\exp\left(-\beta w\left(1-e^{-\xi}\right)\left(1-e^{-a}\right)e^s\right)\right)\mathrm{d}s.$$

By letting ξ go to infinity, we have obtained the desired expression. The proposition is proved.

□

Theorem 17 (Averaging principle)**.** *Under Assumptions L and PNS, as ε goes to 0, the family of processes $(\Omega_{\varepsilon,p}(t), \Omega_{\varepsilon,d}(t), W_\varepsilon(t))$ of Relation* (2.7) *converges in distribution to $(\omega_p(t), \omega_d(t), w(t))$, the unique solution of the ODE*

$$\begin{cases} \omega_a(t) &= \displaystyle\int_0^t e^{-\alpha(t-s)} \int_{\mathbb{R}_+^5} (\beta(x)\Phi_{a,1}(z_1)+\lambda\Phi_{a,2}(z_2))\, \Pi^{\mathrm{PS}}_{w(s)}(\mathrm{d}x, \mathrm{d}z)\, \mathrm{d}s, \quad a\in\{p,d\}, \\ \dfrac{\mathrm{d}w(t)}{\mathrm{d}t} &= M\left(\omega_p(t), \omega_d(t), w(t)\right), \end{cases}$$

where Π^{PS}_w is defined in Proposition 16.

Proof. For $w\geqslant 0$, let $(X^w_\infty, Z^w_{\infty,1}, Z^w_{\infty,2})$ be random variables with distribution Π_w, and, for $a\in\{p,d\}$, let

$$\Psi_a(w) \stackrel{\text{def.}}{=} \mathbb{E}\left[\beta(X^w_\infty)\Phi_{a,1}(Z^w_{\infty,1})\right] + \lambda\mathbb{E}\left[\Phi_{a,2}(Z^w_{\infty,2})\right].$$

The ODE can be rewritten as

$$\frac{\mathrm{d}w(t)}{\mathrm{d}t} = M\left(\int_0^t e^{-\alpha(t-s)}\Psi_p(w(s))\,\mathrm{d}s, \int_0^t e^{-\alpha(t-s)}\Psi_d(w(s))\,\mathrm{d}s, w(t)\right).$$

With Theorem 12, all we have to prove is that this ODE has a unique solution. This is a simple consequence of the Lipschitz property of Ψ_a. Indeed, first, the distribution of $Z^w_{\infty,1}$ does not depend on w and $\beta(\cdot)$ is an affine function of X^w_∞ given by Relation (2.13). Finally, the identity

$$\mathbb{E}\left[\Phi_{a,2}(Z^w_{\infty,2})\right] = -\int_0^{+\infty} \dot{\Phi}_{a,2}(u)\mathbb{P}(Z^w_{\infty,2}\leqslant u)\,\mathrm{d}u,$$

Proposition 16, and simple estimations give that the function Ψ_a has the Lipschitz property. The theorem is proved. □

Links with models of physics

In this section, averaging principles for STDP rules of [KGH99] are discussed. We start by characterizing which type of STDP rules are used, in particular, their model takes into account all pairing of pre- and postsynaptic spikes that last less than the interval of the experiment T. It is supposed that T is really large compared to the neuronal dynamics. Accordingly, in the limit of large T, it corresponds to the pair-based all-to-all model of Assumptions PA.

After adapting notation, the main equation for the asymptotic behavior of the synaptic weight dynamics (Relation (4) of this reference) is expressed, via a separation of timescale argument, as

$$\frac{\mathrm{d}\widetilde{w}}{\mathrm{d}t} = w^1\nu^1(t) + w^2\nu^2(t) + \int_{-\infty}^{+\infty} \widetilde{\Phi}(s)\widetilde{\mu}(s,t)\,\mathrm{d}s, \tag{2.19}$$

where S^1 (resp., S^2) is the process of presynaptic spikes (resp., postsynaptic spikes),

— $\nu^1(t) = \overline{\langle S^1(t)\rangle}$, the presynaptic spike rate and w^1 the intensity of synaptic plasticity triggered by presynaptic spikes only;

— $\nu^2(t) = \overline{\langle S^2(t)\rangle}$, the postsynaptic spike rate and w^2 the intensity of synaptic plasticity triggered by postsynaptic spikes only;

— $\widetilde{\Phi}(t)$ represents the STDP curve;

— $\widetilde{\mu}(s,t)=\overline{\langle S^1(t+s)S^2(t)\rangle}$, the correlation between the spike trains.

The quantity $\overline{\langle\cdots\rangle >}$ is defined in terms of *temporal and ensemble averages* that are not completely clear from a mathematical point of view, $\langle\cdots\rangle$ is the ensemble average and $\overline{\cdots}$ is the temporal average over the spike trains. The model of [KGH99] is without exponential filtering; see Section 2.A.

In our setting, we choose $\overline{M}(\Gamma_p,\Gamma_d,w)=\Gamma_p-\Gamma_d$, $n_{a,0}(z)=0$, $n_{a,1}(z)=D_{a,1}+z_{a,2}$ and $n_{a,2}(z)=D_{a,2}+z_{a,1}$, where $z_{a,i}$ are defined as in Assumptions PA. Theorem 24 gives the following equation:

$$\frac{\mathrm{d}\overline{w}}{\mathrm{d}t} = (D_{p,1}-D_{d,1})\lambda + (D_{p,2}-D_{d,2})\int_{\mathbb{R}_+}\beta(x)\Pi^{\mathrm{PA}}_{\overline{w}(t)}(\mathrm{d}x) + \int_{\mathbb{R}_+}(\lambda z_2+\beta(x)z_1)\,\Pi^{\mathrm{PA}}_{\overline{w}(t)}(\mathrm{d}x,\mathrm{d}z_1,\mathrm{d}z_2), \quad (2.20)$$

where Π^{PA}_w is defined in Proposition 14.

We then have the following equivalence:

	[KGH99]	Our model
Presynaptic plasticity	w^1	$D_{p,1}-D_{d,1}$
Presynaptic rate	$\nu^1(t)$	λ
Postsynaptic plasticity	w^2	$D_{p,2}-D_{d,2}$
Postsynaptic rate	$\nu^2(t)$	$\displaystyle\int_{\mathbb{R}_+}\beta(x)\Pi^{\mathrm{PA}}_{\overline{w}(t)}(\mathrm{d}x)$
STDP	$\displaystyle\int_{-\infty}^{+\infty}\widetilde{\Phi}(s)\widetilde{\mu}(s,t)\,\mathrm{d}s$	$\displaystyle\int_{\mathbb{R}_+}(\lambda z_2+\beta(x)z_1)\,\Pi^{\mathrm{PA}}_{\overline{w}(t)}(\mathrm{d}x,\mathrm{d}z_1,\mathrm{d}z_2)$

The equivalence of the last row can be explained as follows.

We set

$$\Phi_a(t) = B_{a,1}\exp(-\gamma_{a,1}t)\mathbb{1}_{\{t>0\}} + B_{a,2}\exp(\gamma_{a,2}t)\mathbb{1}_{\{t<0\}},$$

and

$$\overline{\mu}(t,w) = \begin{cases} \displaystyle\lim_{h\searrow 0}\frac{\mathbb{E}_{\Pi^{\mathrm{PA}}_w}(\mathcal{N}_\lambda[0,h]\mathcal{N}_{\beta,X}[t,t+h])}{h^2}, & \text{for } t>0;\\ \displaystyle\lim_{h\searrow 0}\frac{\mathbb{E}_{\Pi^{\mathrm{PA}}_w}(\mathcal{N}_\lambda[0,h]\mathcal{N}_{\beta,X}[t,t+h])}{h^2}, & \text{for } t<0, \end{cases}$$

provided that the limits related to second order properties of the point processes $\mathcal{N}_\lambda$ and $\mathcal{N}_{\beta,X}$ exist.

In Section 2.B, a heuristic argument shows that

$$\int_{\mathbb{R}_+}(\lambda z_2+\beta(x)z_1)\,\Pi^{\mathrm{PA}}_{\overline{w}(t)}(\mathrm{d}x,\mathrm{d}z_1,\mathrm{d}z_2) = \int_{-\infty}^{+\infty}(\Phi_p(s)-\Phi_d(s))\overline{\mu}(s,\overline{w}(t))\,\mathrm{d}s,$$

leading to the equivalence between both models.

2.4 Calcium-based rules

We investigate scaled models of calcium-based rules introduced in Section 3.1.1 of [RV21b]. In this section, we show that the asymptotic equation (2.10) has a unique solution. Some regularity properties of the invariant distribution of the operator B_w^F, with respect to the variable w, have to be obtained.

Assumptions C In this case, the vector $(Z(t))$ is a nonnegative one-dimensional process $(C(t))$. For $w{\in}K_W$, the fast process associated to the operator B_w^F of Relation (2.8) can be expressed as $(X^w(t), C^w(t))$, where, as before, $(X^w(t))$ is the solution of Relation (2.11) and the SDE for $(C^w(t))$ is

$$\mathrm{d}C^w = -\gamma C^w(t)\,\mathrm{d}t + C_1\mathcal{N}_\lambda(\mathrm{d}t) + C_2\mathcal{N}_{\beta,X^w}(\mathrm{d}t), \tag{2.21}$$

where C_1 and $C_2{\geqslant}0$, $\gamma{>}0$. For $a{\in}\{p,d\}$, the process $(\Omega_a(t))$ is such that

$$\mathrm{d}\Omega_a(t) = (-\alpha\Omega_a(t){+}h_a(C(t)))\,\mathrm{d}t,$$

i.e., $n_{a,0}(c){=}h_a(c)$, $n_{a,1}(c){=}0$, and $n_{a,2}(c){=}0$ for $c{\in}\mathbb{R}_+$. The functions h_p and h_d are assumed to be L-Lipschitz. They represent, respectively, the influence of the calcium concentration C on potentiation and depression.

Proposition 18. *For $w{\in}K_W$, the Markov process $(X^w(t), C^w(t))$ has a unique invariant distribution Π_w^{C}, and its Laplace transform is given by, for a and $b{\geqslant}0$,*

$$-\ln\int_{\mathbb{R}_+^2} e^{-ax-bc}\Pi_w^{\mathsf{C}}(\mathrm{d}x,\mathrm{d}c) = \nu\int_{-\infty}^0\left(1{-}e^{-bC_2e^{\gamma u}}\right)\mathrm{d}u$$
$$+\lambda\int_{-\infty}^0\left(1{-}\exp\left(-awe^u{-}bC_1e^{\gamma u}-\beta w\int_0^u\left(1{-}e^{-bC_2e^{\gamma(u-s)}}\right)e^s\,\mathrm{d}s\right)\right)\mathrm{d}u.$$

Proof. The existence and uniqueness of Π_w^{C} is a direct consequence of Theorem 12 since Assumptions B hold in this case and Proposition 4 of Section 5 of [RV21a] can be used.

With Proposition 13 and Lemma 2.1 of [RV21b], a stationary version $(X_\infty^w(t), C_\infty^w(t))$ of the fast process $(X^w(t), C^w(t))$ can be represented as

$$\left(w\int_{-\infty}^t e^{-(t-s)}\mathcal{N}_\lambda(\mathrm{d}s), C_1\int_{-\infty}^t e^{-\gamma(t-s)}\mathcal{N}_\lambda(\mathrm{d}s){+}C_2\int_{-\infty}^t e^{-\gamma(t-s)}\mathcal{N}_{\beta,X_\infty^w}(\mathrm{d}s)\right). \tag{2.22}$$

Hence, we have to calculate $\mathbb{E}\left[\exp(-aX_\infty^w(0){-}bC_\infty^w(0))\right]$, that is,

$$\Psi(a,b)\overset{\text{def.}}{=}\mathbb{E}\left[\exp\left(-\int_{-\infty}^0(awe^s{+}bC_1e^{\gamma s})\,\mathcal{N}_\lambda(\mathrm{d}s){-}bC_2\int_{-\infty}^0 e^{\gamma s}\mathcal{N}_{\beta,X_\infty^w}(\mathrm{d}s)\right)\right].$$

We proceed as in the proof of Proposition 13. By the independence of $\mathcal{P}$ and $\mathcal{N}_\lambda$,

$$\mathbb{E}\left[\exp\left(-bC_2\int_{-\infty}^0 e^{\gamma s}\mathcal{N}_{\beta,X_\infty^w}(\mathrm{d}s)\right)\middle|\,\mathcal{N}_\lambda\right] = \exp\left(-\int_{-\infty}^0\left(1{-}e^{-bC_2e^{\gamma s}}\right)\beta(X_\infty^w(s))\,\mathrm{d}s\right)$$

and, with the help of Relation (2.14), we follow the same methods to obtain the desired result.

□

Theorem 19. *Under Assumptions L and C, if the functions h_p and h_d are Lipschitz then, as ε goes to 0, the family of processes $(\Omega_{\varepsilon,p}(t), \Omega_{\varepsilon,d}(t), W_\varepsilon(t))$ converges in distribution to the unique solution $(\omega_p(t), \omega_d(t), w(t))$ of the relations*

$$\begin{cases} \omega_a(t) &= \displaystyle\int_0^t e^{-\alpha(t-s)} \int_{\mathbb{R}_+^2} h_a(c) \Pi^{\mathsf{C}}_{w(s)}(\mathrm{d}x, \mathrm{d}c)\, \mathrm{d}s, \quad a \in \{p,d\}, \\ \dfrac{\mathrm{d}w(t)}{\mathrm{d}t} &= M\left(\omega_p(t), \omega_d(t), w(t)\right), \end{cases} \tag{2.23}$$

almost surely, where, for $w \in K_W$, Π^{C}_w is the probability distribution defined in Proposition 18.

Proof. The application of Theorem 12 is straightforward. All we have have to prove now is that ODE (2.23) has a unique solution.

From the representation (2.22), for any $0 \leqslant w \leqslant w'$, the random variables $C^w_\infty(0)$ and $C^{w'}_\infty(0)$ can be constructed on the same probability space. The Lipschitz property of h_a, with the constant L, gives

$$\begin{aligned} d_a(w,w') \stackrel{\text{def.}}{=} \left| \mathbb{E}\left[h_a(C^w_\infty(0))\right] - \mathbb{E}\left[h_a(C^{w'}_\infty(0))\right] \right| &\leqslant L \mathbb{E}\left[\left| C^w_\infty(0) - C^{w'}_\infty(0) \right| \right] \\ &= C_2 L \mathbb{E}\left[\left| \int_{-\infty}^0 e^{\gamma s} \mathcal{N}_{\beta, X^w_\infty}(\mathrm{d}s) - \int_{-\infty}^0 e^{\gamma s} \mathcal{N}_{\beta, X^{w'}_\infty}(\mathrm{d}s) \right| \right]. \end{aligned}$$

with (2.13), we have $X^w_\infty(t) = w X^1_\infty(t)$ for all t and, therefore,

$$\begin{aligned} \frac{d_a(w,w')}{C_2 L} &\leqslant \mathbb{E}\left[\int_{-\infty}^0 e^{\gamma s} \mathcal{P}\left[\left(\beta(w X^1_\infty(s)), \beta(w' X^1_\infty(s)) \right], \mathrm{d}s \right] \right] \\ &= \beta(w'-w) \mathbb{E}\left[\int_{-\infty}^0 e^{\gamma s} X^1_\infty(s)\, \mathrm{d}s \right] = \frac{\beta}{\gamma}(w'-w) \end{aligned}$$

Let $(w(t))$, $(w'(t))$ be two solutions of ODE (2.23) with the same initial point; then

$$\begin{aligned} \Delta_a(t) &\stackrel{\text{def.}}{=} \left| \int_0^t e^{-\alpha(t-s)} \left[\int_{\mathbb{R}_+^2} h_a(c) \Pi^{\mathsf{C}}_{w(s)}(\mathrm{d}x, \mathrm{d}c) - \int_{\mathbb{R}_+^2} h_a(c) \Pi^{\mathsf{C}}_{w'(s)}(\mathrm{d}x, \mathrm{d}c) \right] \mathrm{d}s \right| \\ &\leqslant \int_0^t \left| \mathbb{E}\left[h_a(C^{w(s)}_\infty(0))\right] - \mathbb{E}\left[h_a(C^{w'(s)}_\infty(0))\right] \right| \mathrm{d}s \leqslant C_2 L \frac{\beta}{\gamma} \int_0^t |w(s) - w'(s)|\, \mathrm{d}s. \end{aligned}$$

With Relation (2.23) and the Lipschitz property of M, we get, for $t \leqslant T$,

$$\begin{aligned} \|w - w'\|_t \stackrel{\text{def.}}{=} \sup_{s \leqslant t} |w(s) - w'(s)| &\leqslant L_M \int_0^t e^{-\mu(t-s)} (\Delta_p(s) + \Delta_d(s))\, \mathrm{d}s \\ &\leqslant 2T L_M C_2 L \frac{\beta}{\gamma} \int_0^t \|w - w'\|_s\, \mathrm{d}s. \end{aligned}$$

This implies that $(\|w - w'\|_t)$ is identically 0. The theorem is proved.

□

The Lipschitz assumptions for the functions (h_p, h_d) of Assumptions C do not apply to the classical threshold functions (S_p, S_d) from [GB12] defined by

$$S_a(x) = \mathbb{1}_{\{x \geqslant \theta_a\}}, \quad x \geqslant 0. \tag{2.24}$$

Additionally, even in the case of Lipschitz functions, the quantities

$$\int_{\mathbb{R}\times\mathbb{R}_+} h_a(c)\Pi_w^{\mathsf{C}}(\mathrm{d}x,\mathrm{d}c), \quad a\in\{p,d\},$$

of the ODE (2.23) do not have a closed form expression in general.

Theorem 19 highlights the importance of the calcium concentration on the dynamics of the synaptic weight. Interestingly, calcium has been the subject of a wide array of experimental studies, and biologists have developed several means to follow its concentration both locally and globally during experiments. In particular, it is now possible to monitor calcium concentration in dendrites of postsynaptic neurons during stimulations with calcium fluorescence indicators, such as GCaMP for example [NOI01], See [HS08]. It may be therefore possible to infer these cumulative functions from such experiments and study the dynamics of Theorem 19 for those realistic calcium concentrations.

From the point of view of numerical analysis, it is quite difficult to obtain some simple numerical results to express solutions of the ODE (2.23). It could be done, by simulations, to estimate the quantities $\mathbb{E}_{\Pi_w^{\mathsf{C}}}(h_a(C))$, $a\in\{p,d\}$ for a large number of values for w. A recent article (see [GWO16]) has derived some approximations for specific cases.

For this reason, the next section investigates a class of discrete calcium-based models for which the invariant distributions have an explicit expression which can be used in practice.

2.5 Discrete models of calcium-based rules

In this section, we study a simple model of plasticity where the membrane potential X, the calcium concentration C, and the synaptic weight W are integer-valued variables. It amounts to representing these three quantities X, C, and W as multiples of a "quantum" instead of a continuous variable. A general class of such discrete models has been introduced in Section 4 of [RV21b].

This amounts to describing the model of plasticity as a chemical reaction network of interacting chemical species: $\mathcal{C}$ (calcium), $\mathcal{W}$ synaptic quanta, $\mathcal{X}$ ions. The associated chemical reactions could be described as

$$\begin{cases} \varnothing \xrightarrow{\lambda} W\mathcal{X}+C_1\mathcal{C}, \\ \mathcal{X} \xrightarrow{\beta} C_2\mathcal{C}, \end{cases} \quad \begin{cases} B_d\mathcal{W} \rightharpoonup \varnothing \rightharpoonup B_p\mathcal{W}, \\ \mathcal{W} \xrightarrow{\mu} \varnothing, \end{cases} \quad \begin{cases} \mathcal{X} \xrightarrow{1} \varnothing, \\ \mathcal{C} \xrightarrow{\gamma} \varnothing. \end{cases}$$

In this setting, the state variable is the vector of the number of copies of the different chemical species. See [Fei19] for a general introduction to chemical reaction networks and also Chapter 2 of [AK15]. It should be noted that our model is not strictly speaking a chemical reaction network since some reactions rates are defined by the processes $(\Omega_a(t))$, $a\in\{p,d\}$.

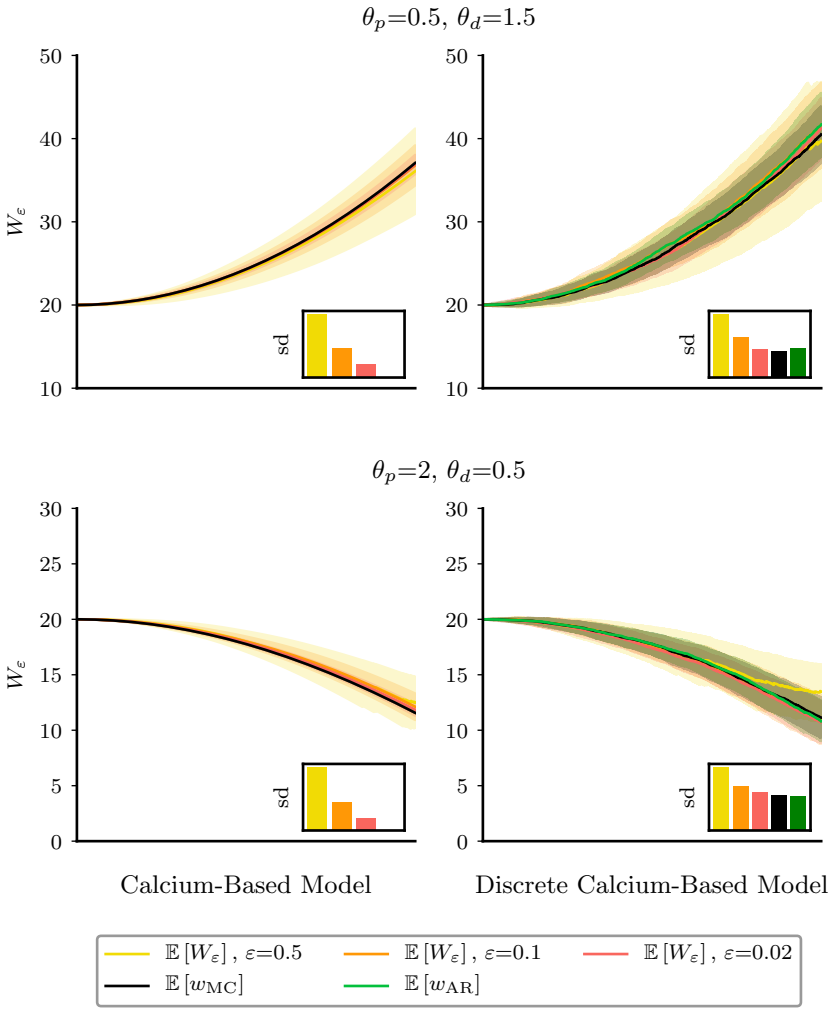

Figure 2.2: **Comparison between continuous and discrete calcium-based models.**
λ=0.1, γ=2, C_1=C_2=1, B_p=2, B_d=1, $\beta(x)$=$(0.01x)^+$, α=0.01 and δ=0.
For the continuous model, we took $M(\omega_p, \omega_d, w)$=ω_p−ω_d.
Inset, standard deviations, sd, of W_ε and w at the end of the simulations.
The expected value of w_{MC} is computed with Monte Carlo estimations of Π_w^{CQ}.
The expected value of w_{AR} is computed with estimated Π_w^{CQ} with the expressions of Section 2.C.

The state of the system is associated to the solution of the following SDEs;

$$\left\{\begin{array}{rcl} \mathrm{d}X(t) &=& -\displaystyle\sum_{i=1}^{X(t-)} \mathcal{N}_{1,i}(\mathrm{d}t) + W(t-)\mathcal{N}_\lambda(\mathrm{d}t) - \sum_{i=1}^{X(t-)} \mathcal{N}_{\beta,i}(\mathrm{d}t), \\ \mathrm{d}C(t) &=& -\displaystyle\sum_{i=1}^{C(t-)} \mathcal{N}_{\gamma,i}(\mathrm{d}t) + C_1\mathcal{N}_\lambda(\mathrm{d}t) + C_2 \sum_{i=1}^{X(t-)} \mathcal{N}_{\beta,i}(\mathrm{d}t), \\ \mathrm{d}\Omega_a(t) &=& \Big[-\alpha\Omega_a(t)+h_a(C(t))\Big]\,\mathrm{d}t, \quad a\in\{p,d\}, \\ \mathrm{d}W(t) &=& -\displaystyle\sum_{i=1}^{W(t-)} \mathcal{N}_{\mu,i}(\mathrm{d}t) + B_p\mathcal{N}_{\Omega_p(t-)}(\mathrm{d}t) - B_d\mathbb{1}_{\{W(t-)\geqslant B_d\}}\mathcal{N}_{\Omega_d(t-)}(\mathrm{d}t), \end{array}\right.$$

where C_1, $C_2\in\mathbb{N}$ and, for $a\in\{p,d\}$, $B_a\in\mathbb{N}$ and h_a is a nonnegative function. For $\xi>0$, $\mathcal{N}_\xi$ (resp., $(\mathcal{N}_{\xi,i})$) is a Poisson process on $\mathbb{R}_+$ with rate ξ (resp., an i.i.d. sequence of such point processes). For $a\in\{p,d\}$, as before, the notation $\mathcal{N}_{\Omega_a(t-)}(\mathrm{d}t)$ stands for $\mathcal{P}\left[(0,\Omega_a(t-)),\mathrm{d}t\right]$, where $\mathcal{P}$ is a Poisson process in $\mathbb{R}_+^2$ with rate 1. All Poisson processes are assumed to be independent.

Outside the leaking mechanism, the time evolution of the discrete random variable $(W(t))$ is driven by two inhomogeneous Poisson processes, one for potentiation and the other for depression with respective intensity functions $(\Omega_p(t))$ and $(\Omega_d(t))$.

The scaling is done in an analogous way as in Section 2.2. The corresponding SDEs are then expressed as

$$\left\{\begin{array}{rcl} \mathrm{d}X_\varepsilon(t) &=& -\displaystyle\sum_{i=1}^{X_\varepsilon(t-)} \mathcal{N}_{1/\varepsilon,i}(\mathrm{d}t) + W_\varepsilon(t-)\mathcal{N}_{\lambda/\varepsilon}(\mathrm{d}t) - \sum_{i=1}^{X_\varepsilon(t-)} \mathcal{N}_{\beta/\varepsilon,i}(\mathrm{d}t), \\ \mathrm{d}C_\varepsilon(t) &=& -\displaystyle\sum_{i=1}^{C_\varepsilon(t-)} \mathcal{N}_{\gamma/\varepsilon,i}(\mathrm{d}t) + C_1\mathcal{N}_{\lambda/\varepsilon}(\mathrm{d}t) + C_2 \sum_{i=1}^{X_\varepsilon(t-)} \mathcal{N}_{\beta/\varepsilon,i}(\mathrm{d}t), \\ \mathrm{d}\Omega_{\varepsilon,a}(t) &=& -\alpha\Omega_{\varepsilon,a}(t)\,\mathrm{d}t+h_a(C_\varepsilon(t))\,\mathrm{d}t, \quad a\in\{p,d\}, \\ \mathrm{d}W_\varepsilon(t) &=& -\displaystyle\sum_{i=1}^{W_\varepsilon(t-)} \mathcal{N}_{\mu,i}(\mathrm{d}t)+B_p\mathcal{N}_{\Omega_{\varepsilon,p}(t)}(\mathrm{d}t)-B_d\mathbb{1}_{\{W_\varepsilon(t-)\geqslant B_d\}}\mathcal{N}_{\Omega_{\varepsilon,d}(t)}(\mathrm{d}t), \end{array}\right. \tag{2.25}$$

Definition 20 (Fast processes)**.** *For a fixed $W=w$, the fast variables of the SDEs* (2.25) *are associated to a Markov process $(X^w(t),C^w(t))$ on $\mathbb{N}^2$ whose transition rates are given by, for $(x,c)\in\mathbb{N}^2$,*

$$(x,c)\longrightarrow\left\{\begin{array}{ll}(x+w,c+C_1) & \lambda,\\ (x-1,c) & x,\end{array}\right. \qquad \longrightarrow\left\{\begin{array}{ll}(x,c-1) & \gamma c,\\ (x-1,c+C_2) & \beta x.\end{array}\right.$$

The next result is the equivalent of Theorem 19 in a discrete setting.

Theorem 21 (Averaging principle for discrete calcium-based model)**.** *If h_p and h_d are functions on $\mathbb{N}$ with a finite range of values, as ε goes to 0, the family of processes $(\Omega_{\varepsilon,p}(t),\Omega_{\varepsilon,d}(t),W_\varepsilon(t))$ defined by Relations* (2.25) *converges in distribution to the unique solution $(\omega_p(t),\omega_d(t),w(t))$ of the relations*

$$\left\{\begin{array}{rcl} \omega_a(t) &=& \displaystyle\int_0^t e^{-\alpha(t-s)}\int_{\mathbb{N}^2} h_a(c)\Pi^{\mathrm{CQ}}_{w(s)}(\mathrm{d}x,\mathrm{d}c)\;\mathrm{d}s, \quad a\in\{p,d\}, \\ \mathrm{d}w(t) &=& -\displaystyle\sum_{i=1}^{w(t-)} \mathcal{N}_{\mu,i}(\mathrm{d}t)+B_p\mathcal{N}_{\omega_p(t)}(\mathrm{d}t)-B_d\mathbb{1}_{\{w(t-)\geqslant B_d\}}\mathcal{N}_{\omega_d(t)}(\mathrm{d}t), \end{array}\right. \tag{2.26}$$

where Π^{CQ}_w is the invariant distribution of the Markov process of Definition 20.

The threshold functions (S_p, S_d) defined by Relations (2.24) and used in classical models of calcium-based STDP [GB12] satisfy the conditions of the theorem. For the proof, see the appendix of [RV21a].

The theorem shows that the limiting process $(w(t))$ is a jump process on $\mathbb{N}$ driven by two nonhomogeneous Poisson processes whose intensity functions $(\omega_a(t))$, $a\in\{p,d\}$ are continuous.

The explicit expression of the invariant distribution of $(C^w(t))$ is given in Proposition 4.3 of [RV21b]. Only the distribution of the calcium variable C^w is considered due to its role in the expression of $(\omega_a(t))$, $a\in\{p,d\}$ in Theorem 21.

Proposition 22 (Equilibrium of fast process)**.** *For $w\in\mathbb{N}$, the Markov process on $\mathbb{N}^2$ of Definition 20 has a unique invariant distribution Π_w^{CQ}, and the generating function of C^w is given by, for $u\in[0,1]$,*

$$E\left(u^{C^w}\right) = \exp\left(-\lambda\int_0^{+\infty}(1-\Delta(u,s,w))\,\mathrm{d}s\right) \tag{2.27}$$

with

$$\Delta(u,s,w) = \Big(1+(u-1)p_1(s)\Big)^{C_1}\left(1+\sum_{i=1}^{C_2}(u-1)^k p_2(s,k)\right)^w$$

$$p_1(s) = e^{-\gamma s} \text{ and } p_2(s,k) = \frac{\beta}{\beta+1-\gamma k}\binom{C_2}{k}\left(e^{-\gamma k s}-e^{-(\beta+1)s}\right).$$

We present in Figure 2.2 simulations for different values of θ_p and θ_d of the continuous model (Section 2.4) with step functions S_a (left) and of the discrete model (right). In particular, we simulate the scaled system for different values of ε and we also estimate the solution of (2.23) and (2.26), w_{MC}, using Monte Carlo estimations to compute $\Pi_w^{\mathrm{C/CQ}}(C\geqslant\theta_a)$.

Moreover, for the discrete case, we are able to compute $\Pi_w^{\mathrm{CQ}}(C\geqslant n)$ for $n=0,1,2$; see Section 2.C. Based on these analytical results, we are able to obtain the numerical values of the parameters of the dynamic of the asymptotic process $(w_{\mathrm{AR}}(t))$. Simulations of the expected values of $(w_{\mathrm{AR}}(t))$ are represented in green in Figure 2.2.

These simulations illustrate Theorems 19 and 21, with the convergence of the scaled processes W_ε towards our asymptotic process. For the continuous case, we observe that even if the step function S_a does not verify the conditions of 19, convergence seems to hold anyway. This is also illustrated by the decrease in standard deviations (inset) as ε goes to 0. For the discrete case, we note the same phenomenon for the expected value and the standard deviation. Recall that the limiting process is stochastic in this context. Finally, it also shows that, qualitatively, the two classes of models continuous/discrete behave quite similarly.

Appendix

2.A Averaging principles for models without exponential filtering

In Section SM2 of [RV21b] more "direct" dynamics for the time evolution of synaptic weight have been presented. For $a\in\{p,d\}$, the update at time t depends only on the instantaneous synaptic plastic processes

$$\Gamma_a(\mathcal{N}_\lambda,\mathcal{N}_{\beta,\overline{X}})(\mathrm{d}t) = n_{a,0}(Z(t-))\,\mathrm{d}t + n_{a,1}(Z(t-))\mathcal{N}_\lambda(\mathrm{d}t) + n_{a,2}(Z(t-))\mathcal{N}_{\beta,X}(\mathrm{d}t)$$

at time t. The corresponding synaptic weight process $(\overline{W}(t))$ satisfies the relation

$$\mathrm{d}\overline{W}(t) = \overline{M}\left(\Gamma_p(\mathcal{N}_\lambda,\mathcal{N}_{\beta,\overline{X}}),\Gamma_d(\mathcal{N}_\lambda,\mathcal{N}_{\beta,\overline{X}}),\overline{W}(t-)\right)(\mathrm{d}t),$$

for some functional $\overline{M}$.

Recall that for our model, the dynamic of the synaptic weight $(W(t))$ is defined by,

$$\mathrm{d}W(t) = M\left(\Omega_p(t),\Omega_d(t),W(t)\right)\mathrm{d}t,$$

where $(\Omega_a(t))$, $a\in\{p,d\}$, is a filtered/smoothed version of $\Gamma_a(\mathcal{N}_\lambda,\mathcal{N}_{\beta,\overline{X}})$,

$$\mathrm{d}\Omega_a(t) = -\alpha\Omega_a(t)\,\mathrm{d}t + n_{a,0}(Z(t))\,\mathrm{d}t + \Gamma_a(\mathcal{N}_\lambda,\mathcal{N}_{\beta,X})(\mathrm{d}t)$$

It turns out that a stochastic averaging principles also holds for the model without an exponential filtering. We first introduced the scaled version of this system.

Definition 23 (Scaled dynamical system for instantaneous plasticity)**.** *We define the stochastic process $(\overline{X}(t),\overline{W}(t))$ with initial state (x_0,w_0), satisfying the evolution equations, for $t>0$,*

$$\begin{cases} \mathrm{d}\overline{X}_\varepsilon(t) = -\dfrac{1}{\varepsilon}\overline{X}_\varepsilon(t)\,\mathrm{d}t + \overline{W}_\varepsilon(t-)\mathcal{N}_{\lambda/\varepsilon}(\mathrm{d}t) - g(\overline{X}_\varepsilon(t-))\mathcal{N}_{\beta/\varepsilon,\overline{X}_\varepsilon}(\mathrm{d}t), \\ \mathrm{d}\overline{Z}_\varepsilon(t) = \dfrac{1}{\varepsilon}\left(-\gamma\odot\overline{Z}_\varepsilon(t)+k_0\right)\mathrm{d}t \\ \qquad +k_1(\overline{Z}_\varepsilon(t-))\mathcal{N}_{\lambda/\varepsilon}(\mathrm{d}t)+k_2(\overline{Z}_\varepsilon(t-))\mathcal{N}_{\beta/\varepsilon,\overline{X}_\varepsilon}(\mathrm{d}t), \\ \mathrm{d}\overline{W}_\varepsilon(t) = \varepsilon\overline{M}\left(\Gamma_p(\mathcal{N}_\lambda,\mathcal{N}_{\beta,\overline{X}}),\Gamma_d(\mathcal{N}_\lambda,\mathcal{N}_{\beta,\overline{X}}),\overline{W}(t)\right)(\mathrm{d}t), \end{cases} \tag{2.28}$$

where Γ_p and Γ_d are plasticity kernels. The functional $\overline{M}$ is defined by

$$\begin{aligned} \overline{M}\colon\quad & \mathcal{M}_+(\mathbb{R}_+)^2\times\mathbb{R}\mapsto\mathcal{M}_+(\mathbb{R}_+) \\ & (\Gamma_p,\Gamma_d,w)\to\overline{M}(\Gamma_p,\Gamma_d,w). \end{aligned} \tag{2.29}$$

We have to modify Assumptions B-(d) by Assumptions B*-(d), in the following way, $\overline{M}$ can be decomposed as, $\overline{M}(\Gamma_p,\Gamma_d,w)=\overline{M}_p(w)\Gamma_p-\overline{M}_d(w)\Gamma_d-\mu w$, where $\overline{M}_a(w)$ is non-negative continuous function, and,

$$\overline{M}_a(w)\leqslant C_M,$$

for all $w\in K_W$, for $a\in\{p,d\}$.

An analogue of Theorem 12 in this context is the following result.

Theorem 24 (Averaging principle for instantaneous plasticity)**.** *Under Assumptions A and B* and for initial conditions satisfying Relation* (2.6)*, there exists* $S_0 \in (0, +\infty]$*, such that the family of processes* $(\overline{W}_\varepsilon(t), t<S_0)$ *associated to Relations* (2.28) *and* (2.29)*, is tight for the convergence in distribution as* ε *goes to* 0*. Almost surely, any limiting point* $(\overline{w}(t), t<S_0)$ *satisfies the relation*

$$\mathrm{d}\overline{w}(t) = \int_{\mathbb{R}\times\mathbb{R}_+^\ell} \overline{M}\left(\left[(n_{a,0}(z)+\lambda n_{a,1}(z)+\beta(x) n_{a,2}(z))\,\mathrm{d}t \right]_{a\in\{p,d\}}, \overline{w}(t) \right) \Pi_{\overline{w}(t)}(\mathrm{d}x, \mathrm{d}z). \quad (2.30)$$

where, for $w \in K_W$*,* Π_w *is the invariant measure* Π_w *of the operator* B_w^F *of Relation* (2.8)*.*

Proof. Due to the specific expression of $\overline{M}$, the arguments follow the ones used in [RV21a]. The proof is skipped. □

Comparison with Theorem 12

Both theorems show that the dynamics of the synaptic weight w in the decoupled stochastic system depend on an integral over the stationary distribution of the fast process. However, in Theorem 12, the averaging property occurs at the level of the synaptic plasticity processes ω_a,

$$\frac{\mathrm{d}\omega_a(t)}{\mathrm{d}t} = -\alpha\omega_a(t) + \int_{\mathbb{R}\times\mathbb{R}_+^\ell} \Big[n_{a,0}(z)+\lambda n_{a,1}(z)+\beta(x) n_{a,2}(z) \Big]\, \mathrm{d}\Pi_{w(t)}(x,z),$$

and, the function M is applied afterwards to have the update of the synaptic weight w,

$$\frac{\mathrm{d}w(t)}{\mathrm{d}t} = M(\omega_p(t), \omega_d(t), w(t)).$$

In Theorem 24, with no exponential filtering, the averaging is applied directly at the level of the synaptic update,

$$\mathrm{d}\overline{w}(t) = \int_{\mathbb{R}\times\mathbb{R}_+^\ell} \overline{M}\left(\left[(n_{a,0}(z)+\lambda n_{a,1}(z)+\beta(x) n_{a,2}(z))\,\mathrm{d}t \right]_{a\in\{p,d\}}, \overline{w}(t) \right) \Pi_{\overline{w}(t)}(\mathrm{d}x, \mathrm{d}z).$$

In particular, with a linear function M, both models are equivalent except for the exponential filtering of the plasticity kernels.

2.B Links with models of physics: a heuristic approach

In this section we give a, non-rigorous, derivation of Relation (2.19) of [KGH99] to establish a connection with our main results in this specific case. For $w \in K_W$, from the definition of Φ_a, $a \in \{p, d\}$,

$$\begin{aligned}
&\int_{-\infty}^0 \Phi_a(s) \mathbb{E}_{\Pi_w^{\mathrm{PA}}} \left(\frac{\mathcal{N}_{\beta,X}[0,h]}{h} \frac{\mathcal{N}_\lambda[s, s+h]}{h} \right) \mathrm{d}s \\
&= B_{a,1} \mathbb{E}_{\Pi_w^{\mathrm{PA}}} \left(\int_{-\infty}^0 \exp(\gamma_{a,1} s) \mathbb{E}_{\Pi_w^{\mathrm{PA}}} \left[\frac{\mathcal{N}_{\beta,X}[0,h]}{h} \frac{\mathcal{N}_\lambda[s, s+h]}{h} \middle| \mathcal{F}_0 \right] \mathrm{d}s \right) \\
&= B_{a,1} \mathbb{E}_{\Pi_w^{\mathrm{PA}}} \left(\mathbb{E}_{\Pi_w^{\mathrm{PA}}} \left[\frac{\mathcal{N}_{\beta,X}[0,h]}{h} \middle| \mathcal{F}_0 \right] \int_{-\infty}^{-h} \exp(\gamma_{a,1} s) \frac{\mathcal{N}_\lambda[s, s+h]}{h} \mathrm{d}s \right)
\end{aligned}$$

$$\sim B_{a,1}\mathbb{E}_{\Pi_w^{\mathrm{PA}}}\left(\beta(X(0))\int_{-\infty}^{-h}\exp(\gamma_{a,1}s)\frac{\mathcal{N}_\lambda[s,s+h]}{h}\,\mathrm{d}s\right)$$

and, if $\mathcal{N}_\lambda{=}(t_n, n{\in}\mathbb{Z})$, with $t_0{\leqslant}0{<}t_1$,

$$= B_{a,1}\mathbb{E}_{\Pi_w^{\mathrm{PA}}}\left(\beta(X(0))\sum_{t_n\leqslant -h}\frac{1}{h}\int_{t_n}^{t_n+h}\exp(\gamma_{a,1}s)\,\mathrm{d}s\right)$$

$$\sim B_{a,1}\mathbb{E}_{\Pi_w^{\mathrm{PA}}}\left(\beta(X(0))\sum_{n\leqslant 0}\exp(\gamma_{a,1}t_n)\right)$$

$$= \mathbb{E}_{\Pi_w^{\mathrm{PA}}}\left(\beta(X(0))Z_{a,1}(0)\right) = \int_{\mathbb{R}_+^5}\beta(x)z_{a,1}\Pi_w^{\mathrm{PA}}(\mathrm{d}x,\mathrm{d}z)$$

by using a representation of $Z_{a,1}(0)$ similar to that of $X_\infty^w(0)$ with Relation (2.13). Similarly,

$$\int_0^{+\infty}\Phi_a(s)\mathbb{E}_{\Pi_w^{\mathrm{PA}}}\left(\frac{\mathcal{N}_{\beta,X}[0,h]}{h}\frac{\mathcal{N}_\lambda[s,s{+}h]}{h}\right)\mathrm{d}s \sim \int_{\mathbb{R}_+^5}\lambda z_{a,2}\Pi_w^{\mathrm{PA}}(\mathrm{d}x,\mathrm{d}z).$$

Extensions

The interest of Relation (2.19) is that it may be formulated for a general plasticity curve Φ_a for all-to-all pair-based models. Recall that the corresponding plasticity kernels are of class $\mathcal{M}$ only for exponential functions. We conjecture that under the conditions, for $a{\in}\{p,d\}$,

— $\displaystyle\int_{-\infty}^{+\infty}|\Phi_a(s)|\,\mathrm{d}s < +\infty$;

— $\lim_{t\to 0+}\Phi_a(t)$ and $\lim_{t\to 0-}\Phi_a(t)$ exist;

the convergence of the scaled process to the ODE (2.19) with a convenient $\widetilde{\mu}$ should hold. For Markovian plasticity kernels, this is done by using Markov properties of the fast processes $(X_\varepsilon(t), Z_\varepsilon(t))$. See [RV21a]. We do not have this tool in the case of a general plasticity curve. The proof of such an extension should require an additional analysis.

2.C Computation of Π_w^{CQ} for $C_1{=}C_2{=}1$

Proposition 25 (Equilibrium of fast process)**.** *For $C_1{=}C_2{=}1$ and $w{\in}\mathbb{N}$, the Markov process on $\mathbb{N}^2$ of Definition 20 has a unique invariant distribution Π_w, and if the distribution of (X_w, C_w) is Π_w, the generating function of C_w is given by, for $u{\in}[0,1]$,*

$$g_w(u) = E\left(u^{C_w}\right) = \exp\left(-\lambda\int_0^{+\infty}\left(1{-}\left(1{-}e^{-\gamma s}{+}ue^{-\gamma s}\right)\left(1{-}p(s)+up(s)\right)^w\right)\mathrm{d}s\right), \quad (2.31)$$

with

$$p(s) = \left(e^{-\gamma s}{-}e^{-(\beta+1)s}\right)/\left(\beta{+}1{-}\gamma\right).$$

In particular, knowing that,

$$\Pi_w^{\mathrm{CQ}}(C{\geqslant}0) = 1,$$

we can easily compute,

$$\Pi_w^{\mathrm{CQ}}(C{\geqslant}1) = 1 - \Pi_w^{\mathrm{CQ}}(C{=}1)$$

with,

$$g_w(0) = \exp\left(-\lambda \int_0^{+\infty} \left(1{-}\left(1{-}e^{-\gamma s}\right)\left(1{-}p(s)\right)^w\right) \mathrm{d}s\right)$$

and,

$$\Pi_w^{\mathrm{CQ}}(C{\geqslant}2) = 1 - g_w(0) - g'_w(0)$$

with,

$$g'_w(0) = \lambda \left[\int_0^{+\infty} \left(e^{-\gamma s}\left(1{-}p(s)\right)^w + wp(s)\left(1{-}e^{-\gamma s}\right)\left(1{-}p(s)\right)^{w-1}\right) \mathrm{d}s\right] g_w(0).$$

BIBLIOGRAPHY

[AFH12] A. Abbassian, M. Fotouhi, and M. Heidari. Neural fields with fast learning dynamic kernel. *Biological cybernetics* **106** (2012), 15–26.

[AK15] D. F. Anderson and T. G. Kurtz. Stochastic Analysis of Biochemical Systems. Mathematical Biosciences Institute Lecture Series. Springer Publishing Company, Incorporated, 2015.

[ARJ20] A. E. Akil, R. Rosenbaum, and K. Josić. Synaptic Plasticity in Correlated Balanced Networks. *bioRxiv* (2020). eprint: `https://doi.org/10.1101/2020.04.26.061515`.

[BA16] B. Babadi and L. F. Abbott. Stability and Competition in Multi-spike Models of Spike-Timing Dependent Plasticity. *PLoS computational biology* **12** (Mar. 2016), e1004750.

[Bal+06] K. Ball, T. G. Kurtz, L. Popovic, G. Rempala, et al. Asymptotic analysis of multiscale approximations to reaction networks. *The Annals of Applied Probability* **16** (2006), 1925–1961.

[BG06] N. Berglund and B. Gentz. Noise-induced phenomena in slow-fast dynamical systems: a sample-paths approach. Springer Science & Business Media, 2006.

[BP98] G.-q. Bi and M.-m. Poo. Synaptic Modifications in Cultured Hippocampal Neurons: Dependence on Spike Timing, Synaptic Strength, and Postsynaptic Cell Type. *Journal of Neuroscience* **18** (Dec. 1998), 10464–10472.

[Che+15] J. Chevallier, M. J. Cáceres, M. Doumic, and P. Reynaud-Bouret. Microscopic approach of a time elapsed neural model. *Mathematical Models and Methods in Applied Sciences* **25** (2015), 2669–2719.

[Clo+10] C. Clopath, L. Büsing, E. Vasilaki, and W. Gerstner. Connectivity reflects coding: a model of voltage-based STDP with homeostasis. *Nature Neuroscience* **13** (Mar. 2010), 344–352.

[Daw93] D. A. Dawson. Measure-valued Markov processes. *École d'Été de Probabilités de Saint-Flour XXI—1991*. Vol. 1541. Lecture Notes in Math. Berlin: Springer, Nov. 1993, 1–260.

[Eur+99] C. W. Eurich, K. Pawelzik, U. Ernst, J. D. Cowan, and J. G. Milton. Dynamics of self-organized delay adaptation. *Physical Review Letters* **82** (1999), 1594.

[Fei19] M. Feinberg. Foundations of chemical reaction network theory. Vol. 202. Applied Mathematical Sciences. Springer, Cham, 2019, xxix+454.

[Fel12] D. E. Feldman. The spike-timing dependence of plasticity. *Neuron* **75** (Aug. 2012), 556–571.

[FGV05] E. Fino, J. Glowinski, and L. Venance. Bidirectional activity-dependent plasticity at corticostriatal synapses. *The Journal of Neuroscience: The Official Journal of the Society for Neuroscience* **25** (Dec. 2005), 11279–11287.

[FW98] M. I. Freidlin and A. D. Wentzell. Random perturbations of dynamical systems. Second Edition edition. New York: Springer-Verlag, 1998.

[Gal+19] A. Galves, E. Löcherbach, C. Pouzat, and E. Presutti. A System of Interacting Neurons with Short Term Synaptic Facilitation. *Journal of Statistical Physics* **178** (Dec. 2019), 869–892.

[Gar10] C. Gardiner. Stochastic Methods: A Handbook for the Natural and Social Sciences (Springer Series in Synergetics). Softcover reprint of hardcover 4th ed. 2009 edition. Springer Series in Synergetics. Springer, 2010.

[GB10] M. Graupner and N. Brunel. Mechanisms of induction and maintenance of spike-timing dependent plasticity in biophysical synapse models. *Frontiers in Computational Neuroscience* **4** (2010).

[GB12] M. Graupner and N. Brunel. Calcium-based plasticity model explains sensitivity of synaptic changes to spike pattern, rate, and dendritic location. *Proceedings of the National Academy of Sciences of the United States of America* **109** (Mar. 2012), 3991–3996.

[GK02b] W. Gerstner and W. M. Kistler. Spiking Neuron Models: Single Neurons, Populations, Plasticity. Cambridge University Press, Aug. 2002.

[GP60] E. N. Gilbert and H. O. Pollak. Amplitude Distribution of Shot Noise. *Bell System Technical Journal* **39** (Mar. 1960), 333–350.

[GWO16] M. Graupner, P. Wallisch, and S. Ostojic. Natural Firing Patterns Imply Low Sensitivity of Synaptic Plasticity to Spike Timing Compared with Firing Rate. *Journal of Neuroscience* **36** (Nov. 2016), 11238–11258.

[Has80] R. Z. Has'minskiĭ. Stochastic stability of differential equations. Alphen aan den Rijn: Sijthoff & Noordhoff, 1980, xvi+344.

[Hel18] P. Helson. A new stochastic STDP Rule in a neural Network Model. *arXiv:1706.00364 [math]* (Mar. 2018).

[Hor+00] D. Horn, N. Levy, I. Meilijson, and E. Ruppin. Distributed synchrony of spiking neurons in a Hebbian cell assembly. *Advances in neural information processing systems*. 2000, 129–135.

[HS08] M. J. Higley and B. L. Sabatini. Calcium signaling in dendrites and spines: practical and functional considerations. *Neuron* **59** (Sept. 2008), 902–913.

[KGH99] R. Kempter, W. Gerstner, and J. L. van Hemmen. Hebbian learning and spiking neurons. *Physical Review E* **59** (Apr. 1999), 4498–4514.

[KH00] W. M. Kistler and J. L. v. Hemmen. Modeling Synaptic Plasticity in Conjunction with the Timing of Pre- and Postsynaptic Action Potentials. *Neural Computation* **12** (Feb. 2000), 385–405.

[Kin92] J. F. C. Kingman. Poisson Processes. Clarendon Press, Dec. 1992.

[KK+13] H.-W. Kang, T. G. Kurtz, et al. Separation of time-scales and model reduction for stochastic reaction networks. *The Annals of Applied Probability* **23** (2013), 529–583.

[KP17] R. Kumar and L. Popovic. Large deviations for multi-scale jump-diffusion processes. *Stochastic Processes and their Applications* **127** (2017), 1297–1320.

[Kur92] T. G. Kurtz. Averaging for martingale problems and stochastic approximation. *Applied Stochastic Analysis*. Ed. by I. Karatzas and D. Ocone. Vol. 177. Berlin/Heidelberg: Springer-Verlag, 1992, 186–209.

[LF12] T. K. Leen and R. Friel. Stochastic Perturbation Methods for Spike-Timing-Dependent Plasticity. *Neural Comput.* **24** (May 2012), 1109–1146.

[MDG08] A. Morrison, M. Diesmann, and W. Gerstner. Phenomenological models of synaptic plasticity based on spike timing. *Biological Cybernetics* **98** (June 2008), 459–478.

[NOI01] J. Nakai, M. Ohkura, and K. Imoto. A high signal-to-noise Ca(2+) probe composed of a single green fluorescent protein. *Nature Biotechnology* **19** (Feb. 2001), 137–141.

[Paw67] R. Pawula. Generalizations and extensions of the Fokker-Planck-Kolmogorov equations. *IEEE Transactions on Information Theory* **13** (1967), 33–41.

[PSV77] G. Papanicolalou, D. W. Stroock, and S. R. S. Varadhan. Martingale approach to some limit theorems. *Proc. 1976. Duke Conf. On Turbulence*. III. Duke Univ. Math, 1977.

[PSW17] B. Perthame, D. Salort, and G. Wainrib. Distributed synaptic weights in a LIF neural network and learning rules. *Physica D: Nonlinear Phenomena* **353** (2017), 20–30.

[RBT00a] M. C. van Rossum, G. Q. Bi, and G. G. Turrigiano. Stable Hebbian learning from spike timing-dependent plasticity. *The Journal of Neuroscience: The Official Journal of the Society for Neuroscience* **20** (Dec. 2000), 8812–8821.

[RKO18] J. Rubin, B. Krauskopf, and H. Osinga. Natural extension of fast-slow decomposition for dynamical systems. *Physical Review E* **97** (2018), 012215.

[RLS01] J. Rubin, D. D. Lee, and H. Sompolinsky. Equilibrium properties of temporally asymmetric Hebbian plasticity. *Physical Review Letters* **86** (Jan. 2001), 364–367.

[Rob00] P. D. Roberts. Dynamics of temporal learning rules. *Phys. Rev. E* **62** (3 Sept. 2000), 4077–4082.

[Rob03] P. Robert. Stochastic Networks and Queues. Stochastic Modelling and Applied Probability. Berlin Heidelberg: Springer-Verlag, 2003.

[Rob99] P. D. Roberts. Computational Consequences of Temporally Asymmetric Learning Rules: I. Differential Hebbian Learning. *Journal of Computational Neuroscience* **7** (Nov. 1999), 235–246.

[RT16] P. Robert and J. Touboul. On the Dynamics of Random Neuronal Networks. *Journal of Statistical Physics* **165** (Nov. 2016), 545–584.

[RV21a] P. Robert and G. Vignoud. Averaging Principles for Markovian Models of Plasticity. *Journal of Statistical Physics* **183** (June 2021), 47–90.

[RV21b] P. Robert and G. Vignoud. Stochastic Models of Neural Plasticity. *SIAM Journal on Applied Mathematics* **81** (Sept. 2021), 1821–1846.

[ZR02] R. S. Zucker and W. G. Regehr. Short-term synaptic plasticity. *Annual Review of Physiology* **64** (2002), 355–405.

CHAPTER 3

AVERAGING PRINCIPLES FOR MARKOVIAN MODELS OF PLASTICITY

ABSTRACT

In this paper we consider a stochastic system with two connected nodes, whose unidirectional connection is variable and depends on point processes associated to each node. The *input* node is represented by an homogeneous Poisson process, whereas the *output* node jumps with an intensity that depends on the jumps of the input node and the connection intensity. We study a scaling regime when the rate of both point processes is large compared to the dynamics of the connection. In neuroscience, this system corresponds to a neural network composed by two neurons, connected by a single synapse. The strength of this synapse depends on the past activity of both neurons, the notion of *synaptic plasticity* refers to the associated mechanism. A general class of such stochastic models has been introduced in [RV20] to describe most of the models of long-term synaptic plasticity investigated in the literature. The scaling regime corresponds to a classical assumption in computational neuroscience that cellular processes evolve much more rapidly than the synaptic strength.

The central result of the paper is an averaging principle for the time evolution of the connection intensity. Mathematically, the key variable is the point process, associated to the output node, whose intensity depends on the past activity of the system. The proof of the result involves a detailed analysis of several of its unbounded additive functionals in the slow-fast limit, and technical results on interacting shot-noise processes.

3.1 Introduction

Neurons exchange electrical and chemical signals at specific spots, called synapses. The synaptic transmission between neural cells is unidirectional, in the sense that, the signal goes from the pre-synaptic neuron towards the post-synaptic neuron. This interaction is modulated over time, and particularly by the concomitant activity of both neurons. In [RV20] we have introduced a general class of mathematical models to represent and study synaptic plasticity mechanisms.

A basic model to investigate such phenomenon consists of a pre-synaptic neuron connected through a synapse to a post-synaptic neuron. The associated stochastic process is described by two random variables (X, W) and the spiking activity of each neuron is represented by a point process.

a. Point process for pre-synaptic spikes: $\mathcal{N}_\lambda$.
This point process is associated to the instants when the pre-synaptic neuron is spiking, i.e. when it transmits a chemical/electrical signal to the post-synaptic neuron via the synapse. We assume that $\mathcal{N}_\lambda$ is an homogeneous Poisson process with rate λ.

b. Synaptic weight: W.
It describes the strength of the connection from the pre-synaptic neuron to the post-synaptic neuron.

c. Post-synaptic membrane potential: X.
This variable is for the current activity of the post-synaptic neuron. At a jump of $\mathcal{N}_\lambda$, the membrane potential X is incremented by W, where W is the current synaptic weight.

d. Point process for post-synaptic spikes: $\mathcal{N}_{\beta,X}$.
In state $X{=}x$, the post-synaptic neuron emits a spike at rate $\beta(x)$, where β is *the activation function* of the neural cell. The point process associated to these instants is an inhomogeneous Poisson process denoted by $\mathcal{N}_{\beta,X}$. This is a key variable of the stochastic model. See Relation (3.6) for a formal definition.

As explained in [RV20], for some synaptic mechanisms, the time evolution of W may depend, in a complex way, on past spiking times of both adjacent neurons. In our model it is a functional of the point processes $\mathcal{N}_\lambda$ and $\mathcal{N}_{\beta,X}$. The model relies on two clearly stated hypotheses: the effect of plasticity only depends on the *relative timing of the activity of both neuronal cells* and is seen over the synaptic strength on *long timescales*.

Accordingly, the purpose of the current paper is to prove limit theorems for a scaled version of the corresponding stochastic processes $(X(t), W(t))$.

A simple model

We begin by the description of a simplified model to highlight the role of the different components in these stochastic models. We consider the following set of Stochastic Differential Equations (SDEs),

$$\begin{cases} \mathrm{d}X(t) &= -X(t)\,\mathrm{d}t + W(t-)\mathcal{N}_\lambda(\mathrm{d}t), \\ \mathrm{d}Z(t) &= -\gamma Z(t)\,\mathrm{d}t + B_1\mathcal{N}_\lambda(\mathrm{d}t) + B_2\mathcal{N}_{\beta,X}(\mathrm{d}t), \\ \mathrm{d}W(t) &= Z(t-)\mathcal{N}_{\beta,X}(\mathrm{d}t), \end{cases} \tag{3.1}$$

where $h(t-)$ is the left-limit of the function h at $t{>}0$ and, for $i{=}\{1,2\}$, $B_i{\in}\mathbb{R}_+$.

In this model, the time evolution of $(W(t))$ is overly simplified, plasticity processes are modeled by an increase of the synaptic weight W at each jump of $\mathcal{N}_{\beta,X}$ by the value of $(Z(t))$.

The process $(Z(t))$ encodes the past spiking activity of both neurons through an additive functional of $\mathcal{N}_\lambda$ and $\mathcal{N}_{\beta,X}$ with an exponential decay factor $\gamma{>}0$. The process $(Z(t))$ is associated to a cellular process, in the general model this is a multi-dimensional process.

The main process of interest is the strength of the synaptic connection $(W(t))$. It has been extensively studied both in experimental neuroscience and in physics, there are nevertheless few rigorous mathematical results on the dynamical evolution of W.

From a mathematical perspective, the variables $(X(t), Z(t), W(t))$, solutions of SDE (3.1) are central to the model. The point process $\mathcal{N}_{\beta,X}$ is nevertheless the key component of the system since it drives the time evolution of $(Z(t))$ and $(W(t))$ and, consequently, of $(X(t))$. Most of the mathematical difficulties of our paper are related to asymptotic estimates of linear functionals of $\mathcal{N}_{\beta,X}$.

The scaling approach of this paper follows from the fact that the model can be expressed as a *slow-fast* system. An important property of this system is that neuronal processes, associated to the point processes $\mathcal{N}_\lambda$ and $\mathcal{N}_{\beta,X}$, occur on a timescale which is much faster than the timescale of the evolution of $(W(t))$. See Sections 1 and 4.1 of [RV20] and the references therein for a discussion on this topic.

Using this scaling for the simple model, SDE (3.1) becomes, for $\varepsilon>0$,

$$\begin{cases} \mathrm{d}X_\varepsilon(t) &= -X_\varepsilon(t)\,\mathrm{d}t/\varepsilon + W_\varepsilon(t-)\mathcal{N}_{\lambda/\varepsilon}(\mathrm{d}t), \\ \mathrm{d}Z_\varepsilon(t) &= -\gamma Z_\varepsilon(t)\,\mathrm{d}t/\varepsilon + B_1\mathcal{N}_{\lambda/\varepsilon}(\mathrm{d}t) + B_2\mathcal{N}_{\beta/\varepsilon,X_\varepsilon}(\mathrm{d}t), \\ \mathrm{d}W_\varepsilon(t) &= Z_\varepsilon(t-)\varepsilon\mathcal{N}_{\beta/\varepsilon,X_\varepsilon}(\mathrm{d}t). \end{cases} \tag{3.2}$$

Pre-synaptic spikes occur at rate λ/ε and when the membrane potential of the post-synaptic cell is x, a post-synaptic spike occurs at rate $\beta(x)/\varepsilon$. The variables $(X_\varepsilon(t))$ and $(Z_\varepsilon(t))$ evolve on the timescale $t\mapsto t/\varepsilon$, with ε small, they are *fast variables*.

Conversely, the increments of the variable W are scaled with the parameter ε, the integration of the differential element $\varepsilon\mathcal{N}_{\beta/\varepsilon,X_\varepsilon}(\mathrm{d}s)$ on a bounded time-interval is $O(1)$. For this reason, $(W_\varepsilon(t))$ is described as a *slow process*.

This is a classical assumption in the corresponding models of statistical physics. Approximations of $(W_\varepsilon(t))$ when ε is small are discussed and investigated with ad hoc methods, see [KGH99] for example.

Averaging principles

The main goal of the present paper is to establish a limit result, or averaging principle, for $(W_\varepsilon(t))$ when ε goes to 0 for a general class of synaptic plasticity models.

We denote by (X^w, Z^w) the solution $(X(t), Z(t))$ of Relation (3.2) when the process $(W(t))$ is constant and equal to w. Under appropriate conditions, it has a unique equilibrium distribution Π_w. The averaging principle for the simple model can be expressed as follows.

There exists $S_0\in(0,+\infty]$, such that the processes $(W_\varepsilon(t), 0\leqslant t<S_0)$ is tight for the convergence in distribution when ε goes to 0, and any limiting point $(w(t), 0\leqslant t<S_0)$ satisfies the following integral equation,

$$w(t) = w(0) + \int_0^t \int_{\mathbb{R}_+^2} z\beta(x)\Pi_{w(s)}(\mathrm{d}x,\mathrm{d}z)\;\mathrm{d}s, \quad t\in[0,S_0). \tag{3.3}$$

See Section 5 of Chapter 1 of [Bil99] for general results on tightness properties and convergence in distribution.

We discuss now some of the technical difficulty to derive such results for our model. The integration of SDE (3.2) gives the relation

$$W_\varepsilon(t) = W_\varepsilon(0) + \int_0^t Z_\varepsilon(s-)\varepsilon\mathcal{N}_{\beta/\varepsilon,X_\varepsilon}(\mathrm{d}s).$$

The tightness of the family of processes $(W_\varepsilon(t))$ is equivalent to the tightness of

$$\left(\int_0^t Z_\varepsilon(s)\varepsilon\mathcal{N}_{\beta/\varepsilon,X_\varepsilon}(\mathrm{d}s)\right) \tag{3.4}$$

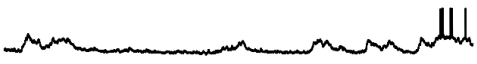

A general approach to prove averaging principles is presented in [Kur92] for jump processes. See Chapter 7 of [FW98] and especially [PSV77] for an introduction to averaging principles. If we had an expression of the type

$$\left(\int_0^t F(X_\varepsilon(s), Z_\varepsilon(s))\,\mathrm{d}s\right),$$

where $s \to F(X_\varepsilon(s), Z_\varepsilon(s))$ is a bounded continuous function on $\mathbb{R}_+$, a direct use of the results of [Kur92], Lemma 1.3 and 1.5, would give the desired tightness. This is the case of [Hel18] for the time-elapsed model of plasticity for which this representation holds, one of the few rigorous results in this domain.

It does not seem to be possible to handle functionals of the form (3.4) in this way. The process $(Z_\varepsilon(s))$ is clearly not bounded and neither is the intensity of the point process $\mathcal{N}_{\beta/\varepsilon, X_\varepsilon}$, since $(\beta(X_\varepsilon(s))$ is also not bounded. Remember that fast processes are on a rapid time scale so visit their state space "quickly", the values of the integrals of (3.4) can be large and therefore must be controlled in an appropriate way.

Two other interesting properties emerge from the stochastic averaging result from Section 3.4.

a. Uniqueness.
If Relation (3.3) has a unique solution for a given initial state, a result for the convergence in distribution of $(W_\varepsilon(t))$ when ε goes to 0 is therefore obtained. Uniqueness holds if the integrand, with respect to s, of the right-hand side of Relation (3.3) is locally Lipschitz as a function of $w(s)$. Regularity properties of the invariant distribution Π_w as a function of w need to be verified and this is not a concern in the case of our simple model. We will consider in fact much more general models for (X^w, Z^w), when Z^w a multi-dimensional process in particular. We did not try to state a set of conditions that can ensure the desired regularity properties of the corresponding Π_w. The proof of the Harris ergodicity of (X^w, Z^w) for a fixed w of Section 3.C of Appendix, though not really difficult, is already cumbersome.

The proof of Proposition 45 for the simple model gives an example of how this property can be established. In a general context, this kind of result is generally proved via the use of a common Lyapounov function for (X^w, Z^w) for all w is in the neighborhood of some $w_0 > 0$. See [Has80], for example. Uniqueness results have already been obtained in Sections 5 and 6 of [RV20] for several important practical cases. In Section 3.8 we investigate these questions for our simple model.

b. Blow-up phenomenon.
The convergence properties are stated on *a fixed time interval* $[0, S_0)$. For some models, the variable S_0 cannot be taken as $+\infty$, see the example of Section 3.4 and Proposition 47. More specifically, the limit in distribution of $(W_\varepsilon(t))$ as ε goes to 0 blows-up, i.e. hits infinity in finite time. An analogue property holds for some mathematical models of large populations of neural cells with fixed synaptic strengths. See [CCP11] for example, where the blow-up phenomenon is the result of mutually exciting dynamics of populations of neural cells. In our case, the strengthening of the connection may grow without bounds when the activation function β has a linear growth. See Proposition 47 of Section 3.8.

A brief description of the general model of synaptic plasticity

We shortly describe the general setting of the models investigated in this paper. See Section 3.2 for a detailed presentation.

a. The process $(X(t))$.
The output neuron follows leaky-integrate dynamics as in Equation (3.1). In addition, the influence of a post-synaptic spike $\mathcal{N}_{\beta,X}$ at time $t>0$ is represented as a drop $-g(X(t-))$ of the post-synaptic potential after the spike.

b. The process $(Z(t))=(Z_i(t))$ is a multi-dimensional process satisfying the same type of ODE as in our simple case but with the constants B_1 and B_2 being replaced by functions k_1 and k_2 of $Z(t)$. A constant drift term k_0 is also added to the dynamics. The ith component $(Z_i(t))$ satisfies an SDE of the type

$$\mathrm{d}Z_i(t) = (-\gamma_i Z_i(t)+k_{0,i})\,\mathrm{d}t+k_{1,i}(Z(t-))\mathcal{N}_\lambda(\mathrm{d}t)+k_{2,i}(Z(t-))\mathcal{N}_{\beta,X}(\mathrm{d}t).$$

c. Evolution of $(W(t))$.
The dependence is more sophisticated since it involves two additional processes (Ω_p, Ω_d). The first one, $(\Omega_p(t))$ integrates, with an exponential decay α a linear combination of the processes leading to potentiation, i.e. to increase the synaptic weight. The process $(\Omega_d(t))$ has a similar role for depression, i.e. to decrease the synaptic weight. They are expressed as, for $a\in\{p,d\}$,

$$\Omega_a(t)=\int_0^t e^{-\alpha(t-s)}\left[n_{0,a}(Z(s))\,\mathrm{d}s+n_{1,a}(Z(s-))\mathcal{N}_\lambda(\mathrm{d}s)+n_{2,a}(Z(s-))\mathcal{N}_{\beta,X}(\mathrm{d}s)\right].$$

The changes of $(Z(t))$ are thus integrated "smoothly" in the evolution of $(W(t))$ in agreement with measurements of the biological literature. See Appendix A of [RV20]. Finally, $(W(t))\in K_W$ verifies

$$\mathrm{d}W(t) = M\left(\Omega_p(t), \Omega_d(t), W(t)\right)\mathrm{d}t,$$

where $K_W\subset\mathbb{R}$ represents the synaptic weight domain, and the functional M is such that $W(t)$ stays in K_W for all $t\geqslant 0$.

It has been shown in Section 3 of [RV20] that these models encompass most classical STDP models from statistical physics. The multiple coordinates of $(Z(t))$ can be interpreted as the concentrations of chemical components implicated in plasticity, that are created/suppressed by spiking mechanisms

Links to non-linear Hawkes point processes

The spiking instants of a neuron can also be seen as a self-exciting point process since its instantaneous jump rate depends on past instants of its jumps. This corresponds to the class of Hawkes point process $\mathcal{M}$ on $\mathbb{R}_+$ associated to a function ϕ and exponential decay γ. More precisely, it is a non-homogeneous Poisson point process $\mathcal{M}$ whose intensity function $(\lambda(t))$ is given by

$$(\lambda(t)) = \left(\phi\left(\int_0^t e^{-\gamma(t-s)}\mathcal{M}(\mathrm{d}s)\right)\right).$$

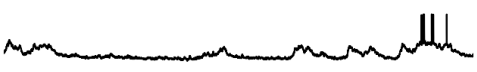

These processes have received of lot of attention from the mathematical literature, for some time now. They are mainly used in models of mathematical finance, but also in neurosciences. See the pioneering works of [HO74] and [Ker64].

A special case of the first equation of Relation (3.1) is, for $w \geqslant 0$,

$$\mathrm{d}X(t) = -X(t)\,\mathrm{d}t + w\mathcal{N}_\lambda(\mathrm{d}t) - \mathcal{N}_{\beta,X}(\mathrm{d}t),$$

if $X(0)=0$, Lemma 30 below gives the representation

$$X(t) = w\int_0^t e^{-(t-s)}\mathcal{N}_\lambda(\mathrm{d}s) - \int_0^t e^{-(t-s)}\mathcal{N}_{\beta,X}(\mathrm{d}s),\ \forall t \geqslant 0.$$

Hence, $\mathcal{N}_{\beta,X}$ can be seen as an extended Hawkes process with activation function β and exponential decay 1.

In the system of equations (3.1), $(X(t))$ and $(Z(t))$ can also be represented as a multi-dimensional Hawkes processes. See [Haw71]. However in our model, an important feature not present in studies of Hawkes processes has been added: the synaptic weight process $(W(t))$ is not constant.

Extensions

The stochastic model with plastic connections presented in this paper may also be used in other contexts than neuroscience. Auto-exciting processes, Hawkes process, used in finance [ELL11], genomics [GS05; RS10], sociology [CS08] suppose, in general, that the influence of each point process on the others is constant over time. For example in [CS08], a Hawkes process is defined to describe the cascade of influences that exist in a social network, taking the example of Youtube videos views. The coefficients that model interactions between different individuals are constant. One could extend this model by taking into account the fact that individuals who watch repeatedly videos at the same time, may develop a stronger interaction. It should be therefore possible to extend these classes of models by adding a dependence of the connections on the past activity of the Hawkes process as for our models. Using classical results on stationary distributions of Hawkes processes with fixed connectivity, a slow-fast analysis similar to the one developed here should then be possible for these models.

Organization of the paper

In Section 3.2, the main processes and definitions are introduced as well as assumptions to prove an averaging principle. The scaling is presented in Section 3.3 and the averaging principle in Section 3.4. In this section the general strategy for the proof of the main theorem is detailed. Section 3.5 investigates monotonicity properties and a coupling result, crucial in the proof of tightness, is proved. Section 3.6 is devoted to the proof of tightness results when the process $(W_\varepsilon(t))$ is assumed to be bounded. Finally, the proof of the main theorem is completed in Section 3.7. In Section 3.B of Appendix, several useful tightness results are proved for interacting shot-noise processes. The ergodicity properties of fast processes are analyzed in Section 3.C of Appendix. Section 3.D of the Appendix discusses averaging principles for related discrete models of synaptic plasticity.

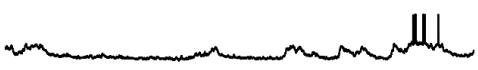

3.2 A stochastic model for plasticity

We define the stochastic model associated to Markovian plasticity kernels introduced in [RV20]. The probabilistic setting of these models along with formal definitions are detailed in the following section.

Definitions and notations

The space of Borelian subsets of a topological space H, is denoted as $\mathcal{B}(H)$. Let $(\Omega, \mathcal{F}, (\mathcal{F}_t), \mathbb{P})$ be a filtered probability space. We assume that two independent Poisson processes, $\mathcal{P}_1$ and $\mathcal{P}_2$ on $\mathbb{R}_+^2$, with intensity $\mathrm{d}x \times \mathrm{d}y$ are defined on $(\Omega, \mathcal{F}, (\mathcal{F}_t), \mathbb{P})$. See [Kin92] for example. For $\mathcal{P} \in \{\mathcal{P}_1, \mathcal{P}_2\}$ and $A, B \in \mathcal{B}(\mathbb{R}_+)$ and a Borelian function f on $\mathbb{R}_+$,

$$\mathcal{P}(A \times B) \overset{\text{def.}}{=} \int_{A \times B} \mathcal{P}(\mathrm{d}x, \mathrm{d}y), \int_{\mathbb{R}_+} f(y) \mathcal{P}(A, \mathrm{d}y) \overset{\text{def.}}{=} \int_{A \times \mathbb{R}_+} f(y) \mathcal{P}(\mathrm{d}x, \mathrm{d}y).$$

For $t \geqslant 0$, the σ-field $\mathcal{F}_t$ of the filtration $(\mathcal{F}_t)_{t \geqslant 0}$ is assumed to contain all events before time t for both point processes, i.e.

$$\sigma\left(\mathcal{P}_1(A \times (s,t]), \mathcal{P}_2(A \times (s,t]), A \in \mathcal{B}(\mathbb{R}_+), s \leqslant t\right) \subset \mathcal{F}_t. \tag{3.5}$$

A stochastic process $(H(t))$ is *adapted* if, for all $t \geqslant 0$, $H(t)$ is $\mathcal{F}_t$-measurable. It is a *càdlàg process* if, almost surely, it is right continuous and has a left limit at every point $t > 0$, $H(t-)$ denotes the left limit of $(H(t))$ at t. The Skorohod space of càdlàg functions from $[0,T]$ to S is denoted as $\mathcal{D}([0,T], S)$. See [Bil99] and [EK09]. The mention of adapted stochastic processes, or of martingale, will be implicitly associated to the filtration $(\mathcal{F}_t)_{t \geqslant 0}$.

The set of real continuous bounded functions on the metric space $\mathcal{S} \subset \mathbb{R}^d$ is denoted by $\mathcal{C}_b(\mathcal{S})$. $\mathcal{C}_b^k(\mathcal{S}) \subset \mathcal{C}_b(\mathcal{S})$ is the set of bounded, k-differentiable functions on $\mathcal{S}$ with respect to each coordinate, with all derivatives bounded and continuous. The multi-dimensional extensions to $\mathcal{S}$ are denoted by $\mathcal{C}_b^k(\mathcal{S}, \mathcal{S})$.

Inhomogeneous Poisson Process for the Output Node. We introduce an important point process $\mathcal{N}_{\phi,H}$, that represents the jumps of a node whose activity process is $(H(t))$, with activation function ϕ. ϕ is a non-negative càdlàg function on $\mathbb{R}$, it is defined by

$$\int_{\mathbb{R}_+} f(u) \mathcal{N}_{\phi,H}(\mathrm{d}u) \overset{\text{def.}}{=} \int_{\mathbb{R}_+} f(u) \mathcal{P}_2\left((0, \phi(H(u-))], \mathrm{d}u\right), \tag{3.6}$$

for any Borelian function f on $\mathbb{R}_+$.

The plasticity process

In the rest of the paper, we will consider a more generic connected system with plasticity, inspired from the neuronal example given in the Introduction. An *input* node will be represented by an homogeneous Poisson process with intensity λ, taking up the role of the pre-synaptic neuron. This input node will interact with an *output* node, whose activity X (i.e. membrane potential) integrates over time the jumps of the input node, with an amplitude W and an exponential decay taken with time constant 1. The output

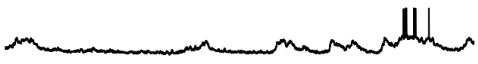

node jumps with an inhomogeneous rate $\beta(X)$ that depends on the output node activity X. The connection intensity W is plastic and depends on previous interactions between both nodes, through a Markovian multi-dimensional variable Z, in the same way that the synaptic weight undergoes synaptic plasticity in the neuronal model.

Definition 26 (Time evolution)**.** *The càdlàg process*

$$(U(t))=(X(t),Z(t),\Omega_p(t),\Omega_d(t),W(t))\in\mathbb{R}\times\mathbb{R}_+^\ell\times\mathbb{R}_+^2\times K_W,$$

is solution of the following Stochastic Differential Equations (SDE), starting from some initial state $U(0)=U_0=(x_0,z_0,\omega_{0,p},\omega_{0,d},w_0)$*.*

$$\begin{cases}\mathrm{d}X(t) &= -X(t)\,\mathrm{d}t+W(t)\mathcal{N}_\lambda(\mathrm{d}t)-g\left(X(t-)\right)\mathcal{N}_{\beta,X}\left(\mathrm{d}t\right),\\ \mathrm{d}Z(t) &= (-\gamma\odot Z(t)+k_0)\,\mathrm{d}t+k_1(Z(t-))\mathcal{N}_\lambda(\mathrm{d}t)+k_2(Z(t-))\mathcal{N}_{\beta,X}(\mathrm{d}t),\\ \mathrm{d}\Omega_a(t) &= -\alpha\Omega_a(t)\,\mathrm{d}t+n_{a,0}(Z(t))\,\mathrm{d}t\\ &\qquad +n_{a,1}(Z(t-))\mathcal{N}_\lambda(\mathrm{d}t)+n_{a,2}(Z(t-))\mathcal{N}_{\beta,X}(\mathrm{d}t),\quad a\in\{p,d\},\\ \mathrm{d}W(t) &= M\left(\Omega_p(t),\Omega_d(t),W(t)\right)\mathrm{d}t,\end{cases}\tag{3.7}$$

with the notation $a\odot b=(a_kb_k)$ *for the* Hadamard *product, for* $a=(a_k)$, $b=(b_k)\in\mathbb{R}_+^\ell$.

Recall that, see Section 3.1, K_W is an interval of $\mathbb{R}$ which contains the range of values for the connection intensity.

We now state the assumptions used for the proof of Theorem 29.

Inputs jumps

The jumps of the input node are given by a Poisson process with rate $\lambda>0$,

$$\mathcal{N}_\lambda(\mathrm{d}t)\overset{\text{def.}}{=}\mathcal{P}_1\left((0,\lambda],\mathrm{d}t\right),\tag{3.8}$$

where $\mathcal{P}_1$ is the Poisson point process introduced in Section 3.2.

Output jumps

When the output node activity is x, a jump of the output node occurs at rate $\beta(x)$ and leads to a decrease of output activity $x-g(x)$:

— It is assumed that β is a non-negative, continuous function on $\mathbb{R}$ and that $\beta(x)=0$ for $x\leqslant -c_\beta\leqslant 0$. Additionally, there exists a constant $C_\beta\geqslant 0$ such that

$$\beta(x)\leqslant C_\beta(1+|x|),\quad \forall x\in\mathbb{R}.\tag{3.9}$$

— The function g is continuous on $\mathbb{R}$ and $0\leqslant g(x)\leqslant\max(c_g,x)$ holds for all $x\in\mathbb{R}$, for some $c_g\geqslant 0$.

The jumps of the output node are represented by the point process $\mathcal{N}_{\beta,X}$. Recall that

$$\mathcal{N}_{\beta,X}(\mathrm{d}t)=\mathcal{P}_2\left((0,\beta(X(t-))],\mathrm{d}t\right).$$

The process $(Z(t))$

The process $(Z(t))$ is a multi-dimensional process, with values in $\mathbb{R}_+^\ell$, it is driven by the general spiking activity of the system, and therefore, depends only on the point processes $\mathcal{N}_\lambda$ and $\mathcal{N}_{\beta,X}$. For some models it describes the time evolution of chemical components within the synapse. $(Z(t))$ is a càdlàg function with values in $\mathbb{R}_+^\ell$, solution of the stochastic differential equation

$$\mathrm{d}Z(t) = (-\gamma \odot Z(t) + k_0)\,\mathrm{d}t + k_1(Z(t-))\mathcal{N}_\lambda(\mathrm{d}t) + k_2(Z(t-))\mathcal{N}_{\beta,X}, \tag{3.10}$$

where, as before, $\odot$ is for the Hadamard product, $k_0 \in \mathbb{R}_+^\ell$ is a constant and k_1 and k_2 are measurable functions from $\mathbb{R}_+^\ell$ to $\mathbb{R}^\ell$. Furthermore, the (k_i) are chosen such that $(z(t))$ has values in $\mathbb{R}_+^\ell$ whenever $z(0) \in \mathbb{R}_+^\ell$.

It is assumed that

a. all coordinates of the vector γ are positive;

b. the non-negative functions k_i, $i=\{0,1,2\}$, are $\mathcal{C}_b^1(\mathbb{R}_+^\ell, \mathbb{R}_+^\ell)$ and bounded by $C_k \geqslant 0$.

The process $(\Omega_p(t), \Omega_d(t))$

These variables, in $\mathbb{R}_+^2$ encode, with an exponential decay, the total memory of instantaneous plasticity processes represented by the process $(Z(t))$. The process $(\Omega_p(t))$ is driving potentiation of the connection, i.e. the derivative of the connection intensity is an increasing function of this variable. In an analogous way, $(\Omega_d(t))$ is associated to depression, i.e. the derivative of the connection intensity is a decreasing function of this variable. The system of equations for $(\Omega_p(t), \Omega_d(t))$ is a set of two one-dimensional SDEs, for $a \in \{p, d\}$,

$$\mathrm{d}\Omega_a(t) = -\alpha\Omega_a(t)\,\mathrm{d}t + n_{a,0}(Z(t))\,\mathrm{d}t + n_{a,1}(Z(t-))\mathcal{N}_\lambda(\mathrm{d}t) + n_{a,2}(Z(t-))\mathcal{N}_{\beta,X}(\mathrm{d}t).$$

We suppose that there exists a constant C_n such that, for $j \in \{0,1,2\}$, $a \in \{p,d\}$, $n_{a,j}$ verifies,

$$n_{a,j}(z) \leqslant C_n(1 + \|z\|), \tag{3.11}$$

where, for $z \in \mathbb{R}_+^\ell$, $\|z\| = z_1 + \cdots + z_\ell$.

For any $w \in K_W$ and $a \in \{p,d\}$, the discontinuity points of

$$(x,z) \mapsto (n_{a,0}(z), n_{a,1}(z), \beta(x)n_{a,2}(z))$$

are negligible for the invariant probability distribution Π_w of $(X(t), Z(t))$ when $(W(t))$ is constant equal to w. See Section 3.C.

When $(W(t))$ is constant, the process $(X(t), Z(t))$ can be seen as generalized shot-noise processes, see Section 3.B. It is well-known that the invariant distribution of the classical, one-dimensional, shot-noise process is absolutely continuous w.r.t Lebesgue's measure. See examples of Sections 5 and 6 of [RV20] and the reference [BCR19] for criteria in this domain.

Dynamics of the connection intensity

The functional M drives the dynamics of the connection intensity, the corresponding equation is given by Relation (3.7). In particular, for any $w{\in}K_W$ and any càdlàg piecewise-continuous functions h_1 and h_2 on $\mathbb{R}_+$, the ODE

$$\frac{\mathrm{d}w}{\mathrm{d}t}(t){=}M(h_1(t),h_2(t),w(t)) \text{ with } w(0){=}w, \tag{3.12}$$

for all points of continuity of h_1 and h_2, has a unique continuous solution denoted by $(S[h_1,h_2](w,t))$ in K_W. We assume that M can be decomposed as $M(\omega_p,\omega_d,w){=}M_p(\omega_p,w){-}M_d(\omega_d,w)-\mu w$, where $M_a(\omega_a,w)$ is non-negative continuous function, non-decreasing on the first coordinate for a fixed $w{\in}K_w$, and,

$$M_a(\omega_a,w)\leqslant C_M(1+\omega_a),$$

for all $w{\in}K_W$, for $a{\in}\{p,d\}$.

Discrete models of plasticity

A model of plasticity with discrete state space has been introduced in [RV20]. The proof of the associated averaging principles for the continuous case can be adapted to such systems. Relevant parts of the proof are briefly presented in Section 3.D of the Appendix.

3.3 The scaled process

The SDEs of Definition 26 are difficult to study without any additional hypothesis. Existence and uniqueness of solutions to this system are guaranteed by Proposition 1 of [RV20]. It can be seen as an intricate fixed point equation for the processes $(X(t),W(t))$ involving functionals of these processes like $\mathcal{N}_{\beta,X}$ defined by Relation (3.6).

As explained in Section 4 of [RV20], $(X(t),Z(t))$ are associated to fast dynamics at the cellular level while the process $(W(t))$ evolves on a much longer timescale. For this reason, a scaling parameter $\varepsilon{>}0$ is introduced so that $(X(t),Z(t))$ evolves on the timescale $t{\mapsto}t/\varepsilon$. More precisely:

— Fast Processes: $(X(t))$ and $(Z(t))$.
The point processes associated to input and output jumps driving the time evolution of $(X(t))$ and $(Z(t))$ are sped-up by a factor $1/\varepsilon$: $\mathcal{N}_\lambda{\to}\mathcal{N}_{\lambda/\varepsilon}$ and $\mathcal{N}_{\beta,X}{\to}\mathcal{N}_{\beta/\varepsilon,X}$. The deterministic part of the evolution is changed accordingly $\mathrm{d}t{\to}\,\mathrm{d}t/\varepsilon$.

— Slow Processes: $(W(t))$ and $(\Omega_p(t),\Omega_d(t))$.
Update of $(\Omega_p(t))$ and $(\Omega_d(t))$ due to fast jump processes have a small amplitude, $\mathcal{N}_\lambda{\to}\varepsilon\mathcal{N}_{\lambda/\varepsilon}$ and $\mathcal{N}_{\beta,X}{\to}\varepsilon\mathcal{N}_{\beta/\varepsilon,X}$.

Formally, we define the scaled process $(U_\varepsilon(t)){=}(X_\varepsilon(t),Z_\varepsilon(t),\Omega_{\varepsilon,p}(t),\Omega_{\varepsilon,d}(t),W_\varepsilon(t))$, the evolution equations of Definition 26 become

$$\mathrm{d}X_\varepsilon(t) = -X_\varepsilon(t)\,\mathrm{d}t/\varepsilon{+}W_\varepsilon(t)\mathcal{N}_{\lambda/\varepsilon}(\mathrm{d}t){-}g\left(X_\varepsilon(t{-})\right)\mathcal{N}_{\beta/\varepsilon,X_\varepsilon}\left(\mathrm{d}t\right), \tag{3.13}$$

$$\mathrm{d}Z_\varepsilon(t) = (-\gamma{\odot}Z_\varepsilon(t){+}k_0)\,\mathrm{d}t/\varepsilon{+}k_1(Z_\varepsilon(t{-}))\mathcal{N}_{\lambda/\varepsilon}(\mathrm{d}t) \tag{3.14}$$

$$
\begin{aligned}
&\qquad\qquad + k_2(Z_\varepsilon(t-))\mathcal{N}_{\beta/\varepsilon,X_\varepsilon}(\mathrm{d}t),\\
\mathrm{d}\Omega_{\varepsilon,a}(t) &= -\alpha\Omega_{\varepsilon,a}(t)\,\mathrm{d}t + n_{a,0}(Z_\varepsilon(t))\,\mathrm{d}t \qquad (3.15)\\
&\quad + \left(n_{a,1}(Z_\varepsilon(t-))\varepsilon\mathcal{N}_{\lambda/\varepsilon}(\mathrm{d}t) + n_{a,2}(Z_\varepsilon(t-))\varepsilon\mathcal{N}_{\beta/\varepsilon,X_\varepsilon}(\mathrm{d}t)\right), \quad a\in\{p,d\}\\
\mathrm{d}W_\varepsilon(t) &= M\left(\Omega_{\varepsilon,p}(t),\Omega_{\varepsilon,d}(t),W(t)\right)\mathrm{d}t. \qquad (3.16)
\end{aligned}
$$

For simplicity, the initial condition of $(U_\varepsilon(t))$ is assumed to be constant,

$$U_\varepsilon(0) = U_0 = (x_0, z_0, \omega_{p,0}, \omega_{d,0}, w_0). \qquad (3.17)$$

Some simplifications of this (heavy) mathematical framework can be expected when ε goes to 0. We first introduce the notion of fast variables which correspond to the processes $(X(t), Z(t))$ with the connection intensity process $(W(t))$ taken as constant.

Fast processes

Definition 27. *For $w\in K_W$, $(X^w(t), Z^w(t))$ is the Markov process in $\mathbb{R}\times\mathbb{R}_+^\ell$ defined by the SDEs*

$$
\begin{cases}
\mathrm{d}X^w(t) &= -X^w(t)\,\mathrm{d}t + w\mathcal{N}_\lambda(\mathrm{d}t) - g\left(X^w(t-)\right)\mathcal{N}_{\beta,X^w}\left(\mathrm{d}t\right),\\
\mathrm{d}Z^w(t) &= (-\gamma\odot Z^w(t) + k_0)\,\mathrm{d}t\\
&\qquad\qquad + k_1(Z^w(t-))\mathcal{N}_\lambda(\mathrm{d}t) + k_2(Z^w(t-))\mathcal{N}_{\beta,X^w}(\mathrm{d}t).
\end{cases}
$$

Let $f\in\mathcal{C}_b^1(\mathbb{R}\times\mathbb{R}_+^\ell)$, then, with Equations (3.13) and (3.14), we have that

$$(M_{f,\varepsilon}^F(t)) \overset{\text{def.}}{=} \left(f(X_\varepsilon(t),Z_\varepsilon(t)) - f(x_0,z_0) - \frac{1}{\varepsilon}\int_0^t B^F_{W_\varepsilon(s)}(f)(X_\varepsilon(s),Z_\varepsilon(s))\,\mathrm{d}s\right)$$

is a local martingale, where, for $v=(x,z)\in\mathbb{R}\times\mathbb{R}_+^\ell$ and,

$$
\begin{aligned}
B_w^F(f)(v) &\overset{\text{def.}}{=} -x\frac{\partial f}{\partial x}(x,z) + \left\langle -\gamma\odot z + k_0, \frac{\partial f}{\partial z}(x,z)\right\rangle\\
&\quad + \lambda\left(f(x+w, z+k_1(z)) - f(u)\right) + \beta(x)\left(f(x-g(x), z+k_2(z)) - f(u)\right), \qquad (3.18)
\end{aligned}
$$

with

$$\frac{\partial f}{\partial z}(x,z) = \left(\frac{\partial f}{\partial z_i}(x,z), i\in\{1,\ldots,\ell\}\right)$$

and $\langle z, z'\rangle$ is the usual scalar product of z and $z'\in\mathbb{R}_+^\ell$. The operator B_w^F is called the *infinitesimal generator* of the fast processes $(X^w(t), Z^w(t))$.

In Proposition 50 of Appendix 3.C, we establish that, under the conditions of Sections 3.2 and 3.2, the fast process $(X^w(t), Z^w(t))$ has a unique invariant distribution Π_w.

Functionals of the occupation measure

We start with a rough, non-rigorous, picture of results that are usually established for *slow-fast* systems.

Definition 28 (Occupation measure). *The occupation measure is the non-negative measure ν_ε on $[0,T]\times\mathbb{R}\times\mathbb{R}_+^\ell$ such that*

$$\nu_\varepsilon(G) \overset{\text{def.}}{=} \int_{[0,T]\times\mathbb{R}\times\mathbb{R}_+^\ell} G(s,x,z)\nu_\varepsilon(\mathrm{d}s,\mathrm{d}x,\mathrm{d}z) \overset{\text{def.}}{=} \int_{[0,T]} G(s,X_\varepsilon(s),Z_\varepsilon(s))\,\mathrm{d}s. \tag{3.19}$$

for any non-negative Borelian function G on $[0,T]\times\mathbb{R}\times\mathbb{R}_+^\ell$.

The integration of Relation (3.15) gives the identity, for $a=\{p,d\}$

$$\Omega_{\varepsilon,a}(t) = \omega_{0,a} - \alpha\int_0^t \Omega_{\varepsilon,a}(s)\,\mathrm{d}s + \int_0^t n_{a,0}(Z_\varepsilon(s))\,\mathrm{d}s + \int_0^t n_{a,1}(Z_\varepsilon(s-))\varepsilon\mathcal{N}_{\lambda/\varepsilon}(\mathrm{d}s) + \int_0^t n_{a,2}(Z_\varepsilon(s-))\varepsilon\mathcal{N}_{\beta/\varepsilon,X_\varepsilon}(\mathrm{d}s).$$

An averaging principle is said to hold when the convergence in distribution

$$\lim_{\varepsilon\to 0}\left(\int_0^t G(X_\varepsilon(s),Z_\varepsilon(s))\,\mathrm{d}s\right) = \lim_{\varepsilon\to 0}\left(\int_{\mathbb{R}\times\mathbb{R}_+^\ell} G(x,z)\nu_\varepsilon(\mathrm{d}s,\mathrm{d}x,\mathrm{d}z)\right) = \left(\int_0^t\int_{\mathbb{R}\times\mathbb{R}_+^\ell} G(x,z)\Pi_{w(s)}(\mathrm{d}x,\mathrm{d}z)\,\mathrm{d}s\right), \tag{3.20}$$

holds for a sufficiently rich class of Borelian functions G. Usually, it is enough to prove the weak convergence of the occupation measure for bounded Borelian functions G.

In our case, there are important examples where G has a linear growth with respect to the coordinates x or $z=(z_j)$. The all-to-all models of pair-based rules for example, which are widely used in computational neuroscience lead to unbounded functionals of the occupation measure. See Section 3.3 of [RV20]. Additionally, convergence results in distribution of the jump processes such as,

$$\lim_{\varepsilon\to 0}\left(\int_0^t G(X_\varepsilon(s),Z_\varepsilon(s))\varepsilon\mathcal{N}_{\lambda/\varepsilon}(\mathrm{d}s)\right) = \left(\lambda\int_0^t\int_{\mathbb{R}\times\mathbb{R}_+^\ell} G(x,z)\Pi_{w(s)}(\mathrm{d}x,\mathrm{d}z)\,\mathrm{d}s\right),$$

and

$$\lim_{\varepsilon\to 0}\left(\int_0^t G(X_\varepsilon(s),Z_\varepsilon(s))\varepsilon\mathcal{N}_{\beta/\varepsilon,X_\varepsilon}(\mathrm{d}s)\right) = \left(\int_0^t\int_{\mathbb{R}\times\mathbb{R}_+^\ell} G(x,z)\beta(x)\Pi_{w(s)}(\mathrm{d}x,\mathrm{d}z)\,\mathrm{d}s\right)$$

are also required. They are not straightforward consequences of Relation (3.20) as it is usually the case for bounded G. See [Kur92] for example. These technical difficulties have to be overcome to establish the tightness of the processes $(\Omega_\varepsilon(t))$, and consequently of $(W_\varepsilon(t))$. As a result, additional limit results have to be established at this point, see Section 3.6. Furthermore, as ε goes to 0, the process $(\Omega_{\varepsilon,p}(t),\Omega_{\varepsilon,d}(t),W_\varepsilon(t))$ should converge to a process $(\omega_p(t),\omega_d(t),w(t))$ satisfying the relation,

$$\begin{cases} \omega_a(t) = \omega_{a,0} - \alpha\displaystyle\int_0^t \omega(s)\,\mathrm{d}s + \int_0^t\int_{\mathbb{R}_+^\ell} n_{a,0}(z)\Pi_{w(s)}(\mathbb{R}_+,\mathrm{d}z)\,\mathrm{d}s \\ \quad + \lambda\displaystyle\int_0^t\int_{\mathbb{R}_+^\ell} n_{a,1}(z)\Pi_{w(s)}(\mathbb{R}_+,\mathrm{d}z)\,\mathrm{d}s + \int_0^t\int_{\mathbb{R}\times\mathbb{R}_+^\ell}\beta(x)n_{a,2}(z)\Pi_{w(s)}(\mathrm{d}x,\mathrm{d}z)\,\mathrm{d}s. \\ \dfrac{\mathrm{d}w}{\mathrm{d}t}(t) = M(\omega_p(t),\omega_d(t),w(t)) \end{cases}$$

3.4 Averaging principles results

We fix $T>0$, throughout the paper the convergence in distribution of processes is considered on the bounded interval $[0,T]$.

Main result

We start by reviewing the assumptions detailed in Section 3.2 on the different parameters of the stochastic model.

Assumptions.

a. It is assumed that β is a non-negative, continuous function on $\mathbb{R}$ and that $\beta(x)=0$ for $x\leqslant -c_\beta\leqslant 0$. Additionally, there exist a constant $C_\beta\geqslant 0$ such that

$$\beta(x)\leqslant C_\beta(1+|x|), \quad \forall x\in\mathbb{R}.$$

b. g is continuous function on $\mathbb{R}$ and $0\leqslant g(x)\leqslant \max(c_g,x)$ holds for all $x\in\mathbb{R}$, for some $c_g\geqslant 0$.

c. All coordinates of the vector γ are positive.

d. There exists a constant $C_k\geqslant 0$ such that $0\leqslant k_0\leqslant C_k$ and functions k_i, $i=1,\ 2$, in $\mathcal{C}^1_b(\mathbb{R}^\ell_+,\mathbb{R}^\ell_+)$, are upper-bounded by $C_k\geqslant 0$.

e. There exists a constant C_n such that, for $j\in\{0,1,2\}$, $a\in\{p,d\}$, $n_{a,j}$ verifies,

$$n_{a,j}(z)\leqslant C_n(1+\|z\|),$$

where, for $z\in\mathbb{R}^\ell_+$, $\|z\|=z_1+\cdots+z_\ell$. Moreover, for any $w\in K_W$, the discontinuity points of

$$(x,z)\mapsto(n_{a,0}(z),n_{a,1}(z),\beta(x)n_{a,2}(z))$$

for $a\in\{p,d\}$, are negligible for the probability distribution Π_w of Section 3.C.

f. M can be decomposed as,

$$M(\omega_p,\omega_d,w)=M_p(\omega_p,w)-M_d(\omega_d,w)-\mu w,$$

where $M_a(\omega_a,w)$ is non-negative continuous function, non-decreasing on the first coordinate for a fixed $w\in K_w$, and,

$$M_a(\omega_a,w)\leqslant C_M(1+\omega_a),$$

for all $w\in K_W$, for $a\in\{p,d\}$.

The main result of the paper is the following theorem.

Theorem 29 (Asymptotic time evolution of plasticity)**.** *Under the conditions of Section 3.2 and for initial conditions satisfying Relation* (3.17)*, there exists* $S_0 \in (0, +\infty]$*, such that the family of processes* $(\Omega_{\varepsilon,p}(t), \Omega_{\varepsilon,d}(t), W_\varepsilon(t), t<S_0)$*,* $\varepsilon \in (0,1)$*, of the system of Section 3.3, is tight for the convergence in distribution. As* ε *goes to* 0*, any limiting point* $(\omega_p(t), \omega_d(t), w(t), t<S_0)$*, satisfies the ODEs, for* $a \in \{p, d\}$*,*

$$\begin{cases} \dfrac{\mathrm{d}\omega_a}{\mathrm{d}t}(t) &= -\alpha\omega_a(t) + \displaystyle\int_{\mathbb{R}\times\mathbb{R}_+^\ell} \Big(n_{a,0}(z) + \lambda n_{a,1}(z) + \beta(x) n_{a,2}(z) \Big)\, \Pi_{w(t)}(\mathrm{d}x, \mathrm{d}z), \\ \dfrac{\mathrm{d}w}{\mathrm{d}t}(t) &= M(\omega_p(t), \omega_d(t), w(t)), \end{cases} \tag{3.21}$$

where, for $w \in K_W$*,* Π_w *is the unique invariant distribution* Π_w *on* $\mathbb{R}\times\mathbb{R}_+^\ell$ *of the Markovian operator* B_w^F*. If* K_W *is bounded, then* $S_0 = +\infty$ *almost-surely.*

Convergence in distribution. As already mentioned, most of the efforts in this paper are devoted to the proof of the tightness property of $(\Omega_{\varepsilon,p}(t), \Omega_{\varepsilon,d}(t), W_\varepsilon(t))$. We note that our result identifies the limiting points, but it does not state any weak convergence results for the scaled processes. Regularity properties are actually required on (Π_w) to have such results. For example, it would be sufficient to have that the mapping,

$$\Psi_a : w \mapsto \int_{\mathbb{R}\times\mathbb{R}_+^\ell} (n_{a,0}(z) + \lambda n_{a,1}(z) + \beta(x) n_{a,2}(z))\, \Pi_w(\mathrm{d}x, \mathrm{d}z),$$

locally Lipschitz for w, for $a \in \{p, d\}$, so that Relation (3.21) has a unique solution.

Due to the generality of our model, we did not try to state a set of conditions that can ensure the desired regularity properties of the corresponding Π_w. Uniqueness results are obtained in Sections 5 and 6 of [RV20] for several important cases. The same properties for the simple model are worked out in Section 3.8. However at this stage, a case by case analysis seems mandatory.

A blow-up phenomenon. As it can be seen, when $S_0 < +\infty$ the convergence is only proved on a bounded time interval. In the proof, the variable S_0 results from the domain definition of the solution to a deterministic differential equation. This is not an artifact of our methods, see Proposition 47 in Section 3.8 for an example.

Steps of the proof

The proof of the theorem is organized as follows. See also Figure 3.1 of Appendix.

a. Section 3.5. A stochastic upper-bound $\overline{U}$ of the original process is introduced and a coupling argument is used to control $(W_\varepsilon(t))$. This is an important ingredient in the proof of tightness results for $(\Omega_{\varepsilon,p}(t), \Omega_{\varepsilon,d}(t), W_\varepsilon(t))$.

b. Section 3.6. Under the temporary assumption that the process $(\overline{W}(t))$ is bounded by K, we establish tightness results for the truncated process $\overline{U}^K$, when ε goes to 0, of variables associated to fast processes $(\overline{X}_\varepsilon^K(t), \overline{Z}_\varepsilon^K(t))$ of the type

$$\left(\int_{[0,T]} G\left(s, \overline{X}_\varepsilon^K(s), \overline{Z}_\varepsilon^K(s) \right) \mathrm{d}s \right)$$

where G is a continuous Borelian function with a linear growth with respect to the coordinates $x \in \mathbb{R}$ and $z \in \mathbb{R}_+^\ell$. An averaging principle is shown for this truncated process.

c. In Theorem 43 of Section 3.7, using monotonicity arguments, we are able to obtain a *deterministic, analytical bound*, uniform in K, for the limiting points of the truncated process. From there, we prove an averaging principle for the dominating process $\overline{U}$ (without truncation) in Proposition 44 where the explicit form of the ODE verified by the limiting points is known. As a direct consequence, we are able to prove that this limit is unique and that the scaled dominating process converges to the solution. Using the fact that the process $W(t)$ is bounded by $\overline{W}(t)$ and the previous convergence, we establish the desired results for the process $U_\varepsilon(t)$ of Theorem 29.

Technical results on shot-noise processes

The processes $(X(t))$ and $(Z(t))$ are closely related to shot-noise processes and their generalizations. See for example [Sch18], [Ric44] and [GP60] for an introduction. We give a quick overview of their use in our proofs. In Appendix 3.B, the results below and several technical lemmas for these processes are detailed and proved.

The following lemma gives an elementary representation result for general shot-noise process associated to a positive Radon measure. See Lemma 1 of [RV20].

Lemma 30. *If μ is a positive Radon measure on $\mathbb{R}_+$ and $\gamma > 0$, the unique càdlàg solution of the ODE*

$$\mathrm{d}Z(t) = -\gamma Z(t) + \mu(\mathrm{d}t),$$

with initial point $z_0 \in \mathbb{R}_+$ is given by

$$Z(t) = z_0 e^{-\gamma t} + \int_{(0,t]} e^{-\gamma(t-s)} \mu(\mathrm{d}s). \tag{3.22}$$

In view of SDEs (3.2) it is natural to introduce a scaled version of these processes.

Definition 31 (Scaled shot-noise process)**.** *For $\varepsilon > 0$, we define the shot-noise process $(S_\varepsilon^x(t))$, solution of the SDE*

$$\mathrm{d}S_\varepsilon^x(t) = -S_\varepsilon^x(t)\,\mathrm{d}t/\varepsilon + \mathcal{N}_{\lambda/\varepsilon}(\mathrm{d}t),$$

where the initial point is $x \geqslant 0$.

Proposition 32. *For $\xi \in \mathbb{R}$ and $x \geqslant 0$, the convergence in distribution of the processes*

$$\lim_{\varepsilon \searrow 0} \left(\int_0^t e^{\xi S_\varepsilon^x(u)}\,\mathrm{d}u \right) = \left(\mathbb{E}\left[e^{\xi S(\infty)} \right] t \right)$$

holds, and

$$\sup_{\substack{0<\varepsilon<1 \\ 0 \leqslant t \leqslant T}} \mathbb{E}\left[e^{\xi S_\varepsilon(t)} \right] < +\infty. \tag{3.23}$$

Proof. See Section 3.B of Appendix. □

We now introduce another shot-noise process $(R_\varepsilon(t))$ associated to the point process $\mathcal{N}_{I/\varepsilon,S_\varepsilon}$ defined by Relation (3.6) where $I(x)=x$, $x\in\mathbb{R}_+$. It is in fact a shot-noise process whose intensity function is $(S_\varepsilon(t))$,

$$\mathrm{d}R_\varepsilon(t) = -\gamma R_\varepsilon(t)\,\mathrm{d}t/\varepsilon + \mathcal{N}_{I/\varepsilon,S_\varepsilon}(\mathrm{d}t), \tag{3.24}$$

with the initial condition $R_\varepsilon(0)=0$.

It turns out that tightness properties of three families of linear functionals of such processes

$$\left(\int_0^t R_\varepsilon(s)\ \mathrm{d}s\right), \left(\int_0^t R_\varepsilon(s)\varepsilon\mathcal{N}_{\lambda/\varepsilon}(\mathrm{d}s)\right), \left(\int_0^t R_\varepsilon(s)\varepsilon\mathcal{N}_{I/\varepsilon,S_\varepsilon}(\mathrm{d}s)\right),$$

are central to establish Theorem 29. The motivation comes from the three terms in the expression of $(\Omega_{\varepsilon,a}(t))$, $a\in\{p,d\}$ of Relation (3.15) and the fact that, with the condition of Relation (3.11), for $j\in\{0,1,2\}$, $n_j(z)\leqslant C_n^0+C_n z$ for $z\in\mathbb{R}_+$.

The necessary results are stated in Proposition 33 which is used in Section 3.7.

Proposition 33. *For $H_\varepsilon\in\{S_\varepsilon,R_\varepsilon\}$, the families of processes*

$$\left(\int_0^t H_\varepsilon(u)\ \mathrm{d}u\right), \left(\int_0^t H_\varepsilon(u)^2\ \mathrm{d}u\right) \text{ and } \left(\int_0^t R_\varepsilon(u)S_\varepsilon(u)\ \mathrm{d}u\right),\ \varepsilon\in(0,1),$$

are tight for the convergence in distribution.

Proof. We first prove the tightness of the second family of processes. With Cauchy-Schwartz' Inequality, we have

$$\int_s^t H_\varepsilon(u)^2\ \mathrm{d}u \leqslant \sqrt{t-s}\sqrt{\int_s^t H_\varepsilon(u)^4\ \mathrm{d}u}.$$

Moreover, Relation (3.23) gives an estimate of S_ε moments and Proposition 49 of Appendix states that

$$\sup_{\varepsilon\in(0,1),t\geqslant 0}\mathbb{E}\left[R_\varepsilon(t)^4\right] < +\infty$$

Gathering up previous estimates, we show that there exists a constant C independent of ε and s, t such that

$$\mathbb{E}\left[\left(\int_s^t H_\varepsilon(u)^2\ \mathrm{d}u\right)^2\right] \leqslant C(t-s)^2.$$

Kolmogorov-Čentsov's Criterion, see Theorem 2.8 and Problem 4.11 of [KS98], implies that the family of variables

$$\left(\int_0^t H_\varepsilon(u)^2\ \mathrm{d}u\right)$$

is tight.

By using repeatedly Cauchy-Schwartz' Inequality, for $0\leqslant s\leqslant t$, we have

$$\mathbb{E}\left[\left(\int_s^t H_\varepsilon(u)\ \mathrm{d}u\right)^4\right] \leqslant (t-s)^2\mathbb{E}\left[\left(\int_s^t H_\varepsilon(u)^2\ \mathrm{d}u\right)^2\right] \leqslant C(t-s)^4$$

and

$$\mathbb{E}\left[\left(\int_s^t R_\varepsilon(u)S_\varepsilon(u)\,\mathrm{d}u\right)^2\right] \leqslant \sqrt{\mathbb{E}\left[\left(\int_s^t R_\varepsilon(u)^2\,\mathrm{d}u\right)^2\right]}\sqrt{\mathbb{E}\left[\left(\int_s^t S_\varepsilon(u)^2\,\mathrm{d}u\right)^2\right]} \leqslant C(t-s)^2$$

Kolmogorov-Čentsov's Criterion can then also be applied to the two other families of processes of the proposition. The proposition is proved.

□

3.5 A coupling property

In this section a process

$$(\overline{U}(t))=(\overline{X}(t),\overline{Z}(t),\overline{\Omega}(t),\overline{W}(t))$$

in $\mathcal{D}\left([0,T],\mathbb{R}_+^4\right)$ is introduced. It has similarities with the process $(U(t))$ of Definition 26 but fewer coordinates and simpler parameters. More importantly, all its coordinates are non-negative. We first prove, via a coupling, that the sample paths of the processes $(U(t))$ and $(\overline{U}(t))$ can be compared in a sense to be made precise. Secondly, we derive several technical estimates for $(\overline{U}(t))$ which are important to prove the tightness of the scaled processes $((\overline{\Omega}_\varepsilon(t),\overline{W}_\varepsilon(t)))$ defined in Section 3.3.

The process $(\overline{U}(t))$ is the solution of the SDEs

$$\begin{cases} \mathrm{d}\overline{X}(t) &= -\overline{X}(t)\,\mathrm{d}t + \overline{W}(t)\mathcal{N}_\lambda(\mathrm{d}t), \\ \mathrm{d}\overline{Z}(t) &= \left(-\underline{\gamma}\overline{Z}(t) + C_k\right)\mathrm{d}t + C_k\mathcal{N}_\lambda(\mathrm{d}t) + C_k\mathcal{N}_{\overline{\beta},\overline{X}}(\mathrm{d}t), \\ \mathrm{d}\overline{\Omega}(t) &= -\alpha\overline{\Omega}(t)\,\mathrm{d}t + C_n\left(1+\ell\overline{Z}(t)\right)\mathrm{d}t + C_n\left(1+\ell\overline{Z}(t-)\right)\mathcal{N}_\lambda(\mathrm{d}t) \\ &\qquad + C_n\left(1+\ell\overline{Z}(t-)\right)\mathcal{N}_{\overline{\beta},\overline{X}}(\mathrm{d}s) \\ \mathrm{d}\overline{W}(t) &= C_M\left(1+\overline{\Omega}(t)\right)\mathrm{d}t, \end{cases} \tag{3.25}$$

with $\overline{\beta}(x)=C_\beta(1+x)$ and with initial condition $\overline{U}(0)$ given by

$$(\overline{x}_0,\overline{z}_0,\overline{\omega}_0,\overline{W}_0)=(\max(x_0,0),\max_{i\in\{1,\dots,\ell\}}\{z_{0,i}\},\max_{a\in\{a,p\}}\{\omega_{0,a}\},|w_0|).$$

C_β, C_n, C_k and C_M are non-negative constants associated to the conditions of Section 3.2, and $\underline{\gamma}\overset{\text{def.}}{=}\min(\gamma_i : i=1,\dots,\ell)$.

Throughout this section, for $t\geqslant 0$, if $(U(t))$ is a solution of Relations (3.7), the inequality $U(t)\leqslant\overline{U}(t)$ will stand for the four relations, $X(t)\leqslant\overline{X}(t)$,

$$\max_{i\in\{1,\dots,\ell\}}\{Z_i(t)\}\leqslant\overline{Z}(t),\ \max_{a\in\{p,d\}}\{\Omega_a(t)\}\leqslant\overline{\Omega}(t),\ \text{and}\ |W(t)|\leqslant\overline{W}(t).$$

A coupling property

We start by proving a monotonicity property of the behavior of both systems "between" jumps.

Define $u(t) = (x(t), z(t), \omega_p(t), \omega_d(t), w(t))$ that follows,

$$\begin{cases} \mathrm{d}x(t) &= -x(t)\,\mathrm{d}t, \\ \mathrm{d}z_i(t) &= (-\gamma_i z_i(t) + k_0)\,\mathrm{d}t, \quad i \in \{1, \dots, \ell\}, \\ \mathrm{d}\omega_a(t) &= -\alpha\omega_a(t)\,\mathrm{d}t + n_{0,a}(z(t))\,\mathrm{d}t, \quad a \in \{p, d\}, \\ \mathrm{d}w(t) &= M\left(\omega_p(t), \omega_d(t), w(t)\right)\mathrm{d}t. \end{cases}$$

and $\overline{u}(t) = (\overline{x}(t), \overline{z}(t), \overline{\omega}(t), \overline{w}(t))$ with,

$$\begin{cases} \mathrm{d}\overline{x}(t) &= -\overline{x}(t)\,\mathrm{d}t, \\ \mathrm{d}\overline{z}(t) &= \left(-\underline{\gamma}\overline{z}(t) + C_k\right)\mathrm{d}t, \\ \mathrm{d}\overline{\omega}(t) &= -\alpha\overline{\omega}(t)\,\mathrm{d}t + C_n\left(1 + \ell\overline{z}(t)\right)\mathrm{d}t, \\ \mathrm{d}\overline{w}(t) &= C_M\left(1 + \overline{\omega}(t)\right)\mathrm{d}t. \end{cases}$$

Lemma 34. *Under the conditions of Sections 3.2, 3.2, and 3.2 and if the initial conditions are such that $u(0) \leqslant \overline{u}(0)$, then for all $t \geqslant 0$, $u(t) \leqslant \overline{u}(t)$.*

Proof. The result is clear for the function $(x(t))$ and also for the functions $(z_i(t))$. For $(\omega_a(t))$, with $a \in \{p, d\}$, we have

$$\mathrm{d}\left(\overline{\omega}(t) - \omega_a(t)\right) = -\alpha\left(\overline{\omega}(t) - \omega_a(t)\right)\mathrm{d}t + \left(C_n(1 + \ell\overline{z}(t)) - n_{0,a}(z(t))\right)\mathrm{d}t,$$

by Condition (3.11), we obtain

$$C_n(1 + \ell\overline{z}(t)) - n_{0,a}(z(t)) \geqslant C_n(1 + \|z(t)\|) - n_{0,a}(z(t)) \geqslant 0.$$

Lemma 30 gives the relation

$$e^{\alpha t}\left(\overline{\omega}(t) - \omega_a(t)\right) = \left(\overline{\omega}(0) - \omega_a(0)\right) + \int_0^t e^{-\alpha s} C_n\left(1 + \ell\overline{z}(s) - n_{0,a}(z(s))\right)\mathrm{d}s \geqslant 0.$$

Finally, again with Lemma 30, Condition 3.2 and the last inequality, we have, for $t \geqslant 0$,

$$\mathrm{d}(\overline{w}(t) - w(t)) = -\mu(\overline{w}(s) - w(s))\,\mathrm{d}t + \left(C_M(1 + \overline{\omega}(s)) - M_p(\omega_p(s), w(s))\right)\mathrm{d}t$$

This leads to,

$$w(t) \leqslant \overline{w}(t).$$

In the same way, we can prove that,

$$w(t) \geqslant -\overline{w}(t).$$

The lemma is proved. □

Proposition 35 (Coupling)**.** *Under the conditions of Section 3.2, there exists a coupling of $(\overline{U}(t))$ and $(U(t))$ such that, almost surely, for all $t > 0$, $(U(t)) \leqslant (\overline{U}(t))$, in particular*

$$|W(t)| \leqslant \overline{W}(t), \quad \forall t \geqslant 0.$$

Proof. All we have to prove is that if $U(0)\leqslant\overline{U}(0)$ and if τ is the first jump of either $(U(t))$ or $(\overline{U}(t))$, then $U(t)\leqslant\overline{U}(t)$ for $t\leqslant\tau$. Our statement is then easily proved by induction on the sequence of jumps of both processes.

Since $(\overline{U}(t))$ and $(U(t))$ are governed by the deterministic ODEs of Lemma 34, the relation $U(t)\leqslant\overline{U}(t)$ holds for $0\leqslant t<\tau$. The processes $(W(t))$ and $(\overline{W}(t))$ being continuous, $|W(\tau)|=|W(\tau-)|\leqslant\overline{W}(\tau-)=\overline{W}(\tau)$.

The instant of jump τ is the minimum of τ_1, τ_2 and $\overline{\tau}_2$, with

$$\begin{cases} \tau_1 = \inf\{t>0 : \mathcal{N}_\lambda((0,t])\neq 0\}, \\ \tau_2 = \inf\left\{t>0 : \mathcal{N}_{\beta,X}((0,t]) = \displaystyle\int_{(0,t]} \mathcal{P}_2\left((0,\beta(X(s-)\right],\mathrm{d}s\right)\neq 0\right\}, \\ \overline{\tau}_2 = \inf\left\{t>0 : \mathcal{N}_{\overline{\beta},\overline{X}}((0,t]) = \displaystyle\int_{(0,t]} \mathcal{P}_2\left(\left(0,\overline{\beta}(\overline{X}(s-))\right],\mathrm{d}s\right)\neq 0\right\}. \end{cases}$$

Since, for $x\leqslant\overline{x}$, $\beta(x)\leqslant\overline{\beta}(x)\leqslant\overline{\beta}(\overline{x})$ is a non-decreasing function and that $X\leqslant\overline{X}$ holds until the first jump, the inequality $\overline{\tau}_2\leqslant\tau_2$ holds almost surely.

If $\tau_1<\overline{\tau}_2$, then

$$X(\tau)=X(\tau-)+W(\tau-)\leqslant\overline{X}(\tau-)+\overline{W}(\tau-)=\overline{X}(\tau).$$

For $i\in\{1,\ldots,\ell\}$,

$$Z_i(\tau)=Z_i(\tau-)+k_i(Z(\tau-)) \leqslant \overline{Z}(\tau-)+C_k=\overline{Z}(\tau)$$

and

$$\begin{aligned}\Omega_a(\tau) = \Omega_a(\tau-)+n_{a,1}(Z(\tau-)) &\leqslant \Omega_a(\tau-)+C_n\left(1+\|Z(\tau)\|\right) \\ &\leqslant \overline{\Omega}(\tau-)+C_n\left(1+\ell\overline{Z}(\tau)\right) = \overline{\Omega}(\tau).\end{aligned}$$

Thus we have $U(\tau)\leqslant\overline{U}(\tau)$. The same arguments work in a similar way when $\tau_2=\overline{\tau}_2<\tau_1$.

In this case, we have

$$X(\tau)=X(\tau-)-g(X(\tau-)) \leqslant \overline{X}(\tau-)=\overline{X}(\tau).$$

The last case $\overline{\tau}_2<\min(\tau_2,\tau_1)$ is not more difficult, since the components of $(U(t))$ do not experience jumps and those of $(\overline{U}(t))$ have positive jumps due to $\mathcal{N}_{\beta,\overline{X}}$. The proposition is proved. □

The process $(\overline{U}_\varepsilon(t))$ is defined by the SDEs,

$$\begin{cases} \mathrm{d}\overline{X}_\varepsilon(t) &= -\overline{X}_\varepsilon(t)\,\mathrm{d}t/\varepsilon + \overline{W}_\varepsilon(t)\mathcal{N}_{\lambda/\varepsilon}(\mathrm{d}t), \\ \mathrm{d}\overline{Z}_\varepsilon(t) &= \left(-\gamma\overline{Z}_\varepsilon(t)+C_k\right)\mathrm{d}t/\varepsilon + C_k\mathcal{N}_{\lambda/\varepsilon}(\mathrm{d}t) + C_k\mathcal{N}_{\overline{\beta}/\varepsilon,\overline{X}_\varepsilon}(\mathrm{d}t), \\ \mathrm{d}\overline{\Omega}_\varepsilon(t) &= -\alpha\overline{\Omega}_\varepsilon(t)\,\mathrm{d}t + C_n\left(1+\ell\overline{Z}_\varepsilon(t)\right)\mathrm{d}t \\ &\qquad + C_n\left(1+\ell\overline{Z}_\varepsilon(t-)\right)\left(\varepsilon\mathcal{N}_{\lambda/\varepsilon}(\mathrm{d}t)+\varepsilon\mathcal{N}_{\overline{\beta}/\varepsilon,\overline{X}_\varepsilon}(\mathrm{d}t)\right) \\ \mathrm{d}\overline{W}_\varepsilon(t) &= C_M\left(1+\overline{\Omega}_\varepsilon(t)\right)\mathrm{d}t, \end{cases} \tag{3.26}$$

and with $\overline{U}_\varepsilon(0)=\overline{U}(0)=(\overline{x}_0,\overline{z}_0,\overline{\omega}_0,\overline{w}_0)$.

The infinitesimal generator $\overline{B}_w^F$ of Relation (3.18) is given by, for $v=(x,z)$ and $f\in\mathcal{C}_b^1(\mathbb{R}\times\mathbb{R}_+)$,

$$\begin{aligned}\overline{B}_w^F(f)(v) \overset{\text{def.}}{=} &-x\frac{\partial f}{\partial x}(v)+(-\gamma z+C_k)\frac{\partial f}{\partial z}(v) \\ &+\lambda\left(f(v+we_1+C_ke_2)-f(v)\right)+C_\beta(x+1)\left(f(v+C_ke_2)-f(v)\right),\end{aligned} \tag{3.27}$$

where $e_1=(1,0)$ and $e_2=(0,1)$.

3.6 Asymptotic results for the truncated process

In this section we study the scaling properties of fast processes of $(\overline{U}(t))$ defined by Relation (3.26). In this section, we fix $K>0$ and consider an analogue process for which the impact of the connection intensity is truncated at K. In Section 3.6 an averaging principle will be established for this process as a first step in the proof of the main result of the paper.

Definition of the truncated process

We define $(\overline{U}^K(t))$ as the solution of the SDEs,

$$\begin{cases} \mathrm{d}\overline{X}_\varepsilon^K(t) &= -\overline{X}_\varepsilon^K(t)\,\mathrm{d}t/\varepsilon + K\wedge\overline{W}_\varepsilon^K(t)\mathcal{N}_{\lambda/\varepsilon}(\mathrm{d}t), \\ \mathrm{d}\overline{Z}_\varepsilon^K(t) &= \left(-\gamma\overline{Z}_\varepsilon^K(t)+C_k\right)\mathrm{d}t/\varepsilon + C_k\mathcal{N}_{\lambda/\varepsilon}(\mathrm{d}t) + C_k\mathcal{N}_{\overline{\beta}/\varepsilon,\overline{X}_\varepsilon^K}(\mathrm{d}t), \\ \mathrm{d}\overline{\Omega}_\varepsilon^K(t) &= -\alpha\overline{\Omega}_\varepsilon^K(t)\,\mathrm{d}t + C_n\left(1+\ell\overline{Z}_\varepsilon^K(t)\right)\mathrm{d}t \\ &\qquad + C_n\left(1+\ell\overline{Z}_\varepsilon^K(t-)\right)\left(\varepsilon\mathcal{N}_{\lambda/\varepsilon}(\mathrm{d}t)+\varepsilon\mathcal{N}_{\overline{\beta}/\varepsilon,\overline{X}_\varepsilon^K}(\mathrm{d}t)\right) \\ \mathrm{d}\overline{W}_\varepsilon^K(t) &= C_M\left(1+\overline{\Omega}_\varepsilon^K(t)\right)\mathrm{d}t, \end{cases} \tag{3.28}$$

and with $\overline{U}_\varepsilon^K(0)=\overline{U}(0)=(\overline{x}_0,\overline{z}_0,\overline{\omega}_0,\overline{w}_0)$.

We begin with a lemma giving a stochastic upper bound of $(\overline{X}_\varepsilon^K(t))$ in terms of a standard shot-noise process.

Lemma 36. *There exists a constant $C_X>0$ independent of ε such that the relation*

$$\overline{X}_\varepsilon^K(t) \leqslant C_X + KS_\varepsilon(t) \tag{3.29}$$

holds for $t\geqslant 0$, where $(S_\varepsilon(t))$ is the shot-noise process of Definition 31.

For any $\eta>0$, there exists a compact subset $\mathcal{K}$ of $\mathbb{R}_+^2$ such that,

$$\sup_{\substack{0<\varepsilon<1\\0\leqslant t\leqslant T}} \mathbb{P}\left(\left(\overline{X}_\varepsilon^K(t),\overline{Z}_\varepsilon^K(t)\right)\notin\mathcal{K}\right)\leqslant\eta.$$

Proof. With Relation (3.22), we have, for $t\geqslant 0$,

$$\overline{X}_\varepsilon^K(t) = x_0e^{-t} + \int_0^t e^{-(t-u)/\varepsilon}K\wedge W_\varepsilon(u-)\mathcal{N}_{\lambda/\varepsilon}(\mathrm{d}u).$$

Which gives, for $s\leqslant t\leqslant T$,

$$\overline{X}_\varepsilon^K(t) \leqslant x_0e^{-t/\varepsilon} + K\int_0^t e^{-(t-u)/\varepsilon}\mathcal{N}_{\lambda/\varepsilon}(\mathrm{d}u) \leqslant x_0 + KS_\varepsilon(t),$$

and therefore

$$\mathbb{E}\left[\overline{X}_\varepsilon^K(t)\right]\leqslant C_X + K\mathbb{E}\left[S_\varepsilon(t)\right]\leqslant C_X+\lambda KT.$$

Relation (3.22) gives the inequality

$$\mathbb{E}\left[\overline{Z}_\varepsilon^K(t)\right]\leqslant z_0 + C_k\int_0^t\exp(-\gamma(t-s))\left(1+\lambda+C_\beta(1+\mathbb{E}\left[\overline{X}_\varepsilon^K(s)\right])\right)\mathrm{d}s$$

which leads to,

$$\sup_{\substack{0<\varepsilon<1\\0\leqslant t\leqslant T}}\mathbb{E}\left[\overline{Z}_\varepsilon^K(t)\right]<+\infty.$$

We conclude by using Markov's inequality. □

Tightness of the truncated process

The next important lemma is used to prove tightness properties of the processes $(\Omega_\varepsilon(t))$.

Lemma 37 (Tightness of linear functionals of the fast processes)**.** *The family of processes*

$$\left(\int_0^t \overline{X}_\varepsilon^K(u)\,\mathrm{d}u\right),\left(\int_0^t \overline{Z}_\varepsilon^K(u)\,\mathrm{d}u\right),\left(\int_0^t \overline{X}_\varepsilon^K(u)\overline{Z}_\varepsilon^K(u)\,\mathrm{d}u\right),\ \varepsilon\in(0,1),$$

are tight for the convergence in distribution. The processes

$$(\overline{M}_{\varepsilon,1}^K(t))\stackrel{\text{def.}}{=}\left(\int_0^t \overline{Z}_\varepsilon^K(u-)\left[\varepsilon\mathcal{N}_{\lambda/\varepsilon}(\mathrm{d}u)-\lambda\,\mathrm{d}u\right]\right)$$
$$(\overline{M}_{\varepsilon,2}^K(t))\stackrel{\text{def.}}{=}\left(\int_0^t \overline{Z}_\varepsilon^K(u-)\left[\varepsilon\mathcal{N}_{\overline{\beta}/\varepsilon,\overline{X}_\varepsilon^K}(\mathrm{d}u)-\overline{\beta}\left(\overline{X}_\varepsilon^K(u)\right)\mathrm{d}u\right]\right)$$

converge in distribution to 0 *as* ε *goes to* 0*.*

Proof. Relation (3.29) gives for $0\leqslant s\leqslant t$,

$$\int_s^t \overline{X}_\varepsilon^K(u)\,\mathrm{d}u\leqslant C_X(t-s)+K\int_s^t S_\varepsilon(u)\,\mathrm{d}u,$$

The tightness of the three processes results from this relation and Proposition 33.

Indeed, Relation (3.22) shows that, for $t\geqslant 0$,

$$\begin{aligned}\overline{Z}_\varepsilon^K(t)-z_0 &= C_k\int_0^t e^{-\gamma(t-s)/\varepsilon}\,\mathrm{d}s+C_k\int_0^t e^{-\gamma(t-s)/\varepsilon}\mathcal{N}_{\lambda/\varepsilon}(\mathrm{d}s)\\ &\quad+C_k\int_0^t e^{-\gamma(t-s)/\varepsilon}\mathcal{P}_2\left(\left(0,C_\beta\frac{1+\overline{X}_\varepsilon^K(s)}{\varepsilon}\right],\mathrm{d}s\right)\\ &\leqslant \frac{C_k}{\gamma}+C_k\int_0^t e^{-\gamma(t-s)/\varepsilon}\mathcal{N}_{\lambda/\varepsilon}(\mathrm{d}s)\\ &\quad+C_k\int_0^t e^{-\gamma(t-s)/\varepsilon}\mathcal{P}_2\left(\left(0,C_\beta\frac{1+C_X}{\varepsilon}\right],\mathrm{d}s\right)\\ &\quad+C_k\int_0^t e^{-\gamma(t-s)/\varepsilon}\mathcal{P}_2\left(\left(C_\beta\frac{1+C_X}{\varepsilon},C_\beta\frac{1+C_X}{\varepsilon}+C_\beta K\frac{S_\varepsilon(s)}{\varepsilon}\right],\mathrm{d}s\right).\end{aligned}$$

The first two terms of the right-hand side of last relation are, up to the constants γ instead of 1 and $C_\beta(1+C_X)$ instead of λ, equal to $S_\varepsilon(t)$. Similarly, up to the constant $C_\beta K$ of $S_\varepsilon(t)$ instead of 1, the last term is equal to $R_\varepsilon(t)$.

The two processes $(\overline{M}_{\varepsilon,i}^K(t))$, $i=\{1,2\}$ are martingales with predictable increasing processes

$$\left(\varepsilon\lambda\int_0^t \overline{Z}_\varepsilon^K(u)^2\,\mathrm{d}u\right)\ \text{and}\ \left(\varepsilon\int_0^t \overline{Z}_\varepsilon^K(u)^2C_\beta\left(1+\overline{X}_\varepsilon^K(u)\right)\mathrm{d}u\right).$$

For $t\geqslant 0$, we have

$$\mathbb{E}\left[\overline{M}_{\varepsilon,1}^K(t)^2\right]\leqslant\int_0^t\mathbb{E}\left[\overline{Z}_\varepsilon^K(u)^2\right]\mathrm{d}u,$$

and,

$$\mathbb{E}\left[\overline{M}^K_{\varepsilon,2}(t)^2\right] = \varepsilon C_\beta \left(\mathbb{E}\left[\overline{M}^K_{\varepsilon,1}(t)^2\right] + \int_0^t \mathbb{E}\left[\overline{Z}^K_\varepsilon(u)^2 \overline{X}^K_\varepsilon(u)\right] \mathrm{d}u\right)$$
$$\leqslant \varepsilon C_\beta \int_0^t \left(\mathbb{E}\left[\overline{Z}^K_\varepsilon(u)^2\right] + \sqrt{\mathbb{E}\left[\overline{Z}^K_\varepsilon(u)^4\right]}\sqrt{\mathbb{E}\left[\overline{X}^K_\varepsilon(u)^2\right]}\right) \mathrm{d}u,$$

with Cauchy-Schwartz' inequality.

Using the upper-bounds for $(\overline{X}^K_\varepsilon(t))$ and $(\overline{Z}^K_\varepsilon(t))$ and Relation (3.23) for S_ε and Proposition 49 of the Appendix for R_ε, we obtain that the quantity $\mathbb{E}\left[\overline{M}^K_{\varepsilon,2}(t)^2\right]$ converges to 0 as ε goes to 0. The last statement of the lemma follows from Doob's inequality. □

We now define the associated occupation measure $\overline{\nu}^K_\varepsilon$ in the same way as in Section 28. Let G be a non-negative Borelian function on $[0,T]\times\mathbb{R}^2_+$, define $\overline{\nu}^K_\varepsilon$ the non-negative measure on $[0,T]\times\mathbb{R}^2_+$ by

$$\int_{[0,T]\times\mathbb{R}^2_+} G(s,x,z)\overline{\nu}^K_\varepsilon(\mathrm{d}s,\mathrm{d}x,\mathrm{d}z) \stackrel{\text{def.}}{=} \int_{[0,T]} G\left(s,\overline{X}^K_\varepsilon(s),\overline{Z}^K_\varepsilon(s)\right)\mathrm{d}s.$$

Lemma 38. *The family of random Radon measures $\overline{\nu}^K_\varepsilon$, $\varepsilon\in(0,1)$, is tight for the convergence in distribution and for any bounded Borelian function on $[0,T]\times\mathbb{R}^2_+$, the set of processes*

$$(I_G(t)) \stackrel{\text{def.}}{=} \left(\int_0^t G\left(u,\overline{X}^K_\varepsilon(u),\overline{Z}^K_\varepsilon(u)\right)\,\mathrm{d}u, 0\leqslant t\leqslant T\right)$$

is tight for the convergence in distribution.

Proof. For $a>0$, $\varepsilon\in(0,1)$, and $\mathcal{K}$ a Borelian subset of $\mathbb{R}^2_+$, we have

$$\mathbb{P}\left(\overline{\nu}^K_\varepsilon([0,T]\times\mathcal{K}^c)>a\right) \leqslant \frac{1}{a}\mathbb{E}\left[\overline{\nu}^K_\varepsilon([0,T]\times\mathcal{K}^c)\right]$$
$$\leqslant \frac{T}{a}\sup_{\substack{0<\varepsilon<1\\0\leqslant t\leqslant T}}\mathbb{P}\left(\left(\overline{X}^K_\varepsilon(t),\overline{Z}^K_\varepsilon(t)\right)\notin\mathcal{K}\right)$$

Lemma 36 shows the existence of a compact set $\mathcal{K}\subset\mathbb{R}^2_+$ such that the last term of the right-hand side of this inequality can be made arbitrarily small. Lemma 1.3 of [Kur92] gives that the family of random measures $(\overline{\nu}^K_\varepsilon, 0<\varepsilon<1)$ is tight.

for the last part of the proposition, we use the criterion of modulus of continuity, see [Bil99]. This is a simple consequence of the inequality, for $0\leqslant s,t\leqslant T$, $|I_G(t)-I_G(s)|\leqslant\|G\|_\infty|t-s|$. The lemma is proved. □

Proposition 39. *The family of random variables $(\overline{\Omega}^K_\varepsilon(t),\overline{W}^K_\varepsilon(t),\overline{\nu}^K_\varepsilon)$, $\varepsilon\in(0,1)$, is tight.*

Proof. Tightness properties of $(\overline{\nu}^K_\varepsilon)$ have been proved in Lemma 38. Relation (3.22) gives the relation, for $t\geqslant 0$,

$$\overline{\Omega}^K_\varepsilon(t)-\overline{\omega}_0 e^{-\alpha t} = \int_0^t e^{-\alpha(t-s)}C_n\left(1+\ell\overline{Z}^K_\varepsilon(s)\right)\left(1+\lambda+C_\beta(1+\overline{X}^K_\varepsilon(s))\right)\mathrm{d}s$$

$$+\int_0^t e^{-\alpha(t-s)}C_n\Big(1+\ell\overline{Z}_\varepsilon^K(s-)\Big)\Big[\varepsilon\mathcal{N}_{\lambda/\varepsilon}(\mathrm{d}s)-\lambda\,\mathrm{d}s+\varepsilon\mathcal{N}_{\overline{\beta}/\varepsilon,\overline{X}_\varepsilon^K}(\mathrm{d}s)-\overline{\beta}\left(\overline{X}_\varepsilon^K(s)\right)\mathrm{d}s\Big]. \quad (3.30)$$

Lemma 37 shows that the family of processes associated to the first term of the right-hand side of this identity is tight, and that the process of the second term is vanishing in distribution as ε goes to 0. The family of processes $(\overline{\Omega}_\varepsilon^K(t))$ is therefore tight and the tightness of $(\overline{W}_\varepsilon^K(t))$ follows from its representation with $(\overline{\Omega}_\varepsilon^K(t))$. The proposition is proved. □

Averaging principle for the truncated process $(\overline{U}^K(t))$

The goal of this section is to prove the following averaging principles for the truncated process. We start by stating the two following lemmas that are proved in Appendix 3.A and that are essential to the proof of averaging principle.

We fix a sequence (ε_n) such that $(\overline{\nu}_{\varepsilon_n}^K)$ is converging in distribution to $\overline{\nu}^K$. The first result focus on identifying the limiting linear functional of $\overline{\nu}^K$.

Lemma 40. *For any continuous bounded Borelian function G and a, b, $c\in\mathbb{R}_+$, the sequence of processes*

$$\left(\int_0^t\left(a\overline{X}_{\varepsilon_n}^K(s)+b\overline{Z}_{\varepsilon_n}^K(s)+c\overline{X}_{\varepsilon_n}^K(s)\overline{Z}_{\varepsilon_n}^K(s)\right)G\left(\overline{X}_{\varepsilon_n}^K(s),\overline{Z}_{\varepsilon_n}^K(s)\right)\mathrm{d}s\right)$$

converges in distribution to

$$\left(\int_0^t\int_{\mathbb{R}^2}(ax+bz+cxz)G(x,z)\overline{\nu}^K(\mathrm{d}s,\mathrm{d}x,\mathrm{d}z)\right).$$

The second lemma shows that $\overline{\nu}^K$ can be expressed as the product of the invariant measure Π_w and the Lebesgue measure. This is Lemma (1.4) of [Kur92].

Lemma 41. *For any non-negative Borelian function F on $\mathbb{R}_+\times\mathbb{R}_+^2$, almost surely,*

$$\int_0^T F(s,x,z)\overline{\nu}^K(\mathrm{d}s,\mathrm{d}x,\mathrm{d}z)=\int_0^T F(s,x,z)\Pi_{K\wedge\overline{w}^K(s)}(\mathrm{d}x,\mathrm{d}z)\,\mathrm{d}s,$$

where, for $w\in\mathbb{R}_+$, Π_w is the unique invariant distribution of the Markov process associated to the infinitesimal generator B_w^F defined by Relation (3.27).

With these two lemmas, Proposition 42 can be established.

Proposition 42. *Any limiting point $(\overline{\omega}^K(t),\overline{w}^K(t))$ of the family of processes $(\overline{\Omega}_\varepsilon^K(t),\overline{W}_\varepsilon^K(t))$, when ε goes to 0, verifies, almost surely for all $t\geqslant 0$, the ODE*

$$\begin{cases}\overline{\omega}^K(t) &= \overline{\omega}_0-\alpha\displaystyle\int_0^t\overline{\omega}^K(s)\,\mathrm{d}s\\ &\quad+\displaystyle\int_0^t\int_{\mathbb{R}^2}C_n(1+\ell z)(1+\lambda+C_\beta(1+x))\Pi_{\overline{w}^K(s)\wedge K}(\mathrm{d}x,\mathrm{d}z)\,\mathrm{d}s\\ \overline{w}^K(t) &= \overline{w}_0+\displaystyle\int_0^t C_M\left(1+\overline{\omega}^K(s)\right)\mathrm{d}s,\end{cases}$$

holds, where Π_w is the unique invariant distribution of the Markov process associated to the infinitesimal generator B_w^F defined by Relation (3.27).

Proof. Relation (3.30) gives the identity, for $t \geqslant 0$,

$$\overline{\Omega}_\varepsilon^K(t) = \overline{\omega}_0 e^{-\alpha t} + e^{-\alpha t}\overline{M}_\varepsilon^K(t) + e^{-\alpha t}\int_0^t e^{\alpha s} C_n(1+\ell \overline{Z}_\varepsilon(s))\left(1+\lambda+C_\beta(1+\overline{X}_\varepsilon^K(s))\right)\,\mathrm{d}s,$$

with

$$\overline{M}_\varepsilon^K(t) \stackrel{\text{def.}}{=} \int_0^t e^{\alpha s} C_n\left(1+\ell\overline{Z}_\varepsilon^K(s)\right)\left[\varepsilon\mathcal{N}_{\lambda/\varepsilon}(\mathrm{d}s) + \varepsilon\mathcal{N}_{\overline{\beta}/\varepsilon, \overline{X}_\varepsilon^K}(\mathrm{d}s) - (\lambda+\overline{\beta}(\overline{X}_\varepsilon^K(s)))\,\mathrm{d}s\right].$$

Lemma 37 shows that $(\overline{M}_\varepsilon^K(t))$ is converging in distribution to 0 when ε goes to 0. We now use Lemmas 40 and 41 and we get that $(\overline{\omega}^K(t), \overline{w}^K(t))$ satisfies the desired relation. □

3.7 Proof of an averaging principle

Finally, this section gathers all the results from the previous sections to prove Theorem 29. The proof is done in two steps:

a. Using an analytical result, an averaging principle for $(\overline{U}(t))$ is proved.

b. The coupling of Section 3.5 is then used to show that a stochastic averaging result also holds in the general case.

Averaging principle for the coupled process $(\overline{U}(t))$

We now turn to an analytical result by considering the dynamical system of Proposition 42 when $K = +\infty$ and by showing an existence and uniqueness results which will be crucial in the proof of the general theorem.

For $w \geqslant 0$, $\overline{\Pi}_w$ is the invariant distribution of the Markov process $(\overline{X}^w(t), \overline{Z}^w(t))$ satisfying the SDE

$$\begin{aligned}
\mathrm{d}\overline{X}^w(t) &= -\overline{X}^w(t)\,\mathrm{d}t + w\mathcal{N}_\lambda(\mathrm{d}t),\\
\mathrm{d}\overline{Z}^w(t) &= \left(-\gamma\overline{Z}^w(t)+C_k\right)\mathrm{d}t + C_k\mathcal{N}_\lambda(\mathrm{d}t) + C_k\mathcal{N}_{\overline{\beta},\overline{X}^w}(\mathrm{d}t).
\end{aligned}$$

Its existence is a consequence of Proposition 50.

Theorem 43. *Under conditions of Section 3.2, there exists $S_0 \in (0, +\infty]$ and a unique continuous function $(\overline{\omega}(t), \overline{w}(t))$ on $[0, S_0)$, solution of the ODE, for $0 \leqslant t < S_0$,*

$$\begin{cases}
\overline{\omega}(t) = \overline{\omega}_0 - \alpha\displaystyle\int_0^t \overline{\omega}(s)\,\mathrm{d}s + \int_0^t\int_{\mathbb{R}_+^2} C_n(1+\ell z)(1+\lambda+C_\beta(1+x))\overline{\Pi}_{\overline{w}(s)}(\mathrm{d}x,\mathrm{d}z)\,\mathrm{d}s,\\
\overline{w}(t) = \overline{w}_0 + \displaystyle\int_0^t C_M\left(1+\overline{\omega}_p(s)\right)\,\mathrm{d}s,
\end{cases} \tag{3.31}$$

with $(\overline{\omega}_0, \overline{w}_0) \in \mathbb{R}_+^2$

Any limiting point $(\overline{\omega}^K(t), \overline{w}^K(t)))$ of the family of processes $(\overline{\Omega}_\varepsilon^K(t), \overline{W}_\varepsilon^K(t))$, when ε goes to 0 is such that, for all $0 \leqslant t < S_0$,

$$\overline{\omega}^K(t) \leqslant \overline{\omega}(t) \text{ and } \overline{w}^K(t) \leqslant \overline{w}(t).$$

Proof. The existence of limiting points of the processes $(\overline{\Omega}_\varepsilon^K(t), \overline{W}_\varepsilon^K(t))$ is due to Proposition 42. If $(\overline{X}^w, \overline{Z}^w)$ is a random variable with distribution $\overline{\Pi}_w$, we have

$$\overline{X}^w \overset{\text{dist.}}{=} w \int_0^{+\infty} e^{-s} \mathcal{N}_\lambda(\mathrm{d}s),$$

and, with standard calculations, we obtain the relations

$$\mathbb{E}\left[\overline{X}^w\right] = \lambda w, \qquad \mathbb{E}\left[\left(\overline{X}^w\right)^2\right] = \left(\lambda^2 + \frac{\lambda}{2}\right) w^2, \tag{3.32}$$

and, consequently,

$$\gamma \mathbb{E}\left[\overline{Z}^w\right] = C_k\left(1+\lambda+C_\beta\left(1+\mathbb{E}\left[\overline{X}^w\right]\right)\right) = C_k\left(1+\lambda+C_\beta(1+\lambda w)\right).$$

The SDEs for $(\overline{X}^w(t))$ and $(\overline{Z}^w(t))$ give

$$\begin{aligned}\mathrm{d}\overline{X}^w\overline{Z}^w(t) = &\left(-(\gamma+1)\overline{X}^w(t)\overline{Z}^w(t) + C_k\overline{X}^w(t)\right)\mathrm{d}t \\ &+ (w\overline{Z}^w(t-) + C_k\overline{X}^w(t-) + C_k w)\mathcal{N}_\lambda(\mathrm{d}t) + C_k\overline{X}^w(t-)\mathcal{N}_{\overline{\beta},\overline{X}^w}(\mathrm{d}t),\end{aligned}$$

and thus, at equilibrium, we obtain the relation

$$\mathbb{E}\left[\overline{X}^w\overline{Z}^w\right] = C_k\frac{1}{\gamma+1}\left(\lambda w\left(1+\mathbb{E}\left[\overline{Z}^w\right]\right) + (1+\lambda+C_\beta)\mathbb{E}\left[\overline{X}^w\right] + C_\beta\mathbb{E}\left[\left(\overline{X}^w\right)^2\right]\right).$$

We have therefore that the function

$$w \mapsto C_n \int_{\mathbb{R}_+^2} (1+\ell z)(1+\lambda+C_\beta(1+x))\overline{\Pi}_w(\mathrm{d}x, \mathrm{d}z)$$

is a non-decreasing and locally Lipschitz function. The existence and uniqueness follows from standard results for ODEs. There exists some $S_0>0$, such that, on the time interval $[0, S_0)$, the solution $(\overline{\omega}(t), \overline{w}(t))$ of the ODE is the limit of a Picard's scheme $(\overline{\omega}_n(t), \overline{w}_n(t))$ associated to Relation (3.31) with

$$(\overline{\omega}_0(t), \overline{w}_0(t)) = (\overline{\omega}^K(t), \overline{w}^K(t)),$$

for all $K\in\mathbb{R}_+$. See Section 3 of Chapter 8 of [HS74] for example. We now prove by induction that $(\overline{\omega}^K(t), \overline{w}^K(t)) \leqslant (\overline{\omega}_n(t), \overline{w}_n(t))$ holds on $[0, S_0)$ for all $n\geqslant 1$. If this is true for n, then

$$\begin{aligned}\overline{\omega}_{n+1}(t) &= \overline{\omega}_0 e^{-\alpha t} + \int_0^t e^{-\alpha(t-s)} \int_{\mathbb{R}^2} C_n(1+\ell z)(1+\lambda+C_\beta(1+x))\Pi_{\overline{w}_n(s)}(\mathrm{d}x, \mathrm{d}z)\ \mathrm{d}s \\ &\geqslant \overline{\omega}_0 e^{-\alpha t} + \int_0^t e^{-\alpha(t-s)} \int_{\mathbb{R}^2} C_n(1+\ell z)(1+\lambda+C_\beta(1+x))\Pi_{\overline{w}^K(s)\wedge K}(\mathrm{d}x, \mathrm{d}z)\ \mathrm{d}s \\ &= \overline{\omega}^K(t),\end{aligned}$$

and the relation $\overline{w}_{n+1}(t) \geqslant \overline{w}^K(t)$ follows directly. The proof by induction is completed. We just have to let n go to infinity to obtain the last statement of our proposition. □

Proposition 44. *Under conditions of Section 3.2, for the convergence in distribution,*

$$\lim_{\varepsilon\to 0}((\overline{\Omega}_\varepsilon(t),\overline{W}_\varepsilon(t)),t<S_0)=((\overline{\omega}(t),\overline{w}(t)),t<S_0),$$

where $(\overline{\Omega}_\varepsilon(t),\overline{W}_\varepsilon(t))$ *is the process defined by SDEs* (3.26) *and* $((\overline{\omega}(t),\overline{w}(t)),t<S_0)$ *by ODE* (3.31).

Proof. From Proposition 42, let $(\overline{\omega}^K(t),\overline{w}^K(t))$ be a limiting point, there exists a sequence (ε_n) such that the sequence of processes $(\overline{\Omega}^K_{\varepsilon_n}(t),\overline{W}^K_{\varepsilon_n}(t))$ is converging to a continuous process $(\overline{\omega}^K(t),\overline{w}^K(t))$.

With the same notations as in Proposition 43, for any $T<S_0$, by continuity of $(\overline{\omega}(t),\overline{w}(t))$ on $[0,T]$, the quantity

$$K_0\stackrel{\text{def.}}{=}1+\sup_{t\leqslant T}\overline{w}(t)$$

is finite. Since $\overline{w}^K(t)\leqslant\overline{w}(t)$ holds for all $t\geqslant 0$, the uniqueness result of Proposition 43 gives the identity

$$((\overline{\omega}^K(t),\overline{w}^K(t)),t\leqslant T)=((\overline{\omega}(t),\overline{w}(t)),t\leqslant T)$$

for all $K\geqslant K_0$. Consequently, for any $\eta>0$, there exists $n_0>0$ such that for $n\geqslant n_0$,

$$\mathbb{P}\left(\sup_{s\leqslant T}\overline{W}^{K_0}_{\varepsilon_n}(s)\geqslant K_0\right)\leqslant\mathbb{P}\left(\sup_{s\leqslant T}\overline{W}^{K_0}_{\varepsilon_n}(s)\geqslant 1+\sup_{t\leqslant T}\overline{w}^{K_0}(t)\right)\leqslant\eta,$$

since the process $(\overline{\omega}^{K_0}(t),\overline{w}^{K_0}(t))$ is upper-bounded, coordinate by coordinate on the time interval $[0,S_0)$, by $(\omega(t),w(t))$, defined by Relation (3.31). Note that S_0 is independent of the sequence (ε_n). Hence, for $n\geqslant n_0$, Relation (3.28) gives

$$\mathbb{P}\left(\begin{array}{c}\overline{X}_{\varepsilon_n}(s)=\overline{X}^{K_0}_{\varepsilon_n}(s),\overline{Z}_{\varepsilon_n}(s)=\overline{Z}^{K_0}_{\varepsilon_n}(s),\\ \overline{\Omega}_{\varepsilon_n}(s)=\overline{\Omega}^{K_0}_{\varepsilon_n}(s),\overline{W}_{\varepsilon_n}(s)=\overline{W}^{K_0}_{\varepsilon_n}(s),\forall s\leqslant T\end{array}\right)$$
$$\geqslant\mathbb{P}\left(\sup_{s\leqslant T}\overline{W}^{K_0}_{\varepsilon_n}(s)\leqslant K_0\right)\geqslant 1-\eta. \quad (3.33)$$

This shows that the sequence of processes $((\overline{\Omega}_{\varepsilon_n}(t),\overline{W}_{\varepsilon_n}(t)),t\leqslant T)$ is converging in distribution to $((\overline{\omega}(t),\overline{w}(t)),t\leqslant T)$. The proposition is proved. □

Averaging principle for the process $(U_\varepsilon(t))$

We now conclude this section with the proof of Theorem 29. We fix $T<S_0$.

The coupling property of Proposition 35 and Relation (3.33) give the existence of K_0 and n_0 such that for $n\geqslant n_0$, the inequality

$$\mathbb{P}\left(\sup_{t\leqslant T}|W_{\varepsilon_n}(t)|\leqslant K_0\right)\geqslant 1-\eta$$

holds.

We get that the results of Lemma 37 hold with $\overline{X}^K_{\varepsilon_n}$ and $\overline{Z}^K_{\varepsilon_n}$ replaced by X_{ε_n} and $\|Z_{\varepsilon_n}\|$, and $\overline{\beta}$ by β. With the same arguments as in the proof of Lemma 38, the family

of random measures (ν_{ε_n}) defined by Relation (3.19) is tight and Lemma 40 holds for $(X_{\varepsilon_n}(t))$ and $(\|Z_{\varepsilon_n}\|(t))$.

With Relations (3.15) and (3.16), we get, for $a\in\{p,d\}$ and $t\geqslant 0$,

$$\Omega_{\varepsilon,a}(t) = \omega_{0,a} + \int_0^t e^{-\alpha(t-s)} n_{a,0}(Z_\varepsilon(s))\,\mathrm{d}s + \int_0^t e^{-\alpha(t-s)} n_{a,1}(Z_\varepsilon(s-))\varepsilon\mathcal{N}_{\lambda/\varepsilon}(\mathrm{d}s) + \int_0^t e^{-\alpha(t-s)} n_{a,2}(Z_\varepsilon(s-))\varepsilon\mathcal{N}_{\beta/\varepsilon,X_\varepsilon}(\mathrm{d}s),$$

and

$$W_\varepsilon(t) = W_\varepsilon(0) + \int_0^t M\left(\Omega_{\varepsilon,p}(s), \Omega_{\varepsilon,d}(s), W(t)\right)\mathrm{d}s.$$

Relation (3.11) of the assumptions of Section 3.2 gives that $n_{a,j}(z)\leqslant C_n(1+\|z\|)$ for $z\in\mathbb{R}^\ell$, $a\in\{p,d\}$ and $j\in\{0,1,2\}$. Lemma 37 applied to $(X_{\varepsilon_n}(t))$ and $(\|Z_{\varepsilon_n}\|(t))$ shows that the family of processes $(\Omega_{\varepsilon,a}(t))$ is tight, consequently that the same property hold for $(W_\varepsilon(t))$ due to the relation satisfied by M of Section 3.2. We have thus obtained the tightness of the sequence of processes

$$(\Omega_{\varepsilon_n,p}(t), \Omega_{\varepsilon_n,d}(t), W_{\varepsilon_n}(t), \nu_{\varepsilon_n}).$$

By taking a subsequence, we can assume it is converging in distribution to some process $(\omega_p(t), \omega_d(t), w(t), \nu)$.

We now identify the measure ν. Lemma (1.4) of [Kur92] shows that, for any bounded Borelian function G on $\mathbb{R}_+\times\mathbb{R}\times\mathbb{R}_+^\ell$,

$$\int_0^T G(s,x,z)\nu(\mathrm{d}s,\mathrm{d}x,\mathrm{d}z) = \int_0^T \int_{\mathbb{R}\times\mathbb{R}_+^\ell} G(s,x,z)\gamma(s)(\mathrm{d}x,\mathrm{d}z)\,\mathrm{d}s,$$

where $(\gamma(s))$ is a predictable measure-valued process.

The continuity of the different functions $g(\cdot)$ and $k_i(\cdot)$ give that, for $f\in\mathcal{C}_b^1(\mathbb{R}\times\mathbb{R}_+^\ell)$, $(x,z,w)\mapsto B_w^F(f)(x,z)$ is continuous, where B_w^F is the operator defined by Relation (3.18).

Moreover, using

— condition of Section 3.2 for the growth of the function β;

— the boundedness of k_i, $i\in\{1,2\}$ of Condition of Section 3.2,

we have that, for $f\in\mathcal{C}_b^1(\mathbb{R}\times\mathbb{R}_+^\ell)$, there exists a constant C_0 such that, for $(x,z)\in\mathbb{R}\times\mathbb{R}_+^\ell$,

$$|B_w^F(f)(x,z)| \leqslant C_0(1+|x|+\|z\|)\left(\|f\|_\infty + \|\nabla f\|_\infty\right).$$

We apply the equivalent of Lemma 40 to $(X_{\varepsilon_n}(t))$ and $(Z_{\varepsilon_n}(t))$ to get the relation, for $T>0$,

$$\lim_{n\to+\infty}\int_0^T B^F_{W_{\varepsilon_n}(s)}(f)\left(X_{\varepsilon_n}(s), Z_{\varepsilon_n}(s)\right)\mathrm{d}s = \int_0^T\int_{\mathbb{R}\times\mathbb{R}_+^\ell} B^F_{w(s)}(f)(x,z)\nu(\mathrm{d}s,\mathrm{d}x,\mathrm{d}z).$$

From the SDEs (3.14) and (3.14) we have

$$f\left(X_{\varepsilon_n}(s), Z_{\varepsilon_n}(s)\right) = f(x_0,z_0) + M^f_{\varepsilon_n}(t)$$

$$+\frac{1}{\varepsilon}\int_0^t B^F_{W_{\varepsilon_n}(s)}(f)\left(X_{\varepsilon_n}(s),Z_{\varepsilon_n}(s)\right)\mathrm{d}s, \quad (3.34)$$

where $(M^f_{\varepsilon_n}(t))$ is the associated martingale.

In the same way as in the proof of Lemma 41, we show that $(\varepsilon_n M^f_{\varepsilon_n}(t))$ is converging in distribution to 0 which leads to the identity, almost surely for any $t\leqslant T$,

$$\int_0^t\int_{\mathbb{R}\times\mathbb{R}^\ell_+} B^F_{w(s)}(f)(x,z)\nu(\mathrm{d}s,\mathrm{d}x,\mathrm{d}z)=0,$$

for f in a countable dense subset S of the functions of $\mathcal{C}^1_b(\mathbb{R}\times\mathbb{R}^\ell_+)$ with compact support. Consequently,

$$\int_0^t\int_{\mathbb{R}\times\mathbb{R}^\ell_+} B^F_{w(s)}(f)(x,z)\gamma(s)(\mathrm{d}x,\mathrm{d}z)\,\mathrm{d}s = 0,$$

which gives that for almost all $t\in[0,T]$

$$\int_{\mathbb{R}\times\mathbb{R}^\ell_+} B^F_{w(t)}(f)(x,z)\gamma(t)(\mathrm{d}x,\mathrm{d}z) = 0, \quad \forall f\in S.$$

Proposition 50 of the Appendix gives therefore that, $\gamma(t)=\Pi_{w(t)}$, for almost all $t\in[0,T]$ (for Lebesgue's measure), so that

$$\int_0^T G(s,x,z)\nu(\mathrm{d}s,\mathrm{d}x,\mathrm{d}z) = \int_0^T\int_{\mathbb{R}\times\mathbb{R}^\ell_+} G(s,x,z)\Pi_{w(s)}(\mathrm{d}x,\mathrm{d}z)\,\mathrm{d}s,$$

holds almost surely for all bounded continuous functions on $\mathbb{R}_+\times\mathbb{R}\times\mathbb{R}^\ell_+$.

To establish the first identity of Relation (3.31), we need the convergence in distribution

$$\lim_{n\to+\infty}\left(\int_0^t e^{-\alpha(t-u)}\begin{pmatrix} n_0\left(Z_{\varepsilon_n}(u)\right)\\ n_1\left(Z_{\varepsilon_n}(u)\right)\\ \beta\left(X_{\varepsilon_n}(u)\right)n_2\left(Z_{\varepsilon_n}(u)\right)\end{pmatrix}\mathrm{d}u\right) = \left(\int_0^t e^{-\alpha(t-u)}\int_{\mathbb{R}\times\mathbb{R}^\ell_+}\begin{pmatrix} n_0\left(z\right)\\ n_1\left(z\right)\\ \beta\left(x\right)n_2\left(z\right)\end{pmatrix}\Pi_{w(u)}(\mathrm{d}x,\mathrm{d}z)\,\mathrm{d}u\right).$$

This is consequence of the fact that $(w(t))$ is almost surely continuous and that, with the conditions of Section 3.2, for any $w\in K_W$,

$$(x,z)\mapsto(n_0(z),n_1(z),\beta(x)n_2(z)),$$

is Π_w almost everywhere continuous.

The theorem is therefore proved.

3.8 The simple model

In this section we consider the simple model defined in Section 3.1. Recall that the associated SDEs are

$$\begin{cases}\mathrm{d}X(t) = -X(t)\,\mathrm{d}t + W(t-)\mathcal{N}_\lambda(\mathrm{d}t),\\ \mathrm{d}Z(t) = -\gamma Z(t)\,\mathrm{d}t + B_1\mathcal{N}_\lambda(\mathrm{d}t) + B_2\mathcal{N}_{\beta,X}(\mathrm{d}t),\\ \mathrm{d}W(t) = Z(t-)\mathcal{N}_{\beta,X}(\mathrm{d}t),\end{cases}$$

with $\gamma>0$, B_1, $B_2\in\mathbb{R}_+$, and β is assumed to be a Lipschitz function on $\mathbb{R}_+$.

This is not, strictly speaking, a special case of the processes defined by Relations (3.7), but the tightness results of Section 3.A of Appendix concerning occupation times of fast processes can obviously be used.

Let, for $w\geqslant 0$, $(X^w(t), Z^w(t))$ be the fast processes associated to the model of Definition 27. Proposition 50 shows that $(X^w(t), Z^w(t))$ has a unique invariant distribution Π_w. We denote by (X^w_∞, Z^w_∞) a random variable with distribution Π_w.

Proposition 45. *The function*

$$w \mapsto \mathbb{E}\left[Z^w_\infty \beta(X^w_\infty)\right] = \int_{\mathbb{R}^2_+} z\beta(x)\Pi_w(\mathrm{d}x, \mathrm{d}z)$$

is locally Lipschitz on $\mathbb{R}_+$.

Proof. Assuming $X^w(0)=Z^w(0)=0$, Lemma 30 and Definition 3.6 give the relations

$$\begin{cases} X^w(t) = w\displaystyle\int_0^t e^{-(t-s)}\mathcal{N}_\lambda(\mathrm{d}s) = wX^1(t) \\ Z^w(t) = B_1\displaystyle\int_0^t e^{-\gamma(t-s)}\mathcal{N}_\lambda(\mathrm{d}s) + B_2\int_0^t e^{-\gamma(t-s)}\mathcal{P}_2((0,\beta(wX^1(s-)),\mathrm{d}s). \end{cases}$$

the random variable $(X^w(t), Z^w(t))$ is converging in distribution to (X^w_∞, Z^w_∞) as well as any of its moments. Define

$$\Psi_t(w) \stackrel{\text{def.}}{=} \mathbb{E}\left[\beta\left(wX^1(t)\right)\int_0^t e^{-\gamma(t-s)}\mathcal{P}_2((0,\beta(wX^1(s-)),\mathrm{d}s)\right],$$

for $x,y\geqslant 0$,

$$\begin{aligned} |\Psi_t(x)-\Psi_t(y)| &\leqslant \mathbb{E}\left[\left|\beta\left(xX^1(t)\right)-\beta\left(yX^1(t)\right)\right|\int_0^t e^{-\gamma(t-s)}\mathcal{P}_2((0,\beta(xX^1(s-)),\mathrm{d}s)\right] \\ &\quad + \left|\mathbb{E}\left[\beta\left(yX^1(t)\right)\int_0^t e^{-\gamma(t-s)}\mathcal{P}_2((\beta(xX^1(s-)),\beta(yX^1(s-)),\mathrm{d}s)\right]\right|. \end{aligned}$$

We note that $(X^1(t))$ is a functional of $\mathcal{N}_\lambda$ and is therefore independent of the Poisson process $\mathcal{P}_2$. We now take care of the two terms of the right-hand side of the last expression.

For the first term, if L_β is the Lipschitz constant of the function β, we obtain

$$\begin{aligned} &\mathbb{E}\left[\left|\beta\left(xX^1(t)\right)-\beta\left(yX^1(t)\right)\right|\int_0^t e^{-\gamma(t-s)}\mathcal{P}_2((0,\beta(xX^1(s)),\mathrm{d}s)\right] \\ &\qquad = \mathbb{E}\left[\left|\beta\left(xX^1(t)\right)-\beta\left(yX^1(t)\right)\right|\int_0^t e^{-\gamma(t-s)}\beta(xX^1(s))\,\mathrm{d}s\right] \\ &\qquad\leqslant L_\beta|x-y|\mathbb{E}\left[X^1(t)\int_0^t e^{-\gamma(t-s)}\beta(xX^1(s))\,\mathrm{d}s\right], \quad (3.35) \end{aligned}$$

and, for the second term, if $|y-x|\leqslant 1$,

$$\left|\mathbb{E}\left[\beta\left(yX^1(t)\right)\int_0^t e^{-\gamma(t-s)}\mathcal{P}_2((\beta(xX^1(s)),\beta(yX^1(s)),\mathrm{d}s)\right]\right|$$
$$\leqslant \mathbb{E}\left[\beta\left(yX^1(t)\right)\int_0^t e^{-\gamma(t-s)}\left|\beta(xX^1(s))-\beta(yX^1(s))\right|\mathrm{d}s\right]$$
$$\leqslant L_\beta|x-y|\mathbb{E}\left[\left(\beta(0)+L_\beta(1+x)X^1(t)\right)\int_0^t e^{-\gamma(t-s)}X^1(s))\,\mathrm{d}s\right]. \quad (3.36)$$

Fubini's Theorem gives the relation,

$$\mathbb{E}\left[X^1(t)\int_0^t e^{-\gamma(t-s)}\beta(xX^1(s))\,\mathrm{d}s\right]=\int_0^t e^{-\gamma s}\mathbb{E}\left[X^1(t)\beta(xX^1(t-s))\right]\mathrm{d}s,$$

and the convergence in distribution of the Markov process $(X^1(t))$ implies the convergence of $(\mathbb{E}\left[X^1(t)\beta(xX^1(t-s))\right])$ to a finite limit when t goes to infinity. With Relations (3.35) and (3.36) and the expressions of $(X^w(t))$ and $(Z^w(t))$, we deduce that for $x\geqslant 0$, there exists a constant F_x independent of t such that

$$\left|\mathbb{E}\left[Z^x(t)\beta\left(X^x(t)\right)\right]-\mathbb{E}\left[Z^y(t)\beta\left(X^y(t)\right)\right]\right|\leqslant F_x|x-y|$$

holds for all $t\geqslant 0$ and y such that $|y-x|\leqslant 1$. We conclude the proof of the proposition by letting t go to infinity.

□

The averaging principle for the simple model, announced in Section 3.1 of the introduction can now be stated.

Theorem 46. *If the function β is Lipschitz, there exists some $S_0(w_0)>0$, such that the family of processes $(W_\varepsilon(t), t<S_0(w_0))$ defined by Relation* (3.2) *converges in distribution to $(w(t), t<S_0(w_0))$, the unique solution of the ODE*

$$\frac{\mathrm{d}w}{\mathrm{d}t}(t)=\int_{\mathbb{R}_+^2} z\beta(x)\Pi_{w(t)}(\mathrm{d}x,\mathrm{d}z)$$

with $w(0)=w_0$.

Proof. For $t\geqslant 0$,

$$W_\varepsilon(t)=w_0+\int_0^t Z_\varepsilon(s-)\varepsilon\mathcal{N}_{\beta/\varepsilon,X_\varepsilon}(\mathrm{d}s),$$

we then proceed as in Section 3.7 by using in particular the analogue of Lemma 37 and 40. □

An explicit representation of the limiting connection intensity process can be obtained when linear activation functions.

Proposition 47. *If the activation function β is such that $\beta(x)=\nu+\beta_0 x$ and*

$$\Lambda_2=\lambda\beta_0^2B_2\left(\frac{\lambda}{\gamma}+\frac{1}{2(\gamma+1)}\right),\ \Lambda_1=\lambda\beta_0\left(\frac{B_1}{\gamma+1}+\frac{\lambda B_1+2\nu B_2}{\gamma}\right),\Lambda_0=\frac{\nu}{\gamma}(\lambda B_1+\nu B_2),$$

then if $\Lambda_2>0$, the asymptotic weight process $(w(t), 0\leqslant t<S_0(w_0))$ of Theorem 46 with initial point $w_0\geqslant 0$ can be expressed as:

a. If $\Delta \overset{\text{def.}}{=} \Lambda_1^2 - 4\Lambda_2\Lambda_0 > 0$, *then*

$$w(t) = \frac{s_2(w_0+s_1)e^{\sqrt{\Delta}t} - s_1(w_0+s_2)}{(w_0+s_2)-(w_0+s_1)e^{\sqrt{\Delta}t}}, \quad S_0(w_0) = \frac{1}{\sqrt{\Delta}} \ln\left(\frac{w_0+s_2}{w_0+s_1}\right),$$

with

$$s_1 \overset{\text{def.}}{=} \frac{\Lambda_1 - \sqrt{\Delta}}{2\Lambda_2} \text{ and } s_2 \overset{\text{def.}}{=} \frac{\Lambda_1 + \sqrt{\Delta}}{2\Lambda_2}.$$

b. If $\Delta = 0$, *then*

$$w(t) = \frac{2w_0\Lambda_2 + \Lambda_1}{\Lambda_2(2-(2\Lambda_2 w_0 + \Lambda_1)t)} - \frac{\Lambda_1}{2\Lambda_2}, \quad S_0(w_0) = \frac{2}{2w_0\Lambda_2 + \Lambda_1}.$$

c. If $\Delta < 0$, *then*

$$w(t) = \frac{\sqrt{-\Delta}}{2\Lambda_2}\left(\tan\left(\frac{1}{2}\sqrt{-\Delta}\cdot t + \arctan(z_0)\right) + \left\lfloor \frac{z_0}{\pi} + \frac{1}{2} \right\rfloor \pi\right) - \frac{\Lambda_1}{2\Lambda_2},$$

with

$$S_0(w_0) = \frac{2}{\sqrt{-\Delta}}\left(\frac{\pi}{2} - \arctan(z_0)\right) \text{ and } z_0 \overset{\text{def.}}{=} \frac{2w_0\Lambda_2 + \Lambda_1}{\sqrt{-\Delta}}.$$

It should be noted that under the conditions of this proposition, this model always exhibits a blow-up phenomenon.

Proof. The SDEs give the relation

$$\begin{aligned} \mathrm{d}X^w Z^w(t) = &-(\gamma+1)X^w Z^w(t)\,\mathrm{d}t \\ &+ (wZ^w(t-) + B_1 w + B_1 X^w(t-))\mathcal{N}_\lambda(\mathrm{d}t) + B_2 X^w(t-)\mathcal{N}_{\beta,X^w}(\mathrm{d}t). \end{aligned}$$

If the initial point has the same distribution as (X_∞^w, Z_∞^w), by integrating and by taking the expected valued of this SDE, we obtain the identity

$$(\gamma+1)\mathbb{E}\left[X_\infty^w Z_\infty^w\right] = \lambda w B_1 + (\lambda B_1 + \nu B_2)\mathbb{E}\left[X_\infty^w\right] + \beta_0 B_2 \mathbb{E}\left[(X_\infty^w)^2\right] + \lambda w \mathbb{E}[Z_\infty^w].$$

With Relations (3.32), we have

$$\mathbb{E}\left[X_\infty^w\right] = \lambda w, \quad \mathbb{E}\left[(X_\infty^w)^2\right] = \left(\lambda^2 + \frac{\lambda}{2}\right) w^2,$$

and, similarly,

$$\gamma\mathbb{E}[Z_\infty^w] = \lambda B_1 + B_2(\nu + \beta_0\mathbb{E}[X_\infty^w]) = \lambda B_1 + B_2(\nu + \beta_0\lambda w).$$

By using Theorem 46, with these identities, we obtain that $(w(t))$ satisfies the ODE

$$\frac{\mathrm{d}w}{\mathrm{d}t}(t) = \mathbb{E}\left[Z_\infty^w(\nu + \beta_0 X_\infty^w)\right] = \Lambda_2 w^2 + \Lambda_1 w + \Lambda_0, \tag{3.37}$$

on its domain of definition. We conclude the proof with trite calculations. □

Appendix

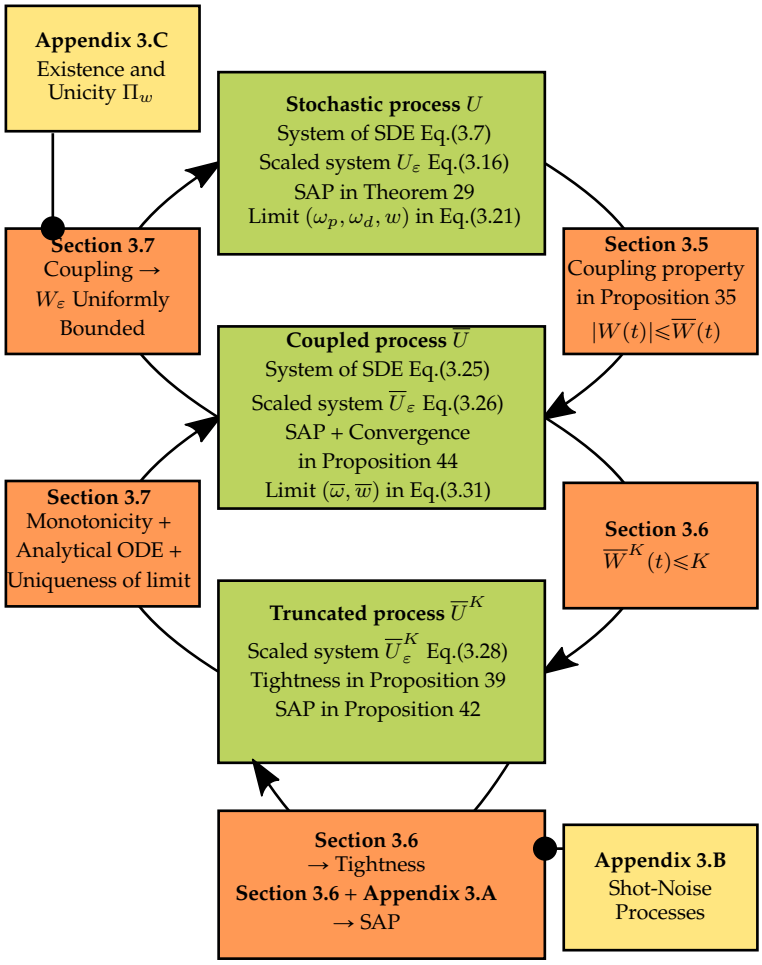

Figure 3.1: **Graphical representation of the steps of the proof of averaging principles.**

3.A Proofs of technical results for occupation times

Proof of Lemma 40

Denote, for $t \geqslant 0$, a, b, $c \in \mathbb{R}_+$, and $\varepsilon > 0$,

$$L_\varepsilon(t) \overset{\text{def.}}{=} a\overline{X}_\varepsilon^K(t) + b\overline{Z}_\varepsilon^K(t) + c\overline{X}_\varepsilon^K(t)\overline{Z}_\varepsilon^K(t).$$

Let G be a continuous bounded Borelian function. From Proposition 37, we can extract a sub-sequence (ε_n) such that, for the convergence in distribution

$$\lim_{n \to +\infty} \left(\int_0^t L_{\varepsilon_n}(u) G\left(\overline{X}_{\varepsilon_n}^K(u), \overline{Z}_{\varepsilon_n}^K(u) \right) \mathrm{d}u \right) = (L(t)),$$

where $(L(t))$ is a continuous càdlàg process.

We will now prove that the process $(L(t))$ is such that,

$$(L(t)) = \left(\int_0^t \int_{\mathbb{R}^2} (ax + bz + cxz) G(x, z) \overline{\nu}^K(\mathrm{d}s, \mathrm{d}x, \mathrm{d}z) \right)$$

holds almost-surely for $t\in[0,T]$.

For $A>0$, the convergence of $(\overline{\nu}^K_{\varepsilon_n})$ to $\overline{\nu}^K$ gives the convergence in distribution,

$$\lim_{n\to+\infty}\left(\int_0^t A\wedge L_{\varepsilon_n}(s)G\left(\overline{X}^K_{\varepsilon_n}(s),\overline{Z}^K_{\varepsilon_{k_n}}(s)\right)\mathrm{d}s\right) = \left(\int_0^t\int_{\mathbb{R}^2_+} A\wedge(ax+bz+cxz)G(x,z)\overline{\nu}^K(\mathrm{d}s,\mathrm{d}x,\mathrm{d}z)\right). \quad (3.38)$$

Using again the upper-bound, Relation (3.29), for $(\overline{X}^K_\varepsilon(t))$ with Relation (3.23), and Proposition 49 for R_ε, we obtain that

$$C_L \overset{\text{def.}}{=} \sup_{\substack{0<\varepsilon<1\\0\leqslant t\leqslant T}}\mathbb{E}\left[L_\varepsilon(s)^2\right]<+\infty,$$

hence, for $\eta>0$,

$$\mathbb{P}\left(\int_0^T(L_\varepsilon(s)-A)^+\,\mathrm{d}s\geqslant\eta\right)\leqslant\frac{1}{\eta}\int_0^T\mathbb{E}\left[(L_\varepsilon(s)-A)^+\right]\mathrm{d}s \leqslant\frac{1}{\eta A}\int_0^T\mathbb{E}\left[L_\varepsilon(s)^2\right]\mathrm{d}s\leqslant\frac{C_LT}{\eta A}.$$

Since G is bounded, with the elementary relation $x=x\wedge A+(x-A)^+$, $x\geqslant0$, then, for $n\geqslant1$,

$$\mathbb{P}\left(\sup_{0\leqslant t\leqslant T}\left|\int_0^t L_{\varepsilon_n}(u)G\left(\overline{X}^K_{\varepsilon_n}(u),\overline{Z}^K_{\varepsilon_n}(u)\right)\mathrm{d}u - \int_0^t A\wedge L_{\varepsilon_n}(u)G\left(\overline{X}^K_{\varepsilon_n}(u),\overline{Z}^K_{\varepsilon_n}(u)\right)\mathrm{d}u\right|\geqslant\eta\right)\leqslant\frac{C_LT}{\eta A}\|G\|_\infty. \quad (3.39)$$

For any $A>0$ and $n\geqslant1$, Cauchy-Schwartz's inequality gives the relation

$$\mathbb{E}\left[\int_0^T A\wedge L_{\varepsilon_n}(u)G\left(\overline{X}^K_{\varepsilon_n}(u),\overline{Z}^K_{\varepsilon_n}(u)\right)\mathrm{d}u\right]\leqslant\sqrt{C_L}T\|G\|_\infty.$$

With Relation (3.38) and the fact that the left-hand side of (3.38) has a bounded second moment, by letting n go to infinity, we get the inequality

$$\mathbb{E}\left[\int_0^T\int_{\mathbb{R}^2_+} A\wedge(ax+bz+cxz)G(x,z)\overline{\nu}^K(\mathrm{d}s,\mathrm{d}x,\mathrm{d}z)\right]\leqslant\sqrt{C_L}T\|G\|_\infty.$$

By letting A go to infinity, the monotone convergence theorem shows that

$$\lim_{A\to+\infty}\mathbb{E}\left[\int_0^T\int_{\mathbb{R}^2_+} A\wedge(ax+bz+cxz)G(x,z)\overline{\nu}^K(\mathrm{d}s,\mathrm{d}x,\mathrm{d}z)\right] = \mathbb{E}\left[\int_0^T\int_{\mathbb{R}^2_+}(ax+bz+cxz)G(x,z)\overline{\nu}^K(\mathrm{d}s,\mathrm{d}x,\mathrm{d}z)\right]\leqslant\sqrt{C_L}T\|G\|_\infty.<+\infty.$$

With Relation (3.39) and the integrability properties proven just above, we obtain that, for $\varepsilon>0$, there exists n_0 such that if $n\geqslant n_0$, then the relation

$$\mathbb{P}\left(\sup_{0\leqslant t\leqslant T}\left|\int_0^t L_{\varepsilon_n}(u)G\left(\overline{X}^K_{\varepsilon_n}(u),\overline{Z}^K_{\varepsilon_n}(u)\right)\mathrm{d}u \right.\right.$$
$$\left.\left. -\int_0^T\int_{\mathbb{R}_+^2}(ax+bz+cxz)G(x,z)\overline{\nu}^K(\mathrm{d}s,\mathrm{d}x,\mathrm{d}z)\right|\geqslant\eta\right)\leqslant\varepsilon$$

holds. Lemma 40 is proved.

Proof of Lemma 41

Following [PSV77] and [Kur92], we first show that there exists an optional process $(\overline{\Gamma}^K_s)$, with values in the set of probability distributions on $\mathbb{R}_+^2$ such that, almost surely, for any bounded Borelian function G on $\mathbb{R}_+\times\mathbb{R}_+^2$,

$$\int_{\mathbb{R}_+\times\mathbb{R}_+^2}G(s,x,z)\overline{\nu}^K(\mathrm{d}s,\mathrm{d}x,\mathrm{d}z)=\int_{\mathbb{R}_+\times\mathbb{R}_+^2}G(s,x,z)\overline{\Gamma}^K_s(\mathrm{d}x,\mathrm{d}z)\,\mathrm{d}s. \tag{3.40}$$

Recall that the optional σ-algebra is the smallest σ-algebra containing adapted càdlàg processes. See Section VI.4 of [RW00] for example. This is a simple consequence of Lemma 1.4 of [Kur92] and the fact that, due to Relation (3.19), the measure $\overline{\nu}^K(\mathrm{d}s,\mathbb{R}^2)$ is the Lebesgue measure on $[0,T]$.

Let $f\in\mathcal{C}^1_b(\mathbb{R}_+^2)$ be a bounded $\mathcal{C}^1$-function on $\mathbb{R}_+^2$ with bounded partial derivatives, we have the relation

$$\varepsilon f\left(\overline{X}^K_\varepsilon(t),\overline{Z}^K_\varepsilon(t)\right)=\varepsilon f(\overline{x}_0,\overline{z}_0)+\varepsilon\overline{M}^f_\varepsilon(t)$$
$$+\int_0^t B^F_{K\wedge\overline{W}^K_\varepsilon(s)}(f)\left(\overline{X}^K_\varepsilon(s),\overline{Z}^K_\varepsilon(s)\right)\mathrm{d}s, \tag{3.41}$$

where, for $t\geqslant0$, if $(\overline{V}^K_\varepsilon(s))\overset{\text{def.}}{=}(\overline{X}^K_\varepsilon(s),\overline{Z}^K_\varepsilon(s))$,

$$\overline{M}^f_\varepsilon(t)\overset{\text{def.}}{=}\int_0^t\left(f\left(\overline{V}^K_\varepsilon(s-)+\left(K\wedge\overline{W}^K_\varepsilon(s),1\right)\right)-f\left(\overline{V}^K_\varepsilon(s-)\right)\right)\left[\mathcal{N}_{\lambda/\varepsilon}(\mathrm{d}s)-\frac{\lambda}{\varepsilon}\mathrm{d}s\right]$$
$$+\int_0^t\left(f\left(\overline{V}^K_\varepsilon(s-)+(0,1)\right)-f\left(\overline{V}^K_\varepsilon(s-)\right)\right)\left[\mathcal{N}_{\overline{\beta}/\varepsilon,\overline{X}^K_\varepsilon}(\mathrm{d}s)-\frac{\overline{\beta}\left(\overline{X}^K_\varepsilon(s)\right)}{\varepsilon}\mathrm{d}s\right],$$

Proposition 37 shows that the martingale $(\varepsilon\overline{M}^f_\varepsilon(t))$ is converging in distribution to 0 as ε goes to 0.

Relation (3.41) gives therefore the convergence in distribution

$$\lim_{\varepsilon\to0}\left(\int_0^t B^F_{K\wedge\overline{W}^K_\varepsilon(s)}(f)\left(\overline{X}^K_\varepsilon(s),\overline{Z}^K_\varepsilon(s)\right)\mathrm{d}s\right)=0.$$

The convergence in distribution of $(\overline{\Omega}^K_{\varepsilon_n}(t),\overline{W}^K_{\varepsilon_n}(t),\overline{\nu}^K_{\varepsilon_n})$, Proposition 40 and Relation (3.40) give that, for any f in $\mathcal{C}^1_b(\mathbb{R}_+^2)$, the relation

$$\left(\int_0^t\int_{\mathbb{R}_+^2}B^F_{K\wedge\overline{w}^K(s)}(f)(x,z)\overline{\Gamma}^K_s(\mathrm{d}x,\mathrm{d}z)\,\mathrm{d}s,\ 0\leqslant t\leqslant T\right)=(0,\ 0\leqslant t\leqslant T). \tag{3.42}$$

holds with probability 1.

Let (f_n) be a dense countable sequence in $\mathcal{C}_b^1(\mathbb{R}_+^2)$ and $\mathcal{E}_1$ be the event, where Relation (3.42) holds for all $f=f_n$, $n\geqslant 1$. Note that that $\mathbb{P}(\mathcal{E}_1)=1$. On $\mathcal{E}_1$, there exists a (random) subset S_1 of $[0,T]$ with Lebesgue measure T such that

$$\int_{\mathbb{R}_+^2} B^F_{K\wedge\overline{w}^K(s)}(f_n)(x,z)\overline{\Gamma}^K_s(\mathrm{d}x,\mathrm{d}z)=0, \forall s\in S_1 \text{ and } \forall n\geqslant 1,$$

and, consequently,

$$\int_{\mathbb{R}_+^2} B^F_{K\wedge\overline{w}^K(s)}(f)(x,z)\overline{\Gamma}^K_s(\mathrm{d}x,\mathrm{d}z)=0, \forall s\in S_1 \text{ and } \forall f\in\mathcal{C}_b^1(\mathbb{R}_+^2).$$

By Proposition 50, for $s\in S_1$, the probability distribution $\overline{\Gamma}^K_s$ is the invariant distribution $\Pi_{K\wedge\overline{w}^K(s)}$. Lemma 41 is proved.

3.B Shot-noise processes

This section presents several technical results on *shot-noise* processes which are crucial for the proof of Theorem 29. See [Sch18], [Ric44] and [GP60] for an introduction.

A scaled shot-noise process

Recall that $(S^x_\varepsilon(t))$, with initial point $x\geqslant 0$, has been introduced by Definition 31. We will have the following conventions,

$$(S_\varepsilon(t)) \overset{\text{def.}}{=} \left(S^0_\varepsilon(t)\right), (S^x(t)) \overset{\text{def.}}{=} (S^x_1(t)) \text{ and } (S(t)) \overset{\text{def.}}{=} \left(S^0_1(t)\right).$$

The process $(S(t))$ is in fact the standard shot-noise process of Lemma 30 associated to the Poisson process $\mathcal{N}_\lambda$, for $t\geqslant 0$,

$$S(t)=\int_0^t e^{-(t-s)}\mathcal{N}_\lambda(\mathrm{d}s) \overset{\text{dist.}}{=} \int_0^t e^{-s}\mathcal{N}_\lambda(\mathrm{d}s). \tag{3.43}$$

In particular $(S(t))$ is a stochastically non-decreasing process, i.e. for $y\geqslant 0$ and $s\leqslant t$,

$$\mathbb{P}(S(s)\geqslant y)\leqslant\mathbb{P}(S(t)\geqslant y). \tag{3.44}$$

A classical formula for Poisson processes, see Proposition 1.5 of [Rob03] for example, gives the relation, for $\xi\in\mathbb{R}$,

$$\mathbb{E}\left[e^{\xi S(t)}\right]=\exp\left(-\lambda\int_0^t\left(1-\exp\left(\xi e^{-s}\right)\right)\mathrm{d}s\right), \tag{3.45}$$

in particular $\mathbb{E}[S^x(t)]=x\exp(-t)+\lambda(1-\exp(-t))$. It also shows that $(S^x(t))$ is converging in distribution to $S(\infty)$ such that,

$$\mathbb{E}\left[e^{\xi S(\infty)}\right]=\exp\left(-\lambda\int_0^{+\infty}\left(1-\exp\left(\xi e^{-s}\right)\right)\mathrm{d}s\right)<+\infty.$$

It is easily seen that $(S^x_\varepsilon(t)) \overset{\text{dist.}}{=} (S^x(t/\varepsilon))$and thus with Relation (3.22), $(S^x_\varepsilon(t))$ can be represented as, for $t \geqslant 0$,

$$S^x_\varepsilon(t) \overset{\text{def.}}{=} xe^{-t/\varepsilon} + \int_0^t e^{-(t-s)/\varepsilon} \mathcal{N}_{\lambda/\varepsilon}(\mathrm{d}s) = xe^{-t/\varepsilon} + S_\varepsilon(t). \tag{3.46}$$

We remind here the results of Proposition 32, that will be proved in the following paragraph. For $\xi \in \mathbb{R}$ and $x \geqslant 0$, the convergence in distribution of the processes

$$\lim_{\varepsilon \searrow 0} \left(\int_0^t e^{\xi S^x_\varepsilon(u)} \, \mathrm{d}u \right) = \left(\mathbb{E}\left[e^{\xi S(\infty)} \right] t \right)$$

holds, and

$$\sup_{\substack{0 < \varepsilon < 1 \\ 0 \leqslant t \leqslant T}} \mathbb{E}\left[e^{\xi S_\varepsilon(t)} \right] < +\infty.$$

Proof of Proposition 32. Let T_1 and T_2 be two stopping times bounded by N, $\theta > 0$, and verifying $0 \leqslant T_2 - T_1 \leqslant \theta$. Using Relation (3.46) and the strong Markov property of Poisson processes, we have that

$$\begin{aligned}
\mathbb{E}\left[\int_{T_1}^{T_2} e^{\xi S^x_\varepsilon(u)} \, \mathrm{d}u \right] &= \varepsilon \mathbb{E}\left[\int_{T_1/\varepsilon}^{T_2/\varepsilon} e^{\xi S^x(u)} \, \mathrm{d}u \right] \\
&= \varepsilon \mathbb{E}\left[\int_0^{(T_2 - T_1)/\varepsilon} e^{\xi S^{S^x(T_1/\varepsilon)}(u)} \, \mathrm{d}u \right] \leqslant \varepsilon \mathbb{E}\left[e^{\xi S^x(T_1/\varepsilon)} \mathbb{E}\left[\int_0^{\theta/\varepsilon} e^{\xi S(u)} \, \mathrm{d}u \right] \right] \\
&\leqslant \theta e^{\xi x} \mathbb{E}\left[e^{\xi S(N/\varepsilon)} \right] \mathbb{E}\left[e^{\xi S(\infty)} \right] \leqslant \theta e^{\xi x} \mathbb{E}\left[e^{\xi S(\infty)} \right]^2,
\end{aligned}$$

holds, by stochastic monotonicity of $(S(t))$ of Relation (3.44).

Aldous' Criterion, see Theorem VI.4.5 of [JS87] gives that the family of processes

$$\left(\int_0^t e^{\xi S_\varepsilon(u)} \, \mathrm{d}u \right),$$

is tight when ε goes to 0. For $p \geqslant 1$ and a fixed vector $(t_i) \in \mathbb{R}^p_+$, the ergodic theorem for the Markov process $(S(t))$ gives the almost-sure convergence of

$$\begin{aligned}
\lim_{\varepsilon \to 0} \left(\int_0^{t_i} e^{\xi S_\varepsilon(u)} \, \mathrm{d}u, i = 1, \ldots, p \right) &= \lim_{\varepsilon \to 0} \left(\varepsilon \int_0^{t_i/\varepsilon} e^{\xi S(u)} \, \mathrm{d}u, i = 1, \ldots, p \right) \\
&= \left(\mathbb{E}\left[e^{\xi S(\infty)} \right] t_i, i = 1, \ldots, p \right).
\end{aligned}$$

Hence, due to the tightness property, the convergence also holds in distribution for the processes

$$\lim_{\varepsilon \to 0} \left(\int_0^t e^{\xi S_\varepsilon(u)} \, \mathrm{d}u \right) = \left(\mathbb{E}\left[e^{\xi S(\infty)} \right] t \right).$$

The last part is a direct consequence of the identity $(S^x_\varepsilon(t)) \overset{\text{dist.}}{=} (S^x(t/\varepsilon))$, and of Relation (3.45), which gives

$$\begin{aligned}
\mathbb{E}\left[e^{\xi S_\varepsilon(t)} \right] &= \exp\left(-\lambda \int_0^{t/\varepsilon} \left(1 - \exp\left(\xi e^{-s} \right) \right) \mathrm{d}s \right) \\
&\leqslant \exp\left(-\lambda \int_0^{+\infty} \left(1 - \exp\left(\xi e^{-s} \right) \right) \mathrm{d}s \right).
\end{aligned}$$

The proposition is proved. □

Interacting shot-noise processes

Recall that $(R_\varepsilon(t))$ defined by Relation (3.24) is a shot-noise process with intensity equal to the shot-noise process $(S_\varepsilon(t))$.

We start with a simple result on moments of functionals of Poisson processes.

Lemma 48. *If $\mathcal{Q}$ is a Poisson point process on $\mathbb{R}_+$ with a positive Radon intensity measure μ and f is a Borelian function such that*

$$I_k(f) \stackrel{\text{def.}}{=} \int f(u)^k \mu(\mathrm{d}u) < +\infty, 1 \leqslant k \leqslant 4,$$

then

$$\mathbb{E}\left[\left(\int f(u)\mathcal{Q}(\mathrm{d}u)\right)^4\right] = \left(I_4 + 6I_1^2 I_2 + 4I_1 I_3 + 3I_2^2 + I_1^4\right)(f).$$

Proof. It is enough to prove the inequality for non-negative bounded Borelian functions f with compact support on $\mathbb{R}_+$.

The formula for the Laplace transform of Poisson point processes, see Proposition 1.5 of [Rob03], gives for $\xi \geqslant 0$,

$$\mathbb{E}\left[\exp\left(\xi \int_0^{+\infty} f(u)\mathcal{Q}(\mathrm{d}u)\right)\right] = \exp\left(\int_0^{+\infty} \left(e^{\xi f(u)} - 1\right) \mu(\mathrm{d}u)\right).$$

The proof is done in a straightforward way by differentiating the last identity with respect to ξ four times and then set $\xi = 0$. □

Proposition 49. *The inequality*

$$\sup_{\varepsilon \in (0,1), t \geqslant 0} \mathbb{E}\left[R_\varepsilon(t)^4\right] < +\infty$$

holds.

Proof. Denote, for $t \geqslant 0$,

$$J_{k,\varepsilon}(t) \stackrel{\text{def.}}{=} \int_0^t e^{-\gamma k(t-u)/\varepsilon} \frac{S_\varepsilon(u)}{\varepsilon}\, \mathrm{d}u,$$

the identity $(S_\varepsilon(t)) \stackrel{\text{dist.}}{=} (S(t/\varepsilon))$ and Relation (3.43) coupled with Fubini's Theorem give the relations

$$\begin{aligned} J_{k,\varepsilon}(t) = \int_0^{t/\varepsilon} e^{-\gamma k(t/\varepsilon - u)} S(u)\, \mathrm{d}u &= \frac{1}{\gamma k - 1} \int_0^{t/\varepsilon} \left(e^{-(t/\varepsilon - v)} - e^{-\gamma k(t/\varepsilon - v)}\right) \mathcal{N}_\lambda(\mathrm{d}v) \\ &\stackrel{\text{dist.}}{=} \frac{1}{\gamma k - 1} \int_0^{t/\varepsilon} \left(e^{-v} - e^{-\gamma k v}\right) \mathcal{N}_\lambda(\mathrm{d}v) \leqslant \frac{1}{|\gamma k - 1|} \overline{J}_k \end{aligned}$$

with

$$\overline{J}_k \stackrel{\text{def.}}{=} \int_0^{+\infty} \left(e^{-k\gamma v} + e^{-v}\right) \mathcal{N}_\lambda(\mathrm{d}v).$$

Relation (3.22) applied to $R_\varepsilon(t)$ gives

$$R_\varepsilon(t) = \int_0^t e^{-\gamma(t-u)/\varepsilon} \mathcal{P}_2\left(\left(0, \frac{S_\varepsilon(u-)}{\varepsilon}\right], \mathrm{d}u\right).$$

The quantity $S_\varepsilon(u)$ is a functional of the point process $\mathcal{P}_1$ and is therefore independent of the Poisson point process $\mathcal{P}_2$. Lemma 48 gives therefore that

$$\mathbb{E}\left[R_\varepsilon(t)^4 \mid \mathcal{P}_1\right] = J_{4,\varepsilon}(t)+6J_{1,\varepsilon}(t)^2J_{2,\varepsilon}(t)+4J_{1,\varepsilon}(t)J_{3,\varepsilon}(t)+3J_{2,\varepsilon}(t)^2+J_{1,\varepsilon}(t)^4,$$

hence,

$$\mathbb{E}\left[R_\varepsilon(t)^4\right] \leqslant \mathbb{E}\left[\frac{\overline{J}_4}{|4\gamma-1|}+\frac{6\overline{J}_1^2\overline{J}_2}{|\gamma-1|^2|2\gamma-1|}+\frac{4\overline{J}_1\overline{J}_3}{|\gamma-1||3\gamma-1|}+\frac{3\overline{J}_2^2}{|2\gamma-1|^2}+\frac{\overline{J}_1^4}{|\gamma-1|^4}\right].$$

Again with Proposition 32 we obtain that, for $k\geqslant 1$, the variable $\overline{J}_k$ has finite moments of all orders, therefore by Cauchy-Shwartz' Inequality, the right-hand side of the last inequality is finite. The proposition is proved. □

3.C Equilibrium of fast processes

For $w\in K_W$, recall that the Markov process $(X^w(t), Z^w(t))$ of Definition 27 is such that

$$\mathrm{d}X^w(t) = -X^w(t)\,\mathrm{d}t+w\mathcal{N}_\lambda(\mathrm{d}t)-g\left(X^w(t-)\right)\mathcal{N}_{\beta,X^w}(\mathrm{d}t) \tag{3.47}$$

$$\mathrm{d}Z^w(t) = (-\gamma\odot Z^w(t)+k_0)\,\mathrm{d}t+k_1(Z^w(t-))\mathcal{N}_\lambda(\mathrm{d}t)+k_2(Z^w(t-))\mathcal{N}_{\beta,X^w}(\mathrm{d}t). \tag{3.48}$$

Proposition 50. *Under the conditions of Sections 3.2 and 3.2, the Markov process $(X^w(t), Z^w(t))$ solution of the SDEs* (3.47) *and* (3.48) *has a unique invariant distribution Π_w, i.e. the unique probability distribution μ on $\mathbb{R}\times\mathbb{R}_+^\ell$ such that*

$$\left\langle \mu, B_w^F(f)\right\rangle = \int_{\mathbb{R}\times\mathbb{R}_+^\ell} B_w^F(f)(x,z)\mu(\mathrm{d}x,\mathrm{d}z) = 0, \tag{3.49}$$

for any $f\in\mathcal{C}_b^1(\mathbb{R}\times\mathbb{R}_+^\ell)$, where B_w^F is the operator defined by Relation (3.18).

Proof. We denote by (X_n^w, Z_n^w) the embedded Markov chain of the Markov process $(X^w(t), Z^w(t))$, i.e. the sequence of states visited by $(X^w(t), Z^w(t))$ after each jump, of either $\mathcal{N}_\lambda$ or $\mathcal{N}_{\beta,X}$.

The proof of the proposition is done in three steps. We first show that the return time of $(X^w(t), Z^w(t))$ to a compact set of $\mathbb{R}\times\mathbb{R}_+^\ell$ is integrable. Then we prove that the Markov chain (X_n^w, Z_n^w) is Harris ergodic, and consequently that it has a unique invariant measure. For a general introduction on Harris Markov chains, see [Num04; MT93]. Finally, the proof of the proposition uses the classical framework of stationary point processes.

Integrability of return times to a compact subset

Suppose that $w\geqslant 0$. The conditions of Section 3.2 on the functions β and g, and Relation (3.47) show that $X^w(t)\geqslant -c_0$, for all $t\geqslant 0$, if $X^w(0)\geqslant -c_0$, with $c_0=c_\beta+c_g$. The state space of the Markov process $(X^w(t), Z^w(t))$ can be taken as $\mathcal{S}\overset{\text{def.}}{=}[-c_0,+\infty)\times\mathbb{R}_+^\ell$.

Define, for $(x,z)\in\mathcal{S}$ and $0<a\leqslant 1$,

$$H(x,z)\overset{\text{def.}}{=} x+a\|z\|, \text{ with } \|z\|\overset{\text{def.}}{=}\sum_{i=1}^{\ell} z_i,$$

we get that

$$B_w^F(H)(x,z) = -x + \left(-a\sum_{i=1}^{\ell}\gamma_i z_i + k_{0,i}\right) + \lambda\left(w + a\sum_{i=1}^{\ell} k_{1,i}(z)\right) + \beta(x)\left(-g(x) + a\sum_{i=1}^{\ell} k_{2,i}(z)\right)$$

hence, with the assumptions of Section 3.2 and 3.2 on the function $k_{\cdot}$ and β, and $a \leqslant 1$,

$$\begin{aligned} B_w^F(H)(x,z) &\leqslant -x - a\underline{\gamma}\|z\| + \ell C_k + \lambda(w + \ell a C_k) + C_\beta\,(1+x)\,\ell a C_k \\ &\leqslant (\ell a C_\beta C_k - 1)x - a\underline{\gamma}\|z\| + (\ell C_k + \lambda w + \lambda\ell C_k + \ell C_\beta C_k) \\ &\leqslant (\ell a C_\beta C_k - 1)x - a\underline{\gamma}\|z\| + C, \end{aligned}$$

where $\underline{\gamma}>0$ is the minimum of the coordinates of γ and C is a constant independent of x, z and a. We fix $0<a\leqslant 1$ sufficiently small so that $\ell a C_\beta C_k<1$ and $K>c_0$ such that

$$C<\underline{\gamma}K/2-1 \text{ and } C<(1-\ell a C_\beta C_k)K/2-1.$$

If $H(x,z)>K$ then $\max(x, a\|z\|)>K/2$ and therefore $B_w^F(H)(x,z)\leqslant -1$, H is therefore a Lyapounov function for B_w^F. One deduces that the same result holds for the return time of Markov chain, (X_n^w, Z_n^w) in the set $I_K = \{(x,z) : H(x,z)\leqslant K\}$.

Harris ergodicity of (X_n^w, Z_n^w)

Proposition 5.10 of [Num04] is used to show that I_K is a recurrent set. A *regeneration property* would be sufficient to conclude. In particular, we can prove that I_K is a *small set*, that is, there exists some positive, non-trivial, Radon measure ν on $\mathcal{S}$ such that,

$$\mathbb{P}_{(x_0,z_0)}\left((X_1^w, Z_1^w)\in S\right) \geqslant \nu(S), \tag{3.50}$$

for any Borelian subset S of $\mathcal{S}$ and all $(x_0,z_0)\in I_K$.

We denote by s_1, resp. t_1, the first instant of $\mathcal{N}_\lambda$, resp. of $\mathcal{N}_{\beta,X^w}$, then, for $(X_0^w, Z_0^w)=(x_0,z_0)\in I_K$, by using the deterministic differential equations between jumps, we get

$$\mathbb{P}_{(x_0,z_0)}\,(s_1<t_1) = \mathbb{E}\left[\exp\left(-\int_0^{s_1}\beta(x_0\exp(-s))\,\mathrm{d}s\right)\right] \geqslant \mathbb{E}\left[\exp(-c_\beta^1 s_1)\right] = p_0 \overset{\text{def.}}{=} \frac{\lambda}{\lambda + c_\beta^1},$$

since β is bounded by some constant c_β^1 on the interval $[-c_0, K]$.

In the following argument, we restrict X to be non-negative, the extension to $[-c_0,+\infty]$ is straightforward. For $\mathcal{A}=[0,A]\in\mathcal{B}(\mathbb{R}_+)$ and $\mathcal{B}=[0,B]\in\mathcal{B}(\mathbb{R}_+^\ell)$, from Equations (3.47) and (3.48), we obtain the relation

$$\begin{aligned} \mathbb{P}_{(x_0,z_0)}\left((X_1^w, Z_1^w)\in\mathcal{A}\times\mathcal{B}\right) &\geqslant p_0\mathbb{P}\left((X_1^w, Z_1^w)\in\mathcal{A}\times\mathcal{B} \mid s_1<t_1\right) \\ &= p_0\mathbb{P}\left(\begin{array}{c} x_0 e^{-s_1} + w\in\mathcal{A}, \\ (z_0-k_0)\odot e^{-\gamma_i s_1} + k_0 + k_1\left((z_0-k_0)\odot e^{-\gamma_i s_1} + k_0\right)\in\mathcal{B} \end{array}\middle|\, s_1<t_1\right) \end{aligned}$$

$$\geqslant \mathbb{P}\left(\begin{array}{c} x_0 e^{-s_1}+w\in\mathcal{A}, \\ H\left((z_0-k_0)\odot e^{-\gamma_i s_1}+k_0\right)\in\mathcal{B}\end{array}\middle| \, s_1<t_1\right)$$
$$= p_0\mathbb{P}\left(\begin{array}{c} x_0 e^{-\bar{s}_1}+w\in\mathcal{A}, \\ H\left((z_0-k_0)\odot e^{-\gamma_i \bar{s}_1}+k_0\right)\in\mathcal{B}\end{array}\right),$$

where $H(z)=z+k_1(z)$, $\bar{s}_1 \overset{\text{dist.}}{=} (s_1|s_1\leqslant t_1)$. By using the fact that k_1 is in $\mathcal{C}_b^1(\mathbb{R}_+^\ell,\mathbb{R}_+^\ell)$ by the conditions of Section 3.2 and in the same way as Example of Section 4.3.3 page 98 of [MT93], we can prove that the random variable

$$\left(x_0 e^{-\bar{s}_1}+w, H\left((z_0-k_0)\odot e^{-\gamma_i \bar{s}_1}+k_0\right)\right)$$

has a density, uniformly bounded below by a positive function h on $\mathbb{R}_+\times\mathbb{R}_+^\ell$, so that

$$\mathbb{P}_{(x_0,z_0)}\left((X_1^w,Z_1^w)\in A\times B\right)\geqslant \int_{A\times B} h(x,z)\,\mathrm{d}x\,\mathrm{d}z, \forall A\in\mathcal{B}(\mathbb{R}_+), B\in\mathcal{B}(\mathbb{R}_+^\ell),$$

for all $(x_0,z_0)\in I_K$). This relation is then extended to all Borelian subsets S of $\mathcal{S}$, so that Relation (3.50) holds. Proposition 5.10 of [Num04] gives therefore that (X_n^w,Z_n^w) is Harris ergodic.

If $w<0$, the last two steps can be done in a similar way. In this case, the process $(-X^w(t))$ satisfies an analogous equation with the difference that the process $\mathcal{N}_{\beta,X^w}$ does not jump when $-X^w(t)>c_\beta$ since $\beta(x)=0$ for $x\leqslant -c_\beta$.

Characterization of Π_w

Let $\widehat{\Pi}_w$ be the invariant probability distribution of (X_n^w,Z_n^w). With the above notations,

$$\mathbb{E}_{\hat{\Pi}_w}\left[\min(s_1,t_1)\right]\leqslant \mathbb{E}_{\hat{\Pi}_w}\left[s_1\right]=\frac{1}{\lambda}<+\infty,$$

the probability defined by the classical cycle formula,

$$\frac{1}{\mathbb{E}_{\hat{\Pi}_w}\left[\min(s_1,t_1)\right]}\mathbb{E}_{\hat{\Pi}_w}\left[\int_0^{\min(s_1,t_1)} f(X^w(u),Z^w(u))\,\mathrm{d}u\right],$$

for any bounded Borelian function on $\mathbb{R}\times\mathbb{R}_+^\ell$ is an invariant distribution for the process $(X^w(t),Z^w(t))$.

Proposition 9.2 of [EK09] shows that any distribution is invariant for $(X^w(t),Z^w(t))$ if and only if it satisfies Relation (3.49). It remains to prove the uniqueness of the invariant distribution, using the fact that the embedded Markov chain has a unique invariant distribution.

Although this is a natural result, we have not been able to find a reference in the literature. Most results are stated for discrete time, the continuous time is usually treated by looking at the process on a "discrete skeleton", i.e. at instants multiple of some positive constant. See Proposition 3.8 of [Asm03] for example. As this technique is not adapted to our system, we derive a different proof using the Palm measure of the associated stationary point process.

If μ is some invariant distribution of the Markov process $(X^w(t),Z^w(t))$, we build a stationary version $((X^w(t),Z^w(t)),t\in\mathbb{R})$ of it on the whole real line. In particular, we have that $(X^w(t),Z^w(t))\overset{\text{dist.}}{=}\mu$, for all $t\in\mathbb{R}$.

We denote by $(S_n, n\in\mathbb{Z})$ the non-decreasing sequence of the jumps (due to $\mathcal{N}_\lambda$ and $\mathcal{N}_{\beta,X^w}$), with the convention $S_0\leqslant 0<S_1$ The sequence $((X^w(S_n), Z^w(S_n)), n\geqslant 0)$ has the same distribution as the process $((X^w_n, Z^w_n), n\geqslant 0)$, the Markov chain with initial state $(X^w(S_0), Z^w(S_0))$. Since, for any $t\in\mathbb{R}$,

$$\left((X^w(s+t), Z^w(s+t)), s\in\mathbb{R}\right) \overset{\text{dist.}}{=} \left((X^w(s), Z^w(s)), s\in\mathbb{R}\right),$$

the marked point process $\mathcal{T} \overset{\text{def.}}{=} \left(S_n, (X^w(S_n), Z^w(S_n)\right), n\in\mathbb{Z})$ is a stationary point process, i.e.

$$((S_n, X^w(S_n), Z^w(S_n), n\in\mathbb{Z}) \overset{\text{dist.}}{=} ((S_n - t, X^w(S_n), Z^w(S_n), n\in\mathbb{Z}), \quad \forall t\in\mathbb{R}.$$

The *Palm measure* of $\mathcal{T}$ is a probability distribution $\widehat{Q}$ such that the sequence $((S_n - S_{n-1}, X^w(S_n), Z^w(S_n), n\in\mathbb{Z})$ is stationary. See Chapter 11 of [Rob03] for a quick presentation of stationary point processes and Palm measures.

Under $\widehat{Q}$, the Markov chain $((X^w(S_n), Z^w(S_n)), n\geqslant 0)$ is at equilibrium. Using Harris ergodicity, we have proved in the previous section that the Markov chain $((X^w_n, Z^w_n), n\geqslant 0)$ has a unique invariant measure. Considering that both sequences $((X^w_n, Z^w_n), n\geqslant 0)$ and $((X^w(S_n), Z^w(S_n)), n\geqslant 0)$ have the same distribution, we have that $\widehat{Q}\left(\mathbb{R}_+^{\mathbb{Z}}, \cdot\right)$ is uniquely determined.

Moreover, remembering that,

$$\widehat{Q}\left(S_n - S_{n-1} > t\right) = \mathbb{E}_{\widehat{Q}}\left[\exp\left(-\int_0^t \beta\left(X^w(S_{n-1})e^{-s}\right)\mathrm{d}s\right)\right]$$

We have that $\widehat{Q}$ is entirely determined by the ergodic distribution of the embedded Markov chain and consequently that the Palm measure $\widehat{Q}$ is unique. By Proposition 11.5 of [Rob03], the distribution of $\mathcal{T}$ is expressed with $\widehat{Q}$.

We have, for every bounded function f,

$$\mathbb{E}_\mu\left[f(X^w(0), Z^w(0))\right] = \mathbb{E}_{\mathcal{T}}\left[f(X^w(S_0)e^{S_0}, Z^w(S_0)\odot e^{\gamma S_0})\right],$$

which uniquely determines the invariant distribution μ.

The proposition is proved. □

3.D Averaging principles for discrete models of plasticity

In this section, we present a general discrete model of plasticity, state the associated averaging principle theorem and give a sketch of its proof. We will only point out the differences with the proof of the main result of this paper, Theorem 29.

For this model of plasticity, the membrane potential X, the plasticity processes Z and the synaptic weight W are integer-valued variables. This system is illustrated in Section 7 of [RV20] for calcium-based models. It amounts to represent these three quantities X, Z and W as multiple of a "quantum" instead of a continuous variable. The leaking mechanism in particular, the term corresponding to $-\gamma Y(t)\,\mathrm{d}t$ in the continuous model, $Y\in\{X, Z, W\}$ and $\gamma>0$, in the SDEs, is represented by the fact that each quantum leaves the system at a fixed rate γ.

The main advantage of this model is that simple analytical expressions of the invariant distribution are available.

Definition 51. *The SDEs for the discrete model are*

$$\left\{\begin{array}{ll} \mathrm{d}X(t) & = -\mathcal{N}_{I,X}(\mathrm{d}t) + W(t-)\mathcal{N}_\lambda(\mathrm{d}t) - \mathcal{N}_{I,\beta X}(\mathrm{d}t), \\ \mathrm{d}Z(t) & = -\mathcal{N}_{I,\gamma Z}(\mathrm{d}t) + B_1\mathcal{N}_\lambda(\mathrm{d}t) + B_2\mathcal{N}_{I,\beta X}(\mathrm{d}t), \\ \mathrm{d}\Omega_a(t) & = -\alpha\Omega_a(t)\,\mathrm{d}t + n_{a,0}(Z(t))\,\mathrm{d}t \\ & \quad + n_{a,1}(Z(t-))\mathcal{N}_\lambda(\mathrm{d}t) + n_{a,2}(Z(t-))\mathcal{N}_{I,\beta X}(\mathrm{d}t), \quad a\in\{p,d\}, \\ \mathrm{d}W(t) & = -\mathcal{N}_{I,\mu W}(\mathrm{d}t) + A_p\mathcal{N}_{I,\Omega_p}(\mathrm{d}t) - A_d\mathbb{1}_{\{W(t-)\geqslant A_d\}}\mathcal{N}_{I,\Omega_d}(\mathrm{d}t), \end{array}\right. \tag{3.51}$$

where β,γ,μ are non-negative real numbers, B_1, $B_2\in\mathbb{N}^\ell$ and, for $a\in\{p,d\}$, $A_a\in\mathbb{N}$. The functions $n_{a,i}$ are assumed to be bounded by C_n.

For $a\in\{p,d\}$, the function I of $\mathcal{N}_{I,G}$ for $G\in\{X,\beta X,\gamma Z,\mu W,\Omega_p,\Omega_d\}$, defined by relation (3.6), is the identity function $I(x)=x$, $x\in\mathbb{R}$ and $\mathcal{N}_\lambda$ is a Poisson process on $\mathbb{R}_+$ with rate λ. All associated Poisson processes are assumed to be independent.

Definition 52. *For a fixed w, the process of the fast variables $(X^w(t),Z^w(t))$ on $\mathbb{N}\times\mathbb{N}^\ell$ of the SDEs is the Markov process whose transition rates are given by, for $(x,z)\in\mathbb{N}\times\mathbb{N}^\ell$,*

$$(x,z)\longrightarrow\left\{\begin{array}{ll}(x+w,z+B_1) & \lambda,\\ (x-1,z) & x,\end{array}\right. \qquad \longrightarrow\left\{\begin{array}{ll}(x,z-1) & \gamma z,\\ (x-1,z+B_2) & \beta x.\end{array}\right.$$

Theorem 53 (Averaging Principle for a Discrete Model)**.** *If the assumptions of Definition 51 are verified, the family of scaled processes $(W_\varepsilon(t))$ associated to Relations* (3.51) *is converging in distribution, as ε goes to 0, to the càdlàg integer-valued process $(w(t))$ satisfying the ODE*

$$\mathrm{d}w(t) = -\mathcal{N}_{I,\gamma w}(\mathrm{d}t) + A_p\mathcal{N}_{I,\omega_p}(\mathrm{d}t) - A_d\mathbb{1}_{\{w(t-)\geqslant A_d\}}\mathcal{N}_{I,\omega_d}(\mathrm{d}t), \tag{3.52}$$

and, for $a\in\{p,d\}$,

$$\frac{\mathrm{d}\omega_a}{\mathrm{d}t}(t) = -\alpha\omega_a(t) + \int_{\mathbb{N}\times\mathbb{N}^\ell}(n_{a,0}(z)+\lambda n_{a,1}(z)+\beta(x)n_{a,2}(z))\,\Pi_{w(t)}(\mathrm{d}x,\mathrm{d}z),$$

where Π_w is the invariant distribution of the Markov process of Definition 52.

Proof. Again, we have to show that, on a fixed finite interval, the process $(W(t))$ is bounded with high probability. A coupled process that stochastically bounds from above the discrete process is also defined.

Definition 54. *The process $(\overline{X}(t),\overline{Z}(t),\overline{\Omega}(t),\overline{W}(t))$ satisfies the following SDEs*

$$\left\{\begin{array}{ll} \mathrm{d}\overline{X}(t) & = -\mathcal{N}_{I,\overline{X}}(\mathrm{d}t) + \overline{W}(t-)\mathcal{N}_\lambda(\mathrm{d}t) - \mathcal{N}_{I,\beta\overline{X}}(\mathrm{d}t), \\ \mathrm{d}\overline{Z}(t) & = -\mathcal{N}_{I,\gamma\overline{Z}}(\mathrm{d}t) + B_1\mathcal{N}_\lambda(\mathrm{d}t) + B_2\mathcal{N}_{I,\beta\overline{X}}(\mathrm{d}t), \\ \mathrm{d}\overline{\Omega}(t) & = -\alpha\overline{\Omega}(t)\,\mathrm{d}t + C_n\,\mathrm{d}t + C_n\mathcal{N}_\lambda(\mathrm{d}t) + C_n\mathcal{N}_{I,\beta\overline{X}}(\mathrm{d}t), \\ \mathrm{d}\overline{W}(t) & = A_p\mathcal{N}_{I,\overline{\Omega}}(\mathrm{d}t), \end{array}\right. \tag{3.53}$$

where B_1, $B_2\in\mathbb{N}^\ell$ and, for $a\in\{p,d\}$, $A_p\in\mathbb{N}$.

It is not difficult to prove that this process is indeed a coupling that verifies the relation $W(t)\leqslant\overline{W}(t)$, for all $t\geqslant 0$ and that the process $(\overline{W}(t))$ is non-decreasing.

From the SDEs governing the scaled version of the coupled system, we obtain

$$\begin{aligned}
\mathbb{E}\left[\overline{W}_\varepsilon(t)-w_0\right] &\leqslant A_p\mathbb{E}\left[\int_0^t \mathcal{N}_{I,\overline{\Omega}_{\varepsilon,p}}\,\mathrm{d}s\right] \leqslant A_p t\mathbb{E}\left[\sup_{s\leqslant t}\overline{\Omega}_{\varepsilon,p}(s)\right] \\
&\leqslant A_p t\mathbb{E}\left[\omega_0+C_n\sup_{s\leqslant t}\int_0^s e^{-\alpha(s-u)}\left(\mathrm{d}u+\varepsilon\mathcal{N}_{\lambda/\varepsilon}(\mathrm{d}u)+\varepsilon\mathcal{N}_{I,\beta\overline{X}/\varepsilon}(\mathrm{d}u)\right)\right] \\
&\leqslant A_p t\left(\omega_0+\frac{C_n}{\alpha}(1+\lambda)+\mathbb{E}\left[\int_0^t \beta\overline{X}_\varepsilon(u)\right]\mathrm{d}u\right) \\
&\leqslant A_p t\left(\omega_0+\frac{C_n}{\alpha}(1+\lambda)+\lambda\beta\mathbb{E}\left[\int_0^t \overline{W}_\varepsilon(u)\,\mathrm{d}u\right]\right) \leqslant D+D\int_0^t \mathbb{E}\left[\overline{W}_\varepsilon(u)\right]\mathrm{d}u,
\end{aligned}$$

for all $t\leqslant T$, for some constant $D\geqslant 0$. Gronwall's Lemma gives a uniform bound, with respect to ε,

$$\mathbb{E}\left[\sup_{t\leqslant T}\overline{W}_\varepsilon(t)\right] = \mathbb{E}\left[\overline{W}_\varepsilon(T)\right]) \leqslant (D+w_0)e^{DT}.$$

Using Markov inequality, we have then that, for any $\eta>0$, the existence of K_0 and n_0 such that $n\geqslant n_0$, the inequality

$$\mathbb{P}\left(\sup_{t\leqslant T}\overline{W}_{\varepsilon_n}(t)\leqslant K_0\right)\geqslant 1-\eta$$

holds. We can then finish the proof in the same way as in Section 3.7. The tightness property of the family of càdlàg processes $(\overline{W}_\varepsilon(t))$, $\varepsilon\in(0,1)$ are proved with Aldous' criterion, see Theorem VI.4.5 of [JS87].

We have to prove the uniqueness of the solution of Relation (3.52) and the convergence in distribution of the scaled process to the process $w(t)$. For this, we need to have some Lipschitz property on the limiting system, and finite first moments for the invariant distribution of $(X^w(t), Z^w(t))$. This is proved in Section 7 of [RV20] for the case where Z is a one-dimensional process, the extension to multi-dimensional Z is straightforward. □

BIBLIOGRAPHY

[Asm03] S. Asmussen. Applied Probability and Queues. 2nd ed. Stochastic Modelling and Applied Probability. New York: Springer-Verlag, 2003.

[BCR19] L. Beznea, I. Cîmpean, and M. Röckner. A new approach to the existence of invariant measures for Markovian semigroups. *Annales de l'Institut Henri Poincaré, Probabilités et Statistiques*. Vol. 55. 2019, 977–1000.

[Bil99] P. Billingsley. Convergence of Probability Measures. John Wiley & Sons, 1999.

[CCP11] M. J. Cáceres, J. A. Carrillo, and B. Perthame. Analysis of nonlinear noisy integrate & fire neuron models: blow-up and steady states. *The Journal of Mathematical Neuroscience* **1** (2011), 7.

[CS08] R. Crane and D. Sornette. Robust dynamic classes revealed by measuring the response function of a social system. *Proceedings of the National Academy of Sciences* **105** (2008), 15649–15653. eprint: `https://www.pnas.org/content/105/41/15649.full.pdf`.

[EK09] S. N. Ethier and T. G. Kurtz. Markov Processes: Characterization and Convergence. John Wiley & Sons, Sept. 2009.

[ELL11] P. Embrechts, T. Liniger, and L. Lin. Multivariate Hawkes processes: an application to financial data. *Journal of Applied Probability* **48** (2011), 367–378.

[FW98] M. I. Freidlin and A. D. Wentzell. Random perturbations of dynamical systems. Second Edition edition. New York: Springer-Verlag, 1998.

[GP60] E. N. Gilbert and H. O. Pollak. Amplitude Distribution of Shot Noise. *Bell System Technical Journal* **39** (Mar. 1960), 333–350.

[GS05] G. Gusto and S. Schbath. FADO: A Statistical Method to Detect Favored or Avoided Distances between Occurrences of Motifs using the Hawkes' Model. *Statistical Applications in Genetics and Molecular Biology* **4** (2005).

[Has80] R. Z. Has'minskiĭ. Stochastic stability of differential equations. Alphen aan den Rijn: Sijthoff & Noordhoff, 1980, xvi+344.

[Haw71] A. G. Hawkes. Spectra of Some Self-Exciting and Mutually Exciting Point Processes. *Biometrika* **58** (1971), 83–90.

[Hel18] P. Helson. A new stochastic STDP Rule in a neural Network Model. *arXiv:1706.00364 [math]* (Mar. 2018).

[HO74] A. G. Hawkes and D. Oakes. A Cluster Process Representation of a Self-Exciting Process. *Journal of Applied Probability* **11** (1974), 493–503.

[HS74] M. W. Hirsch and S. Smale. Differential equations, dynamical systems, and linear algebra. Academic Press [A subsidiary of Harcourt Brace Jovanovich, Publishers], New York-London, 1974, xi+358.

[JS87] J. Jacod and A. N. Shiryaev. Limit theorems for stochastic processes. Vol. 288. Grundlehren der Mathematischen Wissenschaften. Berlin: Springer-Verlag, 1987, xviii+601.

[Ker64] J. Kerstan. Teilprozesse Poissonscher Prozesse. *Trans. Third Prague Conf. Information Theory,Statist. Decision Functions, Random Processes*. Liblice: House Czech. Acad.Sci., Jan. 1964, 377–403.

[KGH99] R. Kempter, W. Gerstner, and J. L. van Hemmen. Hebbian learning and spiking neurons. *Physical Review E* **59** (Apr. 1999), 4498–4514.

[Kin92] J. F. C. Kingman. Poisson Processes. Clarendon Press, Dec. 1992.

[KS98] I. Karatzas and S. Shreve. Brownian Motion and Stochastic Calculus. 2nd ed. Vol. 113. Graduate Texts in Mathematics. New York, NY: Springer, 1998.

[Kur92] T. G. Kurtz. Averaging for martingale problems and stochastic approximation. *Applied Stochastic Analysis*. Ed. by I. Karatzas and D. Ocone. Vol. 177. Berlin/Heidelberg: Springer-Verlag, 1992, 186–209.

[MT93] S. Meyn and R. Tweedie. Markov chains and stochastic stability. Communications and control engineering series. Springer, 1993.

[Num04] E. Nummelin. General Irreducible Markov Chains and Non-Negative Operators. Cambridge University Press, June 2004.

[PSV77] G. Papanicolalou, D. W. Stroock, and S. R. S. Varadhan. Martingale approach to some limit theorems. *Proc. 1976. Duke Conf. On Turbulence*. III. Duke Univ. Math, 1977.

[Ric44] S. O. Rice. Mathematical analysis of random noise. *Bell System Technical Journal* **23** (1944), 282–332.

[Rob03] P. Robert. Stochastic Networks and Queues. Stochastic Modelling and Applied Probability. Berlin Heidelberg: Springer-Verlag, 2003.

[RS10] P. Reynaud-Bouret and S. Schbath. Adaptive estimation for Hawkes processes; application to genome analysis. *Annals of Statistics* **38** (Nov. 2010), 2781–2822.

[RV20] P. Robert and G. Vignoud. Stochastic Models of Neural Synaptic Plasticity. 2020. arXiv: `2010.08195 [math.PR]`.

[RW00] L. C. G. Rogers and D. Williams. Diffusions, Markov Processes and Martingales: Volume 2, Itô Calculus. Cambridge University Press, Sept. 2000.

[Sch18] W. Schottky. Über spontane Stromschwankungen in verschiedenen Elektrizitätsleitern. *Annalen der physik* **362** (1918), 541–567.

CHAPTER 4

ON THE SPONTANEOUS DYNAMICS OF SYNAPTIC WEIGHTS IN STOCHASTIC MODELS WITH PAIR-BASED STDP

ABSTRACT

We investigate spike-timing dependent plasticity (STPD) in the case of a synapse connecting two neuronal cells. We develop a theoretical analysis of several STDP rules using Markovian theory. In this context there are two different timescales, fast neuronal activity and slower synaptic weight updates. Exploiting this timescale separation, we derive the long-time limits of a single synaptic weight subject to STDP. We show that the pairing model of presynaptic and postsynaptic spikes controls the synaptic weight dynamics for small external input, on an excitatory synapse. This result implies in particular that mean-field analysis of plasticity may miss some important properties of STDP. Anti-Hebbian STDP favors the emergence of a stable synaptic weight. In the case of an inhibitory synapse the pairing schemes matter less, and we observe convergence of the synaptic weight to a non-null value only for Hebbian STDP. We extensively study different asymptotic regimes for STDP rules, raising interesting questions for future works on adaptative neuronal networks and, more generally, on adaptative systems.

4.1 Introduction

Neuronal networks, through the dynamics of their connections, are able to store complex patterns over long periods of time, and as such are good candidates for the establishment of memory. In particular, the intensity W of the connection between two neurons, *the synaptic weight*, is seen as an essential building block to explain learning and memory formation [TDM14].

Synaptic plasticity (processes that can modify the synaptic weight) is a complex mechanism [CM08], but general principles have been inferred from experimental data and used for a long time in computational models. Spike-timing dependent plasticity (STDP) refers to plasticity processes that depend on the timing of presynaptic and postsynaptic spiking activity [Fel12].

Experiments show that long-term synaptic plasticity is characterized by the coexistence of two different timescales. Membrane potential and pre/postsynaptic interspike intervals evolve on the order of several milliseconds, see [GK02b]. Synaptic weights W change on a slower timescale ranging from seconds to minutes before observing an effect of STDP protocols on the synaptic weights. The analysis of slow-fast limits for a general class of STDP models is detailed in [RV21b; RV21c; RV21a]. Computational models of synaptic plasticity have also used similar scaling principles, see [KGH99; Rob99; KH00; RBT00a].

In pair-based models, the synaptic weight updates depend only on $\Delta t{=}t_{\text{post}} - t_{\text{pre}}$ for a subset of instants of pre/postsynaptic spikes $t_{\text{pre}}/t_{\text{post}}$.

Hebbian STDP plasticity occurs when

— a *pre-post pairing*, $t_{\text{pre}}<t_{\text{post}}$ leads to an increase of the synaptic weight value (potentiation), which translates into $\Delta W>0$;

— a *post-pre pairing*, $t_{\text{post}}<t_{\text{pre}}$, leads to a smaller synaptic weight (depression), and therefore $\Delta W<0$.

Hebbian STDP has been observed at many different synapses [BP98; Fel12] and is extensively studied in computational models [KGH99; Rob99; KH00; RBT00a; KGH01; RLS01; GK02a; BMG04; RA04; SJT07; GMH11].

Other types of polarity have been observed experimentally, they are often neglected in theoretical studies of STDP. For example, *Anti-Hebbian STDP* follows the opposite principles and has been observed experimentally in the striatum, see [FGV05; RL10]. Different types of STDP rules were analyzed in [Rob00; CF03; RA04; ZD07; RL10; BK12].

In theoretical works, the system, in general, is reduced to a single neuron receiving a large number of excitatory inputs subject to STDP, leading to a Fokker-Plank approach [RBT00a; RLS01; BMG04].

The pre-/postsynaptic spike correlation function [KGH99; KGH01; GK02a] is used to study the influence of STDP with high correlated inputs. However, this method relies on the assumption that all pairs of pre- and postsynaptic spikes impact the synaptic weight update. Several studies have questioned this hypothesis [ID03; MAD07; MDG08], and its influence on the synaptic weight dynamics has not been discussed in theoretical works, except in [BMG04].

Finally, most studies focus on excitatory inputs, whereas inhibitory synapses also exhibit STDP [HNA06; Fel12], but few theoretical works exist [LS14].

Here we develop a theoretical study of a large class of rules, for a system with two neurons and a single synapse. This simple setting is used to test the influence of STDP on an excitatory and an inhibitory synapse, for three different classes of pairing interactions leading to an extensive categorization of the different dynamics. We question in particular if several interesting properties of the synaptic weight dynamics are lost when using classical models with numerous excitatory inputs, leading to an underestimation of the role of STDP in learning systems.

4.2 Theoretical analysis

Spiking neurons and Poisson processes

The spike train of the presynaptic neuron is represented by an homogeneous Poisson process $\mathcal{N}_\lambda=(t_{\text{pre,n}})_{1\leqslant n}$, where $(t_{\text{pre,n+1}}-t_{\text{pre,n}})_{1\leqslant n}$ is a sequence of i.i.d. exponential random variables with parameter λ. The quantity $\mathcal{N}_\lambda(a,b)$ denotes the number of $(t_{\text{pre},n})$ in the interval $[a,b]$, in particular,

$$\mathbb{P}\left(\mathcal{N}_\lambda(t,t+\mathrm{d}t)\neq 0\right)=\lambda\,\mathrm{d}t+o(\mathrm{d}t).$$

We define a stochastic process $(X(t))$ following leaky-integrate dynamics:

a. It decays exponentially to 0 with a fixed exponential decay, set to 1.

b. It is incremented by the synaptic weight $W>0$ at each presynaptic spike, i.e. at each jump of $\mathcal{N}_\lambda$.

The firing mechanism of the postsynaptic neuron is driven by an *activation function* β, when X is x, the output neuron fires at rate $\beta(x)$. The sequence of instants of postsynaptic spikes $(t_{\text{post},n})$ is a point process $\mathcal{N}_{\beta,X}$ on $\mathbb{R}_+$ such that

$$\mathbb{P}\left(\mathcal{N}_{\beta,X}(t,t+\mathrm{d}t)\neq 0 \,\middle|\, X(t-)=x\right)=\beta(x)\,\mathrm{d}t+o(\mathrm{d}t).$$

The notation $f(t-)$ is the left-limit of f at t.

For simplicity, we chose to differentiate between excitatory and inhibitory synapses at the level of the activation function, instead of allowing for negative W. Indeed, for an excitatory synapse, the activation function $\beta(x)=\nu+\beta x$ is used, ν is the rate of the external input to the postsynaptic neuron, it models external noise. For inhibitory synapses, we consider $\beta(x)=\max(\nu-\beta x,0)$. A linear activation function has been used, mainly to enable explicit analytical computations, and for comparison with other computational studies with similar hypotheses, see [KGH99].

Pair-based STDP rules

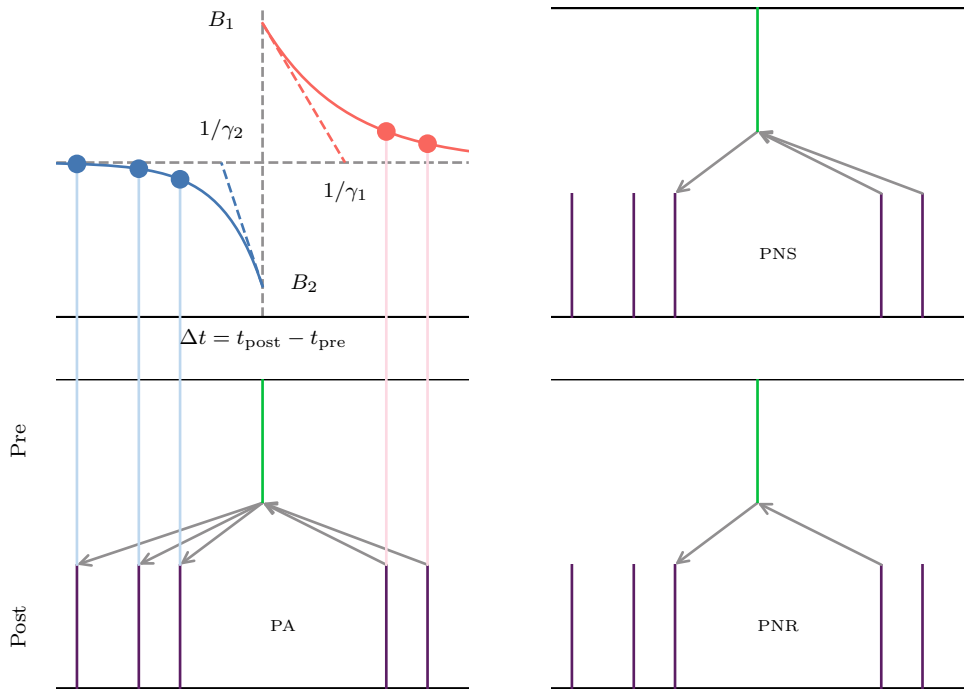

Figure 4.1: **Synaptic plasticity kernels for pair-based rules.**
Example of an exponential plasticity curve as a function of Δt, with different parameters (top left). Examples of pre- and postsynaptic pairings for all-to-all (PA, bottom left), nearest neighbor symmetric (PNS, top right) and nearest neighbor symmetric reduced (PNR, bottom right) STDPs.

We study an important implementation of STDP referred to as pair-based rules. For a pair $(t_{\text{pre}}, t_{\text{post}})$ of instants of pre- and postsynaptic spikes, the synaptic weight update ΔW depends only on $\Delta t=t_{\text{post}}-t_{\text{pre}}$, as illustrated in Figure 4.1.

An important choice for the model is to decide which pairings to take into account in the plasticity update. A large choice of different schemes have been analyzed in the literature [MDG08]. We have chosen to focus on three versions, that are summarized in Figure 4.1:

— *All-to-all* pair-based model (PA): all pairs of spikes are taken into account in the synaptic plasticity rule.

— *Nearest neighbor symmetric* model (PNS): whenever one neuron spikes, the synaptic weight is updated by only taking into account the last spike of the other neuron.

— *Nearest neighbor symmetric reduced* model (PNR): only consecutive pairs of spikes are used to update the synaptic weight.

The synaptic weight update is therefore composed of the sum over relevant spikes, of a kernel $\Phi(\Delta t)$ known as the plasticity curve, here we chose an exponential kernel, given by,

$$\Phi(\Delta t) = \begin{cases} B_2 \exp(\gamma_2 \Delta t) & \Delta t < 0, \\ B_1 \exp(-\gamma_1 \Delta t) & \Delta t > 0. \end{cases}$$

where $B_1, B_2 \in \mathbb{R}$ represents the amplitude of the STDP and $\gamma_1, \gamma_2 > 0$ the characteristic time of interaction, see Figure 4.1 (top left).

All-to-all model (PA)

The *all-to-all* pair-based model supposes that all pairs of spikes are taken into account in the synaptic plasticity rule. The synaptic weight is updated at each postsynaptic spike occurring at time t_{post}, by taking into account all presynaptic spikes before time t_{post}:

$$\Delta W(t_{\text{post}}) = B_1 \sum_{t_{\text{pre},n} < t_{\text{post}}} e^{-\gamma_1 (t_{\text{post}} - t_{\text{pre},n})} = Z_1^{\text{PA}}(t_{\text{post}})$$

and conversely,

$$\Delta W(t_{\text{pre}}) = B_2 \sum_{t_{\text{post},n} < t_{\text{pre}}} e^{-\gamma_2 (t_{\text{pre}} - t_{\text{post},n})} = Z_2^{\text{PA}}(t_{\text{pre}})$$

The processes $(Z_i^{\text{PA}}(t))$, $i=1, 2$ can be expressed as solutions of the stochastic differential equations,

$$\begin{cases} \mathrm{d}Z_1^{\text{PA}}(t) = -\gamma_1 Z_1^{\text{PA}}(t)\,\mathrm{d}t + B_1 \mathcal{N}_\lambda(\mathrm{d}t), \\ \mathrm{d}Z_2^{\text{PA}}(t) = -\gamma_2 Z_2^{\text{PA}}(t)\,\mathrm{d}t + B_2 \mathcal{N}_{\beta,X}(\mathrm{d}t), \end{cases}$$

they are two shot-noise processes, see [GP60; RV21b].

The synaptic weight updates correspond to the evaluation of $(Z_1^{\text{PA}}(t))$ at jumps of the point process $\mathcal{N}_{\beta,X}$ for postsynaptic activity, and similarly for $(Z_2^{\text{PA}}(t))$ with $\mathcal{N}_\lambda$,

$$\mathrm{d}W^{\text{PA}}(t) = \sum_{t_{\text{pre},n} \leqslant t} Z_2^{\text{PA}}(t_{\text{pre},n}-)\delta_{t_{\text{pre},n}} + \sum_{t_{\text{post},n} \leqslant t} Z_1^{\text{PA}}(t_{\text{post},n}-)\delta_{t_{\text{post},n}},$$

where δ_a is the Dirac mass at a. Equivalently,

$$\mathrm{d}W^{\text{PA}}(t) = Z_2^{\text{PA}}(t-)\mathcal{N}_\lambda(\mathrm{d}t) + Z_1^{\text{PA}}(t-)\mathcal{N}_{\beta,X}(\mathrm{d}t).$$

Nearest-neighbor symmetric model (PNS)

In the *nearest neighbor symmetric* model, whenever one neuron spikes, the synaptic weight is updated by only taking into account the last spike of the other neuron, as can be seen in Figure 4.1 (top right). If the presynaptic neuron fires at time $t_{\rm pre}$, the contribution to the plasticity kernel is $\Phi(t_{\rm pre}-t_{\rm post})$, where $t_{\rm post}$ is the last postsynaptic spike before $t_{\rm pre}$ and similarly for postsynaptic spikes.

The nearest neighbor symmetric rule leads to,

$$\begin{cases} \mathrm{d}Z_1^{\rm PNS}(t) &= -\gamma_1 Z_1^{\rm PNS}(t)\,\mathrm{d}t \\ &\qquad +(B_1 - Z_1^{\rm PNS}(t-))\mathcal{N}_\lambda(\mathrm{d}t), \\ \mathrm{d}Z_2^{\rm PNS}(t) &= -\gamma_2 Z_2^{\rm PNS}(t)\,\mathrm{d}t \\ &\qquad +(B_2 - Z_2^{\rm PNS}(t-)))\mathcal{N}_{\beta,X}(\mathrm{d}t). \end{cases}$$

At each presynaptic spike, $(Z_1^{\rm PNS}(t))$, resp. $(Z_2^{\rm PNS}(t))$, is reset to B_1, resp. B_2.

Nearest-neighbor symmetric reduced model (PNR)

Finally, for the *nearest neighbor symmetric reduced* scheme, only consecutive pairs of spikes are used to update the synaptic weight. The synaptic weight is updated at presynaptic spike time $t_{\rm pre}$ only if there are no presynaptic spikes since the last postsynaptic spike. And similarly for postsynaptic spike times. See Figure 4.1 (bottom right).

This rule leads to $(Z_i^{\rm PNR}(t))$, i=1, 2, solutions of

$$\begin{cases} \mathrm{d}Z_1^{\rm PNR}(t) &= -\gamma_1 Z_1^{\rm PNR}(t)\,\mathrm{d}t \\ &\qquad +(B_1 - Z_1^{\rm PNR}(t-))\mathcal{N}_\lambda(\mathrm{d}t) \\ &\qquad -Z_1^{\rm PNR}(t-))\mathcal{N}_{\beta,X}(\mathrm{d}t), \\ \mathrm{d}Z_2^{\rm PNR}(t) &= -\gamma_2 Z_2^{\rm PNR}(t)\,\mathrm{d}t \\ &\qquad +(B_2 - Z_2^{\rm PNR}(t-)))\mathcal{N}_{\beta,X}(\mathrm{d}t) \\ &\qquad -Z_2^{\rm PNR}(t-)\mathcal{N}_\lambda(\mathrm{d}t). \end{cases}$$

A general formulation for pair-based rules with exponential kernels

All these pair-based rules can be represented by a system of the form

$$\begin{cases} \mathrm{d}X(t) &= -X(t)\,\mathrm{d}t + W(t-)\mathcal{N}_\lambda(\mathrm{d}t), \\ \mathrm{d}Z_1(t) &= -\gamma_1 Z_1(t)\,\mathrm{d}t \\ &\qquad +(B_1 - K_{1,1}Z_1(t-))\mathcal{N}_\lambda(\mathrm{d}t) \\ &\qquad -K_{1,2}Z_1(t-)\mathcal{N}_{\beta,X}(\mathrm{d}t), \\ \mathrm{d}Z_2(t) &= -\gamma_2 Z_2(t)\,\mathrm{d}t \\ &\qquad +(B_2 - K_{2,2}Z_2(t-))\mathcal{N}_{\beta,X}(\mathrm{d}t) \\ &\qquad -K_{2,1}Z_2(t-)\mathcal{N}_\lambda(\mathrm{d}t), \\ \mathrm{d}W(t) &= Z_1(t-)\mathcal{N}_{\beta,X}(\mathrm{d}t) + Z_2(t-)\mathcal{N}_\lambda(\mathrm{d}t) \end{cases} \tag{4.1}$$

where $\gamma_1, \gamma_2 > 0$, $B_1, B_2 \in \mathbb{R}$, $\mathbf{K} = (K_{ij}) \in \{0,1\}^{2\times 2}$.

For the three pair-based STDP rules detailed, we have,

$$\mathbf{K}^{\mathrm{PA}}=\begin{pmatrix}0 & 0\\ 0 & 0\end{pmatrix},\quad \mathbf{K}^{\mathrm{PNS}}=\begin{pmatrix}1 & 0\\ 0 & 1\end{pmatrix},\quad \mathbf{K}^{\mathrm{PNR}}=\begin{pmatrix}1 & 1\\ 1 & 1\end{pmatrix}.$$

See Supplemental Material for Figure 4.5 at [URL will be inserted by publisher] for an example of dynamics for each pairing scheme.

A slow-fast system

We consider that the processes $(X(t))$ and $(Z_1(t), Z_2(t))$ evolve on a fast time scale $t\mapsto t/\varepsilon$ for some small $\varepsilon>0$. The increments of the variable W are scaled with the parameter ε, $(W_\varepsilon(t))$ is described as the *slow* process.

For ε small, on a short time interval, the slow process $(W_\varepsilon(t))$ is almost constant, and, due to its faster dynamics, the process $(X_\varepsilon(t), Z_{1,\varepsilon}(t), Z_{2,\varepsilon}(t))$ is "almost" at its equilibrium distribution associated to the current value of $W_\varepsilon(t)\approx w$. This corresponds to the equilibrium of the process $(X^w(t), Z_1^w(t), Z_2^w(t))$, where $W(t)=w$ is at a constant value. Classical results on Markov systems imply that there is unique stationary distribution $\Pi_w^{\mathbf{K}}$ on $\mathbb{R}_+\times\mathbb{R}^2$, for simplicity we will denote $\Pi_w^{\mathrm{PX}}=\Pi_w^{K^{\mathrm{PX}}}$, see [RV21b]

Using averaging principle arguments, the asymptotic dynamic of $(W_\varepsilon(t))$ is given by the ordinary differential equation,

$$\begin{aligned}\frac{\mathrm{d}w}{\mathrm{d}t}(t) &= \int_{\mathbb{R}_+\times\mathbb{R}^2}(\lambda z_2+\beta(x)z_1)\Pi^{\mathbf{K}}_{w(t)}(\mathrm{d}x,\mathrm{d}z)\\ &= \mathbb{E}_{\Pi^{\mathbf{K}}_{w(t)}}\left[\lambda Z_2+\beta(X)Z_1\right]=f^{\mathbf{K}}(w(t)).\end{aligned}\tag{4.2}$$

A more rigorous development of this result is given in Supplemental Material 4.B at [URL will be inserted by publisher], as is a comparison with computational models in Supplemental Material 4.C. Five different asymptotic behaviors for w, solution of (4.2) are defined using analytical asymptotic properties in Table 4.1. We define numerical approximates of these possible behaviors, depending on the values of $p_{+\infty}=\mathbb{P}\left(W_\varepsilon(t)=+\infty\right)$, $p_0=\mathbb{P}\left(W_\varepsilon(t)=0\right)$ and $p_{\text{stable}}=1-p_{+\infty}-p_0$, and a fixed parameters p_{bif}, see Appendix 4.A.

4.3 Results

In the following section, we study the dynamics of the synaptic weight, using analytical computations and numerical simulations. We investigate the influence of B_1 and B_2 because they represent biologically relevant parameters. Indeed most experimental studies only focus on the polarity of STDP, i.e the signs of B_1 and B_2 in the present model. In particular, we will focus on four different types of STDP classified as follow, *Hebbian* STDP ($B_1>0,\quad B_2<0$), *anti-Hebbian* STDP ($B_1<0,\quad B_2>0$), *symmetric LTD* (S-LTD, $B_1<0,\quad B_2<0$) and *symmetric LTP* (S-LTP, $B_1>0,\quad B_2>0$), which have all been shown to exist experimentally [Fel12]. We also choose to study the relative importance of the external firing rate ν, compared to other rate-related variables λ,β. Accordingly, analytical expressions are given for general parameters, while simulations are always realized with $\gamma_1=\gamma_2=\beta=\lambda=1$. See Supplemental Material 4.D at [URL will be inserted by publisher] for proofs and lengthy analytical expressions.

LTD (long-term depression)	$\forall w_0, \lim_{t\to+\infty} w(t) = 0$	$p_{+\infty} < p_{\text{bif}}$ $p_0 \geqslant p_{\text{bif}}$ $p_{\text{stable}} < p_{\text{bif}}$
LTP (long-term potentiation)	$\forall w_0, \lim_{t\to+\infty} w(t) = +\infty$	$p_{+\infty} \geqslant p_{\text{bif}}$ $p_0 < p_{\text{bif}}$ $p_{\text{stable}} < p_{\text{bif}}$
UFP (unstable fixed point	$\exists w_{\text{eq}}, \forall w_0 < w_{\text{eq}}, \lim_{t\to+\infty} w(t) = 0$ and $\forall w_0 > w_{\text{eq}}, \lim_{t\to+\infty} w(t) = +\infty$	$p_{+\infty} \geqslant p_{\text{bif}}$ $p_0 \geqslant p_{\text{bif}}$ $p_{\text{stable}} < p_{\text{bif}}$
SFP (stable fixed point)	$\exists w_{\text{eq}}, \forall w_0, \lim_{t\to+\infty} w(t) = w_{\text{eq}}$	$p_{+\infty} < p_{\text{bif}}$ $p_0 < p_{\text{bif}}$ $p_{\text{stable}} \geqslant p_{\text{bif}}$
MFP (multiple fixed points)	Other behaviors	Complementary set

Table 4.1: **Different behaviors, theoretical definitions and numerical estimations.**

In this framework, we study the asymptotic behavior of the dynamical system (4.2) for the three pair-based rules.

We will show that the synaptic weight $w(t)$ usually exhibits one of three different asymptotic behaviors, which all have a biological interpretation:

— Convergence of $w(t)$ towards 0, which corresponds the disconnection (or pruning) of the synapse: the presynaptic neuron loses its ability to influence the postsynaptic neuron.

— Divergence of $w(t)$ to infinity, leading to a perfect coupling between the pre- and postsynaptic neurons, through an unstable system which, in a biological system, will be stopped by saturation mechanisms.

— Convergence to a non null value w_{eq}, resulting in self-sustained activity, i.e., pre- and postsynaptic activities coupled with STDP are sufficient to have a bounded stable synaptic weight.

Stability and divergence depends on the polarity of STDP

Starting with the all-to-all scheme for an excitatory synapse, i.e. $\beta(x)=\nu+\beta x$, we have,

$$\frac{\mathrm{d}w}{\mathrm{d}t}(t) = f^{\text{PA}}(w) = A_0^{\text{PA}} + A_1^{\text{PA}} w = A_1^{\text{PA}} \left(w - w^{\text{PA}}\right).$$

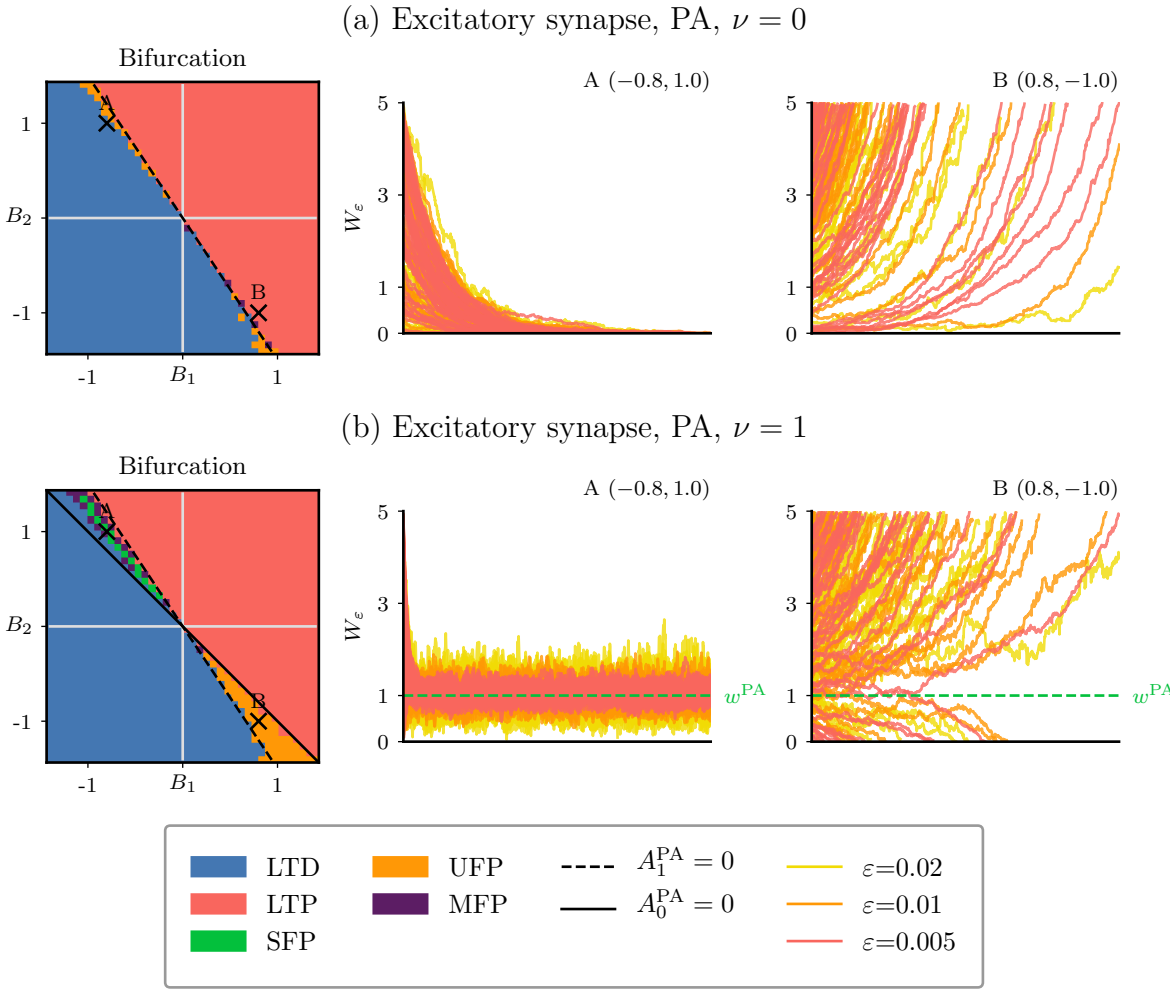

Figure 4.2: **All-to-all pair-based STDP for an excitatory synapse.**
(a) Dynamics of the synaptic weight as a function of B_1 and B_2 for ν=0. (left) Classification based on numerical simulations for different asymptotic dynamics of the synaptic weights (see different colors). Theoretical boundaries are also drawn (see legend for their expressions). (right) Two examples of temporal evolutions of the synaptic weights, for different values of ε. (b) Same as (a) for ν=1.
(γ_1=γ_2=β=λ=1)

with

$$A_0^{\mathrm{PA}} \stackrel{\text{def.}}{=} \nu\lambda\left(\frac{B_1}{\gamma_1}+\frac{B_2}{\gamma_2}\right),$$

$$A_1^{\mathrm{PA}} \stackrel{\text{def.}}{=} \beta\lambda^2\left(\frac{B_1}{\gamma_1}+\frac{B_2}{\gamma_2}+\frac{B_1}{\lambda(1+\gamma_1)}\right) \text{ and}$$

$$w^{\mathrm{PA}} \stackrel{\text{def.}}{=} -A_0^{\mathrm{PA}}/A_1^{\mathrm{PA}}.$$

The signs of A_0^{PA} and A_1^{PA} determine the asymptotic behavior of w. We study the impact of B_1 and B_2 with, or without, external input rate ν on the dynamics in Figure 4.2.

If ν=0, then w^{PA}=0. Without external input ν, the synaptic weights cannot converge to a positive stable solution.

— If $A_1^{\text{PA}}<0$, $(w(t))$ converges to 0, as shown by the blue region of Figure 4.2 (a), with some examples of dynamics at point A.

— If $A_1^{\text{PA}}>0$, $(w(t))$ diverges to $+\infty$, the red region of Figure 4.2 (a) and example B.

If $\nu>0$, w^{PA} is a non-null fixed point. This gives two new behaviors in the bifurcation map, see Figure 4.2 (b).

— If $A_1^{\text{PA}}<0$ and $A_0^{\text{PA}}>0$, the fixed point is stable (green region) and all simulations converge to w^{PA} independently of the initial point. See example A.

— If $A_1^{\text{PA}}>0$ and $A_0^{\text{PA}}<0$, the fixed point is unstable (orange region), example B shows that in that case, the dynamics depends on the initial value of synaptic weight. It diverges to $+\infty$ if starting above w^{PA}, and converges to 0 otherwise.

Influence of pairing scheme

Nearest neighbor symmetric STDP

For nearest neighbor symmetric STDP with $\beta(x)=\nu+\beta x$, the associated dynamical system is given by,

$$\frac{\mathrm{d}w}{\mathrm{d}t}(t) = f^{\text{PNS}}(w) \overset{\text{def.}}{=} A_0^{\text{PNS}}+A_1^{\text{PNS}}w+A_2^{\text{PNS}}h^{\text{PNS}}(w),$$

with,

$$A_0^{\text{PNS}} \overset{\text{def.}}{=} \frac{\nu\lambda}{\lambda+\gamma_1}B_1+\frac{\nu\lambda}{\nu+\gamma_2}B_2,$$
$$A_1^{\text{PNS}} \overset{\text{def.}}{=} \lambda\beta\frac{1+\lambda}{1+\lambda+\gamma_1}B_1,\ A_2^{\text{PNS}}=\lambda B_2,$$

and

$$h^{\text{PNS}}(w) \overset{\text{def.}}{=} \gamma_2\int_{\mathbb{R}_+} e^{-\gamma_2\tau}\left(1-\exp\left(-\nu\tau\right.\right.$$
$$-\lambda\int_0^\tau\left(1-\exp\left(-\beta w\left(1-e^{s-\tau}\right)\right)\right)\mathrm{d}s$$
$$\left.\left.-\lambda\int_{-\infty}^0\left(1-\exp\left(-\beta w\left(1-e^{-\tau}\right)e^s\right)\right)\mathrm{d}s\right)\right)\mathrm{d}\tau-\frac{\nu}{\nu+\gamma_2}.$$

The asymptotic behavior of $(w(t))$ can be analyzed rigorously in this case.
If $\nu=0$, let

$$A_3^{\text{PNS}} \overset{\text{def.}}{=} f^{\text{PNS}\prime}(0)=\lambda\beta\left(\frac{1+\lambda}{1+\lambda+\gamma_1}B_1+\frac{\lambda}{\gamma_2}B_2\right)$$

— If $A_1^{\text{PNS}}<0$ and $A_3^{\text{PNS}}<0$, $(w(t))$ converges to 0 in finite time (blue).

— If $A_1^{\text{PNS}}>0$ and $A_3^{\text{PNS}}>0$, The system diverges to infinity when both parameters are positive (red).

— If $A_1^{\text{PNS}}<0$ and $A_3^{\text{PNS}}>0$, a stable fixed point w^{PNS} exists (green), see example A.

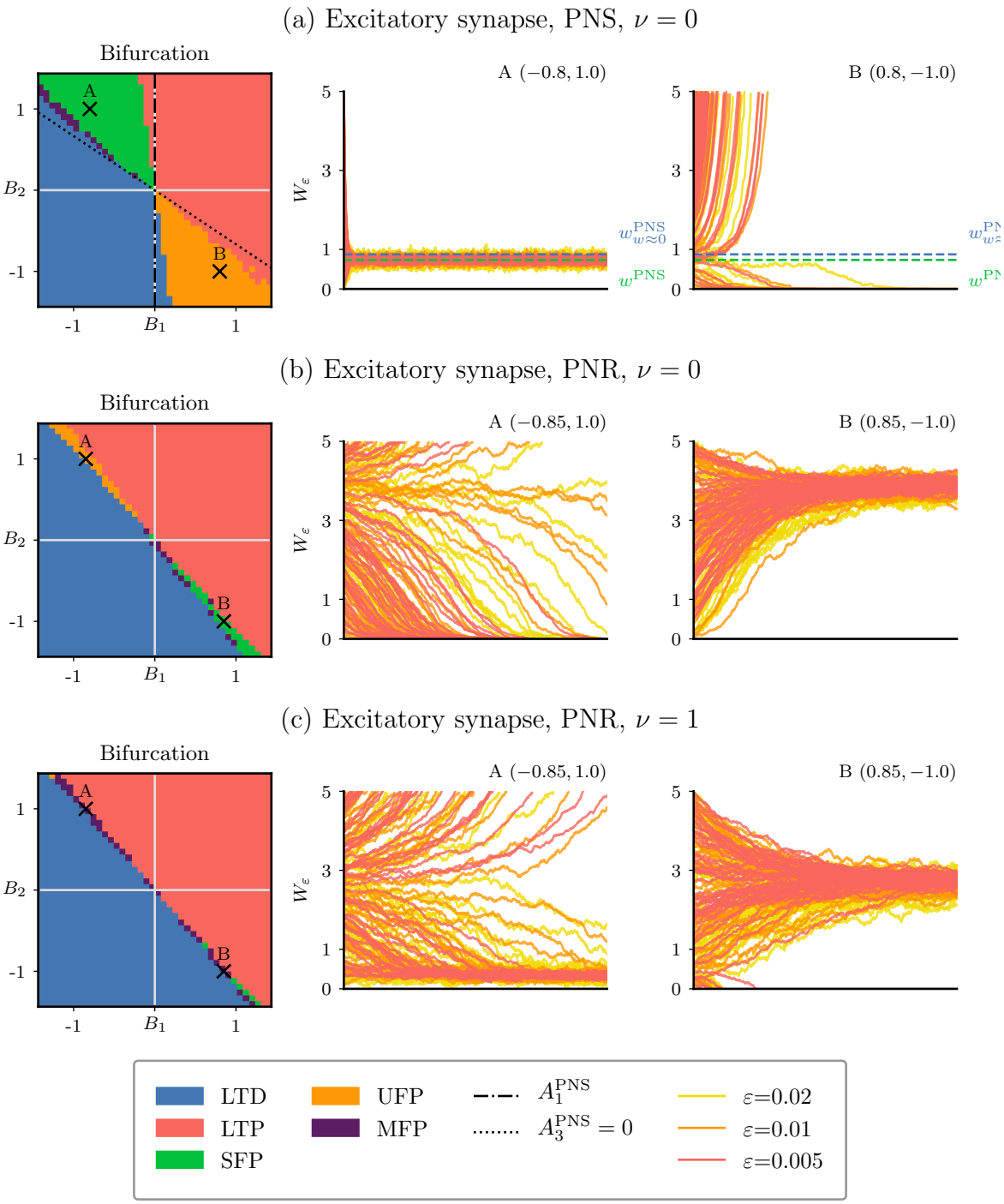

Figure 4.3: **Different pairing schemes leads to diverse dynamics.**
(a) Dynamics of the synaptic weight as a function of B_1 and B_2 for nearest neighbor symmetric STDP and ν=0. (left) Classification based on numerical simulations for different asymptotic dynamics of the synaptic weights (see different colors). Theoretical boundaries are also drawn (see legend for their expressions). (right) Two examples of temporal evolutions of the synaptic weights, for different values of ε. (b) Same as (a) for nearest neighbor symmetric reduced STDP and ν=0. (c) Same as (a) for nearest neighbor symmetric reduced STDP and ν=0.2. (γ_1=γ_2=β=λ=1)

— If $A_1^{\text{PNS}}>0$ and $A_3^{\text{PNS}}<0$, an unstable fixed point w^{PNS} exists (orange), example B.

We prove the existence of the fixed point w^{PNS}, provide a numerical estimation, and compute an approximation of w^{PNS} when $w\approx 0$, Figure 4.3(a) shows a comparison with numerical experiments.

The picture is similar for the case $\nu>0$, with slightly different conditions, where the same dynamics are verified except that $A_3^{\text{PNS}}<0$ is replaced by $A_0^{\text{PNS}}<0$ (see Figure 4.6 Supplemental Material at [URL will be inserted by publisher] for a comparison).

Discussion. Nearest neighbor symmetric STDP has significant differences with the all-to-all scheme. First, a positive stable fixed point may exist in the absence of external noise. The condition on A_1^{PNS} is a condition on B_1 only: if $B_1<0$ the system either converges to 0 or to a positive fixed point. The all-to-all case does not exhibit such a simple behavior, because A_0^{PA} and A_1^{PA} both depend on B_1 and B_2.

Nearest neighbor symmetric reduced STDP

A theoretical study of $(w(t))$ solution of (4.2) with $\beta(x)=\nu+\beta x$ is possible, but more involved than for PA and PNS. Computer simulations were done using this scheme, and the results are illustrated in Figure 4.3(b) and (c).

For $\nu=0$, there exists a (narrow) range of parameters in the Hebbian region (bottom right) where a stable fixed point occurs, see example B in Figure 4.3(b). Symmetrically, an unstable fixed point seems to exist in the anti-Hebbian region (top left) and example A.

For $\nu>0$, a second fixed point appears leading to more complex behaviors characterized by the presence of a stable and an unstable fixed point at the same time Figure 4.3(c). If the stable fixed point is lower than the unstable one, see example A and (top left) in Figure 4.3(c), the synaptic weight either converges to a non null value or diverges to infinity. For Hebbian parameters (bottom right), the situation is reversed, see example B in Figure 4.3(c). The spectrum of values with this complex behavior narrows when ν is increasing. In particular, for large values of ν, only a perfect balance in the parameters may lead to other behaviors than whole depression or potentiation. See Figure 4.7 in Supplemental Material at [URL will be inserted by publisher] for examples of the influence of ν on the dynamics.

Discussion. There are several differences of interest with the two other STDP pair-based rules for an excitatory synapse. First, for all-to-all and nearest neighbor symmetric pairings at an excitatory synapse, the stable fixed point only appears for anti-Hebbian parameters, whereas an unstable one exists for Hebbian STDP. With nearest neighbor symmetric reduced STDP, we have numerically shown that a more complex behavior with several fixed points may occur. Second, the nearest neighbor symmetric reduced STDP needs an almost exact balance of the parameters to enable convergence of the system toward a fixed point.

Table 4.2 gathers all results for an excitatory synapse as a function of the different types of biologically-relevant STDPs.

All-to-all STDP with an inhibitory synapse

We now study the dynamics (4.2) of the synaptic weight for an inhibitory synapse, i.e. when $\beta(x)=(\nu-\beta x)^+$.

	ν	Symmetric LTD	Symmetric LTP	Hebbian	Anti-Hebbian
PA	$=0$	LTD	LTP	LTD if $A_0^{\text{PA}}<0$ LTP if $A_0^{\text{PA}}>0$	LTD if $A_0^{\text{PA}}<0$ LTP if $A_0^{\text{PA}}>0$
	>0	LTD	LTP	LTD if $A_0^{\text{PA}}<0$ LTP if $A_1^{\text{PA}}>0$ UFP if not	LTD if $A_1^{\text{PA}}<0$ LTP if $A_0^{\text{PA}}>0$ SFP if not
PNS	$=0$	LTD	LTP	LTP if $A_3^{\text{PNS}}>0$ UFP if not	LTD if $A_3^{\text{PNS}}<0$ SFP if not
	>0	LTD	LTP	LTP if $A_0^{\text{PNS}}>0$ UFP if not	LTD if $A_0^{\text{PNS}}<0$ SFP if not
PNR*	$=0$	LTD	LTP	LTD/LTP/SFP	LTD/LTP/UFP
	>0	LTD	LTP	LTD/LTP/MFP	LTD/LTP/MFP

Table 4.2: **Different pairing schemes lead to diverse dynamics for an excitatory synapse.**
(S-LTD: symmetric LTD, S-LTP: symmetric LTP, * with simulations and $\gamma_1{=}\gamma_2{=}\beta{=}\lambda{=}1$).

We restrict our study to two cases.
For small w,

$$\begin{aligned}\frac{\mathrm{d}w}{\mathrm{d}t}(t) = f^{\text{PA}}(w) &= A_0^{\text{PA}} - A_1^{\text{PA}} w + o(w) \\ &= -A_1^{\text{PA}}\left(w + w^{\text{PA}}\right) + o(w).\end{aligned}$$

with $A_{0/1}^{\text{PA}}$ defined before.
When $w \geqslant \nu/\beta$, we have

$$\frac{\mathrm{d}w}{\mathrm{d}t}(t) = \frac{A^{\text{PAI}}}{w(t)^{\lambda+\gamma_1}}\left(1+\eta^{\text{PAI}}\left[\frac{w(t)}{w^{\text{PAI}}}\right]^{\gamma_1}\right)$$

with

$$A^{\text{PAI}} \stackrel{\text{def.}}{=} \left[\frac{\nu}{\beta}\right]^{\lambda+\gamma_1} \frac{c(\lambda) B_1 \nu}{(\lambda+\gamma_1)(\lambda+\gamma_1+1)},$$

$$w^{\text{PAI}} \stackrel{\text{def.}}{=} \frac{\beta}{\nu}\left(\left|\frac{B_2}{B_1}\right| \frac{(\lambda+\gamma_1)(\lambda+\gamma_1+1)}{\gamma_2(\lambda+1)}\right)^{1/\gamma_1},$$

$$\eta^{\text{PAI}} \stackrel{\text{def.}}{=} \left|\frac{B_2}{B_1}\right| \frac{B_1}{B_2}.$$

Using arguments on the monotony of the functionals, it should be possible to prove the stability properties, only using the two extreme cases defined above. In particular, the two relevant parameters are A_0^{PA} and B_2.

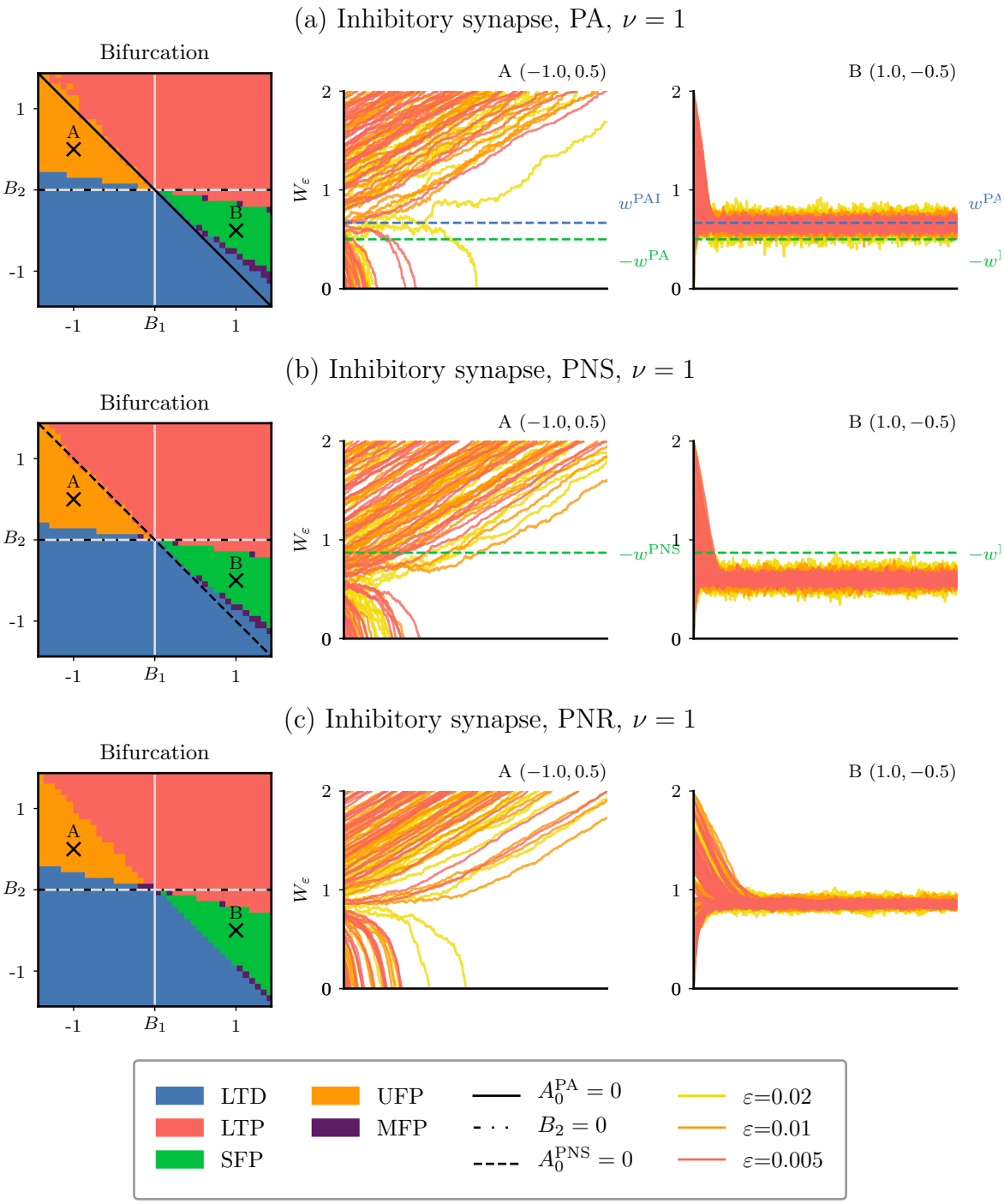

Figure 4.4: **Pair-based STDP for an inhibitory synapse.**
(a) Dynamics of the synaptic weight as a function of B_1 and B_2 for all-to-all STDP and ν=1. (left) Classification based on numerical simulations for different asymptotic dynamics of the synaptic weights (see different colors). Theoretical boundaries are also drawn (see legend for their expressions). (right) Two examples of temporal evolutions of the synaptic weights, for different values of ε. (b) Same as (a) for nearest neighbor symmetric STDP and ν=1. (c) Same as (a) for nearest neighbor symmetric reduced STDP and ν=1.
(γ_1=γ_2=β=λ=1)

	Symmetric LTD	Symmetric LTP	Hebbian	Anti-Hebbian
PA*	LTD	LTP	LTD if $A_0^{\text{PA}}<0$ SFP if not	LTP if $A_0^{\text{PA}}>0$ UFP if not
PNS/PNR*	LTD	LTP	LTD/SFP	LTP/UFP

Table 4.3: **Different pairing schemes lead to diverse dynamics for an inhibitory synapse.**
(S-LTD: symmetric LTD, S-LTP: symmetric LTP, * with simulations and $\gamma_1=\gamma_2=\beta=\lambda=1$).

— For $B_2>0$ and $A_0^{\text{PA}}>0$, the synaptic weight diverges to infinity (in red).

— For $B_2<0$ and $A_0^{\text{PA}}<0$, it converges to 0 in finite time (in blue).

— For $B_2>0$ and $A_0^{\text{PA}}<0$, there is an unstable fixed point (orange, example A).

— For $B_2<0$ and $A_0^{\text{PA}}>0$, the system exhibits a stable equilibrium (green, example B).

We note here an inversion with the properties observed for the excitatory synapse, where only anti-Hebbian STDP led to a stable fixed point, compared to the inhibitory case where only Hebbian STDP elicits this type of behavior.

This analysis is completed with the other schemes in Figure 4.4(b) for PNS and Figure 4.4(c) for PNR. The dynamics are similar to the all-to-all case for this range of parameters, only the values of the fixed points seems to change (compare B for the three cases).

All these behaviors are gathered in Table 4.3.

It is striking that the pairing scheme does not seem to have a decisive impact on the dynamics for an inhibitory synapse, considering the important impact displayed for an excitatory synapse.

4.4 Conclusion

We have developed a simple and rigorous analysis of synaptic weight dynamics via a slow-fast approximation and numerical simulations. For an excitatory synapse, anti-Hebbian STDP can lead to a stable fixed point, with some slight variations depending on the pairing scheme used. For an inhibitory synapse, numerical arguments showed that all schemes were similar, with the existence of a stable fixed point for Hebbian STDP.

This study investigates rigorously the synaptic weight dynamics for several pairing schemes, for all polarities of STDP, and for excitatory/inhibitory inputs. As such, it extends and complete previous results that only focus on all-to-all Hebbian STDP at excitatory synapses.

The nervous system is characterized by its diversity, and in particular, by the existence of many types of neurons which display different properties. Several models in theoretical neuroscience consider neurons that integrate a large quantity of random

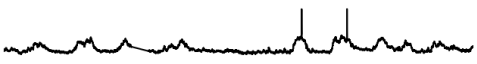

inputs approximated by a Brownian diffusion and the postsynaptic spikes result mainly from noise and not from correlated presynaptic inputs [RLS01; RBT00b]. When the impact of the presynaptic spikes is lost in the external noise (consistent with a large number of external uncorrelated inputs), pairing schemes do not influence the type of dynamics observed see [BMG04] for example. These assumptions often lead to a mean-field formulation where the synaptic weight dynamics is essentially driven by the *mean* global synaptic weight, see [BMG04; BA16].

However, neurons, in the striatum [MDC01; Pid+11] or in the cortex [AG00], need short bursts of presynaptic concentrated activity for their membrane potential to be depolarized enough to trigger spikes. In particular, pattern learning tasks, where a set of highly correlated inputs is repeated and learn to trigger/or not trigger a postsynaptic spike, are a good example of systems where presynaptic inputs cannot be reduced to a diffusive process. In this article, we have focused on similar network dynamics, where the postsynaptic spike train is determined by the presynaptic spike train, and not just a diffusive process. When considering such dynamics, as we have seen, the different STDP schemes have an important impact. A potential mean-field approximation in this context seems therefore to be unlikely.

It is not a surprise that this regime of activity leads to diverse interesting behaviors for the synaptic weight dynamics, where the asymptotic behavior strongly depends on the polarity of the STDP curve and the pairing scheme. We have shown, using analytical and numerical arguments, that several key parameters need to be taken into account while implementing STDP in networks with correlated dynamics, and in particular in recurrent networks [BGH07; GBV10; TAG18]. This conclusion should also apply to more complex pairing schemes such as triplets rules [PG06b; BA16].

Theoretical studies of plasticity in networks are quite scarce. Recently, [Löc17] studies short-term plasticity in a large network, and [Luc+16] the noise-enhanced coupling of two excitatory neurons subject to STDP, which can be extended to the formation of multiclusters in adaptive networks [BSY19]. The need for a general theory is great and this work is a first step in developing a rigorous framework to investigate the role of STDP in network dynamics

Appendix

4.A Computer methods

For each set of parameters, we have run several simulations, with different initial weight values uniformly taken in $[0, w_{\max}]$. We have tested the dynamics of the synaptic weight for the different pairing schemes defined before for a wide range of parameters. Simulations have been done using Python 3.X for the simple network of a presynaptic and a postsynaptic neuron. We used a discrete Euler scheme for the dynamics of the membrane potential X and the plasticity variables Z_1 and Z_2. Whenever the synaptic weight was either 0 or reached the maximal value $w_{\max}$ the dynamics was stopped, and the synaptic weight state recorded.

To compare different dynamics, synapses and pairing schemes, we perform, for each set of parameters, independent simulations and from this array of dynamics we compute several variables:

— The probability of diverging to infinity, $p_{+\infty}=\mathbb{P}\left(W_\varepsilon(t)=+\infty\right)$, approximated by the proportion of simulations where the synaptic weight goes above $w_{\max}$.

— The probability of converging to 0, $p_0=\mathbb{P}\left(W_\varepsilon(t)=0\right)$, approximated by the proportion of simulations whose synaptic weight goes below 0.

— The probability to have a stable fixed point defined by the complementary probability $p_{\text{stable}}=1-p_{+\infty}-p_0$.

While varying B_1 and B_2, we simulated $P=500$ neuronal networks for each condition with $\mathrm{d}t=0.0005$. We also plot the temporal dynamics for specific values of B_1 and B_2, typically used $P=50$ simulations for each scaling ε with $\mathrm{d}t=0.0002$. The following parameters are fixed in the simulations $\gamma_1=\gamma_2=\beta=\lambda=1$.

Simulations were run on the INRIA CLEPS cluster and HPC resources from GENCI-IDRIS (Grant 2022-A0100612385), using GNU parallel (Tange, O. (2020, May 22). GNU Parallel 20200522 ('Kraftwerk'). Zenodo. https://doi.org/10.5281/zenodo.3841377).

4.B Slow-fast approximations, averaging principles

We have the scaled system, for $\varepsilon>0$,

$$\begin{cases} \mathrm{d}X_\varepsilon(t) &= -1/\varepsilon X_\varepsilon(t)\,\mathrm{d}t + W_\varepsilon(t-)\mathcal{N}_{\lambda/\varepsilon}(\mathrm{d}t), \\ \mathrm{d}Z_{1,\varepsilon}(t) &= -\gamma_1 Z_{1,\varepsilon}(t)\,\mathrm{d}t/\varepsilon + (B_1 - K_{1,1}Z_{1,\varepsilon}(t-))\mathcal{N}_{\lambda/\varepsilon}(\mathrm{d}t) \\ &\qquad -K_{1,2}Z_{1,\varepsilon}(t-)\mathcal{N}_{\beta/\varepsilon,X_\varepsilon}(\mathrm{d}t), \\ \mathrm{d}Z_{2,\varepsilon}(t) &= -\gamma_2 Z_{2,\varepsilon}(t)\,\mathrm{d}t/\varepsilon + (B_2 - K_{2,2}Z_{2,\varepsilon}(t-))\mathcal{N}_{\beta/\varepsilon,X_\varepsilon}(\mathrm{d}t) \\ &\qquad -K_{2,1}Z_{2,\varepsilon}(t-)\mathcal{N}_{\lambda/\varepsilon}(\mathrm{d}t), \\ \mathrm{d}W_\varepsilon(t) &= Z_{1,\varepsilon}(t-)\varepsilon\mathcal{N}_{\beta/\varepsilon,X_\varepsilon}(\mathrm{d}t) + Z_{2,\varepsilon}(t-)\varepsilon\mathcal{N}_{\lambda/\varepsilon}(\mathrm{d}t) \end{cases} \tag{4.3}$$

where $\gamma_1, \gamma_2>0$, $B_1, B_2\in\mathbb{R}$, $\mathbf{K}=(K_{ij}, i, j\in\{1,2\})\in\{0,1\}^{2\times 2}$.

Approximations of $(W_\varepsilon(t))$ when ε is small are discussed and investigated with ad hoc methods. The corresponding scaling results, known as separation of timescales,

are routinely used in approximations in mathematical models of computational neuroscience, for example [KGH99].

We first need to define the processes $(X^w(t), Z_1^w(t), Z_2^w(t))$ which follow the fast processes dynamics with a constant synaptic weight w and prove that a unique invariant distribution exists for the associated dynamics. This corresponds to the equilibrium of the process $(X^w(t), Z_1^w(t), Z_2^w(t))$ such that

$$\begin{cases} \mathrm{d}X^w(t) &= -X^w(t)\,\mathrm{d}t + w\mathcal{N}_\lambda(\mathrm{d}t), \\ \mathrm{d}Z_1^w(t) &= -\gamma Z_1^w(t)\,\mathrm{d}t + (B_1 - K_{1,1}Z_1^w(t-))\mathcal{N}_\lambda(\mathrm{d}t) \\ &\qquad -K_{1,2}Z_1^w(t-)\mathcal{N}_{\beta,X^w}(\mathrm{d}t), \\ \mathrm{d}Z_2^w(t) &= -\gamma Z_2^w(t)\,\mathrm{d}t + (B_2 - K_{2,2}Z_2^w(t-))\mathcal{N}_{\beta,X^w}(\mathrm{d}t) \\ &\qquad -K_{2,1}Z_2^w(t-)\mathcal{N}_\lambda(\mathrm{d}t). \end{cases} \tag{4.4}$$

This is the purpose of Proposition 55.

Proposition 55 (Equilibrium of fast processes)**.** *For* $\mathbf{K}=(K_{ij}, i,j\in\{1,2\})\in\{0,1\}^{2\times 2}$, $\gamma_1,\gamma_2>0$, $B_1, B_2\in\mathbb{R}$, *and each* $w\geqslant 0$, *the Markov process* $(X^w(t), Z_1^w(t), Z_2^w(t))$ *solution of* (4.4) *has a unique stationary distribution* $\Pi_w^{\mathbf{K}}$ *on* $\mathbb{R}_+\times\mathbb{R}^2$.

Proof. See Proposition 25 of [RV21a]. □

Theorem 56 (Averaging principle)**.** *There exists* $S_0\in(0,+\infty]$ *such that, when* ε *goes to* 0, *the process* $(W_\varepsilon(t), t<S_0)$ *is converging in distribution to* $(w(t), t<S_0)$, *solution of the equation*

$$\frac{\mathrm{d}w}{\mathrm{d}t}(t) = \mathbb{E}_{\Pi^{\mathbf{K}}_{w(t)}}\left[\lambda Z_2 + \beta(X)Z_1\right], \tag{4.5}$$

where Π_w^K *is defined in Proposition 55.*

Proof. See [RV21c] and [RV21a]. □

4.C Comparison to classical computational models

In this section, we compare averaging principles for STDP rules leading to Relation (4.5) with the results of [KGH99] in the all-to-all pair-based scheme.

The asymptotic behavior of the synaptic weight dynamics, Relation (4) of [KGH99], is a consequence of a similar slow-fast argument,

$$\frac{\mathrm{d}\widetilde{w}}{\mathrm{d}t}(t) = \int_{-\infty}^{+\infty} \widetilde{\Phi}(s)\widetilde{\mu}(s,t)\,\mathrm{d}s, \tag{4.6}$$

where,

— $\widetilde{\Phi}(s)$ represents the STDP curve;

— $\widetilde{\mu}(s,t)=\overline{<S^1(t+s)S^2(t)>}$, the correlation between the spike trains.

The quantity $\overline{\langle \cdots \rangle}$ is defined in terms of *temporal and ensemble averages*, $\langle \cdots \rangle$ is the ensemble average and $\overline{\cdots}$ the temporal average over the spike trains.

In our setting, Theorem 56 gives the following equation,

$$\frac{\mathrm{d}w}{\mathrm{d}t}(t) = \mathbb{E}_{\Pi^{\mathrm{PA}}_{w(t)}}\left[\lambda Z_2 + \beta(X) Z_1\right],$$

with

$$\Phi(t) \overset{\text{def.}}{=} B_1 \exp(-\gamma_1 t)\mathbb{1}_{\{t>0\}} + B_2 \exp(\gamma_2 t)\mathbb{1}_{\{t<0\}}.$$

We have, using simple calculus,

$$\lambda \mathbb{E}_{\Pi^{\mathrm{PA}}_{w(t)}}\left[Z_2\right] = \int_{-\infty}^{0} B_2 \exp(\gamma_2 \tau)\lambda \mathbb{E}_{\Pi^{\mathrm{PA}}_{w(t)}}\left[\beta(x)\right] \mathrm{d}\tau$$

We denote by $\Pi^{\mathrm{PA}}_{2\mapsto 1,t}(\tau)$ the rate of having a post-pre pairing with delay τ at time t. For the post-pre pairing, we can consider that $\Pi^{\mathrm{PA}}_{2\mapsto 1,t}(\tau)$ does not depend on τ and that it is just equal to the product of both rates, i.e there is no causality, and

$$\Pi^{\mathrm{PA}}_{2\mapsto 1,t}(\tau) = \lambda \mathbb{E}_{\Pi^{\mathrm{PA}}_{w(t)}}\left[\beta(x)\right].$$

We easily conclude that,

$$\lambda \mathbb{E}_{\Pi^{\mathrm{PA}}_{w(t)}}\left[Z_2\right] = \int_{-\infty}^{0} \Phi(\tau)\Pi^{\mathrm{PA}}_{2\mapsto 1,t}(\tau)\, \mathrm{d}\tau,$$

with $\Pi^{\mathrm{PA}}_{2\mapsto 1,t}(\tau) \approx \overline{<S^1(t+\tau)S^2(t)>}$.

Similarly, we have

$$\mathbb{E}_{\Pi^{\mathrm{PA}}_{w(t)}}\left[\beta(X)Z_1\right] = \mathbb{E}_{\Pi^{\mathrm{PA}}_{w(t)}}\left[\sum_{t_{\mathrm{pre}}<t_{\mathrm{post}}} B_1 \exp(-\gamma_1(t_{\mathrm{post}} - t_{\mathrm{pre}}))\beta(X)\right]$$

We denote by $\Pi^{\mathrm{PA}}_{1\mapsto 2,t}(\tau)$ the rate of having a pre-post pairing with delay τ at time t. For the pre-post pairing, this quantity depends on τ because spikes of the presynaptic neuron influence the spiking of the postsynaptic one, so we have, by using the fact that Π^{PA} is the invariant distribution,

$$\mathbb{E}_{\Pi^{\mathrm{PA}}_{w(t)}}\left[\sum_{t_{\mathrm{pre}}<t_{\mathrm{post}}} B_1 \exp(-\gamma_1(t_{\mathrm{post}} - t_{\mathrm{pre}}))\beta(X)\right] = \int_0^{+\infty} B_1 \exp(-\gamma_1 \tau)\Pi^{\mathrm{PA}}_{1\mapsto 2,t}(\tau)\, \mathrm{d}\tau.$$

See SM2 of [RV21c], hence

$$\mathbb{E}_{\Pi^{\mathrm{PA}}_{w(t)}}\left[\beta(X)Z_1\right] = \int_0^{+\infty} \Phi(\tau)\Pi^{\mathrm{PA}}_{1\mapsto 2,t}(\tau)\, \mathrm{d}\tau,$$

with $\Pi^{\mathrm{PA}}_{1\mapsto 2,t}(\tau) \approx \overline{<S^1(t)S^2(t+\tau)>}$. This shows the equivalence between [KGH99] and our result for the all-to-all pair-based STDP rules.

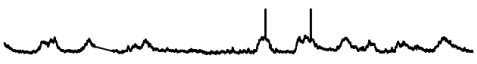

4.D Proofs

All-to-all STDP at an excitatory synapse

We prove that,

$$\mathbb{E}_{\Pi^{\mathrm{PA}}_{w(t)}}\left[\lambda Z_2+\beta(X)Z_1\right] = A_0^{\mathrm{PA}}+A_1^{\mathrm{PA}}w = A_1^{\mathrm{PA}}\left(w-w^{\mathrm{PA}}\right).$$

where,

$$A_0^{\mathrm{PA}} = \nu\lambda\left(\frac{B_1}{\gamma_1}+\frac{B_2}{\gamma_2}\right),\ A_1^{\mathrm{PA}} = \beta\lambda^2\left(\frac{B_1}{\gamma_1}+\frac{B_2}{\gamma_2}+\frac{B_1}{\lambda(1+\gamma_1)}\right)$$

Proof. First, it is easy to show that,

$$\mathbb{E}\left[Z_1^{\mathrm{PA},w}\right] = \lambda\frac{B_1}{\gamma_1},\ \text{and}\ \mathbb{E}\left[Z_2^{\mathrm{PA},w}\right] = \nu\frac{B_2}{\gamma_2}+\beta\lambda\frac{B_2}{\gamma_2}w$$

Moreover, denoting $(Y^w(t))=(X^w(t)Z_1^{\mathrm{PA},w}(t))$, we get

$$\mathrm{d}Y^w(t) = -(1+\gamma_1)Y^w(t)\,\mathrm{d}t + \left(wZ_1^{\mathrm{PA},w}(t-)+B_1X^w(t-)+wB_1\right)\mathcal{N}_\lambda(\mathrm{d}t),$$

by integrating this ODE on $[0,t]$ and taking the expected value, we obtain

$$\mathbb{E}\left[X^wZ_1^{\mathrm{PA},w}\right] = \frac{\lambda w\mathbb{E}\left[Z_1^{\mathrm{PA},w}\right]+\lambda B_1\mathbb{E}\left[X^w\right]+\lambda wB_1}{1+\gamma_1} = \left(\frac{\lambda^2}{\gamma_1}+\frac{\lambda}{1+\gamma_1}\right)B_1w.$$

□

Nearest neighbor symmetric STDP at an excitatory synapse

Estimation of f^{PNS}

$$\mathbb{E}_{\Pi^{\mathrm{PNS}}_{w(t)}}\left[\lambda Z_2+\beta(X)Z_1\right] = A_0^{\mathrm{PNS}}+A_1^{\mathrm{PNS}}w+A_2^{\mathrm{PNS}}h^{\mathrm{PNS}}(w)$$

with,

$$A_0^{\mathrm{PNS}}=\frac{\nu\lambda}{\lambda+\gamma_1}B_1+\frac{\nu\lambda}{\nu+\gamma_2}B_2,\ A_1^{\mathrm{PNS}}=\lambda\beta\frac{1+\lambda}{1+\lambda+\gamma_1}B_1,\ A_2^{\mathrm{PNS}}=\lambda B_2,$$

and,

$$h^{\mathrm{PNS}}(w) = \gamma_2\int_{\mathbb{R}_+}e^{-\gamma_2\tau}\left(1-\exp\left(-\nu\tau-\lambda\int_0^\tau\left(1-\exp\left(-\beta w\left(1-e^{s-\tau}\right)\right)\right)\mathrm{d}s\right.\right.$$
$$\left.\left.-\lambda\int_{-\infty}^0\left(1-\exp\left(-\beta w\left(1-e^{-\tau}\right)e^s\right)\right)\mathrm{d}s\right)\right)\mathrm{d}\tau-\frac{\nu}{\nu+\gamma_2}.$$

For the proof, see Section 3.2 [RV21c].

Dynamics of w

We start with some calculations for h^{PNS} of Section 4.3.

Lemma 57. *h^{PNS} is a convex function, and,*

$$h^{\text{PNS}}(0)=0,\ h^{\text{PNS}}(+\infty)=1-\frac{\nu}{\nu+\gamma_2},\ h^{\text{PNS}\prime}(0)=\frac{\lambda\beta\gamma_2}{(\nu+\gamma_2)^2}$$

Proof. We compute,

$$h^{\text{PNS}\prime}(w)=\lambda\beta\gamma_2\int_{\mathbb{R}_+}e^{-(\nu+\gamma_2)\tau}\left(\int_0^\tau\left(1-e^{s-\tau}\right)\exp\left(-\beta w\left(1-e^{s-\tau}\right)\right)\mathrm{d}s\right.$$
$$\left.+\int_{-\infty}^0\left(1-e^{-\tau}\right)e^s\exp\left(-\beta w\left(1-e^{-\tau}\right)e^s\right)\mathrm{d}s\right)$$
$$\exp\left(-\lambda\int_0^\tau\left(1-\exp\left(-\beta w\left(1-e^{s-\tau}\right)\right)\right)\mathrm{d}s-\lambda\int_{-\infty}^0\left(1-\exp\left(-\beta w\left(1-e^{-\tau}\right)e^s\right)\right)\mathrm{d}s\right)\mathrm{d}\tau.$$

We have $h'(w)$ is an increasing function in w, so $h(w)$ is convex. □

The system

$$\frac{\mathrm{d}w}{\mathrm{d}t}(t)=A_0^{\text{PNS}}+A_1^{\text{PNS}}w+A_2^{\text{PNS}}h^{\text{PNS}}(w)$$

has the following dynamics.

ν	LTD	LTP	STABLE FP	UNSTABLE FP
0	$A_3^{\text{PNS}}<0$	$A_3^{\text{PNS}}>0$	$A_3^{\text{PNS}}<0$	$A_3^{\text{PNS}}>0$
	$A_1^{\text{PNS}}<0$	$A_1^{\text{PNS}}>0$	$A_1^{\text{PNS}}>0$	$A_1^{\text{PNS}}<0$
>0	$A_0^{\text{PNS}}<0$	$A_0^{\text{PNS}}>0$	$A_0^{\text{PNS}}<0$	$A_0^{\text{PNS}}>0$
	$A_1^{\text{PNS}}<0$	$A_1^{\text{PNS}}>0$	$A_1^{\text{PNS}}>0$	$A_1^{\text{PNS}}<0$

Table 4.4: **Bifurcations parameters for the nearest neighbor symmetric scheme.**

where

$$A_3^{\text{PNS}}=\lambda\beta\left(\frac{1+\lambda}{1+\lambda+\gamma_1}B_1+\frac{\lambda}{\gamma_2}B_2\right)=f^{\text{PNS}\prime}(0)_{\nu=0}.$$

Proof.
Case $\nu=0$

We have $f^{\text{PNS}}(0)=0$ and $\lim_{w\to+\infty}f^{\text{PNS}}(w)=\text{sign}(A_1^{\text{PNS}})\times\infty$. We need to look then at the sign of $f^{\text{PNS}\prime}(0)=A_3^{\text{PNS}}$.

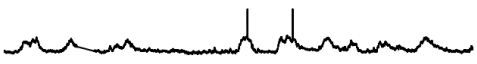

If A_1^{PNS} and A_3^{PNS} are of the same sign, f_1^{PNS} has no positive roots. Therefore, if $A_1^{\text{PNS}}>0$ and $A_3^{\text{PNS}}>0$, we have $\lim_{t\to+\infty} w(t) = +\infty$. Reciprocally, if $A_1^{\text{PNS}}>0$ and $A_3^{\text{PNS}}<0$, we have $\lim_{t\to+\infty} w(t) = 0$.

If A_1^{PNS} and A_3^{PNS} are not of the same sign, f_1^{PNS} has a unique positive root w^{PNS}. Then, if $A_1^{\text{PNS}}<0$ and $A_3^{\text{PNS}}>0$, w^{PNS} is a stable fixed point and $A_1^{\text{PNS}}>0$ and $A_3^{\text{PNS}}<0$, it is an unstable fixed point.

Case $\nu > 0$

We have $f^{\text{PNS}}(0) = A_0^{\text{PNS}}$ and $\lim_{w\to+\infty} f^{\text{PNS}}(w) = \text{sign}(A_1^{\text{PNS}})\times\infty$

Similarly as for ν=0, if A_0^{PNS} and A_1^{PNS} are not of the same sign, f_1^{PNS} has a unique positive root w^{PNS}, following the convexity of f^{PNS}. Then, if $A_0^{\text{PNS}}>0$ and $A_1^{\text{PNS}}<0$, w^{PNS} is a stable fixed point and $A_0^{\text{PNS}}<0$ and $A_1^{\text{PNS}}>0$, it is an unstable fixed point.

It is slightly more complex for the other cases. We will focus on the case, $A_0^{\text{PNS}}>0$ and $A_1^{\text{PNS}}>0$. We have that $f^{\text{PNS}}(0) > 0$ and that $\lim_{w\to+\infty} f^{\text{PNS}}(w) = +\infty$. As f^{PNS} is convex, two cases are possible. Either f^{PNS} has no positive root, and in that case, it is easy to see that $\lim_{t\to+\infty} w(t) = +\infty$. However, it is also possible that f^{PNS} has two positive roots and in that case it would lead to more complex dynamics. we just need to look at $f^{\text{PNS}'}(0)$ and show that it is positive to prove that this case does not happen.

$A_0^{\text{PNS}}>0$ leads to a first inequality,

$$B_1 \geqslant -B_2\frac{\lambda+\gamma_1}{\nu+\gamma_2} \geqslant 0.$$

We can then say that,

$$\begin{aligned} f^{\text{PNS}'}(0) &= A_1^{\text{PNS}}+A_2^{\text{PNS}}\frac{\lambda\beta\gamma_2}{(\nu+\gamma_2)^2} = B_1\lambda\beta\frac{1+\lambda}{1+\lambda+\gamma_1}+B_2\frac{\lambda^2\beta\gamma_2}{(\nu+\gamma_2)^2} \\ &\geqslant -B_2\lambda\beta\frac{(\lambda+\gamma_1)\frac{1+\lambda}{1+\lambda+\gamma_1}-\frac{\lambda\gamma_2}{\nu+\gamma_2}}{\nu+\gamma_2} = -B_2\lambda\beta\frac{\lambda\nu+\lambda^2\nu+\gamma_1\nu+\gamma_1\gamma_2+\lambda\nu\gamma_1}{(\nu+\gamma_2)^2(1+\lambda+\gamma_1)} \geqslant 0 \end{aligned}$$

The same arguments are true for the other case. □

Approximation for w small

We have the following expansion for w small,

$$f^{\text{PNS}}(w) = \nu B_1\frac{\lambda}{\lambda+\gamma_1}+\lambda\beta w B_1\frac{1+\lambda}{1+\lambda+\gamma_1}+\lambda B_2\frac{\nu+\lambda\beta w}{\gamma_2+\nu+\lambda\beta w}+o(w).$$

Leading to the following differential system,

$$\frac{\mathrm{d}w}{\mathrm{d}t}(t) = \frac{a^{\text{PNS}}w(t)^2 + b^{\text{PNS}}w(t) + c^{\text{PNS}}}{w(t) - w_{\text{approx}}^{\text{PNS}}} + o(w(t)),$$

where,

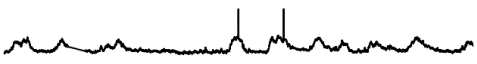

$$a^{\text{PNS}} = B_1\frac{\lambda^2\beta^2(1+\lambda)}{1+\lambda+\gamma_1},\ b^{\text{PNS}} = B_1\frac{\nu\lambda^2\beta}{\lambda+\gamma_1}+B_1\frac{\lambda\beta(1+\lambda)(\gamma_2+\nu)}{1+\lambda+\gamma_1}+B_2\lambda,$$
$$c^{\text{PNS}} = B_1\frac{\nu\lambda(\gamma_2+\nu)}{\lambda+\gamma_1}+B_2\frac{\nu}{\beta} \text{ and } w^{\text{PNS}}_{\text{approx}} = -\frac{\gamma_2+\nu}{\lambda\beta}.$$

Proof.

$$f^{\text{PNS}}(w) = \nu B_1\frac{\lambda}{\lambda+\gamma_1}+\lambda\beta w B_1\frac{1+\lambda}{1+\lambda+\gamma_1}$$
$$+\lambda B_2-\lambda\gamma_2 B_2\int_{\mathbb{R}_+}\exp\left(-\tau\left(\gamma_2+\nu+\lambda\beta w\right)\right)\mathrm{d}\tau+o(w).$$

□

Therefore, if

$$\Delta^{\text{PNS}} = {b^{\text{PNS}}}^2 - 4a^{\text{PNS}}c^{\text{PNS}} > 0,$$

we have an analytical expression for the fixed points of the dynamics $w^{\text{PNS}}_{w\approx 0}$,

$$w^{\text{PNS}}_{w\approx 0} = \frac{-b^{\text{PNS}} + / - \sqrt{\Delta^{\text{PNS}}}}{2a^{\text{PNS}}}.$$

Nearest neighbor symmetric reduced STDP at an excitatory synapse

To study the invariant distribution, we need to use a different formulation of the nearest reduced symmetric rule.

For $w\geqslant 0$, we can define $(X^w(t), T_1^{\text{PNR},w}, T_2^{\text{PNR},w}(t))$, the solution of the SDEs,

$$\begin{cases}\mathrm{d}X^w(t) = -X^w(t)\,\mathrm{d}t + w\mathcal{N}_\lambda(\mathrm{d}t),\\ \mathrm{d}T_1^{\text{PNR},w}(t) = \mathrm{d}t - T_1^{\text{PNR},w}(t-)\,\mathcal{N}_\lambda(\mathrm{d}t),\\ \mathrm{d}T_2^{\text{PNR},w}(t) = \mathrm{d}t - T_2^{\text{PNR},w}(t-)\,\mathcal{N}_{\beta,X^w}(\mathrm{d}t).\end{cases} \tag{4.7}$$

and,

$$\frac{\mathrm{d}w}{\mathrm{d}t}(t) = f^{\text{PNR}}(w) = \mathbb{E}_{\Pi^{\text{PNR}}_{w(t)}}\left[\lambda Z_2+\beta(X)Z_1\right]$$
$$= \mathbb{E}_{\Pi^{\text{PNR}}_{w(t)}}\left[\mathbb{1}_{\{T_1<T_2\}}B_1\beta(X)\exp(-\gamma_1 T_1)\right.$$
$$\left.+\ \mathbb{1}_{\{T_2<T_1\}}B_2\lambda\exp(-\gamma_2 T_2)\right]$$

All-to-all STDP at an inhibitory synapse

Definition 58. *We define the density of probability $Q(y)$ of the exponential Shot-Noise process Y associated to $\mathcal{N}_\lambda$, according to Gilbert and Pollack (1960). A general expression of $Q(y)$ can be found in Gilbert and Pollack (1960). In our case, we will use,*

$$\begin{cases}Q(y) & = c(\lambda)y^{\lambda-1} \quad ,0\leqslant y\leqslant 1,\\ \lim\limits_{y\to+\infty}Q(y) & = 0,\end{cases}$$

with,

$$c(\lambda) = \frac{e^{-\gamma_e\lambda}}{\Gamma(\lambda)}$$

where, γ_e Euler constant and Γ Euler function.

We have the two following limits, for small w,

$$\frac{\mathrm{d}w}{\mathrm{d}t}(t) = f^{\mathrm{PA}}(w) = A_0^{\mathrm{PA}} - A_1^{\mathrm{PA}} w = -A_1^{\mathrm{PA}} \left(w + w^{\mathrm{PA}}\right).$$

where,

$$A_0^{\mathrm{PA}} = \nu\lambda \left(\frac{B_1}{\gamma_1} + \frac{B_2}{\gamma_2}\right) \text{ and } A_1^{\mathrm{PA}} = \beta\lambda^2 \left(\frac{B_1}{\gamma_1} + \frac{B_2}{\gamma_2} + \frac{B_1}{\lambda(1+\gamma_1)}\right).$$

We can compute, when $w \geqslant \nu/\beta$,

$$\frac{\mathrm{d}w}{\mathrm{d}t}(t) = \frac{A^{\mathrm{PAI}}}{w(t)^{\lambda+\gamma_1}} \left(1 + \eta^{\mathrm{PAI}} \left[\frac{w(t)}{w^{\mathrm{PAI}}}\right]^{\gamma_1}\right)$$

where,

$$A^{\mathrm{PAI}} = \left[\frac{\nu}{\beta}\right]^{\lambda+\gamma_1} \frac{c(\lambda) B_1 \nu}{(\lambda+\gamma_1)(\lambda+\gamma_1+1)},\ w^{\mathrm{PAI}} = \frac{\beta}{\nu} \left(\left|\frac{B_2}{B_1}\right| \frac{(\lambda+\gamma_1)(\lambda+\gamma_1+1)}{\gamma_2(\lambda+1)}\right)^{1/\gamma_1},$$

and,

$$\eta^{\mathrm{PAI}} = \left|\frac{B_2}{B_1}\right| \frac{B_1}{B_2}.$$

Proof. For $w \geqslant 0$, we have to calculate,

$$I_1 \overset{\text{def.}}{=} \int (\nu - \beta x)^+ z_1 \Pi_w^{\mathrm{PA}}(\mathrm{d}x, \mathrm{d}z), \text{ and } I_2 \overset{\text{def.}}{=} \lambda \int z_2 \Pi_w^{\mathrm{PA}}(\mathrm{d}x, \mathrm{d}z).$$

We have,

$$I_2 = \frac{\lambda B_2}{\gamma_2} \int (\nu - \beta x)^+ \Pi_w^{\mathrm{PA}}(\mathrm{d}x, \mathrm{d}z) = \frac{\lambda B_2}{\gamma_2} \int_0^{\frac{\nu}{\beta w}} (\nu - \beta w y)\, Q(y)\, \mathrm{d}y$$

We have two cases, if $w \ll \nu/\beta$, then,

$$I_2 = \frac{\lambda B_2}{\gamma_2} (\nu - \beta w \lambda).$$

And, if $w \geqslant \nu/\beta$,

$$\begin{aligned} I_2 &= c(\lambda) \frac{\lambda B_2}{\gamma_2} \int_0^{\frac{\nu}{\beta w}} (\nu - \beta w y)\, y^{\lambda-1}\, \mathrm{d}y \\ &= c(\lambda) \frac{\lambda B_2}{\gamma_2} \nu \left[\frac{\nu}{\beta w}\right]^{\lambda} \left(\frac{\nu}{\lambda} - \frac{1}{\lambda+1}\right) = c(\lambda) \frac{B_2}{\gamma_2} \frac{\nu}{\lambda+1} \left[\frac{\nu}{\beta w}\right]^{\lambda} \end{aligned}$$

Then,

$$I_1 = \int \max(0, \nu - \beta x) z_1 \Pi_w^{\mathrm{PA}}(\mathrm{d}x, \mathrm{d}z) = \int_0^{\frac{\nu}{\beta w}} (\nu - \beta w y)\, B_1 y^{\gamma_1} Q(y)\, \mathrm{d}y$$

We have two cases again, if $w \ll \nu/\beta$, then,

$$I_1 = \frac{\lambda B_1}{\gamma_1} (\nu - \beta w \lambda) - \frac{\lambda B_1}{\gamma_1 + \lambda + 1} \beta w$$

Again, if $w \geqslant \nu/\beta$,

$$\begin{aligned} I_1 &= \int \max(0, \nu - \beta x) z_1 \Pi_w^{\mathrm{PA}}(\mathrm{d}x, \mathrm{d}z) = c(\lambda) \int_0^{\frac{\nu}{\beta w}} (\nu - \beta w y)\, B_1 y^{\gamma_1} y^{\lambda-1}\, \mathrm{d}y \\ &= \frac{c(\lambda) B_1 \nu}{(\lambda+\gamma_1)(\lambda+\gamma_1+1)} \left[\frac{\nu}{\beta w}\right]^{\lambda+\gamma_1} \end{aligned}$$

□

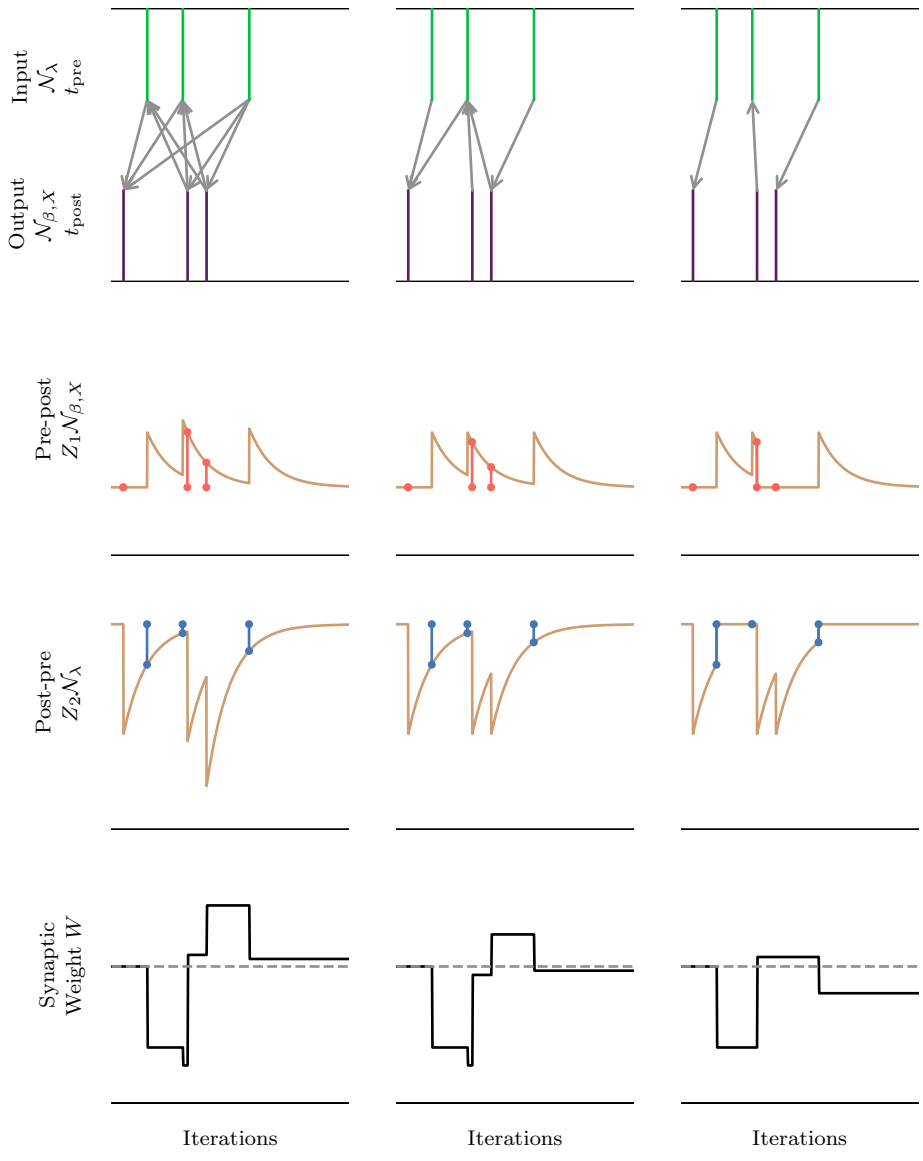

(a) Hebbian all-to-all pair-based rules

(b) Hebbian nearest neighbor symmetric pair-based rules

(c) Hebbian nearest neighbor symmetric reduced pair-based rules

Figure 4.5: **Markovian formulation of pair-based models.**
(a) Temporal dynamics of (X, Z_1, Z_2, W) with a specific pre- and postsynaptic spike trains for all-to-all STDP. (first line) Pre- and postsynaptic spike trains, with associated pairings. (second line) Presynaptic plasticity variable Z_1 (in brown) with value at jumps of the postsynaptic neuron (in red). (third line) Postsynaptic plasticity variable Z_2 (in brown) with value at jumps of the presynaptic neuron (in blue). (fourth line) Resulting dynamics of the synaptic weight W. (b) Same as (a) for nearest neighbor symmetric STDP. (c) Same as (a) for nearest neighbor symmetric reduced STDP.

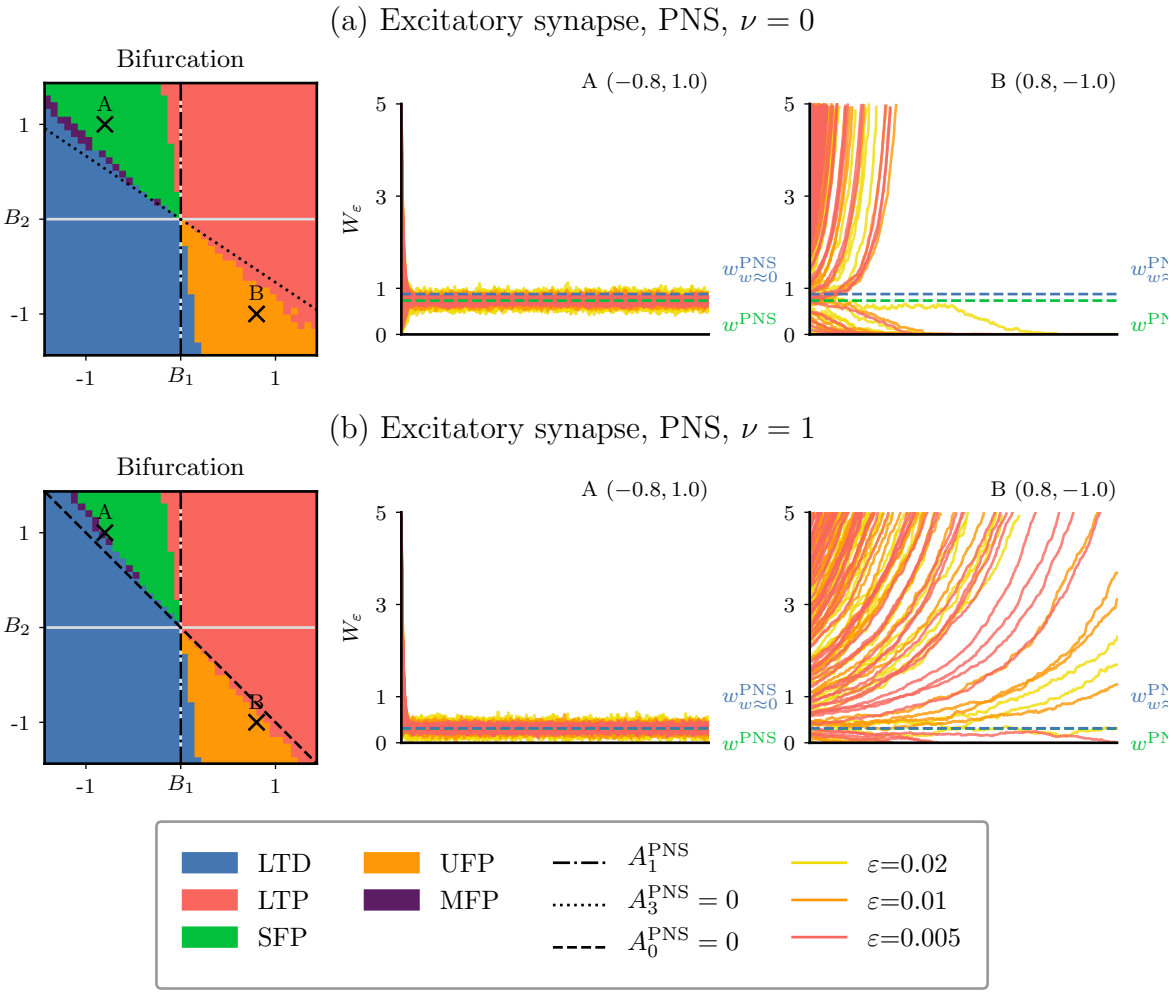

Figure 4.6: **Nearest neighbor symmetric pair-based STDP for an excitatory synapse.** (a) Dynamics of the synaptic weight as a function of B_1 and B_2 for ν=0. (left) Classification based on numerical simulations for different asymptotic dynamics of the synaptic weights (see different colors). Theoretical boundaries are also drawn (see legend for their expressions). (right) Two examples of temporal evolutions of the synaptic weights, for different values of ε. (b) Same as (a) for ν=1.
(γ_1=γ_2=β=λ=1)

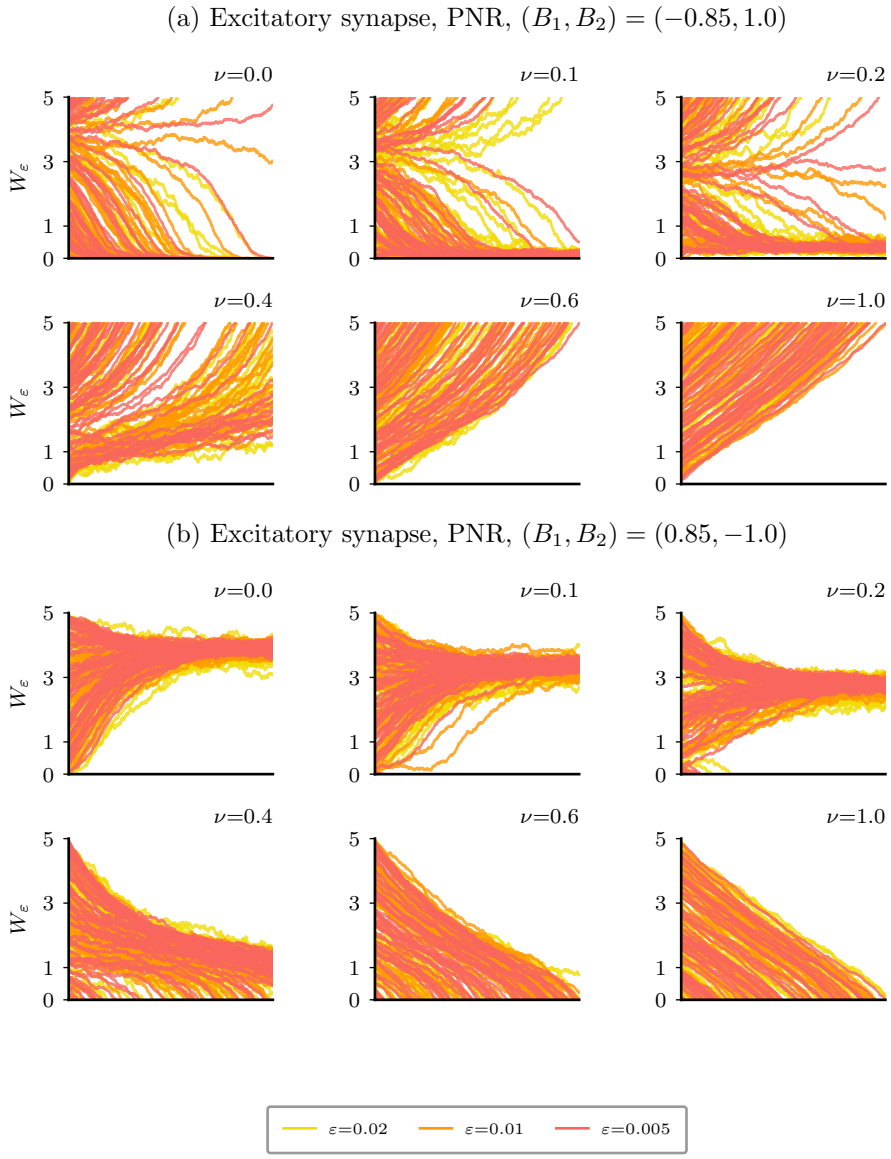

Figure 4.7: **Influence of ν on dynamics with the pair-based nearest-neighbor reduced symmetric scheme.**
(a) Dynamics of the synaptic weight for different values of ϵ (change of color) and values of external input ν (different plots, increasing from left to right, top to down) for anti-Hebbian STDP. (b) Same as (a) for Hebbian STDP.
(γ_1=γ_2=β=λ=1)

BIBLIOGRAPHY

[AG00] R. Azouz and C. M. Gray. Dynamic spike threshold reveals a mechanism for synaptic coincidence detection in cortical neurons in vivo. *Proceedings of the National Academy of Sciences* **97** (July 2000), 8110–8115.

[BA16] B. Babadi and L. F. Abbott. Stability and Competition in Multi-spike Models of Spike-Timing Dependent Plasticity. *PLoS computational biology* **12** (Mar. 2016), e1004750.

[BGH07] A. N. Burkitt, M. Gilson, and J. L. van Hemmen. Spike-timing-dependent plasticity for neurons with recurrent connections. *Biological Cybernetics* **96** (May 2007), 533–546.

[BK12] K. S. Burbank and G. Kreiman. Depression-biased reverse plasticity rule is required for stable learning at top-down connections. *PLoS computational biology* **8** (2012), e1002393.

[BMG04] A. N. Burkitt, H. Meffin, and D. B. Grayden. Spike-timing-dependent plasticity: the relationship to rate-based learning for models with weight dynamics determined by a stable fixed point. *Neural Computation* **16** (May 2004), 885–940.

[BP98] G.-q. Bi and M.-m. Poo. Synaptic Modifications in Cultured Hippocampal Neurons: Dependence on Spike Timing, Synaptic Strength, and Postsynaptic Cell Type. *Journal of Neuroscience* **18** (Dec. 1998), 10464–10472.

[BSY19] R. Berner, E. Schöll, and S. Yanchuk. Multiclusters in Networks of Adaptively Coupled Phase Oscillators. *SIAM Journal on Applied Dynamical Systems* **18** (Jan. 2019), 2227–2266.

[CF03] H. Câteau and T. Fukai. A stochastic method to predict the consequence of arbitrary forms of spike-timing-dependent plasticity. *Neural Computation* **15** (Mar. 2003), 597–620.

[CM08] A. Citri and R. C. Malenka. Synaptic plasticity: multiple forms, functions, and mechanisms. *Neuropsychopharmacology: Official Publication of the American College of Neuropsychopharmacology* **33** (Jan. 2008), 18–41.

[Fel12] D. E. Feldman. The spike-timing dependence of plasticity. *Neuron* **75** (Aug. 2012), 556–571.

[FGV05] E. Fino, J. Glowinski, and L. Venance. Bidirectional activity-dependent plasticity at corticostriatal synapses. *The Journal of Neuroscience: The Official Journal of the Society for Neuroscience* **25** (Dec. 2005), 11279–11287.

[GBV10] M. Gilson, A. Burkitt, and L. J. Van Hemmen. STDP in Recurrent Neuronal Networks. *Frontiers in Computational Neuroscience* **4** (2010).

[GK02a] W. Gerstner and W. M. Kistler. Mathematical formulations of Hebbian learning. *Biological Cybernetics* **87** (Dec. 2002), 404–415.

[GK02b] W. Gerstner and W. M. Kistler. Spiking Neuron Models: Single Neurons, Populations, Plasticity. Cambridge University Press, Aug. 2002.

[GMH11] M. Gilson, T. Masquelier, and E. Hugues. STDP allows fast rate-modulated coding with Poisson-like spike trains. *PLoS computational biology* **7** (Oct. 2011), e1002231.

[GP60] E. N. Gilbert and H. O. Pollak. Amplitude Distribution of Shot Noise. *Bell System Technical Journal* **39** (Mar. 1960), 333–350.

[HNA06] J. S. Haas, T. Nowotny, and H. D. I. Abarbanel. Spike-timing-dependent plasticity of inhibitory synapses in the entorhinal cortex. *Journal of Neurophysiology* **96** (Dec. 2006), 3305–3313.

[ID03] E. M. Izhikevich and N. S. Desai. Relating STDP to BCM. *Neural Computation* **15** (July 2003), 1511–1523.

[KGH01] R. Kempter, W. Gerstner, and J. L. van Hemmen. Intrinsic stabilization of output rates by spike-based Hebbian learning. *Neural Computation* **13** (Dec. 2001), 2709–2741.

[KGH99] R. Kempter, W. Gerstner, and J. L. van Hemmen. Hebbian learning and spiking neurons. *Physical Review E* **59** (Apr. 1999), 4498–4514.

[KH00] W. M. Kistler and J. L. v. Hemmen. Modeling Synaptic Plasticity in Conjunction with the Timing of Pre- and Postsynaptic Action Potentials. *Neural Computation* **12** (Feb. 2000), 385–405.

[Löc17] E. Löcherbach. Large deviations for cascades of diffusions arising in oscillating systems of interacting Hawkes processes. *arXiv:1709.09356 [math]* (Sept. 2017).

[LS14] Y. Luz and M. Shamir. The Effect of STDP Temporal Kernel Structure on the Learning Dynamics of Single Excitatory and Inhibitory Synapses. *PLoS ONE* **9** (July 2014), e101109.

[Luc+16] L. Lucken, O. V. Popovych, P. A. Tass, and S. Yanchuk. Noise-enhanced coupling between two oscillators with long-term plasticity. *Physical Review E* **93** (Mar. 2016), 032210.

[MAD07] A. Morrison, A. Aertsen, and M. Diesmann. Spike-timing-dependent plasticity in balanced random networks. *Neural Computation* **19** (June 2007), 1437–1467.

[MDC01] S. Mahon, J. M. Deniau, and S. Charpier. Relationship between EEG potentials and intracellular activity of striatal and cortico-striatal neurons: an in vivo study under different anesthetics. *Cerebral Cortex (New York, N.Y.: 1991)* **11** (Apr. 2001), 360–373.

[MDG08] A. Morrison, M. Diesmann, and W. Gerstner. Phenomenological models of synaptic plasticity based on spike timing. *Biological Cybernetics* **98** (June 2008), 459–478.

[PG06b] J.-p. Pfister and W. Gerstner. Beyond Pair-Based STDP: a Phenomenological Rule for Spike Triplet and Frequency Effects. *Advances in Neural Information Processing Systems*. Vol. 18. MIT Press, 2006.

[Pid+11] M. Pidoux, S. Mahon, J.-M. Deniau, and S. Charpier. Integration and propagation of somatosensory responses in the corticostriatal pathway: an intracellular study in vivo. *The Journal of Physiology* **589** (Jan. 2011), 263–281.

[RA04] C. C. Rumsey and L. F. Abbott. Equalization of synaptic efficacy by activity- and timing-dependent synaptic plasticity. *Journal of Neurophysiology* **91** (May 2004), 2273–2280.

[RBT00a] M. C. van Rossum, G. Q. Bi, and G. G. Turrigiano. Stable Hebbian learning from spike timing-dependent plasticity. *The Journal of Neuroscience: The Official Journal of the Society for Neuroscience* **20** (Dec. 2000), 8812–8821.

[RBT00b] M. C. W. v. Rossum, G. Q. Bi, and G. G. Turrigiano. Stable Hebbian Learning from Spike Timing-Dependent Plasticity. *Journal of Neuroscience* **20** (Dec. 2000), 8812–8821.

[RL10] P. D. Roberts and T. K. Leen. Anti-Hebbian spike-timing-dependent plasticity and adaptive sensory processing. *Frontiers in Computational Neuroscience* **4** (2010), 156.

[RLS01] J. Rubin, D. D. Lee, and H. Sompolinsky. Equilibrium properties of temporally asymmetric Hebbian plasticity. *Physical Review Letters* **86** (Jan. 2001), 364–367.

[Rob00] P. D. Roberts. Dynamics of temporal learning rules. *Phys. Rev. E* **62** (3 Sept. 2000), 4077–4082.

[Rob99] P. D. Roberts. Computational Consequences of Temporally Asymmetric Learning Rules: I. Differential Hebbian Learning. *Journal of Computational Neuroscience* **7** (Nov. 1999), 235–246.

[RV21a] P. Robert and G. Vignoud. Averaging Principles for Markovian Models of Plasticity. *Journal of Statistical Physics* **183** (June 2021), 47–90.

[RV21b] P. Robert and G. Vignoud. Stochastic Models of Neural Plasticity. *SIAM Journal on Applied Mathematics* **81** (Sept. 2021), 1821–1846.

[RV21c] P. Robert and G. Vignoud. Stochastic Models of Neural Synaptic Plasticity: A Scaling Approach. *SIAM Journal on Applied Mathematics* **81** (2021), 2362–2386.

[SJT07] D. Standage, S. Jalil, and T. Trappenberg. Computational consequences of experimentally derived spike-time and weight dependent plasticity rules. *Biological Cybernetics* **96** (June 2007), 615–623.

[TAG18] M. A. Triplett, L. Avitan, and G. J. Goodhill. Emergence of spontaneous assembly activity in developing neural networks without afferent input. *PLoS Computational Biology* **14** (Sept. 2018), e1006421.

[TDM14] T. Takeuchi, A. J. Duszkiewicz, and R. G. M. Morris. The synaptic plasticity and memory hypothesis: encoding, storage and persistence. *Philosophical Transactions of the Royal Society of London. Series B, Biological Sciences* **369** (Jan. 2014), 20130288.

[ZD07] Q. Zou and A. Destexhe. Kinetic models of spike-timing dependent plasticity and their functional consequences in detecting correlations. *Biological Cybernetics* **97** (July 2007), 81–97.

CHAPTER 5

A MARKOVIAN APPROACH TO HAWKES PROCESSES

ABSTRACT

In this paper, stationary non-linear Hawkes processes are revisited by formulating the Hawkes dependence as a Markovian property on the space of non-negative sequences. A characterization of the associated point process is obtained in terms of the solution of stochastic differential equations. When the influence of past jumps decreases exponentially over time, the Palm measure of the associated stationary point process is expressed with the distribution of the stationary version of a one-dimensional Harris ergodic Markov chain. Finally a scaling result for some Hawkes processes exhibiting a blow-up phenomenon is derived.

5.1 Introduction

The references [RV21b; RV21c; RV21a; RV22b] have introduced a class of general stochastic models describing the influence synaptic plasticity in stochastic neuronal networks. In such models, the firing rate of the postsynaptic neuron depends on the postsynaptic potential membrane, which is driven by the spiking activity of the presynaptic neuron, $\mathcal{N}_\lambda$, and also by its own spiking activity, $\mathcal{N}_{\beta,X}$.

An important class of mathematical models, Hawkes processes, has a similar feature: given the past instants t_n, $n\geqslant 1$ of a *Hawkes process* up to time t, the rate at which a new jump occurs in the time interval $(t, t+\mathrm{d}t)$ is given by

$$\Phi\left(\sum_{n:t_n\leqslant t} h(t-t_n)\right).$$

The function h, the memory function, expresses the impact at time t of a jump which has occurred at time $s<t$ with the quantity $h(t-s)$. The function h is assumed to be non-increasing converging to 0, the influence of a jump in the distant past vanishes. The activation function Φ modulates the global impact of past jumps.

This class of models has been used in various situations such as, mathematical finance, [BH09], population dynamics, [Bou16], biology, [RS10], queueing systems, [DP18], learning theory, [Ete+16], or neurosciences, [GDT17], ...

From a mathematical point of view, these processes have generated, and still generates, a considerable interest. The pioneering works are:

— [HO74] which shows that when the activation function is linear, these processes can be represented by an age-dependent branching process, a special class of the so-called Crump-Mode-Jagers models.

— [Ker64] shows in a more general context, that the functional relation defining stationary Hawkes processes can be expressed as a fixed point equation which can be

solved through a Picard scheme, thereby proving the existence and uniqueness of such processes. [BM96] has considerably developed this approach in a stochastic calculus context.

Up to now, these are in fact the two main approaches to investigate Hawkes processes. Appendix 5.B tries to present some aspects of the overwhelming literature of this domain.

In this work, we reformulate the Hawkes property using the jumps times of the point process. For a stationary Hawkes process, this amounts to investigate the properties of its Palm measure. See Appendix 5.A for a quick introduction and references. This is a preliminary work to investigate Hawkes processes in a multi-dimensional framework where the literature is quite scarce due to the fact that the Picard scheme give only rough conditions for the existence of stationary Hawkes processes.An advantage of this approach is that the Hawkes property can be described in terms of a Markov chain in an infinite dimensional state space for which some tools are available. In the following the term stability will refer to the existence and uniqueness of a stationary Hawkes process.

This paper is organized as follows. Section 5.2 presents some basic definitions, Section 5.3 introduces the Hawkes property in terms of a stochastic differential equation and Section 5.4 gives a characterization of the Palm measure of a stationary Hawkes process as an invariant measure of a Markov chain in the state space of non-negative sequences. Section 5.5 uses this approach to investigate Hawkes process with an exponential memory function. A new, weaker, stability condition is derived and a representation of the Palm measure is obtained in this case. The transient behavior is also analyzed, i.e. when the Hawkes process starting from the null measure blows-up in finite time almost surely. A scaling result for the points of the point process is obtained, it described the accumulation of the points in terms of a Poisson process. Appendix 5.A presents the main definitions and results concerning point processes and the stationarity property.

We conclude this section with a formulation of some conditions for the functions h and Φ that will be used in the rest of the paper.

Assumptions A.

A-1. The memory function. The non-negative function h is continuous on $\mathbb{R}_+$, non-increasing, converging to 0 at infinity and

$$\alpha \stackrel{\text{def.}}{=} \int_0^{+\infty} h(t)\,\mathrm{d}t < +\infty.$$

A-2. The activation function. The non-negative function Φ is continuous and such that,

a) $\Phi(0)>0$;

b) the quantity

$$\beta \stackrel{\text{def.}}{=} \limsup_{y\to+\infty} \frac{\Phi(y)}{y}$$

is finite.

A-3 The constants α and β are such that $\alpha\beta<1$.

5.2 Definitions

Probability space

It is assumed that on the probability space $(\Omega, \mathbb{P})$ is defined a Poisson point process on $\mathbb{R}_+ \times \mathbb{R}$ with intensity measure $\mathrm{d}x \otimes \mathrm{d}y$ and that $(\mathcal{F}_t)$ is a filtration such that, for $t \in \mathbb{R}$, $\mathcal{F}_t$ is the σ-field generated by the random variables $\mathcal{P}(A \times (s,t])$, where A is a Borelian set of $\mathbb{R}_+$ and $s \leqslant t$. If λ and f are non-negative Borelian functions f on $\mathbb{R}$, we define

$$\int_{\mathbb{R}} f(s)\mathcal{P}((0,\lambda(s)],\mathrm{d}s) \stackrel{\text{def.}}{=} \int_{\mathbb{R}_+\times\mathbb{R}} f(s)\mathbb{1}_{\{v\leqslant\lambda(s)\}}\mathcal{P}(\mathrm{d}v,\mathrm{d}s).$$

Without any indication on the filtration, the martingale properties in the paper are understood with respect to this filtration.

State space of non-negative sequences

We refer to Appendix 5.A for general definitions concerning point processes. We denote by $\mathcal{S}$ the space of sequences of non-negative real numbers

$$\mathcal{S} \stackrel{\text{def.}}{=} \left\{x=(x_k)\in(\mathbb{R}_+\cup\{+\infty\})^{\mathbb{N}\setminus\{0\}} : x_{k_0}=+\infty \Rightarrow x_k=+\infty,\ \forall k\geqslant k_0\right\}. \tag{5.1}$$

A functional from $\mathcal{S}$ to the space of positive measures with a mass at 0 is introduced as follows, if $x=(x_k)\in\mathcal{S}$, the positive measure m_x on $\mathbb{R}_-$ is defined by

$$m_x = \delta_0 + \sum_{k=1}^{+\infty}\delta_{t_k}, \quad \text{with } t_k=-\sum_{i=1}^{k}x_i,\ k\geqslant 1, \tag{5.2}$$

with the convention that $\delta_{-\infty}\equiv 0$.

The measure m_x is a positive measure carried by points associated to $x\in\mathcal{S}$. It should be stressed that m_x is not necessarily a point measure, i.e it may not have Radon property, since we do not exclude the fact that the sequence (x_k) converges to 0 sufficiently fast so that the measure m_x may have a finite accumulation point.

Let $x=(x_k)_{k>0}$ be an element of $\mathcal{S}$. Note that 0 is always a point of m_x and that the coordinates of x are the inter-arrivals times of m_x, in particular x_1 is the distance to the first point of m_x on the left of 0. The point measures with a finite number of points correspond to sequences (x_k) which are constant and equal to $+\infty$ after some finite index. In this case, if k_0 is the first index where $x_{k_0}=+\infty$, with a slight abuse of notation we write it as a finite vector $x=(x_1,x_2,\ldots,x_{k_0-1},+\infty)$.

On $\mathcal{S}$, the distance, for $x=(x_k)$, $y=(y_k)\in\mathcal{S}$,

$$d(x,y) = \sum_{1}^{+\infty}\frac{1}{2^k}\,\min(|x_k-y_k|,1), \tag{5.3}$$

with the convention, for $u\in\mathbb{R}_+$, $|u-\infty|=|\infty-u| = +\infty$ and $|\infty-\infty|=0$. It easily checked that $\mathcal{S}$ is a separable Polish space, i.e. a complete separable metric space.

An important subset of $\mathcal{S}$ is

$$\mathcal{S}_h \stackrel{\text{def.}}{=} \left\{x=(x_k)\in\mathcal{S} : h(0) + \sum_{k=1}^{+\infty}h\left(\sum_{i=1}^{k}x_i\right) = \int_0^{+\infty}h(u)\,\breve{m}_x(\mathrm{d}u)<+\infty\right\}, \tag{5.4}$$

with Definition (5.30) of $\breve{m}$ of the Appendix, we have $x\in\mathcal{S}_h$ if $h\in L_1(\breve{m}_x)$.

Definition 59. *For $x\in\mathcal{S}$ and $a\geqslant 0$, we set*

$$\mathcal{T}(x,a) \stackrel{\text{def.}}{=} \inf_{t\geqslant 0}\left\{\int_0^t \Phi\left(h(0)+\sum_{k\geqslant 1} h\left(s+\sum_{i=1}^k x_i\right)\right)\,\mathrm{d}s \geqslant a\right\} \tag{5.5}$$
$$= \inf_{t\geqslant 0}\left\{\int_0^t \Phi\left(\int h\,(s-u)\; m_x(\mathrm{d}u)\right)\mathrm{d}s \geqslant a\right\},$$

if $x\in\mathcal{S}_h$ and $\mathcal{T}(x,a)\stackrel{\text{def.}}{=}0$ if $x\in\mathcal{S}\backslash\mathcal{S}_h$, with the convention $h(+\infty)=0$.

Lemma 60. *Under Assumptions A-1 and A-2-a, if $x\in\mathcal{S}_h$, then*

$$\lim_{t\to+\infty}\int_0^t \Phi\left(\int h\,(s-u)\right)\, m(\mathrm{d}u)\,\mathrm{d}s = +\infty.$$

In particular, for $x\in\mathcal{S}_h$ and $a\geqslant 0$, the variable $\mathcal{T}(x,a)$ is finite.

Proof. Note that, for any $t\geqslant 0$, the monotonicity property of h gives the relation

$$\int_{(-\infty,0)} h(t-u)m_x(\mathrm{d}u) \leqslant \int_{(-\infty,0)} h(-u)m_x(\mathrm{d}u) < +\infty,$$

and with Lebesgue's Theorem we obtain the identity

$$\lim_{t\to+\infty}\int_{(-\infty,0)} h(t-u)m_x(\mathrm{d}x) = 0. \tag{5.6}$$

Our lemma is proved since Φ is continuous with $\Phi(0)>0$. □

5.3 Hawkes SDEs

We first recall the classical definition of an Hawkes process, see [HO74].

Definition 61. *A* Hawkes process *is a point process $\mathcal{N}$ on $\mathbb{R}$ such that, for any $s\in\mathbb{R}$, the process*

$$\left(\mathcal{N}((s,t])-\int_s^t \Phi\left(\int_{(-\infty,u)} h(u-x)\mathcal{N}(\mathrm{d}x)\right)\mathrm{d}u, t\geqslant s\right)$$

is a local martingale with respect to the filtration $(\mathcal{F}_t, t\geqslant s)$, where, for $t\in\mathbb{R}$, $\mathcal{F}_t$ is the σ-field containing the σ-field associated to the random variables $\mathcal{N}((u,v])$, $u\leqslant v\leqslant t$.

If $\mathcal{N}$ is a Hawkes process, for any $s\in\mathbb{R}$ the dual predictable projection of the process of $(\mathcal{N}((s,t]), t\geqslant s)$ is almost surely,

$$\left(\int_s^t \Phi\left(\int_{(-\infty,u)} h(u-x)\mathcal{N}(\mathrm{d}x)\right)\mathrm{d}u, t\geqslant s\right),$$

see Theorem VI (21.7) of [RW00] for example. In the terminology of random measures, see [Jac79], the *stochastic intensity* of $\mathcal{N}$ is

$$\left(\Phi\left(\int_{(-\infty,u)} h(u-x)\mathcal{N}(\mathrm{d}x)\right), u\in\mathbb{R}\right).$$

We now introduce a dynamical system extending a Radon measure on $\mathbb{R}_-$ into a measure on $\mathbb{R}$ exhibiting a Hawkes property on $\mathbb{R}_+$. The Markovian approach used in this paper relies heavily on this construction.

Proposition 62 (Hawkes SDE)**.** *If $m\in\mathcal{M}_p(\mathbb{R}_-)$ verifies $h\in L_1(\breve{m})$, then there exists a unique positive random measure $\mathcal{N}_m$ on $\mathbb{R}$ such that $\mathcal{N}_m\equiv m$ on $\mathbb{R}_-$, the counting measure $(\mathcal{N}_m((0,t]), t\geqslant 0)$ satisfies the stochastic differential equation*

$$\mathrm{d}\mathcal{N}_m((0,t]) = \mathcal{P}\left(\left(0, \Phi\left(\int_{(-\infty,t)} h(t-x)\mathcal{N}_m(\mathrm{d}x)\right)\right), \mathrm{d}t\right), \tag{5.7}$$

for all $t>0$.

Under Assumptions A-1 and A-2-(a), the points of $\mathcal{N}_m$ on $\mathbb{R}_+$ form a non-decreasing sequence of stopping times (T_n), such that if

$$E_1 \overset{\text{def.}}{=} \int_0^{T_1} \Phi\left(\int_{(-\infty,s)} h\left(s-x\right)\mathcal{N}_m(\mathrm{d}x)\right)\mathrm{d}s$$
$$\text{and } E_{n+1} \overset{\text{def.}}{=} \int_{T_n}^{T_{n+1}} \Phi\left(\int_{(-\infty,s)} h\left(s-x\right)\mathcal{N}_m(\mathrm{d}x)\right)\mathrm{d}s, \quad n\geqslant 1, \tag{5.8}$$

then $(E_n, n\geqslant 1)$ is an i.i.d. sequence of exponential random variables with parameter 1 and E_1 is independent of $\mathcal{F}_0$ and, for $n\geqslant 1$, the sequence $(E_k, k>n)$ is independent of $\mathcal{F}_{T_n}$.

Proof. The proof is done by constructing by induction the sequence of points (T_n) of $\mathcal{N}_m$.

$$T_1 \overset{\text{def.}}{=} \inf\left\{t\geqslant 0 : \int_{(0,t]} \mathcal{P}\left(\left(0, \Phi\left(\int_{(-\infty,0]} h(s-x)m(\mathrm{d}x)\right)\right), \mathrm{d}s\right) \neq 0\right\},$$

Two cases are then possible, either $T_1=+\infty$, and, in this case $\mathcal{N}_m=m$, or $T_1<+\infty$ and we can go on to the next iteration.

By induction, for $n\geqslant 1$, if $T_1\leqslant T_2\leqslant\cdots\leqslant T_n<+\infty$, it is possible to define

$$T_{n+1} \overset{\text{def.}}{=} \inf\left\{t\geqslant T_n :\right.$$
$$\left.\int_{(T_n,t]} \mathcal{P}\left(\Phi\left(\int_{(-\infty,0]} h(s-x)m(\mathrm{d}x)\right) + \sum_{k=1}^{n} h\left(s-T_k\right), \mathrm{d}s\right) \neq 0\right\}, \tag{5.9}$$

Again, if $T_{n+1}=+\infty$, we have,

$$\mathcal{N}_m = m + \sum_{k=1}^{n} \delta_{T_k},$$

if not, we can build T_{n+2}. The first part of the proposition is proved, as $\mathcal{N}_m$ has been build verifying (5.7) directly proving existence and uniqueness.

For $t\geqslant 0$, the independence properties of the Poisson process $\mathcal{P}$ give

$$\mathbb{P}(T_1\geqslant t \mid \mathcal{F}_0) = \exp\left(-\int_0^t \Phi\left(\int_{(-\infty,0]} h(s-x)m(\mathrm{d}x)\right)\mathrm{d}s\right). \tag{5.10}$$

From Lemma 60, we obtain

$$\lim_{t\to+\infty} \mathbb{P}(T_1\geqslant t) = 0,$$

so that the variable T_1 is almost surely finite and it clearly has the stopping time property.

Define

$$E_1 \stackrel{\text{def.}}{=} \int_0^{T_1} \int_{(-\infty,0]} h(s-x)m(\mathrm{d}x)\,\mathrm{d}s,$$

from Relation (5.10), we get

$$\mathbb{P}(E_1 \geqslant t \mid \mathcal{F}_0) = \mathbb{P}\left(\int_0^{T_1} \Phi\left(\int_{(-\infty,0]} h(s-x)m(\mathrm{d}x)\right)\mathrm{d}s \geqslant t\right) = e^{-t},$$

hence E_1 is exponentially distributed with parameter 1 and independent of $\mathcal{F}_0$. Using Definition (5.5), the random variable T_1 has the same distribution as the random variable $\mathcal{T}(x, E_1)$ where x is the unique element of $\mathcal{S}$ such that $m{=}m_x$.

If by induction, for $n{\geqslant}1$, the n stopping times $T_1{\leqslant}T_2{\leqslant}\cdots{\leqslant}T_n$ are defined almost surely, T_{n+1} as defined by (5.9) is clearly a stopping time, it is almost surely finite with the same argument as for T_1, and, with the strong Markov property of $\mathcal{P}$ for the stopping time T_n,

$$\mathbb{P}(T_{n+1}{-}T_n \geqslant t \mid \mathcal{F}_{T_n}) = \exp\left(-\int_{T_n}^{T_n+t} \Phi\left(\int_{(-\infty,0]} h(s-x)m(\mathrm{d}x) + \sum_{k=1}^{n} h(s-T_k)\right)\mathrm{d}s\right),$$

hence,

$$\mathbb{P}(E_{n+1} \geqslant t \mid \mathcal{F}_{T_n}) = \mathbb{P}\left(\int_{T_n}^{T_{n+1}} \Phi\left(\int_{(-\infty,0]} h(s-x)\mathcal{N}_m(\mathrm{d}x)\right)\mathrm{d}s \geqslant t \,\middle|\, \mathcal{F}_{T_n}\right) = e^{-t}.$$

proving that E_{n+1} is an exponential random variable.

The strong Markov property of the Poisson process $\mathcal{P}$ gives that E_{n+1} is independent of $\mathcal{F}_{T_n}$. The second part of the proposition is proved. □

In the proof we have seen that the condition $\Phi(0){>}0$ in Lemma 60 guarantees that there is almost surely an infinite number of points in $\mathbb{R}_+$ for SDE (5.7).

Note that it cannot be excluded that this non-decreasing sequence of points may have a finite limit with positive probability and therefore that $\mathcal{N}_m$ is not necessarily a point process. As it will be seen, it can blow-up in finite time, i.e. the limit of its sequence (T_n) of points in $\mathbb{R}_+$ may be finite with positive probability. Proposition 68 gives a condition for which the sequence (T_n) converges almost surely to infinity when m is the null measure. Proposition 77 considers a case when there is such a blow-up and derives a limiting result for the accumulation of points.

However, when the sequence (T_n) is converging almost surely to infinity, $\mathcal{N}_m$ is a point process, and it is not difficult to see that the dual predictable projection of the process of $(\mathcal{N}_m((0,t]), t{\geqslant}0)$ is

$$\left(\int_0^t \Phi\left(\int_{(-\infty,s)} h(s-x)\mathcal{N}_m(\mathrm{d}x)\right)\mathrm{d}s, t{\geqslant}0\right).$$

see Theorem VI (27.1) of [RW00]. Consequently, the stochastic intensity function of $\mathcal{N}_m$ on $\mathbb{R}_+$ is indeed

$$\left(\Phi\left(\int_{(-\infty,s)} h(s-x)\mathcal{N}_m(\mathrm{d}x)\right)\right).$$

Proposition 62 extends a point measure m on $\mathbb{R}_-$ to a point process on $\mathbb{R}$, it can be also seen as a dynamical system on point processes on $\mathbb{R}_-$ in the following way.

A dynamical system

If $m \in \mathcal{M}_p(\mathbb{R}_-)$ is such that $h \in L_1(\check{m})$ and $\mathcal{N}_m$ defined by Relation (5.7) is a point process, for $t \geqslant 0$, we introduce a (random) dynamical system $(T_t(m))$ in $\mathcal{M}_p(\mathbb{R}_-)$ as,

$$\int_{(-\infty,0]} f(x) T_t(m)(\mathrm{d}x) = \int f(x) \theta_t \circ \mathcal{N}_m(\mathrm{d}x) = \int_{(-\infty,t]} f(x-t) \mathcal{N}_m(\mathrm{d}x), \tag{5.11}$$

for any non-negative Borelian function on $\mathbb{R}_-$, $T_t(m)$ is the point process $\mathcal{N}_m$ seen from the point t.

A stationary Hawkes point process is in particular associated to a distribution Q on $\mathcal{M}_p(\mathbb{R}_-)$ which is invariant distribution for the group of transformations (θ_t) on $\mathcal{M}_p(\mathbb{R})$. See Definition 78 in Section 5.A.

When $\Phi(0)=0$, the null measure is clearly a solution of Relation (5.7). The next proposition shows that, under some mild condition, the null point process is the unique stationary Hawkes process in such a case.

Proposition 63. *Under Assumptions A-1 and*

$$\int_{\mathbb{R}_+} t h(t)\, \mathrm{d}t < +\infty,$$

if for some $K \geqslant 0$, the non-negative function Φ satisfies the relation $\Phi(x) \leqslant Kx$, for all $x \geqslant 0$, then there does not exist a stationary Hawkes process $\mathcal{N}$ which is non-trivial, i.e. such that $\mathbb{P}(\mathcal{N} \neq 0) > 0$.

Under the additional condition that the function Φ is Lipschitz with constant K such that $\alpha K < 1$, this result is given by Theorem 1 of [BM96; BM01].

Proof. Fix $\lambda > 0$. Since the set of the distributions of stationary Hawkes processes whose intensity is less than $\lambda > 0$ is a convex and closed subset of the unit ball of $\mathcal{P}(\mathcal{M}_p(\mathbb{R}))$, it is therefore compact by the Banach-Alaoglu theorem. See [Rud73]. If there is a non-trivial stationary Hawkes processes, by Choquet's Theorem, there exists a non-trivial ergodic distribution with respect to the flow (θ_t). See Proposition 12.4 and Choquet's Theorem of [Phe01]. The Birkhoff-Khinchin ergodic theorem, see [CFS82], gives the almost sure convergence

$$\lim_{t \to +\infty} \frac{\mathcal{N}((0,t])}{t} = \mathbb{E}(\mathcal{N}((0,1]) > 0,$$

since $\mathcal{N}$ is non-trivial, we obtain therefore that $\mathbb{P}(\mathcal{N}(\mathbb{R}_+) = +\infty) = 1$. If T_1 is the first positive point of $\mathcal{N}$, the variable T_1 is in particular finite with probability 1.

As in the proof of Proposition 62, we have

$$\mathbb{P}(T_1 \geqslant t \mid \mathcal{F}_0) = \exp\left(- \int_0^t \Phi\left(\int_{(-\infty,0]} h(s-x) \mathcal{N}(\mathrm{d}x) \right) \mathrm{d}s \right)$$

By Fubini's Theorem, we have

$$\begin{aligned} V \overset{\text{def.}}{=} \int_0^{+\infty} \Phi\left(\int_{(-\infty,0]} h(s-x) \mathcal{N}(\mathrm{d}x) \right) \mathrm{d}s &\leqslant K \int_0^{+\infty} \int_{(-\infty,0]} h(s-x) \mathcal{N}(\mathrm{d}x)\, \mathrm{d}s \\ &= K \int_0^{+\infty} \mathcal{N}([-s,0]) h(s)\, \mathrm{d}s. \end{aligned}$$

The stationary property of the point process $\mathcal{N}$ shows that there exists some $\lambda>0$ such that $\mathbb{E}(\mathcal{N}([-s,0]))=\lambda s$, for all $s\geqslant 0$. The integrability of $(th(t))$ gives that V is an integrable random variable, and therefore, is almost surely finite. As a consequence we have that, almost surely, $\mathbb{P}(T_1=+\infty|\mathcal{F}_0)>0$. This is a contradiction. The proposition is proved. □

5.4 A Markov chain formulation

A different formulation of the stationary Hawkes process

In this section, we give an alternative version of Proposition 62 in terms of a Markovian dependence on the state space of sequences. We begin by a characterization of the Palm measure of a stationary Hawkes process.

Proposition 64. *If Conditions A-1 and A-2 a) hold and if Q is the distribution on $\mathcal{M}_p(\mathbb{R})$ of a stationary Hawkes process $\mathcal{N}=(t_n, n\in\mathbb{Z})$ associated to Φ and h then, the sequence of inter-arrivals $(\tau_n, n\in\mathbb{Z})\stackrel{\text{def.}}{=}(t_n-t_{n-1}, n\in\mathbb{Z})$ is a stationary sequence under its associated Palm measure $\widehat{Q}$. Moreover, the sequence of random variables*

$$\left(\int_0^{\tau_{n+1}}\Phi\left(\sum_{k\leqslant n}h\left(s+\sum_{i=k+1}^{n}\tau_i\right)\right)\,\mathrm{d}s,\quad n\in\mathbb{Z}\right), \tag{5.12}$$

is i.i.d. with a common exponential distribution with parameter 1.

If there exists a stationary sequence $(\tau_n, n\in\mathbb{Z})$ satisfying Relation (5.12), then there exists a stationary Hawkes process associated to Φ and h.

Proof. From the point of view of Proposition 62 this proposition is quite intuitive, one has nevertheless to be careful, as always in this setting since Proposition 62 is stated under the distribution Q.

The stationary property of the sequence $(\tau_n, n\in\mathbb{Z})\stackrel{\text{def.}}{=}(T_n-T_{n-1})$ under $\widehat{Q}$ is clear, by definition of $\widehat{Q}$. To prove the second part of the proposition, we use Proposition 11.8, page 315 of [Rob03] which gives that

$$\lim_{t\searrow 0}\mathbb{E}_Q\left(f\mid\mathcal{N}([-t,0])\neq 0\right)=E_{\widehat{Q}}(f),$$

where $\mathbb{E}_R$ denotes the expectation with respect to the distribution R on $\mathcal{M}_p(\mathbb{R})$ and f is a bounded Borelian function on $\mathcal{M}_p(\mathbb{R})$ such that $t\mapsto f(\theta_t(m))$ is Q-almost surely right continuous at $t=0$.

For $n\in\mathbb{Z}$ and $m\in\mathcal{M}_p(\mathbb{R})$, define

$$\Psi_n(m)\stackrel{\text{def.}}{=}\int_{t_n(m)}^{t_{n+1}(m)}\Phi\left(\int_{(-\infty,0]}h(s-x)m(\mathrm{d}x)\right)\,\mathrm{d}s,$$

then, since , Q-almost surely, we have $t_0(m)<0<t_1(m)$ and $t_n(m)<t_{n+1}(m)$, for $t\geqslant 0$ sufficiently small,

$$\Psi_n(\theta_t(m))=\int_{t_n(m)-t}^{t_{n+1}(m)-t}\Phi\left(\int_{(-\infty,-t]}h(s-x+t)m(\mathrm{d}x)\right)\,\mathrm{d}s.$$

By continuity of Φ and h, we get that

$$\lim_{t\searrow 0} \Psi_n(\theta_t(m)) = \Psi_n(m),$$

Q-almost surely. Let F be a continuous bounded Borelian function on $\mathbb{R}_+^n$ then

$$\lim_{t\searrow 0} \mathbb{E}_Q\left[F\left(\Psi_i\left(\mathcal{N}\right), 1\leqslant i\leqslant n\right) \mid \mathcal{N}([-t,0])\neq 0\right] = \mathbb{E}_{\widehat{Q}}\left[F\left(\Psi_i\left(\mathcal{N}\right), 1\leqslant i\leqslant n\right)\right].$$

Since the event $\{\mathcal{N}([-x,0])\neq 0\}$ is $\mathcal{F}_0$-measurable and that for any $1\leqslant k\leqslant n$, the variable

$$\int_{t_k}^{t_{k+1}} \Phi\left(\int_{(-\infty,s]} h\left(s-x\right)\mathcal{N}(\mathrm{d}x)\right)\,\mathrm{d}s$$

is independent of $\mathcal{F}_{t_k}$, we get with Proposition 62 again, by induction on k for example, that

$$\lim_{t\searrow 0} \mathbb{E}_Q\left[F\left(\Psi_i\left(\mathcal{N}\right), 1\leqslant i\leqslant n\right) \mid \mathcal{N}([-t,0])\neq 0\right] = \mathbb{E}\left[F\left(E_i, 1\leqslant i\leqslant n\right)\right],$$

where $(E_i, 1\leqslant i\leqslant n)$ are n independent random variables with a common exponential distribution with parameter 1. By gathering these results we obtain that

$$\mathbb{E}_{\widehat{Q}}\left[F\left(\Psi_i\left(\mathcal{N}\right), 1\leqslant i\leqslant n\right)\right] = \mathbb{E}\left[F\left(E_i, 1\leqslant i\leqslant n\right)\right].$$

Under the probability distribution $\widehat{Q}$, the random variables $\Psi_i\left(\cdot\right)$, $1\leqslant i\leqslant n$, are i.i.d. with a common exponential distribution with parameter 1 Relation (5.12) is a consequence of the relation

$$\Psi_n(\mathcal{N}) = \int_{t_n}^{t_{n+1}} \Phi\left(\sum_{k\leqslant n} h\left(s-t_k\right)\right)\,\mathrm{d}s = \int_0^{\tau_{n+1}} \Phi\left(\sum_{k\leqslant n} h\left(s+\sum_{i=k+1}^{n}\tau_i\right)\right)\,\mathrm{d}s,$$

by invariance of $\widehat{Q}$ with respect to $\widehat{\theta}$, the sequence $(\Psi_n(\cdot))_{n\geqslant 1}$ is stationary under $\widehat{Q}$ and, therefore, is i.i.d. with a common exponential distribution with parameter 1.

Now we assume that there exists a stationary sequence $\underline{\tau}=(\tau_n, n\in\mathbb{Z})$ of integrable random variables satisfying Relation (5.12). Recall that m_τ is the point process defined by Relation (5.2). Using a similar proof as in Proposition 62, we can show that m_τ satisfies an Hawkes SDE (5.7) on $\mathbb{R}$. For $u\in\mathbb{R}$, the same property clearly holds for $\theta_u(m_\tau)$, the point process m_τ translated at u, see Definition (5.32). For $K>0$, let U_K be an independent uniform random variable on $[-K,K]$, the point process $\theta_{U_K}(m_\tau)$ satisfies the Hawkes property. With the same method used for the proof of Proposition 11.2 of [Rob03], we obtain that, as K goes to infinity, $\theta_{U_K}(m_\tau)$ converges in distribution to a stationary point process whose Palm measure is given by the distribution τ. It is not difficult to show that the Hawkes property is preserved in the limit. The proposition is proved. □

We can now state the main result concerning the relation between the Hawkes SDE and the Markov transition kernel $\mathcal{K}$.

Proposition 65. *The Markov chain associated to transition kernel $\mathcal{K}$ of Definition* (5.14) *has an invariant distribution with integrable coordinates if and only if there exists a stationary Hawkes process.*

Proof. If there exists a stationary Hawkes point process (t_n), Proposition 64 shows that the distribution of $(t_{n+1}-t_n)$ under its Palm distribution is an invariant distribution of the Markov chain $(\mathcal{X}_n)$. Conversely, if the Markov chain associated to transition kernel $\mathcal{K}$ has an invariant distribution, then one can construct a stationary version of the Markov chain $\mathcal{X} \stackrel{\text{def.}}{=} (\mathcal{X}_n)$, in particular $\mathcal{X}$ satisfies Relation (5.12). Proposition 64 shows then that there exists a stationary Hawkes point process in this case. □

A Markov chain on $\mathcal{S}$

The previous proposition has highlighted the importance of the Palm space, and therefore led us to develop a second formulation of the Hawkes process, conditioned to jumping at $t=0$, using Markovian kernels.

Definition 66. *The sequence of random variables $(\mathcal{X}_n^x)$ with initial point $\mathcal{X}_0^x=x\in\mathcal{S}$ is defined by induction, for $n\geqslant 0$,*

$$\mathcal{X}_{n+1}^x=(X_{n+1},\mathcal{X}_n^x)=(\mathcal{T}(\mathcal{X}_n^x,E_{n+1}),\mathcal{X}_n^x), \tag{5.13}$$

where (E_n) is an i.i.d. sequence of exponentially distributed random variables with parameter 1 and $\mathcal{T}$ is defined by Relation (5.5)*.*

The associated Markovian kernel is denoted by $\mathcal{K}$

$$\int_{\mathcal{S}} f(y)\mathcal{K}(x,\mathrm{d}y) = \mathbb{E}_x(f(\mathcal{X}_1^x)), \tag{5.14}$$

for a non-negative Borelian function f on $\mathcal{S}$.

The element $\mathcal{X}_{n+1}^x$ is obtained by shifting $\mathcal{X}_n^x$ and adding $X_{n+1}=\mathcal{T}(\mathcal{X}_n^x,E_{n+1})$ at the beginning of the sequence. The sequence $(\mathcal{X}_n^x)$ clearly has the Markov property.

Proposition 67 (The Markov chain $(\mathcal{X}_n^x)$ and Hawkes SDEs)**.** *If Conditions A-1 and A-2 a) hold and $m\in\mathcal{M}_p(\mathbb{R}_-)$ is such that $m(\{0\})>0$, then the distribution of $\mathcal{N}_m$, the solution of Relation* (5.7) *can be expressed as*

$$\mathcal{N}_m \stackrel{\text{dist.}}{=} m + \sum_{n\geqslant 1}\delta_{T_n}$$

with, $T_0=0$ and, for $n\geqslant 1$, $T_{n+1}-T_n=X_{n+1}$ where the sequence (X_n) is defined by induction by

$$\int_{T_{n-1}}^{T_n}\Phi\left(\int_{\mathbb{R}_-}h(s-u)m(\mathrm{d}u)+\sum_{k=1}^{n-1}h\left(s-T_k\right)\right)\mathrm{d}s$$
$$=\int_0^{X_n}\Phi\left(\int_{\mathbb{R}_-}h(T_{n-1}+s-u)m(\mathrm{d}u)+\sum_{k=1}^{n-1}h\left(s+\sum_{i=k+1}^{n-1}X_i\right)\right)\mathrm{d}s=E_n, \tag{5.15}$$

where (E_n) is an i.i.d. sequence of exponentially distributed random variable with parameter 1. The process $(\mathcal{X}_n^x)=((X_n,\ldots,X_1,\mathcal{X}_0^x))$ is the Markov chain with transition kernel $\mathcal{K}(\cdot,\cdot)$ of Relation (5.14) *and initial point*

$$\mathcal{X}_0^x=(s_{n+1}-s_n),\ \textit{if}\ m=(s_n,n\geqslant 0),\cdots\leqslant s_n\leqslant s_{n-1}\leqslant\cdots\leqslant s_1\leqslant s_0=0.$$

Proof. This is a straightforward consequence that Relation (5.15) is a rewriting of Relation (5.8) of Proposition 62. □

The chain starting from the empty state

We now study the Markov chain $(\mathcal{X}_n^0)$ with transition kernel K defined by Relation (5.14) when the initial state empty, i.e. it is the constant sequence equal to $+\infty$, i.e. $\mathcal{X}_0^0{=}(+\infty)$. This initial state corresponds to the case of an isolated point at time 0 without any point before that, i.e. on the time interval $(-\infty, 0)$.

This Markov chain has the same distribution as the sequence $(\mathcal{X}_n^0)$ defined by, for $n{\geqslant}1$,

$$\mathcal{X}_n^0{=}(X_n^0, X_{n-1}^0, X_{n-2}^0, \ldots, X_2^0, X_1^0, +\infty), \tag{5.16}$$

where the sequence (X_n^0) is defined Relation (5.15). We denote by (T_n^0) is the corresponding non-decreasing sequence of points defined by $T_0^0{=}0$ and, for $n{\geqslant}1$,

$$T_n^0 = \sum_{k=1}^{n} X_k^0.$$

Proposition 68. *Under Conditions A-1, A-2 and A-3, there exists $\nu{>}0$ and $\beta_0{>}0$ such that, $\alpha\beta_0{<}1$ and almost surely for all $n{\geqslant}1$,*

$$T_n^0 = \sum_{k=1}^{n} X_k^0 \geqslant \frac{1}{\nu} \sum_{k=1}^{n} \left(E_k{-}\alpha\beta_0\right),$$

and consequently, the process

$$\mathcal{N}^0 \stackrel{\text{def.}}{=} \delta_0 + \sum_{n=1}^{+\infty} \delta_{T_n^0}$$

is almost surely a point process on $\mathbb{R}_+$.

This proposition shows in particular that the sequence of points of the solution $\mathcal{N}_m$ of Relation (5.7) with $m{=}\delta_0$ is a point process on $\mathbb{R}$, the sequence (T_n^0) converges almost surely to $+\infty$.

Proof. Conditions A-2 and A-3 gives the existence $\nu{>}0$ and β_0 such that $\alpha\beta_0{<}1$ and the relation $\Phi(x){\leqslant}\nu{+}\beta_0 x$ holds for all $x{\geqslant}0$. Equation (5.15) gives, for $n{\geqslant}1$,

$$E_n = \int_{T_{n-1}^0}^{T_n^0} \Phi\left(\sum_{k=0}^{n-1} h\left(s + \sum_{i=k+1}^{n-1} X_i^0\right)\right) \mathrm{d}s \leqslant \nu X_n^0{+}\beta_0 \int_0^{X_n^0} \sum_{k=0}^{n-1} h\left(s + \sum_{i=k}^{n-1} X_i^0\right) \mathrm{d}s \tag{5.17}$$

hence

$$E_n - \alpha\beta_0 \leqslant \nu X_n^0{-}\beta_0\overline{H}(X_n^0){+}\beta_0 \int_{X_{n-1}^0}^{X_{n-1}^0+X_n^0} \sum_{k=0}^{n-2} h\left(s + \sum_{i=k+1}^{n-2} X_i^0\right) \mathrm{d}s.$$

with the notation, for $x{\geqslant}0$,

$$\overline{H}(x){=}\int_x^{+\infty} h(s)\ \mathrm{d}s \text{ and } \alpha{=}\overline{H}(0).$$

By using Inequality (5.17) for the index $n{-}1$ and by adding these relations, we get

$$\sum_{k=n-1}^{n} E_k{-}\alpha\beta_0 \leqslant \nu\left[X_n^0{+}X_{n-1}^0\right]{-}\beta_0\left[\overline{H}(X_n^0){+}\overline{H}(X_n^0{+}X_{n-1}^0)\right]$$

$$+\beta_0\int_{X^0_{n-2}}^{X^0_{n-2}+X^0_{n-1}+X^0_n}\sum_{k=0}^{n-3}h\left(s+\sum_{i=k+1}^{n-3}X^0_i\right)\mathrm{d}s.$$

By proceeding by induction, we finally get the relation

$$\sum_{k=1}^{n}(E_k-\alpha\beta_0)\leqslant\nu\sum_{k=1}^{n}X^0_k-\beta_0\sum_{k=1}^{n}\overline{H}(X^0_n+X^0_{n-1}+\cdots+X^0_k).$$

In particular the sequence (T^0_n) is almost surely converging to infinity. The proposition shows that when the initial state is the empty state, there is no blow up phenomenon, the sequence of points does not converge to some finite value.

To prove the second part of the propostion, i.e that $\mathcal{N}$ is indeed a point process, we need that the sequence (T^0_n) is going to infinity almost surely. This is a direct consequence of Proposition 68 and the law of large numbers. □

5.5 Exponential memory

In this section we assume that the function h associated to the memory of previous jumps is exponentially decreasing.

$$h(u)=\exp(-u/\alpha),$$

for some $\alpha>0$. In this case, the past activity of the Hawkes process can be encoded by a one-dimensional Markov process. One of the early analyses is [Oak75]. [DLO19] considers a more general model for which h is the density of the sum of exponential random variables with different parameters. The trick is to use the method of the stages so that a multi-dimensional Markov process can encode the past activity of the Hawkes process.

In this section, we give a existence and uniqueness result of the stationary Hawkes chain with a weaker condition than the classical relation $\alpha L<1$, where L is the Lipschitz constant associated to Φ. The result is obtained by using the Markov process of Section 5.4. At the same time an explicit representation of the distribution of the corresponding Palm measure in terms of the invariant distribution of a one-dimensional Markov chain is obtained. We conclude this section with non-Lipschitz activation functions Φ for which the solution of the Hawkes SDE blows-up in finite time. A limit result gives a scaling description of how the accumulation of the points of Hawkes process occurs.

Proposition 69. *Let $x\in\mathcal{S}_h$, m_x defined by Relation* (5.2) *and $\mathcal{N}_{m_x}=(T_n)$ of Proposition 62, then*

$$(Z_n)\overset{\text{def.}}{=}\left(\int_{(-\infty,T_n]}h(T_n-s)\mathcal{N}_{m_x}(\mathrm{d}s)\right)$$
$$=\int_{(-\infty,0]}\exp\left(-(T_n-u)/\alpha\right)m_x(\mathrm{d}u)+\sum_{k=1}^{n}\exp\left(-(T_n-T_k)/\alpha\right)$$

is a Markov chain on $(1,+\infty)$ such that, for $n\geqslant 0$,

$$Z_0=\int_{(-\infty,0]}e^{s/\alpha}m_x(\mathrm{d}s),\ \textit{and}\ Z_{n+1}=1+e^{-X_{n+1}/\alpha}Z_n,\tag{5.18}$$

where $X_{n+1}{=}T_{n+1}{-}T_n$ is the unique solution of the equation

$$\int_0^{X_{n+1}} \Phi\left(e^{-s/\alpha} Z_n\right) \mathrm{d}s = E_{n+1}, \tag{5.19}$$

where (E_n) are i.i.d. random variables with an exponential distribution with parameter 1.

Proof.

$$\begin{aligned} Z_{n+1} &= \int_{(-\infty, T_{n+1}]} \exp(-(T_{n+1}-s)/\alpha) \mathcal{N}_{m_x}(\mathrm{d}s) \\ &= 1 + \exp(-(T_{n+1}{-}T_n)/\alpha) \int_{(-\infty, T_n]} \exp(-(T_n-s)/\alpha) \mathcal{N}_{m_x}(\mathrm{d}s) \\ &= 1 + \exp(-X_{n+1}/\alpha) Z_n, \end{aligned}$$

and Relation (5.15) gives that

$$\begin{aligned} E_{n+1} &= \int_{T_n}^{T_{n+1}} \Phi\left(\int_{\mathbb{R}_-} h(s{-}u) m(\mathrm{d}u) + \sum_{k=1}^{n} h\left(s{-}T_k\right)\right) \mathrm{d}s \\ &= \int_0^{T_{n+1}-T_n} \Phi\left(e^{-s/\alpha}\left(\int_{\mathbb{R}_-} h(T_n{-}u) m_x(\mathrm{d}u) + \sum_{k=1}^{n} h\left(T_n{-}T_k\right)\right)\right) \mathrm{d}s \\ &= \int_0^{X_{n+1}} \Phi\left(e^{-s/\alpha} Z_n\right) \mathrm{d}s \end{aligned}$$

is an exponentially distributed random variable with parameter 1 and that the sequence (E_n) is i.i.d. □

Proposition 70 (Harris ergodicity)**.** *If Φ satisfies Condition A-2, and if $\alpha\beta_e{<}1$, where*

$$\beta_e \stackrel{\text{def.}}{=} \limsup_{u \to +\infty} \int_{u-1}^{u} \frac{\Phi(s)}{s} \mathrm{d}s \tag{5.20}$$

then the sequence (Z_n) is a Harris Markov chain on $[1, +\infty)$.

For a general introduction on Harris Markov chains, see [Num04].

Proof. The proof will be in two steps. We will first prove, via a Lyapunov function, that the set $[1, K]$ is recurrent, for some $K{>}0$. Then, we will show that the subset $[1, 2]$ is also recurrent and *small*, see [Num04] for example. Proposition 5.10 of [Num04] gives then that the Markov chain (Z_n) is Harris ergodic.

We first exhibit a Lyapunov function for this Markov chain. Equation (5.19) can be rewritten as, if $Z_0{=}z_0$,

$$E_1 = \int_0^{X_1} \phi\left(e^{-s/\alpha} z_0\right) \mathrm{d}s = \alpha \int_{z_0 e^{-X_1/\alpha}}^{z_0} \frac{\Phi(u)}{u} \mathrm{d}u = \alpha \int_{Z_1-1}^{z_0} \frac{\Phi(u)}{u} \mathrm{d}u. \tag{5.21}$$

Let, for $y{\geqslant}1$,

$$F(y) = \int_1^{y-1} \frac{\Phi(u)}{u} \mathrm{d}u,$$

we thus have

$$\mathbb{E}_{z_0}(F(Z_1)) - \mathbb{E}(F(z_0)) = \int_{z_0-1}^{z_0} \frac{\Phi(u)}{u}\, \mathrm{d}u - \frac{1}{\alpha},$$

hence there exist $\eta>0$ and $K>0$ such that if $z_0 \geqslant K$ then

$$\mathbb{E}_{z_0}(F(Z_1)) - \mathbb{E}(F(z_0)) \leqslant \left(\beta_e+\eta-\frac{1}{\alpha}\right) < 0.$$

The function F is a Lyapunov function for the Markov chain (Z_n). The interval $[1, K]$ is a *recurrent set* for the Markov chain. See Theorem 8.6 of [Rob03].

By using Relation (5.21), we obtain, for $z_0 \in [1, K]$,

$$\mathbb{P}_{z_0}(Z_1 < 2) = \mathbb{P}\left(\frac{E_1}{\alpha} > \int_1^{z_0} \frac{\Phi(u)}{u}\, \mathrm{d}u\right) = \exp\left(-\alpha \int_1^{z_0} \frac{\Phi(u)}{u}\, \mathrm{d}u\right)$$
$$\geqslant \exp\left(-\alpha \int_1^{K} \frac{\Phi(u)}{u}\, \mathrm{d}u\right) > 0,$$

the interval $[1, 2]$ is a recurrent set for the Markov chain (Z_n).

For $0<t\leqslant z_0$, the relation

$$\mathbb{P}(Z_1 - 1 \leqslant t) = \exp\left(-\alpha \int_t^{z_0} \frac{\Phi(u)}{u}\, \mathrm{d}u\right)$$

gives that the density of Z_1 is given by, for $z_0 \leqslant K$,

$$\alpha \frac{\Phi(t)}{t} \exp\left(-\alpha \int_t^{z_0} \frac{\Phi(u)}{u}\, \mathrm{d}u\right) \geqslant \alpha \frac{\Phi(t)}{t} \exp\left(-\alpha \int_t^{K} \frac{\Phi(u)}{u}\, \mathrm{d}u\right).$$

There is a positive lower bound independent of $z_0 \leqslant K$. We can now use the same argument as in example of Section 4.3.3 page 98 of [MT93] to prove that $[1, 2]$ is a small set. The proposition is proved. □

Definition 71. *For $z>1$ and $y>0$, under Assumption A-2, we define $G_\Phi(z, y)$ by the relation*

$$\int_0^{G_\Phi(z,y)} \Phi\left(e^{-s/\alpha} z\right) \mathrm{d}s = y. \tag{5.22}$$

Theorem 72. *[Invariant distribution of $(\mathcal{X}_n)$] Under Assumption A-2, and if $\alpha\beta_e<1$, then for any $x \in \mathcal{S}_h$, the Markov chain $(\mathcal{X}_n)$ of Definition 66 converges in distribution to the law of*

$$\left(G_\Phi\left(Z^*_{-n}, \alpha \int_{Z^*_{-n+1}-1}^{Z^*_{-n}} \frac{\Phi(u)}{u}\, \mathrm{d}u\right), n \geqslant 1\right)$$

where G_Φ is defined by Relation (5.22) *and $(Z^*_n, n \in \mathbb{Z})$ is the stationary version of the Harris Markov chain (Z_n) of Proposition 69.*

Proof. For $n \geqslant 1$, with the above notation, by definition $X_{n+1} = G_\Phi(Z_n, E_{n+1})$, i.e.

$$E_{n+1} = \alpha \int_{Z_{n+1}-1}^{Z_n} \frac{\Phi(u)}{u}\, \mathrm{d}u.$$

For $n \geqslant k \geqslant 1$, $(X_n, X_{n-1}, \ldots, X_{n-k+1})$ are the k-first coordinates of $\mathcal{X}_n$, they can be expressed as

$$(G_\Phi(Z_{n-1}, E_n), G_\Phi(Z_{n-2}, E_{n-1}), \ldots, G_\Phi(Z_{n-k}, E_{n-k+1})) = \left(G_\Phi\left(Z_{n-1}, \alpha \int_{Z_n - 1}^{Z_{n-1}} \frac{\Phi(u)}{u}\, \mathrm{d}u \right), \ldots G_\Phi\left(Z_{n-k-1}, \alpha \int_{Z_{n-k}-1}^{Z_{n-k-1}} \frac{\Phi(u)}{u}\, \mathrm{d}u \right) \right).$$

The Harris ergodicity of (Z_n) implies that the random variable $(Z_n, Z_{n-1}, \ldots, Z_{n-k})$ is converging in distribution to $(Z_0^*, Z_{-1}^*, \ldots, Z_{-k}^*)$. Due to Assumption A-2, the mapping $(z, y) \mapsto G_\Phi(z, y)$ is continuous, the continuous mapping theorem concludes the proof of our result. □

Theorem 72 shows that in the case of exponential memory, the invariant distribution of $(\mathcal{X}_n)$ can be expressed in terms of a one-dimensional stationary Markov chain. The following corollary rephrases this result in terms of Hawkes processes. This is a direct application of Proposition 65.

Corollary 73. *If Φ is a continuous function such that $\Phi(0) > 0$ and $\alpha\beta_e < 1$, where β_e is defined by Relation* (5.20)*, then there exists a unique stationary Hawkes process.*

Note that the condition $\alpha\beta_e < 1$ is weaker than the classical conditions of the literature: Φ Lipschitz with Lipschitz constant β such that $\alpha\beta < 1$.

Transient Hawkes processes

From now on, we assume a polynomial behavior for Φ so that, for $x > 0$,

$$\Phi(x) = (\nu + \beta x)^\gamma,$$

where ν, β and γ are positive real numbers.

Theorem 72 shows that $(\mathcal{X}_n)$ is converging in distribution for all α, ν and β when $\gamma < 1$, and, when $\gamma = 1$, the convergence occurs if $\alpha\beta < 1$.

Proposition 74. *If $\Phi(u) = (\nu + \beta u)^\gamma$ and if $\gamma > 1$ with β, $\nu > 0$, then the Markov process (Z_n) is transient.*

Proof. From Relation (5.21), we have

$$E_1 = \alpha \int_{Z_1 - 1}^{z_0} \frac{\Phi(u)}{u}\, \mathrm{d}u,$$

where E_1 is an exponentially distributed random variable with parameter 1. Let, for $u \geqslant 0$, $\Phi_p(u) \stackrel{\text{def.}}{=} (\beta u)^\gamma$ and, on the event $\{\gamma E_1 < \alpha\beta^\gamma z_0^\gamma\}$, we define the variable $Z_{1,p}$ such that

$$E_1 = \alpha \int_{Z_{1,p}-1}^{z_0} \frac{\Phi_p(u)}{u}\, \mathrm{d}u = \frac{\alpha\beta^\gamma}{\gamma} \left(z_0^\gamma - (Z_{1,p} - 1)^\gamma \right),$$

then, since $\Phi_p \leqslant \Phi$, we have $z_0 - Z_{1,p} + 1 \geqslant z_0 - Z_1 + 1 \geqslant 0$ and $E_2 \stackrel{\text{def.}}{=} \gamma E_1 / (\alpha\beta^\gamma)$, then

$$z_0 - Z_{1,p} + 1 = z_0 \left(1 - \left(1 - \frac{E_2}{z_0^\gamma} \right)^{1/\gamma} \right).$$

The elementary inequality

$$1-(1-h)^{1/\gamma} \leqslant \frac{2}{\gamma}h, \quad 0 \leqslant h \leqslant 1/2,$$

gives the relation, for $a \geqslant 1$

$$\begin{aligned}\mathbb{E}_{z_0}\left((z_0-Z_1+1)^a\right) &\leqslant z_0^a \mathbb{P}(2\gamma E_1 \geqslant \alpha\beta^\gamma z_0^\gamma) + \mathbb{E}\left((z_0-Z_{1,p}+1)^a \mathbb{1}_{\left\{2\gamma E_1 \leqslant \alpha\beta^\gamma z_0^\gamma\right\}}\right) \\ &\leqslant z_0^a \exp\left(-\frac{\alpha\beta^\gamma}{2\gamma} z_0^\gamma\right) + \frac{2^a}{\alpha^a \beta^{a\gamma}} \frac{\mathbb{E}\left(E_1^a\right)}{z_0^{a(\gamma-1)}}.\end{aligned}$$

Since $\gamma > 1$, we deduce that

$$\lim_{z_0 \to +\infty} \mathbb{E}_{z_0}\left(Z_1 - z_0\right) = 1 \text{ and } \sup_{z_0 \geqslant 1} \mathbb{E}_{z_0}\left(\left(Z_1 - z_0\right)^2\right) < +\infty. \tag{5.23}$$

Theorem 8.10 of [Rob03] shows that the Markov chain is transient. Strictly speaking Theorem 8.10 is for a Markov chain with a countable state space, nevertheless a glance at the proof of this result shows that it is also valid in our setting. The proposition is proved. □

Relation (5.19) of Proposition 69 gives that the Hawkes Point Process (T_n) of Proposition 62 is such that

$$E_{n+1} \geqslant \beta^\gamma Z_n^\gamma \int_0^{T_{n+1}-T_n} e^{-s\gamma/\alpha}\, \mathrm{d}s = \frac{\alpha}{\gamma}\beta^\gamma Z_n^\gamma \left(1 - e^{-\gamma(T_{n+1}-T_n)/\alpha}\right), \tag{5.24}$$

where (E_n) is an i.i.d. sequence of exponential random variables with parameter 1. Under the assumptions of Proposition 74 the sequence (Z_n) is converging in distribution to infinity and, with the last relation, the relation

$$\lim_{n \to +\infty} T_{n+1} - T_n = 0$$

holds for the convergence in law. This result suggests that the points (T_n) are closer and closer asymptotically. We investigate this aspect in the rest of the section.

We now study of the asymptotic behavior of (Z_n) in the transient case. We start with a technical lemma.

Lemma 75. *If $\gamma \geqslant 2$ then, for any $\delta > 0$,*

$$\sup_{z_0 > 1} \mathbb{E}_{z_0}\left(e^{\delta|Z_1 - z_0|}\right) < +\infty. \tag{5.25}$$

Proof. From Relation (5.21), we get, for $z_0 \geqslant 1$ and $1 \leqslant t \leqslant z_0$,

$$\begin{aligned}\mathbb{P}_{z_0}\left(z_0 - Z_1 + 1 \geqslant t\right) &= \mathbb{P}\left(E_1 \geqslant \alpha \int_{z_0-t}^{z_0} \frac{\Phi(u)}{u}\right) \\ &\leqslant \exp\left(-b z_0^\gamma \left(1 - \left(1 - \frac{t}{z_0}\right)^\gamma\right)\right), \end{aligned} \tag{5.26}$$

with $b \overset{\text{def.}}{=} \alpha\beta^\gamma/\gamma$. Note that, by Definition (5.18) of Z_1, $z - Z_1 + 1 \geqslant 0$, hence, for $\delta > 0$,

$$\mathbb{E}_{z_0}\left(e^{\delta|Z_1 - z_0 - 1|}\right) - 1 = \delta \int_0^{z_0} e^{\delta t} \mathbb{P}_{z_0}\left(z_0 - Z_1 + 1 \geqslant t\right)\, \mathrm{d}t$$

$$\leqslant \delta \int_0^{z_0} \exp\left(\delta t - b z_0^\gamma \left(1 - \left(1 - \frac{t}{z_0}\right)^\gamma\right)\right) \mathrm{d}t$$
$$= \delta z_0 \int_0^1 \exp\left(\delta u z_0 - b z_0^\gamma \left(1 - (1-u)^\gamma\right)\right) \mathrm{d}u.$$

When z_0 is sufficiently large, we split the integral into two terms,

$$z_0 \int_{1-(1-2\delta/(bz_0^{\gamma-1}))^{1/\gamma}}^1 \exp\left(\delta u z_0 - b z_0^\gamma \left(1 - (1-u)^\gamma\right)\right) \mathrm{d}u \leqslant z_0 \exp\left(-\delta z_0\right),$$

and

$$z_0 \int_0^{1-(1-2\delta/(bz_0^{\gamma-1}))^{1/\gamma}} \exp\left(\delta u z_0 - b z_0^\gamma \left(1 - (1-u)^\gamma\right)\right) \mathrm{d}u$$
$$\leqslant z_0 \left(1 - \left(1 - 2\frac{\delta}{b z_0^{\gamma-1}}\right)^{1/\gamma}\right) \exp\left(\delta z_0 \left(1 - (1 - 2\delta/(bz_0^{\gamma-1}))^{1/\gamma}\right)\right).$$

The lemma is proved. □

Proposition 76. *If $\gamma \geqslant 2$, then, almost surely,*

$$\lim_{n\to+\infty} \frac{Z_n}{n} = 1.$$

Proof. This is a consequence of Relations (5.23) and (5.25). Theorem 8.11 of [Rob03] shows that, almost surely, the relation

$$\liminf_{n\to+\infty} \frac{Z_n}{n} \geqslant 1$$

holds. Condition b) of Proposition 8.11 follows from Lemma 75 and Condition c) of this proposition is replaced in this context by the fact that if $z_0 < K_0$, then there exists $n_0 \geqslant 1$ such that $\mathbb{P}_{z_0}(Z_{n_0} \geqslant K_0) > 0$.

Notice that $Z_n \leqslant n + z_0$ holds for all $n \geqslant 1$, we get therefore that almost surely

$$\lim_{n\to+\infty} \frac{Z_n}{n} = 1.$$

The proposition is proved. □

For $x \in \mathcal{S}_h$ and m_x defined by Relation (5.2), if $\mathcal{N}_{m_x} = (T_n)$ the point process of Proposition 62, we know that the sequence $(T_{n+1} - T_n)$ is converging in distribution to 0. The following proposition gives a much more detailed description of the accumulation of points:

for $n \geqslant 1$, the point process seen from the nth point, i.e. the point process $(T_n - T_k, 1 \leqslant k \leqslant n)$ scaled by the factor n^γ converges in distribution to a Poisson point process.

Proposition 77 (Asymptotic behavior of points of a transient Hawkes process)**.** *Assume that $\Phi(u) = (\nu + \beta u)^\gamma$, and that $\gamma \geqslant 2$ with β, $\nu > 0$, if $x \in \mathcal{S}_h$, m_x defined by Relation* (5.2) *and $\mathcal{N}_{m_x} = (T_n)$ the point process of Proposition 62, then the point process $(n^\gamma(T_n - T_k), 1 \leqslant k < n)$ converges in distribution to a Poisson process with rate β^γ.*

Proof. Define $\mathcal{P}_n=(n^\gamma(T_n-T_k), 1\leqslant k<n)$. The representation of (T_n) in terms of the Markov chain (Z_n) of Proposition 69 and Relation (5.19) give

$$E_{n+1} = \int_0^{X_{n+1}} \left(\nu+\beta Z_n e^{-s/\alpha}\right)^\gamma \mathrm{d}s, \tag{5.27}$$

where (E_n) is an i.i.d. sequence of exponential random variables with parameter 1 and, as before, $X_{n+1}=T_{n+1}-T_n$.

For any $\delta>0$ and $n\geqslant 1$, Relation (5.27) gives the inequality

$$\mathbb{P}\left(X_{n+1}\geqslant\delta\right) \leqslant \mathbb{P}\left(\frac{\alpha}{\gamma}\beta^\gamma\left(1-e^{-\delta\gamma/\alpha}\right) Z_n^\gamma \leqslant E_{n+1}\right). \tag{5.28}$$

On the event $\mathcal{E}_{n,\delta}$,

$$\mathcal{E}_{n,\delta} \stackrel{\text{def.}}{=} \left\{X_{n+1}\leqslant\delta, \frac{\nu}{\beta}e^{\delta/\alpha}\leqslant Z_n\right\},$$

Relation (5.27) shows that

$$\beta^\gamma e^{-\delta\gamma/\alpha} Z_n^\gamma X_{n+1} \leqslant E_{n+1},$$

and therefore that the sequence of random variables $(Z_n^\gamma X_{n+1})$ is therefore tight.

The elementary relation

$$(1+h)^\gamma - 1 \leqslant C_1 h, 0\leqslant h\leqslant 1,$$

with $C_1=\gamma 2^{\gamma-1}$ and Relation (5.27) give the following inequality on the event $\mathcal{E}_{n,\delta}$.

$$0 \leqslant E_{n+1} - \beta^\gamma Z_n^\gamma \int_0^{X_{n+1}} e^{-s\gamma/\alpha}\,\mathrm{d}s$$
$$\leqslant C_1\nu\left(\beta Z_n\right)^{\gamma-1}\int_0^{X_{n+1}} e^{-(\gamma-1)s/\alpha}\,\mathrm{d}s \leqslant C_1\nu\beta^{\gamma-1}X_{n+1}Z_n^{\gamma-1}.$$

Using the fact that $(Z_n^\gamma X_{n+1})$ is tight and the almost sure convergence of (Z_n/n) to 1 of Proposition 76 shows that the random variables $(X_{n+1}Z_n^{\gamma-1})$ is converging in distribution to 0. For a sufficiently large n, Relation (5.28) shows that the probability of the event $\mathcal{E}_{n,\delta}$ is arbitrarily close to 1, we obtain that the sequence of random variables

$$(Y_n) \stackrel{\text{def.}}{=} \left(\beta^\gamma Z_n^\gamma \int_0^{X_{n+1}} e^{-s\gamma/\alpha}\,\mathrm{d}s\right)$$

is converging in law to an exponential distribution with parameter 1.

On the event $\mathcal{E}_{n,\delta}$ we have

$$Y_n \leqslant \beta^\gamma Z_n^\gamma X_{n+1} \leqslant e^{\delta\gamma/\alpha}Y_n,$$

hence, for $x\geqslant 0$,

$$\mathbb{P}(\beta^\gamma Z_n^\gamma X_{n+1} \geqslant x) \leqslant \mathbb{P}\left(e^{\delta\gamma/\alpha}Y_n \geqslant x\right) + \mathbb{P}\left(\mathcal{E}_{n,\delta}^c\right),$$

hence

$$\limsup_{n\to+\infty} \mathbb{P}\left(\beta^\gamma Z_n^\gamma X_{n+1} \geqslant x\right) \leqslant \exp\left(-xe^{-\delta\gamma/\alpha}\right),$$

and, by letting δ go to 0, we obtain

$$\limsup_{n\to+\infty} \mathbb{P}\left(\beta^\gamma Z_n^\gamma X_{n+1} \geqslant x\right) \leqslant e^{-x}.$$

An analogue lower bound holds for the $\liminf$, hence $(\beta^\gamma Z_n^\gamma X_{n+1})$ is converging in distribution to an exponential distribution with parameter 1. By using the almost sure convergence of (Z_n/n) to 1, the same property holds for $(\beta^\gamma n^\gamma X_{n+1})$.

For $p \geqslant 1$, the same argument may be used to prove that the sequence of random variables $(\beta^\gamma n^\gamma X_{n-k}, 0 \leqslant k \leqslant p-1)$ is converging in distribution to the product of p exponential distributions with parameter 1. The key argument is again the almost sure convergence of (Z_n/n) to 1.

Final step. Let f be a continuous function on $\mathbb{R}_+$ with compact support included in $[0, K_0]$ for some $K_0 > 0$. The relations $Z_n \leqslant n + z_0$ and (5.27) give the inequality, for all $n \geqslant 1$,

$$E_{n+1} \leqslant (\nu + \beta(n+z_0))^\gamma X_{n+1} \leqslant C_0 (n+1)^\gamma X_{n+1},$$

for some constant C_0 independent of n.

For $p \leqslant n$, we thus have

$$\mathbb{P}(n^\gamma (T_n - T_{n-p}) \leqslant K_0) \leqslant \mathbb{P}\left(\sum_{k=n-p+1}^{n} k^\gamma X_k \leqslant K_0\right) \leqslant \mathbb{P}\left(\frac{1}{C_0}\sum_{k=1}^{p} E_k \leqslant K_0\right).$$

We denote $\mathcal{N}_{\beta^\gamma}$ a Poisson process with rate β^γ, with associated exponential random variables $(E_n^{\beta^\gamma})$.

The last inequality gives that $\mathcal{P}_n$ is stochastically dominated by $\mathcal{N}_{C_0+\beta^\gamma}$, a Poisson process with rate $C_0 + \beta^\gamma$, in the sense that

$$\mathbb{P}(\mathcal{P}_n((0,K_0]) \geqslant p) \leqslant \mathbb{P}(\mathcal{N}_{C_0+\beta^\gamma}((0,K_0]) \geqslant p), \text{ for } p \leqslant n. \tag{5.29}$$

Clearly $\mathcal{N}_{\beta^\gamma}$ is also stochastically dominated by $\mathcal{N}_{C_0+\beta^\gamma}$.

For $p \geqslant 1$ and $n \geqslant p$,

$$\begin{aligned}
&\left|\mathbb{E}\left(\exp\left(-\int f(u)\mathcal{P}_n(u)\right)\right) - \mathbb{E}\left(\exp\left(-\int f(u)\mathcal{N}_{\beta^\gamma}(u)\right)\right)\right| \\
&\quad\leqslant \left|\mathbb{E}\left(\exp\left(-\int f(u)\mathcal{P}_n(u)\right)\right) - \mathbb{E}\left(\exp\left(-\sum_{k=n-p+1}^{n} f(n^\gamma(T_n - T_{n-k}))\right)\right)\right| \\
&\quad+ \left|\mathbb{E}\left(\exp\left(-\sum_{k=n-p+1}^{n} f(n^\gamma(T_n - T_{n-k}))\right)\right) - \mathbb{E}\left(\exp\left(-\sum_{k=n-p+1}^{n} f\left(n^\gamma E_n^{\beta^\gamma}\right)\right)\right)\right| \\
&\quad\quad+ \left|\mathbb{E}\left(\exp\left(-\sum_{k=n-p+1}^{n} f\left(n^\gamma E_n^{\beta^\gamma}\right)\right)\right) - \mathbb{E}\left(\exp\left(-\int f(u)\mathcal{N}_{\beta^\gamma}(u)\right)\right)\right|.
\end{aligned}$$

The first and third terms of the right hand side of the last inequality are respectively bounded by the quantity $\mathbb{P}(\mathcal{P}_n((0,K_0]) \geqslant p)$ and $\mathbb{P}(\mathcal{N}_{\beta^\gamma}((0,K_0]) \geqslant p)$. With Relation (5.29) we can fix p (not depending on n) sufficiently large such that it is arbitrarily small. The second term can also be made arbitrarily small for n sufficiently large in a similar way.

We have thus proved that

$$\lim_{n\to+\infty} \mathbb{E}\left(\exp\left(-\int_{\mathbb{R}_+} f(u)\mathcal{P}_n(u)\right)\right) = \mathbb{E}\left(\exp\left(-\int_{\mathbb{R}_+} f(u)\mathcal{N}_{\beta^\gamma}(u)\right)\right)$$

holds for all continuous function with compact support. We can use Theorem 3.2.6 of [Daw93] to finish the proof of the proposition. □

Appendix

5.A General results and definitions on point processes

Point Processes

We recall the notations on point measures and the associated random variables, the point processes used throughout this paper. See [Nev77], Chapter 1 and 11 of [Rob03], and [Daw93] for a general introduction on random measures.

If $H \in \{\mathbb{R}, \mathbb{R}_-\}$, we denote by $C_c(H)$ the space of continuous functions on H with compact support and $\mathcal{M}_p(H)$, the set of Radon point measures on H, that is positive Radon measures carried by points, for $m \in \mathcal{M}_p(H)$ then

$$m = \sum_{x \in S} \delta_x,$$

where δ_x is the Dirac measure at $x \in H$ and S is a countable subset of H with no limiting points in H. We may also represent $\mathcal{N}$ as the sequence $(x, x \in S)$ of its points. If A is a subset of H, we denote by

$$m(A) = \int_A m(\mathrm{d}x) = \sum_{x \in S} \mathbb{1}_{\{x \in A\}},$$

the number of points of m in A. A point measure m is *simple* if $m(\{x\}) \in \{0, 1\}$, for all $x \in H$. The space $\mathcal{M}_p(H)$ is endowed with the topology of weak convergence.

If $m \in \mathcal{M}_p(\mathbb{R}_-)$, the point process $\breve{m}$ on $\mathbb{R}_+$ defined by

$$\int_0^{+\infty} f(x) \breve{m}(\mathrm{d}x) = \int_{-\infty}^0 f(-x) m(\mathrm{d}x), \tag{5.30}$$

for any non-negative function f on $\mathbb{R}_+$.

Stationary point processes

If m is a simple point measure on $\mathbb{R}$, the points of m are enumerated by an increasing sequence $(t_k(m), k \in \mathbb{Z})$, numbered so that the relations

$$t_{-1}(m) < t_0(m) \leqslant 0 < t_1(m) < \cdots \tag{5.31}$$

hold, with the convention that $t_k(m) = +\infty$ if there are less than $k \geqslant 1$ points of m in $\mathbb{R}_+$, and similarly on $\mathbb{R}_-$. The flow of translation operators (θ_t) on $\mathcal{M}_p(\mathbb{R})$ is defined by, for $t \in \mathbb{R}$ and $m \in \mathcal{M}_p(\mathbb{R})$,

$$\int_{\mathbb{R}} f(s) \theta_t(m)(\mathrm{d}s) \overset{\text{def.}}{=} \int_{\mathbb{R}} f(s-t) m(\mathrm{d}s), \tag{5.32}$$

for any non-negative Borelian function f on $\mathbb{R}$.

A distribution on $\mathcal{M}_p(H)$, an element of the set $\mathcal{P}(\mathcal{M}_p(H))$, is defined as *a point process* on H.

Definition 78 (Stationarity). *A point process $\mathcal{N}$ on $\mathbb{R}$ is* stationary *with intensity $\lambda > 0$, if the random variable $\mathcal{N}([0,1])$ is integrable and $\mathbb{E}(\mathcal{N}([0,1])) = \lambda$, and if its distribution is invariant by translation, i.e. for $t \in \mathbb{R}$, $\theta_t(\mathcal{N}) \overset{\text{dist.}}{=} \mathcal{N}$, where θ_t is the translation operator defined by Relation* (5.32).

Palm space of point processes

The set $\mathcal{M}_p^0(\mathbb{R}_-)$ is a subset of elements m of $\mathcal{M}_p(\mathbb{R}_-)$ such that $m(0)\neq 0$. If $m\in\mathcal{M}_p^0(\mathbb{R}_-)$ then m can be represented either by the non-decreasing sequence $(t_k, k\geqslant 0)$ of its points, or by the sequence $x=(x_k)=(t_{-k}-t_{-k-1}, k\geqslant 0)$ of increments between them.

An operator $\widehat{\theta}$ on $\mathcal{M}_p^0(\mathbb{R})$ is defined by,

$$\widehat{\theta}(m)\stackrel{\text{def.}}{=}\theta_{t_1(m)}(m)\mathbb{1}_{\{t_1(m)<+\infty\}}, \tag{5.33}$$

for $m\in\mathcal{M}_p^0(\mathbb{R})$, where $t_1(m)$ and (θ_t) by defined respectively by Relations (5.31) and (5.32). A simple point process of $\mathcal{M}_p^0(\mathbb{R})$ can be identified to its sequence of inter-arrival times and it is easily seen that the relation

$$\Big((t_{k+1}-t_k)(\widehat{\theta}(m)), k\in\mathbb{Z}\Big) = \Big((t_{k+2}-t_{k+1})(m), k\in\mathbb{Z}\Big),$$

holds.

The mapping $\widehat{\theta}$ is the classical shift operator on sequences. If $m=(t_n, n\in\mathbb{Z})$ is in $\mathcal{M}_p^0(\mathbb{R})$ and $x=(x_n)=(t_n-t_{n-1}, n\in\mathbb{Z})$, then $m=m_x$ and $\widehat{\theta}(m)=m_{\bar{x}}$, with $\bar{x}=(x_{n+1})$ if $m(\mathbb{R}_-)=m(\mathbb{R}_+)=+\infty$.

Equivalence between stationary point processes and Palm measure

We now recall some classical results on stationary point processes on $\mathbb{R}$. A stationary simple point process with intensity $\lambda>0$ can be equivalently defined by either by

a. a distribution Q on $\mathcal{M}_p(\mathbb{R})$ which is invariant for the continuous flow of translations (θ_t);

b. a distribution $\widehat{Q}$ on $\mathcal{M}_p^0(\mathbb{R})$ called the *Palm measure* of Q which is invariant for the operator $\widehat{\theta}$.

When a) is given, a distribution $\widehat{Q}$ on $\mathcal{M}_p^0(\mathbb{R})$ is constructed via Mecke's Formula so that property b) holds. See Chapter II of [Nev77] or Proposition 11.6 of [Rob03].

If b) holds, i.e. if $\widehat{Q}$ is given, then the construction of Q is done with a fundamental construction of ergodic theory, it is the *special flow* associated to the operator $\widehat{\theta}$ and the function $m\mapsto t_1(m)$ on $\mathcal{M}_p^0$. See Chapter 11 of [CFS82], and Chapter 10 of [Rob03]. The distribution Q is expressed as

$$\int_{\mathcal{M}_p(\mathbb{R})} F(m)\, Q(\mathrm{d}m) = \lambda \int_{\mathcal{M}_p^0(\mathbb{R})} \int_0^{t_1(m)} F(\theta_s(m))\ \mathrm{d}s\, \widehat{Q}(\mathrm{d}m), \tag{5.34}$$

for any non-negative Borelian function on $\mathcal{M}_p(\mathbb{R})$. The probability distribution $\widehat{Q}$ is simply determined by a distribution of the sequence of inter-arrival times which is invariant by the shift operator. The space $(\mathcal{M}_p^0(\mathbb{R}), \widehat{\theta}, \widehat{Q})$ can be seen as a probability space whose elements are positive sequences. It is sometimes called the Palm space of Q.

5.B Hawkes processes: a quick review

Hawkes processes have been introduced by Hawkes in 1974 in [Haw71] as a class of inhomogeneous Poisson processes $\mathcal{N}$, whose stochastic intensity $(\lambda(t))$ depends on previous jumps, i.e through,

$$(\lambda(t)) = \left(\Phi\left(\int_{(-\infty,t)} h(t-s)\mathcal{N}(\mathrm{d}s)\right)\right).$$

The first Hawkes processes investigated were restricted to affine activation function Φ of the form,

$$\Phi(x) = \nu + \beta x,$$

which have a nice representation in terms of age-dependent branching processes, see [Lew64; Ver70; DV03]. The condition of existence and uniqueness of stationary Hawkes process in this case is

$$\beta \int_0^{+\infty} h(s)\,\mathrm{d}s < 1,$$

see [HO74].

The special case where $\nu{=}0$ was investigated in [BM01], where a particular interest was dedicated to the critical Hawkes process,

$$\beta \int_0^{+\infty} h(s)\,\mathrm{d}s = 1.$$

The same critical Hawkes process, with general immigration rate ν is investigated in [Kir17]. A more precise study of the cumulant statistics of stationary Hawkes processes is developed in [Jov15] using a Poisson cluster process representation. The addition of an external jump process to the linearized Hawkes process, in view of applications in neuroscience example, has been considered in [Bou16].

Hawkes processes with exponential functions $h(x){=}\exp(-x/\alpha)$ have attracted a particular interest because the associated counting process has the Markovian property, see [Oak75].

Having a linear activation function Φ is very helpful because of the corresponding branching process representation, However, when studying auto-inhibiting point processes, non-linear activation functions Φ are natural candidates to use. In this setting the investigation of sufficient conditions for the existence of stationary versions is more delicate. Most proofs in this domain are based on the functional relation defining stationary Hawkes processes that can be expressed as a fixed point equation which can be solved through a Picard scheme, see [Ker64] for one of the pioneering papers on this subject. . [BM96] has developed this approach when Φ is supposed to be β-Lipschitz, with the following condition,

$$\beta \int_0^{+\infty} |h(s)|\,\mathrm{d}s < 1.$$

Thinning techniques have been applied to the case of a bounded Lipschitz function Φ in the same reference, where the condition

$$\int_0^{+\infty} s|h(s)|\,\mathrm{d}s < +\infty$$

Branching Processes	
References	[Lew64; Ver70; DV03]
Assumptions 1	
a. $\Phi(x) = \nu + \beta x$ with $\nu > 0$ and $\beta \geqslant 0$.	[Oak75; EGG10]
b. $h(x) = \exp(-x/\alpha)$.	
Assumptions 2	
a. $\Phi(x) = \nu + \beta x$ with $\nu > 0$ and $\beta \geqslant 0$.	[Haw71; HO74; BM01; Jov15; Bou16; Kir17]
b. $h : \mathbb{R}_+ \to \mathbb{R}_+$.	
Analytical Methods	
References	[Ker64]
Assumptions 3	
a. $\Phi : \mathbb{R} \to \mathbb{R}_+$.	[BM96; Che+17]
b. $h : \mathbb{R}_+ \to \mathbb{R}$.	
Markovian Processes	
References	[Lin02; Num04; Hai10]
Assumptions 3	
a. $\Phi : \mathbb{R} \to \mathbb{R}_+$.	[BM96; Kar12; Hod16; RDL20; Gra19; Raa19; Cos+20]
b. $h : \mathbb{R}_+ \to \mathbb{R}$.	
Assumptions 4	
a. $\Phi : \mathbb{R} \to \mathbb{R}_+$.	[DLO19]
b. $h(x) = \exp(-x/\alpha)$.	

Table 5.1: **Overview of works on the existence of stationary Hawkes processes.**

is sufficient to prove the existence and uniqueness of the stationary version of the Hawkes process.

Proofs based on contraction arguments are problematic when looking at inhibitory connections. Other techniques have been developed to circumvent these problems, but always need some additional (sometimes strong) assumptions.

In [BM96], renewal theory is used to investigate Hawkes processes, with finite memory. This approach has been extended in [Gra19; Raa19; Cos+20]. It is also possible to limit the influence of intensity rate to the last jump of the Hawkes process as done in [HL17].A recent study [RDL20] has added a refractory effect to prevent explosion in the study of non-linear Hawkes processes.

To go further, it is interesting to see Hawkes processes, as Markov process in general state spaces, either using counting processes [DLO19] or Markov theory in

the state of càdlàg functions [Kar12]. Coupling methods [Lin02] and general Markov theory [Num04; Hai10] are natural tools in this setting.

BIBLIOGRAPHY

[BH09] L. Bauwens and N. Hautsch. Modelling Financial High Frequency Data Using Point Processes. *Handbook of Financial Time Series*. Ed. by T. Mikosch, J.-P. Kreiß, R. A. Davis, and T. G. Andersen. Berlin, Heidelberg: Springer Berlin Heidelberg, 2009, 953–979.

[BM01] P. Brémaud and L. Massoulié. Hawkes Branching Point Processes without Ancestors. *Journal of Applied Probability* **38** (2001), 122–135.

[BM96] P. Brémaud and L. Massoulié. Stability of Nonlinear Hawkes Processes. *The Annals of Probability* **24** (1996), 1563–1588.

[Bou16] A. Boumezoued. Population viewpoint on Hawkes processes. *Advances in Applied Probability* **48** (June 2016), 463–480.

[CFS82] I. P. Cornfeld, S. V. Fomin, and Y. G. Sinaĭ. Ergodic Theory. Grundlehren der mathematischen Wissenschaften. New York: Springer-Verlag, 1982.

[Che+17] S. Chen, A. Shojaie, E. Shea-Brown, and D. Witten. The Multivariate Hawkes Process in High Dimensions: Beyond Mutual Excitation. *arXiv:1707.04928 [stat]* (July 2017).

[Cos+20] M. Costa, C. Graham, L. Marsalle, and V. C. Tran. Renewal in Hawkes processes with self-excitation and inhibition. *Advances in Applied Probability* **52** (Sept. 2020), 879–915.

[Daw93] D. A. Dawson. Measure-valued Markov processes. *École d'Été de Probabilités de Saint-Flour XXI—1991*. Vol. 1541. Lecture Notes in Math. Berlin: Springer, Nov. 1993, 1–260.

[DLO19] Duarte, Aline, Löcherbach, Eva, and Ost, Guilherme. Stability, convergence to equilibrium and simulation of non-linear Hawkes processes with memory kernels given by the sum of Erlang kernels. *ESAIM: PS* **23** (2019), 770–796.

[DP18] A. Daw and J. Pender. Queues driven by Hawkes processes. *Stochastic Systems* **8** (2018), 192–229.

[DV03] D. J. Daley and D. Vere-Jones. An Introduction to the Theory of Point Processes. Volume 1: Elementary Theory and Methods. Second edition. Probability and its Applications. Springer, Nov. 2003.

[EGG10] E. Errais, K. Giesecke, and L. Goldberg. Affine Point Processes and Portfolio Credit Risk. *SIAM Journal on Financial Mathematics* **1** (Jan. 2010), 642–665.

[Ete+16] J. Etesami, N. Kiyavash, K. Zhang, and K. Singhal. Learning Network of Multivariate Hawkes Processes: A Time Series Approach. *Proceedings of the Thirty-Second Conference on Uncertainty in Artificial Intelligence*. UAI'16. Arlington, Virginia, United States: AUAI Press, 2016, 162–171.

[GDT17] F. Gerhard, M. Deger, and W. Truccolo. On the stability and dynamics of stochastic spiking neuron models: Nonlinear Hawkes process and point process GLMs. *PLOS Computational Biology* **13** (Feb. 2017), e1005390.

[Gra19] C. Graham. Regenerative properties of the linear Hawkes process with unbounded memory. *arXiv:1905.11053 [math, stat]* (May 2019).

[Hai10] M. Hairer. Convergence of Markov processes. 2010.

[Haw71] A. G. Hawkes. Spectra of Some Self-Exciting and Mutually Exciting Point Processes. *Biometrika* **58** (1971), 83–90.

[HL17] P. Hodara and E. Löcherbach. Hawkes processes with variable length memory and an infinite number of components. *Advances in Applied Probability* **49** (2017), 84–107.

[HO74] A. G. Hawkes and D. Oakes. A Cluster Process Representation of a Self-Exciting Process. *Journal of Applied Probability* **11** (1974), 493–503.

[Hod16] P. Hodara. Systèmes de neurones en interactions : modélisation probabiliste et estimation. PhD thesis. 2016.

[Jac79] J. Jacod. Calcul stochastique et problèmes de martingales. Vol. 714. Lecture Notes in Mathematics. Springer, Berlin, 1979, x+539.

[Jov15] S. Jovanović. Cumulants of Hawkes point processes. *Physical Review E* **91** (2015).

[Kar12] D. Karabash. On Stability of Hawkes Process. *arXiv:1201.1573 [math]* (Jan. 2012).

[Ker64] J. Kerstan. Teilprozesse Poissonscher Prozesse. *Trans. Third Prague Conf. Information Theory,Statist. Decision Functions, Random Processes*. Liblice: House Czech. Acad.Sci., Jan. 1964, 377–403.

[Kir17] M. Kirchner. A note on critical Hawkes processes. *arXiv:1706.03975 [math]* (June 2017).

[Lew64] P. A. W. Lewis. A Branching Poisson Process Model for the Analysis of Computer Failure Patterns. *Journal of the Royal Statistical Society. Series B (Methodological)* **26** (1964), 398–456.

[Lin02] T. Lindvall. Lectures on the Coupling Method. Courier Corporation, Jan. 2002.

[MT93] S. Meyn and R. Tweedie. Markov chains and stochastic stability. Communications and control engineering series. Springer, 1993.

[Nev77] J. Neveu. Processus ponctuels. *École d'Été de Probabilités de Saint-Flour*. Ed. by P.-L. Hennequin. Vol. 598. Lecture Notes in Math. Berlin: Springer-Verlag, 1977, 249–445.

[Num04] E. Nummelin. General Irreducible Markov Chains and Non-Negative Operators. Cambridge University Press, June 2004.

[Oak75] D. Oakes. The Markovian Self-Exciting Process. *Journal of Applied Probability* **12** (1975), 69–77.

[Phe01] R. R. Phelps. Lectures on Choquet's Theorem. 2nd ed. Lecture Notes in Mathematics. Berlin Heidelberg: Springer-Verlag, 2001.

[Raa19] M. B. Raad. Renewal Time Points for Hawkes Processes. *arXiv:1906.02036 [math]* (June 2019).

[RDL20] M. B. Raad, S. Ditlevsen, and E. Löcherbach. Stability and mean-field limits of age dependent Hawkes processes. *Annales de l'Institut Henri Poincaré, Probabilités et Statistiques* **56** (2020), 1958–1990.

[Rob03] P. Robert. Stochastic Networks and Queues. Stochastic Modelling and Applied Probability. Berlin Heidelberg: Springer-Verlag, 2003.

[RS10] P. Reynaud-Bouret and S. Schbath. Adaptive estimation for Hawkes processes; application to genome analysis. *Annals of Statistics* **38** (Nov. 2010), 2781–2822.

[Rud73] W. Rudin. Functional analysis. McGraw-Hill, 1973.

[RV21a] P. Robert and G. Vignoud. Averaging Principles for Markovian Models of Plasticity. *Journal of Statistical Physics* **183** (June 2021), 47–90.

[RV21b] P. Robert and G. Vignoud. Stochastic Models of Neural Plasticity. *SIAM Journal on Applied Mathematics* **81** (Sept. 2021), 1821–1846.

[RV21c] P. Robert and G. Vignoud. Stochastic Models of Neural Synaptic Plasticity: A Scaling Approach. *SIAM Journal on Applied Mathematics* **81** (2021), 2362–2386.

[RV22b] P. Robert and G. Vignoud. On the Spontaneous Dynamics of Synaptic Weights in Stochastic STDP Models. *revisions at Physical Review E* (2022).

[RW00] L. C. G. Rogers and D. Williams. Diffusions, Markov Processes and Martingales: Volume 2, Itô Calculus. Cambridge University Press, Sept. 2000.

[Ver70] D. Vere-Jones. Stochastic Models for Earthquake Occurrence. *Journal of the Royal Statistical Society. Series B (Methodological)* **32** (1970), 1–62.

SECOND PART

Influence of STDP in computational models of the striatum

CONTENTS

The following document will be decomposed as follows: a general introduction, a general presentation of my contributions, wo parts gathering a total of seven different chapters, each chapter corresponding to a publication, and a discussion. Each chapter will contain its own appendix and a local bibliography.

CHAPTER 1

A SYNAPTIC THEORY FOR SEQUENCE LEARNING IN THE STRIATUM

ABSTRACT

Spatio-temporal patterns have been observed in a variety of brain areas in response to stimuli, prior or during action, or even in spontaneous activity. However, the biological mechanisms endowing neurons with the ability to distinguish between different sequences remain largely unknown. In fact, learning sequences of spikes raises multiple challenges, such as maintaining in memory spike history and discriminating partially overlapping sequences. Medium spiny neurons (MSN) in the striatum, expressing intense plasticity with cortex, have been reported to play a critical role in integrating context elements and develop sensorimotor associations. We theoretically explore the capacity of anti-Hebbian spike-timing dependent plasticity (STDP), observed at cortico-striatal synapses of MSNs, to drive the learning of sequences. To this purpose, we design a spiking model of the MSN receiving *spike patterns* defined as sequential input from a fixed set of cortical cells. We use a simple three-factor synaptic plasticity rule that combines anti-Hebbian STDP and non-associative potentiation associated to a subset of the presented patterns called *rewarded patterns*. We study, in various situations, the ability of the MSN to discriminate rewarded from non-rewarded patterns by firing only after presentation of a rewarded pattern. In particular, we show that two well-known biological properties of striatal networks, spiking latency and collateral inhibition, contribute to a significant increase in accuracy, by allowing a better discrimination of partially overlapping sequences. Altogether, these results argue that the anti-Hebbian STDP observed at cortico-striatal synapses may serve as a biological substrate for learning sequences of spikes.

1.1 Introduction

Nerve cells generate spatio-temporal patterns of action potentials, generally construed to convey information in the central nervous system. While spiking sequences have indeed been observed on a variety of timescales and in vastly distinct brain areas, the biological mechanisms employed to encode, store a sequence or distinguish between different sequences are still largely unknown. At behavioral timescales (seconds), episodic experiences are by nature a sequence of events [Xie+22]. In brain, these result in the generation of spatio-temporal spike sequences, as for instance with hippocampal place cells activating following the animal's movement [MKM08], parietal cortex sequences emerging in a virtual navigation-decision tasks [HCT12]. Generating dynamical output also require the formation of sequential cortical activity, as observed for instance in bird's ability to repeat spatio-temporal sequences over tens of seconds and with temporal structure maintaining millisecond accuracy within synfire chains [Ike+04], or more generally the generation of sequential activation of neural assemblies [Buz10]. Shorter timescale cortical spike sequences lasting tens of milliseconds were also reported in the relative timing of spikes between sequences in oscillating neural assemblies [WL96],

or in sequential activation after an up state transition [Luc+07], in response to a single spike [Hem+19], or even in spontaneous patterns of activity [LBH09]. Theoretically, Hebbian plasticity was reported to naturally generate sequential activity (see e.g. [PB20] for a recent work in an unsupervised learning setting).

The ubiquity of sequences in brain activity suggests that the nervous system shall have developed the ability to identify and distinguish sequences and spike in response to a given set of sequences (and remain silent for other types of input). Theoretically, this is a complex task. Firstly, identifying a sequence requires the ability to integrate signals on a timescale of several spikes. Moreover, difficulties arise for sequences that share a significant amount of input, overlap except for their last spikes, or even could be seen as incompatible. Interestingly, despite ample work in computational neuroscience and machine learning related to the learning of temporal sequences [Güt14], we did not identify any work dealing with the specific task of identifying specific sequences by firing or not depending on the full pattern of input (and differentially learn sub- or super-patterns)

An ample part of the literature related to learning sequences found solutions to the problem of replicating a target output spike train; algorithms based on error backpropagation [BKL02], high-threshold projection [Mem+14], Remote Supervision Methods (ReSuMe) [PK10], or the Chronotron [Flo12] which uses a modification of the Victor & Purpura distance for spike trains to compute error terms, were shown to be successful in performing those tasks. Closer to the problem at hand, some algorithms were designed to decode statistical information from spike trains, or even to simply spike in response to particular sequences of input spikes. Those techniques, that include the Tempotron [GS06; US09], and its extensions [Güt+13; Güt14], differ from the problem at hand in that the neuron is not required to take a decision at the end of the task but may fire at any point during the presentation of the stimulus. In the context of motor decision making for instance, this would be problematic in that it may trigger movement in response to a part of a stimulus that should, when completed, not give rise to a spike.

Here, we explore whether biological learning rules observed in the striatum allow the acquisition of the ability to discriminate between different sequences. The dorsal striatum, a subcortical nucleus and the main input structure of the basal ganglia, has indeed been shown to play a major role for action selection [YK06; GG15; JC15] and a prominent site for memory formation and procedural learning [PV19; Ath+18; Pet+21]. In this variety of tasks, one may expect that the striatum needs to use information from sequences of evidences to take a decision. In contrast with associative recurrent cortices that are efficient to recollect missing information when presented with partial patterns, the striatum is a largely feedforward network, that combines a variety of cortical input to produce an output. Corticostriatal synapses were shown to be highly plastic. They display anti-Hebbian Spike Timing Dependent Plasticity (STDP) [FGV05; Fin+10; Men+20], whereby a cortical spike followed by a striatal medium spiny neuron (MSN) spike leads to a depression of the associated synaptic weight. While many computational studies have investigated the impact of Hebbian STDP, only a few studies have investigated anti-Hebbian STDP. Those concentrated on the question of stability of synaptic weights [Rob00; CF03; BK12], compensation of dendritic attenuation [RA04], cancellation of correlated signals and novelty detection [ZD07; RL10], in particular in the electrosensory system of the mormyrid electric fish.

As shown in all these works, when presented with correlated activity, anti-Hebbian STDP will generally lead to depression of the associated synapses ; this mechanism

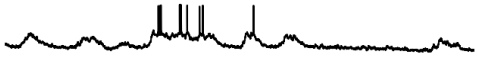

could naturally endow the system with the patience necessary to listen to full sequences and identify specific ones. We will show here that the combination of anti-Hebbian STDP with a simple, non-associative LTP is sufficient for a single MSN neuron to learn and distinguish sequences. We will note that while the simplest model of neuron with instantaneous firing will be able to learn sequences, they will however have a tendency to spike too early, in situations where partial sequences and longer sequences are presented. Going back to biology, we will observe that incorporating two key biological observations from the striatal network, spike latency and collateral inhibition, participate to the remarkable ability to identify and learn sequences of spikes.

1.2 Results

Sequence learning in the striatum

Given a spatio-temporal sequence of cortical spikes, we will say that a MSN has learnt a specific subset of sequences if it acquires the ability to spike in response to a specific subset of sequences, after the end of the correlated activity and not to spike in response to the others.

While basic, this notion of sequence learning is quite distinct from the literature. Indeed, as precisely reviewed in [Güt14], sequence learning has been classically divided into two different types of tasks: (i) reproducing a target spike train or (ii) classify a pattern by spiking, at any time, during the presentation of specific input sequences. The second task relates to the role of the striatal neurons which integrate cortical correlated patterns and then spike to trigger further downstream pathways leading to motor processing and eventually, an action. As such, it is similar to the task we set out to study here.

Since the latter task is not designed to wait until the end of a pattern to fire, when the network classifies a spike pattern B and fires during its presentation (at the end of subpattern A), it will also fire for any pattern that starts by (or just contains) A, and thus the specificity of pattern B and the extra information it contains compared to A is never taken into account. Assuming that the striatum needs to distinguish such patterns in some situations and to possibly respond differently to each of them, we have developed a new task where the striatal network, represented by one or two MSNs, integrates sequences of cortical spikes and naturally learns to spike *at the end* of the patterns.

This task, is different from the two previously defined in the sense that (i) a target spike train is not defined and used in the learning rule, and (ii) because the MSN needs to spike at the end of the pattern presentation and not earlier to produce a correct classification.

This novel tasks raises two main challenges: (i) the neuron shall keep the memory of past spikes for the whole duration of the pattern before firing, and (ii) some combinations of sequences may be harder to learn, for instance when the tasks include a rewarded pattern A that is a sub-pattern of another rewarded or non-rewarded patterns $B \supset A$, since in both cases the neuron will have a tendency to fire in response to the subpattern.

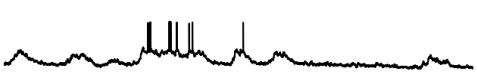

Simple models of striatal dynamics

Our scientific approach will consist in exploring the ability of striatal networks to achieve this task using simple, yet increasingly realistic, mathematical models. The striatum is a complex nucleus, composed primarily of MSNs that are the only cells that project outside of the striatum to other structures. These neurons integrate numerous cortical and thalamic inputs, and have been often described as coincidence detectors, since their high threshold requires the concomitant arrival of many spikes to induce a spike, which are often fired after a period of latency. Those neurons have been described in depth, both biologically and computationally, and several mathematical models were proposed to describe their behavior [Izh07; Hum+09; HWG09; YAK11; GHR15]. Within the striatum, MSNs have been also described to produce sparse inhibitory collateral connections among themselves, which reportedly plays a major role in the regulation of MSN firings or their overall activity [WAS07].

Our approach will consist in starting from the most simple setting of a single MSN receiving many cortical input and expressing the type of cortico-striatal plasticity observed experimentally, and build our way towards more complex models of two-neuron networks with non-linearities and adaptation, and assess in each case the performance of the system.

MSNs as linear leaky-integrate-and-fire neurons

Leaky-integrate-and-fire dynamics. We started by modeling the MSN as a linear leaky integrate-and-fire neuron [YAK11; Bur06; Ger+14], where the MSN integrates cortical and external inputs and fires when hitting a threshold. In detail, between two spikes, the membrane potential V of the neuron satisfies a linear differential equation:

$$\tau \frac{\mathrm{d}V}{\mathrm{d}t} = -(V(t) - V_{\mathrm{eq}}) + RI(t) + \sqrt{\tau} V_{\mathrm{noise}}(t)$$

Spikes are emitted when the voltage exceeds a threshold V_{th}, at which time the neuron's voltage is instantaneously reset to V_{r} and resumes input integration after a delay $\tau_{\mathrm{refractory}}$=10 ms. $V_{\mathrm{noise}}(t)$ represents Gaussian white noise, with a standard deviation of η_{noise}=0.5 mV.

Inference of the parameters from experimental data. In order to fit the model, we used electrophysiological data from MSNs recordings in the mouse dorsolateral striatum in response to steps of input current with increasing amplitude. An example of electrophysiological data is depicted in Figure 1.1a1. These protocols are standard to characterize the neuron spiking properties and are helpful to characterize the neuron type.

In particular, it is possible to extract from these protocols the resting membrane V_{eq}, the threshold V_{th} and the reset V_{r} potentials. Moreover, the R-I curve of the neuron is presented in Figure 1.1a2 (in blue). It represents the change in membrane potential as a function of input current intensity, and is used to compute R after fitting a linear curve to the experimental data (Figure 1.1a2, in green). τ can then be fitted directly on the electrophysiological traces. Once all these parameters are fixed, the model is completely constrained, and we can reproduce the action potential protocol using simulations (Figure 1.1a3). The model simulations reproduce relatively well

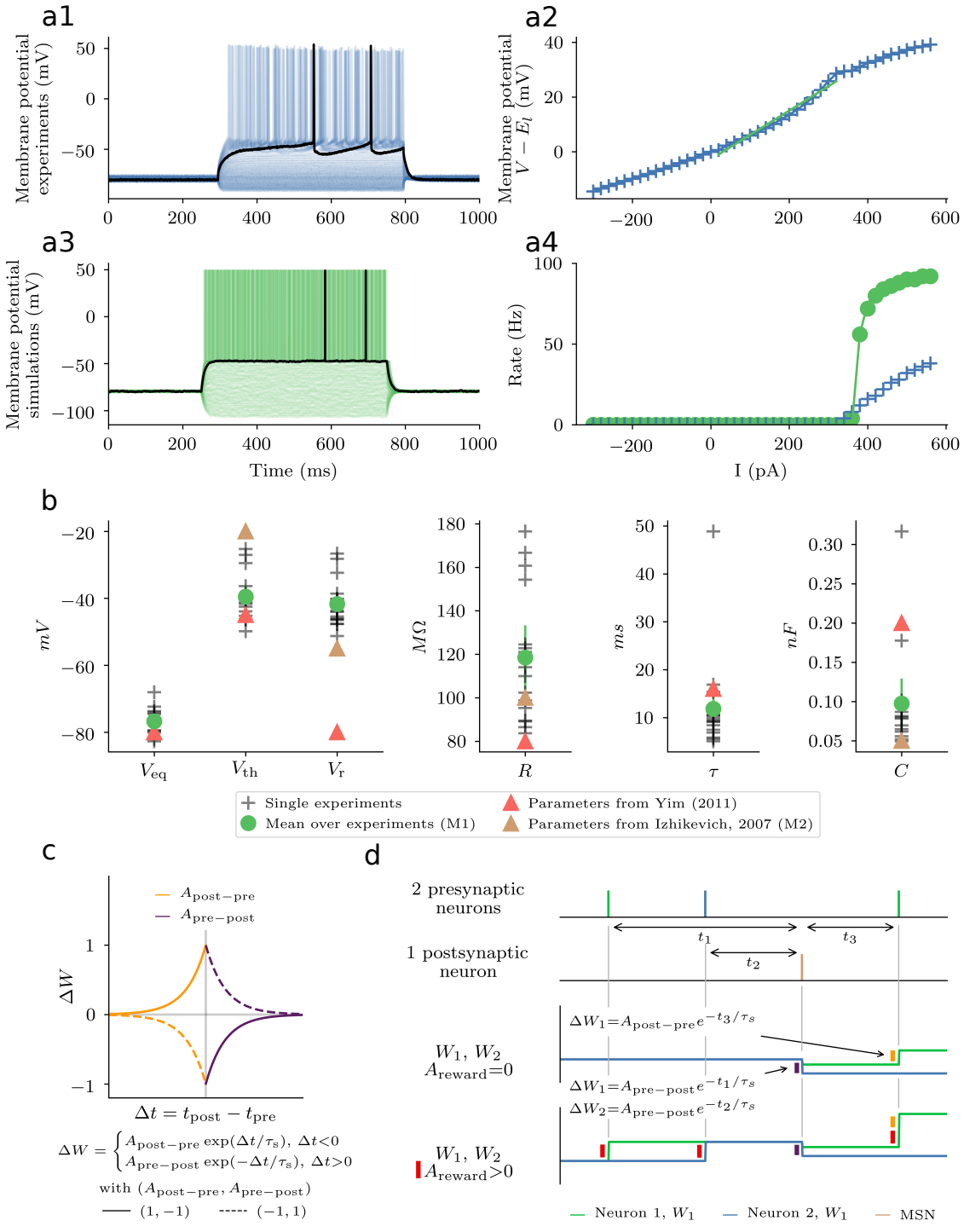

Figure 1.1: **MSNs as integrated-and-fire neurons with two types of synaptic plasticity at corticostriatal synapses.**

Figure 1.1: **MSNs as integrated-and-fire neurons with two types of synaptic plasticity at corticostriatal synapses.**

(a) *Integrate-and-fire model (M1) for the MSN.* (a1) Electrophysiological data (unpublished) from a MSN, recorded during an AP protocol (presentation of current steps with increasing intensity). Membrane potential in mV, first spiking event (in black). (a2) R-I curve from the same MSN, mean membrane potential value as a function of current intensity (in blue). Linear regression to determine R (in green). (a3) Response of an integrate-and-fire model, using values fitted on experimental data, to an AP protocol (presentation of current steps with increasing intensity). Membrane potential in mV, first spiking event (in black). (a4) Firing rates as a function of current intensity, experimental data (in blue), simulations with an integrate-and-fire neuron (green circle), exact FI curve for the integrate-and-fire model (green line).
(b) *Integrate-and-fire parameters, from experiments and previous models.* Values for the integrate-and-fire model parameters, fitted to each electrophysiological experiment (black crosses). Mean values over all experiments (green circles, M1). Values from the integrate-and-fire parameters from [YAK11] (red triangles) and from Izhikevich models [Izh07] (brown triangles, M2).
(c) *STDP applied at corticostriatal synapses.* Synaptic weight update ΔW as a function of Δt, using an exponential function, parametrized by $A_{\mathrm{post-pre}}$, for the change after a post-pre pairing (in orange) and $A_{\mathrm{pre-post}}$ for pre-post pairings (in purple), with exponential decay τ_s. Two examples of STDP are presented, asymmetric Hebbian STDP (dashed line) and anti-Hebbian STDP (solid line).
(d) *Non-associative potentiation to represent reward signals.* Simple example of synaptic updates resulting from spike train from two input neurons (top, neuron 1 in green, neuron 2 in blue) and one output neuron (second line, in brown). Synaptic update resulting from asymmetric anti-Hebbian STDP only (third line) or with non-associative reward-LTP (in red, bottom line).

---

electrophysiological data, considering the restricted numbers of parameters in the model. However, this type of model does not scale properly for high input currents, as can be seen when looking at the F-I curve (firing rate as a function of input intensity, Figure 1.1a4, blue data and green simulations).

Using experimental data from several MSNs, we fitted V_{eq}, V_{th}, V_{r}, R and τ for each neuron and also computed $C{=}\tau/R$. All these parameters are represented in Figure 1.1b, along with their averaged value (green circles) and values from previous studies (red triangles for [YAK11] and brown triangles for a non-linear version by [Izh07]). In particular, we notice that the values inferred from experimental data are consistent with canonical models, except for the reset potential V_{r} which is sometimes taken as equal to the rest potential V_{eq}, notably in [Izh07]. We have chosen to use a different value when modeling the MSN, because MSNs reset to values close to their threshold potential leading to a greater excitability immediately after a spike compared to when they are at their resting potential. In the following sections, MSNs will be modeled either using the linear integrate-and-fire model (M1) with parameters inferred using experimental data (the averages over all experiments, green circles), or the non-linear model (M2) from [Izh07]. Parameters are provided in Table 1.1.

Cortical inputs. In the cortical input received by the MSN (term $I(t)$ in equation 1.2), we explicitly distinguish the spikes received from P cortical neurons, noted $I_{\text{stim}}(t)$ (and with which plasticity will be modeled, see below) and an additional input $I_{\text{ext}}(t)$ modeled as a Poisson process with rate λ_{ext}:

$$I(t) = I_{\text{stim}}(t) + I_{\text{ext}}(t).$$

Each spike induces instantaneous jumps in the MSN membrane potential, with a constant amplitude $W_{\text{ext}}{=}1\,nA$ (high enough to be able to evoke spiking activity in the MSN) for external spikes and synaptic weights $W(t) = (W_i(t))_{1\leqslant i\leqslant P}$ for each of the P cortical neuron considered, that vary through plasticity mechanisms.

$$I_{\text{stim}}(t) = \tau \sum_{1\leqslant i\leqslant P} \sum_{t_i^k\leqslant t} W_i(t_i^k-)\delta(t-t_i^k), \qquad I_{\text{ext}}(t) = \tau W_{\text{ext}} \sum_{t_{\text{ext}}^k\leqslant t} \delta(t-t_{\text{ext}}^k),$$

where we noted, for a function f being potentially discontinuous at time t, $f(t-)$ the value reached immediately before the jump, $(t_i^k)_{k\geqslant 0}$ is the sequence of spikes of neuron i and $(t_{\text{ext}}^k)_{k\geqslant 0}$ the sequence of external spike times, that have exponentially distributed inter-spike intervals. The factor τ allows appropriate scaling of weights for direct comparison with experimentally measured EPSCs (excitory post-synaptic currents).

Synaptic plasticity at cortico-striatal synapses

Spike-timing dependent plasticity. Synaptic weights from the P cortical neurons to the MSN are subject to pair-based STDP, which is modeled as synaptic weight updates arising after each spike according to the spike timing relative to all previous spikes of the other neuron (all-to-all implementation in the parlance of [MDG08]). In detail:

— If the MSN spikes at time t_{post} (postsynaptic spike), then all weights are updated. Noting $t_{\text{pre},i}$ the previous spikes of cortical neuron i, the synaptic weight W_i is updated according to:

$$W_i(t_{\text{post}}) = W_i(t_{\text{post}}-) + \varepsilon \sum_{t_{\text{pre},i}<t_{\text{post}}} \Phi(t_{\text{post}} - t_{\text{pre},i})$$

where ε denotes the plasticity rate, chosen in our simulations as $\varepsilon{=}0.02$.

— If presynaptic cortical neuron $i \in \{1, \cdots, P\}$ spikes at time $t_{\text{pre},i}$, noting t_{post} the times of the MSN spikes, then the synaptic weight W_i is updated as:

$$W_i(t_{\text{pre},i}) = W_i(t_{\text{pre},i}-) + \varepsilon \sum_{t_{\text{post}}<t_{\text{pre},i}} \Phi(t_{\text{post}} - t_{\text{pre},i}).$$

Denoting $\Delta t{=}t_{\text{post}} - t_{\text{pre}}$ the timing between the presynaptic (cortical) spike and the postsynaptic (MSN) spike, we use an exponential STDP kernel [MDG08]:

$$\Phi(\Delta t) = \begin{cases} A_{\text{post-pre}} \exp\left(\frac{\Delta t}{\tau_s}\right) & \text{if } \Delta t < 0 \\ A_{\text{pre-post}} \exp\left(-\frac{\Delta t}{\tau_s}\right) & \text{if } \Delta t > 0 \end{cases}$$

with $\tau_s{=}20$ ms.

An example of this STDP curve and of the impact of each parameter is given in Figure 1.1c.

Non-associative reward-LTP. Anti-Hebbian plasticity and the prominence of depression associated was often combined with non-associative LTP to prevent neurons from becoming silent altogether [RB00; WRL03; RA04]. Indeed, synaptic weights involved in the firing of a postsynaptic neuron are reduced by anti-Hebbian STDP, leading to their decrease, a process that may persist until no postsynaptic spike is produced; in other words, in the absence of an additional LTP, the synaptic weights subject to anti-Hebbian learning decrease until the network becomes silent.

We chose to use non-associative LTP to model rewards signals, leading to the following synaptic update rule, where at each presynaptic spike of cortical neuron i, the associated synaptic weight W_i was updated by,

$$\Delta W_i = \varepsilon \, A_{\text{reward}}.$$

where A_{reward} is either null (corresponding to the absence of any LTP) or positive (corresponding to non-associative potentiation of active presynaptic neurons).

This model offers an approximation of more detailed models proposed in the literature, in particular three-factor learning rules [KIT17; Fon+18; Ger+18], by just considering a simple reward signal consisting in the potentiation of the synaptic weight at each presynaptic spike.

Eventually, synaptic weights are clipped within a realist range $[w_{min}, w_{max}]=[0., 2.]\, nA$. An example of simple synaptic weight dynamics with $P=2$ cortical neurons, with and without reward is presented in Figure 1.1d.

Pattern recognition in the striatum

Patterns of correlated cortical activity. Learning at the level of the striatum is based on the detection of correlated sequences of cortical inputs. We emulated learning through a simple task, where N_p patterns of cortical activity are presented to the MSN, whose spiking models the output of the network. A pattern represents a sequence of cortical activity with duration $t_{\text{duration}}=50\, ms$, and is composed by two different processes (i) correlated activity from a subset of cortical neurons (always present at each presentation of the pattern) (ii) random spiking activity from all cortical neurons.

In Figure 1.2a, a simple learning task is detailed with two patterns: pattern A which corresponds to a spike from cortical neuron 4 happening at time t_{offset}; pattern B where cortical neuron 1 spikes at t_{offset}, followed after a delay t_{delay} by a spike of cortical neuron 3, see Figure 1.2a (top right).

During learning, the network is presented with patterns, chosen randomly from the set of N_p patterns. Among the patterns, a fixed subset was chosen to be rewarded with a probability $1/2$. Accordingly, the rest of the patterns were defined as non-rewarded patterns. In the example of Figure 1.2a, pattern A was chosen to not be rewarded $(-)$ and pattern B rewarded $(+)$. During training, rewarded patterns are subject to a positive potentiation signal ($A_{\text{reward}}>0$) while non-rewarded patterns do not ($A_{\text{reward}}=0$). For all patterns, STDP rules are also applied at the synaptic weight matrix W depending on pre- and postsynaptic spikes.

Accuracy, a measure of the network performance in the classification task. A rewarded pattern was deemed learnt if the MSN fired after the presentation of the whole sequence of correlated cortical activity, while non-rewarded patterns should not elicit any spike. For example, in Figure 1.2a, both patterns were tested, before and after

learning. Before learning, patterns A and B did not trigger any spikes of the MSN, leading to a correct classification for A (as a non-rewarded pattern) and a misclassification for B. After learning, pattern A still did not elicit any spike while the MSN emited a spike after the presentation of all cortical spikes of pattern B, leading to a correct classification.

The accuracy of the learning process was estimated through the averaged numbers of correct responses:

$$\text{Accuracy} = \frac{1}{N_p} \sum_{1 \leqslant k \leqslant N_p} r_k \sigma_k + (1 - r_k)(1 - \nu_k), \tag{1.1}$$

where $r_k{=}1$ if k is a rewarded pattern and 0 otherwise, $\sigma_k{=}1$ if the MSN spiked after the correlated cortical activity and 0 otherwise, and $\nu_k{=}1$ if the neuron spikes, and 0 otherwise.

We stress here that to correctly classify a rewarded pattern, the MSN cannot spike during the cortical pattern, the spike has to be elicited at the end of the sequence. We made this choice to model the capacity of the striatum to take decision based on whole sequences of cortical activity, and not only on the first spikes.

The accuracy (and other network properties) is computed on a frozen network, where all sources of noise have been shut-off. All patterns are presented, and evaluated on this test network, with the MSN membrane potential reset to its resting value between each pattern.

Impact of STDP and reward-LTP on two simple tasks

In order to test whether simple models of cortico-striatal learning perform in learning sequences, we designed two simple tasks. We compared the evolution of different properties as a function of pattern iterations (Figure 1.2b and c), using four different types of STDP:

— Symmetric LTD: $A_{\text{post}-\text{pre}}{=}A_{\text{pre}-\text{post}}{=}-1$, which represents STDP where correlated spiking only leads to depression of the synaptic weight.

— Asymmetric Hebbian STDP: $A_{\text{post}-\text{pre}}{=}-1$ and $A_{\text{pre}-\text{post}}{=}1$, which emulates the classical Hebbian STDP rules where pre-post pairings lead to potentiation, while post-pre pairings lead to depression.

— Asymmetric anti-Hebbian STDP: $A_{\text{post}-\text{pre}}{=}1$ and $A_{\text{pre}-\text{post}}{=}-1$, which is the reverse of the asymmetric Hebbian STDP.

— Symmetric LTP: $A_{\text{post}-\text{pre}}{=}A_{\text{pre}-\text{post}}{=}1$, which represents STDP where correlated spiking only lead to potentiation of the synaptic weight.

We distinguish Hebbian learning rules (asymmetric Hebbian STDP and symmetric LTP), characterized by $A_{\text{pre}-\text{post}}{=}1$, from anti-Hebbian learning rules (asymmetric anti-Hebbian STDP and symmetric LTD) with $A_{\text{pre}-\text{post}}{=}-1$. Finally, we also tested the tasks with or without reward LTP (right or left respectively), and either starting from low or high synaptic weights (solid or dashed lines).

Task A, random inputs. In the first task, we presented the MSN with random activity from the cortical neurons ($100\,Hz$ for each cortical neuron) and studied the norm of the synaptic weight matrix W (Figure 1.2b). We observe in Figure 1.2b (left) that without reward-LTP, symmetric LTD leads to a decrease of the synaptic weight norms (blue line), regardless of the initial values. Conversely, symmetric LTP (red lines) leads to the general potentiation of the synaptic weight, again for both low and high initial synaptic weights. The picture is more complex for asymmetric Hebbian and anti-Hebbian STDP, whose dynamics change depending on the initial values. Asymmetric Hebbian STDP (in green) converges to a stable regime, while asymmetric anti-Hebbian STDP (in brown) either leads to complete depression when starting too low, or to complete potentiation when starting too high.

When adding reward-LTP Figure 1.2b (right), all rules lead to the potentiation of the synaptic weights, except symmetric LTD where depression still dominates.

Task B, learning to respond to one pattern. We next turned to investigate the dynamics of the system in response to a single pattern, obtained as a Poisson process with intensity $\lambda_{\text{poisson}}{=}1\,kHz$ on a time interval of duration $t_{\text{poisson}}{=}5\,ms$, conditioned with having at least two spikes. We computed the probability that the MSN remains silent (top), the relative timing of the first spike of the MSN (middle) and the resulting accuracy (bottom), for both a non-rewarded pattern (left) and a rewarded one (right).

Starting with the non-rewarded patterns, the simulations show several important features. First, when starting from low synaptic weights (not sufficient to trigger spiking), and in the absence of non-associative reward-LTP, the synaptic weights are not updated (indeed the postsynaptic neuron never spikes), and therefore the probability to remain silent is equal to 1 throughout learning, leading to an accuracy of 1 for each type of STDP. The picture is more complex when the network starts with initial synaptic weights high enough to trigger spikes of the postsynaptic neurons (dashed lines). In that case, symmetric LTD is able to reduce the synaptic weight enough to silent them, which translates in an increase in accuracy during learning, reaching maximal accuracy quickly. Asymmetric anti-Hebbian STDP is also able to reduce synaptic weights, also leading to an increase of accuracy. However, this is not as efficient as symmetric LTD, mainly because the network is unstable if the synaptic weights are too high initially, as was observed in Task A. Conversely, when the postsynaptic neuron spikes, symmetric LTP and asymmetric Hebbian STDP only lead to an increase of the synaptic weights involved in spiking, making it impossible for these Hebbian rules to silence the neuron when presented with a non-rewarded pattern. In particular, the accuracy stays equal to zero during all the task, as the MSN always spikes in response to the pattern.

We now present results for Task B with a rewarded pattern, in Figure 1.2c (right). When the network starts with small synaptic weights, the pattern does not trigger any MSN spike, as seen previously for the unrewarded pattern. However, thanks to the reward-LTP mechanism, the presence of presynaptic spikes results in the potentiation of the associated synaptic weight, and therefore leads to the triggering of MSN spikes. When looking at Hebbian rules, numerical experiments show that the MSN starts to spike after a short training (see the decrease in the probability to remain silent, top panel), and once the MSN spikes, the synaptic weights are still potentiated (even more, due to the fact that $A_{\text{pre}-\text{post}}{>}0$), forcing the first postsynaptic spike to be triggered at the beginning of the pattern (the relative timing of the first spike goes to 0, middle

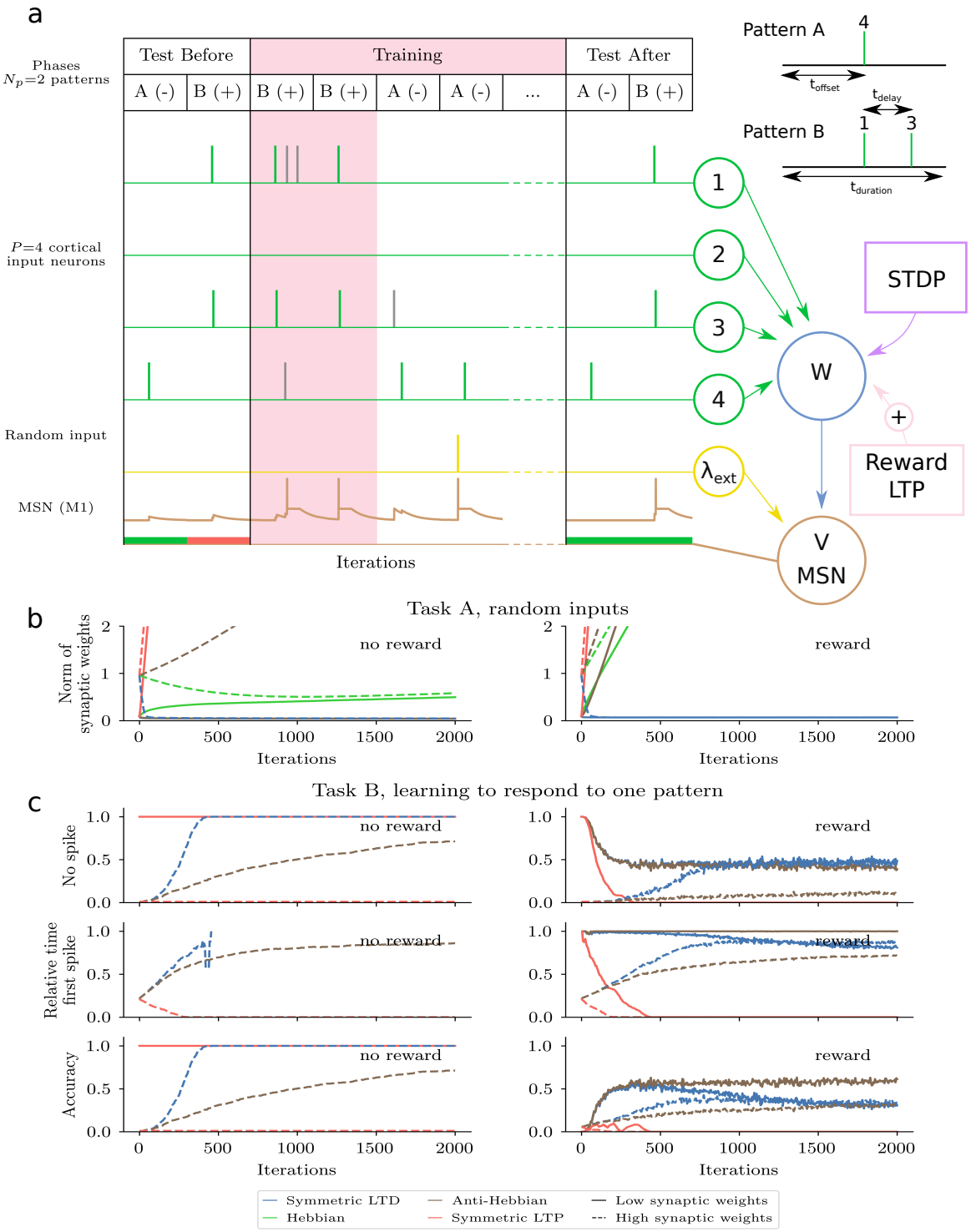

Figure 1.2: **Learning sequences in the striatum, using anti-Hebbian rules and non-associative reward-LTP.**

Figure 1.2: **Learning sequences in the striatum, using anti-Hebbian rules and non-associative reward-LTP.**

(a) *Classification task using the striatal network.* Schematic representation of the striatal network (right) with $P{=}4$ cortical neurons (in green), a random input neuron with rate λ_{ext} (in yellow) and one MSN, represented by its membrane potential V (in brown). Two mechanisms of synaptic plasticity are considered in the dynamics of the synaptic weight W (in blue): STDP (in purple) and LTP related to the reward signal (reward-LTP) (in red). Example of the learning task (left), with test sessions and the training protocol (middle). $N_p{=}2$ patterns A and B are presented to the network, with A being non-rewarded $(-)$ and B rewarded $(+)$. Each pattern represent sequential activity (top right), A with a single cortical spike and B with two spikes separated by a delay t_{delay}. All pattern have a duration of t_{duration}, and correlated cortical spikes are presented at t_{offset}. Spiking activity of the cortical neurons (in green for pattern spikes and grey for random spikes) and the random input neuron (in yellow) are represented along with the membrane potential V of the output neuron (MSN, M1, in brown). In the test sessions, below the MSN potential, are represented accuracy results (correct classification in green, wrong classification in red).
(b) *Dynamics of learning with random noise (Task A).* Evolution of the norm of the synaptic weights, during the presentation of cortical random spikes, with $P{=}10$ cortical neurons, without (left) or with (right) non-associative reward-LTP, for different types of STDP rules (color) and different values of initial synaptic weights (low in solid lines, high in dashed lines).
(c) *Dynamics of learning with a Poisson sequence (Task B).* Different learning properties, during the presentation of a Poisson sequence, with $P{=}10$ cortical neurons, without (left) or with (right) non-associative reward-LTP, for different types of STDP rules (color) and different values of initial synaptic weights (low in solid lines, high in dashed lines). (top) Probability to observe no spike during pattern presentation, (middle) relative timing of the first postsynaptic spike, (bottom) accuracy. (Note: the traces from symmetric LTP and asymmetric Hebbian STDP are superimposed.)

Low synaptic weights $=[0., 0.05]\,nA$ / high synaptic weights $=[0.05, 0.5]\,nA$ / $A_{\text{reward}}{=}0.5$ / $N{=}500$ independent networks / Membrane potential X and plasticity reset between each pattern.

---

panel). In particular, this response (spiking before the end of the pattern) is not the correct behavior, and leads to an accuracy of 0 (bottom panel).

For anti-Hebbian rules, another type of dynamics emerges. At first, only A_{reward} acts on the synaptic weight, leading to the potentiation of W. Once a spike is elicited at the MSN, the associated synaptic weight undergo a combination of potentiation (from A_{reward}) and depression (from $A_{\text{pre-post}}{<}0$), with $A_{\text{reward}}{+}A_{\text{pre-post}}{<}0$. After each postsynaptic spike, synaptic weights are therefore decreased. Several iterations are needed for this resulting depression to decrease the synaptic weight enough to stop triggering spikes at the postsynaptic neuron. When this event arrives, the synaptic weights are again only subject to potentiation, which leads to spiking of the postsynaptic neuron in the following presentation. The MSN therefore alternates between answering correctly to the pattern (by spiking) or not (by remaining silent). Anti-Hebbian rules

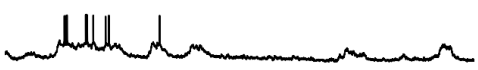

lead to an equilibrium where the MSN oscillates between those two states. This can be seen by the fact, that the probability to remain silent converges to 0.5 in both cases, resulting in an accuracy of 0.5. Asymmetric anti-Hebbian STDP is particularly stable in this regime, while symmetric LTD loses efficacy after extended training.

When starting from higher synaptic weights, symmetric LTD and asymmetric anti-Hebbian STDP are able to displace the postsynaptic spikes to the end of sequence of cortical activity (see blue dotted lines, in middle panel), resulting in a non-zero accuracy.

As a conclusion, only symmetric LTD and asymmetric anti-Hebbian STDP correctly learn to classify both types (rewarded and non-rewarded) of patterns, whereas Hebbian rules perform poorly. It is particularly interesting to notice that anti-Hebbian rules have been shown to be present at corticostriatal synapses [FGV05], and therefore enable the correct classification of patterns of sequential cortical activity. This conclusion results of course from our definition of accuracy, where rewarded patterns are only classified correctly when they spike *after* the pattern.

These simple experiments have however pointed out that the anti-Hebbian rules, coupled with non-associative reward-LTP lead to an equilibrium where the neuron oscillates between sub- and supra-threshold states. In particular, the accuracy, measured as defined above, suffers from this dynamics and does not render the fact that the network has indeed learned the correct combination of weights to elicit a spike at the end of the pattern. In order to compare with systems where a stable equilibrium is reached, we define a new metric that we call MaxAccuracy as,

$$\text{MaxAccuracy}(t) = \max_{[t-T_1, t+T_1]} \{\text{Accuracy}(t)\}$$

where $\text{Accuracy}(t)$ represents the value of accuracy computed at time t, following Eq. 1.1, and $[t-T_1, t+T_1]$ represents an interval of pattern iterations (T_1 will be taken as 10 test iterations in the rest of the paper). In particular, when using this measure, the oscillatory behavior described before is "hidden" thanks to the $\max$, which will be useful when comparing with more stable learning rules. We stress that this equilibrium results from the simple hypotheses of the model, in particular the absence of reward-prediction errors, and other mechanisms that would lead to the convergence of the synaptic weights to stable values.

Sequence learning using anti-Hebbian rules with a single output cell

Now that the setting has been detailed, and after testing the direct influence of both STDP rules and reward signaling, we aim at testing the previous conclusions on more complex tasks.

Task 1, learning sequences of cortical associations

We now focus our attention on the ability of the network to learn to discriminate N_p patterns composed of sequences of cortical spikes.

More practically, the N_p are chosen as follows:

a. Each pattern is assigned to a number n of cortical spikes uniformly (between 1 and N_{stim} inputs).

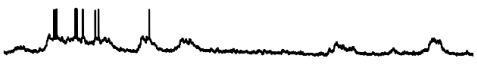

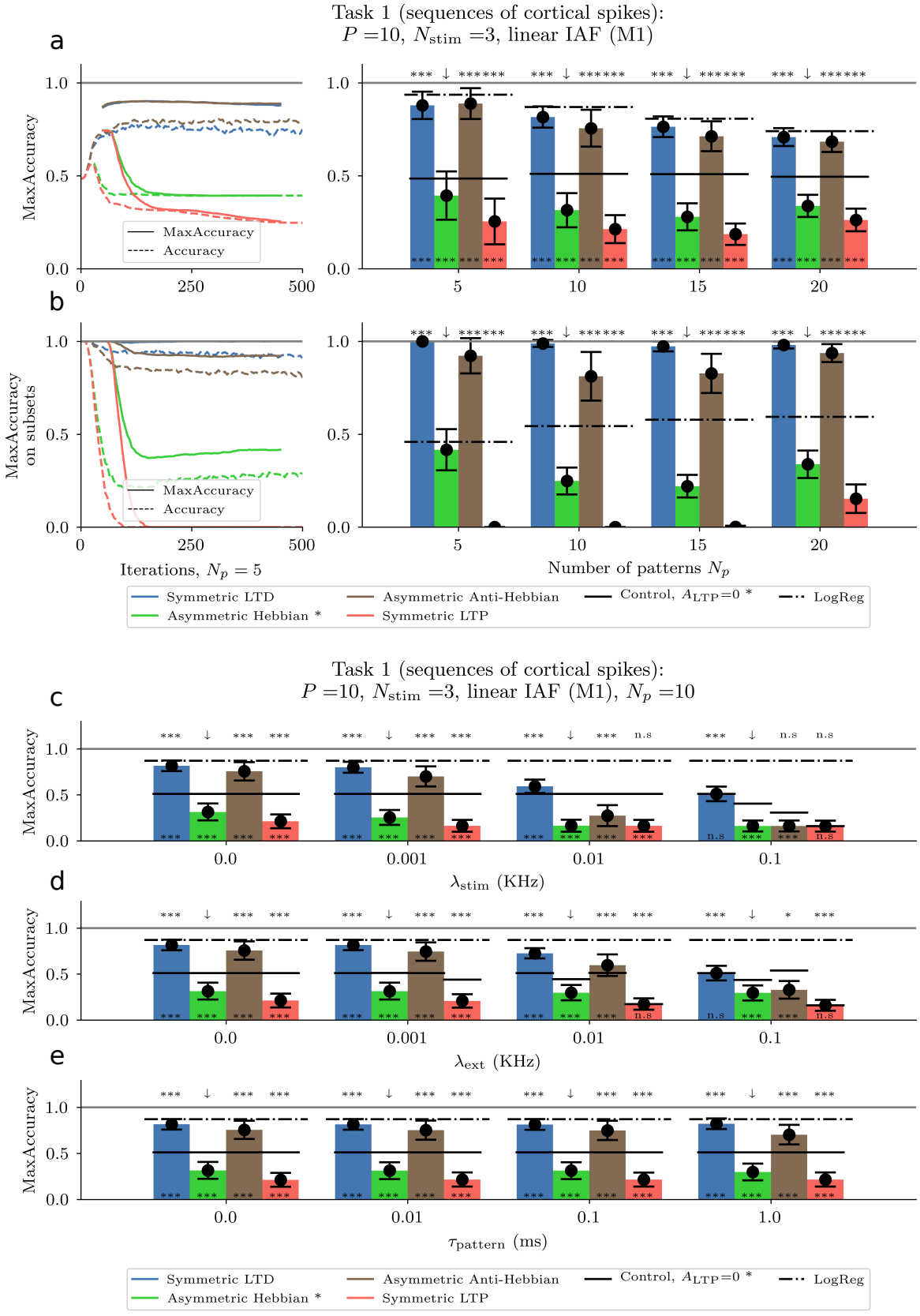

Figure 1.3: **Anti-Hebbian rules and non-associative LTP enable learning with a single linear integrate-and-fire MSN (M1).**

Parameters	(M1)	(M2) [Izh07]	[YAK11]
$V_{\text{eq}}\,(mV)$	-76.72	-80	-80
$V_{\text{th}}\,(mV)$	-39.51	-20	-45
$V_r\,(mV)$	-41.70	-55	-80
$R\,(M\Omega)$	118.50	100	80
$\tau\,(ms)$	11.85		16
$C\,(nF)$	0.098	0.05	0.2
$a\,(ms^{-1})$		0.01	
$b\,(nF\,ms^{-1})$		-0.02	
$d\,(nF\,ms^{-1}\,mV)$		0.15	

Table 1.1: **Parameters of different models for MSNs.**

b. The pattern is associated to a different ordered subset of n neurons from $\{1, P\}$.

c. The temporal sequence is defined with the first spike at time t_{offset}, and the following ones presented with a fixed delay t_{delay}=1 ms.

d. Finally, each pattern is chosen to be rewarded or not, with probability $1/2$.

Patterns A and B from Figure 1.2a where build following this method. For pattern A, we have n=1 spikes of cortical neuron (4) at time (t_{offset}). For pattern B, we have n=2 spikes of cortical neuron $(1,\ 3)$ at time $(t_{\text{offset}},\ t_{\text{offset}}+t_{\text{delay}})$.

During the task, we measure at test protocols (frozen network), the accuracy and MaxAccuracy as defined before. Moreover, for each set of parameters we realize the simulations either with,

— A_{reward}=0.9 for rewarded patterns, and A_{reward}=0 for non-rewarded ones, to emulate supervised learning using the rewarding signal;

— A_{reward}=0 for all patterns, as a control task, where no supervision is given to the network.

In order to compare with more classical algorithms, we have defined an equivalent optimization problem, where the correct classification is learned using logistic regression, implemented with the *lmfit* package. We trained the network taking as inputs a binary version of the $P \times N_p$ matrix $(M_{p,n})$, with $m_{p,n}$=1 if cortical neurons n was spiking during pattern p, and $m_{p,n}$=0 if neuron n does not spike during pattern p. The linear matrix in the logistic regression W is constrained to only have positive coefficients, as would happen for excitatory synapses.

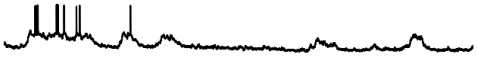

Figure 1.3: **Anti-Hebbian rules and non-associative LTP enable efficient learning with a single linear integrate-and-fire MSN (M1).**

(a) *Only anti-Hebbian rules lead to learning when presenting patterns composed by sequences of cortical inputs* [Task 1] (left) Accuracy (dashed lines) and MaxAccuracy (solid lines) as a function of learning iterations, for different STDP rules, for N_p=5 patterns. (right) MaxAccuracy as a function of the number of presented patterns N_p, for different STDP rules.
(b) *Anti-Hebbian rules lead to a specific equilibrium where smaller subsets of rewarded patterns do not lead to spike of the MSN.* (left) [Task 1] Accuracy (dashed lines) and MaxAccuracy (solid lines) as a function of learning iterations, for different STDP rules, when testing subpattern of N_p=5 learned patterns. (right) MaxAccuracy when testing subpattern of N_p learned patterns, for different STDP rules.
(c-e) *Influence of different types of noise on learning and performance* [Task 1] MaxAccuracy as a function of noise in cortical inputs λ_{stim} (c), of external noise injected directed in the MSN potential λ_{ext} (d) and jitter in spike times during pattern presentation τ_{pattern} (e), for different STDP rules.

Training done for 500 patterns iterations, with test sessions every N_p iterations. Mean results computed over N=250 simulations with errors bars representing $\pm$SD/2.
Statistical t-test from scipy.stats Python library; *: p<0.05, **: p<0.005, ***: p<0.0005.
(below) (H0): networks without supervision (A_{reward}=0), compared with networks with supervision (A_{reward}=0.9).
(above) (H0): networks with asymmetric Hebbian STDP, compared to other STDP rules.

Anti-Hebbian rules enable learning of cortical sequences with fixed delay

The results for Task 1, with P=10, N_p=5 and N_{stim}=3 are presented in Figure 1.3a (left). The temporal evolution of the accuracy (dashed lines) and MaxAccuracy (solid lines) are represented for the four different types of STDP presented before. We observe that both anti-Hebbian rules learn to classify correctly the patterns. As explained in the previous section, the synaptic weights converge to an equilibrium, and then alternate a few correct responses with one wrong response that initializes a new sequence of correct responses. Using the MaxAccuracy quantification, we observe higher levels of performance and more truthfully represent the fact that the network discriminate patterns correctly. Hebbian rules do not perform well in this task, leading to low accuracies. It is interesting to note that MaxAccuracy and accuracy converge to the same values for Hebbian rules, highlighting the fact that MaxAccuracy does not always improve the accuracy value.

Similar results are obtained for various numbers of patterns N_p Figure 1.3a (right). In particular, for all the different tasks presented here, only anti-Hebbian rules perform significantly better than the control without supervision (comparison with black solid lines, significativity at the bottom of each bar plot). More interestingly, Hebbian rules perform significantly worse than without supervision. When comparing with results from the logistic regression, we see that anti-Hebbian rules perform slightly worse than the classical machine learning algorithm. As a conclusion, anti-Hebbian rules enable efficient learning in Task A, while Hebbian rules perform worse than a non-supervised network.

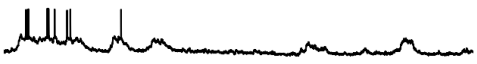

To further investigate the equilibrium reached by anti-Hebbian rules while learning Task A, we have tested the response of the network to randomly selected "subpatterns" of the rewarded patterns. For example, if during the task, the pattern $(1, 3)$ was rewarded, we tested the response of the MSN to the patterns $(1, \varnothing)$, $(\varnothing, 3)$, where $\varnothing$ means that no spike were presented. We computed the accuracy on these subpatterns, a correct classification was defined when the subpattern did not elicit any MSN spike. The results are gathered in Figure 1.3b, and show that anti-Hebbian rules perform significantly better than Hebbian ones, in a task where classical logistic regression produce fewer correct classifications.

To appreciate the robustness of these findings, we changed the number of neurons P, of stimulations by pattern N_{stim}, and found similar results (see Figure 1.7a-b), except for asymmetric anti-Hebbian STDP which performs worse for higher number of stimulations, again due to its unstable behavior. Moreover, we have also tested if changes in $A_{\text{post}-\text{pre}}$ values leads to different dynamics in Figure 1.7c. We showed that learning really depends on $A_{\text{pre}-\text{post}}$ (Hebbian or anti-Hebbian rules) while $A_{\text{post}-\text{pre}}$ influence is less notable. Finally, we tried different values for A_{reward} in Figure 1.7d, two main conclusions can be drawn from these experiments. In order to elicit learning, we need to have $A_{\text{reward}} + A_{\text{pre}-\text{post}} < 0$, which is verified when $A_{\text{pre}-\text{post}} = -1$, for $A_{\text{reward}} < 1$. Moreover, maximal learning is achieved when $A_{\text{reward}} + A_{\text{pre}-\text{post}}$ is small compared to A_{reward}. With this observation in mind, we will choose in the sequel $A_{\text{reward}} = 0.9$ which verifies both of these properties.

Anti-Hebbian rules do not only learn to correctly classify rewarded patterns, but they also converge to an equilibrium where subpatterns of cortical activity are not sufficient to trigger spiking at the MSN. In conclusion, MSNs subject to anti-Hebbian STDP, learn to spike only if the whole pattern is presented.

Robustness to different types of noise

In order to test the robustness of learning to spontaneous activity, we introduced three types of noise in the neuronal network dynamics,

a. random cortical spikes at rate of λ_{stim};

b. random MSN spikes at rate λ_{ext}, implemented thanks to I_{ext} spikes defined in Section 1.2;

c. random jitter in the spike timings during pattern presentation, with standard deviation τ_{pattern}.

MaxAccuracy for $P = 10$, $N_p = 5$ and $N_{\text{stim}} = 3$, with different noise values are presented in Figure 1.3c-e. In all three cases, we start without noise, and test with increasing values of the noise parameter. It is quite interesting to see that learning is robust in the presence of random cortical spikes (Figure 1.3c), up to $1\,Hz$, and that symmetric LTD performs well even with higher noise values. Again this confirms the fact that asymmetric anti-Hebbian STDP leads to more unstable dynamics, and start failing for lower noise intensities than symmetric LTD. We emphasize here that the random presynaptic spikes also leads to potentiation of the associated synaptic weights, through the non-associative reward LTP. The same conclusions can be drawn with random MSN spikes (Figure 1.3d). In both cases, adding noise with higher frequency ($100\,Hz$) quite expectedly makes the network unable to learn. Finally, adding jitter in the timings

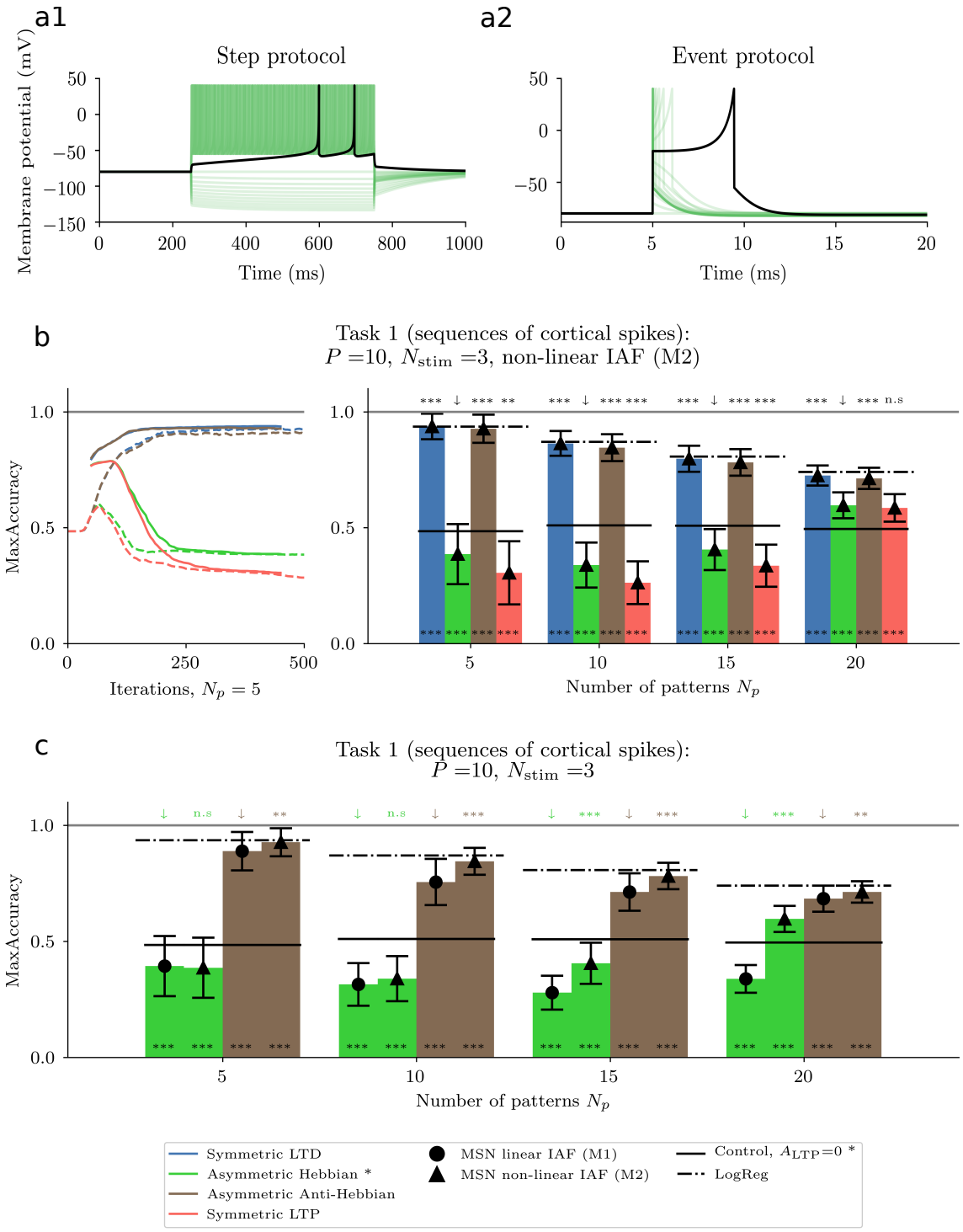

Figure 1.4: **Latency in MSNs enhance the network performance.**

Figure 1.4: **Latency in MSNs enhance the network performance.**

(a) Response of a non-linear Izhikevich model (M2) to an AP protocol (presentation of current steps with increasing intensity) (a1) or presentation of a pulse of current (a2). Membrane potential in mV, first spiking event (in black).
(b) [Task 1] Accuracy (dashed lines) and MaxAccuracy (solid lines) as a function of learning iterations, for different STDP rules, for $N_p{=}5$ patterns for non-linear Izhikevich (M2) model. (right) MaxAccuracy as a function of the number of presented patterns N_p, for different STDP rules.
(c) [Task 1] MaxAccuracy as a function of the number of presented patterns N_p, for asymmetric Hebbian and anti-Hebbian STDP, comparing linear IAF (M1) and non-linear Izhikevich (M2) models.

Training done for 500 patterns iterations, with test sessions every N_p iterations. Mean results computed over $N{=}250$ simulations with errors bars representing $\pm$SD$/2$.
Statistical t-test from scipy.stats Python library; *: $p{<}0.05$, **: $p{<}0.005$, ***: $p{<}0.0005$.
(below) (H0): networks without supervision ($A_{\text{reward}}{=}0$), compared with networks with supervision ($A_{\text{reward}}{=}0.9$).
(b, above) (H0): networks with asymmetric Hebbian STDP, compared to other STDP rules. (c, above) (H0): (M1) compared to (M2) neurons models, for asymmetric Hebbian STDP (green) and asymmetric anti-Hebbian STDP (brown).

---

of cortical spikes in the pattern presentation does not stop anti-Hebbian rules from reaching high accuracy. Jitter leads to more realistic patterns of cortical activity, with a random timing between each cortical stimulation (but with fixed average). As shown in this section, the network is robust to noise, and accordingly in the following experiments, we will suppress all noise processes, to concentrate on the higher bounds of th network's capacity.

Spiking latency enhances the network's performance

Using the previous network, anti-Hebbian rules were able to approach classical machine learning accuracy, but they did not perform as well.

Heuristically, integrate-and-fire models have the drawback to fire instantaneously after the depolarization of the membrane potential. This implies that when presented with overlapping patterns, e.g. patterns $A{=}(1)$ and pattern $B{=}(1,\,2)$, the neuron will not be able to learn to spike after the end of both patterns, because it will either be able to spike in response to pattern A only, and therefore fire before the end of pattern B, or it will spike after pattern B, and thus not spike after pattern A. This *'impatience'* of the MSN described by integrate-and-fire models is in fact an artifact of the simplicity of the integrate-and-fire model. In reality, biological MSNs have been shown to display spike latency: once a spike is triggered, the neuron spikes only after a delay.

In order to test whether the spike latency property in MSN neurons improves their ability to learn sequences, we modified our neuron model to include a nonlinearity and adaptation, following [Izh07]. This neuron model (noted M2) was shown to display spike latency akin to electrophysiological measurements. The equation of the voltage

V and adaptation U are given by:

$$\begin{cases} C\frac{\mathrm{d}V}{\mathrm{d}t} = k(V(t) - V_{\mathrm{c}})(V(t) - V_{\mathrm{eq}}) - U(t) + I(t) \\ \frac{\mathrm{d}U}{\mathrm{d}t} = a(b(V(t) - V_{\mathrm{eq}}) - U(t)). \end{cases}$$

with spike emitted when the voltage exceeds a threshold V_{th}, at which time the neuron's voltage is instantaneously reset to V_{r}. In these models, spike emission is due to a runaway build up of cell membrane potential (or, mathematically, a blow-up of the solutions [Tou08; TB09]) associated with the quadratic nonlinearity in the voltage equation. At the time of a spike, the adaptation variable is updated to $U(t-) \to U(t-) + d$. These models are known to be very versatile depending on the parameter set [Tou08; Rub+17], and we use here the parameters provided in [Izh07] (see Table 1.1). The parameters are compared to the integrate-and-fire model (M1) ones in Figure 1.1b. In order to appropriately scale the input, currents I_{stim} and I_{ext} defined above are scaled by RC, with R a scaling factor set as $R{=}100\,M\Omega$

We present in Figure 1.4a, the MSN membrane potential using the non-linear model (M2), either for step (a1) or pulse (a2) currents. Nonlinear dynamics, and spike latency lead to dynamics of the membrane potentials closer to electrophysiological data (compare Figure 1.1a1 and Figure 1.4a1). The latency property is more clearly visible in the neuron's response to cortical pulses (Figure 1.4a2), where it can be seen that when the current pulse is just sufficient to trigger a spike (black line), initiation of a spike takes several milliseconds.

In Figure 1.4b, we present the resulting MaxAccuracy for Task 1, using neuron model (M2). We show that asymmetric anti-Hebbian STDP performs as well as the logistic regression, which confirms the fact that the lack of latency was responsible for the gap observed with (M1). We more precisely compare both models in Figure 1.4c, and show that with asymmetric anti-Hebbian STDP, (M2) always reaches significantly higher accuracies than (M1).

We have showed in this section, that anti-Hebbian STDP rules coupled with a latency mechanism for spiking make a simple striatal network as efficient as logistic regression to learn a classification task using biological learning rules.

Inhibition in striatal networks improves learning

While taking into account non-linearities and adaptation produce latencies that may allow the appropriate learning of nested rewarded patterns, the excitatory nature of the cortico-striatal input prevents the system from learning rewarded pattern A and a non-rewarded pattern B that contains A (Figure 1.5a). Indeed, either the MSN spikes for pattern A, and it has to spike for pattern B (case of Figure 1.5a, 3rd line), or it does not spike for any of them. We note that a similar issue arises with the logistic regression when we constrain the weights W to be positive. Biologically, as exposed above, the striatum is a complex network made of a large number of MSNs, sharing part of their input, receiving distinct neuromodulation, and interacting together through collateral inhibition. Heuristically, this collateral inhibition could, in nature, provide a mechanism to learn such nested patterns. We explore this hypothesis here in a simple model.

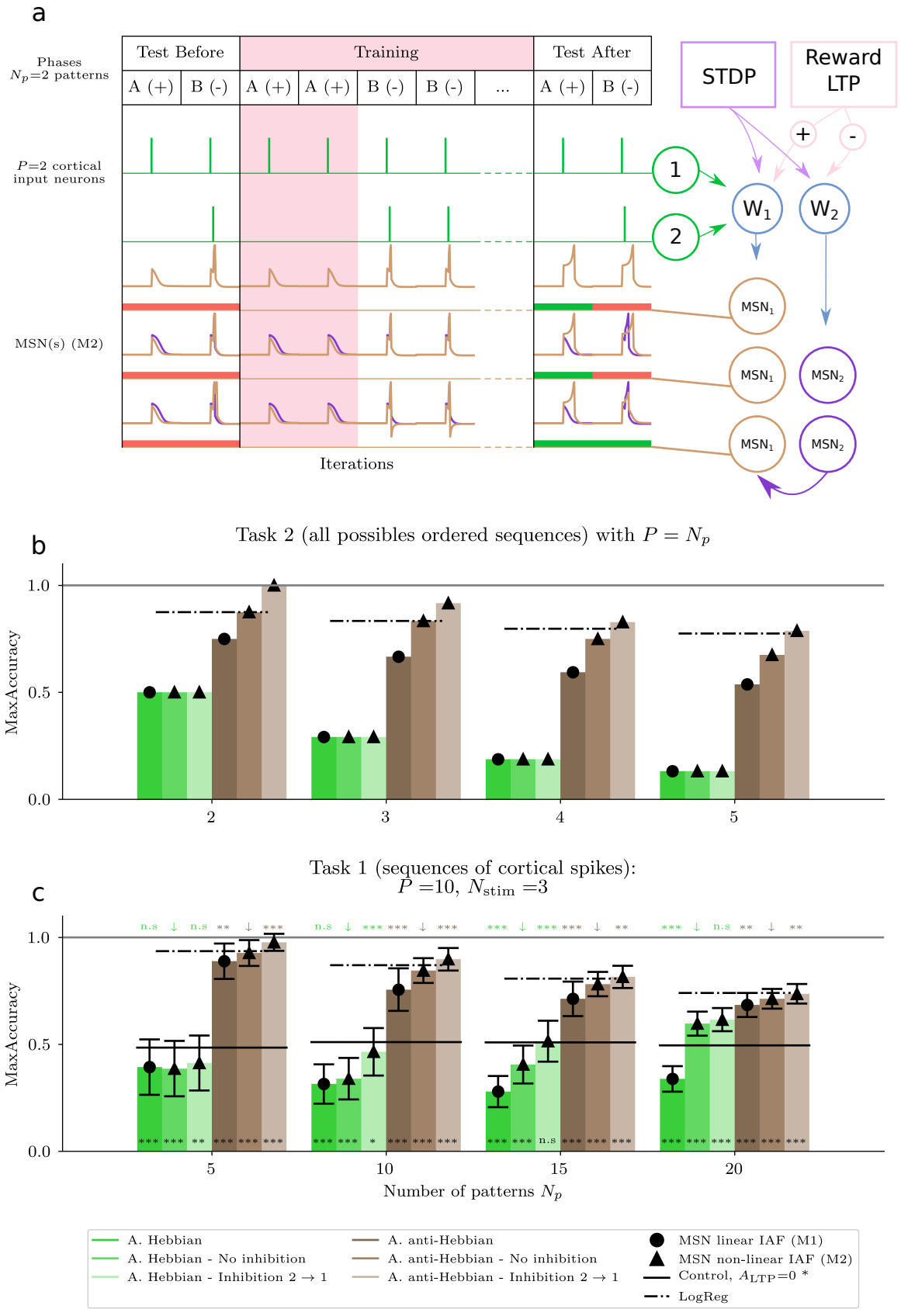

Figure 1.5: **Lateral inhibition facilitates learning of complex pattern sequences.**

Figure 1.5: **Lateral inhibition facilitates learning of complex pattern sequences.**

(a) *Lateral inhibition in the striatal network.* Schematic representation of the striatal network (right) with $P{=}2$ cortical neurons (in green), and three different models for MSN activity: (i) one striatal neuron (MSN) modeled as a non-linear IAF neuron (M2, in brown), (ii) two striatal neurons (MSN_1 in brown, and MSN_2 in purple) without collateral inhibition, (iii) two striatal neurons with collateral inhibition from MSN_2 to MSN_1.
Two mechanisms of synaptic plasticity are considered in the dynamics of the synaptic weight W (in blue): the STDP (in purple) and LTP related to the reward signal (reward-LTP) (in red). Reward-LTP is presented for rewarded patterns at MSN_1 and for non-rewarded patterns at MSN_2. Example of the learning task (left), with test sessions and the training protocol (middle). $N_p{=}2$ patterns A and B are presented to the network, with A being rewarded $(+)$ and B non-rewarded $(-)$ (for MSN_1). In the test sessions, below the MSN potential, are represented accuracy results (correct classification in green, wrong classification in red). Spiking activity of the cortical neurons (in green) are represented along with the membrane potential V of for the output neuron(s) (MSN).
(b) *Advantages of lateral inhibition in learning all possible patterns for a small number of neurons.* [Task 2] MaxAccuracy when learning all possible sequences for P neurons, for asymmetric Hebbian and anti-Hebbian STDP, comparing linear IAF (M1) and non-linear Izhikevich (M2) models, in the absence ($J{=}0$) or presence ($J{=}{-}0.5$) of lateral inhibition.
(c) *Consequence of lateral inhibition when learning sequences of cortical inputs* [Task 1] MaxAccuracy as a function of the number of presented patterns N_p, for asymmetric Hebbian and anti-Hebbian STDP, comparing linear IAF (M1) and non-linear Izhikevich (M2) models, in the absence ($J{=}0$) or presence ($J{=}{-}0.5$) of lateral inhibition.

[Task 2] Training done for 2000 patterns iterations, with test sessions every 5 iterations. [Task 1] Training done for 500 patterns iterations, with test sessions every N_p iterations. Mean results computed over $N{=}250$ simulations with errors bars representing $\pm$SD$/2$. Statistical t-test from scipy.stats Python library; *: $p{<}0.05$, **: $p{<}0.005$, ***: $p{<}0.0005$.
(below) (H0): networks without supervision ($A_{\text{reward}}{=}0$), compared with networks with supervision ($A_{\text{reward}}{=}0.9$).
(above) (H0): (M2) neurons without collateral inhibition ($J{=}0$) for asymmetric Hebbian STDP (green) and asymmetric anti-Hebbian STDP (brown).

A striatal network with two MSNs, connected through collateral inhibition

We considered a simple two-neuron network model (neurons labeled MSN_1 and MSN_2), where each MSN is a non-linear integrate-and-fire neuron (model M2 of section 1.2), which integrates the same cortical activity through two different weight matrices W_1 and W_2 (Figure 1.5a), and MSN_1 may be inhibited by MSN_2 through an additional current:

$$I_2(t) = RCJ \sum_{t^k_{\text{MSN}_2} \leqslant t} \delta(t - t^k_{\text{MSN}_2}),$$

where $(t^k_{\mathrm{MSN}_2})$ are the spike times of MSN_2, and $J = -0.5\,nA$. The absence of inhibition corresponds to $J = 0$. MSN_1 and MSN_2 also differ in their rewards. Here, we assumed for simplicity that MSN_1 and MSN_2 learn opposite tasks (i.e., MSN_2 is rewarded for non-rewarded patterns of MSN_1, see Figure 1.5a (right)), and the accuracy is read out on MSN_1 only. Figure 1.5a illustrates the fact that, in the absence of collateral inhibition (fourth line), MSN_1 learns to respond to pattern A, and as a consequence also spike for pattern $B \supset A$, while MSN_2 spikes after pattern B. Therefore, inhibition from MSN_2 (fifth line) can now induce a strong enough depolarization of MSN_1 potential to prevent it from spiking, leading to the correct classification of both patterns. Beyond this specific case, we investigated in detail how, statistically, collateral inhibition impacted accuracies.

Collateral inhibition enhance the network perfomance above logistic regression

In order to study more extensively this new network property, we consider a second task, Task 2, where patterns are forced to be nested one into another, leading to the misclassifications detailed in the previous section.

In particular, we test for P neurons, how the network is able to correctly discriminate the following P patterns, (1), $(1,\,2)$, ..., $(1,\,2,\,...,\,P)$, when considering all possible combinations of rewarded/non-rewarded patterns. We have tested on all these combinations (so 2^P situations) how the network performs in the discrimination task. For example, for P=2, the network is tested on 4 different sets of 2 patterns, (1) and $(1,\,2)$, with each pattern being either rewarded $(+)$ or non-rewarded $(-)$. For this task only, we have chosen a delay between spikes of t_{delay}=$0.5\,ms$. The results are presented in Figure 1.5b, for several values of P. As could be expected from the example of Figure 1.5a, the network with collateral inhibition is able to correctly classify all sequences of patterns for P=2, and stay close to the optimal performance for higher values of P. In particular, this network completely outperforms either the network without inhibition, or logistic regression.

It is interesting to question our choice of rewards for MSN_2, who rewards patterns that are not rewarded by MSN_1, and conversely, do not reward patterns that are rewarded by MSN_1. Considering the fact that the collateral inhibition is unilateral from MSN_2 to MSN_1, two rewards strategies were possible for MSN_2, either it rewarded as MSN_1 ('same' rewards) or did the reverse ('differential' reward, the one used here). We checked using Task 2, both strategies in Figure 1.8, and found that only the 'differential' strategy led to significant changes when adding collateral inhibition. As a consequence, the 'differential' reward strategy was used in the rest of the paper.

We also tested this network on Task 1 in Figure 1.5c. Collateral inhibition leads to a significantly higher performance for all parameters tested. These results have been confirmed for different sets of P neurons (Figure 1.9a), various N_{stim} (Figure 1.9b) or different values of collateral inhibition (Figure 1.9c).

Overall, it is quite notable to observe that in all cases, asymmetric Hebbian STDP (in green), for Task 1 or 2, still leads to poor performances, while asymmetric anti-Hebbian STDP reaches high accuracy. The two biologically relevant properties that have been added, spiking latency and collateral inhibition, both lead to a significant increase in accuracy.

Classification of more complex patterns

We have finally tested our different neuronal networks against more complex inputs, with two different tasks. First, we define Task 3, where we consider Task 1 patterns, with jittered spikes (the cortical spike times are chosen from uniforms distributions around the delay t_{delay}, kept constant during the whole simulations). Then, we also consider Task 4 where patterns of cortical activity were defined through Poisson processes of intensity λ_{poisson}=1 kHz, on a duration t_{poisson}=2 ms, conditioned to have at least 2 spikes.

We present below the classification results for Task 3 (Figure 1.6a) and Task 4 (Figure 1.6b), for different values of patterns N_p. Global performances are consistent with what was observed for Task 1, in particular with collateral inhibition leading to higher accuracies than logistic regression.

1.3 Discussion

A simple striatal neuronal network, composed of one or two MSNs, integrating spikes from a population of cortical neurons, is presented and trained in a task, specifically defined to emulate the striatum role in procedural learning. The MSNs learn to correctly classify patterns, built on precisely timed sequences of cortical spikes, by spiking at the end of the pattern. We show that this simple striatal network endowed with two types of synaptic plasticity, anti-Hebbian learning rules (either symmetric LTD or asymmetric anti-Hebbian STDP) and non-associative reward-LTP, performs well in this task. When adding spike latency, a prominent characteristic of MSNs, we found that the network was able to achieve similar performance as logistic regression. A second MSN, that learns the reverse associations of patterns, and that inhibits the first MSN through lateral inhibition is incorporated in the striatal network, to model collateral inhibition between MSNs. We show that thanks to this addition, the striatal network outperforms classical algorithms. We prove that several key properties exhibited by MSNs, (anti-Hebbian STDP, latency and collateral inhibition) enable the classification of precisely timed sequences of cortical activity, and more importantly that thanks to the present learning rules, the MSN learns to take into account the complete cortical pattern before taking a decision.

The reward signaling used in the present model was restricted to simple supervision through the potentiation of synaptic weights associated to presynaptic spikes during rewarded patterns. Detailed models, in particular three-factor learning rules [KIT17; Fon+18; Ger+18], can also been used in this context, and in particular by detailing how the reward can be implemented using dopaminergic signaling. A framework for corticostriatal plasticity was developed along with the use of dopamine-dependent STDP curves [GHR15]. It only focused on Hebbian STDP, while here we show that anti-Hebbian STDP plays a significant role during learning. It would be interesting to model the fact that dopaminergic neurons are not only modulated by the value of rewards (or of the reward-prediction error). Indeed, dopaminergic neurons of the SNc (substantia nigra pars-compacta), which are responsible for dopamine in the striatum, are known to be also directly stimulated by MSNs originating from striosomes. The integration of the dopaminergic circuit could therefore lead to more realistic study of the influence of reward on learning in the striatum.

We have considered here that MSNs activity was the relevant quantity to study the impact of striatal dynamics on procedural learning. This restrictive vue can be expanded by integrating downstream pathways, and the rest of the basal ganglia nuclei. In particular, direct and indirect-pathway neurons have different electrophysiological properties, and also exhibit different types of STDP [Per+22]. Building a general model of the striatum, with both pathways, can lead to a better understanding of the striatum participation in learning. Incorporating these two pathways can also be interesting when considering the influence of striatal plasticity in the process of action selection, that heavily rely on the distinctive dynamics specific to each pathway [Dun+19]. A similar dichotomy exists when comparing the dorsomedial (DMS) and dorsolateral (DLS) parts of the striatum. Both regions are involved in different types of learning, specifically goal-directed behavior and habits. Differences in corticostriatal STDP have been shown to exist experimentally, and a similar striatal network is developed in [Per+22] to study the influence of the different types of anti-Hebbian STDP on the flexibility and maintenance of learning.

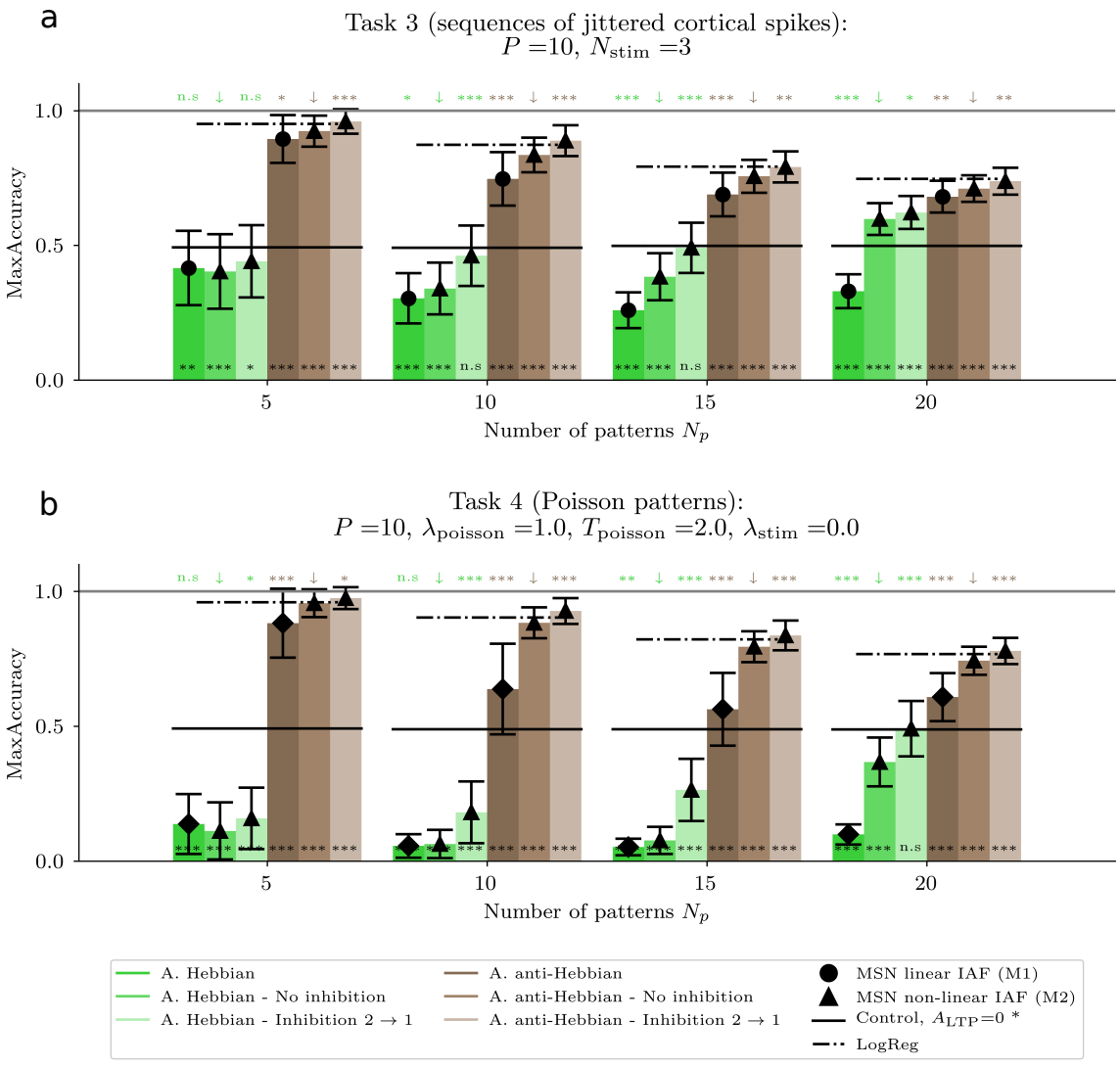

Figure 1.6: **Striatal learning also perform well on more realistic patterns.**

Figure 1.6: **Striatal learning also performs well on more realistic patterns.**

(a) *Learning patterns with jiterred inputs* [Task 3] MaxAccuracy as a function of the number of presented patterns N_p, for asymmetric Hebbian and anti-Hebbian STDP, comparing linear IAF (M1) and non-linear Izhikevich (M2) models, in the absence ($J{=}0$) or presence ($J{=}{-}0.5$) of lateral inhibition. (b) *Learning patterns of Poisson spike trains* [Task 4] MaxAccuracy as a function of the number of presented patterns N_p, for asymmetric Hebbian and anti-Hebbian STDP, comparing linear IAF (M1) and non-linear Izhikevich (M2) models, in the absence ($J{=}0$) or presence ($J{=}{-}0.5$) of lateral inhibition.

Training done for 500 patterns iterations, with test sessions every N_p iterations. Mean results computed over $N{=}250$ simulations with errors bars representing $\pm$SD$/2$.
Statistical t-test from scipy.stats Python library; *: $p{<}0.05$, **: $p{<}0.005$, ***: $p{<}0.0005$.
(below) (H0): networks without supervision ($A_{\text{reward}}{=}0$), compared with networks with supervision ($A_{\text{reward}}{=}0.9$).
(above) (H0): (M2) neurons without collateral inhibition ($J{=}0$) for asymmetric Hebbian STDP (green) and asymmetric anti-Hebbian STDP (brown).

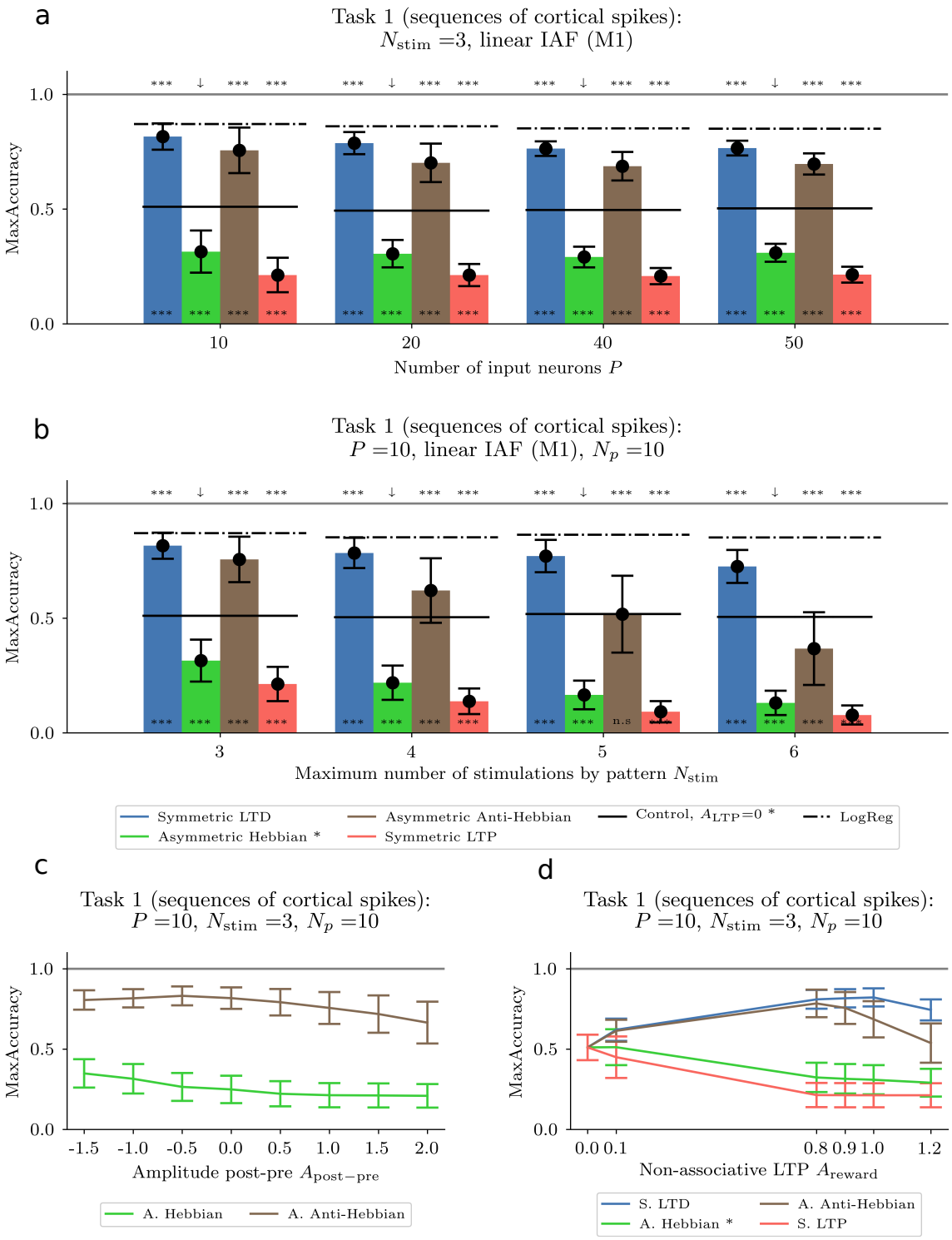

Figure 1.7: **Influence of parameters on learning with linear IAF model (M1).** [Task 1] (a) MaxAccuracy for different number of cortical neurons P, with N_p=P. Training done for [500, 1000, 2000, 2000] patterns iterations for P=[10, 20, 40, 50], with test sessions every N_p=P iterations. (b) MaxAccuracy for different number of cortical stimulations N_{stim}. (c) MaxAccuracy for different values of post-pre amplitude $A_{post-pre}$. (d) MaxAccuracy for different values of reward-LTP A_{reward}. (same as in Figure 1.3)

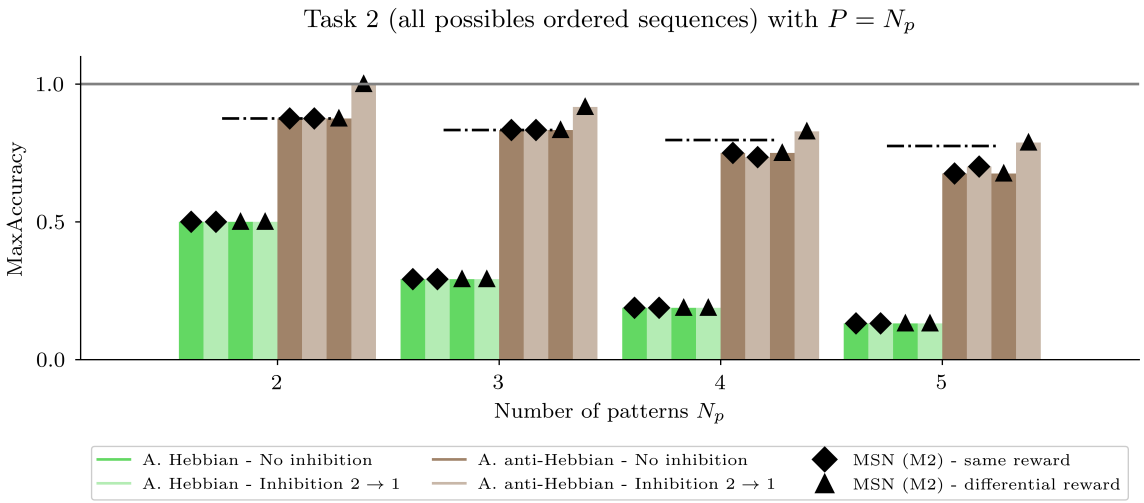

Figure 1.8: **Influence of the strategy of reward with collateral inhibition.** [Task 2] MaxAccuracy for different number of cortical neurons P, with N_p=P for different types of learning stategies and connectivity. (same as in Figure 1.5)

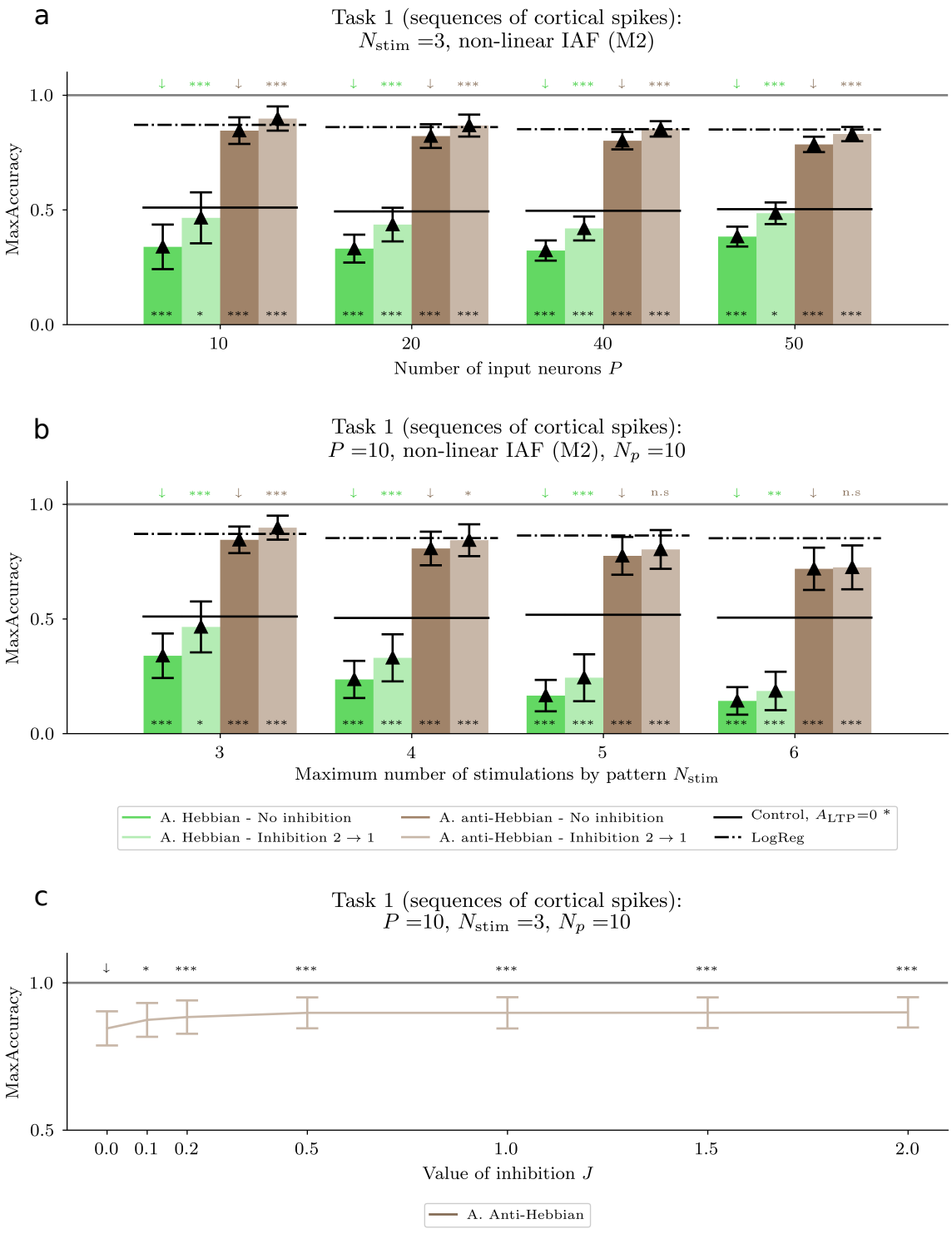

Figure 1.9: **Influence of parameters on learning with non-linear IAF model (M2) and lateral inhibition.**
[Task 1] (a) MaxAccuracy for different number of cortical neurons P, with N_p=P. Training done for [500, 1000, 2000, 2000] patterns iterations for P=[10, 20, 40, 50], with test sessions every N_p=P iterations. (b) MaxAccuracy for different number of cortical stimulations N_{stim}. (c) MaxAccuracy for different values of lateral inhibition J for asymmetric anti-Hebbian STDP. (same as in Figure 1.5).

BIBLIOGRAPHY

[Ath+18] V. R. Athalye, F. J. Santos, J. M. Carmena, and R. M. Costa. Evidence for a neural law of effect. *Science* **359** (Mar. 2018), 1024–1029.

[BK12] K. S. Burbank and G. Kreiman. Depression-biased reverse plasticity rule is required for stable learning at top-down connections. *PLoS computational biology* **8** (2012), e1002393.

[BKL02] S. M. Bohte, J. N. Kok, and H. La Poutré. Error-backpropagation in temporally encoded networks of spiking neurons. *Neurocomputing* **48** (Oct. 2002), 17–37.

[Bur06] A. N. Burkitt. A Review of the Integrate-and-fire Neuron Model: I. Homogeneous Synaptic Input. *Biological Cybernetics* **95** (July 2006), 1–19.

[Buz10] G. Buzsáki. Neural syntax: cell assemblies, synapsembles and readers. *Neuron* **68** (Nov. 2010), 362–385.

[CF03] H. Câteau and T. Fukai. A stochastic method to predict the consequence of arbitrary forms of spike-timing-dependent plasticity. *Neural Computation* **15** (Mar. 2003), 597–620.

[Dun+19] K. Dunovan, C. Vich, M. Clapp, T. Verstynen, and J. Rubin. Reward-driven changes in striatal pathway competition shape evidence evaluation in decision-making. *PLoS computational biology* **15** (May 2019), e1006998.

[FGV05] E. Fino, J. Glowinski, and L. Venance. Bidirectional activity-dependent plasticity at corticostriatal synapses. *The Journal of Neuroscience: The Official Journal of the Society for Neuroscience* **25** (Dec. 2005), 11279–11287.

[Fin+10] E. Fino, V. Paille, Y. Cui, T. Morera-Herreras, J.-M. Deniau, and L. Venance. Distinct coincidence detectors govern the corticostriatal spike timing-dependent plasticity. *The Journal of Physiology* **588** (Aug. 2010), 3045–3062.

[Flo12] R. V. Florian. The Chronotron: A Neuron That Learns to Fire Temporally Precise Spike Patterns. *PLoS ONE* **7** (Aug. 2012), e40233.

[Fon+18] A. Foncelle, A. Mendes, J. Jędrzejewska-Szmek, S. Valtcheva, H. Berry, K. T. Blackwell, and L. Venance. Modulation of Spike-Timing Dependent Plasticity: Towards the Inclusion of a Third Factor in Computational Models. *Frontiers in Computational Neuroscience* **12** (2018), 49.

[Ger+14] W. Gerstner, W. M. Kistler, R. Naud, and L. Paninski. Neuronal Dynamics: From Single Neurons to Networks and Models of Cognition. New York, NY, USA: Cambridge University Press, 2014.

[Ger+18] W. Gerstner, M. Lehmann, V. Liakoni, D. Corneil, and J. Brea. Eligibility Traces and Plasticity on Behavioral Time Scales: Experimental Support of NeoHebbian Three-Factor Learning Rules. *Frontiers in Neural Circuits* **12** (July 2018).

[GG15] A. M. Graybiel and S. T. Grafton. The Striatum: Where Skills and Habits Meet. *Cold Spring Harbor Perspectives in Biology* **7** (Aug. 2015), a021691.

[GHR15] K. N. Gurney, M. D. Humphries, and P. Redgrave. A new framework for cortico-striatal plasticity: behavioural theory meets in vitro data at the reinforcement-action interface. *PLoS biology* **13** (Jan. 2015), e1002034.

[GS06] R. Gütig and H. Sompolinsky. The tempotron: a neuron that learns spike timing-based decisions. *Nature Neuroscience* **9** (Mar. 2006), 420–428.

[Güt+13] R. Gütig, T. Gollisch, H. Sompolinsky, and M. Meister. Computing complex visual features with retinal spike times. *PloS One* **8** (2013), e53063.

[Güt14] R. Gütig. To spike, or when to spike? *Current Opinion in Neurobiology* **25** (Apr. 2014), 134–139.

[HCT12] C. D. Harvey, P. Coen, and D. W. Tank. Choice-specific sequences in parietal cortex during a virtual-navigation decision task. *Nature* **484** (Mar. 2012), 62–68.

[Hem+19] M. Hemberger, M. Shein-Idelson, L. Pammer, and G. Laurent. Reliable Sequential Activation of Neural Assemblies by Single Pyramidal Cells in a Three-Layered Cortex. *Neuron* **104** (Oct. 2019), 353–369.e5.

[Hum+09] M. D. Humphries, N. Lepora, R. Wood, and K. Gurney. Capturing dopaminergic modulation and bimodal membrane behaviour of striatal medium spiny neurons in accurate, reduced models. *Frontiers in Computational Neuroscience* **3** (2009), 26.

[HWG09] M. D. Humphries, R. Wood, and K. Gurney. Dopamine-modulated dynamic cell assemblies generated by the GABAergic striatal microcircuit. *Neural Networks: The Official Journal of the International Neural Network Society* **22** (Oct. 2009), 1174–1188.

[Ike+04] Y. Ikegaya, G. Aaron, R. Cossart, D. Aronov, I. Lampl, D. Ferster, and R. Yuste. Synfire chains and cortical songs: temporal modules of cortical activity. *Science (New York, N.Y.)* **304** (Apr. 2004), 559–564.

[Izh07] E. M. Izhikevich. Dynamical Systems in Neuroscience. MIT Press, 2007.

[JC15] X. Jin and R. M. Costa. Shaping action sequences in basal ganglia circuits. *Current Opinion in Neurobiology* **33** (Aug. 2015), 188–196.

[KIT17] Ł. Kuśmierz, T. Isomura, and T. Toyoizumi. Learning with three factors: modulating Hebbian plasticity with errors. *Current Opinion in Neurobiology* **46** (Oct. 2017), 170–177.

[LBH09] A. Luczak, P. Barthó, and K. D. Harris. Spontaneous events outline the realm of possible sensory responses in neocortical populations. *Neuron* **62** (May 2009), 413–425.

[Luc+07] A. Luczak, P. Barthó, S. L. Marguet, G. Buzsáki, and K. D. Harris. Sequential structure of neocortical spontaneous activity in vivo. *Proceedings of the National Academy of Sciences of the United States of America* **104** (Jan. 2007), 347–352.

[MDG08] A. Morrison, M. Diesmann, and W. Gerstner. Phenomenological models of synaptic plasticity based on spike timing. *Biological Cybernetics* **98** (June 2008), 459–478.

[Mem+14] R.-M. Memmesheimer, R. Rubin, B. P. Olveczky, and H. Sompolinsky. Learning precisely timed spikes. *Neuron* **82** (May 2014), 925–938.

[Men+20] A. Mendes, G. Vignoud, S. Perez, E. Perrin, J. Touboul, and L. Venance. Concurrent Thalamostriatal and Corticostriatal Spike-Timing-Dependent Plasticity and Heterosynaptic Interactions Shape Striatal Plasticity Map. *Cerebral Cortex (New York, N.Y.: 1991)* **30** (June 2020), 4381–4401.

[MKM08] E. I. Moser, E. Kropff, and M.-B. Moser. Place Cells, Grid Cells, and the Brain's Spatial Representation System. *Annual Review of Neuroscience* **31** (2008), 69–89.

[PB20] U. Pereira and N. Brunel. Unsupervised Learning of Persistent and Sequential Activity. *Frontiers in Computational Neuroscience* **13** (2020).

[Per+22] S. Perez, Y. Cui, G. Vignoud, E. Perrin, A. Mendes, Z. Zheng, J. Touboul, and L. Venance. Striatum expresses region-specific plasticity consistent with distinct memory abilities. *Cell Reports* **38** (2022), 110521.

[Pet+21] A. J. Peters, J. M. J. Fabre, N. A. Steinmetz, K. D. Harris, and M. Carandini. Striatal activity topographically reflects cortical activity. *Nature* **591** (Mar. 2021), 420–425.

[PK10] F. Ponulak and A. Kasiński. Supervised learning in spiking neural networks with ReSuMe: sequence learning, classification, and spike shifting. *Neural Computation* **22** (Feb. 2010), 467–510.

[PV19] E. Perrin and L. Venance. Bridging the gap between striatal plasticity and learning. *Current Opinion in Neurobiology*. Neurobiology of Learning and Plasticity **54** (Feb. 2019), 104–112.

[RA04] C. C. Rumsey and L. F. Abbott. Equalization of synaptic efficacy by activity- and timing-dependent synaptic plasticity. *Journal of Neurophysiology* **91** (May 2004), 2273–2280.

[RB00] P. D. Roberts and C. C. Bell. Computational consequences of temporally asymmetric learning rules: II. Sensory image cancellation. *Journal of Computational Neuroscience* **9** (Aug. 2000), 67–83.

[RL10] P. D. Roberts and T. K. Leen. Anti-Hebbian spike-timing-dependent plasticity and adaptive sensory processing. *Frontiers in Computational Neuroscience* **4** (2010), 156.

[Rob00] P. D. Roberts. Dynamics of temporal learning rules. *Phys. Rev. E* **62** (3 Sept. 2000), 4077–4082.

[Rub+17] J. E. Rubin, J. Signerska-Rynkowska, J. D. Touboul, and A. Vidal. Wild oscillations in a nonlinear neuron model with resets: (I) Bursting, spike-adding and chaos. *Discrete & Continuous Dynamical Systems - B* **22** (2017), 3967.

[TB09] J. Touboul and R. Brette. Spiking Dynamics of Bidimensional Integrate-and-Fire Neurons. *SIAM Journal on Applied Dynamical Systems* **8** (Jan. 2009), 1462–1506.

[Tou08] J. Touboul. Bifurcation Analysis of a General Class of Nonlinear Integrate-and-Fire Neurons. *SIAM Journal on Applied Mathematics* **68** (Jan. 2008), 1045–1079.

[US09] R. Urbanczik and W. Senn. A gradient learning rule for the tempotron. *Neural Computation* **21** (Feb. 2009), 340–352.

[WAS07] J. R. Wickens, G. W. Arbuthnott, and T. Shindou. Simulation of GABA function in the basal ganglia: computational models of GABAergic mechanisms in basal ganglia function. *Progress in Brain Research* **160** (2007), 313–329.

[WL96] M. Wehr and G. Laurent. Odour encoding by temporal sequences of firing in oscillating neural assemblies. *Nature* **384** (Nov. 1996), 162–166.

[WRL03] A. Williams, P. D. Roberts, and T. K. Leen. Stability of negative-image equilibria in spike-timing-dependent plasticity. *Physical Review E* **68** (Aug. 2003), 021923.

[Xie+22] Y. Xie et al. Geometry of sequence working memory in macaque prefrontal cortex. *Science* **375** (Feb. 2022), 632–639.

[YAK11] M. Y. Yim, A. Aertsen, and A. Kumar. Significance of Input Correlations in Striatal Function. *PLoS Computational Biology* **7** (Nov. 2011).

[YK06] H. H. Yin and B. J. Knowlton. The role of the basal ganglia in habit formation. *Nature Reviews. Neuroscience* **7** (June 2006), 464–476.

[ZD07] Q. Zou and A. Destexhe. Kinetic models of spike-timing dependent plasticity and their functional consequences in detecting correlations. *Biological Cybernetics* **97** (July 2007), 81–97.

CHAPTER 2

REGION-SPECIFIC ANTI-HEBBIAN PLASTICITY SUBTEND DISTINCT LEARNING STRATEGIES IN THE STRIATUM

ABSTRACT

The striatum mediates two learning modalities: goal-directed behavior in dorsomedial (DMS) and habits in dorsolateral (DLS) striatum. The synaptic bases of these learnings are still elusive. Indeed, while ample research has described DLS plasticity, little is known about DMS plasticity and its involvement in procedural learning.

Experimental results, only summarized in this section, but developed in the corresponding article [Per+22], show that symmetric and asymmetric anti-Hebbian spike-timing-dependent plasticity (STDP) exist in DMS and DLS respectively, with opposite plasticity dominance upon increasing corticostriatal activity. Moreover, behavioral experiments coupled with STDP occlusion protocols show that during motor skill learning, plasticity was engaged in DMS and striatonigral DLS neurons only during early learning stages, whereas striatopallidal DLS neurons were mobilized only during late phases.

In the following report, we developed a mathematical model to study the computational properties of these rules in learning; we found that symmetric anti-Hebbian STDP favored memory flexibility by allowing a rapid forgetting of patterns, while asymmetric anti-Hebbian STDP contributed to memory maintenance, consistent with memory processes at play in procedural learning.

2.1 Introduction

The dorsal striatum is critical for action selection and initiation [YK06; GG15; JC15] and represents a major site for memory formation encoding for procedural learning [PV19]. The dorsal striatum is composed of two main anatomico-functional regions, the dorsolateral striatum (DLS) and dorsomedial striatum (DMS) based on topographic cortical glutamatergic afferents. DLS mainly receives cortical inputs from the premotor and sensorimotor cortices, whereas DMS receives cortical afferents from prefrontal and associative cortices [Hun+16]. Moreover, DLS and DMS appear to engage at different learning phases: the classical view posits that during reward-guided instrumental learning DMS supports goal-directed behavior, while DLS is gradually involved in later learning phases associated with habit formation and performance [YK06; BO10; CJ10; Tho+10; GC13; BNR15; Van+19; CCN04]. Similarly, during motor skill learning DMS appears to play a crucial role during initial phases of fast improvements, while DLS is determinant for slower learning phases as experience accumulates [GG15; JC15; CCN04; Yin+09; XZZ15]. Nevertheless, there is evidence that DLS does not only activate at late learning phases, but is engaged, together with DMS, from early training phases [Tho+10; GC13; Kim+09; Sta+10; Kup+17; Ber+18]. Acquisition and maintenance of motor skills and habits involve corticostriatal long-term synaptic efficacy changes [PV19]. Indeed, in vivo proxies for plasticity, such as changes in firing activity [CCN04; Yin+09; TG14; Bar+11; Kor+12; OHa+16; Ath+18; Pet+21] or in evoked-LFP [XZZ15], were detected

in the corticostriatal pathway throughout procedural learning. Conversely, triggering corticostriatal synaptic plasticity was shown to modify habitual behavior [XZZ15; Ma+18]. Although these findings clearly highlight a causal and/or correlative link between corticostriatal plasticity and procedural learning, the nature and contribution of DLS and DMS long-term plasticity remain to be fully determined. To investigate plasticity properties at corticostriatal synapses and their potential implication in memory storage and relearning in DMS and DLS, we characterized the spike-timing-dependent plasticity (STDP) [Fel12], in both dorsal striatal compartments, in order to characterize the experience-dependent changes in neuronal networks they subtend. Using brain slice preparations preserving afferents from the somatosensory or the cingulate cortex and the corresponding striatal projection domains [Fin+18], we investigated the DMS and DLS corticostriatal STDP in striatal medium-sized spiny neurons (MSNs).

We observed that similar STDP paradigms trigger anti-Hebbian STDP in both DMS and DLS, but the specific profiles of STDP are vastly distinct: symmetric anti-Hebbian STDP arises in DMS (yielding LTD only), contrasting with asymmetric anti-Hebbian STDP in DLS (yielding LTD or LTP depending on spike timings). Moreover, when corticostriatal activity was scaled up, we found that a long-term depression (LTD) prevailed in DMS, while long-term potentiation (LTP) prevailed in DLS. In fact, we further found that MSNs from the DMS exhibited opposite plasticity, in a specific activity regime, depending on whether they belonged to the direct and indirect pathway. During motor skill learning (Rotarod task), we found that during early learning phases, plasticity was engaged for all recorded MSNs in DMS, both belonging to the direct and indirect pathway, and only direct pathway MSNs in DLS. In contrast, during late learning phases, we found that only the indirect pathway MSNs in DLS were mobilized. To appreciate how these distinct plasticity rules may support the different phases of procedural learning, we developed a mathematical model to quantify the capacity of those plasticity rules for memory formation and storage. Our model predicted that asymmetric anti-Hebbian STDP facilitated the maintenance of memory, whereas symmetric LTD allowed reward-dependent learning with a swift turnover of memories, potentially enhancing memory flexibility. These findings therefore reveal how distinct corticostriatal plasticity maps in DLS and DMS, having opposite polarities, could endow the striatum with complementary capacities for procedural learning allowing flexibility in memory acquisition and stabilization of memories potentially allowing the development of habits.

2.2 Summary of experimental results

I reproduce in this section parts of the experimental conclusions from [Per+22]. In particular, I focus on the results pertinent to the computational study that I have devised and studied.

Distinct anti-Hebbian STDP profiles in sensorimotor and associative striatum

We investigated STDP rules at corticostriatal synapses in MSNs located either in DLS or DMS. For this purpose, we used two brain slice preparations that preserved connections between the sensorimotor cortex (S2) and DLS, or between the associative cortex (CG2) and DMS, and allowed to stimulate within cortical layer 5 while recording MSNs (Figure 2.1) [Fin+18]. At both synapses, we first applied the same STDP protocol consisting

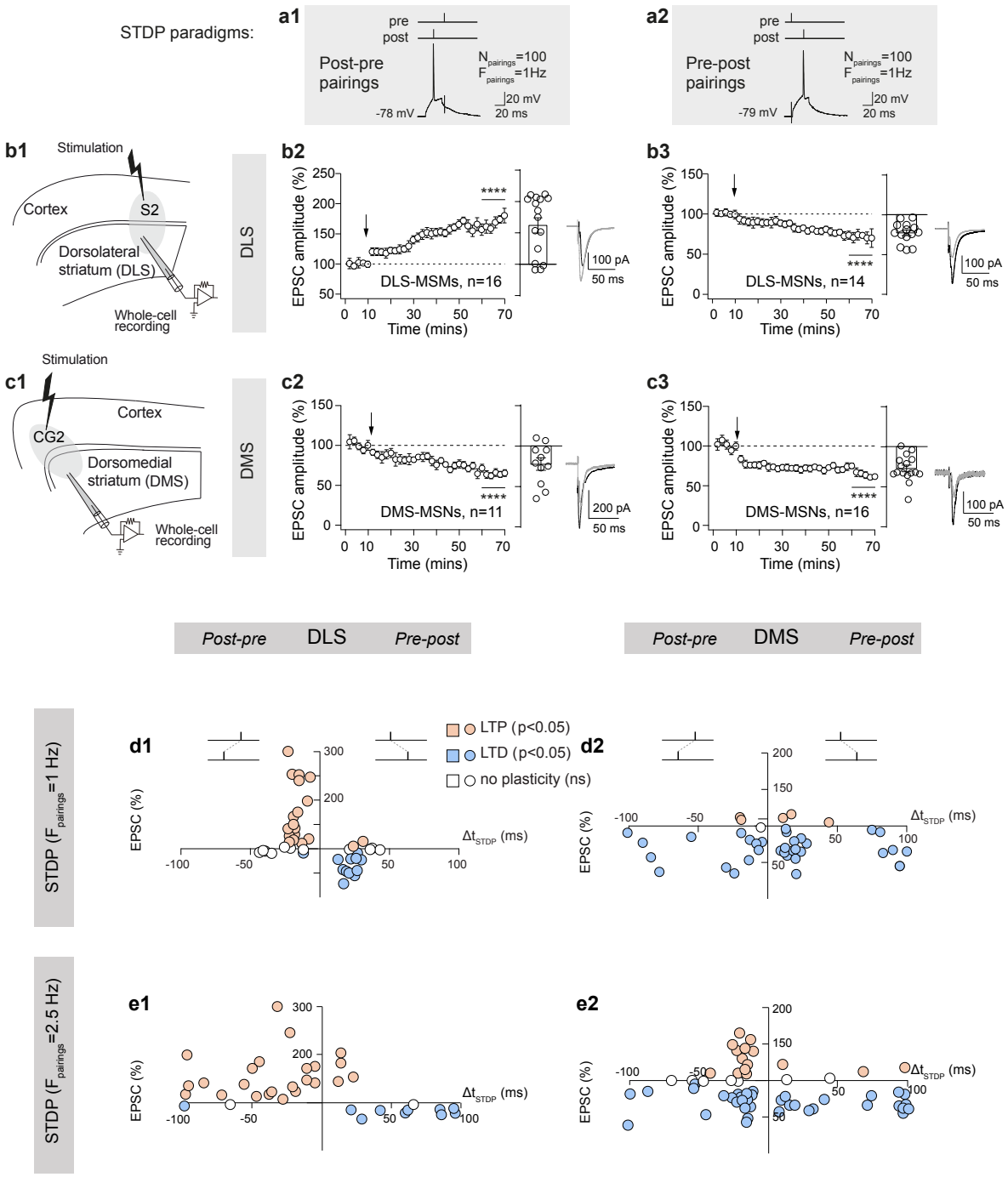

Figure 2.1: **Distinct anti-Hebbian STDP profiles in DLS and DMS**

Figure 2.1: **Distinct anti-Hebbian STDP profiles in DLS and DMS.**
(a) STDP pairings: a single spike evoked in the recorded MSN was paired with a single cortical stimulation. Pairings were repeated 100 times at $1\,Hz$. Δt_{STDP} indicates the time between pre- and postsynaptic stimulations. $\Delta t_{\text{STDP}}<0$ and $\Delta t_{\text{STDP}}>0$ refer to the post-pre (a1) and pre-post (a2) pairings, respectively. Pre- and postsynaptic stimulations were applied either in the sensorimotor (S2) (b) or the associative (CG2) (c) cortical and striatal areas. (b1 and c1) Experimental setup showing the location of the stimulation and recording electrodes in cortical and striatal sensorimotor (b1) and associative (c1) areas.
(b) DLS-STDP displays an asymmetric anti-Hebbian polarity in rats. (b1) Experimental setup. (b2 and b3) Averaged time-courses of (b2) LTP induced by 100 post-pre pairings (n=16) and (b3) LTD induced by 100 pre-post pairings (n=14).
(c) DMS-STDP displays symmetric anti-Hebbian polarity. (c1) Experimental setup. (c2 and c3) Averaged time-courses of LTD induced by (c2) 100 post-pre pairings (n=11) and (c3) 100 pre-post pairings (n=16). Bar graphs represent the average of all STDP experiments and each point represents the percentage of change in EPSC amplitude at 50-60 min after STDP pairings in a single STDP experiment. Insets correspond to the average EPSC amplitude at baseline and at 50-60 min after STDP pairings. Error bars represent the SEM. ****: $p<0.0001$ by one sample t-test.
(d) Summary graphs of STDP in relation with Δt_{STDP} showed at $1\,Hz$, (d1) an asymmetric anti-Hebbian STDP in a restricted time window ($-30<\Delta t_{\text{STDP}}<30\,ms$), (d2) symmetric anti-Hebbian STDP in a broad time window ($-100<\Delta t_{\text{STDP}}<100\,ms$).
(e) Summary graphs of STDP in relation with Δt_{STDP} showed at $2.5\,Hz$, (e1) a widening of the temporal window of STDP expression and in particular of LTP being also induced for short pre-post pairings, (e2) mainly LTD except for narrow ($-30<\Delta t_{\text{STDP}}<0\,ms$) post-pre pairings for which half of the MSNs exhibited LTD while the other half displayed LTP (n=59).

---

of 100 pairings at $1\,Hz$ of pre- and postsynaptic stimulations with prescribed timing Δt=-15 or $+15\,ms$. $\Delta t<0$ indicates that postsynaptic stimulation preceded presynaptic stimulation (post-pre pairings) (Figure 2.1a1) and $\Delta t>0$ indicates that presynaptic stimulation preceded postsynaptic stimulation (pre-post pairings) (Figure 2.1a2).

We investigated corticostriatal STDP in the DLS (Figure 2.1b) and observed asymmetric (i.e distinct plasticity polarity on both sides of Δt=0) anti-Hebbian STDP: spike-timing-dependent long-term potentiation (LTP) for post-pre pairings (Figure 2.1b2) and depression (LTD) for pre-post pairings (Figure 2.1b3). Anti-Hebbian qualifies STDP with pre-post LTD, as defined in [Fel12]. Post-pre pairings induced tLTP ($p<0.0001$, n=16), whereas pre-post pairings induced LTD ($p<0.0001$, n=14). This is in line with DLS-STDP displaying anti-Hebbian polarity in native conditions [FGV05; Fin+10; Men+20]. Striatal DLS-STDP with a Hebbian polarity has also been reported [PK08; She+08], caused by the use of GABAA receptor antagonists. Indeed, GABAergic signaling governs STDP polarity and operates as a Hebbian/anti-Hebbian switch in the DLS [Pai+13; Val+17].

In DMS (Figure 2.1c), post-pre and pre-post pairings induced a symmetric (i.e similar plasticity polarity, here LTD, on both sides of Δt=0) anti-Hebbian STDP (Figure 2.1c2 and c3). Indeed, spike-timing-dependent long-term depression (LTD) was

observed following post-pre pairings ($p<0.0001$, $n=11$) as well as following pre-post pairings ($p<0.0001$, $n=16$).

In conclusion, corticostriatal STDP in DMS and DLS displayed both anti-Hebbian plasticity, and differed significantly in that they displayed symmetric or asymmetric profiles in DMS and DLS respectively.

We also characterized in the associated paper, which pathways were involved in the different STDP rules observed. In particular, after blocking the different pathways specifically, it was shown that post-pre DLS-LTP and DMS-LTD are NMDAR-mediated, whereas pre-post DLS- and DMS-LTD are CB1R-mediated.

Dominance of opposite forms of plasticity in DMS and DLS with increasing corticostriatal activity

Expression map of STDP is not only shaped by spike timing (Δt) but also by the frequency at which pairings are presented (F_{pairings}) [Fel12; Mar+97; STN01]. We further characterized the induction rules of corticostriatal STDP in DLS ($N_{\text{total}}=130$ DLS-MSNs) and DMS ($N_{\text{total}}=125$ DMS-MSNs) by varying together Δt ($-100\leqslant\Delta t\leqslant+100\,ms$) and F_{pairings} ($1\leqslant F_{\text{pairings}}\leqslant 5\,Hz$).

When $F_{\text{pairings}}=1\,Hz$, DLS-MSNs elicit asymmetric anti-Hebbian STDP, as explained in the previous section, characterized by LTD for pre-post pairings ($\Delta t>0$, Figure 2.1d1), and LTP for post-pre pairings ($\Delta t<0$, Figure 2.1d1). Conversely, DMS-MSNs develop symmetric anti-Hebbian STDP, defined by the dominance of LTD, for both pre-post and post-pre pairings (Figure 2.1d2).

When raising the frequency F_{pairings} to $2.5\,Hz$, the STDP profiles changed for both type of neurons. First, DLS-MSNs still exhibit asymmetric anti-Hebbian STDP, but the temporal window of STDP has widened up to $\pm 100\,ms$ (Figure 2.1e1). Second, pre-post pairings in DMS-MSNs are still characterized by LTD at their corticostriatal synapse (Figure 2.1e2) but their behavior for post-pre pairing is less clear with neurons exhibiting LTP or LTD.

In the associated article, a more systematic study is developped on the influence of F_{pairings}, which lead to the following conclusions,

a. the STDP expression domain (Δt) is narrower in DLS than in DMS for low F_{pairings} and is widening with increasing firing activity;

b. the existence of an opposite dominance of LTP and LTD in DLS and DMS, respectively.

The diversity of behaviors observed in DMS-MSNs for post-pre pairings justified further studies on this particular protocol. We analyzed more finely which types of neurons were recorded and postulated that appartenance of the MSN to different pathways could be a possible explanation to the different types of STDP observed.

Two populations of MSNs exist in both DMS and DLS, and are characterized by the structure they are projecting to. On the one hand, dMSNs that project to the GPi (internal globus pallidus) and the SNr (substantia nigra pars reticulata) are part of the direct pathway of the cortico-basal-ganglia network. On the other hand, iMSNs that project to the GPe (external globus pallidus) are part of the indirect pathway. Both types of neurons have been shown to act differently on the processus of action selection and

motor control, and they also respond differently to dopamine. The two MSN subtypes express different dopaminergic receptors, D1R- and D2R-like for the direct and indirect pathways, respectively [Cal+14; Bon+19].

We proved that the observed dichotomy regarding LTP/LTD expression in DMS-MSNs for F_{pairings}=2.5 Hz overlapped that of MSNs belonging in the same proportion to the direct (striatonigral) and the indirect (striatopallidal) pathways using transgenic mice. Indeed, DMS-dMSNs exhibit LTD for post-pre pairings, while DMS-iMSNs display LTP.

Region-specific involvement of STDP during procedural learning

We next investigated the engagement of LTP and LTD in DLS and DMS during motor skill learning, using behavioral experiments (rotarod task).

In order to see if these STDP rules were implicated in learning, we used ex vivo saturation/occlusion experiments: STDP protocols in ex vivo brain slices were realized, at different stages of learning. It is expected that if STDP related process is active during a certain stage of learning, the associated pathways tend to be saturated. When an STDP protocol is subsequently applied in an ex-vivo experiment, it should lead to changes in observed STDP. In particular, synaptic processes active in learning should lead to an absence of plasticity in response to subsequent STDP protocols.

This paradigm was used to test the pathways associated to post-pre pairings for F_{pairings}=2.5 Hz. DLS-MSNs belonging to the direct or indirect pathways are selectively engaged, in terms of STDP, depending on the stages of motor skill learning: only DLS-dMSNs are involved at early stages, and during the late stages only DLS-iMSNs are engaged. DMS-MSN plasticity is mobilized in both MSN populations during early stages and then showed a disengagement during late stages. Interestingly, DLS-dMSNs show the same plasticity profiles, and occlusion, as DMS-iMSNs. All results and methods can be found in the full paper [Per+22].

2.3 Results

Reduced mathematical model of the striatal network.

The observation that corticostriatal synapses to the DMS are subject to symmetric anti-Hebbian STDP distinct from the asymmetric anti-Hebbian STDP at the DLS synapse (at 1 Hz, see Figure 2.1) raises the question of the respective contribution of DMS and DLS plasticity in striatal learning. To investigate whether these two STDP modalities subtend different learning properties, we considered a simplified model of the corticostriatal system, composed of one MSN and a fixed number of cortical neurons. We quantified the capacity of this system to retain memory as a function of the form of corticostriatal STDP, all parameters equal otherwise.

We considered the response of one MSN (Figure 2.2, with MSN activity illustrated in brown), modeled as an integrate-and-fire neuron, receiving inputs from P cortical neurons (Figure 2.2, with their activities in green) and an additional Poisson process modeling input from other cells than the P cortical neurons (Figure 2.2, with its spiking activity in yellow).

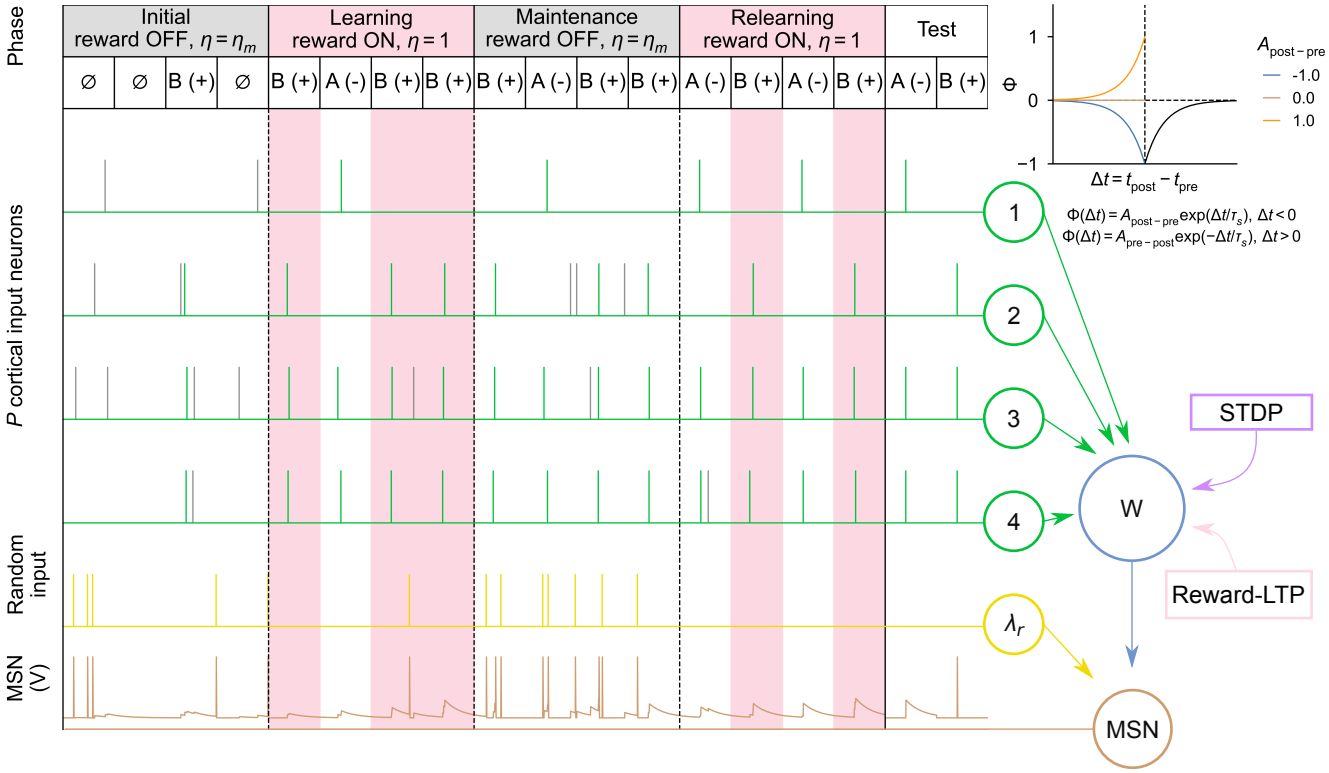

Figure 2.2: **A pattern recognition task to test learning, maintenance and relearning in a computational model of the striatal network.**
Schematic representation of the striatal network (right) with P=4 cortical neurons (in green), a random input neuron with rate λ_r (in yellow) and one striatal neuron (MSN), represented by its membrane potential V (in brown). Two mechanisms of synaptic plasticity are considered in the dynamics of the synaptic weight W (in blue): anti-Hebbian STDP (in purple) and LTP related to the reward signal (reward-LTP) (in red). Anti-Hebbian STDP is modeled using exponential kernels (inset on the top right), with different values for $A_{\text{post-pre}}$ and $A_{\text{pre-post}}=-1$. Example of the learning task (left), separated in four phases with four iterations in each phase. Each learning phase has specific parameters (see Table 2.1). N_p=2 patterns A and B are presented to the network, with A being non-rewarded $(-)$ and B rewarded $(+)$. An iteration with no pattern presentation is represented by $\varnothing$. Spiking activity of the cortical neurons (in green for pattern spikes and grey for random spikes) and the random input neuron (in yellow) are represented along with the membrane potential V of the output neuron (MSN).

The synaptic weight between cortical neuron $i \in \{1, \cdots, P\}$ and the MSN, noted W_i, is subject to plasticity. We used an all-to-all pair-based learning rule corresponding to an instantaneous update of the synaptic weight W_i by an amount ΔW_i given by

$$\Delta W_i = \begin{cases} A_{\text{pre-post}} \sum_{t_{\text{pre},i} < t_{\text{post}}} \exp\left(-\frac{\Delta t}{\tau_s}\right) & \text{for a pre-post pairing,} \\ A_{\text{post-pre}} \sum_{t_{\text{post}} < t_{\text{pre},i}} \exp\left(\frac{\Delta t}{\tau_s}\right) & \text{for a post-pre pairing.} \end{cases}$$

with $\Delta t = t_{\text{post}} - t_{\text{pre},i}$.

By convention, we fixed $A_{\text{pre-post}}=-1$, and varied the parameter $A_{\text{post-pre}}$; $A_{\text{post-pre}}<0$ corresponds to symmetric anti-Hebbian STDP, while $A_{\text{post-pre}}>0$ corresponds to asymmetric anti-Hebbian learning rules (Figure 2.2, top right panel).

The MSN was presented with patterns of cortical activity, built on two different components: (i) a combination of spikes from selected cortical patterns (a set of N_{stim} neurons), which were always triggered synchronously at each pattern iteration according to a normal distribution with standard deviation τ_p (ii) random spikes from all cortical neurons with rate λ_r/P. Examples of such patterns are presented in Figure 2.2: pattern A, whereby cortical neurons 1, 3 and 4 fired and pattern B corresponding to the coordinated spiking of cortical neurons 2, 3 and 4 (spikes in green), with superimposed random spikes (in grey). N_p patterns were built according to these principles and separated into two classes, rewarded and non-rewarded ones, with equal chances (in Figure 2.2, A is a non-reward pattern $(-)$ and B is a rewarded pattern $(+)$).

Because of the prominent role of depression in anti-Hebbian learning, particularly in the symmetric case, potentiation mechanisms are needed in order for the system to maintain some spiking activity [RB00]. We modeled potentiation through a reward signal representing neuromodulation (including, but not limited to, dopaminergic signaling) see [KIT17; Fon+18; Ger+18; BMP19] and Methods for a discussion. Reward-LTP was delivered during rewarded cortical activity patterns (Figure 2.2), and affected the weights corresponding to all presynaptic cells that spiked during the pattern presentation (even if they were noise), (see red region in Figure 2.2).

At each iteration, the system was presented with a prescribed probability η by a pattern composed of synchronous cortical activity and random noise, or with probability $1-\eta$ only with random cortical spikes (see iterations labeled $\varnothing$ in Figure 2.2). We considered that a rewarded cortical pattern is learnt when the MSN spiked in response to the synchronous cortical activity. Conversely, a non-rewarded pattern was learnt if the MSN did not fire during pattern presentation. The accuracy of striatal learning was estimated during test protocols conducted throughout the task on a network devoid of any plasticity and noise, with a metric combining the fraction of rewarded patterns correctly eliciting spikes from the MSN and of non-rewarded ones that did not trigger any spike.

To avoid transient effects associated with the initialization of synaptic variables, we simulated an initial phase of spontaneous activity of the cortical network, defined by the presentation of patterns with probability $\eta=\eta_m$ in the absence of reward-LTP. During the learning phase, patterns are presented at each iteration and rewards were provided for rewarded patterns. It emulates learning, as the output neuron learns to discriminate patterns by spiking in response to rewarded patterns and not spiking in response to non-reward patterns, in the presence of cortical random activity. The capacity of the network to keep patterns in memory was then estimated during a maintenance phase where stimuli were presented again with probability $\eta=\eta_m$ in the absence of reward-LTP (same setup as the initial phase). Finally, the capacity to relearn previously learned patterns was then tested in a protocol where stimuli and reward-LTP were presented just like in the learning phase (see Table 2.1 for detailed parameters for each phase, and Table 2.2 for model parameters).

Random input activity was parametrized by λ_r, which was set up to $\lambda_{\text{MSN}}=5\,Hz$ for the learning and relearning phases (similar to MSN firing rate in non-anesthetized animals [Mah+06]). It was chosen to be higher, $\lambda_r=4\lambda_{\text{MSN}}=20\,Hz$ in the initial and maintenance, for technical reasons (see Methods) that do not influence our results.

Asymmetric anti-Hebbian STDP favors memory maintenance, whereas symmetric LTD allows accrued flexibility.

Numerical experiments showed significant differences between the learning capability with symmetric or asymmetric anti-Hebbian STDP, particularly during the maintenance and relearning phases (Figure 2.3a).

In Figure 2.3a, learning accuracy is plotted as a function of iterations during the four different phases. We present the results for different values of $A_{\text{post-pre}}$ (solid lines), and some controls with $A_{\text{pre-post}}=0$ (dotted lines). We observe that accuracy essentially remains at random levels during the initial phase, as could be expected in the absence of reward. As soon as rewards are provided during the learning phase, we observe a rapid increase and stabilization of learning accuracy. When rewards are no more provided in the maintenance phase, the accuracy drops, with different dynamics depending on $A_{\text{post-pre}}$, as quantified in the next section. Finally, during the relearning phase, the system learns again previously memorized patterns when reward-LTP is applied anew. The kinetics of this relearning are analyzed below. In Figure 2.3b, accuracies at the end of each phase as a function of $A_{\text{post-pre}}$ are presented.

Initial phase

In the initial phase, the network is not able to detect patterns, as could be expected from the fact that it does not receive any supervision, and the computed accuracy remains around chance levels (accuracy of 0.5).

Learning phase

The learning phase led, in all cases, to a rapid rise of the accuracy, highlighting the ability of all tested networks to store patterns. We have previously shown [VTV20] that the combination of anti-Hebbian STDP and reward-LTP allowed a striatal network to correctly classifies rewarded and non-rewarded sequential patterns of cortical inputs. Heuristically, potentiation of the synaptic weights through the reward-LTP causes the MSN to spike in response to the associated pattern. This effect is counterbalanced by the presence of pre-post LTD, which leads to depression of the synaptic weights, and therefore favors an equilibrium where the synaptic weights are high enough to trigger the spike, but still remain bounded. Similarly, if the MSN spikes for non-rewarded patterns, the pre-post LTD in the absence of reward induces a decrease in synaptic weights that results in an absence of MSN firing. The combined action of both types of plasticity, i.e., anti-Hebbian STDP and reward-LTP, enables learning of the rewarded pattern in the learning phase (Figure 2.3a, plain lines). Learning with reward signals relied on the pre-post LTD, since no learning occurred when $A_{\text{pre-post}}=0$ (Figure 2.3a, dotted lines). In fact, the absence of the pre-post LTD leads to a continual growth of the synaptic weights, which results in the MSN spiking for non-rewarded patterns, therefore reducing the accuracy.

Moreover, we note that the final accuracy at the end of the learning phase depends on $A_{\text{post-pre}}$. This is a consequence of the fact that as the system learns a rewarded pattern, we do not reach a fixed equilibrium but a stationary regime: synaptic weights associated with the pattern decrease progressively for each accurate answer (due to the combination of reward LTP and pre-post LTD) until the MSN stops firing, leading to a jump in synaptic weights (only reward LTP). Larger potentiations will thus allow

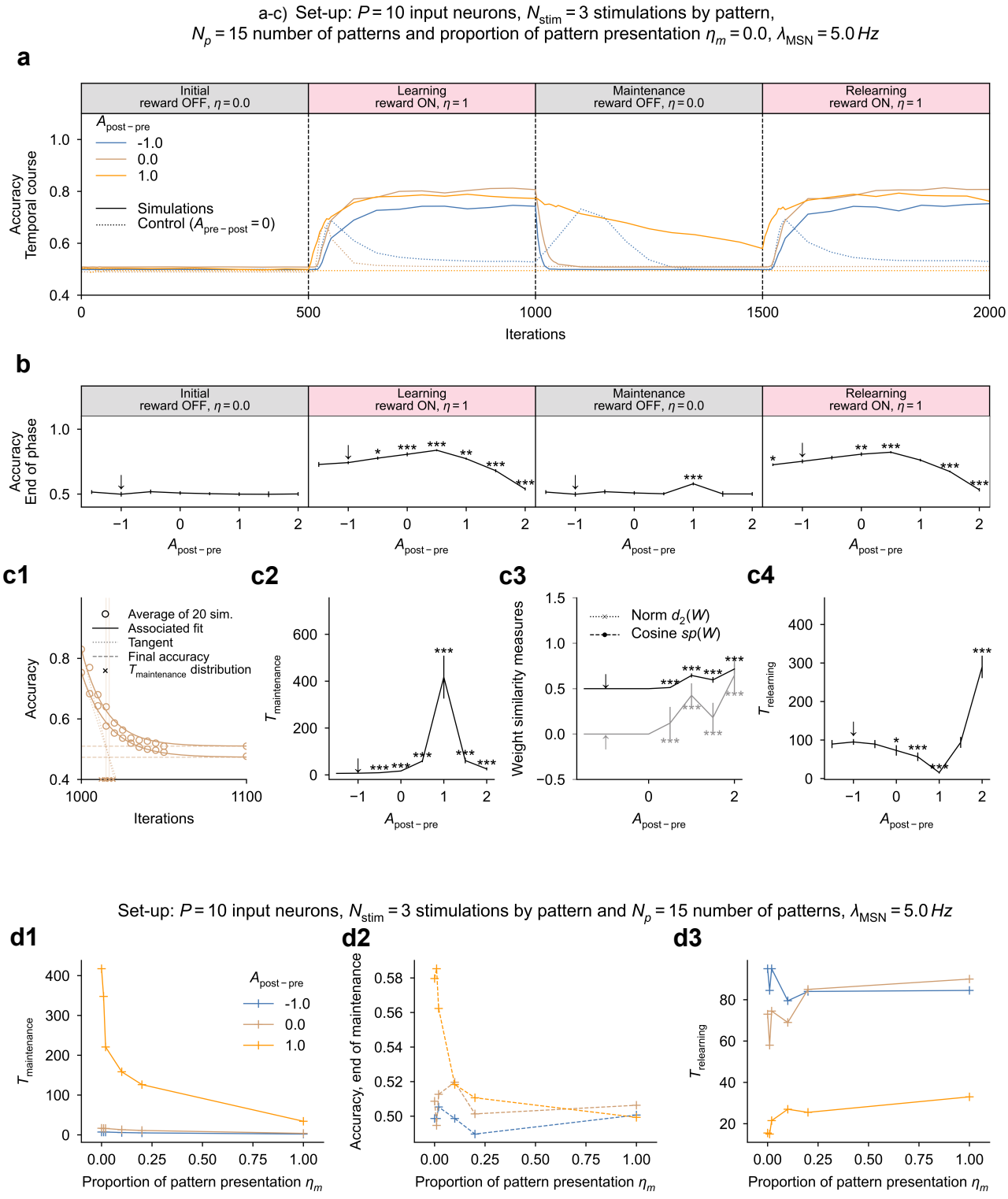

Figure 2.3: **Influence of symmetric and asymmetric anti-Hebbian STDP rules on learning, maintenance and relearning of patterns in a striatal neuronal network.**

Figure 2.3: **Influence of symmetric and asymmetric anti-Hebbian STDP rules on learning, maintenance and relearning of patterns in a striatal neuronal network.**
(a) Learning dynamics for P=10 input neurons, N_{stim}=3 stimulations by pattern, N_p=15 patterns and the proportion of pattern presentation in the initial/maintenance phases η_m=0. Time-evolution of the learning accuracy through an initialization, learning, maintenance and relearning phases, for different anti-Hebbian plasticities (blue: symmetric, brown: no post-pre learning, orange: asymmetric). Averaged simulations results are presented (plain lines) and controls with $A_{\text{pre-post}}$=0 (dotted lines). (b) Accuracy at the end of each phase as a function of the type of plasticity (where $A_{\text{post-pre}}$ parametrizes the plasticity). (c1) Examples of fits obtained from a set of 20 simulations for the accuracy during the maintenance phase. Averaged simulations (for 20 simulations, open circles), associated fit (plain lines), tangent at origin (dashed) and fitted final accuracy (dotted). We represented below the sets of values for $T_{\text{maintenance}}$ obtained with this method for $A_{\text{post-pre}}$=0. (c2) Characteristic time of maintenance $T_{\text{maintenance}}$ as a function of $A_{\text{post-pre}}$. (c3) Weight similarity measures $d_2(W)$ and $sp(W)$ as a function of $A_{\text{post-pre}}$. (c4) Characteristic time of relearning $T_{\text{relearning}}$ as a function of $A_{\text{post-pre}}$. (d) Dependency of characteristic time of maintenance $T_{\text{maintenance}}$ (d1), accuracy at the end of the maintenance phase (d2) and characteristic time of relearning $T_{\text{relearning}}$ (d3) on the type of plasticity $A_{\text{post-pre}}$ and stimulus presentation frequency η_m.
(a) Mean results computed over 200 simulations. (b-d) Mean of results over 10 sets of 20 simulations with errors bars representing $\pm$SD/2. Statistical t-test from scipy.stats Python library; *: p<0.05, **: p<0.005, ***: p<0.0005.

---

for a larger number of accurate responses, in turn increasing accuracy. On the other side, having too much potentiation leads to unstable synaptic weights that diverge, also reducing accuracy. Accordingly, their exist a value of $A_{\text{post-pre}}$ where the accuracy is maximal after learning (in Figure 2.3b, $A_{\text{post-pre}}\approx 0.5$), but all values lead to higher accuracy than in the initial phase.

In conclusion, pre-post LTD and reward LTP enable discrimination of rewarded and non-rewarded patterns, for all values of $A_{\text{post-pre}}$.

Maintenance phase

The drop in accuracy during the maintenance phase was found to be faster for symmetric anti-Hebbian learning than for asymmetric anti-Hebbian learning, with a significant impact of the value of $A_{\text{post-pre}}$ on the accuracy at the end of the maintenance phase (Figure 2.3b). To quantify this difference, we computed the characteristic decay time $T_{\text{maintenance}}$ of accuracy (see Figure 2.3c1). Figure 2.3c2 shows that asymmetric STDP allows for a longer and more precise maintenance of learning even in the absence of rewards. Phenomenologically, symmetric LTD tends to induce a global depression of all synaptic weights in response to random stimuli, which therefore can lead the MSN to stop firing to the patterns rapidly, while the presence of LTP in asymmetric anti-Hebbian STDP limits this phenomenon, allowing for a more durable conservation of the relative magnitudes of the synaptic weight W. In order to show the correlations with synaptic weight dynamics, we computed the deviation from the synaptic weight values at the end of the learning phase in terms of amplitude and change in orientation

(Methods, Figure 2.3c3). These measures show that positive $A_{\text{post-pre}}$ leads to a smaller deviation of the synaptic weights than for negative values.

Relearning phase

We next compared the relearning capacity associated with each of the learning modalities. First, after the relearning phase, the system reaches the same accuracies that were obtained at the end of the first learning paradigm. The network is therefore able to learn again patterns that were previously learned. We evaluated the speed at which the network recalled such previously learned association through the characteristic time of relearning $T_{\text{relearning}}$ (see Methods for its definition, Figure 2.3c4). As could be expected, $T_{\text{relearning}}$ is smaller for positive $A_{\text{post-pre}}$, meaning that relearning is faster for asymmetric anti-Hebbian STDP. These findings are only logical consequence of the fact that asymmetric anti-Hebbian STDP keeps in memory learned patterns for longer times. If $A_{\text{post-pre}}$ is increased too much, this property disappears because the network becomes unstable with too much potentiation.

Influence of the pattern presentation rate

If learnt patterns are presented during the maintenance phase in the absence of reward (when $\eta_m{>}0$), we expect to unlearn those patterns in the long run, i.e., both symmetric and asymmetric anti-Hebbian STDP will be associated to a drop in learning accuracy due the absence of reward-LTP. This decay is expected to be faster with larger values of η_m. This phenomenon was confirmed in our numerical experiments, showing a drop in accuracy in the maintenance phase (Figure 2.3d1), and the characteristic time $T_{\text{maintenance}}$ (Figure 2.3d2), found generally more dramatic for symmetric anti-Hebbian STDP, and occurring faster for larger η_m. The presentation rate η_m of learnt patterns during the maintenance phase was also found to play a significant role in the relearning phase, with higher rates of presentations leading to a slower relearning, potentially indicating a more dramatic deviation of the synaptic weights W from their after-learning values, see Figure 2.3d3. However, we noticed that relearning is still effective, even for higher rate of presentation η_m, when comparing asymmetric and symmetric anti-Hebbian STDP: even if the network loses its capacity to recall correctly the patterns, it stays close (in the synaptic weight parameter space) to the optimal matrix, and therefore relearning is efficient.

Influence of noise

Noise is an important parameter in the model presented here, in particular for its role in the maintenance phase. We have seen that learning occurs in the presence of noise. However, we do expect a strong dependence of final accuracies and learning efficiency on noise levels. To test the influence of noise during the learning phase, we systematically varied the noise frequency λ_{MSN} and replicated our analysis for each value tested (see Figure 2.5). In the absence of noise $\lambda_{\text{MSN}}{=}0$, the system reaches high accuracies in the learning phase, and the maximal value does not depend on $A_{\text{post-pre}}$. Moreover, we observe that the network conserves similar levels of accuracy throughout the maintenance phase when assuming a complete absence of noise. Increasing noise levels impair learning ability, and for high values of noise $\lambda_{\text{MSN}}{>}10\,Hz$, the network shows poor learning and maintenance abilities. Realistic noise levels on the same order

as typical MSN firing rate is between these two regimes and allow both learning and maintenance, with different capacities for symmetric and asymmetric anti-Hebbian STDP as discussed above.

Beyond noise levels, we further confirmed that all observations reported were robust to variations in the number of cortical neurons, patterns presented and number of stimulations (Figure 2.4), with $(P, N_p, N_{\text{stim}})$ equals to $(10, 10, 3)$, $(10, 15, 5)$ and $(20, 30, 3)$.

Conclusions of the model on the impact of different STDP in DMS and DLS.

Our experimental results show the existence of different types of plasticity as a function of the region and pairing frequency, see Figure 2.1. The model therefore suggests that at low frequency, the asymmetric anti-Hebbian STDP observed in DLS at $1\,Hz$ could allow maintaining stimulus associations for longer durations and relearning almost immediately previously learned associations. In contrast, the symmetric LTD observed in DMS at that frequency leads to a faster erasure of associations, making the system available to learn new patterns. At higher frequency, experiments done at $2.5\,Hz$ showed that STDP elicited at iMSN neurons in the DMS switched from a symmetric LTD to an asymmetric anti-Hebbian STDP. We could postulate from our model that in a regime with more frequent stimulations, iMSN neurons adapt their behavior so as to store patterns for longer times than dMSN neurons.

Overall, when presenting patterns at a slow rate, DMS with symmetric LTD, is able to forget quickly, whereas asymmetric anti-Hebbian STDP maintains memory in DLS. This observation on a vastly simplified model agrees with DMS and DLS differential involvement in motor skill learning reported in the literature [YK06; GG15; JC15; BO10; BNR15]: both learn the task during the first trials, and then DMS disengages when habit learning mediated by the DLS takes over initial phases of motor training or goal-directed learning.

2.4 Discussion

To explore how the striatum is able to achieve distinct learning modalities, from goal-directed learning to maintaining habits, we explored long-term plasticity using similar STDP paradigm in both DMS and DLS. DLS had been the focus of most of the plasticity characterization, and in light of the distinct roles of dorsal striatal compartments in procedural learning [YK06; GG15; JC15; BO10; BNR15], we characterized here the STDP at both DMS- and DLS-MSN corticostriatal synapses using specific brain slices [Fin+18] allowing to stimulate in the somatosensory or CG2 layer 5 cortical area. In DMS and DLS, we found distinct anti-Hebbian STDP: symmetric in DMS and asymmetric in DLS. Hebbian and anti-Hebbian STDP have been reported in the dorsal striatum depending on whether GABAergic transmission inhibitor [Pai+13; Val+17] were applied (Hebbian STDP [PK08; She+08]) or not (anti-Hebbian STDP [FGV05; Fin+10; Men+20]). These studies targeted DLS-MSNs, except [She+08] where MSNs were recorded indifferently in DLS and DMS. In vivo recordings in adult rats confirmed the anti-Hebbian polarity of striatal STDP [SRR10; Fis+17; Mor+19]. Interestingly, we found that with increasing cortical activity, plasticity followed opposite polarity in DMS and DLS, with LTD and

LTP dominance, respectively. Another difference between DMS- and DLS-STDP upon increasing the frequency of stimulus presentations F_{pairings}, is that plasticity expression domain (Δt) remained wide in DMS whereas it was broadened in DLS.

We designed a simplified model in order to investigate the potential impact of the different forms of STDP rules on maintenance and relearning in a basic classification task. To specifically analyze the role of learning rules, we have chosen to keep all model parameters identical otherwise. The significant differences found between therefore establish the role of STDP form in learning abilities. Our experiments show that different types of plasticities are expressed in different regions of the striatum and may depend on the connectivity pathway they belong to, where MSNs are known to display distinct electrophysiological properties [Wil+19; Ale+21]. The specific properties of dMSNs and iMSNs or of MSNs in DMS and DLS may also contribute to the variety of learning abilities. Future work will be needed to finely characterize and integrate such differences in models and study how the network combines direct and indirect pathways endowed with distinct plasticity rules for global procedural learning in the striatum.

Anti-Hebbian STDP has been the focus of several experimental and a few computational studies mostly in cerebellum-like structures in fish or mammals [RS11] or other central areas [Fel12]. Different possible roles of anti-Hebbian STDP in adaptive sensory processing have been hypothesized taking the mormyrid electric fish electrosensory system as a central example [RL10]. According to models, Purkinje-like cells in the fish electrosensory lobe can store and retrieve a temporally structured negative image of prior sensory stimuli, through STDP mechanisms [RB00]. Our results possibly shed new light on those findings. Indeed, in [RB00], the ability of the neuronal network to store patterns of cortical activity was tested for different pair-based rules of STDP (see their Figure 7), along with its capacity to forget the negative image after some time without stimulus. The authors conclude that the anti-Hebbian STDP with no plasticity for post-pre pairings, established in vitro in the fish Purkinje-like cells [Bel+97], leads to an efficient cancellation of the stimulus, with rapid adaptation when the pattern is not presented anymore (see Figure 8 [RB00]). The anti-Hebbian symmetric learning rule performs similarly, whereas the asymmetric anti-Hebbian STDP does not perform as well [RB00]. The authors explain the drop in performance of the asymmetric anti-Hebbian STDP because of oscillations in the dynamics, produced by the alternation between potentiation and depression (see their Figure 9 [RB00]). In particular, the authors state that "the system with [asymmetric anti-Hebbian STDP] does not converge onto an accurate negative image". It is however interesting to note that with asymmetric anti-Hebbian STDP, the system is still able to clone partially the stimulus. More importantly, they show that the cloned image is kept in memory for a longer time than with symmetric LTD (compare curves A/B and C in their Figure 8 [RB00]). In our study, the model allows a precise analysis of the role of symmetric versus asymmetric anti-Hebbian STDP in the maintenance of learned patterns. We show that asymmetric anti-Hebbian STDP leads to the maintenance of learned patterns, whereas symmetric LTD causes a rapid decrease in memory performance in the absence of reward. Similar to [RB00], we show that the alternation of potentiation and depression in the asymmetric anti-Hebbian STDP, if correctly tuned, forces the synaptic weights to retain some information on previously learned patterns. On the contrary, with symmetric anti-Hebbian LTD, the synaptic weights indistinctly converge to zero because they are only subject to depression, leaving the system fresh to construct new associations and identify novel stimuli.

Our present experimental work shows that DLS-MSNs exhibit asymmetric anti-Hebbian STDP, consistent with DLS role in habit behavior, where rewards are no longer presented. Conversely, we could hypothesize that thanks to symmetric anti-Hebbian STDP in DMS-MSNs, DMS should be able to adapt quickly between different action-outcome associations and therefore forget rapidly previous information. Our model shows that this role is consistent with anti-Hebbian symmetric STDP. This is in line with the role of DMS which is essential for behavioral flexibility such as strategy-shifting or reversal learning [Bon+19; Rag+02; Rag07].

2.5 Mathematical models

Neuronal network model

To simulate the impact of plasticity on learning, we built a simple neuronal network model that includes P cortical neurons serving as input neurons to one output MSN. The MSN integrated cortical and external input (see section below) and fired when hitting a threshold, according to the classical leaky integrate-and-fire model [Bur06; Ger+14]. In detail, between two spikes, the membrane potential V of the neuron satisfies a linear differential equation:

$$\tau \frac{\mathrm{d}V}{\mathrm{d}t} = -(V(t) - V_{\mathrm{eq}}) + RI(t).$$

Spikes were emitted when the voltage exceeded a threshold V_{th}, at which time the neuron's voltage was instantaneously reset to V_{eq} and resumed input integration. We set τ=16 ms, V_{eq}= $-$ 80 mV and R=80 $M\Omega$, V_{th}= $-$ 45 mV, and the reset potential was chosen equal to the resting potential V_{eq} [YAK11]. In equation 2.5, $I(t)$ represents the synaptic input, which was generated as described below.

Connectivity and input to the MSN

The input $I(t)$ received by the MSN is the superposition of the input received from P cortical neurons, noted $I_{\mathrm{stim}}(t)$, and an external (to the network) input $I_{\mathrm{ext}}(t)$ modeled as a Poisson process with rate λ_r:

$$I(t) = I_{\mathrm{stim}}(t) + I_{\mathrm{ext}}(t).$$

Spikes from cortical neurons and the external source induce instantaneous jumps in the MSN membrane potential. Jumps associated with cortical sources have amplitudes that vary through plasticity mechanisms described in the next section. These amplitudes are modeled through the collection of synaptic weights $W(t) = (W_i(t))_{1 \leqslant i \leqslant P}$. Denoting t_i^k the k-th spike time of input neuron i and δ the Dirac mass, we have

$$I_{\mathrm{stim}}(t) = \tau \sum_{1 \leqslant i \leqslant P} \sum_{t_i^k \leqslant t} W_i(t_i^k-)\delta(t - t_i^k)$$

where we noted, for a function f being potentially discontinuous at time t, $f(t-)$ the value reached immediately before the jump.

Contrasting with the network input described above whose synaptic weights are allowed to vary in time according to plasticity rules described in the next section, the

external input is assumed to induce jumps of fixed amplitude W_{ext}=1 nA (high enough to evoke spiking activity in the MSN):

$$I_{\text{ext}}(t) = \tau W_{\text{ext}} \sum_{t_{\text{ext}}^k \leqslant t} \delta(t - t_{\text{ext}}^k),$$

where $(t_{\text{ext}}^k)_{k\geqslant 0}$ denotes the sequence of external spike times, which have exponentially distributed inter-spike intervals.

The factor τ needs to be added in both currents expressions because we chose to use a simple model of synaptic inputs, where spikes induce a Dirac of activity. Therefore, in order to relate synaptic weight W to EPSC amplitudes measured in experiments, we need this scaling. In particular, the membrane potential has the following expression, between spikes of the postsynaptic neuron,

$$V(t) = V_{\text{eq}} + R \sum_{1\leqslant i\leqslant P} \sum_{t_i^k \leqslant t} W_i(t_i^k-) e^{-(t-t_i^k)/\tau} + RW_{\text{ext}} \sum_{t_{\text{ext}}^k \leqslant t} e^{-(t-t_{\text{ext}}^k)/\tau}.$$

Cortico-striatal plasticity

We implemented a pair-based model of STDP, where synaptic weights W were updated after each spike (all-to-all implementation [MDG08]), according to the spike timing relative to all previous spikes of the other neuron. In detail:

— If the MSN spikes at time t_{post} (postsynaptic spike), then all weights are updated. Noting $t_{\text{pre},i}$ the previous spikes of cortical neuron i, the synaptic weight W_i is updated according to:

$$W_i(t_{\text{post}}) = W_i(t_{\text{post}}-) + \varepsilon \sum_{t_{\text{pre},i} \leqslant t_{\text{post}}} \Phi(t_{\text{post}} - t_{\text{pre},i})$$

where ε denotes the plasticity rate, chosen in our simulations as ε=0.02.

— If presynaptic cortical neuron $i \in \{1, \cdots, P\}$ spikes at time $t_{\text{pre},i}$, noting t_{post} the times of the MSN spikes, then the synaptic weight W_i is updated as:

$$W_i(t_{\text{pre},i}) = W_i(t_{\text{pre},i}-) + \varepsilon \sum_{t_{\text{post}} \leqslant t_{\text{pre},i}} \Phi(t_{\text{post}} - t_{\text{pre},i}).$$

Denoting Δt=$t_{\text{post}} - t_{\text{pre}}$ the timing between the presynaptic (cortical) spike and the postsynaptic (MSN) spike, we use an exponential STDP kernel [MDG08]:

$$\Phi(\Delta t) = \begin{cases} A_{\text{post-pre}} \exp\left(\frac{\Delta t}{\tau_s}\right) & \text{if } \Delta t < 0 \\ A_{\text{pre-post}} \exp\left(-\frac{\Delta t}{\tau_s}\right) & \text{if } \Delta t > 0 \end{cases}$$

with τ_s=20 ms.

Consistent with the anti-Hebbian form of the corticostriatal STDP [FGV05; Men+20], we consider $A_{\text{pre-post}} = -1$ (see e.g. [Fel12]), corresponding to synaptic depression subsequent to a pre-post paired stimulation. The observation of corticostriatal Hebbian and anti-Hebbian STDP results mainly from the use of GABAergic transmission inhibitors [She+08] or not [FGV05; Men+20], as demonstrated thereafter [Pai+13;

Val+17]. The sign of $A_{\text{post-pre}}$ allows distinguishing between symmetric anti-Hebbian STDP ($A_{\text{post-pre}} \leqslant 0$) reported at DMS corticostriatal synapses from asymmetric anti-Hebbian STDP ($A_{\text{post-pre}} \geqslant 0$) reported at DLS corticostriatal synapses. Here, we focused on the influence of $A_{\text{post-pre}}$ on learning and relearning.

During a learning task (see next section), the system is presented with a succession of cortical patterns. Each pattern corresponds to a temporal window of a fixed duration ($100\,ms$), where a subset of N_{stim} cortical neurons spike at time $t_{\text{offset}}=50\,ms$. Two types of noise are modeled at the level of a single cortical neuron. First, each neuron involved in the pattern spikes at a time normally distributed with mean t_{offset} and standard deviation $\tau_p=0.2\,ms$, modeling variability of the spike times. Second, cortical spikes unrelated to the pattern are added through Poisson spikes with rate λ_r/P, representing the random firing of the cortical neuron. Moreover, the influence of external inputs is modeled at the level of the postsynaptic neuron, directly with the spikes of the random input presented above.

In the model presented here, a pattern can either be rewarded or not through a simple additive mechanism. If a pattern is rewarded, then each time a presynaptic neuron i fires during the pattern (even if it is noise), its associated synaptic weight gets potentiated, following,

$$\Delta W_i = \varepsilon\, A_{\text{reward}} > 0.$$

If the pattern is not rewarded, the synaptic weight is not modified.

Detailed models, in particular three-factor learning rules [KIT17; Fon+18; Ger+18], are thus approximated here by the presence of a simple reward signal consisting in the potentiation of the synaptic weight of all presynaptic neurons that spiked during the pattern (both those involved in the pattern and those associated with noisy inputs).

A framework for corticostriatal plasticity was developed along with the use of dopamine-dependent STDP curves [GHR15], but only focused on Hebbian STDP. Following the same principles about the role of dopamine in the reward system, we chose to fix the STDP curves and modeled the reward influence through an additive potentiation as used in most existing models of anti-Hebbian STDP [RB00; WRL03; RA04].

Eventually, synaptic weights are clipped within a realist range $[w_{\min}, w_{\max}] = [0., 2.]\,nA$. The initial synaptic weights are drawn from a uniform distribution on $[0., 0.05]\,nA$.

Learning with anti-Hebbian STDP rules

To characterize the capacity of learning associated with each STDP forms, we defined a fixed set of N_p cortical patterns. The system was presented either with a randomly chosen pattern of correlated cortical activity (from the set N_p patterns) with probability η, or with probability $1-\eta$ only with noise. Among the set of N_p patterns, a fixed subset was chosen to be rewarded (rewarded patterns were randomly chosen among all patterns, each pattern having a probability $1/2$ to be rewarded). A rewarded pattern was deemed learnt if the MSN fired in response to the presentation of the pattern. Moreover, non-rewarded patterns should not elicit any spike.

The accuracy of the learning process was estimated through the averaged numbers of correct responses:

$$\text{Accuracy} = \frac{1}{N_p} \sum_{1 \leqslant k \leqslant N_p} r_k \sigma_k + (1 - r_k)(1 - \sigma_k), \tag{2.1}$$

where r_k=1 if k is a rewarded pattern and 0 otherwise, σ_k=1 if the MSN spiked and 0 otherwise.

Each simulation emulated learning throughout four phases (see parameters in Table 2.1), all of which including STDP and differing in the frequency of pattern presentation and presence of rewards:

a. The initial phase of spontaneous activity, where patterns are presented randomly (η=η_m) and in the presence of noise. This phase is useful to avoid transient effects due to the initialization by reaching a realistic synaptic weight regime based on the plasticity rule. Noise was set to λ_r=$4\lambda_{\text{MSN}}$=20 Hz.

b. The learning phase during which neurons display spontaneous random activity with pattern presented at each iteration (η=1), and Poisson noise with intensity λ_r=λ_{MSN}=5 Hz consistent with firing of the MSNs in the rat striatum [Mah+06]. The reward signal was present and potentiated all synapses of presynaptic neurons active during a rewarded pattern. This phase emulates learning, as the output neuron learns to discriminate patterns by spiking in response to rewarded patterns and not spiking in response to non-rewarded patterns.

c. The maintenance phase models spontaneous activity with λ_r=$4\lambda_{\text{MSN}}$=20 Hz and random presentations of patterns (η=η_m) in the absence of rewards, allowing to evaluate the system's ability to sustain a discrimination between learnt patterns. We chose to take λ_r=$4\lambda_{\text{MSN}}$ in order to shorten our simulations and speed up the decrease of memory. All results are still true for λ_r=λ_{MSN}, except that memory is maintained for longer times than our simulations permitted.

d. The relearning phase, with the same parameters as the learning phase (a), is used to measure the system ability to learn again patterns, after a period of spontaneous activity.

Phase	Initial	Learning	Maintenance	Relearning
Reward	No	Yes	No	Yes
Random Noise λ_r	$4\lambda_{\text{MSN}}$=20 Hz	λ_{MSN}=5 Hz	$4\lambda_{\text{MSN}}$=20 Hz	λ_{MSN}=5 Hz
Rate of Pattern Presentation η	η_m	1	η_m	1

Table 2.1: **Parameters for the different phases of the learning task used in the mathematical model.**
Anti-Hebbian STDP is present in all phases and each phase lasts for 500 iterations.

Model simulations

Simulations were performed on Python 3.X, using the Anaconda suite (Anaconda Software Distribution, Computer software Version 2-2.4.0. Anaconda, Nov. 2016. Web. https ://anaconda.com.). The Python libraries of numeric calculus *numpy* and plotting *matplotlib* were used. Our custom code is freely accessible on https://github.com/gvignoud/striatalLearning. Simulations were run on the INRIA

CLEPS cluster and HPC resources from GENCI-IDRIS (Grant 2022-A0100612385), using GNU parallel (Tange, O. (2020, May 22). GNU Parallel 20200522 ('Kraftwerk'). Zenodo. https ://doi.org/10.5281/zenodo.3841377). We used a Euler scheme to simulate our network and Poisson processes, with $\mathrm{d}t{=}0.2\,ms$.

In order to study the evolution of the network during the different phases and compute learning accuracy, we evaluated some properties of the network every 50 pattern iterations (except at the beginning of each phase, where we recorded every 5 pattern iterations). During these test sessions, we froze the network structure by considering that

— both types of plasticity are turned off;

— the three noise components described above were suppressed ($\lambda_r{=}0$, $\tau_p = 0$);

— all patterns were successively presented to the network, and the accuracy was computed using the responses of the MSN, as described in Eq. (2.1);

— between each pattern, the MSN potential was reset to its equilibrium value, in order to avoid influence of one pattern to another.

For each set of parameters, we ran 200 different simulations. Statistics were computed on a random split of the simulations into 10 sets of 20 simulations, in order to compare statistics of performance of the network across multiple conditions. We use statistical t-test from scipy.stats Python library (* $p{<}0.05$, ** $p{<}0.005$, *** $p{<}0.0005$).

We started by collecting the mean accuracy at the end of each phase A_j for $j{=}1, 2, 3, 4$.

To characterize the kinetics of learning in the maintenance phase, we fitted a sigmoidal function to the curve of accuracy as a function of time. This generic sigmoid with 5 parameters, was given by:

$$S[A_{\text{init}}, t_{\text{init}}, A_{\text{end}}, d, g](t) = A_{\text{end}} + (A_{\text{init}} - A_{\text{end}}) \times \left(1 + \left(\frac{t - t_{\text{init}}}{g}\right)\right)^{-d}$$

where A_{init} is the initial value of the sigmoid, t_{init} the starting time of the second phase (in terms of pattern iterations), A_{end} is the final value, g is a timescale parameter, while d is a shape parameter of the sigmoid. Fitting the sigmoid allows comparing the dynamics in the maintenance phase for various conditions, and in particular the performance of symmetric and asymmetric anti-Hebbian STDP. The initial value was set at $A_{\text{init}}{=}A_2$ and the ending value at $A_{\text{end}}{=}A_1$ The fits were realized by estimating the best values of d and g to reproduce the accuracy dynamics and were performed using the scipy.optimize.curvefit function of the scipy Python library.

We compared maintenance of the learning task through the characteristic time of decay to represent the speed of decrease,

$$T_{\text{maintenance}} = \min\left(\max\left(0, \frac{g}{d}\right), 1000\right).$$

Finally, in order to measure the relearning characteristic time, i.e., the time necessary for the system to relearn patterns after the maintenance phase, we define $T_{\text{relearning}}$ as follows. Remembering that A_1 (resp., A_2) is the accuracy after the initial phase (resp.,

learning phase), we define $T_{\text{relearning}}$ as the time needed in the relearning phase to learn again at least 60% of the previously learned accuracy,

$$T_{\text{relearning}} = \inf \{t > 0 | \text{Accuracy}(t) - A_1 > 0.6 \times (A_2 - A_1)\} .$$

We investigated how synaptic weight during the maintenance phase deviate from those at the end of the learning phase. To this end, we defined W_{ref} the synaptic weights at the end of the learning phase, and used various metrics to analyze the divergence of the weights from this value during maintenance:

— The divergence of the L^2 norm,

$$d_2(W) = \frac{1}{1 + \frac{\sqrt{\sum_i (W_i - W_{\text{ref},i})^2}}{\sqrt{\sum_i W_{\text{ref},i}^2}}}$$

which is equal to 1 when $W = W_{\text{ref}}$ and decays to 0 as the Euclidean distance between the two weight vectors increases. A large $d_2(W)$ (i.e., close to 1) means that weights remained similar to the reference, and a decay of that quantity estimates how quickly the weight vector deviates from reference.

— One may consider that relative values of weights, rather than their absolute amplitude, contain a particularly important information in learning. In that sense, W_{ref} provides a direction in the space of weights, and we estimated the alignment of the weight vector at a given time with W_{ref} through the *cosine similarity* of the centered synaptic weight:

$$sp(W) = \frac{\sum_i (W_i - \overline{W_i}) \times (W_{\text{ref},i} - \overline{W_{\text{ref},i}})}{\sqrt{\sum_i (W_i - \overline{W_i})^2} \sqrt{\sum_i (W_{\text{ref},i} - \overline{W_{\text{ref},i}})^2}}$$

where $\overline{x}$ for $x \in \mathbb{R}^P$ denotes the average of the vector's component.

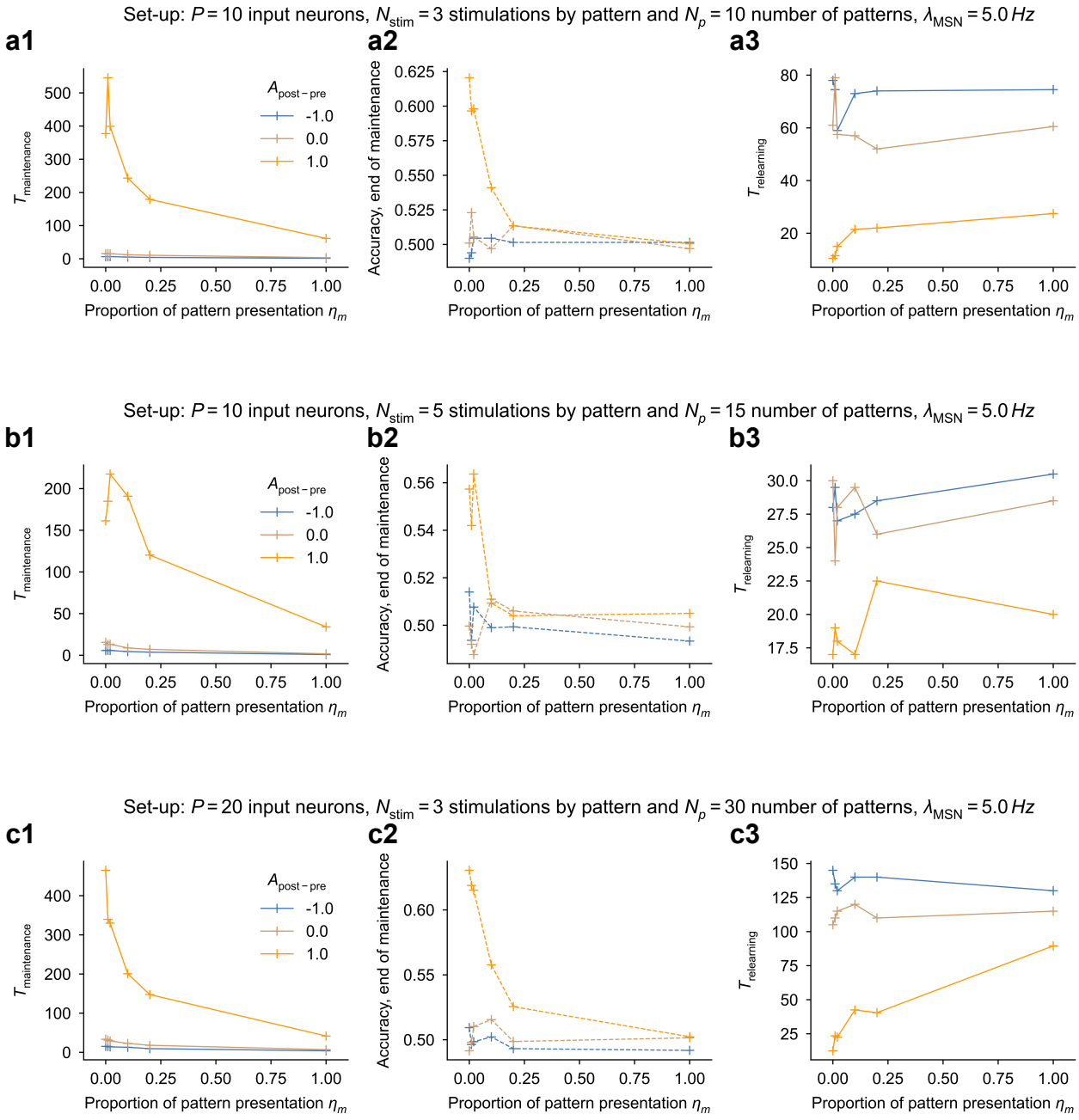

Figure 2.4: **Learning task using various setups** $(P, N_{\text{stim}} and N_p)$ **(related to Figure 2.3).** Influence of η_m on the learning parameters for (a) P=10 input neurons, N_{stim}=3 stimulations by pattern, N_p=10 patterns, (b) P=10 input neurons, N_{stim}=5 stimulations by pattern, N_p=15 patterns and (c) P=20 input neurons, N_{stim}=3 stimulations by pattern, N_p=30 patterns.
(x) Dependance of characteristic time of maintenance $T_{\text{maintenance}}$ (x1), accuracy at the end of the maintenance phase (x2) and characteristic time of relearning $T_{\text{relearning}}$ (x3) on the type of plasticity $A_{\text{post-pre}}$ and stimulus presentation frequency η_m.
Mean of results over 10 sets of 20 simulations with errors bars representing $\pm$SD/2. Statistical t-test from scipy.stats Python library; *: p<0.05, **: p<0.005, ***: p<0.0005.

Parameters	Values
P	$(10, 20)$
τ	$16\,ms$
$V_{\text{eq}} = V_{\text{r}}$	$-80\,mV$
R	$80\,M\Omega$
V_{th}	$-45\,mV$
N_p	$(10, 15)$ for $P = 10$ and (30) for $P = 20$
N_{stim}	$(3, 5)$
$A_{\text{post-pre}}$	$(-1.5, -1.0, -0.5, 0., 0.5, 1.0, 1.5, 2.)$
$A_{\text{pre-post}}$	$(-1.0, 0.)$
τ_s	$20\,ms$
A_{reward}	$(0., 0.95)$
ϵ	0.02
τ_p	$0.2\,ms$
λ_{MSN}	$5\,Hz$
η_m	$(0., 0.01, 0.02, 0.1, 0.2, 1.0)$
$\mathrm{d}t$	0.2

Table 2.2: **Parameters of the mathematical model to study learning features in DMS and DLS.**

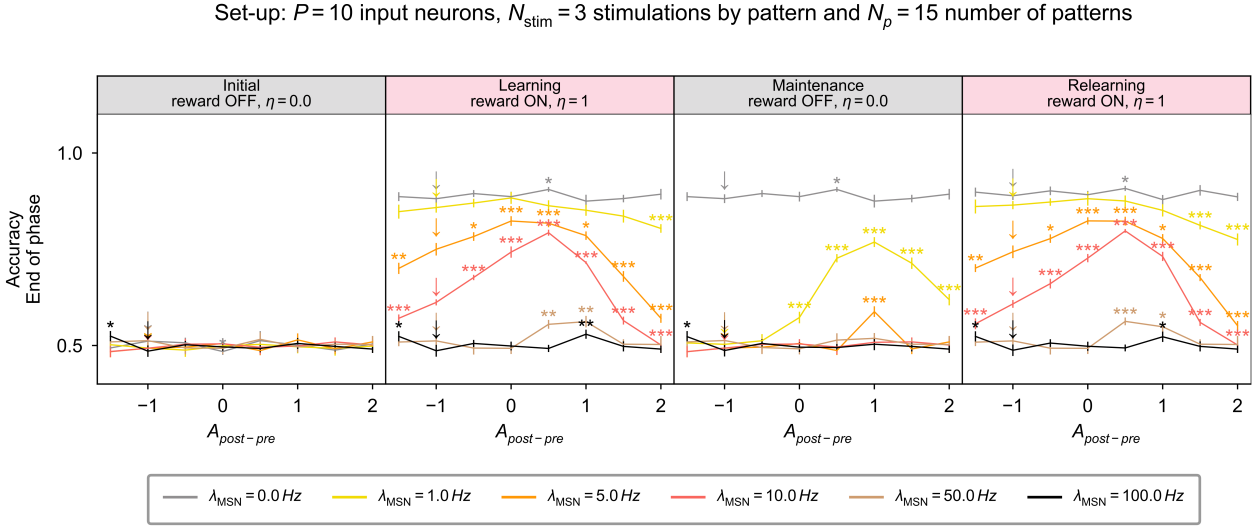

Figure 2.5: **Learning task with different noise values λ_{MSN}.**
Accuracy at the end of each phase as a function of the type of plasticity (where $A_{\text{post}-\text{pre}}$ parameterizes the plasticity). Several values of noise λ_{MSN} are tested (see different colors).
Mean of results over 10 sets of 20 simulations with errors bars representing $\pm$SD/2. Statistical t-test from scipy.stats Python library; *: p<0.05, **: p<0.005, ***: p<0.0005.

BIBLIOGRAPHY

[Ale+21] J. Alegre-Cortés, M. Sáez, R. Montanari, and R. Reig. Medium spiny neurons activity reveals the discrete segregation of mouse dorsal striatum. *eLife* **10** (Feb. 2021), e60580.

[Ath+18] V. R. Athalye, F. J. Santos, J. M. Carmena, and R. M. Costa. Evidence for a neural law of effect. *Science* **359** (Mar. 2018), 1024–1029.

[Bar+11] T. D. Barnes, J.-B. Mao, D. Hu, Y. Kubota, A. A. Dreyer, C. Stamoulis, E. N. Brown, and A. M. Graybiel. Advance cueing produces enhanced action-boundary patterns of spike activity in the sensorimotor striatum. *Journal of Neurophysiology* **105** (Apr. 2011), 1861–1878.

[Bel+97] C. C. Bell, V. Z. Han, Y. Sugawara, and K. Grant. Synaptic plasticity in a cerebellum-like structure depends on temporal order. *Nature* **387** (May 1997), 278–281.

[Ber+18] H. C. Bergstrom et al. Dorsolateral Striatum Engagement Interferes with Early Discrimination Learning. *Cell Reports* **23** (May 2018), 2264–2272.

[BMP19] Z. Brzosko, S. B. Mierau, and O. Paulsen. Neuromodulation of Spike-Timing-Dependent Plasticity: Past, Present, and Future. *Neuron* **103** (Aug. 2019), 563–581.

[BNR15] A. C. Burton, K. Nakamura, and M. R. Roesch. From ventral-medial to dorsal-lateral striatum: neural correlates of reward-guided decision-making. *Neurobiology of Learning and Memory* **117** (Jan. 2015), 51–59.

[BO10] B. W. Balleine and J. P. O'Doherty. Human and rodent homologies in action control: corticostriatal determinants of goal-directed and habitual action. *Neuropsychopharmacology: Official Publication of the American College of Neuropsychopharmacology* **35** (Jan. 2010), 48–69.

[Bon+19] P. Bonnavion, E. P. Fernández, C. Varin, and A. de Kerchove d'Exaerde. It takes two to tango: Dorsal direct and indirect pathways orchestration of motor learning and behavioral flexibility. *Neurochemistry International* **124** (Mar. 2019), 200–214.

[Bur06] A. N. Burkitt. A Review of the Integrate-and-fire Neuron Model: I. Homogeneous Synaptic Input. *Biological Cybernetics* **95** (July 2006), 1–19.

[Cal+14] P. Calabresi, B. Picconi, A. Tozzi, V. Ghiglieri, and M. Di Filippo. Direct and indirect pathways of basal ganglia: a critical reappraisal. *Nature Neuroscience* **17** (Aug. 2014), 1022–1030.

[CCN04] R. M. Costa, D. Cohen, and M. A. L. Nicolelis. Differential corticostriatal plasticity during fast and slow motor skill learning in mice. *Current biology: CB* **14** (July 2004), 1124–1134.

[CJ10] L. H. Corbit and P. H. Janak. Posterior dorsomedial striatum is critical for both selective instrumental and Pavlovian reward learning. *The European Journal of Neuroscience* **31** (Apr. 2010), 1312–1321.

[Fel12] D. E. Feldman. The spike-timing dependence of plasticity. *Neuron* **75** (Aug. 2012), 556–571.

[FGV05] E. Fino, J. Glowinski, and L. Venance. Bidirectional activity-dependent plasticity at corticostriatal synapses. *The Journal of Neuroscience: The Official Journal of the Society for Neuroscience* **25** (Dec. 2005), 11279–11287.

[Fin+10] E. Fino, V. Paille, Y. Cui, T. Morera-Herreras, J.-M. Deniau, and L. Venance. Distinct coincidence detectors govern the corticostriatal spike timing-dependent plasticity. *The Journal of Physiology* **588** (Aug. 2010), 3045–3062.

[Fin+18] E. Fino, M. Vandecasteele, S. Perez, F. Saudou, and L. Venance. Region-specific and state-dependent action of striatal GABAergic interneurons. *Nature Communications* **9** (Aug. 2018), 3339.

[Fis+17] S. D. Fisher, P. B. Robertson, M. J. Black, P. Redgrave, M. A. Sagar, W. C. Abraham, and J. N. J. Reynolds. Reinforcement determines the timing dependence of corticostriatal synaptic plasticity in vivo. *Nature Communications* **8** (Aug. 2017), 334.

[Fon+18] A. Foncelle, A. Mendes, J. Jędrzejewska-Szmek, S. Valtcheva, H. Berry, K. T. Blackwell, and L. Venance. Modulation of Spike-Timing Dependent Plasticity: Towards the Inclusion of a Third Factor in Computational Models. *Frontiers in Computational Neuroscience* **12** (2018), 49.

[GC13] C. M. Gremel and R. M. Costa. Orbitofrontal and striatal circuits dynamically encode the shift between goal-directed and habitual actions. *Nature Communications* **4** (Aug. 2013), 2264.

[Ger+14] W. Gerstner, W. M. Kistler, R. Naud, and L. Paninski. Neuronal Dynamics: From Single Neurons to Networks and Models of Cognition. New York, NY, USA: Cambridge University Press, 2014.

[Ger+18] W. Gerstner, M. Lehmann, V. Liakoni, D. Corneil, and J. Brea. Eligibility Traces and Plasticity on Behavioral Time Scales: Experimental Support of NeoHebbian Three-Factor Learning Rules. *Frontiers in Neural Circuits* **12** (July 2018).

[GG15] A. M. Graybiel and S. T. Grafton. The Striatum: Where Skills and Habits Meet. *Cold Spring Harbor Perspectives in Biology* **7** (Aug. 2015), a021691.

[GHR15] K. N. Gurney, M. D. Humphries, and P. Redgrave. A new framework for cortico-striatal plasticity: behavioural theory meets in vitro data at the reinforcement-action interface. *PLoS biology* **13** (Jan. 2015), e1002034.

[Hun+16] B. J. Hunnicutt, B. C. Jongbloets, W. T. Birdsong, K. J. Gertz, H. Zhong, and T. Mao. A comprehensive excitatory input map of the striatum reveals novel functional organization. *eLife* **5** (Nov. 2016), e19103.

[JC15] X. Jin and R. M. Costa. Shaping action sequences in basal ganglia circuits. *Current Opinion in Neurobiology* **33** (Aug. 2015), 188–196.

[Kim+09] E. Y. Kimchi, M. M. Torregrossa, J. R. Taylor, and M. Laubach. Neuronal correlates of instrumental learning in the dorsal striatum. *Journal of Neurophysiology* **102** (July 2009), 475–489.

[KIT17] Ł. Kuśmierz, T. Isomura, and T. Toyoizumi. Learning with three factors: modulating Hebbian plasticity with errors. *Current Opinion in Neurobiology* **46** (Oct. 2017), 170–177.

[Kor+12] A. C. Koralek, X. Jin, J. D. Long, R. M. Costa, and J. M. Carmena. Corticostriatal plasticity is necessary for learning intentional neuroprosthetic skills. *Nature* **483** (Mar. 2012), 331–335.

[Kup+17] D. A. Kupferschmidt, K. Juczewski, G. Cui, K. A. Johnson, and D. M. Lovinger. Parallel, but Dissociable, Processing in Discrete Corticostriatal Inputs Encodes Skill Learning. *Neuron* **96** (Oct. 2017), 476–489.e5.

[Ma+18] T. Ma, Y. Cheng, E. Roltsch Hellard, X. Wang, J. Lu, X. Gao, C. C. Y. Huang, X.-Y. Wei, J.-Y. Ji, and J. Wang. Bidirectional and long-lasting control of alcohol-seeking behavior by corticostriatal LTP and LTD. *Nature Neuroscience* **21** (Mar. 2018), 373–383.

[Mah+06] S. Mahon, N. Vautrelle, L. Pezard, S. J. Slaght, J.-M. Deniau, G. Chouvet, and S. Charpier. Distinct Patterns of Striatal Medium Spiny Neuron Activity during the Natural Sleep–Wake Cycle. *The Journal of Neuroscience* **26** (Nov. 2006), 12587–12595.

[Mar+97] H. Markram, J. Lübke, M. Frotscher, and B. Sakmann. Regulation of synaptic efficacy by coincidence of postsynaptic APs and EPSPs. *Science (New York, N.Y.)* **275** (Jan. 1997), 213–215.

[MDG08] A. Morrison, M. Diesmann, and W. Gerstner. Phenomenological models of synaptic plasticity based on spike timing. *Biological Cybernetics* **98** (June 2008), 459–478.

[Men+20] A. Mendes, G. Vignoud, S. Perez, E. Perrin, J. Touboul, and L. Venance. Concurrent Thalamostriatal and Corticostriatal Spike-Timing-Dependent Plasticity and Heterosynaptic Interactions Shape Striatal Plasticity Map. *Cerebral Cortex (New York, N.Y.: 1991)* **30** (June 2020), 4381–4401.

[Mor+19] T. Morera-Herreras, Y. Gioanni, S. Perez, G. Vignoud, and L. Venance. Environmental enrichment shapes striatal spike-timing-dependent plasticity in vivo. *Scientific Reports* **9** (Dec. 2019), 19451.

[OHa+16] J. K. O'Hare, K. K. Ade, T. Sukharnikova, S. D. Van Hooser, M. L. Palmeri, H. H. Yin, and N. Calakos. Pathway-Specific Striatal Substrates for Habitual Behavior. *Neuron* **89** (Feb. 2016), 472–479.

[Pai+13] V. Paille, E. Fino, K. Du, T. Morera-Herreras, S. Perez, J. H. Kotaleski, and L. Venance. GABAergic circuits control spike-timing-dependent plasticity. *The Journal of Neuroscience: The Official Journal of the Society for Neuroscience* **33** (May 2013), 9353–9363.

[Per+22] S. Perez, Y. Cui, G. Vignoud, E. Perrin, A. Mendes, Z. Zheng, J. Touboul, and L. Venance. Striatum expresses region-specific plasticity consistent with distinct memory abilities. *Cell Reports* **38** (2022), 110521.

[Pet+21] A. J. Peters, J. M. J. Fabre, N. A. Steinmetz, K. D. Harris, and M. Carandini. Striatal activity topographically reflects cortical activity. *Nature* **591** (Mar. 2021), 420–425.

[PK08] V. Pawlak and J. N. D. Kerr. Dopamine receptor activation is required for corticostriatal spike-timing-dependent plasticity. *The Journal of Neuroscience: The Official Journal of the Society for Neuroscience* **28** (Mar. 2008), 2435–2446.

[PV19] E. Perrin and L. Venance. Bridging the gap between striatal plasticity and learning. *Current Opinion in Neurobiology*. Neurobiology of Learning and Plasticity **54** (Feb. 2019), 104–112.

[RA04] C. C. Rumsey and L. F. Abbott. Equalization of synaptic efficacy by activity- and timing-dependent synaptic plasticity. *Journal of Neurophysiology* **91** (May 2004), 2273–2280.

[Rag+02] M. E. Ragozzino, K. E. Ragozzino, S. J. Y. Mizumori, and R. P. Kesner. Role of the dorsomedial striatum in behavioral flexibility for response and visual cue discrimination learning. *Behavioral Neuroscience* **116** (Feb. 2002), 105–115.

[Rag07] M. E. Ragozzino. The contribution of the medial prefrontal cortex, orbitofrontal cortex, and dorsomedial striatum to behavioral flexibility. *Annals of the New York Academy of Sciences* **1121** (Dec. 2007), 355–375.

[RB00] P. D. Roberts and C. C. Bell. Computational consequences of temporally asymmetric learning rules: II. Sensory image cancellation. *Journal of Computational Neuroscience* **9** (Aug. 2000), 67–83.

[RL10] P. D. Roberts and T. K. Leen. Anti-Hebbian spike-timing-dependent plasticity and adaptive sensory processing. *Frontiers in Computational Neuroscience* **4** (2010), 156.

[RS11] T. Requarth and N. B. Sawtell. Neural mechanisms for filtering self-generated sensory signals in cerebellum-like circuits. *Current Opinion in Neurobiology* **21** (Aug. 2011), 602–608.

[She+08] W. Shen, M. Flajolet, P. Greengard, and D. J. Surmeier. Dichotomous dopaminergic control of striatal synaptic plasticity. *Science (New York, N.Y.)* **321** (Aug. 2008), 848–851.

[SRR10] J. M. Schulz, P. Redgrave, and J. N. J. Reynolds. Cortico-striatal spike-timing dependent plasticity after activation of subcortical pathways. *Frontiers in Synaptic Neuroscience* **2** (2010), 23.

[Sta+10] T. A. Stalnaker, G. G. Calhoon, M. Ogawa, M. R. Roesch, and G. Schoenbaum. Neural Correlates of Stimulus–Response and Response–Outcome Associations in Dorsolateral Versus Dorsomedial Striatum. *Frontiers in Integrative Neuroscience* **4** (May 2010), 12.

[STN01] P. J. Sjöström, G. G. Turrigiano, and S. B. Nelson. Rate, timing, and cooperativity jointly determine cortical synaptic plasticity. *Neuron* **32** (Dec. 2001), 1149–1164.

[TG14] C. A. Thorn and A. M. Graybiel. Differential entrainment and learning-related dynamics of spike and local field potential activity in the sensorimotor and associative striatum. *The Journal of Neuroscience: The Official Journal of the Society for Neuroscience* **34** (Feb. 2014), 2845–2859.

[Tho+10] C. A. Thorn, H. Atallah, M. Howe, and A. M. Graybiel. Differential Dynamics of Activity Changes in Dorsolateral and Dorsomedial Striatal Loops During Learning. *Neuron* **66** (June 2010), 781–795.

[Val+17] S. Valtcheva, V. Paillé, Y. Dembitskaya, S. Perez, G. Gangarossa, E. Fino, and L. Venance. Developmental control of spike-timing-dependent plasticity by tonic GABAergic signaling in striatum. *Neuropharmacology* **121** (July 2017), 261–277.

[Van+19] Y. Vandaele, N. R. Mahajan, D. J. Ottenheimer, J. M. Richard, S. P. Mysore, and P. H. Janak. Distinct recruitment of dorsomedial and dorsolateral striatum erodes with extended training. *eLife* **8** (Oct. 2019), e49536.

[VTV20] G. Vignoud, J. Touboul, and L. Venance. A synaptic theory for procedural and sequence learning in the striatum. *Bernstein Conference 2020*. 2020.

[Wil+19] J. A. Willett, J. Cao, D. M. Dorris, A. G. Johnson, L. A. Ginnari, and J. Meitzen. Electrophysiological Properties of Medium Spiny Neuron Subtypes in the Caudate-Putamen of Prepubertal Male and Female Drd1a-tdTomato Line 6 BAC Transgenic Mice. *eNeuro* **6** (Mar. 2019), ENEURO.0016–19.2019.

[WRL03] A. Williams, P. D. Roberts, and T. K. Leen. Stability of negative-image equilibria in spike-timing-dependent plasticity. *Physical Review E* **68** (Aug. 2003), 021923.

[XZZ15] Q. Xiong, P. Znamenskiy, and A. M. Zador. Selective corticostriatal plasticity during acquisition of an auditory discrimination task. *Nature* **521** (May 2015), 348–351.

[YAK11] M. Y. Yim, A. Aertsen, and A. Kumar. Significance of Input Correlations in Striatal Function. *PLoS Computational Biology* **7** (Nov. 2011).

[Yin+09] H. H. Yin, S. P. Mulcare, M. R. F. Hilário, E. Clouse, T. Holloway, M. I. Davis, A. C. Hansson, D. M. Lovinger, and R. M. Costa. Dynamic reorganization of striatal circuits during the acquisition and consolidation of a skill. *Nature Neuroscience* **12** (Mar. 2009), 333–341.

[YK06] H. H. Yin and B. J. Knowlton. The role of the basal ganglia in habit formation. *Nature Reviews. Neuroscience* **7** (June 2006), 464–476.

Discussion

*

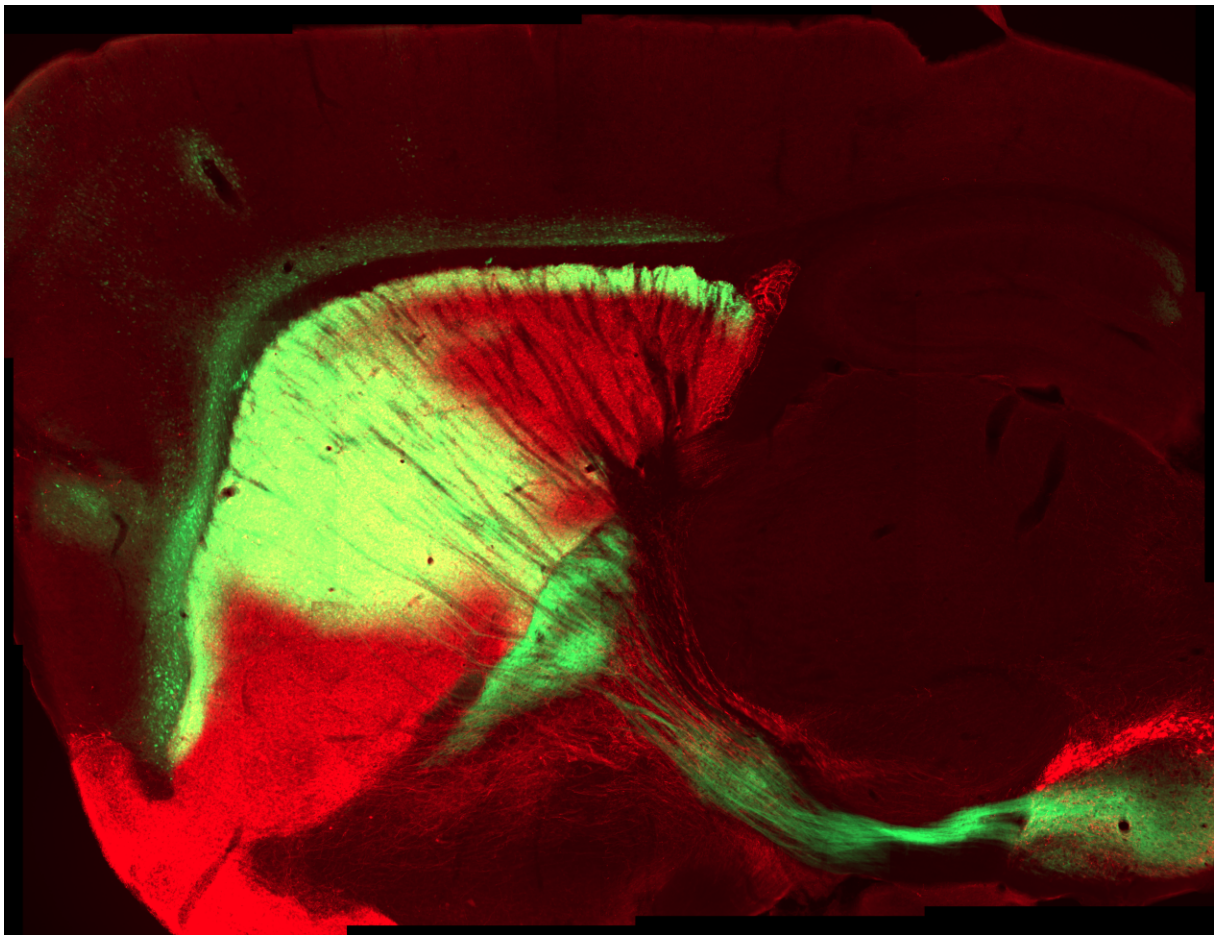

Sagittal section of a mouse brain. A retrograde AAV-GFP was injected in the striatum, revealing mesencephalic projections known as the MFB (medial forebrain bundle), as well as deep-layer cortical pyramidal neurons. GFP in green; Tyrosine Hydroxylase in red [S. Valverde].

We discuss three possible directions for future works, based on the present report.

Beyond spike-timing dependent plasticity

STDP is a synaptic plasticity rule based on the relative pre- and postsynaptic spike timings. As developed in the Introduction, numerous experimental works have shown that STDP can be elicited at different types of synapses. STDP has also been investigated from a computational point of view, in different types of models, and implemented in complex neuronal networks. Considering its simplicity, STDP has also attracted some criticisms almost since its discovery.

Questioning the importance of STDP

Most experimental data on STDP have been obtained using *in vitro* protocols, where pairs of spikes from the pre- and postsynaptic neurons are triggered using electric stimulations. Several authors have pointed out that these protocols do not reproduce realistic conditions of neuronal activity, and have therefore questioned the general definition of STDP [LS10; Suv19]. At first, STDP is defined as a process where local depolarizations of the membrane potential, caused by a backpropagating action potential, could interact with EPSPs (excitatory post-synaptic potentials) resulting from presynaptic spikes, and induce changes in synaptic transmission.

A first crucial issue about *in vitro* experimental protocols concerns the mechanisms used to trigger a postsynaptic spike. Indeed, in most studies, a brief depolarizing current is presented to the postsynaptic neuron soma, which leads to the triggering of a spike. In particular, the spike is not induced through natural processes, resulting from the integration of dendritic currents. This raises the question of which particular mechanism induces the local depolarization needed for plasticity induction, is it Na^+ spikes, calcium Ca^{2+} spikes? Is it possible to have STDP, without having a postsynaptic spike, but simply thanks to local depolarizations?

A second recurrent concern stresses that STDP protocols are not "realistic" when looking at brain activity. *In vivo* recordings do not support the idea that two single neurons repeatedly fire one after the other, with the same delay, at a fixed frequency. For example, bursts of spiking activity, up and down states, oscillations are more characteristic of brain dynamics than protocols of STDP. Even if some studies have succeeded in eliciting STDP in *in vivo* recordings [Mor+19], the results are less clear and more often stress that other paradigms than STDP are needed to fully understand synaptic plasticity.

A third issue, that is already extensively addressed in the current report, is that Hebbian STDP, has been considered, for a long time, as the only version of STDP, while several experiments have since then shown that a great diversity of plasticity curves exists, such as anti-Hebbian STDP at corticostriatal synapses [FGV05; Fel12]. Moreover, with *in vitro* protocols, networks effects are modified, if not deleted, while the influence of local neuromodulators depends highly on the brain slices preparation. In more realistic situations, the synaptic weights are maybe affected as much by those processes, than by STDP, questioning its actual relevance.

Towards biologically-plausible synaptic plasticity

Even if early STDP protocols were not realistic in term of naturalistic activity-pattern at central synapses, experimentalists have been prone to develop more biologically-plausible schemes to trigger synaptic plasticity. As stated in the previous section, the main critics about STDP refer to the induction of the postsynaptic spike directly by an electrical stimulation at the level of the soma. Several studies have tried using presynaptic inputs to trigger the postsynaptic spikes, leading to more realistic spike triggering. These experiments are gathered under the acronym ITDP, for *input-timing dependent plasticity* (ITDP) [Cho+12; Ler+17].

The necessity of having a postsynaptic action potential to induce synaptic plasticity was also recurrently questioned and has been proven false since then. Indeed, in [FDV09], it is shown that brief subthreshold events can act as causal signals for long-term plasticity. Even if the observed plasticity is not as "acute" as the one observed using STDP protocols, subthreshold events are sufficient to trigger long-term synaptic changes. The influence of the postsynaptic membrane potential, and not only of spike trains, has also been considered in a class of computational models of STDP [CG10].

More recently, it was shown in place fields in hippocampal area CA [Bit+17] that it was possible to induce synaptic potentiation different from STDP, considering that its temporal window was wider than in STDP experiments (seconds instead of milliseconds), that a “plateau” of postsynaptic activity replaced the postsynaptic spike, and that the order of the association did not change the polarity of the observed synaptic plasticity. This synaptic learning rule evolves on behavioral timescales, and may be a good surrogate of STDP when looking at *in vivo* activity.

Do we really need STDP to be biologically-plausible?

STDP has been used in a wide range of computational models, and several theoretical studies have used its simple and elegant formulation to investigate the role of synaptic plasticity in learning. Considering the fact that STDP is currently questioned as a relevant mechanism for learning in experimental studies, it seems logical to also interrogate its use in computational models.

First, STDP can be seen as a “building block” of synaptic plasticity, and as such I think that its use is justified when looking at complex models. Indeed, STDP protocols results from pre- and postsynaptic pairings, and gives a real insight on the dynamics of a single synapse, as a function of the pre- and postsynaptic spiking activity. When building complex neuronal networks, where neurons are only represented by their spike trains, neuroscientists need simple learning rules like STDP, and they have been using them for long times. Prior to STDP, many computational models used “Hebbian” synaptic plasticity in their models, where synaptic weight changes depend on the pre- and postsynaptic firing rates, that also has its limits from a biological point of view. This does not mean that all conclusions from computational models with rate-based plasticity, or STDP, are useless just because the synaptic learning rules did not fulfill a never ending (and always growing) list of biological properties. It just needs to be considered when drawing conclusions on large scales systems and learning in general. It is particularly interesting to notice that STDP was first formulated in computational studies [Ger+96] and not from experiments.

Second, I also would like to stress that STDP, even if not fully biologically-based, is still a powerful rule when learning, and as such justifies the amount of theoretical

works that have been published on its properties. For example, it has been recently used in deep learning [Ben+15; Ben+17] in spiking neural networks (SNN), and it could have tremendous applications for the implementations of machine learning algorithms in neuromorphic processors.

Finally, more complex synaptic plasticity rules related to STDP have been developed over the years, and still need theoretical studies to investigate their impact on neuronal networks dynamics. It would be a shame to limit efforts in this direction because STDP may not be the principal synaptic plasticity mechanisms in the brain. I think that computational and theoretical models can be a mean to understand the interactions between the various synaptic plasticity observed in experiments, starting with STDP but also integrating more biological and naturalistic synaptic plasticity rules.

Stochastic neuronal networks with STDP

Theoretical models developed in this report are limited to a simple system, with one presynaptic neuron and one postsynaptic neuron, connected by a single synapse. This framework was useful when studying the direct effects of pre- and postsynaptic spikes on the synaptic weights, and such elementary results are necessary when considering to study larger neuronal networks with synaptic plasticity. In future works, we aim at extending our formalism to recurrent neuronal networks, and prove similar theorems for multidimensional systems.

Nonlinear Hawkes processes

When studying STDP in the slow-fast approximation, we have proven that the invariant distribution of the neuronal dynamics with fixed weights were crucial in determining the system's dynamics. Following this idea, we have developed a new formalism for Hawkes processes, which represent a good model for neuronal activity. However, we restricted ourselves to auto-exciting processes, while neurons are more likely to be auto-inhibiting processes. Indeed, a postsynaptic spike leads to a decrease of the membrane potential value, and consequently, to a decrease of the firing rate.

To reproduce this behavior using Hawkes process, the stochastic intensity λ_{Hawkes} needs to depend on negative functionals of previous jumps, i.e

$$\lambda_{\text{Hawkes}}(t) = \beta\left(\int_{-\infty}^{t} h(t-s)\mathcal{N}_{\text{Hawkes}}(\mathrm{d}s)\right),$$

where h is a negative function, and β the activation function. Nevertheless, the stochastic intensity needs, by definition, to be non-negative, and it would not be possible to use linear Hawkes process where $\beta(x)=\nu+\beta x$. A large literature on linear Hawkes processes exists, usually in the framework of cluster branching processes [Haw71; HO74]. When looking at nonlinear activation functions β, other proofs need to be developed to study the existence of stationary Hawkes processes. Several articles have been dedicated to nonlinear Hawkes processes, usually using Picard iterations and analysis to prove the existence and unicity of a stationary solution [Ker64; BM96]. Recent works have also discussed the possible role of inhibition in Hawkes processes, but focus on simpler kernels h with finite memory in order to use renewal theory [Cos+20]. A global theory of general Hawkes processes, with negative function h is still lacking even if it would be of great interests for neuroscience, epidemiology or population dynamics theory.

Adaptative neuronal networks

Multidimensional Hawkes processes are interesting models to study neuronal dynamics, they can be used to infer the connectivity matrix from the spike trains and as such are of particular interest for neuroscientists [Rey+14]. It is indeed possible to formulate the dynamics of spiking neuronal network as a multidimensional Hawkes process, verifying,

$$\begin{cases} \lambda_{\text{Hawkes,1}}(t) = \beta_1 \left(\sum_{i=0}^{N} \int_{-\infty}^{t} h_{1,i}(t-s) \mathcal{N}_{\text{Hawkes,i}}(\mathrm{d}s) \right) \\ \qquad \vdots \qquad\qquad\qquad\qquad \vdots \\ \lambda_{\text{Hawkes,N}}(t) = \beta_N \left(\sum_{i=0}^{N} \int_{-\infty}^{t} h_{N,i}(t-s) \mathcal{N}_{\text{Hawkes,i}}(\mathrm{d}s) \right) \end{cases}$$

where, the function $H = (t \mapsto h_{i,j}(t))_{1 \leqslant i,j \leqslant N}$ represents the connectivity matrix of the neuronal network. Multidimensional Hawkes processes have been studied, with fixed connectivity H, in the linear case [Haw71] or the nonlinear case [BM96]. Again, as explained in the previous section, most studies do not consider any inhibitory mechanism, and it could be expected that adding inhibition leads to less restrictive conditions for the existence of a stationary solution: it has a stabilizing effect on the point processes dynamics. The importance of the excitation/inhibition balance has been known to be central when studying neuronal dynamics for a long time [Bru00].

In the present report, we have studied the influence of STDP on neuronal dynamics. We claim that an even more general class of Hawkes, where the connectivity matrix H depend on time, through some plasticity mechanisms, can be defined. This would open the door for theoretical studies of adaptative Hawkes processes, which modify their interactions as a function of previous activity. Adaptative cluster processes have recently been introduced, when considering phase-dependent plasticity and are linked to this idea [BSY19].

The influence of STDP on recurrent neuronal networks has been the focus of numerous studies [GBV10], mainly in computational neuroscience. Their approach would benefit from the development of a theoretical framework for adaptative multidimensional processes.

Mean-field analysis of STDP in neuronal networks

When looking at large neuronal networks, it is always tempting to take the limit when the number of neurons goes to infinity, and usually end up with mean-field dynamics. This limit has been largely studied for neuronal networks with fixed connectivity [RT16], and leads to interesting analytical results on the network dynamics. A similar approximation can be envisioned while looking at adaptative neuronal networks with synaptic plasticity. For short-term synaptic plasticity, a recent study looks at the mean-field approximations of the associated dynamics [Löc17].

What would happen when examining long-term synaptic plasticity? Is it possible to couple the mean-field analysis with slow-fast arguments? If yes, in which order should we take the limits? And is this order determinant for the limit's dynamics? All of these questions are still pending, and future works on such processes will be important, not only for neuroscience, but to other adaptative systems, with applications in finance, epidemiology or evolution. A recent article [ARJ20] uses both approximations, but does not consider all the possible problems that can emerge from taking this double limit.

Goal-directed behavior versus habits in the striatum

Computational models developed in the present report have highlighted the crucial role of STDP when learning to recognize patterns of correlated cortical activity. However, as pointed out in this discussion, STDP should not be considered as the only synaptic plasticity mechanism at play when looking at complex tasks, and more importantly network dynamics should also be taken into account. Future works could be devoted to a more realistic model of the striatum, integrating direct- and indirect pathways neurons for example, or inhibitory interneurons. Several striatal models already study those influences separately, without considering anti-Hebbian STDP. A global model of the striatum would be a terrific tool to study the differential influence of each of these processes, and to more clearly understand its role in procedural learning.

DMS and DLS, more differences than just STDP

DMS and DLS differential role in procedural learning could be investigated using such a general striatal system. In the present reports, we only considered disparity in STDP at corticostriatal synapses [Per+22], however the difference between those two regions are not limited to synaptic plasticity. The following properties should be inserted in any striatal network, aiming at studying why DMS and DLS subtend specific types of learning and behaviors, respectively goal-directed behavior and habits:

— Both regions receive inputs from different cortical regions (somato-sensory versus associative areas), and some correlated activity patters may be specific to DMS or DLS.

— MSNs exhibit different electrophysiological properties when located in either of those regions.

— Feedforward inhibition, through the action of fast-spiking or low-threshold spiking interneurons also depends on DMS or DLS [Fin+18].

— STDP at corticostriatal synapses is specific to these regions, as was shown in [Per+22].

Moreover, the dopaminergic signaling pathways should also be modeled, as it is critical in goal-directed behavior [SDM97]. Similarly, in order to model the whole action selection process, MSNs belonging to direct- or indirect pathways, and the subsequent circuits, should be investigated following previous studies [Dun+19].

A global model of the basal ganglia, incorporating those properties, will be needed to directly relate to behavioral experiments, and to predict animal behavior in procedural learning.

Switch between goal-directed behavior and habits

Even if this global model is able to reproduce goal-directed and habitual behavior, thanks to different properties present either in the DMS or the DLS, it may not explain how both regions influence each other. Indeed, the striatum is differentially involved during procedural learning, and studying how the switch between goal-directed behavior and habits occur will be a great advance in our comprehension of the establishment

of procedural memory. A recent article has shown that this question is of interest, both for neuroscientists and experimentalists [PB19]. How is this switch implemented, why and when? are several questions that need to be answered. Computational models are of great help in the study of such topics, because they can emulate dynamics not easily tested in experiments.

BIBLIOGRAPHY

[AFH12] A. Abbassian, M. Fotouhi, and M. Heidari. Neural fields with fast learning dynamic kernel. *Biological cybernetics* **106** (2012), 15–26.

[AG00] R. Azouz and C. M. Gray. Dynamic spike threshold reveals a mechanism for synaptic coincidence detection in cortical neurons in vivo. *Proceedings of the National Academy of Sciences* **97** (July 2000), 8110–8115.

[AK15] D. F. Anderson and T. G. Kurtz. Stochastic Analysis of Biochemical Systems. Mathematical Biosciences Institute Lecture Series. Springer Publishing Company, Incorporated, 2015.

[Ale+21] J. Alegre-Cortés, M. Sáez, R. Montanari, and R. Reig. Medium spiny neurons activity reveals the discrete segregation of mouse dorsal striatum. *eLife* **10** (Feb. 2021), e60580.

[ARJ20] A. E. Akil, R. Rosenbaum, and K. Josić. Synaptic Plasticity in Correlated Balanced Networks. *bioRxiv* (2020). eprint: `https://doi.org/10.1101/2020.04.26.061515`.

[Asm03] S. Asmussen. Applied Probability and Queues. 2nd ed. Stochastic Modelling and Applied Probability. New York: Springer-Verlag, 2003.

[Ath+18] V. R. Athalye, F. J. Santos, J. M. Carmena, and R. M. Costa. Evidence for a neural law of effect. *Science* **359** (Mar. 2018), 1024–1029.

[BA10] B. Babadi and L. F. Abbott. Intrinsic stability of temporally shifted spike-timing dependent plasticity. *PLoS computational biology* **6** (Nov. 2010), e1000961.

[BA16] B. Babadi and L. F. Abbott. Stability and Competition in Multi-spike Models of Spike-Timing Dependent Plasticity. *PLoS computational biology* **12** (Mar. 2016), e1004750.

[Bal+06] K. Ball, T. G. Kurtz, L. Popovic, G. Rempala, et al. Asymptotic analysis of multiscale approximations to reaction networks. *The Annals of Applied Probability* **16** (2006), 1925–1961.

[Bar+11] T. D. Barnes, J.-B. Mao, D. Hu, Y. Kubota, A. A. Dreyer, C. Stamoulis, E. N. Brown, and A. M. Graybiel. Advance cueing produces enhanced action-boundary patterns of spike activity in the sensorimotor striatum. *Journal of Neurophysiology* **105** (Apr. 2011), 1861–1878.

[BC07] M. A. Buice and J. D. Cowan. Field-theoretic approach to fluctuation effects in neural networks. *Physical Review E* **75** (May 2007), 051919.

[BC15] K. R. Brimblecombe and S. J. Cragg. Substance P Weights Striatal Dopamine Transmission Differently within the Striosome-Matrix Axis. *The Journal of Neuroscience* **35** (June 2015), 9017–9023.

[BCR19] L. Beznea, I. Cîmpean, and M. Röckner. A new approach to the existence of invariant measures for Markovian semigroups. *Annales de l'Institut Henri Poincaré, Probabilités et Statistiques*. Vol. 55. 2019, 977–1000.

[Bel+97] C. C. Bell, V. Z. Han, Y. Sugawara, and K. Grant. Synaptic plasticity in a cerebellum-like structure depends on temporal order. *Nature* **387** (May 1997), 278–281.

[Ben+15] Y. Bengio, T. Mesnard, A. Fischer, S. Zhang, and Y. Wu. STDP as presynaptic activity times rate of change of postsynaptic activity. *arXiv:1509.05936 [cs, q-bio]* (Sept. 2015).

[Ben+17] Y. Bengio, T. Mesnard, A. Fischer, S. Zhang, and Y. Wu. STDP-Compatible Approximation of Backpropagation in an Energy-Based Model. *Neural Computation* **29** (2017), 555–577.

[Ber+18] H. C. Bergstrom et al. Dorsolateral Striatum Engagement Interferes with Early Discrimination Learning. *Cell Reports* **23** (May 2018), 2264–2272.

[BG06] N. Berglund and B. Gentz. Noise-induced phenomena in slow-fast dynamical systems: a sample-paths approach. Springer Science & Business Media, 2006.

[BGH07] A. N. Burkitt, M. Gilson, and J. L. van Hemmen. Spike-timing-dependent plasticity for neurons with recurrent connections. *Biological Cybernetics* **96** (May 2007), 533–546.

[BH09] L. Bauwens and N. Hautsch. Modelling Financial High Frequency Data Using Point Processes. *Handbook of Financial Time Series*. Ed. by T. Mikosch, J.-P. Kreiß, R. A. Davis, and T. G. Andersen. Berlin, Heidelberg: Springer Berlin Heidelberg, 2009, 953–979.

[Bil99] P. Billingsley. Convergence of Probability Measures. John Wiley & Sons, 1999.

[Bit+17] K. C. Bittner, A. D. Milstein, C. Grienberger, S. Romani, and J. C. Magee. Behavioral time scale synaptic plasticity underlies CA1 place fields. *Science (New York, N.Y.)* **357** (Sept. 2017), 1033–1036.

[BK12] K. S. Burbank and G. Kreiman. Depression-biased reverse plasticity rule is required for stable learning at top-down connections. *PLoS computational biology* **8** (2012), e1002393.

[BKL02] S. M. Bohte, J. N. Kok, and H. La Poutré. Error-backpropagation in temporally encoded networks of spiking neurons. *Neurocomputing* **48** (Oct. 2002), 17–37.

[BM01] P. Brémaud and L. Massoulié. Hawkes Branching Point Processes without Ancestors. *Journal of Applied Probability* **38** (2001), 122–135.

[BM96] P. Brémaud and L. Massoulié. Stability of Nonlinear Hawkes Processes. *The Annals of Probability* **24** (1996), 1563–1588.

[BMG04] A. N. Burkitt, H. Meffin, and D. B. Grayden. Spike-timing-dependent plasticity: the relationship to rate-based learning for models with weight dynamics determined by a stable fixed point. *Neural Computation* **16** (May 2004), 885–940.

[BMP19] Z. Brzosko, S. B. Mierau, and O. Paulsen. Neuromodulation of Spike-Timing-Dependent Plasticity: Past, Present, and Future. *Neuron* **103** (Aug. 2019), 563–581.

[BNR15] A. C. Burton, K. Nakamura, and M. R. Roesch. From ventral-medial to dorsal-lateral striatum: neural correlates of reward-guided decision-making. *Neurobiology of Learning and Memory* **117** (Jan. 2015), 51–59.

[BO10] B. W. Balleine and J. P. O'Doherty. Human and rodent homologies in action control: corticostriatal determinants of goal-directed and habitual action. *Neuropsychopharmacology: Official Publication of the American College of Neuropsychopharmacology* **35** (Jan. 2010), 48–69.

[Bon+19] P. Bonnavion, E. P. Fernández, C. Varin, and A. de Kerchove d'Exaerde. It takes two to tango: Dorsal direct and indirect pathways orchestration of motor learning and behavioral flexibility. *Neurochemistry International* **124** (Mar. 2019), 200–214.

[Bou16] A. Boumezoued. Population viewpoint on Hawkes processes. *Advances in Applied Probability* **48** (June 2016), 463–480.

[BP01] G. Bi and M. Poo. Synaptic modification by correlated activity: Hebb's postulate revisited. *Annual Review of Neuroscience* **24** (2001), 139–166.

[BP98] G.-q. Bi and M.-m. Poo. Synaptic Modifications in Cultured Hippocampal Neurons: Dependence on Spike Timing, Synaptic Strength, and Postsynaptic Cell Type. *Journal of Neuroscience* **18** (Dec. 1998), 10464–10472.

[Bru00] N. Brunel. Dynamics of sparsely connected networks of excitatory and inhibitory spiking neurons. *Journal of Computational Neuroscience* **8** (June 2000), 183–208.

[BSY19] R. Berner, E. Schöll, and S. Yanchuk. Multiclusters in Networks of Adaptively Coupled Phase Oscillators. *SIAM Journal on Applied Dynamical Systems* **18** (Jan. 2019), 2227–2266.

[Bur06] A. N. Burkitt. A Review of the Integrate-and-fire Neuron Model: I. Homogeneous Synaptic Input. *Biological Cybernetics* **95** (July 2006), 1–19.

[Buz10] G. Buzsáki. Neural syntax: cell assemblies, synapsembles and readers. *Neuron* **68** (Nov. 2010), 362–385.

[Cal+14] P. Calabresi, B. Picconi, A. Tozzi, V. Ghiglieri, and M. Di Filippo. Direct and indirect pathways of basal ganglia: a critical reappraisal. *Nature Neuroscience* **17** (Aug. 2014), 1022–1030.

[CCN04] R. M. Costa, D. Cohen, and M. A. L. Nicolelis. Differential corticostriatal plasticity during fast and slow motor skill learning in mice. *Current biology: CB* **14** (July 2004), 1124–1134.

[CCP11] M. J. Cáceres, J. A. Carrillo, and B. Perthame. Analysis of nonlinear noisy integrate & fire neuron models: blow-up and steady states. *The Journal of Mathematical Neuroscience* **1** (2011), 7.

[CF03] H. Câteau and T. Fukai. A stochastic method to predict the consequence of arbitrary forms of spike-timing-dependent plasticity. *Neural Computation* **15** (Mar. 2003), 597–620.

[CF16] R. Chaudhuri and I. Fiete. Computational principles of memory. *Nature Neuroscience* **19** (Mar. 2016), 394–403.

[CFS82] I. P. Cornfeld, S. V. Fomin, and Y. G. Sinaĭ. Ergodic Theory. Grundlehren der mathematischen Wissenschaften. New York: Springer-Verlag, 1982.

[CG10] C. Clopath and W. Gerstner. Voltage and Spike Timing Interact in STDP – A Unified Model. *Frontiers in Synaptic Neuroscience* **2** (July 2010).

[Che+15] J. Chevallier, M. J. Cáceres, M. Doumic, and P. Reynaud-Bouret. Microscopic approach of a time elapsed neural model. *Mathematical Models and Methods in Applied Sciences* **25** (2015), 2669–2719.

[Che+17] S. Chen, A. Shojaie, E. Shea-Brown, and D. Witten. The Multivariate Hawkes Process in High Dimensions: Beyond Mutual Excitation. *arXiv:1707.04928 [stat]* (July 2017).

[Chi01] E. Chichilnisky. A simple white noise analysis of neuronal light responses. *Network: Computation in Neural Systems* **12** (2001), 199–213.

[Cho+12] J.-H. Cho, I. T. Bayazitov, E. G. Meloni, K. M. Myers, W. A. Carlezon, S. S. Zakharenko, and V. Y. Bolshakov. Coactivation of thalamic and cortical pathways induces input timing–dependent plasticity in amygdala. *Nature Neuroscience* **15** (Jan. 2012), 113–122.

[CJ10] L. H. Corbit and P. H. Janak. Posterior dorsomedial striatum is critical for both selective instrumental and Pavlovian reward learning. *The European Journal of Neuroscience* **31** (Apr. 2010), 1312–1321.

[CJB10] V. S. Chakravarthy, D. Joseph, and R. S. Bapi. What do the basal ganglia do? A modeling perspective. *Biological Cybernetics* **103** (Sept. 2010), 237–253.

[Clo+10] C. Clopath, L. Büsing, E. Vasilaki, and W. Gerstner. Connectivity reflects coding: a model of voltage-based STDP with homeostasis. *Nature Neuroscience* **13** (Mar. 2010), 344–352.

[CM08] A. Citri and R. C. Malenka. Synaptic plasticity: multiple forms, functions, and mechanisms. *Neuropsychopharmacology: Official Publication of the American College of Neuropsychopharmacology* **33** (Jan. 2008), 18–41.

[Cos+20] M. Costa, C. Graham, L. Marsalle, and V. C. Tran. Renewal in Hawkes processes with self-excitation and inhibition. *Advances in Applied Probability* **52** (Sept. 2020), 879–915.

[Cow68] J. D. Cowan. Statistical Mechanics of Nervous Nets. *Neural Networks: Proceedings of the -School on Neural Networks - June 1967 in Ravello*. Ed. by E. R. Caianiello. Berlin, Heidelberg: Springer, 1968, 181–188.

[Cow91] J. Cowan. Stochastic Neurodynamics. *Advances in Neural Information Processing Systems*. Vol. 3. Morgan-Kaufmann, 1991.

[CS08] R. Crane and D. Sornette. Robust dynamic classes revealed by measuring the response function of a social system. *Proceedings of the National Academy of Sciences* **105** (2008), 15649–15653. eprint: `https://www.pnas.org/content/105/41/15649.full.pdf`.

[Cui+16] Y. Cui, I. Prokin, H. Xu, B. Delord, S. Genet, L. Venance, and H. Berry. Endocannabinoid dynamics gate spike-timing dependent depression and potentiation. *eLife* **5** (Feb. 2016), e13185.

[Dav93] M. H. A. Davis. Markov models and optimization. London: Chapman & Hall, 1993.

[Daw93] D. A. Dawson. Measure-valued Markov processes. *École d'Été de Probabilités de Saint-Flour XXI—1991*. Vol. 1541. Lecture Notes in Math. Berlin: Springer, Nov. 1993, 1–260.

[Des+20] C. Desjardins, Q. Salardaine, G. Vignoud, and B. Degos. Movement disorders analysis using a deep learning approach. *Movement Disorders*. Vol. 35. 2020.

[DLO19] Duarte, Aline, Löcherbach, Eva, and Ost, Guilherme. Stability, convergence to equilibrium and simulation of non-linear Hawkes processes with memory kernels given by the sum of Erlang kernels. *ESAIM: PS* **23** (2019), 770–796.

[DP18] A. Daw and J. Pender. Queues driven by Hawkes processes. *Stochastic Systems* **8** (2018), 192–229.

[Dun+19] K. Dunovan, C. Vich, M. Clapp, T. Verstynen, and J. Rubin. Reward-driven changes in striatal pathway competition shape evidence evaluation in decision-making. *PLoS computational biology* **15** (May 2019), e1006998.

[DV03] D. J. Daley and D. Vere-Jones. An Introduction to the Theory of Point Processes. Volume 1: Elementary Theory and Methods. Second edition. Probability and its Applications. Springer, Nov. 2003.

[DV08] D. J. Daley and D. Vere-Jones. An introduction to the theory of point processes. Vol. II. Second edition. Probability and its Applications (New York). New York: Springer, 2008, xviii+573.

[EGG10] E. Errais, K. Giesecke, and L. Goldberg. Affine Point Processes and Portfolio Credit Risk. *SIAM Journal on Financial Mathematics* **1** (Jan. 2010), 642–665.

[EK09] S. N. Ethier and T. G. Kurtz. Markov Processes: Characterization and Convergence. John Wiley & Sons, Sept. 2009.

[ELL11] P. Embrechts, T. Liniger, and L. Lin. Multivariate Hawkes processes: an application to financial data. *Journal of Applied Probability* **48** (2011), 367–378.

[ET10] G. B. Ermentrout and D. H. Terman. Mathematical Foundations of Neuroscience. Springer Science & Business Media, July 2010.

[Ete+16] J. Etesami, N. Kiyavash, K. Zhang, and K. Singhal. Learning Network of Multivariate Hawkes Processes: A Time Series Approach. *Proceedings of the Thirty-Second Conference on Uncertainty in Artificial Intelligence*. UAI'16. Arlington, Virginia, United States: AUAI Press, 2016, 162–171.

[Eur+99] C. W. Eurich, K. Pawelzik, U. Ernst, J. D. Cowan, and J. G. Milton. Dynamics of self-organized delay adaptation. *Physical Review Letters* **82** (1999), 1594.

[FD02] R. C. Froemke and Y. Dan. Spike-timing-dependent synaptic modification induced by natural spike trains. *Nature* **416** (Mar. 2002), 433–438.

[FDV09] E. Fino, J.-M. Deniau, and L. Venance. Brief subthreshold events can act as Hebbian signals for long-term plasticity. *PloS One* **4** (Aug. 2009), e6557.

[Fei19] M. Feinberg. Foundations of chemical reaction network theory. Vol. 202. Applied Mathematical Sciences. Springer, Cham, 2019, xxix+454.

[Fel12] D. E. Feldman. The spike-timing dependence of plasticity. *Neuron* **75** (Aug. 2012), 556–571.

[FG16] N. Frémaux and W. Gerstner. Neuromodulated Spike-Timing-Dependent Plasticity, and Theory of Three-Factor Learning Rules. *Frontiers in Neural Circuits* **9** (2016), 85.

[FGV05] E. Fino, J. Glowinski, and L. Venance. Bidirectional activity-dependent plasticity at corticostriatal synapses. *The Journal of Neuroscience: The Official Journal of the Society for Neuroscience* **25** (Dec. 2005), 11279–11287.

[Fin+10] E. Fino, V. Paille, Y. Cui, T. Morera-Herreras, J.-M. Deniau, and L. Venance. Distinct coincidence detectors govern the corticostriatal spike timing-dependent plasticity. *The Journal of Physiology* **588** (Aug. 2010), 3045–3062.

[Fin+18] E. Fino, M. Vandecasteele, S. Perez, F. Saudou, and L. Venance. Region-specific and state-dependent action of striatal GABAergic interneurons. *Nature Communications* **9** (Aug. 2018), 3339.

[Fis+17] S. D. Fisher, P. B. Robertson, M. J. Black, P. Redgrave, M. A. Sagar, W. C. Abraham, and J. N. J. Reynolds. Reinforcement determines the timing dependence of corticostriatal synaptic plasticity in vivo. *Nature Communications* **8** (Aug. 2017), 334.

[Flo12] R. V. Florian. The Chronotron: A Neuron That Learns to Fire Temporally Precise Spike Patterns. *PLoS ONE* **7** (Aug. 2012), e40233.

[Fon+18] A. Foncelle, A. Mendes, J. Jędrzejewska-Szmek, S. Valtcheva, H. Berry, K. T. Blackwell, and L. Venance. Modulation of Spike-Timing Dependent Plasticity: Towards the Inclusion of a Third Factor in Computational Models. *Frontiers in Computational Neuroscience* **12** (2018), 49.

[FSG10] N. Frémaux, H. Sprekeler, and W. Gerstner. Functional Requirements for Reward-Modulated Spike-Timing-Dependent Plasticity. *Journal of Neuroscience* **30** (2010), 13326–13337. eprint: `https://www.jneurosci.org/content/30/40/13326.full.pdf`.

[FV10] E. Fino and L. Venance. Spike-timing dependent plasticity in the striatum. *Frontiers in Synaptic Neuroscience* **2** (2010), 6.

[FW98] M. I. Freidlin and A. D. Wentzell. Random perturbations of dynamical systems. Second Edition edition. New York: Springer-Verlag, 1998.

[Gal+19] A. Galves, E. Löcherbach, C. Pouzat, and E. Presutti. A System of Interacting Neurons with Short Term Synaptic Facilitation. *Journal of Statistical Physics* **178** (Dec. 2019), 869–892.

[Gar10] C. Gardiner. Stochastic Methods: A Handbook for the Natural and Social Sciences (Springer Series in Synergetics). Softcover reprint of hardcover 4th ed. 2009 edition. Springer Series in Synergetics. Springer, 2010.

[Gar19] J. L. Gardner. Optimality and heuristics in perceptual neuroscience. *Nature Neuroscience* **22** (Apr. 2019), 514–523.

[GB07] M. Graupner and N. Brunel. STDP in a bistable synapse model based on CaMKII and associated signaling pathways. *PLoS computational biology* **3** (Nov. 2007), e221.

[GB10] M. Graupner and N. Brunel. Mechanisms of induction and maintenance of spike-timing dependent plasticity in biophysical synapse models. *Frontiers in Computational Neuroscience* **4** (2010).

[GB12] M. Graupner and N. Brunel. Calcium-based plasticity model explains sensitivity of synaptic changes to spike pattern, rate, and dendritic location. *Proceedings of the National Academy of Sciences of the United States of America* **109** (Mar. 2012), 3991–3996.

[GBV10] M. Gilson, A. Burkitt, and L. J. Van Hemmen. STDP in Recurrent Neuronal Networks. *Frontiers in Computational Neuroscience* **4** (2010).

[GC13] C. M. Gremel and R. M. Costa. Orbitofrontal and striatal circuits dynamically encode the shift between goal-directed and habitual actions. *Nature Communications* **4** (Aug. 2013), 2264.

[GDT17] F. Gerhard, M. Deger, and W. Truccolo. On the stability and dynamics of stochastic spiking neuron models: Nonlinear Hawkes process and point process GLMs. *PLOS Computational Biology* **13** (Feb. 2017), e1005390.

[Ger+14] W. Gerstner, W. M. Kistler, R. Naud, and L. Paninski. Neuronal Dynamics: From Single Neurons to Networks and Models of Cognition. New York, NY, USA: Cambridge University Press, 2014.

[Ger+18] W. Gerstner, M. Lehmann, V. Liakoni, D. Corneil, and J. Brea. Eligibility Traces and Plasticity on Behavioral Time Scales: Experimental Support of NeoHebbian Three-Factor Learning Rules. *Frontiers in Neural Circuits* **12** (July 2018).

[Ger+96] W. Gerstner, R. Kempter, J. L. van Hemmen, and H. Wagner. A neuronal learning rule for sub-millisecond temporal coding. *Nature* **383** (Sept. 1996), 76–81.

[GG15] A. M. Graybiel and S. T. Grafton. The Striatum: Where Skills and Habits Meet. *Cold Spring Harbor Perspectives in Biology* **7** (Aug. 2015), a021691.

[GH92] W. Gerstner and J. L. van Hemmen. Associative memory in a network of 'spiking' neurons. *Network: Computation in Neural Systems* **3** (Jan. 1992), 139–164.

[GHR15] K. N. Gurney, M. D. Humphries, and P. Redgrave. A new framework for cortico-striatal plasticity: behavioural theory meets in vitro data at the reinforcement-action interface. *PLoS biology* **13** (Jan. 2015), e1002034.

[GK02a] W. Gerstner and W. M. Kistler. Mathematical formulations of Hebbian learning. *Biological Cybernetics* **87** (Dec. 2002), 404–415.

[GK02b] W. Gerstner and W. M. Kistler. Spiking Neuron Models: Single Neurons, Populations, Plasticity. Cambridge University Press, Aug. 2002.

[GMH11] M. Gilson, T. Masquelier, and E. Hugues. STDP allows fast rate-modulated coding with Poisson-like spike trains. *PLoS computational biology* **7** (Oct. 2011), e1002231.

[GP60] E. N. Gilbert and H. O. Pollak. Amplitude Distribution of Shot Noise. *Bell System Technical Journal* **39** (Mar. 1960), 333–350.

[Gra19] C. Graham. Regenerative properties of the linear Hawkes process with unbounded memory. *arXiv:1905.11053 [math, stat]* (May 2019).

[GS05] G. Gusto and S. Schbath. FADO: A Statistical Method to Detect Favored or Avoided Distances between Occurrences of Motifs using the Hawkes' Model. *Statistical Applications in Genetics and Molecular Biology* **4** (2005).

[GS06] R. Gütig and H. Sompolinsky. The tempotron: a neuron that learns spike timing-based decisions. *Nature Neuroscience* **9** (Mar. 2006), 420–428.

[Güt+03] R. Gütig, R. Aharonov, S. Rotter, and H. Sompolinsky. Learning input correlations through nonlinear temporally asymmetric Hebbian plasticity. *The Journal of Neuroscience: The Official Journal of the Society for Neuroscience* **23** (May 2003), 3697–3714.

[Güt+13] R. Gütig, T. Gollisch, H. Sompolinsky, and M. Meister. Computing complex visual features with retinal spike times. *PloS One* **8** (2013), e53063.

[Güt14] R. Gütig. To spike, or when to spike? *Current Opinion in Neurobiology* **25** (Apr. 2014), 134–139.

[GWO16] M. Graupner, P. Wallisch, and S. Ostojic. Natural Firing Patterns Imply Low Sensitivity of Synaptic Plasticity to Spike Timing Compared with Firing Rate. *Journal of Neuroscience* **36** (Nov. 2016), 11238–11258.

[Hai10] M. Hairer. Convergence of Markov processes. 2010.

[Has80] R. Z. Has'minskiĭ. Stochastic stability of differential equations. Alphen aan den Rijn: Sijthoff & Noordhoff, 1980, xvi+344.

[Haw71] A. G. Hawkes. Spectra of Some Self-Exciting and Mutually Exciting Point Processes. *Biometrika* **58** (1971), 83–90.

[HCT12] C. D. Harvey, P. Coen, and D. W. Tank. Choice-specific sequences in parietal cortex during a virtual-navigation decision task. *Nature* **484** (Mar. 2012), 62–68.

[Hel18] P. Helson. A new stochastic STDP Rule in a neural Network Model. *arXiv:1706.00364 [math]* (Mar. 2018).

[Hem+19] M. Hemberger, M. Shein-Idelson, L. Pammer, and G. Laurent. Reliable Sequential Activation of Neural Assemblies by Single Pyramidal Cells in a Three-Layered Cortex. *Neuron* **104** (Oct. 2019), 353–369.e5.

[Hen+21] J. A. Hennig, E. R. Oby, D. M. Losey, A. P. Batista, B. M. Yu, and S. M. Chase. How learning unfolds in the brain: toward an optimization view. *Neuron* (Oct. 2021).

[HF17] N. Hiratani and T. Fukai. Detailed Dendritic Excitatory/Inhibitory Balance through Heterosynaptic Spike-Timing-Dependent Plasticity. *The Journal of Neuroscience: The Official Journal of the Society for Neuroscience* **37** (Dec. 2017), 12106–12122.

[HL17] P. Hodara and E. Löcherbach. Hawkes processes with variable length memory and an infinite number of components. *Advances in Applied Probability* **49** (2017), 84–107.

[HNA06] J. S. Haas, T. Nowotny, and H. D. I. Abarbanel. Spike-timing-dependent plasticity of inhibitory synapses in the entorhinal cortex. *Journal of Neurophysiology* **96** (Dec. 2006), 3305–3313.

[HO74] A. G. Hawkes and D. Oakes. A Cluster Process Representation of a Self-Exciting Process. *Journal of Applied Probability* **11** (1974), 493–503.

[Hod16] P. Hodara. Systèmes de neurones en interactions : modélisation probabiliste et estimation. PhD thesis. 2016.

[HOD18] M. D. Humphries, J. A. Obeso, and J. K. Dreyer. Insights into Parkinson's disease from computational models of the basal ganglia. *Journal of Neurology, Neurosurgery, and Psychiatry* **89** (Nov. 2018), 1181–1188.

[Hor+00] D. Horn, N. Levy, I. Meilijson, and E. Ruppin. Distributed synchrony of spiking neurons in a Hebbian cell assembly. *Advances in neural information processing systems*. 2000, 129–135.

[HS08] M. J. Higley and B. L. Sabatini. Calcium signaling in dendrites and spines: practical and functional considerations. *Neuron* **59** (Sept. 2008), 902–913.

[HS74] M. W. Hirsch and S. Smale. Differential equations, dynamical systems, and linear algebra. Academic Press [A subsidiary of Harcourt Brace Jovanovich, Publishers], New York-London, 1974, xi+358.

[Hum+09] M. D. Humphries, N. Lepora, R. Wood, and K. Gurney. Capturing dopaminergic modulation and bimodal membrane behaviour of striatal medium spiny neurons in accurate, reduced models. *Frontiers in Computational Neuroscience* **3** (2009), 26.

[Hun+16] B. J. Hunnicutt, B. C. Jongbloets, W. T. Birdsong, K. J. Gertz, H. Zhong, and T. Mao. A comprehensive excitatory input map of the striatum reveals novel functional organization. *eLife* **5** (Nov. 2016), e19103.

[HWG09] M. D. Humphries, R. Wood, and K. Gurney. Dopamine-modulated dynamic cell assemblies generated by the GABAergic striatal microcircuit. *Neural Networks: The Official Journal of the International Neural Network Society* **22** (Oct. 2009), 1174–1188.

[ID03] E. M. Izhikevich and N. S. Desai. Relating STDP to BCM. *Neural Computation* **15** (July 2003), 1511–1523.

[ID21] Y. Inglebert and D. Debanne. Calcium and Spike Timing-Dependent Plasticity. *Frontiers in Cellular Neuroscience* **15** (2021), 374.

[Ike+04] Y. Ikegaya, G. Aaron, R. Cossart, D. Aronov, I. Lampl, D. Ferster, and R. Yuste. Synfire chains and cortical songs: temporal modules of cortical activity. *Science (New York, N.Y.)* **304** (Apr. 2004), 559–564.

[Izh07] E. M. Izhikevich. Dynamical Systems in Neuroscience. MIT Press, 2007.

[Jac79] J. Jacod. Calcul stochastique et problèmes de martingales. Vol. 714. Lecture Notes in Mathematics. Springer, Berlin, 1979, x+539.

[JC15] X. Jin and R. M. Costa. Shaping action sequences in basal ganglia circuits. *Current Opinion in Neurobiology* **33** (Aug. 2015), 188–196.

[Jov15] S. Jovanović. Cumulants of Hawkes point processes. *Physical Review E* **91** (2015).

[JS87] J. Jacod and A. N. Shiryaev. Limit theorems for stochastic processes. Vol. 288. Grundlehren der Mathematischen Wissenschaften. Berlin: Springer-Verlag, 1987, xviii+601.

[Kar12] D. Karabash. On Stability of Hawkes Process. *arXiv:1201.1573 [math]* (Jan. 2012).

[Ker64] J. Kerstan. Teilprozesse Poissonscher Prozesse. *Trans. Third Prague Conf. Information Theory,Statist. Decision Functions, Random Processes*. Liblice: House Czech. Acad.Sci., Jan. 1964, 377–403.

[KGH01] R. Kempter, W. Gerstner, and J. L. van Hemmen. Intrinsic stabilization of output rates by spike-based Hebbian learning. *Neural Computation* **13** (Dec. 2001), 2709–2741.

[KGH99] R. Kempter, W. Gerstner, and J. L. van Hemmen. Hebbian learning and spiking neurons. *Physical Review E* **59** (Apr. 1999), 4498–4514.

[KH00] W. M. Kistler and J. L. v. Hemmen. Modeling Synaptic Plasticity in Conjunction with the Timing of Pre- and Postsynaptic Action Potentials. *Neural Computation* **12** (Feb. 2000), 385–405.

[Kim+09] E. Y. Kimchi, M. M. Torregrossa, J. R. Taylor, and M. Laubach. Neuronal correlates of instrumental learning in the dorsal striatum. *Journal of Neurophysiology* **102** (July 2009), 475–489.

[Kin92] J. F. C. Kingman. Poisson Processes. Clarendon Press, Dec. 1992.

[Kir17] M. Kirchner. A note on critical Hawkes processes. *arXiv:1706.03975 [math]* (June 2017).

[KIT17] Ł. Kuśmierz, T. Isomura, and T. Toyoizumi. Learning with three factors: modulating Hebbian plasticity with errors. *Current Opinion in Neurobiology* **46** (Oct. 2017), 170–177.

[KK+13] H.-W. Kang, T. G. Kurtz, et al. Separation of time-scales and model reduction for stochastic reaction networks. *The Annals of Applied Probability* **23** (2013), 529–583.

[Kor+12] A. C. Koralek, X. Jin, J. D. Long, R. M. Costa, and J. M. Carmena. Corticostriatal plasticity is necessary for learning intentional neuroprosthetic skills. *Nature* **483** (Mar. 2012), 331–335.

[KP17] R. Kumar and L. Popovic. Large deviations for multi-scale jump-diffusion processes. *Stochastic Processes and their Applications* **127** (2017), 1297–1320.

[KS98] I. Karatzas and S. Shreve. Brownian Motion and Stochastic Calculus. 2nd ed. Vol. 113. Graduate Texts in Mathematics. New York, NY: Springer, 1998.

[Kup+17] D. A. Kupferschmidt, K. Juczewski, G. Cui, K. A. Johnson, and D. M. Lovinger. Parallel, but Dissociable, Processing in Discrete Corticostriatal Inputs Encodes Skill Learning. *Neuron* **96** (Oct. 2017), 476–489.e5.

[Kur92] T. G. Kurtz. Averaging for martingale problems and stochastic approximation. *Applied Stochastic Analysis*. Ed. by I. Karatzas and D. Ocone. Vol. 177. Berlin/Heidelberg: Springer-Verlag, 1992, 186–209.

[LBH09] A. Luczak, P. Barthó, and K. D. Harris. Spontaneous events outline the realm of possible sensory responses in neocortical populations. *Neuron* **62** (May 2009), 413–425.

[Ler+17] F. Leroy, D. H. Brann, T. Meira, and S. A. Siegelbaum. Input-Timing-Dependent Plasticity in the Hippocampal CA2 Region and Its Potential Role in Social Memory. *Neuron* **95** (Aug. 2017), 1089–1102.e5.

[Lew64] P. A. W. Lewis. A Branching Poisson Process Model for the Analysis of Computer Failure Patterns. *Journal of the Royal Statistical Society. Series B (Methodological)* **26** (1964), 398–456.

[LF12] T. K. Leen and R. Friel. Stochastic Perturbation Methods for Spike-Timing-Dependent Plasticity. *Neural Comput.* **24** (May 2012), 1109–1146.

[Lin02] T. Lindvall. Lectures on the Coupling Method. Courier Corporation, Jan. 2002.

[Löc17] E. Löcherbach. Large deviations for cascades of diffusions arising in oscillating systems of interacting Hawkes processes. *arXiv:1709.09356 [math]* (Sept. 2017).

[LS08] E. V. Lubenov and A. G. Siapas. Decoupling through synchrony in neuronal circuits with propagation delays. *Neuron* **58** (Apr. 2008), 118–131.

[LS10] J. Lisman and N. Spruston. Questions about STDP as a General Model of Synaptic Plasticity. *Frontiers in Synaptic Neuroscience* **2** (2010), 140.

[LS14] Y. Luz and M. Shamir. The Effect of STDP Temporal Kernel Structure on the Learning Dynamics of Single Excitatory and Inhibitory Synapses. *PLoS ONE* **9** (July 2014), e101109.

[Luc+07] A. Luczak, P. Barthó, S. L. Marguet, G. Buzsáki, and K. D. Harris. Sequential structure of neocortical spontaneous activity in vivo. *Proceedings of the National Academy of Sciences of the United States of America* **104** (Jan. 2007), 347–352.

[Luc+16] L. Lucken, O. V. Popovych, P. A. Tass, and S. Yanchuk. Noise-enhanced coupling between two oscillators with long-term plasticity. *Physical Review E* **93** (Mar. 2016), 032210.

[Ma+18] T. Ma, Y. Cheng, E. Roltsch Hellard, X. Wang, J. Lu, X. Gao, C. C. Y. Huang, X.-Y. Wei, J.-Y. Ji, and J. Wang. Bidirectional and long-lasting control of alcohol-seeking behavior by corticostriatal LTP and LTD. *Nature Neuroscience* **21** (Mar. 2018), 373–383.

[MAD07] A. Morrison, A. Aertsen, and M. Diesmann. Spike-timing-dependent plasticity in balanced random networks. *Neural Computation* **19** (June 2007), 1437–1467.

[Mah+06] S. Mahon, N. Vautrelle, L. Pezard, S. J. Slaght, J.-M. Deniau, G. Chouvet, and S. Charpier. Distinct Patterns of Striatal Medium Spiny Neuron Activity during the Natural Sleep–Wake Cycle. *The Journal of Neuroscience* **26** (Nov. 2006), 12587–12595.

[Mar+97] H. Markram, J. Lübke, M. Frotscher, and B. Sakmann. Regulation of synaptic efficacy by coincidence of postsynaptic APs and EPSPs. *Science (New York, N.Y.)* **275** (Jan. 1997), 213–215.

[Mat+18] A. Mathis, P. Mamidanna, K. M. Cury, T. Abe, V. N. Murthy, M. W. Mathis, and M. Bethge. DeepLabCut: markerless pose estimation of user-defined body parts with deep learning. *Nature Neuroscience* **21** (Sept. 2018), 1281–1289.

[MDC01] S. Mahon, J. M. Deniau, and S. Charpier. Relationship between EEG potentials and intracellular activity of striatal and cortico-striatal neurons: an in vivo study under different anesthetics. *Cerebral Cortex (New York, N.Y.: 1991)* **11** (Apr. 2001), 360–373.

[MDG08] A. Morrison, M. Diesmann, and W. Gerstner. Phenomenological models of synaptic plasticity based on spike timing. *Biological Cybernetics* **98** (June 2008), 459–478.

[Mem+14] R.-M. Memmesheimer, R. Rubin, B. P. Olveczky, and H. Sompolinsky. Learning precisely timed spikes. *Neuron* **82** (May 2014), 925–938.

[Men+20] A. Mendes, G. Vignoud, S. Perez, E. Perrin, J. Touboul, and L. Venance. Concurrent Thalamostriatal and Corticostriatal Spike-Timing-Dependent Plasticity and Heterosynaptic Interactions Shape Striatal Plasticity Map. *Cerebral Cortex (New York, N.Y.: 1991)* **30** (June 2020), 4381–4401.

[Mes+19] T. Mesnard, G. Vignoud, J. Sacramento, W. Senn, and Y. Bengio. Ghost Units Yield Biologically Plausible Backprop in Deep Neural Networks. 2019. arXiv: 1911.08585 [q-bio.NC].

[MG20] J. C. Magee and C. Grienberger. Synaptic Plasticity Forms and Functions. *Annual Review of Neuroscience* **43** (2020), 95–117.

[Mil07] R. Miller. A Theory of the Basal Ganglia and Their Disorders. CRC Press, Aug. 2007.

[MKM08] E. I. Moser, E. Kropff, and M.-B. Moser. Place Cells, Grid Cells, and the Brain's Spatial Representation System. *Annual Review of Neuroscience* **31** (2008), 69–89.

[Mor+19] T. Morera-Herreras, Y. Gioanni, S. Perez, G. Vignoud, and L. Venance. Environmental enrichment shapes striatal spike-timing-dependent plasticity in vivo. *Scientific Reports* **9** (Dec. 2019), 19451.

[MT93] S. Meyn and R. Tweedie. Markov chains and stochastic stability. Communications and control engineering series. Springer, 1993.

[Nab+14] S. Nabavi, R. Fox, C. D. Proulx, J. Y. Lin, R. Y. Tsien, and R. Malinow. Engineering a memory with LTD and LTP. *Nature* **511** (July 2014), 348–352.

[Nev77] J. Neveu. Processus ponctuels. *École d'Été de Probabilités de Saint-Flour*. Ed. by P.-L. Hennequin. Vol. 598. Lecture Notes in Math. Berlin: Springer-Verlag, 1977, 249–445.

[NOI01] J. Nakai, M. Ohkura, and K. Imoto. A high signal-to-noise Ca(2+) probe composed of a single green fluorescent protein. *Nature Biotechnology* **19** (Feb. 2001), 137–141.

[Num04] E. Nummelin. General Irreducible Markov Chains and Non-Negative Operators. Cambridge University Press, June 2004.

[Oak75] D. Oakes. The Markovian Self-Exciting Process. *Journal of Applied Probability* **12** (1975), 69–77.

[OHa+16] J. K. O'Hare, K. K. Ade, T. Sukharnikova, S. D. Van Hooser, M. L. Palmeri, H. H. Yin, and N. Calakos. Pathway-Specific Striatal Substrates for Habitual Behavior. *Neuron* **89** (Feb. 2016), 472–479.

[Pai+13] V. Paille, E. Fino, K. Du, T. Morera-Herreras, S. Perez, J. H. Kotaleski, and L. Venance. GABAergic circuits control spike-timing-dependent plasticity. *The Journal of Neuroscience: The Official Journal of the Society for Neuroscience* **33** (May 2013), 9353–9363.

[Paw67] R. Pawula. Generalizations and extensions of the Fokker-Planck-Kolmogorov equations. *IEEE Transactions on Information Theory* **13** (1967), 33–41.

[PB19] S. Patrick and D. Bullock. *Graded striatal learning factors enable switches between goal-directed and habitual modes, by reassigning behavior control to the fastest-computed representation that predicts reward*. Tech. rep. Apr. 2019, 619445.

[PB20] U. Pereira and N. Brunel. Unsupervised Learning of Persistent and Sequential Activity. *Frontiers in Computational Neuroscience* **13** (2020).

[Per+22] S. Perez, Y. Cui, G. Vignoud, E. Perrin, A. Mendes, Z. Zheng, J. Touboul, and L. Venance. Striatum expresses region-specific plasticity consistent with distinct memory abilities. *Cell Reports* **38** (2022), 110521.

[Pet+21] A. J. Peters, J. M. J. Fabre, N. A. Steinmetz, K. D. Harris, and M. Carandini. Striatal activity topographically reflects cortical activity. *Nature* **591** (Mar. 2021), 420–425.

[Pez+22] E. Pezé-Heidsieck, S. Valverde, A. Di Nardo, and A. Prochiantz. Non-cell autonomous Engrailed regulates dendritic growth and protects DA neurons from degeneration via physiological eustress. Preprint. 2022.

[PG06a] J.-P. Pfister and W. Gerstner. Triplets of Spikes in a Model of Spike Timing-Dependent Plasticity. *Journal of Neuroscience* **26** (Sept. 2006), 9673–9682.

[PG06b] J.-p. Pfister and W. Gerstner. Beyond Pair-Based STDP: a Phenomenological Rule for Spike Triplet and Frequency Effects. *Advances in Neural Information Processing Systems*. Vol. 18. MIT Press, 2006.

[Phe01] R. R. Phelps. Lectures on Choquet's Theorem. 2nd ed. Lecture Notes in Mathematics. Berlin Heidelberg: Springer-Verlag, 2001.

[Pid+11] M. Pidoux, S. Mahon, J.-M. Deniau, and S. Charpier. Integration and propagation of somatosensory responses in the corticostriatal pathway: an intracellular study in vivo. *The Journal of Physiology* **589** (Jan. 2011), 263–281.

[PK08] V. Pawlak and J. N. D. Kerr. Dopamine receptor activation is required for corticostriatal spike-timing-dependent plasticity. *The Journal of Neuroscience: The Official Journal of the Society for Neuroscience* **28** (Mar. 2008), 2435–2446.

[PK10] F. Ponulak and A. Kasiński. Supervised learning in spiking neural networks with ReSuMe: sequence learning, classification, and spike shifting. *Neural Computation* **22** (Feb. 2010), 467–510.

[PS95] T. A. Poggio and T. J. Sejnowski. Models of Information Processing in the Basal Ganglia. MIT Press, 1995.

[PSV77] G. Papanicolalou, D. W. Stroock, and S. R. S. Varadhan. Martingale approach to some limit theorems. *Proc. 1976. Duke Conf. On Turbulence*. III. Duke Univ. Math, 1977.

[PSW17] B. Perthame, D. Salort, and G. Wainrib. Distributed synaptic weights in a LIF neural network and learning rules. *Physica D: Nonlinear Phenomena* **353** (2017), 20–30.

[PV19] E. Perrin and L. Venance. Bridging the gap between striatal plasticity and learning. *Current Opinion in Neurobiology*. Neurobiology of Learning and Plasticity **54** (Feb. 2019), 104–112.

[RA04] C. C. Rumsey and L. F. Abbott. Equalization of synaptic efficacy by activity- and timing-dependent synaptic plasticity. *Journal of Neurophysiology* **91** (May 2004), 2273–2280.

[Raa19] M. B. Raad. Renewal Time Points for Hawkes Processes. *arXiv:1906.02036 [math]* (June 2019).

[Rag+02] M. E. Ragozzino, K. E. Ragozzino, S. J. Y. Mizumori, and R. P. Kesner. Role of the dorsomedial striatum in behavioral flexibility for response and visual cue discrimination learning. *Behavioral Neuroscience* **116** (Feb. 2002), 105–115.

[Rag07] M. E. Ragozzino. The contribution of the medial prefrontal cortex, orbitofrontal cortex, and dorsomedial striatum to behavioral flexibility. *Annals of the New York Academy of Sciences* **1121** (Dec. 2007), 355–375.

[RB00] P. D. Roberts and C. C. Bell. Computational consequences of temporally asymmetric learning rules: II. Sensory image cancellation. *Journal of Computational Neuroscience* **9** (Aug. 2000), 67–83.

[RBS16] B. S. Robinson, T. W. Berger, and D. Song. Identification of Stable Spike-Timing-Dependent Plasticity from Spiking Activity with Generalized Multilinear Modeling. *Neural Comput.* **28** (Nov. 2016), 2320–2351.

[RBT00a] M. C. van Rossum, G. Q. Bi, and G. G. Turrigiano. Stable Hebbian learning from spike timing-dependent plasticity. *The Journal of Neuroscience: The Official Journal of the Society for Neuroscience* **20** (Dec. 2000), 8812–8821.

[RBT00b] M. C. W. v. Rossum, G. Q. Bi, and G. G. Turrigiano. Stable Hebbian Learning from Spike Timing-Dependent Plasticity. *Journal of Neuroscience* **20** (Dec. 2000), 8812–8821.

[RDL20] M. B. Raad, S. Ditlevsen, and E. Löcherbach. Stability and mean-field limits of age dependent Hawkes processes. *Annales de l'Institut Henri Poincaré, Probabilités et Statistiques* **56** (2020), 1958–1990.

[Rey+14] P. Reynaud-Bouret, V. Rivoirard, F. Grammont, and C. Tuleau-Malot. Goodness-of-Fit Tests and Nonparametric Adaptive Estimation for Spike Train Analysis. *The Journal of Mathematical Neuroscience* **4** (Apr. 2014), 3.

[Ric44] S. O. Rice. Mathematical analysis of random noise. *Bell System Technical Journal* **23** (1944), 282–332.

[RKO18] J. Rubin, B. Krauskopf, and H. Osinga. Natural extension of fast-slow decomposition for dynamical systems. *Physical Review E* **97** (2018), 012215.

[RL10] P. D. Roberts and T. K. Leen. Anti-Hebbian spike-timing-dependent plasticity and adaptive sensory processing. *Frontiers in Computational Neuroscience* **4** (2010), 156.

[RLS01] J. Rubin, D. D. Lee, and H. Sompolinsky. Equilibrium properties of temporally asymmetric Hebbian plasticity. *Physical Review Letters* **86** (Jan. 2001), 364–367.

[Rob00] P. D. Roberts. Dynamics of temporal learning rules. *Phys. Rev. E* **62** (3 Sept. 2000), 4077–4082.

[Rob03] P. Robert. Stochastic Networks and Queues. Stochastic Modelling and Applied Probability. Berlin Heidelberg: Springer-Verlag, 2003.

[Rob99] P. D. Roberts. Computational Consequences of Temporally Asymmetric Learning Rules: I. Differential Hebbian Learning. *Journal of Computational Neuroscience* **7** (Nov. 1999), 235–246.

[RRT13] P. Reynaud-Bouret, V. Rivoirard, and C. Tuleau-Malot. Inference of functional connectivity in Neurosciences via Hawkes processes. *2013 IEEE Global Conference on Signal and Information Processing*. Dec. 2013, 317–320.

[RS10] P. Reynaud-Bouret and S. Schbath. Adaptive estimation for Hawkes processes; application to genome analysis. *Annals of Statistics* **38** (Nov. 2010), 2781–2822.

[RS11] T. Requarth and N. B. Sawtell. Neural mechanisms for filtering self-generated sensory signals in cerebellum-like circuits. *Current Opinion in Neurobiology* **21** (Aug. 2011), 602–608.

[RT16] P. Robert and J. Touboul. On the Dynamics of Random Neuronal Networks. *Journal of Statistical Physics* **165** (Nov. 2016), 545–584.

[Rub+17] J. E. Rubin, J. Signerska-Rynkowska, J. D. Touboul, and A. Vidal. Wild oscillations in a nonlinear neuron model with resets: (I) Bursting, spike-adding and chaos. *Discrete & Continuous Dynamical Systems - B* **22** (2017), 3967.

[Rub17] J. E. Rubin. Computational models of basal ganglia dysfunction: the dynamics is in the details. *Current Opinion in Neurobiology* **46** (2017), 127–135.

[Rud73] W. Rudin. Functional analysis. McGraw-Hill, 1973.

[RV20] P. Robert and G. Vignoud. Stochastic Models of Neural Synaptic Plasticity. 2020. arXiv: 2010.08195 [math.PR].

[RV21a] P. Robert and G. Vignoud. Averaging Principles for Markovian Models of Plasticity. *Journal of Statistical Physics* **183** (June 2021), 47–90.

[RV21b] P. Robert and G. Vignoud. Stochastic Models of Neural Plasticity. *SIAM Journal on Applied Mathematics* **81** (Sept. 2021), 1821–1846.

[RV21c] P. Robert and G. Vignoud. Stochastic Models of Neural Synaptic Plasticity: A Scaling Approach. *SIAM Journal on Applied Mathematics* **81** (2021), 2362–2386.

[RV22a] P. Robert and G. Vignoud. A Markovian approach to Hawkes processes. In writing. 2022.

[RV22b] P. Robert and G. Vignoud. On the Spontaneous Dynamics of Synaptic Weights in Stochastic STDP Models. *revisions at Physical Review E* (2022).

[RW00] L. C. G. Rogers and D. Williams. Diffusions, Markov Processes and Martingales: Volume 2, Itô Calculus. Cambridge University Press, Sept. 2000.

[SBC02] H. Z. Shouval, M. F. Bear, and L. N. Cooper. A unified model of NMDA receptor-dependent bidirectional synaptic plasticity. *Proceedings of the National Academy of Sciences of the United States of America* **99** (Aug. 2002), 10831–10836.

[SBD18] J. Schiller, S. Berlin, and D. Derdikman. The Many Worlds of Plasticity Rules. *Trends in Neurosciences* **41** (Mar. 2018), 124–127.

[Sch18] W. Schottky. Über spontane Stromschwankungen in verschiedenen Elektrizitätsleitern. *Annalen der physik* **362** (1918), 541–567.

[SDM97] W. Schultz, P. Dayan, and P. R. Montague. A neural substrate of prediction and reward. *Science (New York, N.Y.)* **275** (Mar. 1997), 1593–1599.

[Seu00] H. S. Seung. Half a century of Hebb. *Nature Neuroscience* **3** (Nov. 2000), 1166–1166.

[Sha92] C. J. Shatz. The Developing Brain. *Scientific American* **267** (1992), 60–67.

[She+08] W. Shen, M. Flajolet, P. Greengard, and D. J. Surmeier. Dichotomous dopaminergic control of striatal synaptic plasticity. *Science (New York, N.Y.)* **321** (Aug. 2008), 848–851.

[Si+19] G. Si, J. K. Kanwal, Y. Hu, C. J. Tabone, J. Baron, M. Berck, G. Vignoud, and A. D. Samuel. Structured Odorant Response Patterns across a Complete Olfactory Receptor Neuron Population. *Neuron* **101** (2019), 950–962.e7.

[SJT07] D. Standage, S. Jalil, and T. Trappenberg. Computational consequences of experimentally derived spike-time and weight dependent plasticity rules. *Biological Cybernetics* **96** (June 2007), 615–623.

[Smi+16] J. B. Smith, J. R. Klug, D. L. Ross, C. D. Howard, N. G. Hollon, V. I. Ko, H. Hoffman, E. M. Callaway, C. R. Gerfen, and X. Jin. Genetic-Based Dissection Unveils the Inputs and Outputs of Striatal Patch and Matrix Compartments. *Neuron* **91** (Sept. 2016), 1069–1084.

[SRR10] J. M. Schulz, P. Redgrave, and J. N. J. Reynolds. Cortico-striatal spike-timing dependent plasticity after activation of subcortical pathways. *Frontiers in Synaptic Neuroscience* **2** (2010), 23.

[ST16] H. Steiner and K. Y. Tseng. Handbook of Basal Ganglia Structure and Function. Academic Press, 2016.

[Sta+10] T. A. Stalnaker, G. G. Calhoon, M. Ogawa, M. R. Roesch, and G. Schoenbaum. Neural Correlates of Stimulus–Response and Response–Outcome Associations in Dorsolateral Versus Dorsomedial Striatum. *Frontiers in Integrative Neuroscience* **4** (May 2010), 12.

[STN01] P. J. Sjöström, G. G. Turrigiano, and S. B. Nelson. Rate, timing, and cooperativity jointly determine cortical synaptic plasticity. *Neuron* **32** (Dec. 2001), 1149–1164.

[Suv19] A. Suvrathan. Beyond STDP—towards diverse and functionally relevant plasticity rules. *Current Opinion in Neurobiology*. Neurobiology of Learning and Plasticity **54** (Feb. 2019), 12–19.

[SWW10] H. Shouval, S. Wang, and G. Wittenberg. Spike Timing Dependent Plasticity: A Consequence of More Fundamental Learning Rules. *Frontiers in Computational Neuroscience* **4** (2010), 19.

[TAG18] M. A. Triplett, L. Avitan, and G. J. Goodhill. Emergence of spontaneous assembly activity in developing neural networks without afferent input. *PLoS Computational Biology* **14** (Sept. 2018), e1006421.

[TB09] J. Touboul and R. Brette. Spiking Dynamics of Bidimensional Integrate-and-Fire Neurons. *SIAM Journal on Applied Dynamical Systems* **8** (Jan. 2009), 1462–1506.

[TDM14] T. Takeuchi, A. J. Duszkiewicz, and R. G. M. Morris. The synaptic plasticity and memory hypothesis: encoding, storage and persistence. *Philosophical Transactions of the Royal Society of London. Series B, Biological Sciences* **369** (Jan. 2014), 20130288.

[TG14] C. A. Thorn and A. M. Graybiel. Differential entrainment and learning-related dynamics of spike and local field potential activity in the sensorimotor and associative striatum. *The Journal of Neuroscience: The Official Journal of the Society for Neuroscience* **34** (Feb. 2014), 2845–2859.

[Tho+10] C. A. Thorn, H. Atallah, M. Howe, and A. M. Graybiel. Differential Dynamics of Activity Changes in Dorsolateral and Dorsomedial Striatal Loops During Learning. *Neuron* **66** (June 2010), 781–795.

[TMK18] S. Tonegawa, M. D. Morrissey, and T. Kitamura. The role of engram cells in the systems consolidation of memory. *Nature Reviews Neuroscience* **19** (Aug. 2018), 485–498.

[TN04] G. G. Turrigiano and S. B. Nelson. Homeostatic plasticity in the developing nervous system. *Nature Reviews. Neuroscience* **5** (Feb. 2004), 97–107.

[Tou08] J. Touboul. Bifurcation Analysis of a General Class of Nonlinear Integrate-and-Fire Neurons. *SIAM Journal on Applied Mathematics* **68** (Jan. 2008), 1045–1079.

[US09] R. Urbanczik and W. Senn. A gradient learning rule for the tempotron. *Neural Computation* **21** (Feb. 2009), 340–352.

[Val+17] S. Valtcheva, V. Paillé, Y. Dembitskaya, S. Perez, G. Gangarossa, E. Fino, and L. Venance. Developmental control of spike-timing-dependent plasticity by tonic GABAergic signaling in striatum. *Neuropharmacology* **121** (July 2017), 261–277.

[Van+19] Y. Vandaele, N. R. Mahajan, D. J. Ottenheimer, J. M. Richard, S. P. Mysore, and P. H. Janak. Distinct recruitment of dorsomedial and dorsolateral striatum erodes with extended training. *eLife* **8** (Oct. 2019), e49536.

[Ver70] D. Vere-Jones. Stochastic Models for Earthquake Occurrence. *Journal of the Royal Statistical Society. Series B (Methodological)* **32** (1970), 1–62.

[Vig+19] G. Vignoud, S. Perez, E. Perrin, C. Piette, A. Mendes, and L. Venance. D1/D2 detection from action-potential properties using machine learning approach in the dorsal striatum. *International Basal Ganglia Society Meeting (IBAGS)*. 2019.

[VTV20] G. Vignoud, J. Touboul, and L. Venance. A synaptic theory for procedural and sequence learning in the striatum. *Bernstein Conference 2020*. 2020.

[VTV22] G. Vignoud, J. Touboul, and L. Venance. A synaptic theory for sequence learning in the striatum. Preprint. 2022.

[VVT18] G. Vignoud, L. Venance, and J. D. Touboul. Interplay of multiple pathways and activity-dependent rules in STDP. *PLoS computational biology* **14** (2018), e1006184.

[WAS07] J. R. Wickens, G. W. Arbuthnott, and T. Shindou. Simulation of GABA function in the basal ganglia: computational models of GABAergic mechanisms in basal ganglia function. *Progress in Brain Research* **160** (2007), 313–329.

[Wic93] J. Wickens. A Theory of the Striatum. New York, NY, USA: Elsevier Science Inc., 1993.

[Wil+19] J. A. Willett, J. Cao, D. M. Dorris, A. G. Johnson, L. A. Ginnari, and J. Meitzen. Electrophysiological Properties of Medium Spiny Neuron Subtypes in the Caudate-Putamen of Prepubertal Male and Female Drd1a-tdTomato Line 6 BAC Transgenic Mice. *eNeuro* **6** (Mar. 2019), ENEURO.0016–19.2019.

[WL96] M. Wehr and G. Laurent. Odour encoding by temporal sequences of firing in oscillating neural assemblies. *Nature* **384** (Nov. 1996), 162–166.

[WRL03] A. Williams, P. D. Roberts, and T. K. Leen. Stability of negative-image equilibria in spike-timing-dependent plasticity. *Physical Review E* **68** (Aug. 2003), 021923.

[Xie+22] Y. Xie et al. Geometry of sequence working memory in macaque prefrontal cortex. *Science* **375** (Feb. 2022), 632–639.

[XZZ15] Q. Xiong, P. Znamenskiy, and A. M. Zador. Selective corticostriatal plasticity during acquisition of an auditory discrimination task. *Nature* **521** (May 2015), 348–351.

[YAK11] M. Y. Yim, A. Aertsen, and A. Kumar. Significance of Input Correlations in Striatal Function. *PLoS Computational Biology* **7** (Nov. 2011).

[Yin+09] H. H. Yin, S. P. Mulcare, M. R. F. Hilário, E. Clouse, T. Holloway, M. I. Davis, A. C. Hansson, D. M. Lovinger, and R. M. Costa. Dynamic reorganization of striatal circuits during the acquisition and consolidation of a skill. *Nature Neuroscience* **12** (Mar. 2009), 333–341.

[YK06] H. H. Yin and B. J. Knowlton. The role of the basal ganglia in habit formation. *Nature Reviews. Neuroscience* **7** (June 2006), 464–476.

[ZD07] Q. Zou and A. Destexhe. Kinetic models of spike-timing dependent plasticity and their functional consequences in detecting correlations. *Biological Cybernetics* **97** (July 2007), 81–97.

[ZR02] R. S. Zucker and W. G. Regehr. Short-term synaptic plasticity. *Annual Review of Physiology* **64** (2002), 355–405.

LIST OF FIGURES

LIST OF TABLES